BIOLOGICAL AND ECOLOGICAL STUDIES ON MARINE ICHTHYOPLANKTON

EDITED BY: Hui Zhang, Chen Jiang and Yuan Li

PUBLISHED IN: Frontiers in Marine Science

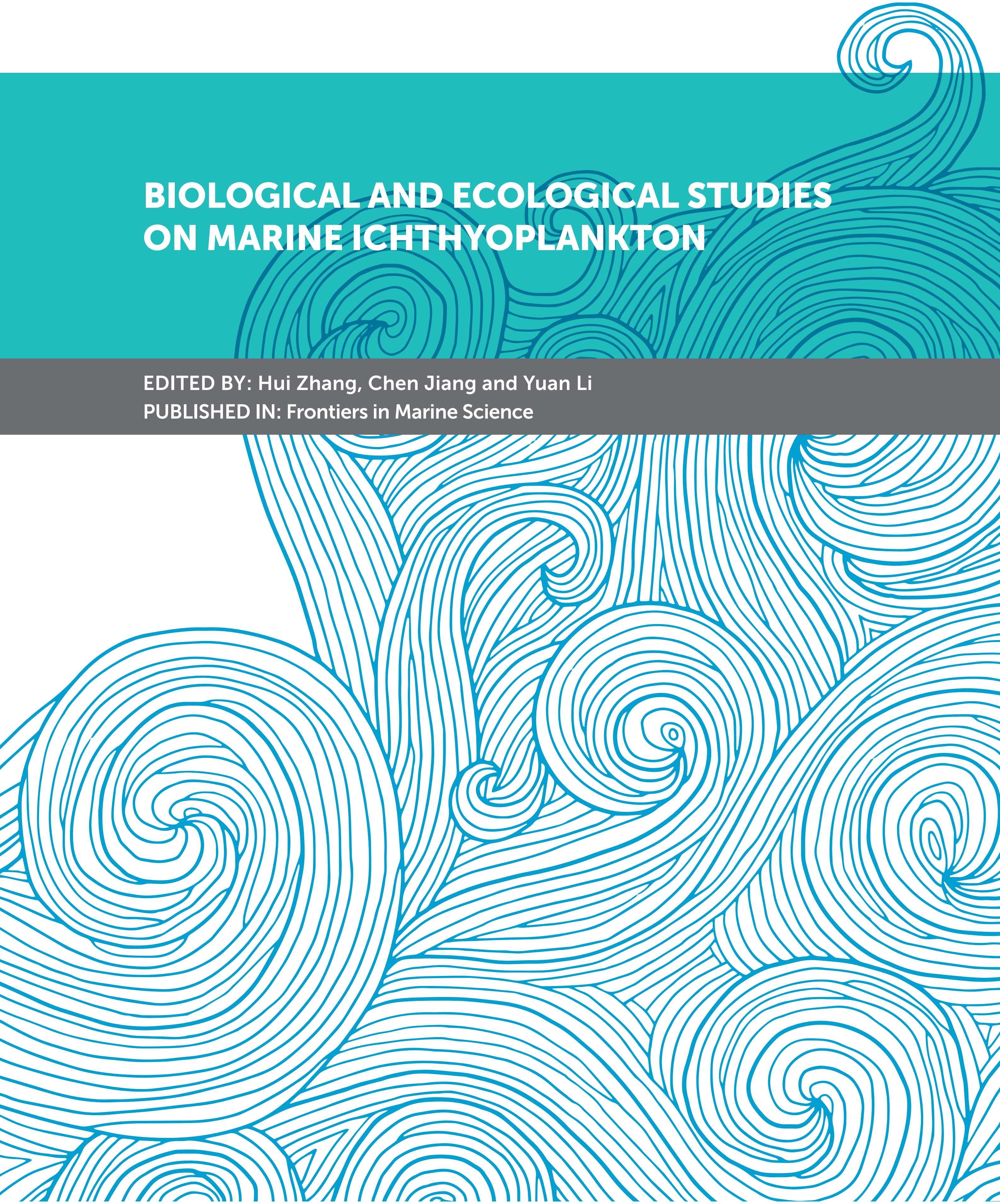

frontiers Research Topics

ISSN 1664-8714
ISBN 978-2-88976-745-8
DOI 10.3389/978-2-88976-745-8

About Frontiers

Frontiers is more than just an open-access publisher of scholarly articles: it is a pioneering approach to the world of academia, radically improving the way scholarly research is managed. The grand vision of Frontiers is a world where all people have an equal opportunity to seek, share and generate knowledge. Frontiers provides immediate and permanent online open access to all its publications, but this alone is not enough to realize our grand goals.

Frontiers Journal Series

The Frontiers Journal Series is a multi-tier and interdisciplinary set of open-access, online journals, promising a paradigm shift from the current review, selection and dissemination processes in academic publishing. All Frontiers journals are driven by researchers for researchers; therefore, they constitute a service to the scholarly community. At the same time, the Frontiers Journal Series operates on a revolutionary invention, the tiered publishing system, initially addressing specific communities of scholars, and gradually climbing up to broader public understanding, thus serving the interests of the lay society, too.

Dedication to Quality

Each Frontiers article is a landmark of the highest quality, thanks to genuinely collaborative interactions between authors and review editors, who include some of the world's best academicians. Research must be certified by peers before entering a stream of knowledge that may eventually reach the public - and shape society; therefore, Frontiers only applies the most rigorous and unbiased reviews.
Frontiers revolutionizes research publishing by freely delivering the most outstanding research, evaluated with no bias from both the academic and social point of view. By applying the most advanced information technologies, Frontiers is catapulting scholarly publishing into a new generation.

What are Frontiers Research Topics?

Frontiers Research Topics are very popular trademarks of the Frontiers Journals Series: they are collections of at least ten articles, all centered on a particular subject. With their unique mix of varied contributions from Original Research to Review Articles, Frontiers Research Topics unify the most influential researchers, the latest key findings and historical advances in a hot research area! Find out more on how to host your own Frontiers Research Topic or contribute to one as an author by contacting the Frontiers Editorial Office: frontiersin.org/about/contacts

BIOLOGICAL AND ECOLOGICAL STUDIES ON MARINE ICHTHYOPLANKTON

Topic Editors:
Hui Zhang, Institute of Oceanology, Chinese Academy of Sciences (CAS), China
Chen Jiang, Dalian Ocean University, China
Yuan Li, Third Institute of Oceanography, Ministry of Natural Resources, China

Citation: Zhang, H., Jiang, C., Li, Y., eds. (2022). Biological and Ecological Studies on Marine Ichthyoplankton. Lausanne: Frontiers Media SA.
doi: 10.3389/978-2-88976-745-8

Table of Contents

frontiers | Frontiers in Marine Science

EDITORIAL
published: 13 July 2022
doi: 10.3389/fmars.2022.948521

Editorial: Biological and Ecological Studies on Marine Ichthyoplankton

Hui Zhang[1,2,3], Yuan Li[4] and Chen Jiang[5]*

[1] CAS Key Laboratory of Marine Ecology and Environmental Sciences, Institute of Oceanology, Chinese Academy of Sciences, Qingdao, China, [2] Laboratory for Marine Ecology and Environmental Science, Qingdao National Laboratory for Marine Science and Technology, Qingdao, China, [3] University of Chinese Academy of Sciences, Beijing, China, [4] Third Institute of Oceanography, Ministry of Natural Resources, Xiamen, China, [5] Key Laboratory of Mariculture & Stock Enhancement in North China's Sea, Ministry of Agriculture, Dalian Ocean University, Dalian, China

Keywords: community structure and its environmental factors, DNA barcoding, China, Eastern Indian Ocean, Mexico, Norway, Barents Sea

Editorial on the Research Topic

Biological and Ecological Studies on Marine Ichthyoplankton

Ichthyoplankton (including fish eggs and larvae), belonging to the early life stages, is important for the growth and development of communities (Shan et al., 2004; Lechner et al., 2016). Although this stage is short for the fish life history, it is the most vulnerable stage in the whole life development cycle, which could change quickly in response to environmental variations (Downie et al., 2020). The quantity and survival of ichthyoplankton reflects the biomass and interannual dynamics of future fish stocks (Butler et al., 2003). It provides the basis for the recruitment of fish stocks and the sustainable use of fishery resources. Therefore, understanding the distribution patterns of ichthyoplankton and exploring the abiotic and biotic factors influencing the distribution patterns are crucial for assessing fish recruitment and stock restoration. Moreover, ichthyoplankton plays an important role in the energy transfer of estuarine ecosystems, which is a key link in the aquatic food web (Wan and Sun, 2006). Despite the fact that ichthyoplankton plays such important role in the ecosystem, researchers have not paid enough attention to it. Possible reasons for this, at least in part, are the difficulties in species identification. At present, more than 36,058 fish species have been identified as adults (Fricke et al., 2021), but only approximately 10% of these can be identified as larvae or postlarvae, while less than 10% of eggs can be identified to species (Shao et al., 2001). Currently, this situation is gradually being improved by the combination of morphology and DNA barcoding identification methods.

However, limited by the life history characteristics of ichthyoplankton, research on sample collection, species identification, community structure changes, and responses to environmental and climate changes at this stage is lagging and weak. Thus, investigating and evaluating the ichthyoplankton community not only could lay a foundation for understanding the status of fish stocks, determining spawning sites and spawning cycles, and explicating fishery management, but also help to clarify the energy flow and material circulation of estuarine ecosystems.

Altogether, thirteen articles are accepted in this topic, covering nine region including Yangtze River Estuary (China), Sansha Bay (China), Beibu Gulf (China), Pearl River Estuary (China), Macclesfield bank (China), Ninety East Ridge (Eastern Indian Ocean), northern Gulf of Mexico (Mexico), Norwegian coast (Norway) and Barents Sea. Among which seven focused on the community structure of ichthyoplankton (Wang et al.; Hou et al.; Jiang et al.; Zhang et al.; Huang et al.; Hou et al.; Vikebø et al.; Chen et al.; Endo et al.; Long et al.; Wang D et al.; Chen et al.), three explored the feeding characteristics of ichthyoplankton (Vikebø et al.; Chen et al.; Endo et al.), one discussed the selection of spawning habitat by ichthyoplankton (Wang et al., 2021), one assessed the

OPEN ACCESS

Edited and reviewed by:
Yngvar Olsen,
Norwegian University of Science and Technology, Norway

****Correspondence:***
Hui Zhang
zhanghui@qdio.ac.cn

Specialty section:
This article was submitted to
Marine Fisheries, Aquaculture and
Living Resources,
a section of the journal
Frontiers in Marine Science

Received: *19 May 2022*
Accepted: *16 June 2022*
Published: *13 July 2022*

Citation:
Zhang H, Li Y and Jiang C (2022)
Editorial: Biological and Ecological
Studies on Marine Ichthyoplankton.
Front. Mar. Sci. 9:948521.
doi: 10.3389/fmars.2022.948521

feasibility of 6 sampling design for ichthyoplankton (Long et al.), and one systematic review of estuarine ichthyoplankton studies (Zhang et al.).

Overall, the studies jointly form the latest advances in current research on the ecology and biology of ichthyoplankton. DNA barcoding, as a complementary tool for morphological identification, is gradually being applied in ichthyoplankton classification (Kerr et al., 2020). It has been affirmed to be effective in identifying fish eggs and larvae and has shown potential in ichthyoplankton assemblage and ecology studies.

Community structure, including species composition and distribution, has long been one of the most important studies on the ichthyoplankton. Temporally, the high abundance of ichthyoplankton (Pearl River Estuary) mainly occurred in spring and autumn (Hou et al.); spatially, the high density of ichthyoplankton (Sansha Bay) occurred near the coastline (Jiang et al.). The species composition of ichthyoplankton communities in different areas differed greatly, which may be related to the ecological habits of ichthyoplankton and environment. Therefore, the factors affecting the community structure of ichthyoplankton have become the other key concerns of researchers. Ichthyoplankton assemblage structure appears to be strongly influenced by temperature, salinity, water depth, distance from shore, Chlorophyll *a*, and sea level anomalies. Interestingly, 80% articles on environmental factors affecting the structure of ichthyoplankton communities concluded that temperature was the main influencing factor. For estuarine or inshore ichthyoplankton community, temperature and salinity were the most important factors (Wang D et al.; Jiang et al.; Wang et al.; Hou et al.); while, for ocean community, sea surface height correlated with ichthyoplankton abundance the most (Zhang et al.); for coral reef community, the larval fish assemblage showed distinct spatial differences responding well with the geographical conditions, and the most reef-associated fish occurred inside the Atoll, and the abyssal fish presented near the edge (Huang et al.). In addition, Wang et al. characterized the dynamics of larval fish assemblages across epipelagic, mesopelagic, and bathypelagic (0-1,500 m) regions of the Gulf of Mexico, which indicated the abundance of ichthyoplankton decreased with increasing depth, and the pelagic upper layer was significantly higher than the pelagic lower layer and the deep sea in terms of abundance and diversity.

Moreover, the spawning habitat selection mechanism under the locally varying environmental conditions was explored based on a case study of *Coilia mystus* in the Yangtze Estuary by Wang et al., which are helpful in gaining a comprehensive understanding of fish spawning habitat selection mechanism in the estuarine areas and conductive to the protection of the population. Long et al. established six stratified schemes for monitoring *C. mystus* in the Yangtze estuary to evaluate its performance in different sample sizes, providing references to future sampling designs for ichthyoplankton in the estuary area.

In addition, quantity, quality and timing of food are critical to the replenishment and survival of juvenile fish populations (Swalethorp et al., 2014). Chen et al. detected the gastrointestinal contents of larvae and early larvae of small yellow croaker in the Yangtze Estuary to reveal its feeding habits during the settlement period. Vikebø et al. and Endo et al. evaluated the effects of food and environmental factors on the growth and survival of Northeast Pacific cod by combining multiple models.

Furthermore, estuarine ichthyoplankton over the last 60 years (1951–2022) were reviewed, it focus on evaluation of ichthyoplankton published studies, community structure and factors affecting community structure. The review emphasized that an increase in the amount of research on estuarine ichthyoplankton over time, but it was mainly concentrated in developed countries. Importantly, climate change indirectly affects the community structure of ichthyoplankton by altering the spawning habitat, spawning time, and egg hatching time. The movement of spawning sites poleward and the advance of spawning time have become a consistent trend (Zhang et al.).

Indeed, the oceanic marine environment is changeable, and ichthyoplankton in different sea areas are affected by different variables, even producing multivariable synergistic effects. Therefore, strengthen long-term monitoring of ichthyoplankton in important marine areas will not only understand the variations in the community structure and protect their spawning sites and habitats, but will also provide a rich theoretical basis for the restoration and sustainable development of fish resources.

AUTHOR CONTRIBUTIONS

All authors listed have made a substantial, direct, and intellectual contribution to the work and approved it for publication.

REFERENCES

Butler, J. L., Jacobson, L. D., Barnes, J. T. and Moser, H. G. (2003). Biology and Population Dynamics of Cowcod (Sebastes Levis) in the Southern California Bight. *Fish. Bull.* 101 (2), 260–280.

Downie, A. T., Illing, B., Faria, A. M. and Rummer, J. L. (2020). Swimming Performance of Marine Fish Larvae: Review of a Universal Trait Under Ecological and Environmental Pressure. *Rev. Fish Biol. Fish.* 30, 93–98. doi: 10.1007/s11160-019-09592-w

Fricke, R., Eschmeyer, W. N. and van der L, R. (2021) *Eschmeyer's Catalog of Fishes: Genera, Species, References*. Available at: http://researcharchive.calacademy.org/research/ichthyology/catalog/fishcatmain.asp.

Kerr, M., Browning, J., Bønnelycke, E. M., Zhang, Y., Hu, C., Armenteros, M., et al. (2020). DNA Barcoding of Fish Eggs Collected Off Northwestern Cuba and Across the Florida Straits Demonstrates Egg Transport by Mesoscale Eddies. *Fish. Oceanogr.* 29, 340–348. doi: 10.1111/fog.12475

Lechner, A., Keckeis, H. and Humphries, P. (2016). Patterns and Processes in the Drift of Early Developmental Stages of Fish in Rivers: A Review. *Rev. Fish Biol. Fish.* 26, 471–498. doi: 10.1007/s11160-016-9437-y

Shan, X. J., Xian, W. W. and Wu, Y. F. (2004). Progress of Studies on Ichthyoplankton Ecology of Changjiang River Estuary. *J. Oceanol. Limnol.* 0 (4), 87–93. doi: 10.13984/j.cnki.cn37-1141.2004.04.015

Shao, G., Yang, R. and Chen, K. (2001). *An Identification Guide of Marine Fish Eggs From Taiwan* (M. Taibei: Academia Sinica).

Swalethorp, R., Kjellerup, S., Malanski, E., Munk, P. and Nielsen, T. G. (2014). Feeding Opportunities of Larval and Juvenile Cod (Gadus Morhua) in a Greenlandic Fjord: Temporal and Spatial Linkages Between Cod and Their Preferred Prey. *Mar. Biol.* 161, 2831–2846. doi: 10.1007/s00227-014-2549-9

Wan, R. and Sun, S. (2006). The Category Composition and Abundance of Ichthyoplankton in the Ecosystem of the Yellow Sea and the East China Sea. *Curr. Zool.* 52 (1), 28–44. doi: 10.3969/j.issn.1674-5507.2006.01.004

Conflict of Interest: The authors declare that the research was conducted in the absence of any commercial or financial relationships that could be construed as a potential conflict of interest.

frontiers in Marine Science

ORIGINAL RESEARCH
published: 16 September 2021
doi: 10.3389/fmars.2021.732970

Assemblage Structure of the Ichthyoplankton and Its Relationship With Environmental Factors in Spring and Autumn off the Pearl River Estuary

Gang Hou[1,2], Jinrun Wang[1], Limei Liu[1], Yanying Chen[1], Chuanhao Pan[1], Jianbin Lin[1] and Hui Zhang[3,4,5]*

[1] College of Fisheries, Guangdong Ocean University, Zhanjiang, China, [2] Marine Resources Big Data Center of South China Sea, Southern Marine Science and Engineering Guangdong Laboratory, Zhanjiang, China, [3] CAS Key Laboratory of Marine Ecology and Environmental Sciences, Institute of Oceanology, Chinese Academy of Sciences (CAS), Qingdao, China, [4] Center for Ocean Mega-Science, Chinese Academy of Sciences (CAS), Qingdao, China, [5] Laboratory for Marine Ecology and Environmental Science, Qingdao National Laboratory for Marine Science and Technology, Qingdao, China

OPEN ACCESS

Edited by:
JInghui Fang,
Yellow Sea Fisheries Research Institute, Chinese Academy of Fishery Sciences (CAFS), China

Reviewed by:
Shuyang Ma,
Ocean University of China, China
Sónia Cotrim Marques,
Center for Marine and Environmental Sciences (MARE-IPLeiria), Portugal

***Correspondence:**
Hui Zhang
zhanghui@qdio.ac.cn

Specialty section:
This article was submitted to Marine Fisheries, Aquaculture and Living Resources, a section of the journal Frontiers in Marine Science

Received: *29 June 2021*
Accepted: *16 August 2021*
Published: *16 September 2021*

Citation:
Hou G, Wang J, Liu L, Chen Y, Pan C, Lin J and Zhang H (2021) Assemblage Structure of the Ichthyoplankton and Its Relationship With Environmental Factors in Spring and Autumn off the Pearl River Estuary. Front. Mar. Sci. 8:732970. doi: 10.3389/fmars.2021.732970

Ichthyoplankton assemblages and their relationship with environmental variables are investigated in waters off the Pearl River Estuary in spring and autumn of 2019. Of 80 ichthyoplankton taxa identified using DNA barcode and morphological methods, 61 are identified to species. The most abundance families (Carangidae, Trichiuridae, Mullidae, and Scombridae) account for 61.34% of the horizontal total catch in spring, while Menidae and Carangidae are the most abundant families identified in autumn, accounting for 89.72% of the horizontal total catch. Cluster analysis identifies three species assemblages in spring, and four in autumn based on horizontal trawls. Relationships between assemblage structure and environmental variables (*in situ* and remote sensed) are determined by canonical correspondence analysis. Ichthyoplankton assemblage structure appears to be strongly influenced by sea level anomalies, salinity, water depth, temperature at 10 m depth, and distance from shore. We demonstrate the efficacy of using DNA barcode to identify ichthyoplankton, and suggest how these data can be used to protect fish spawning grounds in waters off the Pearl River Estuary.

Keywords: ichthyoplankton, DNA barcode, assemblage structure, spawning ground conservation, Pearl River Estuary

INTRODUCTION

Information on the composition, and spatial and temporal distributions of ichthyoplankton assemblages is of value because it can be used to identify fish spawning sites and reproductive seasons, and appropriate areas and strategies for their protection (Potter et al., 1990; Raynie and Shaw, 1994; Oliveira and Ferreira, 2010; Makrakis, 2019). Ichthyoplankton–the early life stages of fish–undergo dynamic changes in morphology, physiological capability, behavior, ecological role, and habitat as they develop. Their natural mortality rate is high (Fuiman, 2003). Being a key life cycle stage, the survival rate of these fish eggs and larvae affects their recruitment and assemblage dynamics (Chambers and Trippel, 1997; Cao et al., 2007). The formation of ichthyoplankton assemblages is regulated by the physical and biological processes, and their distributions are considered to be more important to the survival of larvae than absolute larval abundance (Hewitt, 1981). Because ichthyoplankton assemblage distribution can be correlated with adult spawning phases and biotic/abiotic variables, those conditions suitable for adult reproduction, and mechanisms that affect planktonic early life stages, can be identified (Doyle et al., 1993; Whitfield, 1999; Hare et al., 2001; Mesa et al., 2016).

Ranked as the 13th or 14th largest river in the world and 2nd largest river in China, the Pearl River, has an annual runoff exceeding 33.6×10^9 m^3 (Ou et al., 2007). This river discharges into the South China Sea (SCS) across the Pearl River Delta floodplain, and in doing so transports abundant nutrients into the sea (Lu et al., 2007; Chen et al., 2008). The terrain of the Pearl River Estuary is complex, and the interlaced river network empties into the northern SCS through eight distributaries. This geographic complexity, coupled with variable salinity and high nutrient input, render the Pearl River Estuary and adjacent aquatic environments variable, changeable, and high productive (Zhang et al., 2011; Zhu et al., 2019). Waters of and off the Pearl River Estuary provide habitat for 542 species of fish (287 species in the estuary area, and 330 species in coastal and offshore areas) (Li, 2008). This species richness is more than 36% of the total number of fish species (nearly 1500) reported from the northern SCS (Zhan, 1998; Li, 2008; Sun and Chen, 2013). This high richness and the fish yield from these waters from depths greater than 30 m render this area one of the most important fishing grounds in the SCS (Wang, 2012; Cai et al., 2018). However, fish resources in this region have decreased dramatically in recent decades, largely because of anthropogenic disturbance and climate change (Zeng et al., 2019; Zhou et al., 2019). Meanwhile, the Indo-Pacific humpback dolphin, *Sousa Chinese* Osbeck, 1765, Indo-Pacific finless porpoise *Neophocaena phocaenoides* (Cuvier, 1829), Eden's Whale, *Balaenoptera edeni* Anderson, 1879, Bryde's whale, *B. edeni* Olsen, 1913, and humpback whale *Megaptera novaeangliae* Borowski, 1781, which mainly prey on fishes, have all been reported from waters off the Pearl River Estuary (Jefferson et al., 2012; Peilie, 2012; Lin et al., 2019). Sadly Bryde's and humpback whales have disappeared from these waters, and the population of Indo-Pacific humpback dolphin has continuously declined (Hung et al., 2006; Peilie, 2012; Lin et al., 2019). A shortage of food is considered to be one of the main reasons for these disappearances and population declines (Li et al., 2020).

Understanding the spatial distributions of fish is necessary to understand marine ecosystem dynamics. The Pearl River Estuary and its offshore waters are important spawning, feeding, and nursing ground in the northern SCS (Zhan, 1998; Li et al., 2000; Wang and Lin, 2006; Xiao et al., 2013). Accordingly, understanding how the distributions of ichthyoplankton are linked to environmental variables can provide valuable information to assist with spatial, temporal, and/or ecosystem-based approaches to fishery management (Hsieh C. H. et al., 2010; Laman et al., 2017). However, despite the importance of these waters to fish stocks, due to the difficulties identifying early life stages of fish, only Xiao et al. (2013) has studied the ichthyoplankton fauna from them, wherein the abundance of 113 identified taxa was reported. Anthropogenic disturbance, climate change, and fisheries over-exploitation have all contributed to serious declines in fishery resources in the waters of and off the Pearl River Estuary (Duan et al., 2009; Wang et al., 2016; Zeng et al., 2019; Zhou et al., 2019). Because of this there is a pressing need to investigate the status of fish spawning grounds, and ichthyoplankton assemblages in this area, so that more effective management and/or protection of these resources can be achieved.

Precise identification of species in ichthyoplankton samples is important to understand species reproductive biology, preferred spawning time, and spawning grounds (Baumgartner et al., 2004; Cao et al., 2007; Claydon et al., 2014; Zhang et al., 2015). However, accurately identifying fish eggs and larvae to species is difficult, probably for which reason there have been few empirical studies on ichthyoplankton in the SCS (Li K. Z. et al., 2014; Huang et al., 2017; Hou et al., 2021). DNA barcode, which delimits species using molecular maker (e.g., cytochrome c oxidase subunit I, COI), have been widely applied to facilitate the identification of fish eggs and larvae (Valdez-Moreno et al., 2010; Frantine-Silva et al., 2015; Hubert et al., 2015; Leyva-Cruz et al., 2016; Burrows et al., 2018; Kerr et al., 2020; Chen et al., 2021; Hou et al., 2021). For instance, Leyva-Cruz et al. (2016) identified 42 taxa of fish eggs collected from the waters surrounding Banco Chinchorro in the Mexican Caribbean. Burrows et al. (2018) applied the DNA barcode to identify fish eggs in the Gulf of Mexico, and delimited 709 eggs to 62 species. Kerr et al. (2020) successfully identified 564 fish eggs to 89 taxa collected from northwestern Cuba and across the Florida Straits using DNA barcode. Therefore, it has been demonstrated that DNA barcode can effectively identify fish eggs and larvae, and illustrated the potentiality in the study of ichthyoplankton assemblage and ecology.

To identify fish spawning grounds in waters off the Pearl River Estuary we undertook ichthyoplankton surveys in the spring and autumn of 2019. Our aims were to: (i) identify fish eggs and larvae using DNA barcodes and morphology, and develop a morphological database for the ichthyoplankton in this area, (ii) describe the ichthyoplankton assemblages structure in spring and autumn, and (iii) reveal relationships between environmental variables and ichthyoplankton assemblage structure. By evaluating the influence of human activities on recruitment of fishery resources, the management and conservation of these species and their spawning grounds in waters off the Pearl River Estuary can be improved.

MATERIALS AND METHODS

Study Area and Sample Collection

Surveys occurred at 12 stations in waters off the Pearl River Estuary (112.50–114.50°E, 20.00–21.50°N) in spring (April) and

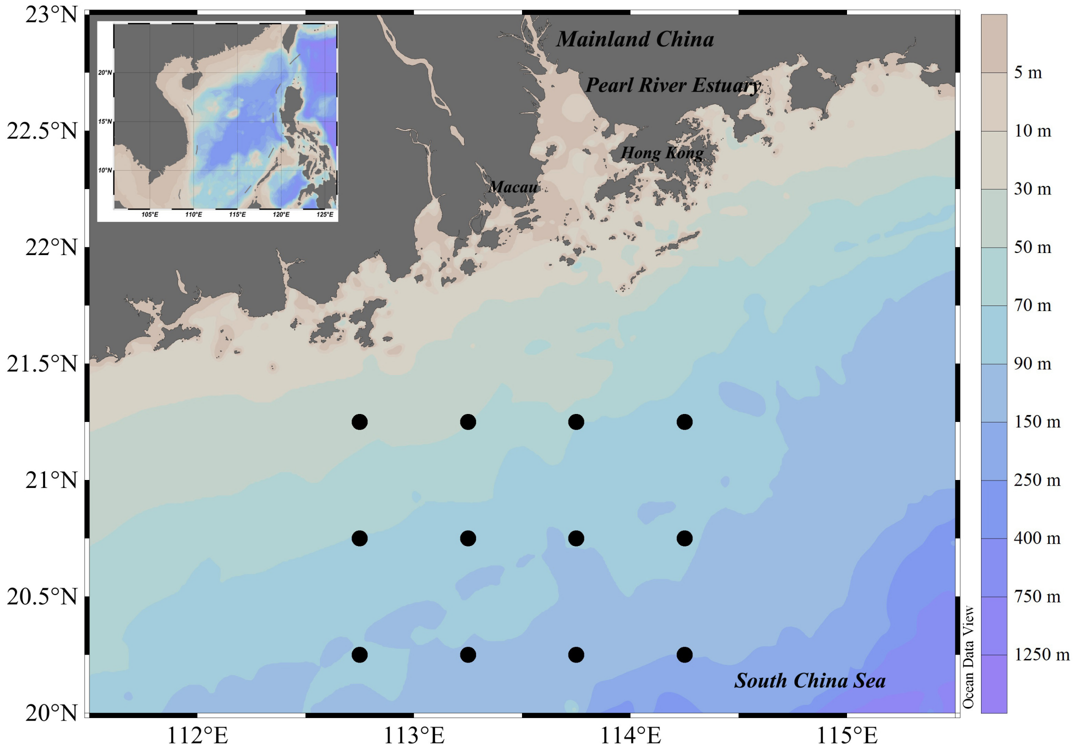

FIGURE 1 | Sampling stations of ichthyoplankton off Pearl River Estuary.

autumn (October) of 2019 (**Figure 1**). Ichthyoplankton samples were collected by zooplankton net (0.8 m diameter, 2.7 m long, 505 μm mesh, with cod-end container mesh of 400 μm) at stations over seabed depths exceeding 30 m. Four zooplankton net deployments were made at each station: two simultaneous horizontal tows at fixed depth (15 min at 1.5–2.2 knots), and two vertical hauls (~sea bed to the surface, hauled at 1.5 m/s). To preserve useful morphological characteristics of fish eggs and larval specimens, and to ensure that we could extract quality COI sequences from samples, we (upon collection) immediately preserved ichthyoplankton samples in 4% neutral formalin for 2 h, then filtered this out and transferred fixed samples to ~75% ethanol.

In the waters off the PER, several oceanographic events occurred, i.e., salinity front, coastal current, river plume, and water masses etc. (Dong et al., 2004; Su, 2004; Li et al., 2018), and these events were evaluated for possible effects on the ichthyoplankton assemblages. Temperature and salinity were considered as key variables in the oceanographic events. In the present study, the surveyed water was at the sea side off the salinity front (>32 PSU, the offshore boundary of the river plume; Ou et al., 2007). Thus, environmental variables included surface sea water temperature (SST, °C), sea water temperature at 10 m (T-10, °C), sea water temperature at 40 m (T-40, °C), sea surface salinity (SSS, PSU) were considered in the present study. In addition, sea level anomaly (SLA, mm), water depth (m), and offshore distance (km) were also adopted (He et al., 2014, 2016). SST and water depth were measured *in situ*. Satellite remote-sensed T-10, T-40, and SSS and SLA data were downloaded from HYCOM model data[1], for which temporal resolution was 1 days, and spatial resolution was 1 km. SLA data were derived from sea surface elevation data of HYCOM, then calculated using the Google Earth Engine, a cloud platform by mean processing algorithm. Minimum offshore distance was calculated in R version 4.0.5 (R Core Team, 2021) using the Sp package (Pebesma and Bivand, 2005).

Laboratory Analyses

Ichthyoplankton were identified in the laboratory by combined the molecular and morphological analyses. Briefly, ichthyoplankton specimens were first identified by cytochrome c oxidase subunit I (COI) to the lowest taxonomic level using a combined local DNA barcode library (Hou et al., 2018) and the Barcode of Life Data (BOLD) system, and the blast search criteria similar to those used in Hubert et al. (2015). Because formalin-fixation can reduce the success rate of DNA extraction and sequence amplification after 10 days (Hou et al., 2021), especially for fish eggs, we quickly picked out the ichthyoplankton specimen beneath a stereomicroscope and randomly selected 15 eggs/larvae in each horizontal and vertical trawl to be DNA extracted and amplified for the first time. If possible we performed this 2 or 3 times for each sample if a sample contained >60/90 specimens. In the 3 times, the success rate of DNA extraction and sequence amplification reduced

---

[1] https://www.hycom.org/global

sharply to below 20%, after which we stopped. For the purpose of developing a morphological database for the ichthyoplankton in the study area, each specimen was photographed by a Zeiss microscope (Axioplan 2 imaging E) before the DNA extraction (**Figure 2**). For the specimens that failed in the DNA extraction were identified by morphology following Okiyama (1989) and Shao et al. (2001).

Data Analysis

Species density (abundance per tow) was standardized to catch per unit effort. Taxa were assigned to different ecological guilds using habitat data for adult fish species in Fishbase[2]. An index of relative importance (IRI) was calculated for each species or taxon using the following function (Zhu et al., 2002; Ren et al., 2016):

$\mathrm{IRI} = \mathrm{N}\% \times \mathrm{F}\% \times 10{,}000$

Where N% and F% are the relative abundance of the total catch and frequency of occurrence. Accordingly, each species or taxon was then defined as dominant ($\mathrm{IRI} \geq 100$), common ($10 \leq \mathrm{IRI} < 100$), or rare ($\mathrm{IRI} < 10$).

Species accumulation curves were used to assess if our sampling effort was sufficient to describe ichthyoplankton species richness. The classic method "random" was used as an accumulator function to determine the means and standard deviations of species accumulation curves from random subsampling of the data without replacement (Gotelli and Colwell, 2001). The species accumulation curves were fitted in the "vegan" package implemented in R version 4.0.5 (Oksanen et al., 2020; R Core Team, 2021).

Species/taxa which accounted for more than 1% of the total catch in averaged horizontal tows were used in seasonal assemblage structure analysis. Data were first square root transformed and standardized to enhance the weighting of rare species (Clarke, 1993), and then clustered using Bray-Curtis similarity (Primer Software, Version 5.2). A non-parametric ANOSIM analysis was performed to examine differences within clusters in seasons (Clarke and Warwick, 2001). SIMPER analysis was used to calculate the contribution of each taxon to the Bray-Curtis similarity within clusters, and dissimilarity among clusters (Clarke and Warwick, 2001). Canonical correspondence analysis (CCA) was used to elucidate relationships between environmental variables and ichthyoplankton assemblages (CCA, CANOCO Software, Version 4.5). A category of sample coded "no fish" was created to prevent CANOCO from eliminating samples containing no ichthyoplankton (Grothues and Cowen, 1999). Down-weighting of rare species was performed. A forward selection was applied to test the statistical significance of environmental variables by a Monte Carlo permutation test (999 permutations) (Ye et al., 2015). Variation inflation factor (VIF) was used to test for collinearity between independent environment variables, with an upper cutoff of 10 (indicating excessive multicollinearity) (Graham, 2003; Kutner et al., 2004). Ordination diagrams of the CCA results were plotted to demonstrate associations between environmental variables and species. The length of a vector of a given variable on the CCA plot indicates the importance of that variable, with any variable having a correlation coefficient $\geq |0.4|$ is considered to be biologically important (Rakocinski et al., 1996; Akin et al., 2005). Species plotted closer to any vector with a longer distance from the origin have a stronger relationship with that vector (Ren et al., 2016). Species located near the origin either do not show a strong relationship to any of the variables, or they are found at average values of environmental variables (Elliott, 1998; Akin et al., 2005).

RESULTS

Ichthyoplankton Species Identification by DNA Barcode and Morphology

Of 4769 ichthyoplankton specimens collected, 2867 were from spring and 1902 from autumn. In all, 931 fish eggs and 229 larvae were selected for photography and DNA extraction, from which high-quality COI sequences were obtained from 308 fish eggs (33.1% of samples) and 125 larvae (54.6% of samples). A total of 75 taxa were identified using BOLD and local DNA barcode libraries (**Supplementary Table 1**). Among the 75 taxa identified by COI sequences, 61 were identified to species (referred to 50 genera, 33 families, and 10 orders), 5 were identified to genus, and 9 could not be identified. Of these, 38 taxa identified from eggs were attributed to species (comprising 31 genera, 20 families, and 8 orders), and 35 larvae were identified to species (comprising 29 genera, 21 families, and 7 orders) (**Supplementary Table 1**). In all, 80 taxa were identified by morphological and molecular analyses (75 taxa by COI sequences, 4 by morphology, and 1 taxon that are unidentified) (**Supplementary Tables 1**, **2**). Our species accumulation curves were non-asymptotic, indicating substantially more taxa would have been encountered with increased sampling effort in spring and autumn (**Figure 3**).

Spatial and Temporal Patterns of Ichthyoplankton in Spring and Autumn

In spring, in horizontal net tows, 11 taxa were categorized as dominant, contributing 82.46% to the total abundance in these samples. In vertically hauled net tows, nine taxa were dominant, contributing 77.18% to vertical samples. In autumn, in horizontal net tows, five taxa were dominant, contributing 92.92% to the total abundance of species in these samples. In vertically hauled net samples, three species were dominant, contributing 79.52% to these samples (**Table 1** and **Supplementary Table 2**). Among these taxa, *Terapon jarbua* (Forsskål, 1775) was dominant in both horizontal and vertical trawls during spring and autumn.

The mean total abundance in spring was 91.7 ind./net in horizontal tows and 27.75 ind./net in vertical hauls. These values were higher than those in autumn: 68.88 ind./net (horizontal tows) and 10.38 ind./net (vertical hauls). However, One-way ANOVA indicated that there are no significant difference for the abundance in horizontal and vertical tows between spring and autumn ($F_{spring} = 0.19$, $F_{autumn} = 2.08$, $P > 0.05$). In the present study, we took horizontal samples to examine differences within clusters in seasons. In spring, ichthyoplankton composition was not very similar, and there was significant

---

[2] https://www.fishbase.in/search.php

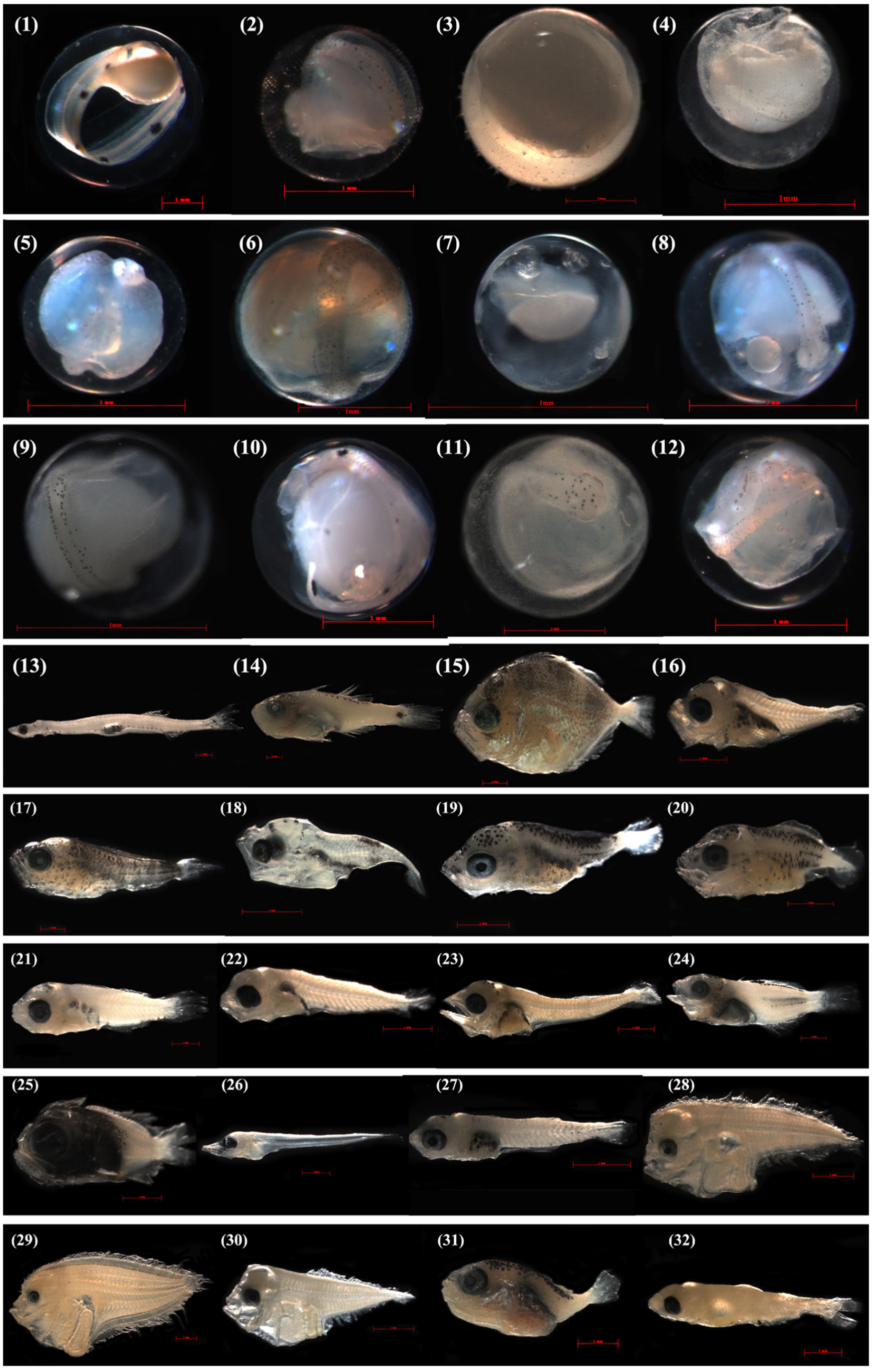

FIGURE 2 | Photographs of the specimens that were identified to species level by COI sequences off Pearl River Estuary. Egg stages, i.e., (1) *Ophichthus erabo*, GDYH4502, 4.102 mm; (2) *Trachinocephalus myops*, GDYH4477, 1.265 mm; (3) *Oxyporhamphus micropterus*, GDYH5679, 2.622 mm; (4) *Seriolina nigrofasciata*, GDYH6025, 1.264 mm; (5) *Psenopsis anomala*, GDYH4493, 1.046 mm; (6) *Coryphaena hippurus*, GDYH4501, 1.593 mm; (7) *Nemipterus virgatus*, GDYH6061, 0.727 mm; (8) *Auxis thazard*, GDYH4497, 1.066 mm; (9) *Auxis rochei*, GDYH5571, 1.007 mm; (10) *Tentoriceps cristatus*, GDYH4597, 1.674 mm; (11) *Uranoscopus oligolepis*, GDYH8442, 1.862 mm; (12) *Heteromycteris japonicus*, GDYH4481, 1.309 mm; larval stages, i.e., (13) *Encrasicholina punctifer*, GDYH8199, 14.133 mm; (14) *Ostorhinchus kiensis*, GDYH8267, 12.468 mm; (15) *Caranx ignobilis*, GDYH8296, 8.153 mm; (16) *Decapterus macrosoma*, GDYH5565, 4.252 mm; (17) *Elagatis bipinnulata*, GDYH8295, 8.941 mm; (18) *Selar crumenophthalmus*, GDYH8440, 3.644 mm; (19) *Seriola dumerili*, GDYH5583, 4.297 mm; (20) *Seriola rivoliana*, GDYH8519, 4.207 mm; (21) *Nemipterus bathybius*, GDYH8463, 7.310 mm; (22) *Nemipterus virgatus*, GDYH6066, 4.368 mm; (23) *Auxis rochei*, GDYH5969, 6.176 mm; (24) *Terapon jarbua*, GDYH8191, 7.725 mm; (25) *Pristigenys niphonia*, GDYH8518, 4.857 mm; (26) *Trichiurus brevis*, GDYH8198, 7.139 mm; (27) *Upeneus japonicus*, GDYH5575, 3.989 mm; (28) *Arnoglossus tenuis*, GDYH5949, 5.459 mm; (29) *Psettina hainanensis*, GDYH6000, 9.746 mm; (30) *Engyprosopon multisquama*, GDYH5869, 4.783 mm; (31) *Lagocephalus spadiceus*, GDYH8268, 4.527 mm; (32) *Diaphus watasei*, GDYH5965, 5.790 mm. The measured length for eggs is egg diameter, for larvae is total length.

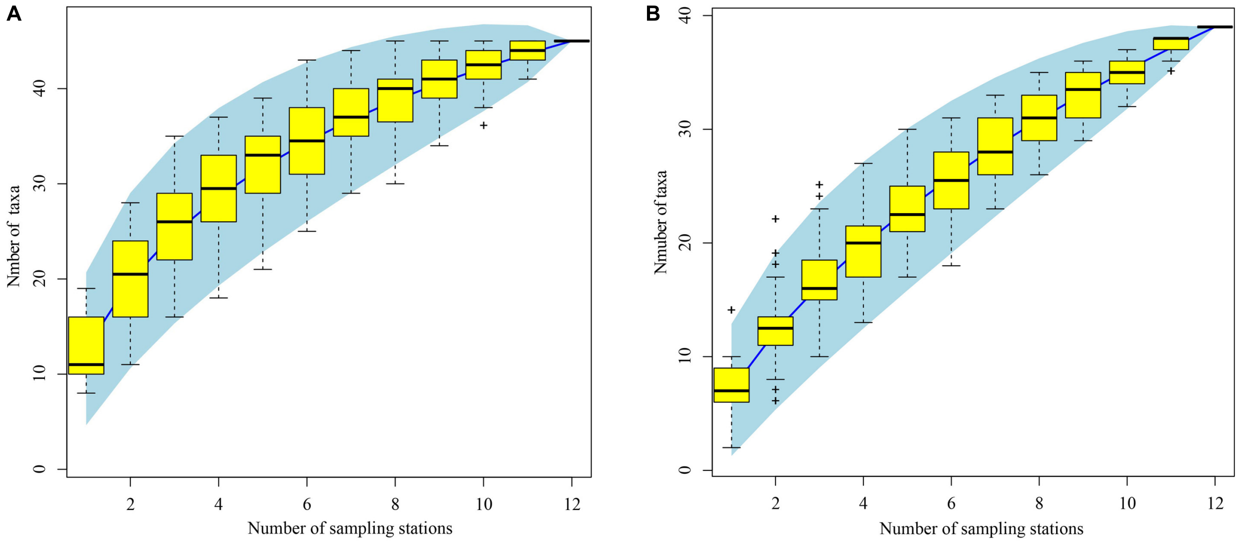

FIGURE 3 | Species accumulation curves of ichthyoplankton off Pearl River Estuary. **(A)** Spring; **(B)** autumn. Light blue area indicates 95% confidence intervals. Yellow boxes are the interquartile ranges, the central bold mark on each box indicates the median, and the bottom and top edges of the box indicate the 25th and 75th percentiles, respectively. The whiskers extend to the most extreme data points not considered outliers, and the outliers are plotted individually using the "+" symbol.

TABLE 1 | Dominant ichthyoplankton species determined by the IRI.

Spring				Autumn			
Horizontal		Vertical		Horizontal		Vertical	
Species	**IRI**	**Species**	**IRI**	**Species**	**IRI**	**Species**	**IRI**
Upeneus japonicus	978.72	*Decapterus maruadsi*	849.60	*Mene maculata*	5275.26	*Mene maculata*	2911.65
Terapon jarbua	947.30	*Terapon jarbua*	716.97	*Decapterus macrosoma*	312.56	*Decapterus macrosoma*	130.52
Selar crumenophthalmus	650.84	*Auxis rochei*	295.30	*Coryphaena hippurus*	173.42	*Terapon jarbua*	110.44
Trichiurus japonicus	641.38	*Selar crumenophthalmus*	285.29	*Terapon jarbua*	108.89		
Decapterus maruadsi	617.90	*Gobiidae gen. spp.*	200.20	*Upeneus japonicus*	102.84		
Decapterus macrosoma	343.03	*Psenopsis anomala*	168.92				
Trichiurus nanhaiensis	235.12	*Trichiurus japonicus*	157.66				
Auxis thazard	220.35	*Ophichthus sp.1*	150.15				
Psenopsis anomala	157.50	*Trachinocephalus myops*	140.14				
Gobiidae gen. spp.	151.45						
Auxis rochei	116.61						

variation among clusters (ANOSIM, $R > 0.41$, $P < 0.05$). In autumn, ichthyoplankton composition was not very similar, however, there was not significant variation among most clusters (ANOSIM, $R > 0.54$), and average dissimilarities among clusters in each seasonal survey were high (SIMPER, average dissimilarity ≥58.29% **Table 2**). The most dominant characteristics taxa in each cluster calculated by SIMPER were unidentified Gobiidae, *Decapterus maruadsi* (Temminck and Schlegel, 1843) and *Upeneus japonicus* (Houttuyn, 1782) in spring, and *Decapterus macrosoma* Bleeker, 1851, *Mene maculata* (Bloch and Schneider, 1801), and *T. jarbua* in autumn (**Supplementary Table 3**). In spring, there were three main clusters of taxa comprising 18 categories of ichthyoplankton, each represented more than 1% of the total abundance (I to III, **Figures 4A,B**). In autumn, there were four clusters indicated by six categories of ichthyoplankton (**Figures 4C,D**).

Relationships of Ichthyoplankton Assemblages to Environmental Variables

Environmental variables off the PER are shown in **Supplementary Table 4**. Because a VIF test indicated that SST and T-40 showed multicollinearity with other environmental variables, we excluded them from subsequent analysis, leaving us with five variables (SLA, SSS, T-10, Depth, and Offshore distance) for CCA analysis. Monte Carlo permutation tests indicated that four (excepting SLA) of these variables contributed significantly to explaining ichthyoplankton assemblage structure ($P < 0.05$).

TABLE 2 | The comparison of the assemblage structure according to one-way ANOSIM and SIMPER analysis.

	ANOSIM			**SIPMER**
Seasons	**Groups**	***R***	***P***	**Average dissimilarity %**
Spring	Global	0.483	0.001	
	1 and 2	0.667	0.027	65.63
	1 and 3	0.487	0.032	70.62
	2 and 3	0.413	0.032	58.29
Autumn	Global	0.606	0.001	
	1 and 2	1	0.333	100
	1 and 3	0.76	0.167	85.91
	1 and 4	0.583	0.2	77.4
	2 and 3	0.636	0.048	76.5
	2 and 4	0.536	0.067	77.99
	3 and 4	0.563	0.008	72.92

According to the rule of correlation coefficient $\geq |0.4|$, SLA was evaluated to be biologically important and used in CCA analysis (**Supplementary Table 5**). Eigenvalues were 0.413 (CCA1), 0.295 (CCA2), 0.132 (CCA3), and 0.095 (CCA4). In brief, the first and second CCA axes accounted for 41.6 and 29.8% of the variance in the species-environment relationship, respectively, with the correlation efficiencies of the first two axes being 0.878 and 0.921, respectively (**Table 3**). The sum of all canonical eigenvalues (0.992) only equaled 33.09% of the unconstrained eigenvalues (2.998), showing the restrictive effect of building environmental relationships into the CCA model. Results obtained from the first two axes were plotted to explain species–environment relationships. The first axis was highly correlated with T-10 and distinguished autumn sampling stations. The second axis was highly correlated with SSS, SLA, and water depth, and distinguished spring sampling stations (**Figure 5A**). The ordination diagram of the first two axes with the scores for environmental variables and species showed that most species scattered near the origin, which indicated average values in relation to environmental variables for these species. However, some species were outliers, e.g., *Pristigenys niphonia* (Cuvier, 1829), *Istiophorus platypterus* (Shaw, 1792), and *Elagatis bipinnulata* (Quoy and Gaimard, 1825), which was separated from the majority of species along the first axis, showing mainly a negative correlation with SSS; *Euthynnus affinis* (Cantor, 1849), *Ophisurus serpens* (Linnaeus, 1758), *Tentoriceps cristatus* (Klunzinger, 1884), and Unidentified Gobiidae, which were separated from most species along the second axis, showing mainly a positive correlation with SLA and a negative correlation with water depth and offshore distance (**Figure 5B**).

DISCUSSION

Performance of Molecular Techniques for Identifying Ichthyoplankton

We identified 75 taxa using DNA barcodes, combining the BOLD system with a local DNA barcode library. Of these taxa, 61 were identified to species, including 38 taxa from eggs, and 35 taxa from larvae; we could not attribute 11 egg or 6 larval COI sequences (3.93% of all sequences) to any taxon, indicating incompleteness of regional barcode libraries (**Supplementary Table 1**). Our study demonstrates the importance of DNA barcoding in studies involving ichthyoplankton identification, especially their egg stages. However, for sequencing large numbers of ichthyoplankton samples this technology is expensive and time consuming, and its application would be impracticable for large spawning-ground surveys. To obtain species-level information from ichthyoplankton using molecular approaches, it proved indispensable to first differentiate morphotypes based on their morphology. Thus, developing a morphological database together with a corresponding DNA barcode library will facilitate identification of fish early life stages (Hubert et al., 2015; Hou et al., 2021). In the present study, we develop a preliminary morphological database of 75 ichthyoplankton taxa for these waters, layed the foundation for the morphological identification in the waters off the PER (**Figure 2**). Compared to the previous study, we improved the preserved method, transferred from the 4% neutral formalin to ∼75% ethanol, which can ensure that we can obtain a certain proportion of COI sequences of both fish larvae and fish eggs, although the morphology quality of larvae is not good as those preserved in formalin solution (Hou et al., 2021). In addition, the present study also represents the first attempt by using the DNA Barcode to provide more detailed information regarding the species composition, occurrence of spawning site and spawning seasons for ichthyoplankton off the PER. However, the present surveys effort were not robust estimates of species richness due to the lack of asymptote in the species accumulation curves (**Figure 3**), indicating that adding more survey stations would added many more ichthyoplankton species.

Spawning Periods and Ichthyoplankton Assemblage Structure off the Pearl River Estuary

Because we surveyed only in spring (April) and autumn (October), we are limited to discussing these two sampling events. The 33 ichthyoplankton taxa that occur in both spring and autumn samples account for 41.25% of all species (80 taxa) that we report from this area. This suggests that many fish species spawn in both spring and autumn. Most species also have spawning peaks in spring, which corresponds to subtropical monsoon characteristics in the northern SCS and adjacent waters (Tzeng et al., 2002; Hsieh et al., 2005; Hsieh H. Y. et al., 2010; Xiao et al., 2013; Li K. Z. et al., 2014). Earlier analyses of fish spawning times were based largely on monitoring gonad development of fishes in the northern SCS (i.e., begin at gonadal maturity stage IV); such an approach is also expensive and requires considerable manpower and logistical resources (Chen et al., 2002, 2003). While spawning periods could be inferred from earlier monitoring work, the spawning locations of fishes remained unknown. Thus, that information we present from this region provides clear evidence of the spatial and temporal

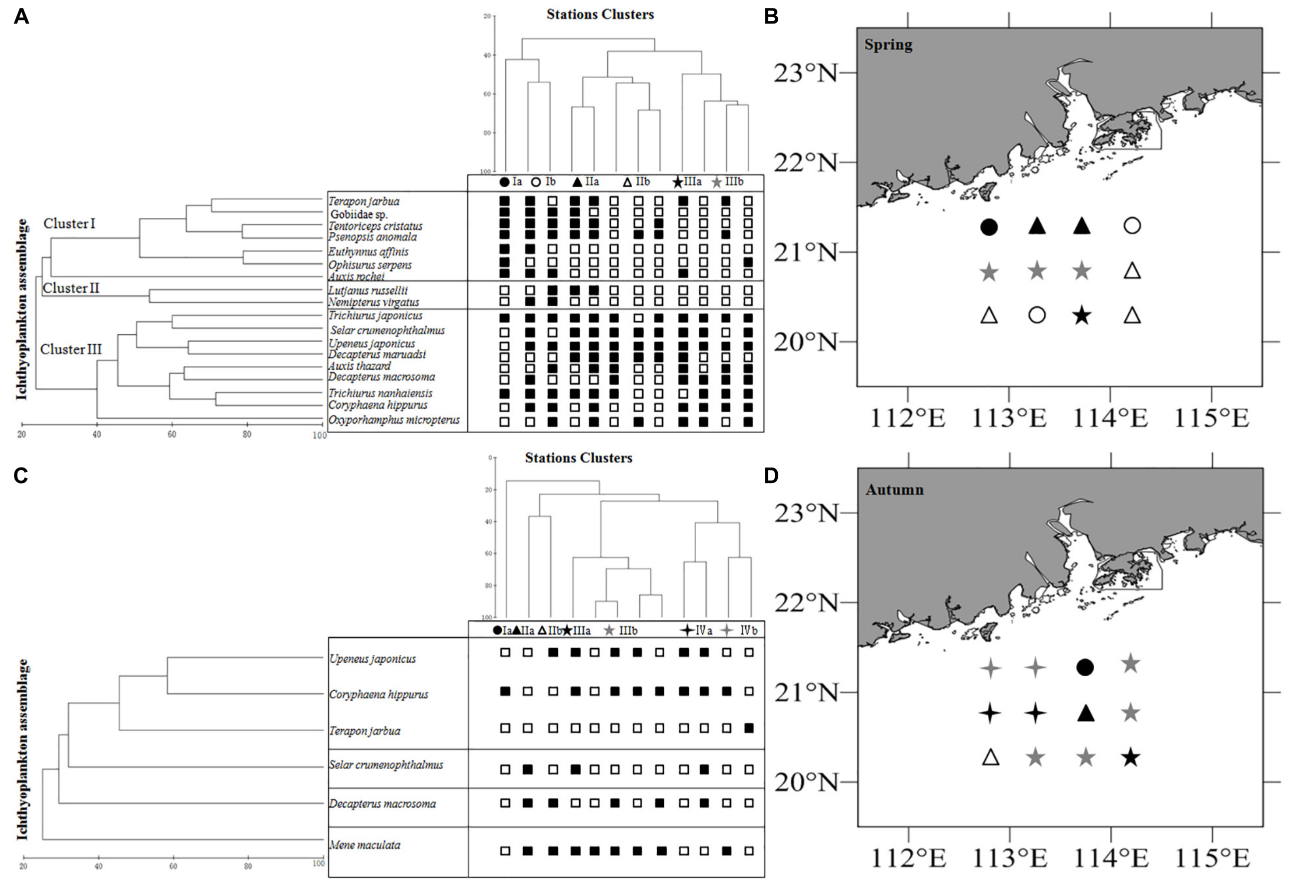

FIGURE 4 | Relationships between station clusters, larval assemblages for ichthyoplankton off Pearl River Estuary. **(A)** Station clusters in spring, **(B)** Mapping of the clusters of stations in spring. **(C)** Station clusters in autumn, **(D)** Mapping of the clusters of stations in autumn. ☐ indicates not occured in the station, and ■ indicates occurred in the station. Symbols indicate the membership to clusters.

TABLE 3 | Results of CCA based on ichthyoplankton abundance collected off the Pearl River Estuary in spring and autumn, 2019.

Axes	CCA axes				Total variance
	1	2	3	4	
Eigenvalues	0.413	0.295	0.132	0.095	2.998
Species-environment corrections	0.878	0.921	0.132	0.812	
Cumulative percentage variance of species data	13.8	23.6	28.0	31.2	
Cumulative percentage variance of species-environment relation	41.6	71.4	84.6	94.2	
Sum of all canonical eigenvalues					0.992

distribution of ichthyoplankton in spring and autumn, and likely presence of spawning grounds nearby.

To protect spawning fish stocks and juveniles, a 2-month (June and July) moratorium on fishing in the SCS was implemented from 1999 to 2008; and extended to 77 days from 16 May to 1 August from 2009 to 2016; since 2017 it was even extended to 3.5 months (1 May to 16 August). Our study indicates that the moratorium in effect from 2017 does not protect spawning fish in this region in spring. For 1 month prior to closure, fishers off the Pearl River Estuary could be catching spawning adults, which intuitively would affect recruitment and exacerbate resource declines. Within Pearl River, a fishing moratorium extends from 1 March to 30 June–a closure which coincides with the spawning periods of freshwater fish, effectively increasing their recruitment (e.g., *Megalobrama hoffmanni* Herre and Myers, 1931) (Li Y. F. et al., 2014). Our data for offshore waters support advancing the fisheries moratorium in waters off the Pearl River Estuary by at least 1 month to April to better protect fishery resources.

Because we used a zooplankton net to collect drifting and suspended eggs, many eggs (e.g., demersal eggs of sea catfish, mouth-hatched eggs such as those of cardinalfish, and adhesive eggs) were not sampled. Accordingly the composition of our ichthyoplankton assemblages is somewhat biased, and not representative of the entire fish community known from these waters. However, we do report several unexpected and most important taxa, such as commercially important

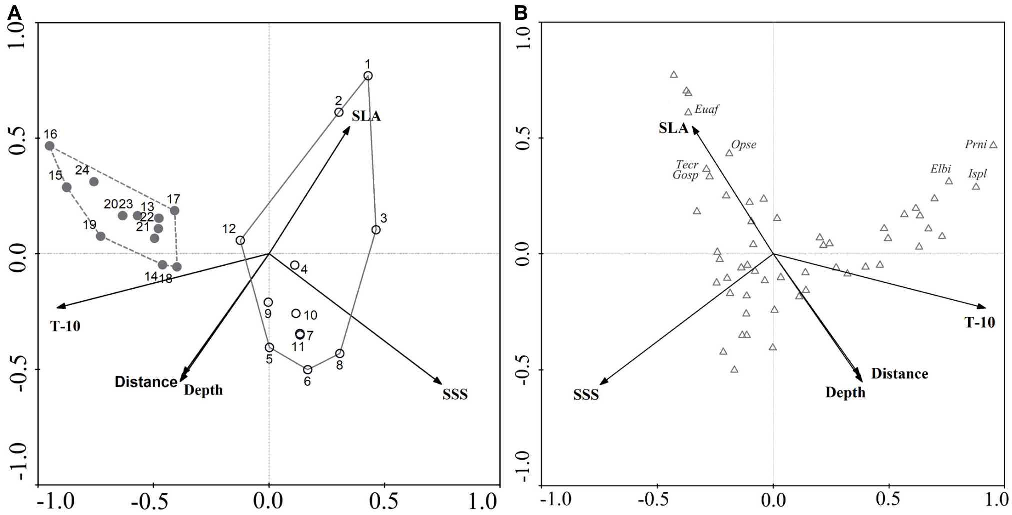

FIGURE 5 | Canonical correspondence analysis ordination plots for ichthyoplankton assemblages and environmental variables off Pearl River Estuary. **(A)** Biplot of sampling stations. The circles represent the stations in spring, and gray represent stations in autumn. **(B)** Biplot of species.

Scombridae species [*Thunnus tonggol* (Bleeker, 1851), *E. affinis* (Cantor, 1849), *Auxis thazard* (Lacepède, 1800), *Auxis rochei* (Risso, 1810)], and Nemipteridae species [*Nemipterus virgatus* (Houttuyn, 1782) and *Nemipterus bathybius* Snyder, 1911], the most caught fish taxon *Decapterus* spp. in the northern SCS, and the new species *Strophidon tetraporus* sp. nov. (Huang et al., 2020). The spawning grounds of these species are not well known, mainly because of difficulties experienced with accurate identification of their eggs and larvae, and lack of any illustrated handbooks. Additionally, benthopelagic fish (e.g., *Diaphus watasei* Jordan and Starks, 1904, and *Cyclothone* sp.) were identified from COI sequences, indicating that waters off the Pearl River Estuary are affected by continental shelf surface water mixing (Zhang et al., 2011).

The Environmental Factors That Affected the Ichthyoplankton Assemblages

Understanding relationships between ichthyoplankton assemblages and physical and biological processes is becoming increasingly important for ecosystem-based fisheries management. Physical process such as the estuaries (Zhang et al., 2015), ocean currents (Doyle et al., 2002; Sassa et al., 2007; Mullaney et al., 2011; Thompson et al., 2014), water mass (Grothues and Cowen, 1999; Hare et al., 2001; Espinosa-Fuentes and Flores-Coto, 2004; Muhling et al., 2010), monsoons (Hsieh et al., 2005; Hsieh H. Y. et al., 2010) can influence the distributions and survival of fish eggs and larvae, and define the structure and diversity of their assemblages. In the present study, the suite of environmental variables that we examined were significantly associated with ichthyoplankton assemblage structure. The first CCA axis (significantly influenced by SSS and T-10) represents a spatial gradient from the distance off the Pearl River Estuary. Increased salinity and temperature at 10 m depth were associated with changes in ichthyoplankton assemblage structure. Salinity and temperature affect fish reproductive activity and the spatial and temporal distribution of ichthyoplankton assemblages (Whitfield, 1999; Fuiman, 2003).

Salinity is inversely related to egg diameter through its influence on the width of the perivitelline space, and it also affects the hatching process and development rate (Fuiman, 2003). Temperature, a potent environmental regulator of fish physiology, can affect production and activity of hatching enzymes, and is strongly, negatively correlated with the duration of incubation (Fuiman, 2003). Thus, temperature and salinity drive reproductively mature fishes to appropriate habitat for spawning. In the nearshore and offshore waters of Pearl River Estuary, the salinity gradually increases from upstream to downstream, ranging (multi-year) 0.03–33.08 PSU through dry and wet seasons (Jia et al., 2011), meanwhile the sanility front discriminate the nearshore waters (with a salinity of <26, the nearshore boundary of the plume, Wong et al., 2003) and offshore waters (with a salinity of >32, the offshore boundary of the plume, Ou et al., 2007). The horizontal structure and shapes of Pearl River buoyant plume varied among monthly and annually, which are driven by the river discharge in different months and years (Ou et al., 2007; Li et al., 2018). This variability provides varied habitat for many (542) fish species (Wang and Lin, 2006; Zhu et al., 2019), which may also accordingly affect the spatial distribution and ichthyoplankton assemblages for this area. In the present study, the surveyed water was at the sea side off the salinity front (>32 PSU), the dominant characteristics taxa in clusters were associate with high salinities and temperature, i.e., *Selar crumenophthalmus* (Bloch, 1793), *D. macrosoma* Bleeker, 1851, *A. thazard* and *A. rochei* in spring, and *M. maculata* and *Coryphaena hippurus* Linnaeus, 1758 in autumn (**Table 1** and **Supplementary Table 3**).

Biological processes, i.e., spawning behavior of adults, duration of the incubation period, metamorphosis, interspecific competition, and predation may also affect ichthyoplankton assemblages (Harden Jones, 1968; Mason and Brandt, 1996; Miller, 2002; Olivar et al., 2010). Fish have evolved a wide range of life-history strategies in response to the environments, and the offspring must be produced at a specific time and locations, delivered to appropriate nursery grounds to survive and grow, and then mature to join the reproductive population at the appropriate place (Harden Jones, 1968). The interspecific competition for zooplankton prey may exist in the larval stages and lead to reduce growth and survival of competitors' larvae, which may disrupt the assemblages. Meanwhile, the predators can reduce the relative larval populations. In the nearshore and offshore waters of PRE, the abundant nutrients transported by river discharges produce high productivity of zooplankton (Li et al., 2006), which attract large number of fishes to spawn and nurse in the coastal waters, i.e., the *D. maruadsi* (South China Sea Fisheries Research Institute, 1966). As the *D. maruadsi* was the dominant prey for genus *Trichiurus* fishes (Yan et al., 2011), the prey availability induced the formation of predators' spawning ground, and then affected the ichthyoplankton assemblages.

Furthermore, variation in species distribution explained by the first four CCA axes was 31.2%, indicating that other factors influence the distribution and composition of ichthyoplankton assemblages off the Pearl River Estuary. The effect of other variables (e.g., chlorophyll-a, and phytoplankton and zooplankton concentration) on ichthyoplankton assemblage structure should be examined in subsequent investigations.

Our analysis of ichthyoplankton assemblages indicates that waters off the Pearl River Estuary are important spawning grounds for many commercially important species. We believe that consideration should be given to protecting this area.

DATA AVAILABILITY STATEMENT

The original contributions presented in the study are included in the article/**Supplementary Material**, further inquiries can be directed to the corresponding author/s.

ETHICS STATEMENT

The animal study was reviewed and approved by Guangdong Ocean University.

AUTHOR CONTRIBUTIONS

GH and HZ analyzed the data and completed the first draft. GH, YC, and JW performed the field survey. GH, JW, LL, YC, and JL conducted the laboratory experiments. CP and HZ provided the guidance on data analysis and structure. All authors contributed to the article and approved the submitted version.

FUNDING

This study was supported by Fund of Southern Marine Science and Engineering Guangdong Laboratory (Zhanjiang) (ZJW-2019-08), the National Natural Science Foundation of China (Nos. 31702347 and 42090044), Youth Innovation Promotion Association CAS (No. 2020211), Undergraduate Innovation and Entrepreneurship Training Program of Guangdong Province (S202010566005), and the Startup Project of Guangdong Ocean University (R19006).

ACKNOWLEDGMENTS

We would like to thank the editor and reviewers for their constructive comments on our manuscript. We also thank numerous members on the survey ship for their help.

SUPPLEMENTARY MATERIAL

The Supplementary Material for this article can be found online at: https://www.frontiersin.org/articles/10.3389/fmars.2021.732970/full#supplementary-material

REFERENCES

Akin, S., Buhan, E., Winemiller, K. O., and Yilmaz, H. (2005). Fish assemblage structure of Koycegiz Lagoon–Estuary, Turkey: spatial and temporal distribution patterns in relation to environmental variation. *Estuar. Coast. Shelf. Sci.* 64, 671–684. doi: 10.1016/j.ecss.2005.03.019

Baumgartner, G., Nakatani, K., Gomes, L., Bialetzki, A., and Sanches, P. (2004). Identification of spawning sites and natural nurseries of fishes in the upper Paraná River. *Brazil. Environ. Biol. Fish.* 71, 115–125. doi: 10.1007/s10641-004-0098-z

Burrows, M., Browing, J. S., Breitbart, M., and Murawski, S. A. (2018). DNA barcoding reveals clear delineation between spawning sites for neritic versus oceanic fishes in the Gulf of Mexico. *Fish. Oceanogr.* 28, 228–239. doi: 10.1111/fog.12404

Cai, Y., Xu, S. N., Chen, Z. Z., Xu, Y. W., Jiang, Y., et al. (2018). Current status of community structure and diversity of fishery resources in offshore northern South China Sea. *South China Fish. Sci.* 14, 10–18. doi: 10.3969/j.issn.2095-0780.2018.02.002

Cao, W., Chang, J., and Duan, Z. (2007). *Fish Resources of Early Life Stages in Yangtze River*. Beijing: China Waterpower Press.

Chambers, R. C., and Trippel, E. A. (1997). "Early life history and recruitment: legacy and challenges," in *Early Life History and Recruitment in Fish Populations* (London: Chapman and Hall), 515–549. doi: 10.1007/978-94-009-1439-1_19

Chen, C., Wang, S. L., Lu, X. X., Zhang, S. R., Lui, H. K., Tseng, H. C., et al. (2008). Hydrogeochemistry and greenhouse gases of the Pearl River, its estuary and beyond. *Quat. Int.* 186, 79–90. doi: 10.1016/j.quaint.2007.08.024

Chen, G. B., Li, Y. Z., and Chen, P. M. (2002). Spawning ground of Nemipterus bathybius in northern continental shelf waters of South China Sea. *J. Zhanjiang. Ocean. Uni.* 22, 20–25.

Chen, G. B., Li, Y. Z., and Chen, P. M. (2003). A study on spawning ground of blue mackerel scad (Decapterus Maruadsi) in continental shelf waters on northern South China Sea. *J. Trop. Oceanogr.* 22, 22–28.

Chen, W. T., Li, C., Yang, J. P., Zhu, S. L., Li, J., Li, Y., et al. (2021). Temporal species-level composition of larvae resources in the lower Pearl River drainage and implications for species' reproductive cycles. *Gene* 776:145351. doi: 10.1016/j.gene.2020.145351

Clarke, K. R. (1993). Non-parametric multivariate analyses of changes in community structure. *Austral. Ecol.* 18, 117–143. doi: 10.1111/j.1442-9993.1993.tb00438.x

Clarke, K. R., and Warwick, R. (2001). Changes in marine communities: an approach to statistical analysis and interpretation.

Mt. Sinai. *J. Med.* 40, 689–692. doi: 10.2337/diacare.26.7.2005

Claydon, J., Mccormick, M. I., and Jones, G. P. (2014). Multispecies spawning sites for fishes on a low-latitude coral reef: spatial and temporal patterns. *J. Fish. Biol.* 84, 1136–1163. doi: 10.1111/jfb.12355

Dong, L. X., Su, J. L., Wong, L. A., Cao, Z. Y., and Chen, J. C. (2004). Seasonal variation and dynamics of the Pearl River plume. *Cont. Shelf Res.* 24, 1761–1777. doi: 10.1016/j.csr.2004.06.006

Doyle, M. J., Mier, K. L., Busby, M. S., and Brodeur, R. D. (2002). Regional variation in springtime ichthyoplankton assemblages in the northeast Pacific Ocean. *Prog. Oceanogr.* 53, 247–281. doi: 10.1016/S0079-6611(02)00033-2

Doyle, M. J., Morse, W. W., and Kendall, A. W. Jr. (1993). A Comparison of larval fish assemblages in the temperate zone of the northeast pacific and northwest atlantic oceans. *Bull. Mar. Sci.* 53, 588–644. doi: 10.1080/07055900.1993.9649474

Duan, L. J., Li, S. Y., Liu, Y., Moreau, J., and Christensen, V. (2009). Modeling changes in the coastal ecosystem of the Pearl River Estuary from 1981 to 1998. *Ecol. Model.* 220, 2802–2818. doi: 10.1016/j.ecolmodel.2009.07.016

Elliott, S. M. (1998). Environmental influences on the fish assemblage of the humber estuary. *UK. Estuar. Coast. Shelf. Sci.* 46, 175–184. doi: 10.1006/ecss.1997.0268

Espinosa-Fuentes, M. L., and Flores-Coto, C. (2004). Cross-shelf and vertical structure of ichthyoplankton assemblages in continental shelf waters of the Southern Gulf of Mexico. *Estuar. Coast. Shelf. Sci.* 59, 333–352. doi: 10.1016/j.ecss.2003.09.006

Frantine-Silva, W., Sofia, S., Orsi, M., and Almeida, F. (2015). DNA barcoding of freshwater ichthyoplankton in the neotropics as a tool for ecological monitoring. *Mol. Ecol. Resour.* 15, 1226–1237. doi: 10.1111/1755-0998.12385

Fuiman, L. A. (2003). "Special considerrations of fish eggs and larvae," in *Fishery Science: The Unique Contributions of Early Life Stages*, eds L. A. Fuiman and R. G. Werner (Hoboken, NJ: Blackwell Science), 1–32.

Gotelli, N. J., and Colwell, R. K. (2001). Quantifying biodiversity: procedures and pitfalls in the measurement and comparison of species richness. *Ecol. Lett.* 4, 379–391. doi: 10.1046/j.1461-0248.2001.00230.x

Graham, M. H. (2003). Confronting multicollinearity in ecological multiple regression. *Ecology* 84, 2809–2815. doi: 10.1890/02-3114

Grothues, T. M., and Cowen, R. K. (1999). Larval fish assemblages and water mass history in a major faunal transition zone. *Cont. Shelf. Res.* 19, 1171–1198. doi: 10.1016/S0278-4343(99)00010-2

Harden Jones, F. R. (1968). *Fish Migrations*. London: Edward Arnold.

Hare, J. A., Fahay, M. P., and Cowen, R. K. (2001). Springtime ichthyoplankton of the slope region off the north-eastern United States of America: larval assemblages, relation to hydrography and implications for larval transport. *Fish. Oceanogr.* 10, 164–192.

He, L., Li, G. S., Li, K., and Shu, Y. Q. (2014). Estimation of regional sea level change in the Pearl River Delta from tide gauge and satellite altimetry data. *Estuar. Coast. Shelf Sci.* 141, 69–77. doi: 10.1016/j.ecss.2014.02.005

He, X. Q., Xu, D. F., Bai, Y., Pan, D. L., Chen, C. T. A., Chen, X., et al. (2016). Eddy-entrained Pearl River plume into the oligotrophic basin of the South China Sea. *Cont. Shelf Res.* 124, 117–124. doi: 10.1016/j.csr.2016.06.003

Hewitt, R. (1981). The value of pattern in the distribution of young fish. *Rapports et Proce′s-Verbaux des Re′unions* 178, 229–236.

Hou, G., Chen, W. T., Lu, H. S., Cheng, F., and Xie, S. G. (2018). Developing a DNA barcode library for perciform fishes in the South China Sea: species identification, accuracy and cryptic diversity. *Mol. Ecol. Resour.* 18, 137–146. doi: 10.1111/1755-0998.12718

Hou, G., Chen, Y. Y., Wang, S. J., Chen, W. T., and Zhang, H. (2021). Formalin-fixed fish larvae could be effectively identified by DNA barcodes: a case study on thousands of specimens in South China Sea. *Front. Mar. Sci.* 8:634575. doi: 10.3389/fmars.2021.634575

Hsieh, C. H., Chen, C. S., and Chiu, T. S. (2005). Composition and abundance of copepods and ichthyoplankton in Taiwan Strait (western North Pacific) are influenced by seasonal monsoons. *Mar. Freshw. Res.* 56, 153–161. doi: 10.1071/MF04058

Hsieh, C. H., Yamauchi, A., Nakazawa, T., and Wang, W. F. (2010). Fishing effects on age and spatial structures undermine population stability of fishes. *Aquat. Sci.* 72, 165–178. doi: 10.1007/s00027-009-0122-2

Hsieh, H. Y., Lo, W. T., Liu, D. C., and Su, W. C. (2010). Influence of hydrographic features on larval fish distribution during the south-westerly monsoon in the waters of Taiwan, western North Pacific Ocean. *J. Fish. Biol.* 76, 2521–2539. doi: 10.1111/j.1095-8649.2010.02643.x

Huang, D. L., Zhang, X., Jiang, Z. J., Zhang, J. P., Arbi, I., Jiang, X., et al. (2017). Seasonal fluctuations of ichthyoplankton assemblage in the northeastern south china sea influenced by the kuroshio intrusion. *J. Geophys. Res. Oceans* 122, 7253–7266. doi: 10.1002/2017JC012906

Huang, W. C., Mohapatra, A., Thu, P. T., Chen, H. M., and Liao, T. Y. (2020). A review of the genus strophidon (anguilliformes: muraenidae), with description of a new species. *J. Fish Biol.* 97, 1462–1480. doi: 10.1111/jfb.14514

Hubert, N., Espiau, B., Meyer, C., and Planes, S. (2015). Identifying the ichthyoplankton of a coral reef using DNA barcodes. *Mol. Ecol. Resour.* 15, 57–67. doi: 10.1111/1755-0998.12293

Hung, C., So, M. K., Connell, D. W., Fung, C. N., Lam, M., Nicholson, S., et al. (2006). A preliminary risk assessment of organochlorines accumulated in fish to the Indo-Pacific humpback dolphin (Sousa chinensis) in the northwestern waters of Hong Kong. *Chemosphere* 144, 190–196. doi: 10.1016/j.envpol.2005.12.028

Jefferson, T. A., Hung, S. K., Robertson, K. M., and Archer, F. I. (2012). Life history of the Indo-Pacific humpback dolphin in the Pearl River Estuary, southern China. *Mar. Mamm. Sci.* 28, 84–104. doi: 10.1111/j.1748-7692.2010.00462.x

Jia, H., Xie, J., Wu, S., and He, G. (2011). Temproral and spatial variations of salinity in peral river estuary in recent years. *Trans. Oceanol. Limnol.* 2, 142–146.

Kerr, M., Browning, J., Bønnelycke, E. M., Zhang, Y., Hu, C., Armenteros, M., et al. (2020). DNA barcoding of fish eggs collected off northwestern Cuba and across the Florida Straits demonstrates egg transport by mesoscale eddies. *Fish. Oceanogr.* 29, 340–348. doi: 10.1111/fog.12475

Kutner, M., Nachtsheim, C., and Neter, J. (2004). *Applied Linear Regression Models*. NewYork, NY: McGraw-Hill/Irwin.

Laman, E. A., Rooper, C. N., Turner, K., Rooney, S., Cooper, D. W., and Zimmermann, M. (2017). Using species distribution models to describe essential fish habitat in Alaska. *Can. J. Fish. Aquat. Sci.* 75, 1230–1255. doi: 10.1139/cjfas-2017-0181

Leyva-Cruz, E., Vásquez-Yeomans, L., Carrillo, L., and Valdez-Moreno, M. (2016). Identifying pelagic fish eggs in the southeast Yucatan Peninsula using DNA barcodes. *Genome* 59, 1117–1129. doi: 10.1139/gen-2015-0151

Li, K. Z., Yin, J. Q., Huang, L. M., and Lin, Z. J. (2014). Seasonal variations in diversity and abundance of surface ichthyoplankton in the northern south china sea. *Acta Oceanol. Sin.* 33, 145–154. doi: 10.1007/s13131-014-0533-3

Li, K. Z., Yin, J. Q., Huang, L. M., and Tan, Y. H. (2006). Spatial and temporal variations of mesozooplankton in the Pearl River estuary. *China. Estuar. Coast. Shelf S* 67, 543–552. doi: 10.1016/j.ecss.2005.12.008

Li, Q. P., Zhou, W. W., Chen, Y. C., and Wu, Z. C. (2018). Phytoplankton response to a plume front in the northern South China Sea. *Biogeosciences* 15, 2551–2563. doi: 10.5194/bg-15-2551-2018

Li, S. H., Lin, M. L., Caruso, F., Dong, L. J., Lin, W. Z., Rosso, M., et al. (2020). Cetaceans under threat in South China Sea. *Science* 368, 1074–1075. doi: 10.1126/science.abc7557

Li, Y. (2008). *Study on Fish Community Strucure in the Pearl River Estuary Waters*. China: Guangdong Ocean university.

Li, Y. F., Li, X. X., Yang, J., Sovan, L., Shuai, F. M., and Li, J. (2014). Effect fo Pearl River closed fishing on Megalobrama hoffmanni recruitment stock. *J. Fish. China* 38, 503–509.

Li, Y. Z., Chen, G. B., and Sun, D. R. (2000). Analysis of the composition of fishes in the Pearl River estuarine waters. *J. Fish. China* 24, 312–317.

Lin, M., Xing, L., Fang, L., Huang, S. L., Yao, C. J., Turvey, S. T., et al. (2019). Can local ecological knowledge provide meaningful information on coastal cetacean diversity? a case study from the northern South China Sea. *Ocean. Coast. Manag.* 172, 117–127. doi: 10.1016/j.ocecoaman.2019.02.004

Lu, X. X., Zhang, S. R., Xie, S. P., and Ma, P. K. (2007). Rapid channel incision of the lower Pearl River (China) since the 1990s as a consequence of sediment depletion. *Hydrol. Earth. Syst. Sci.* 11, 1897–1906. doi: 10.5194/hess-11-1897-2007

Makrakis, S. (2019). Tributaries as biodiversity preserves: An ichthyoplankton perspective from the severely impounded Upper Paraná River. *Aquat. Conserv: Mar. Freshw. Ecosyst.* 29, 258–269. doi: 10.1002/aqc.3037

Mason, D. M., and Brandt, S. B. (1996). Effect of alewife predation on survival of larval yellow perch in an embayment of Lake Ontario. *Can. J. Fish. Aqua. Sci.* 53, 1609–1617. doi: 10.1139/cjfas-53-7-1609

Mesa, M. L., Mesa, G. L., Catalano, B., and Jones, C. D. (2016). Spatial distribution pattern and physical-biological interactions in the larval notothenioid fish assemblages from the Bransfield Strait and adjacent waters. *Fish. Oceanogr.* 25, 624–636. doi: 10.1111/fog.12178

Miller, T. J. (2002). "Assemblages, communities, and species interactions," in *Fishery Science: The Unique Contributions of Early Life Stages*, eds L. A. Fuiman and R. G. Werner (Hoboken, NJ: Blackwell Science), 183–205.

Muhling, B. A., Beckley, L. E., Koslow, J. A., and Pearce, A. F. (2010). Larval fish assemblages and water mass structure off the oligotrophic south-western Australian coast. *Fish. Oceanogr.* 17, 16–31. doi: 10.1111/j.1365-2419.2007.00452.x

Mullaney, T. J., Miskiewicz, A. G., Baird, M. E., Burns, P., and Suthers, I. M. (2011). Entrainment of larval fish assemblages from the inner shelf into the East Australian current and into the western Tasman Front. *Fish. Oceanogr.* 20, 434–447. doi: 10.1111/j.1365-2419.2011.00594.x

Okiyama, M. (1989). *An Etlas of the Early Stages Fishes in Japan*. Tokyo: Tokai Univerisity Press.

Oksanen, J., Blanchet, F. G., Friendly, M., Kindt, R., and Wagner, H. H. (2020). *Package 'vegan': Community Ecology Package. R package Version 2.5-6*. https://github.com/vegandevs/.

Olivar, M. P., Emelianov, M., and Villate, F. (2010). The role of oceanographic conditions and plankton availability in larval fish assemblages off the Catalan coast (NW Mediterranean). *Fish. Oceanogr.* 19, 209–229. doi: 10.1111/j.1365-2419.2010.00538.x

Oliveira, E., and Ferreira, E. (2010). Spawning areas, dispersion and microhabitats of fish larvae in the Anavilhanas Ecological Station, rio Negro, Amazonas State, Brazil. *Neotrop. Ichthyol.* 6, 559–566. doi: 10.1590/s1679-62252008000400003

Ou, S. Y., Zhang, H., Wang, D. X., and He, J. (2007). Horizontal characteristics of buoyant plume off the Pearl River Estuary during summer. *J. Coast Res.* 50, 652–657.

Pebesma, E. J., and Bivand, R. S. (2005). *Classes and Methods for Spatial Data: The sp Package [CP/OL].* Available online at: http://ftp.yz.yamagata-u.ac.jp/pub/cran/web/packages/sp/

Peilie, W. (2012). *Chinese Cetaceans*. Beijing: Chinese industry Press.

Potter, I. C., Beckley, L. E., Whitfield, A. K., and Lenanton, R. (1990). Comparisons between the roles played by estuaries in the life cycles of fishes in temperate western Australia and southern Africa. *Environ. Biol. Fishes.* 28, 143–178. doi: 10.1007/BF00751033

Rakocinski, C. F., Lyczkowski-Shultz, J., and Richardson, S. L. (1996). Ichthyoplankton assemblage structure in mississippi sound as revealed by canonical correspondence analysis. *Estuar. Coast. Shelf. Sci.* 43, 237–257. doi: 10.1006/ecss.1996.0067

Raynie, R. C., and Shaw, R. F. (1994). Ichthyoplankton abundance along a recruitment corridor from offshore spawning to estuarine nursery ground. *Estuar. Coast. Shelf. Sci.* 39, 421–450. doi: 10.1006/ecss.1994.1074

Ren, P., He, H., Song, Y. Q., Cheng, F., and Xie, S. G. (2016). The spatial pattern of larval fish assemblages in the lower reach of the Yangtze River: potential influences of river-lake connectivity and tidal intrusion. *Hydrology* 766, 365–379. doi: 10.1007/s10750-015-2471-2

Sassa, C., Kawaguchi, K., and Taki, K. (2007). Larval mesopelagic fish assemblages in the Kuroshio–Oyashio transition region of the western north pacific. *Mar. Biol.* 150, 1403–1415.

Shao, K.-T., Yang, J.-S., Chen, K.-C., and Lee, Y.-S. (2001). *An Idenfification Guide of Marine Fish Eggs From Taiwan. Institute of Zoology Academia Sinica*. Taibei: Taiwan Power Company.

South China Sea Fisheries Research Institute (1966). *The investigation report of fishery resources by bottom trawl survey in Northern South China Sea*. Guangzhou: South China Sea Fisheries Research Institute.

Su, J. L. (2004). Overview of the South China Sea circulation and its influence on the coastal physical oceanography outside the Pearl River Estuary. *Cont. Shelf Res.* 24, 1745–1760. doi: 10.1016/j.csr.2004.06.005

Sun, D. R., and Chen, Z. (2013). *Fish Categories Books in the South China Sea*. Beijing: Maritime Press.

Thompson, A. R., Auth, T. D., Brodeur, R. D., Bowlin, N. M., and Watson, W. (2014). Dynamics of larval fish assemblages in the California current system: a comparative study between Oregon and southern California. *Mar. Ecol. Prog.* 506, 193–212. doi: 10.3354/meps10801

Tzeng, W. N., Wang, Y. T., and Chang, C. W. (2002). Spatial and temporal variations of the estuarine larval fish community on the west coast of Taiwan. *Mar. Freshw. Res.* 53, 419–430. doi: 10.1071/MF01136

Valdez-Moreno, M., Vásquez-Yeomans, L., Elías-Gutiérrez, M., Ivanova, N. V., and Hebert, P. D. (2010). Using DNA barcodes to connect adults and early life stages of marine fishes from the Yucatan Peninsula, Mexico: potential in fisheries management. *Mar. Freshw. Res.* 61, 655–671. doi: 10.1071/MF 09222

Wang, D., and Lin, Z. J. (2006). Spatial and temporal variations of fish commun ity structure in the PearlRiver Estuary waters. *South China Fish. Sci.* 2, 37–45. doi: 10.3969/j.issn.2095-0780.2006.04.007

Wang, Y. (2012). Fishery policy exploration in the Pearl River Estuary based on an ecosim model. *Ecol. Modell.* 230, 34–43. doi: 10.1016/j.ecolmodel.2012.01.017

Wang, Y., Hu, J., Pan, H., Li, S., and Failler, P. (2016). An integrated model for marine fishery management in the Pearl River Estuary: linking socio-economic systems and ecosystems. *Mar. Policy* 64, 135–147. doi: 10.1016/j.marpol.2015.11.014

Whitfield, A. K. (1999). Ichthyofaunal assemblages in estuaries: a South African case study. *Rev. Fish. Biol. Fish.* 9, 151–186. doi: 10.1023/A:1008994405375

Wong, L. A., Chen, J. C., Xue, H., Dong, L., Guan, W., and Su, J. (2003). A model study of the circulation in the Pearl River Estuary and its adjacent coastal waters: 2 sensitivity experiments. *J. Geophys. Res.* 108, 249–260. doi: 10.1029/2002JC001451

Xiao, Y. Z., Wang, R., Zheng, Y. J., and Wei, H. E. (2013). Species composition and abundance distribution of ichthyoplankton in the Pearl River Estuary. *J. Trop. Oceanogr.* 32, 80–87. doi: 10.3969/j.issn.1009-5470.2013.06.012

Yan, Y., Hou, G., Chen, J., Lu, H., and Jin, X. (2011). Feeding ecology of hairtail trichiurus margarites and largehead hairtail trichiurus lepturus in the Beibu Gulf, the South China Sea. China. *J. Ocean. Limnol.* 29, 174–183. doi: 10.1007/s00343-011-0004-z

Ye, S., Lin, M., Li, L., Liu, J., Song, L., and Li, Z. (2015). Abundance and spatial variability of invasive fishes related to environmental factors in a eutrophic Yunnan Plateau lake, Lake Dianchi, southwestern China. *Environ. Biol. Fish.* 98, 209–224. doi: 10.1007/s10641-014-0252-9

Zeng, Z. Z., Cheung, W. W., Li, S. Y., Hu, J. T., and Wang, Y. (2019). Effects of climate change and fishing on the Pearl River Estuary ecosystem and fisheries. *Rev. Fish Biol. Fisher.* 29, 861–875. doi: 10.1007/s11160-019-09574-y

Zhan, H. (1998). Study on fish community structure in the Zhujiang estuary and adjacent waters. *Acta Oceanol. Sin.* 20, 91–97.

Zhang, H., Xian, W., and Liu, S. (2015). Ichthyoplankton assemblage structure of springs in the Yangtze Estuary revealed by biological and environmental visions. *PeerJ* 3:e1186. doi: 10.7717/peerj.1186

Zhang, Y., Xia, H. Y., Qian, L. B., and Zhu, P. L. (2011). Analysis on hydrological characteristics off the Pearl River Estuary in summer and winter of 2006. *J. Trop. Oceanogr.* 30, 20–28.

Zhou, L., Wang, G., Kuang, T., Guo, D., and Li, G. (2019). Fish assemblage in the Pearl River Estuary: spatial-seasonal variation, environmental influence and trends over the past three decades. *J. Appl. Ichthyol.* 35, 884–895. doi: 10.1111/jai.13912

Zhu, J., Zheng, Q., Hu, J., Lin, H., Chen, D., Chen, Z., et al. (2019). Classification and 3-D distribution of upper layer water masses in the northern South China Sea. *Acta Oceanol. Sin.* 38, 126–135. doi: 10.1007/s13131-019-118-2

Zhu, X. H., Liu, D., and Sha, X. K. (2002). Relationship between community structure of ichthyoplankton and environmental factors in the Estuary of Changjiang River in spring. *Studia Marina Sinica* 5, 169–179.

Conflict of Interest: The authors declare that the research was conducted in the absence of any commercial or financial relationships that could be construed as a potential conflict of interest.

frontiers in Marine Science

BRIEF RESEARCH REPORT
published: 29 October 2021
doi: 10.3389/fmars.2021.764859

Characteristics of Ichthyoplankton Communities and Their Relationship With Environmental Factors Above the Ninety East Ridge, Eastern Indian Ocean

Liyan Zhang[1,2,3], Jing Zhang[4], Shigang Liu[2], Rui Wang[2], Jiali Xiang[1,2], Xing Miao[2], Ran Zhang[2], Puqing Song[2]* and Longshan Lin[1,2]*

[1] College of Marine Sciences, Shanghai Ocean University, Shanghai, China, [2] Third Institute of Oceanography, Ministry of Natural Resources, Xiamen, China, [3] Fujian Institute of Oceanography, Xiamen, China, [4] Fisheries College, Jimei University, Xiamen, China

OPEN ACCESS

Edited by:
Hui Zhang,
Institute of Oceanology, Chinese
Academy of Sciences (CAS), China

Reviewed by:
Sher Khan Panhwar,
University of Karachi, Pakistan
Gang Hou,
Guangdong Ocean University, China

***Correspondence:**
Puqing Song
songpuqing@tio.org.cn
Longshan Lin
lshlin@tio.org.cn

Specialty section:
This article was submitted to
Marine Fisheries, Aquaculture
and Living Resources,
a section of the journal
Frontiers in Marine Science

Received: 26 August 2021
Accepted: 11 October 2021
Published: 29 October 2021

Citation:
Zhang L, Zhang J, Liu S, Wang R, Xiang J, Miao X, Zhang R, Song P and Lin L (2021) Characteristics of Ichthyoplankton Communities and Their Relationship With Environmental Factors Above the Ninety East Ridge, Eastern Indian Ocean. Front. Mar. Sci. 8:764859. doi: 10.3389/fmars.2021.764859

The Ninety East Ridge is a submarine north–south oriented volcanic ridge in the eastern Indian Ocean. Surface-layer ichthyoplankton collected in this area from September to October were identified by combined morphological and molecular (DNA barcoding) techniques, and their species composition, diversity, and abundance, and correlations with environmental variables were described. Collections comprised 109 larvae and 507 eggs, which were identified to 37 taxa in 7 orders, 20 families, and 27 genera, and were dominated by the order Perciformes and species *Vinciguerria* sp., *Oxyporhamphus micropterus*, and *Decapterus macarellus*. Species abundances at each station and of each species were relatively low, suggesting that this area or the time of sampling were not of major importance for fish spawning. Waters above Ninety East Ridge had lower species diversity but higher species richness than waters further offshore. A generalized additive model revealed that high abundance of ichthyoplanktonic taxa occurred in areas with low sea surface height and high sea surface salinity, temperature, and chlorophyll *a* concentration. Of these, sea surface height was most correlated with ichthyoplankton abundance. We provided baseline data on surface-dwelling ichthyoplankton communities in this area to aid in development of pelagic fishery resources in waters around the Ninety East Ridge.

Keywords: ichthyoplankton, species diversity, molecular genetics, DNA barcoding, eastern Indian Ocean

INTRODUCTION

The eastern Indian Ocean is bordered by the Bay of Bengal to the north, Sri Lanka and the Indian Peninsula to the northwest, Sumatra and the Andaman Sea to the east, and the Arabian Sea and South Indian Ocean to the west and south, extending from 65°E–100°E, 10°S–15°N. Except for coastal shelf areas, water depths here exceed 2,000 m; and are up to 5,000 m in the south. This region's location, climate, and currents contribute to its high biodiversity and rich marine biological resources (Wei et al., 2007). Despite this, there has been limited research undertaken on the biodiversity and biological resources of this area compared with elsewhere in the western Indian Ocean near the eastern coast of Africa (Li et al., 2019). Chinese surveys in the eastern Indian Ocean have investigated this region's hydrometeorology, biology, chemistry, geology, and optics. Biological research has focused on bacteria, zooplankton, and phytoplankton (Wang et al., 2016, 2020; Li et al., 2019; Wei et al., 2019).

The Ninety East Ridge is a submarine volcanic ridge about 5,500 km long oriented in a north–south direction, and 100–200 km wide in an east–west direction. The average water depth of this ridge is 2.5 km, about 2 km shallower than that of flanking ocean basins. Open sea areas near the equator are less affected by terrestrial input, and upwellings transport many nutrients into surface layers, resulting in high and stable productivity (Wei et al., 2007). Few studies have reported species in and around the Ninety East Ridge, and there has been no study on the ichthyoplankton (fish eggs and larvae) of this region.

The planktonic stages of fish life cycles are typically very short relative to adult longevity. This developmental period is associated with changes in fish morphology, physiology, and ecology (Zhao and Zhang, 1985), and fish are most vulnerable during it this period, with the highest number of individuals experiencing the greatest mortality (Wan and Zhang, 2016). Ichthyoplankton can passively drift with ocean currents and are particularly sensitive to environmental variation, with subtle changes strongly affecting their survival, development, and growth. Ichthyoplankton survival rates directly affect recruitment and the strength of subsequent generations (Ellis and Nash, 1997; Wan and Zhang, 2016). Ichthyoplankton surveys plays an important role in marine survey, which is mainly reflected in: (1) biological and taxonomic research; (2) exploring and evaluating fishery resources; (3) assessing numbers of fish populations; (4) identifying different groups of the same species; and (5) discussing relationships between the quantity of fishes and environmental variables to assist with forecasts of the number of supplementary resources (Zhao and Zhang, 1985).

In Indian Ocean regions, only few ichthyoplankton identification studies have been described, mostly based on morphological features (Rathnasuriya et al., 2021). In this study, ichthyoplankton samples were collected from the surveyed area above the Ninety East Ridge, and identified by integrating DNA barcoding and morphological characteristics. Species composition, quantitative distribution characteristics of ichthyoplankton community and their relationship to environmental factors were analyzed for the first time. Baseline data are presented to facilitate subsequent exploration and use of pelagic fishery resources in the eastern Indian Ocean, and to predict patterns in the distribution of regional fishery resources.

MATERIALS AND METHODS

Survey and Stations

From September to October 2019, the Third Institute of Oceanography, Ministry of Natural Resources chartered two light-liftnet fishing vessels, "Fuyuanyu 080" and "Fuyuanyu 082," to investigate pelagic fishery resources above the Ninety East Ridge, from 86°E–92°E and 2°N–5°S. These two ships were mechanically comparable, and between them deployed plankton nets in surface waters at 44 stations (**Figure 1**).

Sample Collection and Processing

Samples were collected by a plankton net (opening diameter of 80 cm, mesh size of 505 μm) with a pre-calibrated flow meter, trawled horizontally for about 10 min at 3 kn (Gaqsiq, 2008). Upon collection ichthyoplankton samples were washed and filtered, and fixed in anhydrous ethanol. Fish eggs and fish larvae were subsequently sorted, identified and counted in the laboratory; taxa were first classified using morphological characteristics (Leis and Carson-Ewart, 2004; Wan and Zhang, 2016), after which one or two individuals (eggs and larvae) at each station were chosen for molecular analysis.

Experimental Methods and Data Analysis

Genetics

A DNA Genome Extraction Kit (TIANGEN Marine Biological Co., Ltd.) was used to extract genomic DNA from eggs and larvae. Concentrations of extracted genomic DNA were measured and then stored in a refrigerator at 4°C prior to genetic assays. Common primers for fish mitochondrial cytochrome oxidase subunit I (*COI*) gene fragments (F1: 5′-TCAACCAACCACAAAGACATTGGCAC-3′; R1: 5′-TAGACTTCTGGGTGGCCAAAGAATCA-3′) (Ward et al., 2005) were used to amplify the target fragment. The amplicon length was 655 bp. The polymerase chain reaction (PCR) mixture comprised 2.5 μL dNTP (2 mM), 2 μL 10 × *Taq* buffer (containing Mg^{2+}), 1 μL (2 mM) of each F1 and R1 primer, 1 μL DNA template, 0.15 μL *Taq* DNA polymerase, and double-distilled water to bring the final volume to 25 μL. The PCR program involved a 95°C predenaturation step for 5 min; 30 cycles of 95°C denaturation for 30 s, 52°C annealing for 30 s, and 72°C extension for 30 s; and a 72°C extension for 10 min. A 3 μL sample of PCR amplification product was then separated on a 1.5% agarose gel by electrophoresis, and those products with a concentration sufficiently high for sequencing were sent to Qingdao Personal Gene Biotechnology (Qingdao) for purification and bidirectional DNA sequencing.

All target sequences were first compared with our database constructed based on the catches of the light-liftnet fishing, and then blasted in the NCBI database. Sequences with genetic similarity ≥ 98% were regarded as conspecific, those from 92 to 98% as congeneric, and those from 85 to 92% as confamilial (Ko et al., 2013; Li et al., 2018). To reflect the interspecific relationship, we chosen *Carcharhinus longimanus* (EU398627 and GU440259) as an outgroup. A neighbor-joining (NJ) tree was created using MEGA 5.0 software based on the best selected K2P model. Genetic distances within species, between species, and between genera were calculated (Tamura et al., 2011).

Dominant Species

The index of relative importance (*IRI*) was used to identify dominant taxa (Pinkas et al., 1971) in accordance with the formula $IRI = M\% \times F\%$, where $M\%$ represents the percentage of each species relative to the total number of ichthyoplankton

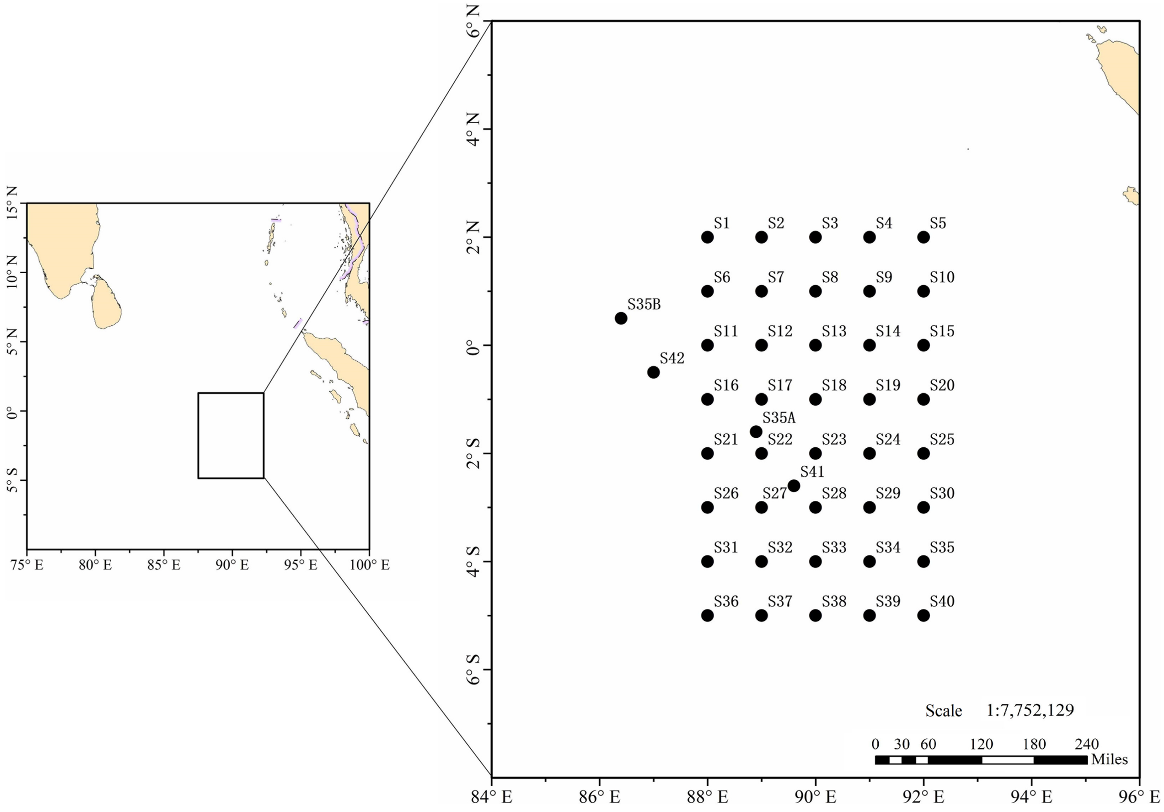

FIGURE 1 | Survey area (Ninety East Ridge) and ichthyoplankton survey stations.

samples, and $F\%$ is the percentage of stations at which a given species appears. We considered species with an $IRI > 200$ to be dominant (Zhang et al., 2019).

Species Diversity

The following formulas were used to analyze species diversity (Shannon and Wiener, 1963; Pielou, 1966; Ludwig and Reynolds, 1988):

Margalef's species richness index:

$$D = S{-}1\ /lnN;$$

Shannon–Weiner diversity index:

$$H^{'} = -\sum P_i lnP_i;$$

Pielou's evenness index:

$$J^{'} = H^{'}/lnS.$$

In these equation, S = the total number of species, and P_i the ratio of the number of samples of ichthyoplankton species i to the total number of ichthyoplankton samples, i.e., $P_i = n_i/N$, where n_i = the number of individuals of species i and N = the total number of ichthyoplankton samples.

Correlating Environmental Variables

Generalized additive model (GAM) was used to analyze the influence of environmental factors on the trends of ichthyoplankton abundance (Hastie and Tibshirani, 1990). Because the distributions of fish eggs and larvae are closely related, we analyze them as a whole in the GAM. Ichthyoplankton abundance at each station was used as a biological indicator; it was log-transformed [Log(AD + 1)] and used as a dependent variable in the model. Our GAM was constructed using the "mgcv" package in R language (R Development Core Team, 2012).

According to net mouth area, trawl speed, trawl time, and numbers of ichthyoplankton caught, we calculated ichthyoplankton abundance per unit volume using $\mathrm{AD} = \frac{T}{O \times L \times C \times 100}$, where AD = ichthyoplankton abundance (ind./100 m^3), T = number of ichthyoplankton per net (ind.), O = net mouth area (m^2), L = flow rate (flow meter), and C = a calibration value of the flow meter.

As all ichthyoplankton samples were collected from sea surface, the selected several environmental variables also come from surface environment, including sea surface temperature (SST), sea surface height (SSH), sea surface salinity (SSS), and sea surface chlorophyll *a* concentration (Chl *a*). To visually present the effect of currents on the distributions of ichthyoplankton, we plotted average geostrophic current during the survey period, and superimposed the distribution of ichthyoplankton abundance onto this. SST, SSS, and Chl *a* were measured on site with a SV48 M probe (German Sea-Sun-Technology), and mean SSH distance and geostrophic flow data (including the variables *u* and *v*) were obtained from the National Oceanic and Atmospheric Administration[1] website.

RESULTS

Species Identification and Composition

We successfully amplified 129 sequences (GenBank with access numbers MZ892544∼MZ892597). The 652 bp target fragment base composition comprised T (29.5%), C (28.0%), A (23.4%), and G (19.1%), and had 318 variable sites, 307 parsimony-informative sites, and 11 single-informative sites. With *C. longimanus* as an outgroup, NJ tree including all sequences (**Figure 2**) formed 31 groups (including one for *C. longimanus*) (**Supplementary Figure 1**). Within-group genetic distances ranged from 0.000 to 0.006, and between-group genetic distances ranged from 0.116 to 0.465 (**Supplementary Figure 2** and **Supplementary Table 1**). These values are generally consistent with the "10× rule" for distance between species, indicating that each group had distinct species.

The NJ tree and genetic distances revealed 30 fish species in the samples. For eggs from which PCR products could not be successfully amplified, we relied upon external morphology for identification. However, because eggs were fixed in ethanol and some taxonomic characteristics were lost, identification of seven taxa was limited to family level. Therefore, 37 species of ichthyoplankton were identified in this survey, belonging to 7 orders, 20 families, and 27 genera (**Supplementary Table 2**), of which 1 species was identified to order, 7 to family, 1 to genus, and 28 to species. The 16 species represented by larvae belonged to 6 orders, 11 families, and 14 genera, and the 24 species identified from eggs belonged to 5 orders, 14 families, and 16 genera. Only three species (*Oxyporhamphus micropterus*, *Thunnus albacares*, *Gempylus serpens*) were represented by both eggs and larvae.

Most species (11 families, 15 genera, 20 species) belonged to the order Perciformes, followed by Myctophiformes (1 family, 3 genera, 5 species), Beloniformes (2 families, 2 genera, 4 species), Stomiiformes (2 families, 3 genera, 3 species), Beryciformes (2 families, 2 genera, 2 species), Tetraodontiformes (1 family, 1 genus, 2 species), and Lophiiformes (1 family, 1 genus, 1 species).

Species Distribution and Abundance

Of 616 ichthyoplankton samples, 109 were represented by larvae and 507 by eggs. Excluding stations S9 and S25 (where no ichthyoplankton were caught), the number of eggs or larvae (samples) collected at a station ranged from 1 (S39) to 79 (S29) (averaged 14, **Figure 3**). At 31 stations there were fewer than 20 ichthyoplankton samples, 8 stations with 21–35 samples, and 3 stations with more than 50 samples. Species and numbers of fish eggs and larvae at each station are detailed in **Supplementary Table 3**. Overall, more ichthyoplankton samples were caught in the central and southern parts of the surveyed sea area.

Ichthyoplankton abundance at each station was low, ranging from 0 to 17.06 ind./100 m^3 (**Supplementary Figure 3**), abundances of 11 stations were < 1 ind./100 m^3, 21 stations were 1–3 ind./100 m^3, 9 stations were 3–10 ind./100 m^3, 3 stations were > 10 ind./100 m^3. Abundances of each species ranged from 0.22 to 33.91 ind./100 m^3, for 33 species (89.2% in abundance percentage), average abundances were < 0.3 ind./100 m^3, only 4 species had abundances ≥ 0.3 ind./100 m^3: *Brama orcini* (0.3), *Decapterus macarellus* (0.34), *O. micropterus* (0.37), and *Vinciguerria* sp. (0.77).

Excluding stations S9 and S25, the number of species caught was low, ranging from 1 to 6 at each station. Only a single species was caught at 4 stations, 2 species were caught at 9 stations, 3 species were caught at 13 stations, 4 species were caught at 8 stations, 5 species were caught at 7 stations, and 6 species were caught at a single (S33) station.

The numbers of individuals per species in all samples combined ranged from 1 to 157. Only a single individual was caught for 13 species (e.g., *Makaira nigricans*, *Caulophryne pelagica*, *Diretmoides pauciradiatus*, *Malacosteus niger*, *Xiphias gladius*), whereas 2–20 individuals was caught for of 15 species (e.g., *Echiostoma barbatum*, *Coryphaena equiselis*, *Diodon hystrix*, *Naucrates ductor*, *Exocoetus volitans*). For *T. albacares*, *Myripristis violacea*, *G. serpens*, *Mulloidichthys vanicolensis*, and *Exocoetidae* sp. 1, 20–45 individuals of each were caught, the numbers of individuals caught of *B. orcini*, *D. macarellus*, and *O. micropterus* were similar. The most abundantly represented taxon was *Vinciguerria* sp., of which 157 individuals were caught.

The number of stations where each species occurred ranged from 1 to 13. Twenty species (e.g., *M. nigricans*, *C. pelagica*, *E. barbatum*, *Taractes rubescens*, *Symbolophorus rufinus*, *Coryphaena hippurus*, *Cubiceps whiteleggii*) were caught at only one station; 12 species (e.g., Myctophidae sp. 2, Exocoetidae sp. 1, *B. orcini*, *D. macarellus*, *M. violacea*) were caught at 2–10 stations; 3 species (*Vinciguerria* sp., *T. albacares,* and *O. micropterus*) were caught at 11–12 stations, and 2 species (*M. vanicolensis* and *G. serpens*) were caught at 13 stations.

Dominant Species and Species Diversity

Species with an *IRI* > 200 were considered dominant (**Supplementary Table 4**), including *Vinciguerria* sp. (637), *O. micropterus* (308), and *D. macarellus* (255); their proportional contributions to total abundance were 25.5, 12.3, and 11.2%, respectively. Moreover, *G. serpens*, *M. vanicolensis*, *T. albacares*, *M. violacea*, and *B. orcini* also had high *IRI* values.

The mean ichthyoplankton Shannon–Weiner diversity index (*H*') was 0.83 (0.00–1.52); for two stations with no samples and four stations where only a single species was caught, this diversity index was 0. At 17 (38.63%) stations this index exceeded 1. Average richness index (*D*) was 1.01 (0.00–2.16), and this index exceeded 1 at 22 (50%) stations. The evenness index (*J*') was 0.79 (0.20–1.00) (**Supplementary Table 5**).

Relationship Between Distribution Characteristics of Ichthyoplankton and Their Environment Variables

The distribution of environmental variables for each station is shown in **Supplementary Figure 4**. SST values ranged from 27.0 to 29.3°C, with peak ichthyoplankton abundance at about 28.4°C.

---

[1] https://www.ngdc.noaa.gov/

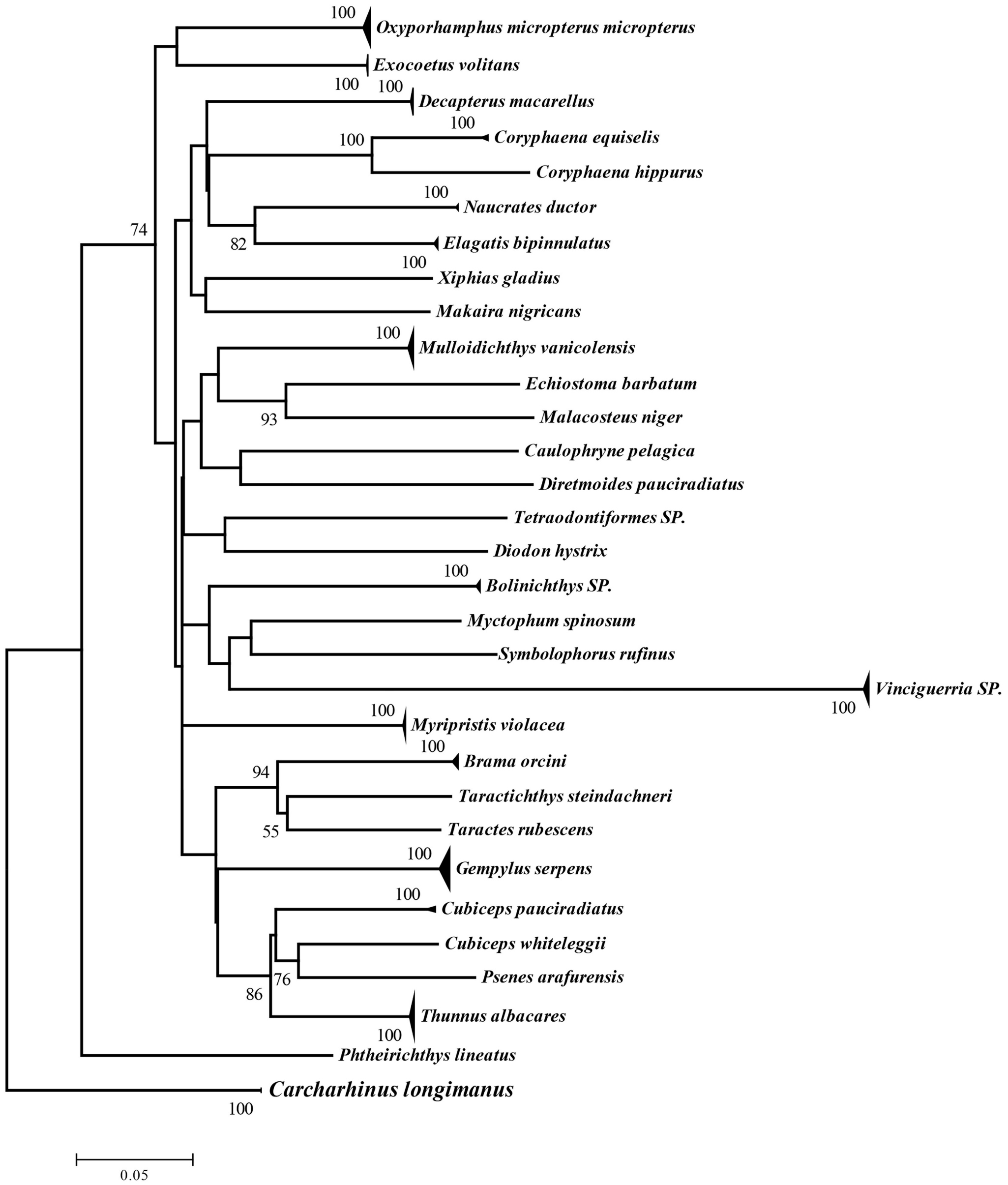

FIGURE 2 | Neighbor-joining phylogenetic tree for surface-dwelling ichthyoplankton from above Ninety East Ridge based on the K2P model.

SSS values ranged from 33.6 to 34.8‰, with peak abundance at about 34.5‰. SSH values ranged from −4.9 to 9.6 cm, with peak abundance at about −2 cm. Chl *a* values ranged from 0.03 to 0.78 mg/m^3, with peak abundance at about 0.15 mg/m^3.

Of the four environmental variables, the GAM revealed that only SSH was significantly correlated with ichthyoplankton abundance ($P < 0.05$). How ichthyoplankton abundance responded to each environmental variable is shown in **Figure 4**. SSH and abundance were negatively correlated. There were no obvious changes in abundance with SSS between 33.6 and 34.2‰, but abundance was positively correlated with SSS at higher values. SST and Chl *a* were positively correlated with abundance.

DISCUSSION

Most ichthyoplankton are small and thus are easily overlooked, and have been regarded as a large subset of zooplankton. However, because ichthyoplankton represent an important stage in the life cycles of fish, they are important in assessments of environmental impact, fishery resources, and responses to climate change. Ichthyoplankton also represent an important food source and link in marine food chains; therefore, their identification is important (Shao et al., 2001). Because of their small size, complex external morphology and anatomy, and ontogenetic variability, the characters used to visually identify ichthyoplankton are

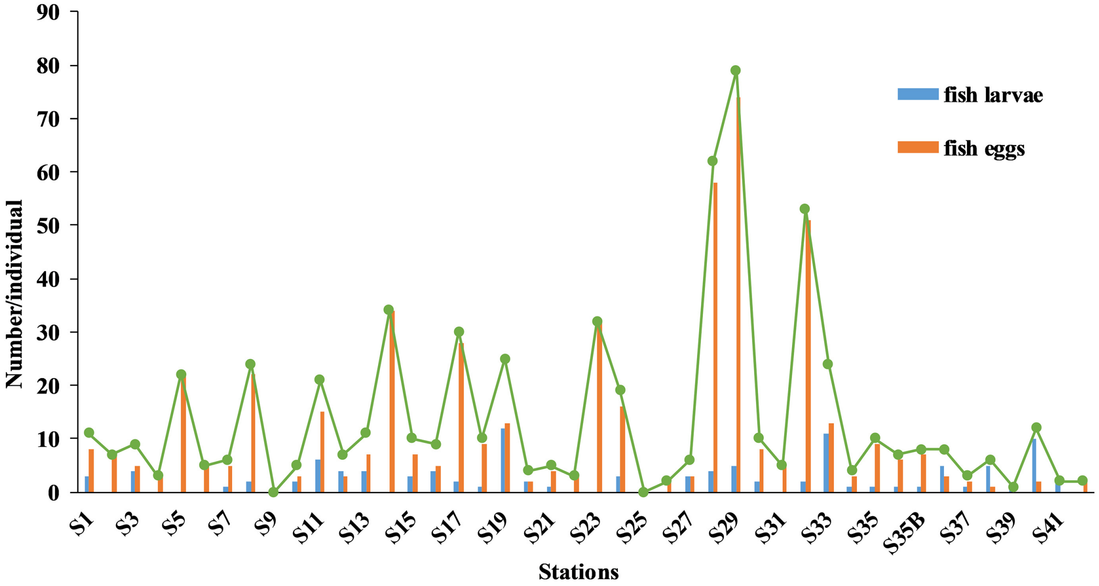

FIGURE 3 | Distributions of fish eggs and larvae, and total numbers of ichthyoplankton caught by stations above Ninety East Ridge.

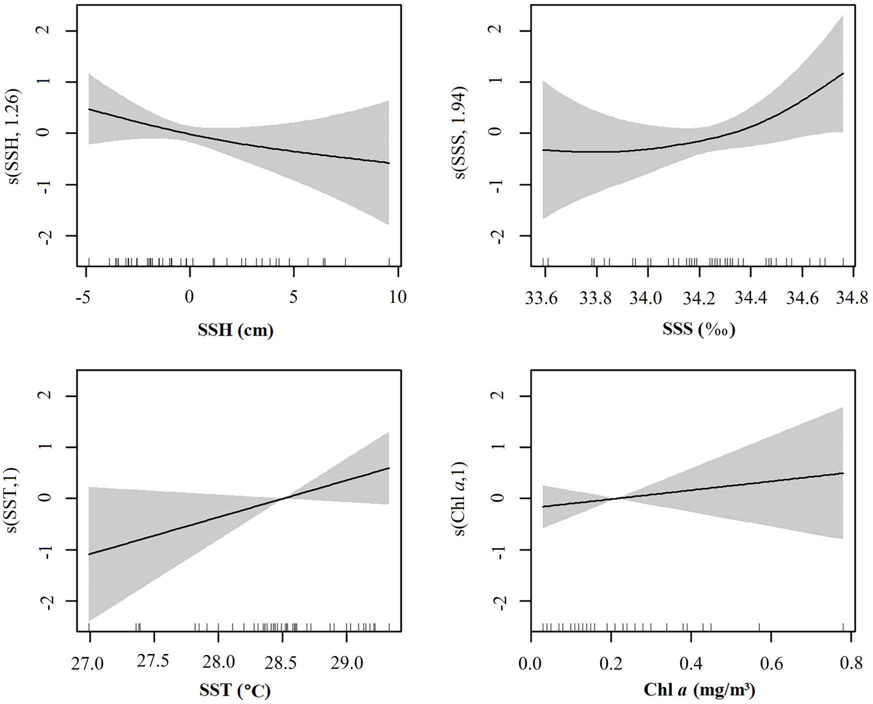

FIGURE 4 | Non-linear responses of ichthyoplankton abundance to environmental variables.

few and difficult to observe, hampering identification. We augmented our morphological identifications with DNA barcoding—a technique that has been successfully applied in other ichthyoplankton studies (Zhou et al., 2015; Ahern et al., 2018; Duke and Burton, 2020)—to improve the accuracy of our identifications.

We used DNA barcoding to identify 27 taxa to species, two species to genus, and one species to order. Of the 37 taxa identified in samples, 24 species were not collected during a field survey of pelagic fishery resources (unpublished data). Identified species included oceanic migrators (*M. nigricans*), nearshore species (*D. hystrix*), uncommon species (*Phtheirichthys lineatus*), common Exocoetidae species (*O. micropterus*), and deep-ocean species (*M. niger*, *D. pauciradiatus*, *E. barbatum*, *C. pelagica*). Among the 10 taxa not identified to species, *Vinciguerria* sp. (family Phosichthyidae) was most abundant (25.5% of all identified specimens), suggesting a potential resource exists in or near the surveyed sea area. *Tetraodontiformes* sp., a suspected cryptic species of Tetraodontiformes, was also detected. Our results confirm the effectiveness of DNA barcoding for ichthyoplankton identification; this technique can increase the known diversity and richness of species in an area and provide a scientific reference for studies on variation in fisheries. Because both the abundance of individuals at each station and the number of species was low (only four species at three stations had abundances that exceeded 10 ind./100 m^3), the surveyed area might not be a main spawning area, or autumn might not be a main spawning period for most of these fish species.

The H' for the surveyed area was lower than that for continental shelf and adjacent east Indian Ocean (Holliday et al., 2012; Beckley et al., 2019; Rathnasuriya et al., 2021), perhaps because that the nearshore sea area has relatively high habitat diversity, rich productivity, and bait resources, and is a spawning and breeding ground for many fishes (Holliday et al., 2012). Meanwhile, the surveyed sea area was located in the open ocean and presented a single habitat and complex ocean currents; most involved species are oceanic migratory fish, or few nearshore species transported by ocean currents.

The temporal and spatial distributions of ichthyoplankton are affected by broodstock reproductive characteristics, and the environment, mainly Chl *a*, temperature, salinity, depth, and ocean currents (Zheng et al., 2003; Xiao et al., 2017). Our GAM model revealed that ichthyoplankton in the surveyed area were concentrated in areas of low SSH and high SSS, SST, and Chl *a* (**Figure 3**), with SSH most strongly correlated with ichthyoplankton abundance. In contrast, the distributions of nearshore ichthyoplankton are mainly affected by other variables such as Chl *a* (Zhang et al., 2019), SSS (Chen et al., 2015), SST, and water depth (Li et al., 2017; Xiao et al., 2017; Chermahini et al., 2021).

Water temperature strongly affects fish spawning and egg development, with high temperatures possibly stimulating both. Fish larval species richness and total abundance increases with water temperature, with species being replaced over time, assisted by increased prey as a consequence of increased water temperature (Meinert et al., 2020). However, our surveyed area is relatively large, and changes in water temperature are relatively small, with maximum SST differences of 2.3°C between stations, and with 75% of stations having SSTs between 28.3 and 29°C. Thus, not surprisingly, we report a low correlation between SST and ichthyoplankton abundance in our GAM.

In addition to seeking suitable water temperatures for survival, marine fishes must find places with better conditions for feeding when migrating. High Chl *a* can improve ocean primary productivity, increasing the probability of fish feeding, and inducing their aggregation. We assume that the spawning probability of aggregating fishes in these environments is increased, which is why we included Chl *a* in our analyses. However, our GAM did not show a high correlation between Chl *a* concentration and fish abundance. Additionally, ichthyoplankton abundance and total species richness at each station (unpublished data) were not obviously correlated either, indicating that areas with many captured individuals may not have more ichthyoplankton.

Variation in SSH is generally caused by a shift in the direction of ocean currents, with low SSHs more often found near where ocean currents change direction or vortices occur (Bakun, 2006; Tittensor et al., 2010; Prants et al., 2014). The average geostrophic flow vector diagram for the survey period revealed that stations S28 and S29 (with the highest ichthyoplankton abundances) are in areas where large ocean currents meander. Vortices forming low SSHs not only gather and passively transport ichthyoplankton, but also increase their feeding opportunities and survival rate (Meinert et al., 2020). Despite this, SSH alone does not adequately explain the distributions of ichthyoplankton across the surveyed sea area, indicating that their abundance is influenced by other variables, such as ocean currents, illuminance, total nitrogen, total phosphorus, pH, suspended matter, dissolved oxygen, and/or chemical oxygen demand (Chen et al., 2015).

The oceanic marine environment is changeable, and ichthyoplankton in different sea areas are affected by different variables, even giving rise to multivariable synergistic effects. Therefore, to truly understand species composition, quantity distribution, and the relationships between ichthyoplankton and environmental variables around the Ninety East Ridge, additional samples collected at different times of the year and more environmental data are needed. Various models could be used to comprehensively analyze biological and environmental data to provide further empirical support for studies on the variation in and development and utilization of fishery resources in this area.

DATA AVAILABILITY STATEMENT

The datasets presented in this study can be found in online repositories. The names of the repository/repositories and accession number(s) can be found in the article/**Supplementary Material**.

ETHICS STATEMENT

The animal study was reviewed and approved by the Ethics Committee of the Laboratory of Animal Welfare and Ethics of Shanghai Ocean University.

AUTHOR CONTRIBUTIONS

LZ performed the data analysis and wrote the manuscript. SL, RW, and XM assisted with GMA model analysis. JZ and JX assisted with molecular analysis. LL and PS conceived and designed the study, and critically revised the manuscript. All authors listed in this manuscript have made a direct and substantial contribution to this work.

FUNDING

This research was funded by the National Programme on Global Change and Air–Sea Interaction (GASI-01-EIND-YD01aut/spr).

ACKNOWLEDGMENTS

The present study could not have been performed without assistance from Liangming Wang, Cheng Liu, Zizi Cai, and Yuanyuan Li during experimentation and data processing. We also thank the editors and reviewers of this manuscript for their constructive comments.

SUPPLEMENTARY MATERIAL

The Supplementary Material for this article can be found online at: https://www.frontiersin.org/articles/10.3389/fmars.2021.764859/full#supplementary-material

REFERENCES

Ahern, A., Gomez-Gutierrez, J., Aburto-Oropeza, O., Saldierna-Martinez, R. J., Johnson, A. F., Harada, A. E., et al. (2018). DNA sequencing of fish eggs and larvae reveals high species diversity and seasonal changes in spawning activity in the southeastern Gulf of California. *Mar. Ecol. Prog. Ser.* 592:12446. doi: 10.3354/meps.2018.12446

Bakun, A. (2006). Fronts and eddies as key structures in the habitat of marine fish larvae: opportunity, adaptive response and competitive advantage. *Sci. Mar.* 70, 105–122. doi: 10.3989/SCIMAR.2006.70S2105

Beckley, L. E., Holliday, D., Sutton, A. L., Weller, E., Olivar, M. P., and Thompson, P. A. (2019). Structuring of larval fish assemblages along a coastaloceanic gradient in the macro-tidal, tropical Eastern Indian Ocean. *Deep Sea Res. Part II Top. Stud. Oceanogr.* 161, 105–119. doi: 10.1016/J.DSR2.2018.03.008

Chen, Y. G., Mao, C. Z., Zhong, J. S., and Xu, Z. L. (2015). Influence of abiotic factors on spatiotemporal patterns of larval fish assemblages in the surf zones of the Yangtze River estuary and Hangzhou Bay. *J. Fish. Sci. China* 22, 780–790. doi: 10.3724/SP.J.1118.2015.140392

Chermahini, A. M., Shabani, A., Naddafi, R., Ghorbani, R., Rabbaniha, M., and Noorinejad, M. (2021). Diversity, distribution, and abundance patterns of ichthyoplankton assemblages in some inlets of the northern Persian Gulf. *J. Sea Res.* 167:101981. doi: 10.1016/j.seares.2020.101981

Duke, E. M., and Burton, R. S. (2020). Efficacy of metabarcoding for identification of fish eggs evaluated with mock communities. *Ecol. Evol.* 10, 3463–3476. doi: 10.1002/ECE3.6144

Ellis, T., and Nash, R. (1997). Predation by sprat and herring on pelagic fish eggs in a plaice spawning area in the Irish Sea. *J. Fish Biol.* 50, 1195–1202. doi: 10.1111/J.1095-8649.1997.TB01647.X

Gaqsiq (2008). GB/T 12763.6-2007, Specification of Oceanographic Investigation – Part 6: Marine Biological Investigation. Beijing: Standards Press of China.

Hastie, T. J., and Tibshirani, R. J. (1990). Generalized additive models. *Stat. Sci.* 1, 297–310. doi: 10.2307/2532174

Holliday, D., Beckley, L. E., Millar, N., Olivar, M. P., Slawinski, D., Feng, M., et al. (2012). Larval fish assemblages and particle back-tracking define latitudinal and cross-shelf variability in an eastern Indian Ocean boundary current. *Mar. Ecol. Prog. Ser.* 460, 127–144. doi: 10.3354/MEPS09730

Ko, H. L., Wang, Y. T., Chiu, T. S., Lee, M. A., Leu, M. Y., Chang, K. Z., et al. (2013). Evaluating the accuracy of morphological identification of larval fishes by applying DNA barcoding. *PLoS One* 8:e53451. doi: 10.1371/journal.2013.pone.0053451

Leis, J. M., and Carson-Ewart, B. M. (2004). *The Larvae of Indo-Pacific Coastal Fishes: A Guide to Identification (Fauna Malesiana handbook 2)*, 2nd Edn. Leiden: Brill.

Li, Y., Sun, P., and Yuan, C. (2019). Phytoplankton assemblage and their inter-annual variation in the south sector of eastern Indian Ocean in spring. *Mar. Environ. Sci.* 38, 825–832.

Li, Y., Zhang, L., Song, P., Zhang, R., Wang, L., and Lin, L. (2018). Fish diversity and molecular taxonomy in the Prydz bay during the 29th CHINARE. *Acta Oceanol. Sin.* 37, 15–20. doi: 10.1007/S13131-018-1228-Y

Li, Z. G., Ye, Z. J., Wan, R., Chen, Y., Tian, Y. J., Ren, Y. P., et al. (2017). Evaluating the relationship between spatial heterogeneity and temporal variability of larval fish assemblages in a coastal marine ecosystem (Haizhou bay, China). *Mar. Ecol.* 38:e12446. doi: 10.1111/maec.2017.12446

Ludwig, J. A., and Reynolds, J. F. (1988). *Statistical Ecology: A Primer in Methods and Computing*. Hoboken: John Wiley & Sons.

Meinert, C. R., Clausen-Sparks, K., Cornic, M., Sutton, T. T., and Rooker, J. R. (2020). Taxonomic richness and diversity of larval fish assemblages in the oceanic Gulf of Mexico: links to oceanographic conditions. *Front. Mar. Sci.* 7:579. doi: 10.3389/fmars.2020.00579

Pielou, E. C. (1966). The use of information theory in the study of ecological succession. *Theor. Biol.* 10, 370–383. doi: 10.1016/0022-5193(66)90133-0

Pinkas, L., Oliphant, M. S., and Iverson, I. L. K. (1971). Food habits of albacore, bluefin tuna, and bonito in California waters. *Fish. Bull.* 52, 11–46.

Prants, S. V., Budyansky, M. V., and Uleysky, M. Y. (2014). Identifying lagrangian fronts with favourable fishery conditions. *Deep Sea Res. Part I. Ocean. Res. Pap.* 90, 27–35. doi: 10.1016/J.DSR.2014.04.012

R Development Core Team (2012). *A Language and Environment for Statistical Computing*. Vienna: R Foundation for Statistical Computing.

Rathnasuriya, M. I. G., Mateos-Rivera, A., Skern-Mauritzen, R., Wimalasiri, H. B. U., Jayasinghe, R. P. P. K., Krakstad, J. O., et al. (2021). Composition and diversity of larval fish in the Indian Ocean using morphological and molecular methods. *Mar. Biodivers.* 51:39. doi: 10.1007/s12526-021-01169-w

Shannon, C. E., and Wiener, W. (1963). *The Mathematical Theory of Communication*. Urbana: University of Illinois Press.

Shao, K. T., Yang, J. S., and Chen, K. C. (2001). *An Identification Guide of Marine Fish Eggs from Taiwan*. Taipei: Boyu Professional Document Processing Center.

Tamura, K., Peterson, D., Peterson, N., Stecher, G., Nei, M., and Kumar, S. (2011). MEGA5: molecular evolutionary genetics analysis using maximum likelihood, evolutionary distance, and maximum parsimony methods. *Mol. Biol. Evol.* 28, 2731–2739. doi: 10.1093/MOLBEV/MSR121

Tittensor, D. P., Mora, C., Jetz, W., Lotze, H. K., Ricard, D., Berghe, E. V., et al. (2010). Global patterns and predictors of marine biodiversity across taxa. *Nature* 466, 1098–1101. doi: 10.1038/nature09329

Wan, R. J., and Zhang, R. Z. (2016). *Fish Eggs, Larvae and Juveniles in the Offshore Waters of China and Their Adjacent Waters*. Shanghai: Shanghai Scientific and Technical Publishers.

Wang, J., Kan, J., Borecki, L., Zhang, X., Wang, D., and Sun, J. (2016). A snapshot on spatial and vertical distribution of bacterial communities in the eastern Indian Ocean. *Acta Oceanol. Sin.* 35, 85–93. doi: 10.1007/S13131-016-0871-4

Wang, X., Li, C., Liu, K., Zhu, L., and Li, D. (2020). Atmospheric microplastic over the South China Sea and East Indian Ocean: abundance, distribution and source. *J. Hazard. Mater.* 389:121846. doi: 10.1016/j.jhazmat.2019.121846

Ward, R., Zemlak, T., Innes, B., Last, P., and Hebert, P. (2005). DNA barcoding Australia's fish species. *Philos. Trans. R. Soc., B.* 360, 1847–1857. doi: 10.1098/RSTB.2005.1716

Wei, H. L., Fang, N. Q., Ding, X., Nie, L. S., and Liu, X. M. (2007). Major environmental events reflected by pelagic records since 3.5 Ma BP in the Ninetyeast ridge at the equator. *Geol. Bull.* 26, 1627–1632. doi: 10.1016/S1872-5791(08)60002-0

Wei, Y., Zhang, G., Chen, J., Wang, J., Ding, C., Zhang, X., et al. (2019). Dynamic responses of picophytoplankton to physicochemical variation in the eastern Indian Ocean. *Ecol. Evol.* 9, 5003–5017. doi: 10.1002/ECE3.5107

Xiao, H. H., Zhang, C. L., Xu, B. D., Xue, Y., and Ren, Y. P. (2017). Spatial pattern of ichthyoplankton assemblage in the coastal waters of central and southern Yellow Sea in spring. *Acta Oceanol. Sin.* 39, 34–47. doi: 10.3969/j.issn.0253-4193.2017.08.004

Zhang, H., Xian, W., and Liu, S. (2019). Seasonal variations of the ichthyoplankton assemblage in the Yangtze estuary and its relationship with environmental factors. *Peer J* 7:e6482. doi: 10.7717/peerj.2019.6482

Zhao, C. Y., and Zhang, R. Z. (1985). *Fish Eggs and Larvae in China Seas*. Shanghai: Shanghai Scientific and Technical Publishers.

Zheng, Y. J., Chen, X. Z., and Cheng, J. H. (2003). *The Biological Resources and Environment in the East China Sea Continental Shelf*. Shanghai: Shanghai Scientific and Technical Publishers.

Zhou, M. Y., Chen, X., and Yang, S. Y. (2015). Identification of several fish eggs and larvae by DNA barcoding in Xiamen water. *Mar. Environ. Sci.* 34, 120–125. doi: CNKI:SUN:HYHJ.0.2015-01-021

Conflict of Interest: The authors declare that the research was conducted in the absence of any commercial or financial relationships that could be construed as a potential conflict of interest.

frontiers in Marine Science

ORIGINAL RESEARCH
published: 08 November 2021
doi: 10.3389/fmars.2021.766616

The Non-stationary Environmental Effects on Spawning Habitat of Fish in Estuaries: A Case Study of *Coilia mystus* in the Yangtze Estuary

Dong Wang[1,2,3], Rong Wan[1,2,3], Zengguang Li[1,2,3]*, Junbo Zhang[1,2,3], Xiangyu Long[4], Pengbo Song[4], Lu Zhai[1,2,3] and Shuo Zhang[1,2,3]

[1] College of Marine Sciences, Shanghai Ocean University, Shanghai, China, [2] National Engineering Research Center for Oceanic Fisheries, Shanghai Ocean University, Shanghai, China, [3] Key Laboratory of Sustainable Exploitation of Oceanic Fisheries Resources, Ministry of Education, Shanghai Ocean University, Shanghai, China, [4] Fisheries College, Ocean University of China, Qingdao, China

OPEN ACCESS

Edited by:
Yuan Li,
Third Institute of Oceanography,
China

Reviewed by:
Cui Liang,
Institute of Oceanology, Chinese
Academy of Sciences (CAS), China
Delian Huang,
South China Sea Fisheries Research
Institute (CAFS), China

***Correspondence:**
Zengguang Li
zgli@shou.edu.cn

Specialty section:
This article was submitted to
Marine Fisheries, Aquaculture
and Living Resources,
a section of the journal
Frontiers in Marine Science

Received: 29 August 2021
Accepted: 11 October 2021
Published: 08 November 2021

Citation:
Wang D, Wan R, Li Z, Zhang J,
Long X, Song P, Zhai L and Zhang S
(2021) The Non-stationary
Environmental Effects on Spawning
Habitat of Fish in Estuaries: A Case
Study of Coilia mystus in the Yangtze
Estuary. Front. Mar. Sci. 8:766616.
doi: 10.3389/fmars.2021.766616

The estuarine areas provide necessary spawning habitat, nursing habitat, and migratory for a variety of fishes and the environmental conditions are of significant heterogeneity. *Coilia mystus* is the key commercial fish that spawns in the Yangtze Estuary and the yield has declined sharply in the past 30 years. In order to understand the spawning habitat selection mechanism of *C. mystus*, the geographically weighted regression (GWR) model was applied to explore the non-stationary effect of environmental variables [e.g., the sea surface temperature (SST) and the sea surface salinity (SSS)] and geographical variables [e.g., the distance to the coast (DTC) and the depth (DEP) of water] on the egg density distribution of *C. mystus*. The data were derived from the spring and summer ichthyoplankton surveys carried out from 2019 to 2020 in the Yangtze Estuary, China. The GWR model results showed that the key variables in different seasons had spatial non-stationary effects on the distribution of spawning habitat of *C. mystus*, which were mainly caused by regional rise in temperature and saltwater intrusion of the South Branch. In the spring, the SSS, the DTC, and the DEP were the main impact factors and saltwater intrusion in the South Branch might lead to the trend that the spawning habitat moved further upstream to the Changxing Island. The SST was most important in the summer and the relatively lower SST was more crucial in the spawning habitat selection than the DTC and the DEP. The GWR model performed well in the study of *C. mystus* potential spawning habitat in the Yangtze Estuary. We recommend that more attention should be paid in regional variation of environmental factors to explore fish potential spawning habitat in the estuarine areas.

Keywords: geographically weighted regression (GWR) model, estuarine areas, *Coilia mystus*, spawning habitat, the Yangtze Estuary

INTRODUCTION

The distribution of fish spawning habitat is usually determined by the adaptation of reproductive physiology and species response to the surrounding environmental conditions (Gallego et al., 2007; Zorica et al., 2013; Gonzalez-Irusta and Wright, 2016; Reglero et al., 2017). The spawning distribution could be influenced by various environmental factors, e.g., temperature, salinity, topography (Opdal, 2010; Dumont et al., 2011; Shi et al., 2014). There is evidence that compared with adults, the early life history stages of fish species seem to be more sensible and vulnerable to the variations in the environmental conditions (Portner and Farrell, 2008). To ensure more survival of eggs and larvae, spawning activity usually happens in the recurrent hydrographic features (Munk et al., 2009) such as estuaries, upwellings, or tidal mixing front (Tian et al., 2009; Zorica et al., 2013; Gibson et al., 2018). The estuaries, as important fish spawning and nursery habitats, are usually characterized by complex hydrological systems and spatially varying environmental conditions (Andrew et al., 2009). A study on fish spawning habitat is the fundamental step for the fish recruitment process (Lelievre et al., 2014), especially for the estuarine species. Examining fish spawning activity and its response to the spatial non-stationary environment is important for gaining a comprehensive understanding of spawning habitat selection mechanism, which helps to understand fish stock fluctuations and, hence, establish appropriate protection strategies for estuarine fish.

To evaluate statistical relationships between the spawning habitat and environmental variables, "global" regression models (Brunsdon et al., 1996; Windle et al., 2010) such as generalized additive model (GAM) and generalized linear model (GLM) are fully developed and used (Bacheler et al., 2010; Asch and Checkley, 2013; Gonzalez-Irusta and Wright, 2016). These models treat the entire data set as "whole map" and function under the assumption of spatial stationarity (Brunsdon et al., 2002; Windle et al., 2010). In the recent years, more and more studies have focused on spatial heterogeneity and the changes in species distribution caused by variations in the environmental conditions (Li et al., 2018). The geographically weighted regression (GWR) model provides a promising approach for investigating spatial non-stationarity effect and could make good predictions of fish species distribution (Lauri et al., 2014). The GWR model has been applied successfully to both the marine and freshwater habitats, e.g., North Atlantic Ocean (Windle et al., 2010), Gulf of Maine (Li et al., 2018), and Lake Malawi (Likongwe et al., 2015). However, rarely study has been reported that applies the GWR model method to demonstrate the non-stationary effect of the environment on the fish spawning habitat.

The Yangtze Estuary in China is the largest estuary in the western Pacific Ocean with three brunches and four outlets to the East China Sea (**Figure 1**). It is characterized by high biological productivity associated with relatively extreme and varying environmental conditions (Shan et al., 2010). It serves as an important spawning habitat, nursing ground, and migration channel for varieties of fish species because of the advantaged conditions (Zhuang et al., 2006; Yu and Zhang, 2017). More than 300 fish species have been found inhabiting the Yangtze Estuary (Zhuang et al., 2006). Among them, *Coilia mystus* is considered one of the most important commercial fish species in the Yangtze Estuary (Shi and Wang, 2002) with an annual yield of more than 1,500 tons in the 1990s (Ni, 1999). However, in 2019, China had to announce that it would stop issuing special fishing licenses for the wild populations of *C. mystus* because of the severe depletion of the resources (Zhai and Pauly, 2019, 2020) caused by overfishing and the habitat degradation (Ni et al., 1999; Liu et al., 2013).

Coilia mystus belongs to Clupeiformes, with a short lifespan, seasonal migrations, and long spawning periods (Zhuang et al., 2006; Zhao et al., 2020). Also, it is a semi-anadromous fish (Elliott et al., 2007) that generally lives in the shallow marine area and spawns in the estuarine area (Zhuang et al., 2006; Zhao et al., 2020). The South Branch of the Yangtze Estuary is considered the main spawning location for *C. mystus* (Ni et al., 1999). The spawning period of *C. mystus* starts from late April to September and peaking in late May and June (Zhuang et al., 2006). In the spawning season, adults of *C. mystus* migrate to the brackish water in the Yangtze Estuary to spawn, but will never enter the freshwater areas above the Jiangyin section of the river (Yang et al., 2006b). There are few studies on the selection mechanism of spawning habitat of *C. mystus* and its response to environmental conditions, except for some previous work examining the migration pattern and biology trait (Yang et al., 2006a; Zhao et al., 2020). It is generally believed that the sea surface temperature (SST) and the sea surface salinity (SSS) would influence the spawning habitat of *C. mystus* (Jiang et al., 2006; Jiang and Shen, 2006). However, some geographical variables such as the distance to the coast (DTC) and the depth (DEP) of water, which were involved in other estuarine ichthyoplankton study (Locke and Courtenay, 1995; Halvor et al., 2007), were barely explored. An updated study on spawning activity and specific locations of spawning habitat in the area is necessary. Especially, understanding how the spawning habitat of *C. mystus* shifts over subtle spatial changes in the environment is the key problem.

In this study, the spawning habitat selection mechanism under the locally varying environmental conditions was explored based on a case study of *C. mystus* in the Yangtze Estuary. The spatial GWR model was applied to investigate the non-stationary effect of the environmental variables, i.e., the SST, the SSS, and geographical variables, i.e., the DTC and the DEP on the distribution of spawning habitat of *C. mystus*. The conclusions are helpful in gaining a comprehensive understanding of fish spawning habitat selection mechanism in the estuarine areas and conductive to the protection of the population.

MATERIALS AND METHODS

Sample Collection and Analysis

The biological and environmental data were collected from four ichthyoplankton surveys carried out in 2019 and 2020 (**Table 1**) covering the peak and end of the spawning period of *C. mystus*. The sampling area covered both the South and North Branches of the Yangtze Estuary and its coastal zones (**Figure 1**). Considering the navigation risk and difficulties, the Deepwater Navigation Channel (DNC) was not involved in the survey. The study area was divided into four subareas (A, B, C, and D) based on the topographic features and salinity condition in the Yangtze Estuary (Luo and Shen, 1994; Yan et al., 2001). Besides, it was divided into 159 oblique grids of equal size $3' \times 3'$ (**Figure 1B**) based on the central axis of the Chongming Island. In each cruise, around 55 stations were chosen from the grids by using a

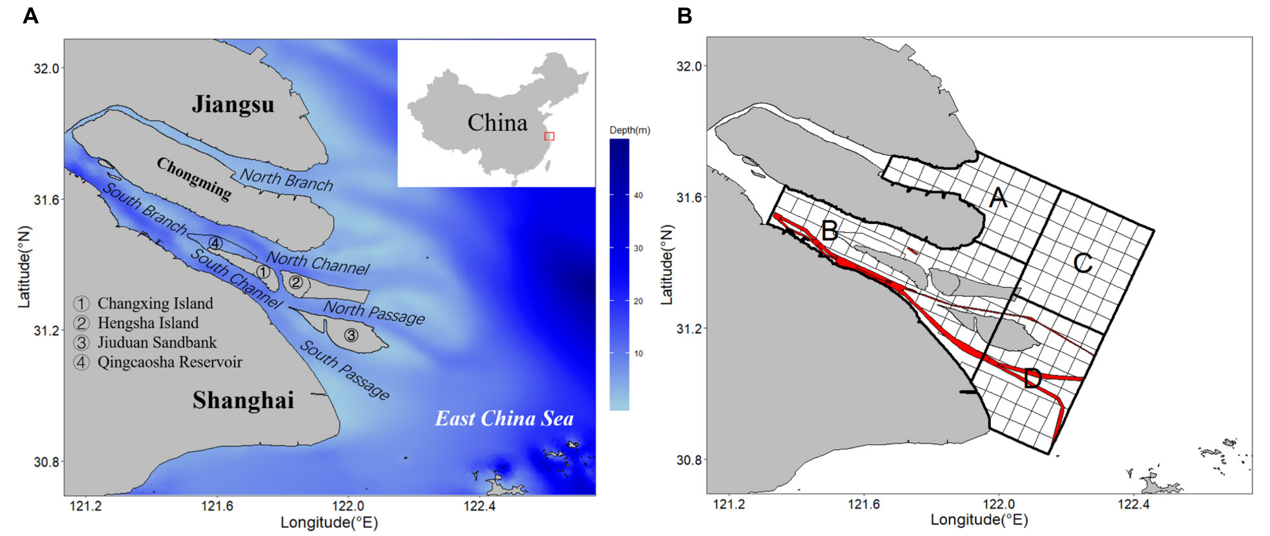

FIGURE 1 | (A) Study area with depth of water in the Yangtze Estuary. The red rectangle on the China map is the location of the Yangtze Estuary. **(B)** Subareas A, B, C, and D. Red line is the Deepwater Navigation Channel (DNC).

stratified random sampling method. A higher weight (25 stations) was allocated in subarea B according to the historical study of *C. mystus* spawning habitat (Ni et al., 1999).

The surveys started around 4 a.m. and were conducted in the day. Eggs were collected by a plankton net with an opening diameter of 80 cm and a mesh size of 505 μm. At each survey station, the net was towed horizontally against the current at a speed of 2–3 knots for a duration of 10 min and a calibrated flow meter was mounted in the net opening to capture the filtered water volume. Samples were gathered from the net and fixed in a 5% buffered formalin seawater solution immediately for further identification in the laboratory. Eggs of *C. mystus* have distinguishing features such as spherical with a diameter of 0.83–1.03 mm, transparent, and contain multiple oil globules with different sizes (Zhang et al., 1985). The eggs were identified by morphology observation under a microscope according to the study by Thompson and Riley (1981) and Zhang et al. (1985). The identified eggs were standardized in terms of number of specimens per cubic meter (ind m^{-3}). The stations where no specimens were found were recorded as zero. The environmental profile was recorded by the SBE 19plus V2 SeaCAT conductivity-temperature-depth system (CTD). SST (°C) and SSS were defined by mean data of 3 m below the sea surface. Spatial data such as the DEP (m) was derived by the electronic charts and the DTC (km), the shortest distance from the station to the coast or islands, was calculated in use of the R package "raster."

TABLE 1 | Summary of the surveys and the average value (± SD) of data collected.

Cruise	Season	Stations	SST (°C)	SSS	Egg density (ind.m^{-3})
May 2019	Spring	57	22.08 ± 0.87	6.01 ± 8.27	0.060 ± 0.096
Aug. 2019	Summer	55	28.96 ± 0.90	6.04 ± 7.45	0.004 ± 0.013
May 2020	Spring	56	22.48 ± 0.96	7.16 ± 7.31	0.122 ± 0.496
Aug. 2020	Summer	55	29.14 ± 1.42	4.30 ± 6.52	0.027 ± 0.059

Data Analysis

Model Development

The GWR model was applied to evaluate the relationship between the distribution of spawning habitat of *C. mystus* and the environmental constraints for each month. The square root of egg density with corresponding independent variables was formulated as below (Gollini et al., 2015):

$$y_i = \beta_{i0} + \sum_{k=1}^{m} \beta_{ik} x_{ik} + \epsilon_i \tag{1}$$

Where, y_i is the dependent variable at location i, x_{ik} is the value of kth independent variable at location i, m is the number of independent variables, β_{ik} is the local regression coefficient for the kth independent variable at location i, and ϵ_i is random error at location i. All the model development is based on the R package "GWmodel".

The spatial weighting matrix of the GWR model was built of three key elements: the type of distance, the kernel function, and the bandwidth. In this study, a great circle distance matrix, bisquare kernels function, and "adaptive" bandwidth (number of local data) were applied. Besides, bandwidth was obtained via cross-validation. For more detail, please see Gollini et al. (2015).

Before model development, collinearity between explanatory variables in four months was tested based on variance inflation factors (VIFs). By using a GLM model including all the independent variables (e.g., SST, SSS, DTC, DEP), a given predictor with VIFs greater than 10 should be removed from the model development (O'Brien, 2007). The result of the diagnostics of collinearity (**Figure 2**) showed that only SSS in August 2019

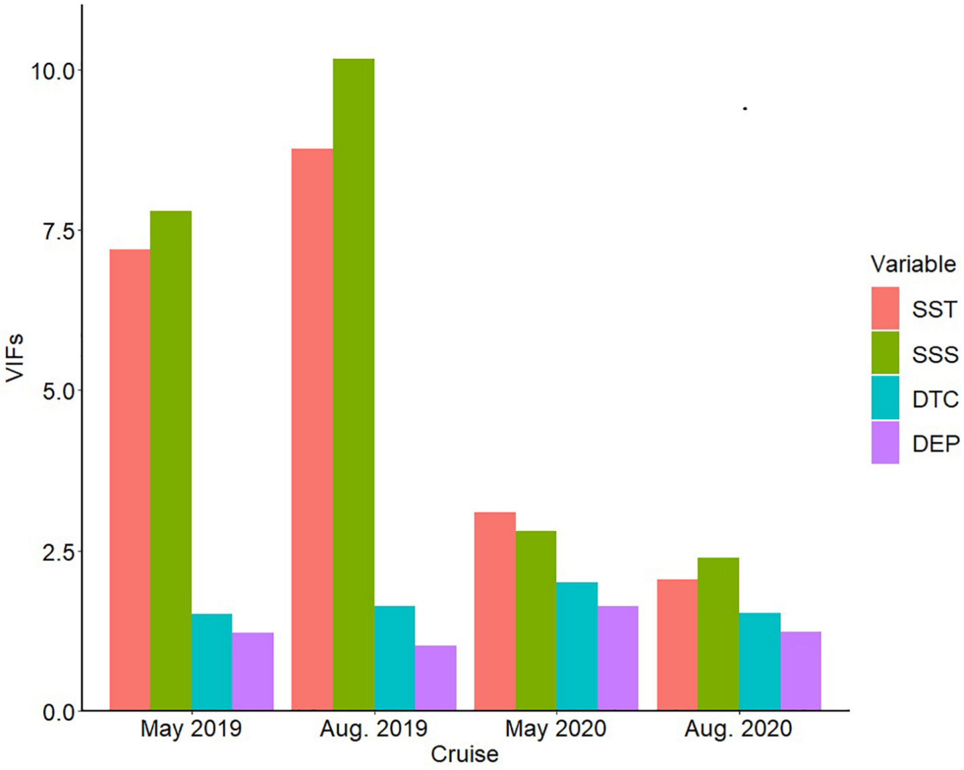

FIGURE 2 | Monthly variance inflation factor (VIFs) of all the selected abiotic variables in the Yangtze Estuary in 2019 and 2020.

had a collinearity relationship with other indicators. However, the VIFs (10.16) were close to 10, so it was still involved in the following model development.

A global selection procedure (Brooks et al., 2014) was conducted by the GWR model to find the optimal model for each month and the best performing model comes to a variable combination that produces the minimum akaike information criterion (AIC) value among all the regressing models. Among four independent variables analyzed (SSS, SST, DTC, and DEP), the optimal independent variable subset for models showed both the consistency and difference. The DTC was subsequently involved in all the four models. The DEP was included in all the models, except for May 2020. The SSS was only removed from the model in August 2020 and the SST was included in August 2019 and 2020.

Model Fit and Prediction

The GWR model fit was tested by the Pearson correlation coefficient (r^2). Significant levels (p) of spatial autocorrelation in regression residuals were evaluated by the Moran's I statistics. As the quantity of data in each month is small, the leave-one-out cross-validation (LOOCV) procedure was used to obtain test errors (Molinaro et al., 2005). In this procedure, each station was sequentially picked to be the validation data and the remaining data were used as the training data. Meanwhile, the root mean square error (RMSE) was used to validate the model (Christoph and Jose, 2012). The RMSE can be calculated as follows:

$$RMSE = \sqrt{\frac{1}{N}\sum_{i=1}^{N}(y_i - \hat{y}_i)^2} \qquad (2)$$

Where, N is the number of samples and $\hat{y}_i$ is the predicted value from the model for the ith observation. In the GWR model prediction, the entire survey area was divided into 6,000 oblique grids of equal size $0.52' \times 0.52'$ and the selected environmental variables were evaluated by inverse distance weighting based on the survey data from each cruise.

RESULTS

Model Performance and Validation

Based on the minimum AIC scores, the GWR models that best approximated the observed distribution of *C. mystus* eggs were listed in **Table 2**. Compared to the total number of stations (**Table 1**), the year 2019 required a larger bandwidth size than the year 2020 to develop the GWR model, in which model of August 2019 yielded results increasingly close to the universal model. Smaller bandwidth for models in other months might lead to more rapid spatial variations in the results. Moran's I of residuals for the GWR models were randomly structured and the relevant p-value (0.13–0.78) indicated that spatial autocorrelation was not significant (Windle et al., 2010). In addition, the GWR models had good performance according to r^2 (0.53–0.69).

The GWR models had reasonable prediction skills with RMSE ranging from 0.05 to 0.24 (**Table 2**). In general, the observed *C. mystus* eggs were confined in the South Branch, near the Chongming, Changxing, and Hengsha Islands (**Figure 3**). The predicted distribution of egg concentration was broadly consistent with the pattern where most *C. mystus* eggs appeared. The monthly and interannual variations in the predicted egg density basically corresponded to that of the survey data. There were far more eggs collected in May than in August. In May 2019, the highest egg density was up to 0.34 ind.m^{-3} (predicted 0.26 ind.m^{-3}), while it was only 0.07 ind.m^{-3} (predicted 0.08 ind.m^{-3}) in August. Besides, the egg density sampled in 2020 was higher compared with that in the same month in 2019. Of the four months compared, the highest egg density was 2.72 ind.m^{-3} (predicted 1.61 ind.m^{-3}) in May 2020 and eggs were highly aggregated in the upper end of the Changxing Island. In August 2020, the highest egg density was as much as 0.32 ind.m^{-3} (predicted 0.14 ind.m^{-3}). Although there were a few eggs sampled in the North Branch (3 eggs in May 2019 and 2 eggs in May 2020) and subarea C (16 eggs in May 2019 and 1 egg in August 2020), no obvious egg concentration was predicted in these areas.

Environmental Variables and Non-stationary Environmental Effects

In this study, the coefficients estimated of each independent variable determined in the GWR models were mapped to explore the non-stationary environmental effects. The value of coefficients is not limited between −1 and 1 (Li et al., 2018). All the independent variables showed non-stationary effects on the dependent variable.

TABLE 2 | Summary of optimal bandwidth and model performance for the geographically weighted regression (GWR) models.

Date	Model	Bandwidth	AIC	R^2	RMSE	Moran's *I* of residuals
May 2019	y~SSS+DTC+DEP	32	−81.00	0.69	0.13	−0.06
Aug. 2019	y~SST+SSS+DTC+DEP	40	−182.13	0.55	0.05	−0.14
May 2020	y~SSS+DTC	19	−14.71	0.68	0.24	0.24
Aug. 2020	y~SST+DTC+DEP	27	0.50	0.53	0.13	0.16

y is square root of egg density.

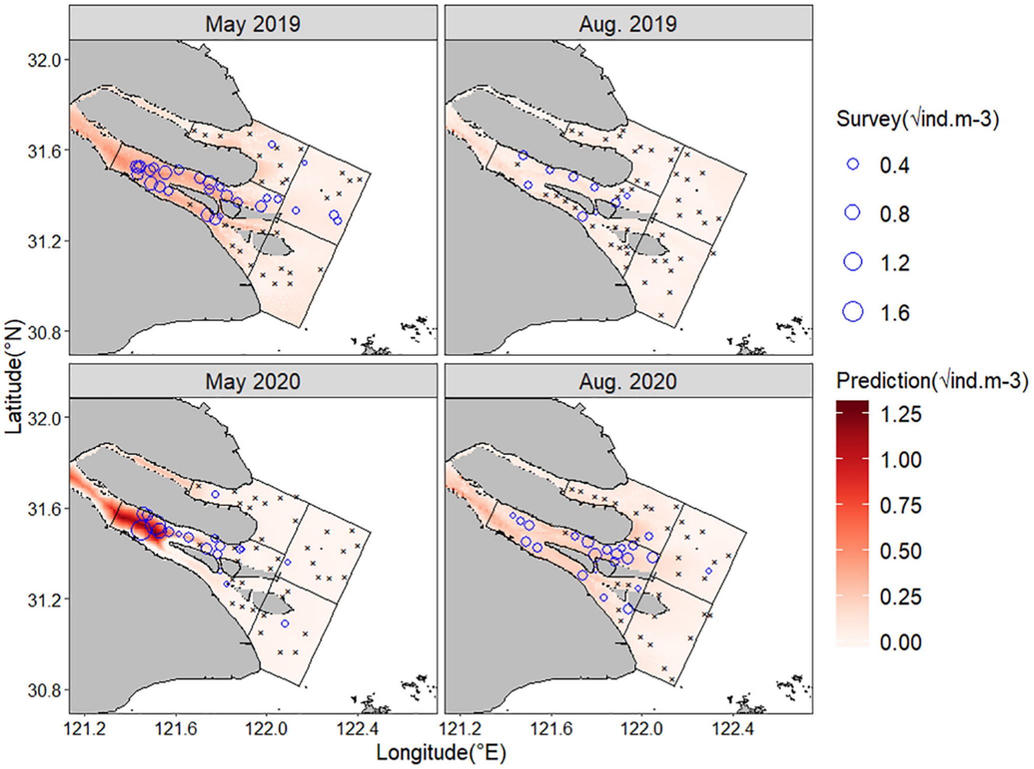

FIGURE 3 | The distribution of eggs sampled and predicted in each survey. The blue circle is egg density sampled in each station and the black × denotes stations with zero egg sampled. The color gradation represents the prediction result.

The overall SST in the Yangtze Estuary showed a decreasing trend from the South to the North Branch and from the branch to the offshore area (**Figure 4A**). The SST in May 2019 and 2020 ranged from 20 to 24°C. SST in August was included in best performing models in both 2019 and 2020 models. In August 2019, the SST exceeded 25°C in all the sites and ranged from 28 to 30°C in the South Branch and the surrounding waters. The positive relationship between SST and egg density widely occupied the study area (coefficients up to 0.037), except for a slight negative relationship near the Hengsha Island (**Figure 5**). August 2020 had a general higher SST across the South Branch and the highest SST (34.17°C) showed up in the North Channel. Meanwhile, the relationship between SST and egg density was negative in the North Channel and waters around the Changxing Island and positive in the rest of the study area. The whole estimated coefficients ranged from −0.029 to 0.04 in August 2020.

The SSS ranged from 0.01 to 28.5 in the study area showing an opposite distribution pattern to SST (**Figure 4B**). The salinity of water between the South Branch and the North Branch was of significant heterogeneity as the brackish water (salinity < 2) occupied most of the South Branch and the high salinity water (salinity > 10) distributed mainly in the North Branch and the offshore area. In May 2019 and 2020, the estimated coefficients of SSS were generally negative upstream of the Hengsha Island and upstream of the North Branch and close to zero in the rest of the study area (**Figure 5**). The strength of the negative effect of SSS was stable and the coefficients were approximately −0.022 in May 2019. However, it had an unstable negative effect on egg density in May 2020, as the strength of the negative effect in the upstream of the Changxing Island (coefficients up to −0.275) was stronger than that around the Hengsha Island (coefficients up to −0.1). The salinity in August 2019 had a weaker effect and the estimated coefficients were close to 0.

The relationship between DTC and egg density was obvious in subareas A and B (**Figure 5**). In May 2019 and 2020, the distribution pattern of a positive relationship between DTC and egg density was similar to that of a negative effect of SSS. The magnitude of positive coefficients in May 2020 (up to 0.249) was much higher than that (up to 0.04) in May 2019. The negative coefficients were in the rest of subareas A and B and the negative effect of SSS in May 2019 took up a wider area than that in May 2020 (**Figure 5**). In August 2020, the relationship between DTC and egg density showed high spatial variability in subarea B and the coefficients were from −0.019 to 0.039.

The DEP showed strong heterogeneity across the whole study area, especially in subarea B. The upstream of the Hengsha Island was occupied by both the water depths up to 25 m deep and shallow waters less than 5 m. Most of the waters in the rest area were less than 5 m deep, except for the right side of subarea C, which was appropriately 20 m deep. The mapping of estimated coefficients of DEP showed a wide range of positive relationships with egg density in the three models. In May 2019, it had positive coefficients in subareas A, B, and D, except for a weak negative effect in the bottom of subarea C. The positive strength in the upstream of the Hengsha Island (coefficients up to 0.015) was weaker than that in the rest of subareas A and B and the South Passage (coefficients up to 0.025). The DEP in August 2019 was completely positively related to egg density and displayed a weaker effect with coefficients around 0.005. The coefficients ranged from −0.20 to 0.040 in August 2020 and negative effects were located in the middle of the Changxing Island and the right end of the Hengsha Island.

DISCUSSION

The spatial regression GWR model was used to explore the spawning habitat of *C. mystus* and its response to the rapidly changing abiotic variables in the Yangtze Estuary. The estimated coefficients of each variable changed locally across the study

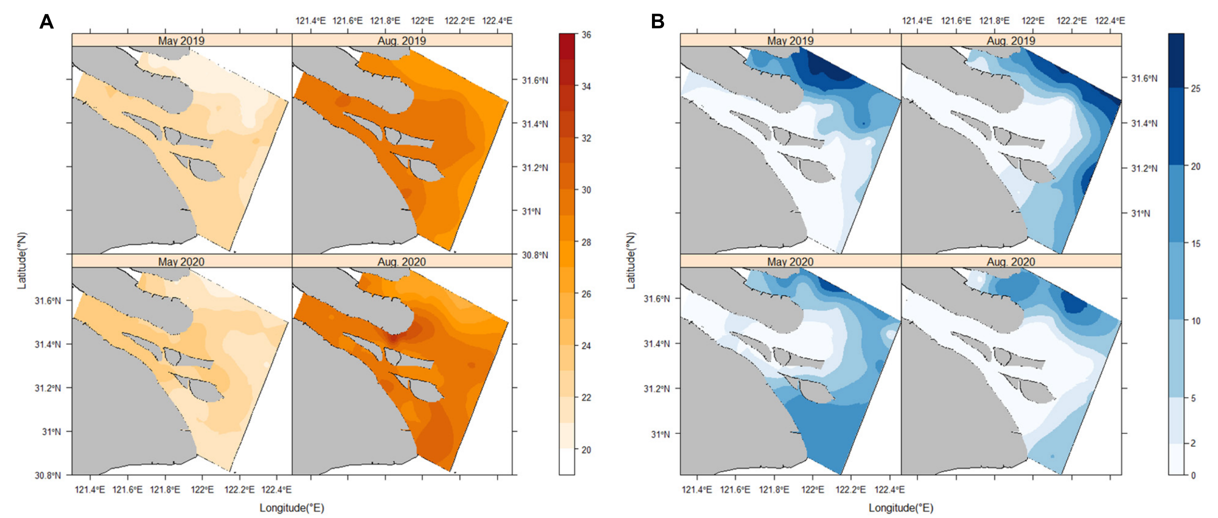

FIGURE 4 | (A) Distribution patterns of the sea surface temperature for each cruise. **(B)** Distribution patterns of the sea surface salinity for each cruise in the study area.

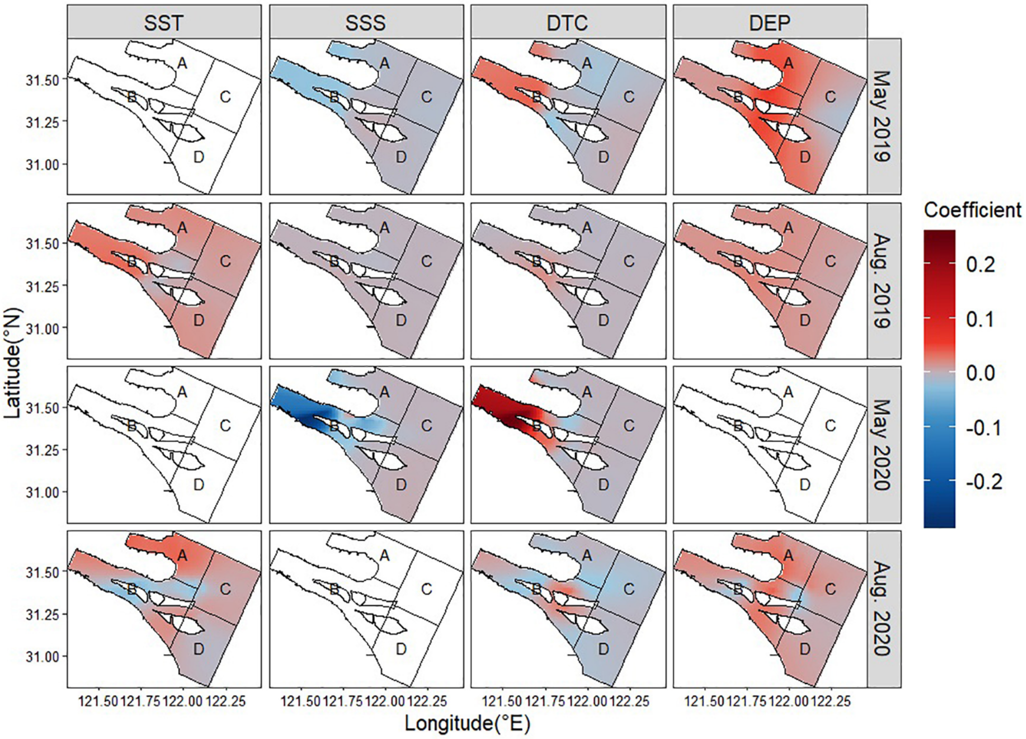

FIGURE 5 | Distribution of coefficients estimated for each cruise. The red color represents a positive relationship with the square root of egg density and the blue color represents a negative relationship with the square root of egg density. The blank figure represents independent variables that were not involved in the model.

area, indicating non-stationary effects caused by environment heterogeneity in the Yangtze Estuary. Seasonal variations can be found in environmental factors that affect the distribution of the spawning habitat of *C. mystus*. In the spring, SSS, DTC, and DEP were the main impact factors and saltwater intrusion in the South Branch might lead to the trend that the spawning habitat moved further upstream to the Changxing Island. SST was most important in the summer and the relatively lower SST was more crucial in the spawning habitat selection than DTC and DEP. The predicted spawning habitat of *C. mystus* was mainly distributed in the middle of the South Branch, near the Chongming, Changxing, and Hengsha Islands, which basically corresponded with the known area of spawning habitat defined in previous studies (Ni et al., 1999; Zhuang et al., 2006). However, there was possibility that the spawning habitat of *C. mystus* moved further upstream (**Figure 3**: May 2020) and adults of *C. mystus* might have the habit of spawning in the freshwater (Yang et al., 2006a,b).

The non-stationary effects of abiotic variables were reflected by the spatially varying relationship between the independent variables and dependent variables (Li et al., 2018). Both SST and SSS represented the primary habitat environment in defining *C. mystus* spawning habitat (Jiang et al., 2006; Jiang and Shen, 2006; Shi et al., 2014). In the reproductive season, adults of *C. mystus* would spawn to the brackish water with salinity from 0.14 to 7.51 and temperature of 18–28°C in the Yangtze Estuary (Ni et al., 1999; Zhuang et al., 2006; Ding, 2011).

The temperature across the study area in May 2019 and May 2020 (19–24°C) was within the range of suitable temperature for spawning, resulting in SSS the decisive environmental factor in defining the spawning habitat in the spring (Jiang and Shen, 2006). Although SSS was also involved in August 2019, the non-stationary effect of SSS was only significant in spring. Several studies based on the stepwise model and GAM have shown a universal negative correlation between SSS and the number of *C. mystus* eggs (Jiang et al., 2006; Ding, 2011; Hu et al., 2021). However, results from the GWR models indicated that the strength of the negative relationship between SSS and egg density varied spatially upstream of the Hengsha Island in May 2020 (**Figure 5**). There was saltwater intrusion of the South Branch in this month, as high salinity water was found along the Jiuduan sandbank (**Figure 4B**; Chen and Zhu, 2014). To avoid that eggs being transported to the unfavorable salinity waters (Fortier and Gagné, 1990), more adult fish might choose to spawn further upstream of the Changxing Island (**Figure 3**) and resulted in the strength difference. There was also a strong difference in the negative effect of SSS between May 2020 and May 2019. Overfishing and environmental degradation were the main reasons for the resource decline of *C. mystus* (Ni et al., 1999; Liu et al., 2013). The policy that stopping issuing special fishing licenses of *C. mystus* in 2019 might contribute to more egg production in 2020 and lead to the strength difference.

Sea surface temperature was the dominant environmental factor in summer, as the strength of the effect of SST was much stronger than that of SSS in August 2019. The conclusion was contradicted with that of Jiang and Shen (2006), who thought that SSS influenced greater than SST in summer. It might because the average SST in the summer of 2002 was lower than 28°C (Jiang and Shen, 2006). Previous studies have proved that the increase of temperature would accelerate fish gonadal maturation and, thus, promoting spawning activity (Jiang et al., 2006; Jiao et al., 2019). The widely distributed positive coefficients estimated of SST in August 2019 agreed with the conclusion. However, under higher SST in the North Channel, the area around the Changxing Island, and the South Passage in August 2020 (**Figure 4A**), the relationship between SST and egg density was negative (**Figure 5**), which indicated that the "extreme" temperature might restrain the spawning activity or harm the survival of eggs. Ni et al. (2020) reported that under the gradual warming of the Yangtze Estuary, the yield of adults of *C. mystus* have declined dramatically since a surge by 2°C occurred in 1997 and did not recover in the recent years. The regional temperature rise in the South Branch might be one of the reasons that influence the recruitment success of *C. mystus*. More attention should be paid to such areas in the future surveys.

There has been no obvious alteration in the distribution of *C. mystus* spawning habitat over the years. Homing of mature adults to their natal area is observed in a huge variety of migratory fishes such as diadromous fish and Gadiformes (Stabell, 1984; Robichaud and Rose, 2001; Knutsen et al., 2007). However, cues for the homing behavior were still uncertain and complex to explain. In this study, DTC and DEP were applied to explore the geographic effect on the distribution of spawning. It was shown that the relationship between DTC and egg density is positive in the upstream of the Hengsha Island and negative in the rest of subareas A and B (**Figure 5**). The spatially varying relationship suggests that adult *C. mystus* might prefer to spawn in the middle of the river upstream of the Hengsha Island, while close to the coast near waters around the Hengsha Island (Yang et al., 1990). The less egg production around the Hengsha Island caused by weaker runoff in May 2020 might also account for the smaller area of the negative effect of DTC in the North Channel (**Figure 5**). In August 2020, the non-stationary effect of DTC around the Changxing and Hengsha Islands was different from that in the other months. The choice of relatively lower temperature areas in August 2020 rather than the suitable DTC might be the main reason for the "abnormal" phenomenon. Since it is possible to ensure the survival of eggs under "extreme" temperature, the environmental condition of SST would determine the spawning habitat of *C. mystus*. The reproductive migration process of *C. mystus* was from offshore to inshore waters and finally stopped upstream of the Hengsha Island (Zhuang et al., 2006); based on the relationship analyzed above, the gradually reducing DTC might be one cue for the homing process of adults of *C. mystus*.

It was shown that the estimated coefficients of DEP were positively correlated to egg density in most of the study areas (**Figure 5**) in all the 3 months, which validated the result that *C. mystus* would spawn in deep waters (Zhou et al., 2011). The non-stationary effect caused by DEP was obvious in May 2019 and August 2020. As the deepest DEP yielded approximately the same level of egg density as other areas where water depth was relatively shallow (**Figures 1A**, **3**), the strength of the positive effect of DEP was weaker in the upstream of the Hengsha Island in May 2019 (**Figure 5**). The negative relationship between DEP and egg density was due to the eggs found in the shallow waters at the bottom of subarea C in May 2019. However, these eggs might be a result of the transport of local current (Ye et al., 2004; Wan and Wang, 2018) rather than a choice of spawning, as the environmental conditions are unsuitable for spawning. In August 2020, there were small areas of negative relationship in waters near the Changxing and Hengsha Islands. Such a phenomenon might also be the result of lower temperature preference in summer, as eggs were found in the shallow water of relatively lower SST rather than the deep water with "extreme" waters.

CONCLUSION

In conclusion, the specific location of the spawning habitat of *C. mystus* was predicted and defined by the GWR model in the Yangtze Estuary. The GWR model showed capability in explaining the response of species to the environmental variation in an estuarine habitat and the non-stationary effect of local variables had been analyzed for better understanding the spawning habitat selection mechanism of *C. mystus*. However, it was difficult to predict the actual spawning habitat specifically based on our limited data. In the future, more surveys covering the upstream of the South and North Branch throughout the spawning season should be carried out. Meanwhile, there was inference about the potential spawning habitat of *C. mystus* in the North Branch (Zhao et al., 2020). The potential spawning habitat can be defined as "a habitat where the environmental conditions are suitable for spawning" (Planque et al., 2010). We have collected a few eggs in the North Branch and subarea C; however, such phenomenon did not appear repeatedly and the environmental condition in the North Branch seemed unsuitable for spawning. The member/vagrant hypothesis proposed that the successful stock recruitment depended heavily on the local current system for preventing the eggs from being dispersed to unfavorable conditions (Fortier and Gagné, 1990). The eggs found might be under the transport of local currents to the nursing ground (Hu et al., 2021), as residual currents in the North Channel to the offshore area have the direction first to East then to the North (Ye et al., 2004; Wan and Wang, 2018). Thus, a study on the transport mechanism of the early life stage of *C. mystus* is necessary to verify the inference and hypothesis.

DATA AVAILABILITY STATEMENT

The raw data supporting the conclusions of this article will be made available by the authors, without undue reservation.

AUTHOR CONTRIBUTIONS

DW and ZL conceived and designed the study. RW, JZ, LZ, and SZ were involved in revising the manuscript for important intellectual content. XL and PS collected the data. DW compiled and analyzed the data and drafted the manuscript. All authors approved the final version of the manuscript and agreed to be accountable for all the aspects of the work.

FUNDING

This work was funded by projects: the Tracking Evaluation on Recovery Effect of Fishing Ban in Key Water Areas of the Yangtze River Basin (Grant No. D-8021-20-0073), the Estimation of Spawning Population Biomass of *Coilia mystus* in the Yangtze Estuary Based on Daily Egg Production Method (Grant No. A2-2006-21-200309), the Scientific Research Foundation for the Imported Talent by RW (Grant No. A1-2006-21-7009), and the Population Dynamics Mechanism and Maintenance Management Strategy of Important Fish Species in the Yangtze Estuary and Adjacent Waters (Grant No. 21010502200).

ACKNOWLEDGMENTS

We are indebted to the vessels and colleagues who contributed to collecting the data used for this study. Additionally, we thank Bai Li for her valuable and constructive comments on the manuscript.

REFERENCES

Andrew, M. W., Charles, E. T., William, B. D., and James, A. S. (2009). Observations on the distribution of ichthyoplankton within the saco river estuary system. *Northeastern Naturalist* 16, 647–654. doi: 10.1656/045.016.n414

Asch, R. G., and Checkley, D. M. (2013). Dynamic height: a key variable for identifying the spawning habitat of small pelagic fishes. *Deep Sea Res. 1 Oceanogr. Res. Pap.* 71, 79–91. doi: 10.1016/j.dsr.2012.08.006

Bacheler, N. M., Ciannelli, L., Bailey, K. M., and Duffy-Anderson, J. (2010). Spatial and temporal patterns of walleye pollock (*Theragra chalcogramma*) spawning in the eastern Bering Sea inferred from egg and larval distributions. *Fish. Oceanogr.* 19, 107–120. doi: 10.1111/j.1365-2419.2009.00531.x

Brooks, W., Zhu, J., and Lu, Z. (2014). *Local Adaptive Grouped Regularization and its Oracle Properties for Varying Coefficient Regression.* arXiv [Preprint]. Available online at: https://arxiv.org/pdf/1411.5725.pdf (accessed October 27, 2021).

Brunsdon, C., Fotheringham, A. S., and Charlton, M. (2002). Geographically weighted summary statistics-a framework for localised exploratory data analysis. *Comput. Environ. Urban Syst.* 26, 501–524.

Brunsdon, C., Fotheringham, A. S., and Charlton, M. E. (1996). Geographically weighted regression: a method for exploring spatial nonstationarity. *Geogr. Anal.* 28, 281–298. doi: 10.1111/j.1538-4632.1996.tb00936.x

Chen, J., and Zhu, J. R. (2014). Sources for saltwater intrusion at water intake of qingcaosha reservoir in the yangtze estuary. *Acta Oceanol. Sin.* 36, 131–141.

Christoph, B., and Jose, M. B. (2012). On the use of cross-validation for time series predictor evaluation. *Inf. Sci.* 191, 192–213. doi: 10.1016/j.ins.2011.12.028

Ding, Y. W. (2011). *The Temporal And Spatial Variation Of The Fish Recruitment Resource In Yangtze River Estuary.* [Master's thesis]. Qingdao: University of Chinese Academy of Sciences.

Dumont, P., D'Amours, J., Thibodeau, S., Dubuc, N., Verdon, R., Garceau, S., et al. (2011). Effects of the development of a newly created spawning ground in the Des Prairies River (Quebec, Canada) on the reproductive success of lake sturgeon (*Acipenser fulvescens*). *J. Appl. Ichthyol.* 27, 394–404. doi: 10.1111/j.1439-0426.2011.01718.x

Elliott, M., Whitfield, A. K., Potter, I. C., Blaber, S. J. M., Cyrus, D. P., Nordlie, F. G., et al. (2007). The guild approach to categorizing estuarine fish assemblages: a global review. *Fish Fish.* 8, 241–268. doi: 10.1111/j.1467-2679.2007.00253.x

Fortier, L., and Gagné, J. A. (1990). Larval Herring (*Clupea harengus*) Dispersion. Growth, and Survival in the St, Lawrence Estuary: match/Mismatch or Membership/Vagrancy?.*Can. J. Fish. Aquat. Sci.* 47, 1898–1912. doi: 10.1139/f90-214

Gallego, A., North, E. W., and Petitgas, P. (2007). Introduction: status and future of modelling physical-biological interactions during the early life of fishes. *Mar. Ecol. Prog. Ser.* 347, 122–126.

Gibson, G. A., Stockhausen, W. T., Coyle, K. O., Hinckley, S., Parada, C., Hermann, A. J., et al. (2018). An individual-based model for sablefish: exploring the connectivity between potential spawning and nursery grounds in the Gulf of Alaska. *Deep Sea Res. 2 Top. Stud. Oceanogr.* 165, 89–112. doi: 10.1016/j.dsr2.2018.05.015

Gollini, I., Lu, B. B., Charlton, M., Brunsdon, C., and Harris, P. (2015). GWmodel: an R package for exploring spatial heterogeneity using geographically weighted models. *J. Stat. Softw.* 63, 1–52. doi: 10.18637/jss.v063.i17

Gonzalez-Irusta, J. M., and Wright, P. J. (2016). Spawning grounds of Atlantic cod (*Gadus morhua*) in the North Sea. *ICES J. Mar. Sci.* 73, 1–12. doi: 10.1093/icesjms/fsv180

Halvor, K., Esben, M. O., Lorenzo, C., Sigurd, H. E., Jan, A. K., Jan, H. S., et al. (2007). Egg distribution, bottom topography and small-scale cod population structure in a coastal marine system. *Mar. Ecol. Prog. Ser.* 2007, 249–255.

Hu, L. J., Song, C., Geng, Z., Zhao, F., Jiang, J., Liu, R. H., et al. (2021). Temporal and spatial distribution of Coilia mystus larvae and juveniles in the Yangtze Estuary during the main breeding season. *J. Fish. Sci. China* 28, 1152–1161.

Jiang, M., and Shen, X. Q. (2006). Abundance distributions of pelagic fish eggs and larva in the Changjiang River estuary and vicinity waters in summer. *Mar. Sci.* 30, 92–97.

Jiang, M., Shen, X. Q., and Chen, L. F. (2006). Relationship between with abundance distribution of fish eggs, larvae and environmental factors in the Changjiang Estuary and vicinity waters in spring. *Mar. Environ. Sci.* 25, 37–44.

Jiao, W. J., Zhang, P., Chang, J. B., Tao, J. P., Liao, X. L., and Zhu, B. (2019). Variation in the suitability of Chinese sturgeon spawning habitat after construction of dams on the Yangtze River. *J. Appl. Ichthyol.* 35, 637–643. doi: 10.1111/jai.13914

Knutsen, H., Olsen, E. M., Ciannelli, L., Espeland, S. H., Knutsen, J. A., Simonsen, J. H., et al. (2007). Egg distribution, bottom topography and small-scale cod population structure in a coastal marine system. *Mar. Ecol. Prog. Ser.* 333, 249–255. doi: 10.3354/meps333249

Lauri, L. S., Nathan, J. M., Timothy, E., Barbara, H., and Steven, H. (2014). Distribution patterns of Pacific halibut (*Hippoglossus stenolepis*) in relation to environmental variables along the continental shelf waters of the US West Coast and southern British Columbia. *Fish. Oceanogr.* 23, 225–241. doi: 10.1111/fog.12057

Lelievre, S., Vaz, S., Martin, C. S., and Loots, C. (2014). Delineating recurrent fish spawning habitats in the North Sea. *J. Sea Res.* 91, 1–14. doi: 10.1016/j.seares.2014.03.008

Li, B., Cao, J., Guan, L. S., Mazur, M., Chen, Y., and Wahle, R. A. (2018). Estimating spatial non-stationary environmental effects on the distribution of species: a case study from American lobster in the Gulf of Maine. *ICES J. Mar. Sci.* 1473–1482. doi: 10.1093/icesjms/fsy024

Likongwe, P., Kihoro, J., Ngigi, M. M., and Jamu, D. (2015). Modeling spatial non-stationarity of Chambo in South-East Arm of Lake Malawi. *Asian J. Appl. Sci. Eng.* 4, 81–90.

Liu, K., Xu, D. P., Duan, J. R., Zhang, M. Y., Fang, D. A., Zhou, Y. F., et al. (2013). Fluctuation of biological characteristics and yield of *Coilia mystus* in fishing season after impoundment of the Three Gorges Dam in Yangtze River Estuary. *Resour. Environ. Yangtze Basin* 22, 1282–1288.

Locke, A., and Courtenay, S. C. (1995). Effects of environmental factors on ichthyoplankton communities in the Miramichi estuary, Gulf of St Lawrence. *J. Plankton Res.* 17, 333–349. doi: 10.1093/plankt/17.2.333

Luo, B., and Shen, H. (eds) (1994). The Three Gorges Project and Ecology in Estuaries. Beijing: China Science Publishing & Media LTD.

Molinaro, A. M., Simon, R., and Pfeiffer, R. (2005). Prediction error estimation: a comparison of resampling methods. *Bioinformatics* 21, 3301–3307. doi: 10.1093/bioinformatics/bti499

Munk, P., Fox, C. J., Bolle, L. J., Damme, C. J. G., Fossum, P., and Kraus, G. (2009). Spawning of North Sea fishes linked to hydrographic features. *Fish. Oceanogr.* 18, 458–469. doi: 10.1111/j.1365-2419.2009.00525.x

Ni, J. F., Guo, H. Y., Tang, W. Q., Zhang, Y., and Zhang, X. G. (2020). On interannual variations of *Coilia mystus* catches in the Yangtze River Estuary. *Mar. Fish.* 42, 192–204.

Ni, Y. (1999). Fishery resources conservation for *Coilia mystus* in the Changjiang estuary. *J. Fish. Sci. China* 6, 75–77.

Ni, Y., Wang, Y. L., Jiang, M., and Chen, Y. Q. (1999). Biological characteristics of *Coilia mystus* in the Changjiang estuary. *J. Fish. Sci. China* 6, 69–71.

O'Brien, R. M. (2007). A Caution Regarding Rules of Thumb for Variance Inflation Factors. *Qual. Quant.* 41, 673–690.

Opdal, A. F. (2010). Fisheries change spawning ground distribution of northeast Arctic cod. *Biol. Lett.* 6, 261–264. doi: 10.1098/rsbl.2009.0789

Planque, B., Bellier, E., and Lazure, P. (2010). Modelling potential spawning habitat of sardine (*Sardina pilchardus*) and anchovy (*Engraulis encrasicolus*) in the Bay of Biscay. *Fish. Oceanogr.* 16, 16–30. doi: 10.1111/j.1365-2419.2006.00411.x

Portner, H. O., and Farrell, A. P. (2008). Ecology: physiology and climate change. *Science* 322, 690–692. doi: 10.1126/science.1163156

Reglero, P., Santos, M., Balbin, R., Laiz-Carrion, R., Alvarez-Berastegui, D., Ciannelli, L., et al. (2017). Environmental and biological characteristics of Atlantic bluefin tuna and albacore spawning habitats based on their egg distributions. *Deep Sea Res. 2 Top Stud. Oceanogr.* 140, 105–116. doi: 10.1016/j.dsr2.2017.03.013

Robichaud, D., and Rose, G. A. (2001). Multiyear homing of Atlantic cod to a spawning ground. *Can. J. Fish. Aquat. Sci.* 58, 2325–2329. doi: 10.1139/cjfas-58-12-2325

Shan, X. J., Jin, X. S., and Yuan, W. (2010). Fish assemblage structure in the hypoxic zone in the Changjiang (Yangtze River) estuary and its adjacent waters. *Chin. J. Oceanol. Limnol.* 28, 459–469. doi: 10.1007/s00343-010-9102-6

Shi, W. G., and Wang, B. (2002). Status quo of tapertail anchovy resource in the estuaries of the Yangtze River. *Acta Hydrobiol. Sin.* 26, 648–653.

Shi, Y. R., Chao, M., Quan, W. M., and Shen, X. Q. (2014). Spatial and seasonal variations in fish assemblages of the Yangtze River estuary. *J. Appl. Ichthyol.* 30, 844–852. doi: 10.1111/jai.12448

Stabell, O. B. (1984). Homing and olfaction in salmonds: a critical review with special reference to the atlantic salmon. *Biol. Rev.* 59, 333–388. doi: 10.1111/j.1469-185X.1984.tb00709.x

Thompson, B. M., and Riley, J. D. (1981). Egg and larval development studies in the North Sea cod (*Gadus morhua L.*). *Rapports et Proce's-Verbaux des Re'unions du Conseil International pour l'Exploration de la Mer* 178, 553–559.

Tian, R. C., Chen, C., Stokesbury, K. D. E., Rothschild, B. J., Cowles, G. W., Xu, Q., et al. (2009). Dispersal and settlement of sea scallop larvae spawned in the fishery closed areas on Georges Bank. *ICES J. Mar. Sci.* 66, 2155–2164. doi: 10.1093/icesjms/fsp175

Wan, Y., and Wang, L. (2018). Study on the seasonal estuarine turbidity maximum variations of the Yangtze Estuary, China. *J. Waterw. Port Coast. Ocean Eng.* 144:05018002. doi: 10.1061/(ASCE)WW.1943-5460.0000442

Windle, M. J. S., Rose, G. A., Devillers, R., and Fortin, M. J. (2010). Exploring spatial non-stationarity of fisheries survey data using geographically weighted regression (GWR): an example from the Northwest Atlantic. *ICES J. Mar. Sci.* 67, 145–154. doi: 10.1093/icesjms/fsp224

Yan, Y., Gao, J., Zhu, Y., and Zheng, J. (2001). Preliminary study on relationship between Deepwater Channel regulation and riverbed evolution. *J. Hohai Univ.* 29, 7–12.

Yang, D., Wu, G., and Sun, J. (1990). The investigation of pelagic eggs, larvae and juveniles of fishes at the mouth of the Changjiang River and adjacent areas. *Oceanol. Limnol. Sin.* 21, 346–355.

Yang, J., Arai, T., Liu, H., and Miyazaki, N. (2006a). Environmental signature in the otolith elemental fingerprint of the tapertail anchovy, *Coilia mystus*, from the Changjiang estuary, China. *J. Appl. Ichthyol.* 22, 459–462. doi: 10.1111/j.1439-0426.2006.00776.x

Yang, J., Arai, T., Liu, H., Miyazaki, N., and Tsukamoto, K. (2006b). Reconstructing habitat use of *Coilia mystus* and *Coilia ectenes* of the Yangtze River estuary, and of *Coilia ectenes* of Taihu Lake, based on otolithstrontium and calcium. *J. Fish Biol.* 69, 1120–1135. doi: 10.1111/j.1095-8649.2006.01186.x

Ye, S., Lv, J., Ding, D., and Huang, X. (2004). A preliminary study on the impacts of large-scale estuarine engineering on habitat fragmentation in the Yangtze River estuary. *Ocean Eng.* 22, 41–47.

Yu, W., and Zhang, Z. (2017). Recognition of tide and tidal current movement in the Yangtze Estuary. *J. Water Resour. Res.* 6, 475–485.

Zhai, L., and Pauly, D. (2019). Yield-per-recruit, utility-per-recruit, and relative biomass of 21 exploited fish species in China's coastal seas. *Front. Mar. Sci.* 6:724. doi: 10.3389/fmars.2019.00724

Zhai, L., and Pauly, D. (2020). Construction and interpretation of particle size distribution spectra from 19 Ecopath Models of Chinese coastal ecosystems. *Front. Mar. Sci.* 7:298. doi: 10.3389/fmars.2020.00298

Zhang, R., Lu, S., Zhao, C., Chen, L., Zang, Z., and Jiang, Y. (1985). *Fish Eggs and Larvae in the Offshore Waters of China.* Shanghai: Shanghai Scientific & Technical Publishers.

Zhao, F., Yang, Q., Song, C., Zhang, T., and Zhaung, P. (2020). Biological characteristics and resource utilization of *Coilia mystus* in the Yangtze Estuary. *Mar. Fish.* 42, 110–119.

Zhou, Y., Jin, H., Zhang, H., Zhang, Y., Jiang, R., and Xu, K. (2011). Distribution of Ichthyoplankton of *Coilia mystus* in the coast of north Zhejiang Province in spring and summer. *J. Zhejiang Ocean Univ. (Nat. Sci.)* 30, 307–312.

Zhuang, P., Wang, Y., Li, S., Deng, S., Li, C., Ni, Y., et al. (2006). *Fishes Of The Yangtze Estuary*. Shanghai: Shanghai Scientific & Technical Publishers.

Zorica, B., Vilibic, I., Kec, V. C., and Sepic, J. (2013). Environmental conditions conducive to anchovy (*Engraulis encrasicolus*) spawning in the Adriatic Sea. *Fish. Oceanogr.* 22, 32–40. doi: 10.1111/fog.12002

Conflict of Interest: The authors declare that the research was conducted in the absence of any commercial or financial relationships that could be construed as a potential conflict of interest.

ORIGINAL RESEARCH
published: 18 November 2021
doi: 10.3389/fmars.2021.766369

Assemblage Structure of Larval Fishes in Epipelagic and Mesopelagic Waters of the Northern Gulf of Mexico

Verena H. Wang*†, Carley R. Zapfe and Frank J. Hernandez

Division of Coastal Sciences, School of Ocean Sciences and Engineering, University of Southern Mississippi, Ocean Springs, MS, United States

OPEN ACCESS

Edited by:
Hui Zhang,
Institute of Oceanology, Chinese Academy of Sciences (CAS), China

Reviewed by:
Simon Geist,
Texas A&M University Corpus Christi, United States
Khor Waiho,
University of Malaysia Terengganu, Malaysia

***Correspondence:**
Verena H. Wang
wangv21@ecu.edu

†Present address:
Verena H. Wang,
Department of Biology, Coastal Studies Institute, East Carolina University, Wanchese, NC, United States

Specialty section:
This article was submitted to Marine Fisheries, Aquaculture and Living Resources, a section of the journal Frontiers in Marine Science

Received: *29 August 2021*
Accepted: *19 October 2021*
Published: *18 November 2021*

Citation:
Wang VH, Zapfe CR and Hernandez FJ (2021) Assemblage Structure of Larval Fishes in Epipelagic and Mesopelagic Waters of the Northern Gulf of Mexico. Front. Mar. Sci. 8:766369. doi: 10.3389/fmars.2021.766369

The early life stages of fishes play a critical role in pelagic food webs and oceanic carbon cycling, yet little is known about the taxonomic composition and distribution of larval fishes in the northern Gulf of Mexico (GOM) below the epipelagic (<200 m). Here, we provide the first large-scale characterization of larval fish assemblages in the GOM across epipelagic, mesopelagic, and bathypelagic regions (0–1,500 m), using samples collected during the Natural Resource Damage Assessment conducted following the Deepwater Horizon oil spill (DWHOS). These data contain > 130,000 ichthyoplankton specimens from depth-discrete plankton samples collected across 48 stations in the GOM during six cruises conducted in 2010 and 2011. We examined indices of abundance and diversity, and used a multivariate regression tree approach to model the relationship between larval fish assemblages and environmental conditions. The total abundance of larval fish followed a generally decreasing trend with increasing depth, and family-level richness and diversity were significantly higher in the epipelagic than mesopelagic and bathypelagic regions. Fourteen distinct assemblage groups were identified within the epipelagic, with depth, surface salinity, and season contributing to the major branches separating groups. Within the mesopelagic, seven distinct assemblage groups were identified and were largely explained by variation in depth, season, and surface temperature. Bathypelagic assemblages were poorly described by environmental conditions. The most common epipelagic assemblage groups were widely distributed across the GOM, as were all mesopelagic assemblage groups, suggesting limited horizontal structuring of GOM larval fishes. Of the mesopelagic-associated fish taxa, four dominant families (Myctophidae, Gonostomatidae, Sternoptychidae, Phosichthyidae) comprised the majority of the catch in both the epipelagic (63%) and combined mesopelagic and bathypelagic (97%) regions. Dufrêne-Legendre indicator analysis confirmed that these dominant families were characteristic of epipelagic and mesopelagic assemblages; the larvae of less common mesopelagic-associated families largely identified with epipelagic assemblage groups. A lack of baseline data about the distribution patterns of early life stages of mesopelagic fishes in the GOM was apparent following the DWHOS, and these findings provide a valuable reference point in the face of future ecosystem stressors.

Keywords: ichthyoplankton, plankton survey, MOCNESS, deep sea, multivariate regression tree, Dufrêne-Legendre

INTRODUCTION

Open ocean ecosystems are dominated by mesopelagic fishes, which occupy depths between 200 and 1,000 m and collectively comprise the largest proportion of global fish biomass (Irigoien et al., 2014). As both major consumers of microzooplankton and key prey for pelagic predators, including commercially important species, mesopelagic fishes provide an important intermediate link in the pelagic food web (Choy et al., 2013; Young et al., 2015; Drazen and Sutton, 2017). Additionally, the diel vertical migration behavior characteristic of many mesopelagic fish taxa contributes to the global carbon cycle, actively transporting carbon consumed in the epipelagic to the mesopelagic, where it is deposited via respiration, fecal material, or mortality (Davison et al., 2013). While the importance of mesopelagic fishes to ecosystem function is now well recognized, the early life history stages of these taxa remain understudied.

Larval mesopelagic fishes are a large, often numerically dominant, component of oceanic ichthyoplankton catch in regions worldwide (e.g., eastern North Pacific, Moser and Smith, 1993; western North Pacific, Sassa et al., 2004; northwest Mediterranean, Olivar et al., 2010; equatorial and tropical Atlantic, Olivar et al., 2018; southern Gulf of Mexico, Daudén-Bengoa et al., 2020). Mesopelagic larvae are thought to be largely constrained to productive epipelagic regions of the water column (<200 m) with limited or small-scale diel vertical movements relative to adults (Ahlstrom, 1959; Sassa et al., 2002). However, broad-scale surveys of ichthyoplankton rarely sample at depths exceeding 200 m (exceptions include Moser and Smith, 1993; Sassa and Kawaguchi, 2006; Olivar et al., 2018; Dove et al., 2021), so mesopelagic larval dynamics throughout the water column remain largely unknown.

Understanding the spatial and temporal distributions of larval fish assemblages and the physical processes that shape them can provide insights into the patterns that structure adult populations (Fuiman and Werner, 2002). Indeed, the geographic distributions of adult mesopelagic fishes have been found to reflect larval fish distributions accurately, relative to the dispersal potential of the larval stage (Olivar et al., 2017, 2018). Because of their limited mobility and high vulnerability (Houde, 1989), larval fish assemblage dynamics are heavily influenced by oceanographic features and often reflect changes in the marine environment (Kingsford, 1993; Brodeur et al., 2008; Hsieh et al., 2009). This makes the early life stages of fishes uniquely susceptible to environmental perturbations, which can have impacts on adult recruitment, food web dynamics, and broader ecosystem services.

In the northern Gulf of Mexico (GOM), the Deepwater Horizon Oil Spill (DWHOS) occurred at ~1,500 m depth in April 2010 and exposed a deficiency in baseline data for deep-sea ecosystems in the GOM and beyond (Ramirez-Llodra et al., 2011; Fisher et al., 2016). The adult stages of mesopelagic fishes have long been studied in the GOM, albeit on a limited spatial scale (see Hopkins et al., 1996) or without depth-discrete sampling (Murdy et al., 1983); focus on quantifying the ecology of the mesopelagic GOM, including fishes, has increased dramatically in the wake of DWHOS (Cook et al., 2020). Mesopelagic fish larvae, however, receive little targeted attention in the GOM. Studies of broad-scale ichthyoplankton assemblages in the GOM that include (but are not focused on) mesopelagic fish taxa are constrained to sampling of the epipelagic region (Muhling et al., 2012; Lyczkowski-Shultz et al., 2013; Meinert et al., 2020) and to coastal waters (Rakocinski et al., 1996; Carassou et al., 2012). High abundances of mesopelagic larvae in the mixed layer (0–100 m) of the open ocean GOM suggest that epipelagic regions represent important habitat for these taxa during early development (Meinert et al., 2020), but questions remain about larval distribution patterns and usage of mesopelagic portions of the water column.

Adult mesopelagic fish assemblages have been found to lack geographic and temporal patterns of structure in the GOM, suggesting that these assemblages are well-mixed and highly dispersed over large distances despite variation in local oceanographic features (Ross et al., 2010; Milligan and Sutton, 2020). On the continental shelf, distributions of larval mesopelagic fishes in the GOM were largely explained by sampling depth and were not associated with environmental factors, despite strong correlation of epipelagic-associated larval fishes to sea surface temperature (Muhling et al., 2012). These previous findings suggest that mesopelagic larval fishes in the oceanic GOM may have limited spatial assemblage structure, although the response of vertical assemblage distribution to environmental drivers remains unknown.

Here, we characterize the dynamics of larval fish assemblages across epipelagic, mesopelagic, and bathypelagic (0–1,500 m) regions of the GOM, encompassing both epipelagic- and mesopelagic-associated fish families. We examine indices of abundance and diversity, as well as environmental drivers of larval fish assemblage structure in the different pelagic zones. Insights into the spatial and temporal scale of variability in pelagic ichthyoplankton communities in the GOM will provide a reference point for a previously unstudied ecosystem that may guide response efforts to future environmental perturbations.

MATERIALS AND METHODS

Sample Collection

Sample collection and specimen identification were conducted as part of the Deepwater Horizon Oil Spill Natural Resource Damage Assessment (DWH NRDA) effort. Our study focused on six deep-pelagic plankton cruises conducted during Fall 2010 and Spring 2011 (**Table 1**), encompassing 48 stations in the northern Gulf of Mexico (**Figure 1**). Samples were collected using a multiple opening/closing net and environmental sensing system (MOCNESS) with a 1 m^2 opening and 333 μm mesh nets. The MOCNESS simultaneously collects plankton while using mounted sensors to measure conductivity, temperature, and depth, and a flowmeter to record the volume of water filtered for each net sample. Paired day and night oblique MOCNESS tows were conducted at each sampling location, with each tow consisting of eight sequentially collected depth-discrete net samples targeting depth bins ranging from 0 to 1,500 m (**Table 1**). Upon recovery of the MOCNESS, nets were rinsed with seawater and the contents of each cod end were preserved in 10% buffered formalin.

Ichthyoplankton from the MOCNESS samples were sorted and identified to the lowest possible taxonomic level. During the sorting procedure, ichthyoplankton specimens were separated roughly into two size classes (<25 mm or > 25 mm, TL). Only specimens from the < 25 mm size category were retained for this analysis, as they represented the majority of the data and reduced the likelihood of confounding distribution patterns by including later life stages. Ichthyoplankton specimens were not consistently identified to the genus or species level, so all analyses were conducted at the family level. Occasionally, the complete set of eight nets within a MOCNESS deployment was not successfully collected due to weather or equipment malfunction. Because the analyses conducted here are largely based on comparisons among depth-discrete samples (nets) rather than tows, ichthyoplankton and environmental data from MOCNESS tows with missing nets were retained for analysis. Nets with missing environmental data were excluded from all analyses.

TABLE 1 | Ichthyoplankton samples collected using a 1 m^2 MOCNESS with 333 μm mesh nets in the northern Gulf of Mexico during the Deepwater Horizon Oil Spill Natural Resource Damage Assessment effort.

	Survey campaign					
	WS1	**WS3**	**NSPC3**	**NSPC4**	**WS4**	**NS9**
Start date	9/9/10	9/26/10	9/25/10	10/16/10	4/20/11	4/18/11
End date	9/16/10	10/1/10	10/2/10	10/23/10	5/27/11	6/26/11
Season	Fall	Fall	Fall	Fall	Spring	Spring
Stations	8	5	8	8	9	42
Tows	12	10	15	16	25	82
Nets per depth bin (m)						
0–25	12	10	15	16	25	81
25–200	12	10	15	16	26	81
200–400	12	10	15	16	25	78
400–600	12	10	15	16	24	79
600–800	10	10	15	16	25	75
800–1,000	8	10	12	13	14	71
1,000–1,200	5	9	10	10	7	64
1,200–1,500	3	6	6	4	5	45
Total	74	75	103	107	151	574

Six survey campaigns were conducted aboard the R/V F. G. Walton Smith (WS) and R/V Nick Skansi (NS). Sampling dates (MM/DD/YY), season, and number of stations, tows, and depth-discrete net samples (nominally eight depth bins sampled per tow) are indicated for each survey.

Ichthyoplankton Data

Raw ichthyoplankton counts were standardized by the volume of water filtered, resulting in larval fish concentration (larvae 1,000 m^{-3}) for each depth-discrete net sample, hereafter referred to as "abundance." Extremely rare families were excluded prior to all analyses. Due to the patchy nature of ichthyoplankton distribution, rare taxa may represent sampling error rather than truly rare taxa that are indicators of site-specific conditions (Legendre and Gallagher, 2001). While the treatment of rare taxa for multivariate analyses is certainly a matter of debate (Poos and Jackson, 2012), we conservatively removed families that did not exceed 1% of the catch in any net and families with < 5 total individuals across all nets to avoid the undue influence of rare families on distance measures.

Family-level abundance (log-transformed), richness, and diversity were compared among depth-bins using a one-way analysis of variance (ANOVA), followed by Tukey's honestly significant difference (HSD) test to determine a posteriori differences among pairwise means. Richness was defined as the number of families present in a net sample. Diversity was estimated using the Shannon Diversity index:

$$H = -\sum p_i ln(p_i) \qquad (1)$$

where p_i represents the proportion of the net sample represented by the ith family relative to the total number of families present in a net sample.

Environmental and Spatiotemporal Data

Environmental variables consist of a suite of *in-situ* measurements collected simultaneously with MOCNESS ichthyoplankton sampling, derived variables, and spatiotemporal descriptors. For each depth-discrete net sample, temperature, salinity, and density (sigma-t) were reported as the mean of all observations recorded while each net was actively sampling, and depth was reported as the midpoint between the depth measured at net opening and closing. Surface temperature, surface salinity, and mixed layer depth were reported from surface (0–25 m) net observations only, and were used to represent surface features for all subsurface nets within each respective tow deployment. Mixed layer depth was calculated following Levitus (1982) as the depth at which density (sigma-t) increases by 0.125 kg m^{-3} from a surface reference point at 10 m. Spatial variability was represented by geographic coordinates (latitude and longitude recorded at net opening), as well as general proximity to the continental slope. Sampling locales were grouped by bathymetry

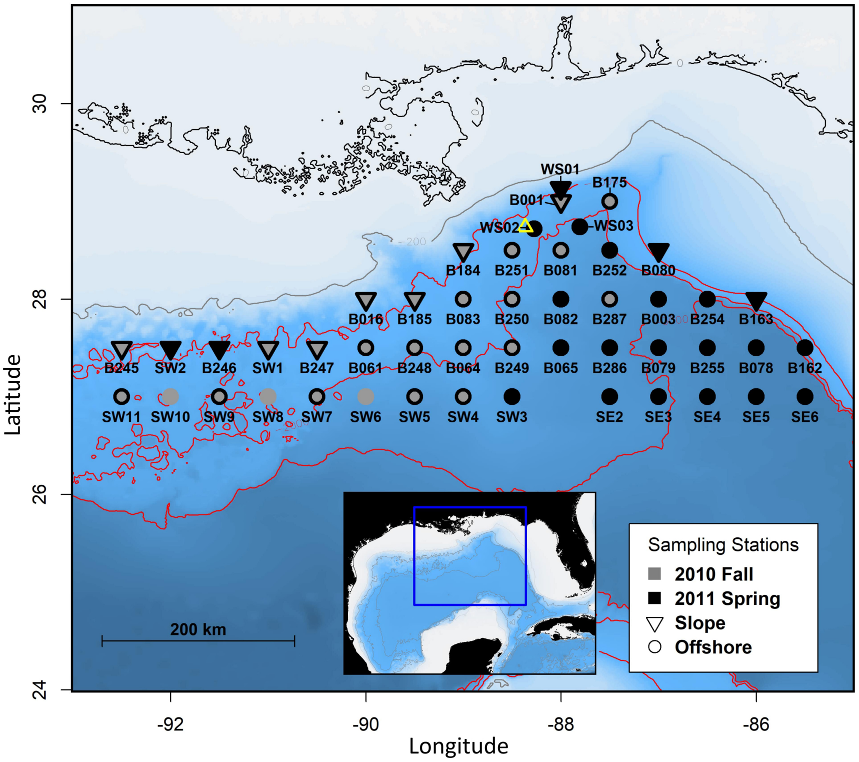

FIGURE 1 | Map of deep-pelagic plankton sampling stations in the northern Gulf of Mexico, distinguishing between sampling period (year, season) and slope vs. offshore locations. The gray line represents the 200 m isobath, red lines represent 1,000 m isobath increments, and the open yellow triangle marks the location of the Deepwater Horizon wellhead.

into "slope" and "offshore" stations (**Figure 1**), loosely following Burdett et al. (2017). Slope stations were on or adjacent to the 1,000 m isobath, and offshore stations were seaward of the 1,000 m isobath. Stations directly adjacent to the 1,000 m isobath but also encompassing steep bathymetric features were considered offshore stations. Season (fall/spring) and diel periodicity (day/night) were also included to account for multiple scales of temporal variability.

Assemblage Analyses

We used a multivariate regression tree (MRT) approach to model the relationship between the abundance of larval fish families and the environment (De'ath, 2002). The MRT classifies samples (multivariate ichthyoplankton family abundances from an individual net sample) by recursive partitioning, with each node of the tree defined by a rule for a single environmental variable, culminating in terminal nodes containing clusters of samples (hereafter, assemblage groups) represented by a suite of environmental characters. MRT analyses generate easily interpretable visual representations of taxon-environment relationships, and are well-suited to analyze imbalanced or incomplete datasets, mixtures of continuous and categorical explanatory environmental variables, and are robust to the collinearity of explanatory variables (De'ath, 2002).

Ichthyoplankton abundance data were Hellinger-transformed prior to MRT analyses. Hellinger transformations are appropriate for community composition data containing numerous zeros, do not assign high weights to rare taxa, and allow dissimilarity measures among sites to be calculated using Euclidean distances (Legendre and Gallagher, 2001). MRT analyses were conducted using all families (after removal of rare families) as well as with the 30 most abundant families after Hellinger transformation. MRT was conducted separately on four depth-defined subsets of ichthyoplankton and environmental data—all pelagic zones combined, epipelagic, mesopelagic, bathypelagic. For each depth-defined data subset, independent MRT trials were run for all possible combinations of the 12 explanatory environmental and spatiotemporal variables described above (temperature, salinity, density, depth, surface temperature, surface salinity, mixed layer depth, latitude, longitude, slope/offshore, season, diel periodicity), each with 10 cross-validations. The best predictive trees were selected by minimizing cross-validated relative error (CVRE) while maximizing relevance, or the ratio of the number of explanatory variables appearing on the tree relative to the number of variables included in each analysis (De'ath, 2002; Carassou et al., 2012).

After identifying the best fit trees, Dufrêne-Legendre (DL) indicator values were calculated to describe the families that were characteristic of each MRT-defined assemblage group. For each family and assemblage group within a tree, the DL index is the product of "specificity" and "fidelity," where specificity is the mean family abundance in the assemblage group relative to the mean family abundance across all assemblage groups, and fidelity is the frequency of occurrence of the family within the assemblage group (Dufrêne and Legendre, 1997). The DL index is at a maximum (DL = 1) when a family occurs in all samples in an assemblage group and is absent from all other assemblage groups, and at a minimum (DL = 0) when a family does not occur in an assemblage group. Following De Cáceres et al. (2010), DL indices were assessed for all combinations of assemblage groups, and the combination that yielded the maximum indicator value was retained. This method accounts for varying niche breadths among families and allows for families to be representative of multiple assemblage groups, which may be particularly relevant for mesopelagic environments with ubiquitous fish taxa. The statistical significance for each DL index value and association with assemblage groups was assessed with permutation tests (n = 1,000 permutations) (De Cáceres and Legendre, 2009). All analyses were conducted using R v.3.6.2 (R Core Team, 2019), with MRT and DL analyses implemented with the "mvpart" and "indicspecies" packages, respectively.

RESULTS

Ichthyoplankton

Over the six deep-pelagic survey campaigns included in this study, 160 tows were sampled, encompassing 1,084 depth-discrete nets (**Table 1**). A total of 134,610 fish larvae were collected and identified to at least the family level, belonging to 149 families (**Supplementary Table 1**). Only 66% of these larvae were identified to genus (251 genera) and 16% to species (256 species), thus all subsequent results are from family-level analyses. Of the mesopelagic fish taxa, the four most common families were Myctophidae, Gonostomatidae, Sternoptychidae, and Phosichthyidae, hereafter referred to as the dominant mesopelagic families. These dominant mesopelagic families were common in both the epipelagic (0–200 m), comprising 63.4% of the catch, as well as the meso- and bathypelagic (200–1,500 m), where they comprised 97.4% of all larvae. After removing rare taxa, 93 families were retained for abundance, diversity, richness, and assemblage analyses (**Supplementary Table 1**).

Larval fish abundance varied significantly among depth bins [$F_{(7,1075)}$ = 827.3, $P < 0.0001$], as did family richness [$F_{(7,1076)}$ = 466.3, $P < 0.0001$], and family diversity [$F_{(7,1076)}$ = 288.3, $P < 0.0001$]. The abundance of larval fish followed a generally decreasing trend with increasing depth, and *post hoc* comparisons using Tukey's HSD test showed that mean abundance differed significantly among all depth bin pairs ($P < 0.0001$) except for two bins within the mesopelagic (200–400 m vs. 600–800 m; $P = 0.947$; **Figure 2**). Family richness was higher overall in epipelagic depth bins than in meso- and bathypelagic depth bins ($P < 0.0001$), and a larger number of families were detected in the lower epipelagic (25–200 m) than in the upper epipelagic (0–25 m; **Figure 2**). Shannon diversity at the family level was highest in the epipelagic and was significantly different among epipelagic, mesopelagic, and bathypelagic depth zones ($P < 0.0001$), although differences in family diversity among depth bins within pelagic zones was less common (**Figure 2**).

Ichthyoplankton Assemblage Structure

The MRT trials conducted with all 93 larval fish families (after removal of rare taxa) and with the 30 most abundant families resulted in identical tree structures and assemblage groups for three of the four depth-defined subsets of ichthyoplankton and environmental data (all pelagic zones combined, mesopelagic, bathypelagic), with minor differences in tree structure and group assignment for the epipelagic subset. For ease of interpretation, only MRT analyses for the 30 most abundant families are presented here. Among the environmental variables included in the MRT analyses, clear trends of decreasing temperature and increasing density were detected with increasing depth, and surface features (surface temperature, surface salinity, mixed layer depth) varied between seasons (**Figure 3**). Overall, the best-fit trees for the four depth-defined MRT analyses included various combinations of depth, season, surface salinity, surface temperature, mixed layer depth, and longitude as predictors of larval fish assemblage structure. Mean salinity and temperature of each depth-discrete net, latitude, slope/offshore station locale, and diel periodicity never appeared on the selected trees, and thus did not influence the structure of larval fish assemblages.

All Pelagic Zones

When considering all pelagic zones combined (0–1,500 m), depth and season were the most important predictors of larval fish assemblage structure, explaining 51.6% of the variability [(1 – CVRE) × 100] in assemblage structure (CVRE = 0.484, relevance = 2/2, **Supplementary Figure 1**). Eight larval fish assemblage groups were identified, corresponding largely to variation among broad pelagic regions: upper epipelagic (0–25 m), lower epipelagic (25–200 m), upper mesopelagic (200–400 m), lower mesopelagic (400–1,000 m), bathypelagic (1,000–1,500 m). Assemblage groups in the upper epipelagic and lower mesopelagic were both further distinguished by season. Patterns of association between families and assemblage groups for all pelagic zones combined (**Supplementary Table 2** and **Supplementary Figure 1**) were largely in agreement with broad-scale patterns identified in epipelagic and mesopelagic MRT analyses, which are discussed in further detail below.

Epipelagic

When examining the epipelagic (0–200 m), the largest predictors of larval fish assemblage structure were depth, surface salinity, season, mixed layer depth, and longitude, resulting in 14 distinct assemblage groups (Epi-A – Epi-N) and explaining 38.3% of the of the variability in assemblage structure (CVRE = 0.617, relevance = 5/5; **Figure 4**). Assemblage groups Epi-A – Epi-J were associated with the upper epipelagic (0–25 m), and Epi-K – Epi-N were associated with the lower epipelagic (25–200 m). Following the main branch separating the upper and lower epipelagic, assemblages in both depth regions were further structured by surface salinity, season, and mixed layer depth, while upper epipelagic assemblages were additionally

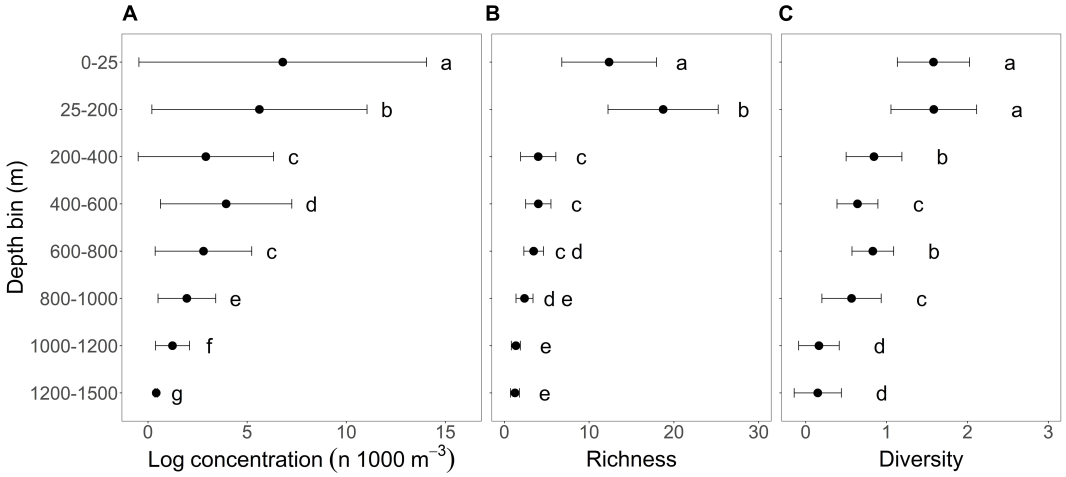

FIGURE 2 | Variation in **(A)** total ichthyoplankton abundance (log number of larvae 1,000 m^{-3}), **(B)** family-level richness (number of families), and **(C)** family-level Shannon diversity index among depth bins sampled in the northern Gulf of Mexico. Points represent mean values and horizontal bars indicate standard deviations. Within each larval measure, lower case letters indicate significant differences among depth bins resulting from *post-hoc* Tukey's HSD tests.

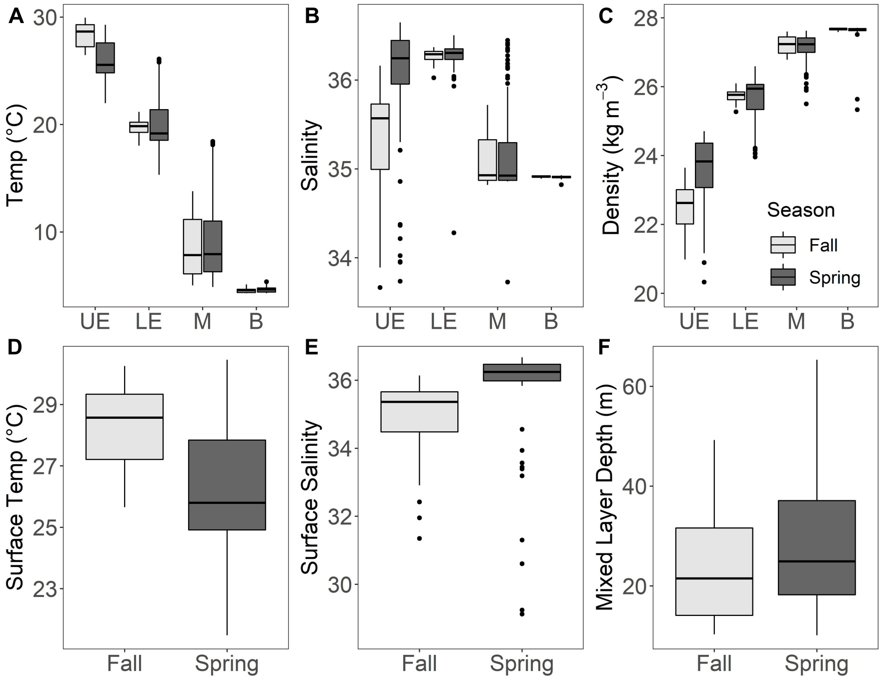

FIGURE 3 | Environmental variability in the northern Gulf of Mexico among pelagic zones and seasons for **(A)** temperature, **(B)** salinity, and **(C)** density measured with each net sample. Surface feature variability between seasons was shown for **(D)** surface temperature, **(E)** surface salinity, and **(F)** mixed layer depth associated with each tow. UE, upper epipelagic (0–25 m); LE, lower epipelagic (25–200 m); M, mesopelagic (200–1,000 m); B, bathypelagic (1,000–1,500 m). Boxplots display the median value (horizontal line), 25th and 75th percentiles (lower and upper hinges, respectively), and the extent of the whiskers from each hinge represents 1.5 × IQR (inter-quartile range; distance between 25th and 75th percentiles), with outliers beyond the whiskers shown as filled symbols. A small number of outlier values for salinity, density, and surface salinity were truncated here for ease of visualization, but retained in all analyses.

distinguished by station locale (longitude). Assemblage groups that were not defined by seasonal branches (Epi-A, Epi-B, Epi-K) were nonetheless comprised of nearly all spring samples (with the exception a single fall sample in Epi-A). The most common epipelagic assemblage groups (Epi-A, Epi-K, Epi-M, Epi-N) were broadly distributed across the spatial extent of GOM sampling (**Supplementary Figure 2**).

Mesopelagic-associated families were found to be characteristic of larval assemblage groups within both the upper and lower regions of the epipelagic. The families

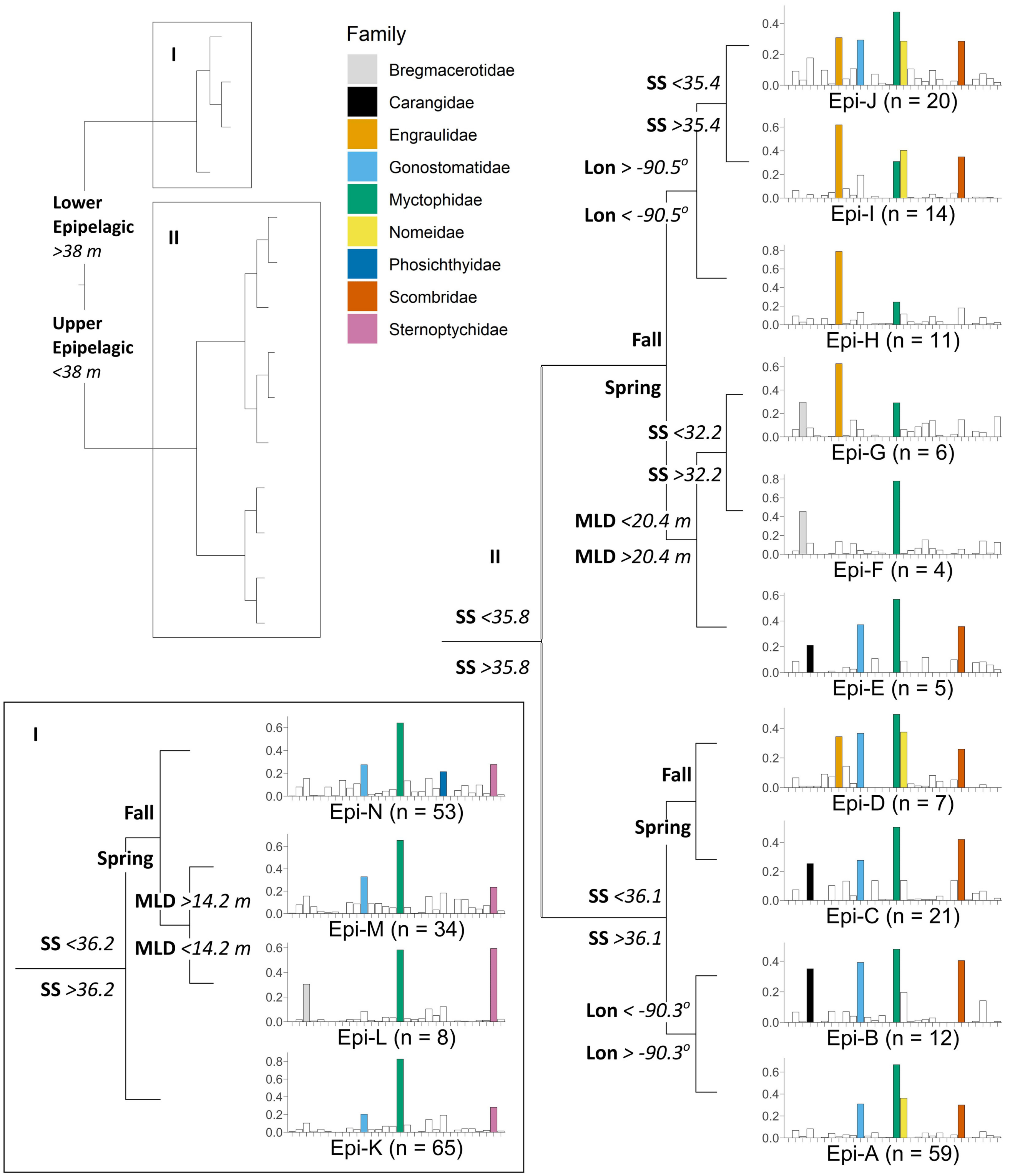

FIGURE 4 | Multivariate regression tree illustrating the effect of depth, surface salinity (SS), season (fall/spring), mixed layer depth (MLD), and longitude (Lon) on the structure of epipelagic (0–200 m) larval fish assemblages in the northern Gulf of Mexico. The full tree structure is depicted in the upper left, with (I) lower epipelagic and (II) upper epipelagic branches detailed separately. Each node represents a diverging environmental or spatiotemporal variable, resulting in terminal nodes with distinct assemblage groups (Epi-A – Epi-N). Barplots represent mean square root relative abundance (i.e., Hellinger-transformed larval abundance; *y*-axis) for each of 30 families (*x*-axis) in alphabetical order from left to right (see **Table 2** for list of family names), with the most abundant families (abundance > 0.2) in each assemblage group highlighted in color for clarity. Sample size (n) for each assemblage group is indicated next to the group name.

TABLE 2 | Dufrêne-Legendre (DL) indicator values characterizing the association of larval fish families with epipelagic assemblage groups (or combinations of assemblage groups) following De Cáceres et al. (2010).

	Epipelagic assemblage group (Epi-)														Index	
Family	**A**	**B**	**C**	**D**	**E**	**F**	**G**	**H**	**I**	**J**	**K**	**L**	**M**	**N**	**DL**	***P***
Alepisauridae											X		X		0.084	0.437
Bothidae	X	X	X	X	X	X	X	X	X	X			X	X	0.585	**0.004**
Bregmacerotidae						X	X				X	X	X	X	0.787	**0.001**
Carangidae		X	X		X	X	X			X					0.634	**0.001**
Chauliodontidae				X			X				X	X	X		0.344	**0.003**
Congridae				X				X		X				X	0.468	**0.001**
Coryphaenidae		X	X	X					X						0.464	**0.001**
Engraulidae				X		X	X	X	X	X					0.856	**0.001**
Gempylidae		X	X	X	X		X		X	X	X	X	X	X	0.583	**0.001**
Gobiidae		X		X	X	X	X	X		X		X	X	X	0.587	**0.001**
Gonostomatidae	X	X	X	X	X	X	X	X	X	X	X	X	X	X	0.947	NA
Howellidae		X				X						X	X		0.372	**0.003**
Labridae			X		X	X	X			X			X		0.423	**0.002**
Melamphaidae		X				X		X			X	X	X	X	0.501	**0.001**
Microstomatidae											X	X	X	X	0.607	**0.001**
Myctophidae	X	X	X	X	X	X	X	X	X	X	X	X	X	X	0.987	NA
Nomeidae	X	X	X	X	X		X	X	X	X				X	0.804	**0.001**
Ophichthidae				X		X	X	X		X					0.290	**0.006**
Ophidiidae						X	X								0.367	**0.001**
Paralepididae					X	X	X				X	X	X	X	0.776	**0.001**
Paralichthyidae				X		X	X	X	X	X		X		X	0.481	**0.001**
Phosichthyidae				X		X					X	X	X	X	0.737	**0.001**
Platytroctidae															**–**	**–**
Scaridae			X	X	X		X		X				X		0.445	**0.002**
Scombridae	X	X	X	X	X	X	X	X	X	X			X		0.875	**0.001**
Scopelarchidae											X		X	X	0.485	**0.001**
Scorpaenidae			X		X	X	X			X		X	X	X	0.447	**0.001**
Serranidae		X	X		X	X	X	X		X			X		0.503	**0.001**
Sternoptychidae					X						X	X	X	X	0.873	**0.001**
Synodontidae						X	X								0.513	**0.001**

*Epipelagic assemblage groups (Epi-A – Epi-N) were identified using the multivariate regression tree in **Figure 4**. The most likely combination of assemblage groups associated with each family are indicated by the symbol "X," with blank cells indicating no association. Significant DL indicator values ($P < 0.05$) are denoted in bold; P = NA when all assemblage groups are associated with a family (permutation tests cannot be conducted because there are no external groups for comparison). The symbol "–" indicates that the family was not present in any sample in the epipelagic region.*

Gonostomatidae (DL = 0.95, *P* = NA) and Myctophidae (DL = 0.99, *P* = NA) were ubiquitous and were strongly characteristic of all 14 epipelagic assemblage groups (Epi-A – Epi-N; **Table 2** and **Figure 4**). Assessment of significance was not possible for these two families because permutation tests cannot be conducted when all assemblage groups are included (i.e., no external groups for comparison). The families Sternoptychidae (DL = 0.87, *P* = 0.001), Paralepididae (DL = 0.78, *P* = 0.001), Phosichthyidae (DL = 0.74, *P* = 0.001), Bregmacerotidae (DL = 0.79, *P* = 0.001), and Microstomatidae (DL = 0.61, *P* = 0.001) were strongly associated with all lower epipelagic assemblage groups (Epi-K – Epi-N; **Table 2** and **Figure 4**). However, only Microstomatidae were exclusive in their association with lower epipelagic assemblage groups. The families Sternoptychidae, Paralepididae, Phosichthyidae, and Bregmacerotidae were also occasionally characteristic of upper epipelagic (0–25 m) assemblage groups, although these assemblage groups represented small sample sizes and were relatively small contributors (3.0–8.6%) to the overall DL indicator group assignment for each family.

Epipelagic-associated taxa were mostly frequently found to be characteristic of larval assemblage groups within the upper region of the epipelagic. The families Scombridae (DL = 0.88, *P* = 0.001) and Nomeidae (DL = 0.80, *P* = 0.001) were strong indicators of all upper epipelagic assemblage groups (Epi-A – Epi-J), with the exception of the minor assemblage group Epi-F ($n = 4$) for Nomeidae (**Table 2** and **Figure 4**). Scombridae were also associated with the lower epipelagic assemblage group Epi-M, which was characterized by lower surface salinity during the spring season when the depth of the mixed layer is large. Nomeidae were also associated with a large lower epipelagic assemblage group (Epi-N), which was characterized by lower surface salinity during the fall. The family Engraulidae (DL = 0.86, *P* = 0.001) was largely characteristic of upper epipelagic assemblage groups where the surface salinity was < 36.1, nearly all of which were fall samples (Epi-D, Epi-F – Epi-J; **Table 2** and **Figure 4**). The family Carangidae (DL = 0.63, *P* = 0.001) was associated with six upper epipelagic assemblage groups (Epi-B, Epi-C, Epi-E – Epi-G, Epi-J), although these assemblage groups were spread among the upper epipelagic branches of the tree and environmental patterns were less clear (**Table 2** and **Figure 4**).

While most upper epipelagic larval assemblage groups were defined by variability in season or surface features, minor spatial structure was also identified. Two upper epipelagic assemblage groups (Epi-B and Epi-H) were defined by longitude and associated with western sampling stations (delineated at and inclusive of stations B247 and SW7; **Figure 1**). Epi-B was distinguished from its closest neighboring assemblage group (Epi-A), which was comprised of samples collected at eastern stations, by its association with seven additional DL indicator families, including Carangidae, Gempylidae, Gobiidae, Melamphaidae, and Serranidae (**Table 2** and **Figure 4**). Epi-H was associated with seven fewer DL indicator families than its nearest pair of neighboring assemblage groups combined (Epi-I and Epi-J), although only the families Gempylidae (Epi-I and Epi-J) and Melamphaidae (Epi-H) were uniquely characteristic of each branch (**Table 2** and **Figure 4**). Nearly all of the families included in the epipelagic MRT analyses had high DL values (DL = 0.29–0.99) and significant associations with assemblage groups or combinations of assemblage groups, with the exception of the family Alepisauridae (DL = 0.08, *P* = 0.437) and Platytroctidae, which was not present in epipelagic samples.

Mesopelagic

Mesopelagic (200–1,000 m) larval fish assemblage structure was largely explained by depth, season, surface temperature, and mixed layer depth (although mixed layer depth did not appear on any tree nodes), resulting in seven distinct assemblage groups (Meso-A – Meso-G) and explaining 46.7% of the variability in larval fish assemblage structure (CVRE = 0.533, relevance = 3/4, **Figure 5**). Assemblage groups Meso-A – Meso-D were associated with the lower mesopelagic (400–1,000 m), and were further separated by season and depth. Assemblage groups Meso-E – Meso-G were associated with the upper mesopelagic (200–400 m), and assemblages within this region were distinguished additionally by season and surface temperature (**Figure 5**). Seasonal separation of mesopelagic assemblage groups was complete, with no overlap between spring and fall samples within assemblage groups. Broadly, more taxa were associated with upper mesopelagic assemblages (16–19 families) than lower mesopelagic assemblages (6–9 families), although most associations with families outside of the dominant mesopelagic taxa were weak (**Table 3**). All mesopelagic assemblage groups were widely distributed across sampling locales (**Supplementary Figure 3**).

Presence of the family Gonostomatidae was strongly characteristic of all mesopelagic assemblage groups (DL = 0.94, *P* = NA; **Table 3** and **Figure 5**). The family Myctophidae was associated with the combination of three lower mesopelagic (Meso-B – Meso-D) and two upper mesopelagic (Meso-F and Meso-G) assemblage groups (DL = 0.79, *P* = 0.001; **Table 3** and **Figure 5**), and was not associated with fall assemblage groups at 200–400 or 800–1,000 m depths. The families Sternoptychidae (DL = 0.81, *P* = 0.001) and Phosichthyidae (DL = 0.49, *P* = 0.001) were indicative of all upper mesopelagic assemblage groups (Meso-E – Meso-G), the spring assemblage group representing the 400–600 m depth strata (Meso-D), and the fall assemblage group representing 400–800 m depths (Meso-B, Sternoptychidae only; **Table 3** and **Figure 5**). Sternoptychidae and Phosichthyidae were not characteristic of the 800–1,000 m portion of the mesopelagic (**Table 3** and **Figure 5**). The family Microstomatidae, while lower in relative abundance than the aforementioned dominant mesopelagic families, was associated with the upper mesopelagic assemblage groups (Meso-E – Meso-G; DL = 0.33, *P* = 0.001; **Table 3** and **Figure 5**). All other families had relatively low DL indicator values (DL < 0.2) and lacked strong association with assemblage groups.

Bathypelagic

Bathypelagic (1,000–1,500 m) larval fish assemblage structure was explained by density, surface salinity, and mixed layer depth, resulting in four assemblage groups (Bathy-A – Bathy-D). However, only 8.6% of the variability in assemblage structure was explained by these environmental predictors (CVRE = 0.914, relevance = 3/3), and the majority of samples (87%) fell into a single assemblage group (Bathy-A). Because these environmental variables were such poor predictors of bathypelagic assemblage structure, the bathypelagic MRT and indicator values will not be described further here (**Supplementary Table 3** and **Supplementary Figure 4**).

DISCUSSION

Mesopelagic-associated taxa comprised the majority of ichthyoplankton in both the epipelagic and mesopelagic regions of the northern Gulf of Mexico. Four dominant mesopelagic families (Myctophidae, Gonostomatidae, Sternoptychidae, Phosichthyidae) were particularly common, with few other families making significant contributions to larval assemblage groups within mesopelagic waters. Mesopelagic-associated families outside of the four dominant taxa (e.g., Chauliodontidae, Melamphaidae, Paralepididae) were largely constrained to larval assemblage groups within epipelagic waters, and while these families were occasionally found in the mesopelagic, catches were minimal in comparison to the epipelagic and associations with mesopelagic assemblage groups were weak. Overall, larval abundance declined steeply with increasing depth and even the dominant mesopelagic families were most abundant in epipelagic regions. In both epipelagic and mesopelagic regions, the distinct larval assemblage groups identified were predominantly structured by depth and season, with surface conditions (temperature, salinity, mixed layer depth) and geographic locale (longitude) providing some finer-scale distinctions among assemblages. The most common (largest) epipelagic assemblage groups consisted of samples distributed widely across the GOM, as did all mesopelagic assemblage groups (southeastern gap in

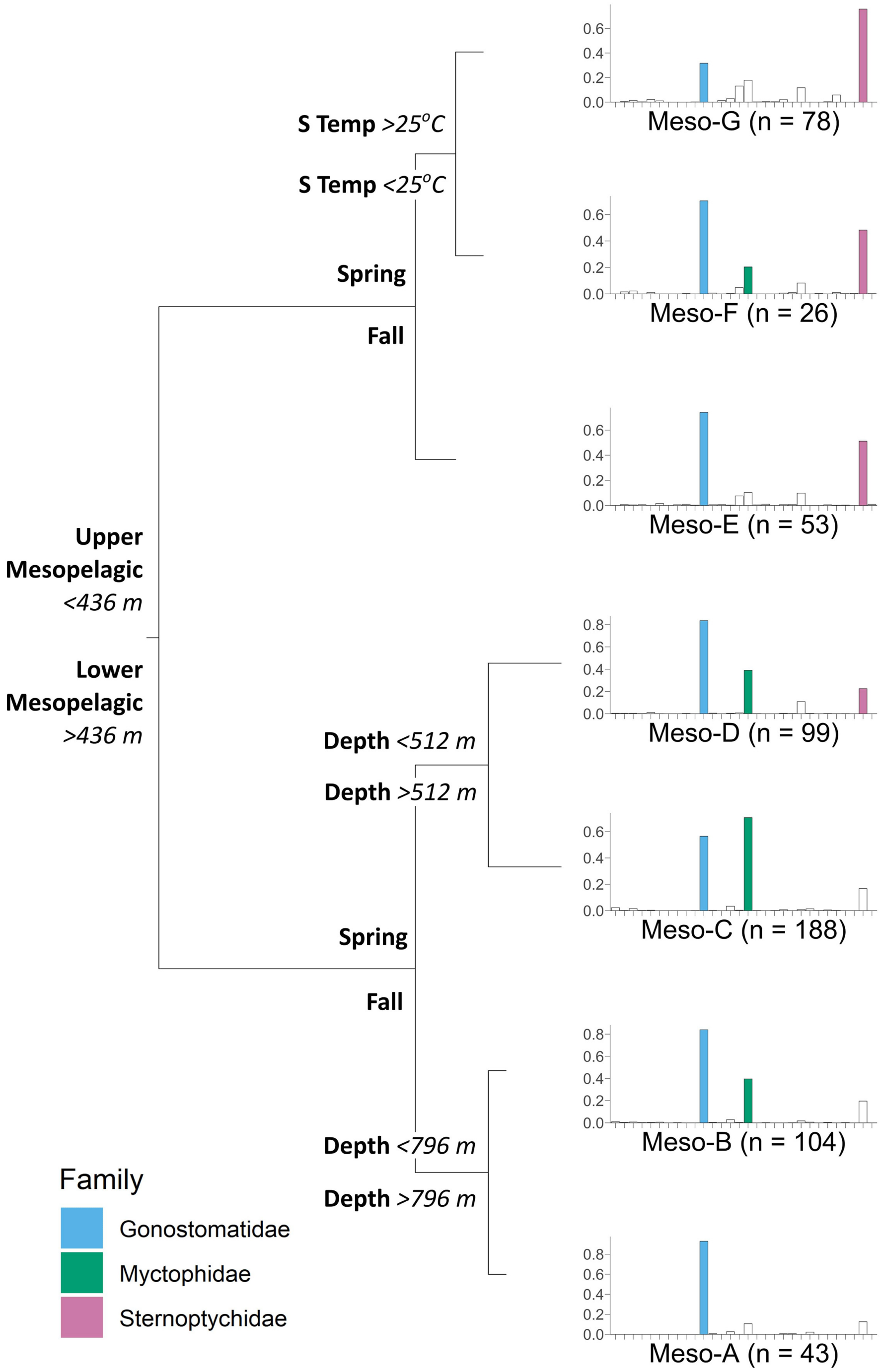

FIGURE 5 | Multivariate regression tree illustrating the effect of depth, season (fall/spring), and surface temperature (S Temp) on the structure of mesopelagic (200–1,000 m) larval fish assemblages in the northern Gulf of Mexico. Each node represents a diverging environmental or spatiotemporal variable, resulting in terminal nodes with distinct assemblage groups (Meso-A – Meso-G). Barplots represent mean square root relative abundance (i.e., Hellinger-transformed larval abundance; *y*-axis) for each of 30 families (*x*-axis) in alphabetical order from left to right (see **Table 2** for list of family names), with the most abundant families (abundance > 0.2) in each assemblage group highlighted in color for clarity. Sample size (n) for each assemblage group is indicated next to the group name.

sampling coverage during the fall notwithstanding). Meaningful assemblage structure was not detected in the bathypelagic region, which is not surprising given the environmental stability of the pelagic realm beyond 1,000 m depth.

The ubiquity of the dominant mesopelagic ichthyoplankton families detected aligns with prior surveys of adult mesopelagic fishes in the GOM, where Gonostomatidae, Myctophidae, Phosichthyidae, and Sternoptychidae accounted for 96% of all

TABLE 3 | Dufrêne-Legendre (DL) indicator values characterizing the association of larval fish families with mesopelagic assemblage groups (or combinations of assemblage groups) following De Cáceres et al. (2010).

	Mesopelagic assemblage group (Meso-)							**Index**	
Family	**A**	**B**	**C**	**D**	**E**	**F**	**G**	**DL**	***P***
Alepisauridae		X	X					0.079	**0.006**
Bothidae		X		X	X	X	X	0.029	0.375
Bregmacerotidae		X	X			X	X	0.056	0.274
Carangidae					X			0.017	0.870
Chauliodontidae				X		X	X	0.087	**0.010**
Congridae					X		X	0.042	**0.046**
Coryphaenidae								–	–
Engraulidae					X			0.016	0.307
Gempylidae				X	X	X		0.022	0.196
Gobiidae					X		X	0.013	0.506
Gonostomatidae	X	X	X	X	X	X	X	0.944	NA
Howellidae	X			X	X	X		0.029	0.367
Labridae					X		X	0.029	0.078
Melamphaidae	X	X	X				X	0.123	**0.005**
Microstomatidae					X	X	X	0.326	**0.001**
Myctophidae		X	X	X		X	X	0.791	**0.001**
Nomeidae					X		X	0.011	0.859
Ophichthidae					X			0.035	**0.042**
Ophidiidae							X	0.010	0.732
Paralepididae	X		X	X	X	X	X	0.035	0.486
Paralichthyidae	X				X	X		0.037	0.064
Phosichthyidae				X	X	X	X	0.485	**0.001**
Platytroctidae	X		X					0.048	0.087
Scaridae						X		0.032	0.072
Scombridae		X	X		X		X	0.019	0.905
Scopelarchidae							X	0.163	**0.001**
Scorpaenidae					X	X		0.016	0.437
Serranidae						X		0.038	**0.039**
Sternoptychidae		X		X	X	X	X	0.813	**0.001**
Synodontidae					X	X		0.038	**0.022**

Mesopelagic assemblage groups (Meso-A – Meso-G) were identified using the multivariate regression tree in ***Figure 5****. The most likely combination of assemblage groups associated with each family are indicated by the symbol "X," with blank cells indicating no association. Significant DL indicator values ($P < 0.05$) are denoted in bold; P = NA when all assemblage groups are associated with a family (permutation tests cannot be conducted because there are no external groups for comparison). The symbol "–" indicates that the family was not present in any sample in the mesopelagic region.*

specimens collected (Ross et al., 2010). Ichthyoplankton surveys encompassing outer shelf and oceanic regions of the GOM also found high abundances of these dominant mesopelagic families when sampling epipelagic waters (Muhling et al., 2012; Meinert et al., 2020). Among the few ichthyoplankton surveys sampling to depths (800–1,000 m) comparable to this study, similar broad patterns of distribution were detected in the equatorial and tropical Atlantic when accounting for both epipelagic and mesopelagic waters, with prevalence of the same four dominant families and decreasing abundance and richness with increasing depth (Olivar et al., 2018; Dove et al., 2021).

We found that larval fish assemblages in the oceanic GOM were largely structured by depth and season, which is consistent with patterns from other regions and often reflect the spawning habitat preferences of adults (Doyle et al., 1993; Duffy-Anderson et al., 2006; Muhling et al., 2012). Adult mesopelagic fish assemblages in the GOM were found to lack spatial structure despite the presence of distinct physical oceanographic features among widely separated sampling sites (Ross et al., 2010; Milligan and Sutton, 2020), so it is not unexpected that the epipelagic and mesopelagic larval assemblage groups identified here were broadly distributed across the GOM with little horizontal differentiation. Adult distributions have been found to be important in structuring patterns of larval distribution in mesopelagic fishes in other regions (tropical and equatorial Atlantic, Olivar et al., 2017, 2018; southern Gulf of Mexico, Daudén-Bengoa et al., 2020). While the extent of larval distribution often mirrors patterns of adult distribution, larval assemblages are subsequently subject to strong influence by oceanographic conditions (Grothues and Cowen, 1999). Surface salinity was identified by MRT as the primary environmental variable responsible for differentiating larval fish assemblages within upper and lower epipelagic regions. In the GOM, freshwater and high nutrient discharge from the Mississippi River interact with the Loop Current system to influence salinity variability in the GOM (Dagg and Breed, 2003; Brokaw et al., 2019), resulting in salinity-driven variability in ichthyoplankton diversity and taxonomic richness in the GOM, both of which were highest during low salinity conditions (Meinert et al., 2020). We did not examine Loop Current and Mississippi River influences directly, but variability in salinity was high in the GOM both within and between seasons in surface and upper epipelagic waters, and strongly influenced epipelagic larval fish assemblage structure.

While surface features (surface salinity and temperature) were found to define ichthyoplankton assemblages, mean salinity and temperature for depth-discrete nets were not identified by MRT as structuring environmental variables. The MRT technique is robust to collinearity (De'ath, 2002), and the best fit trees typically remove variables that are redundant. Temperature and depth are not independent, with temperature decreasing as depth increases. Similarly, salinity varies with season in upper epipelagic waters. Both temperature and salinity have limited variability within depth bins in mesopelagic waters. Depth and season are strong drivers of ichthyoplankton assemblage structure in the selected trees, so temperature and salinity may not contribute to additional definition of assemblage groups. Indeed, substituting temperature as a proxy for depth (or including temperature in addition to depth) in our final analyses did not result in appreciably different tree structures. The importance of surface feature variability in defining assemblage structure in both epipelagic and mesopelagic regions here is not surprising, considering that primary productivity is tightly linked to mesopelagic fish biomass in the open ocean (Irigoien et al., 2014). Primary productivity at the surface can impact the mesopelagic food web via vertical migration of fishes and zooplankton prey, as well as sinking particles (Kelly et al., 2019). Larval mesopelagic fishes are weak vertical migrators relative to adults (Sassa et al., 2002), so larvae distributed in mesopelagic waters are likely to benefit from the downward export of surface productivity rather than active migration to feed at the surface. The larvae of common mesopelagic fish species have been found to display different diel patterns of vertical distribution, but migration in the water column was constrained within ∼20–200 m (Sabatés, 2004). Diel periodicity was not identified by MRT as a structuring factor for GOM larval fish assemblages, likely due to our broad epipelagic depth bins precluding detection of any fine scale differences in diel distribution patterns.

Outside of the GOM, the structure of mesopelagic larval fish assemblages has been influenced by currents (Sassa et al., 2004; Olivar et al., 2010), availability of planktonic prey (Olivar et al., 2010; Koslow et al., 2014), oxygen minimum zones (Koslow et al., 2011; Dove et al., 2021), as well as bathymetry (Olivar et al., 2010). Distinct larval fish assemblages have been identified between oceanic and continental shelf waters in the GOM (Richards et al., 1993), and bottom topography can influence the abundance and distributions of mesopelagic fauna by modifying local hydrography (Fock et al., 2004; Sutton et al., 2008; De Forest and Drazen, 2009). Significantly higher abundance and diversity were identified in the offshore GOM when compared to the slope environment in other mesopelagic taxa (Frank et al., 2020). Here, MRT analyses did not distinguish between larval fish assemblages in slope and offshore sampling locales in the GOM. Ichthyoplankton in the GOM were largely concentrated in epipelagic waters, so it is possible that beyond the continental shelf, bathymetric features have minimal influence on the surface conditions that appear to drive assemblage structure for the early life history stages of fishes.

Epipelagic-associated larval fishes were not the primary focus of this study, but the broad distribution patterns found here were generally in agreement with previous studies of common epipelagic larval fishes in the GOM. In particular, we found that larval Engraulidae in oceanic GOM waters are largely associated with fall assemblage groups (September–October). Analyses of long time series of GOM ichthyoplankton on the continental shelf found that Engraulidae were strongly associated with late summer and fall sampling periods (August–October), suggesting that spawning peaks during summer in shallow inshore waters (Muhling et al., 2012; Lyczkowski-Shultz et al., 2013) before dispersing to slope and offshore GOM environments. This timing is further supported by the lack of detection of larval Engraulidae in offshore GOM ichthyoplankton samples during early summer (June–July) (Meinert et al., 2020), although we did occasionally detect low concentrations of larval Engraulidae in spring samples. Engraulidae have previously been associated with western GOM locales (Muhling et al., 2012; Lyczkowski-Shultz et al., 2013). While a weak western pattern can be seen in the epipelagic assemblage groups strongly associated with Engraulidae in this study, these assemblage groups were not defined by longitude in the MRT analysis. Additionally, a lack of sampling effort during fall in the eastern portion of the GOM sampling range precludes us from drawing any conclusions about spatial distributions of larval Engraulidae here.

While our analyses generally indicate broad GOM distribution for most larval assemblages, MRT analysis identified two small assemblage groups (Epi-B and Epi-H) in upper epipelagic waters that were defined by their geographic location (encompassing the westernmost sampling stations, delineated at approximately 90°W). In a study encompassing both shelf and slope ichthyoplankton samples in the GOM, a faunal discontinuity was identified at 87°W with breaks in species distribution and distinct eastern and western patterns of abundance between common species (Lyczkowski-Shultz et al., 2013). This longitudinal differentiation in distribution patterns was attributed to distinct bottom topography (i.e., DeSoto Canyon) driving local circulation, as well as differences in riverine influence (i.e., Mississippi River outflow) (Lyczkowski-Shultz et al., 2013). Single-species evaluations of the larvae of commercially important fisheries species in the GOM have found higher larval abundance in the western GOM (delineated at 89.25°W) when assessing regional patterns of distribution (Hanisko et al., 2017a,b). Eastern and western differentiation in larval fish distribution and abundance in the GOM is well documented, so our finding of a pair of small western assemblage groups certainly warrant further evaluation beyond our family-level analyses.

Assemblage analyses in this study were conducted at the family level, which is not uncommon for studies of ichthyoplankton communities (e.g., in the GOM alone: Richards et al., 1993; Carassou et al., 2012; Muhling et al., 2012; Meinert et al., 2020). It is possible that with improved taxonomic resolution, additional structure could have been detected among GOM larval fish communities. The most common assemblage groups in both epipelagic and mesopelagic regions were largely structured by depth and season, suggesting that ichthyoplankton within families may respond similarly to broad-scale habitat changes. However, many families were associated with multiple assemblage groups, both large and small and across seasons and depth regions, so it is certainly feasible that the finer scale assemblage structure we detected may be attributable to varying environmental tolerances among species within families. It is important to note that MRT assemblage groupings result from evaluations of multivariate abundance and are not defined by the presence or absence of prominent indicator families, but by variation in the relative proportions of abundance of all families in the assemblage. Families that occur across assemblages with disparate environmental characters may differ in proportion of abundance or in coincidence with other families, in addition to potentially reflecting species-specific differences in environmental response that are masked by poor taxonomic resolution. The oceanic GOM is known to support one of the most speciose ichthyofaunas in the world (Sutton et al., 2017), and the ubiquitous family Myctophidae is known to be particularly diverse, with the early life stages of approximately 50 species from 18 genera identified in the GOM (Richards, 2005). Outside of the GOM, both adult and larval myctophids have demonstrated species-specific or subfamily-specific patterns of vertical distribution (Watanabe et al., 1999; Sassa et al., 2002; Collins et al., 2008; Olivar et al., 2018). Within the GOM, it is possible that improved taxonomic resolution could reveal that larval myctophid species are occupying different portions of the water column and contributing to vertical assemblage differentiation. Horizontally, assemblages of adult myctophid species in the GOM were found to be well-mixed, with limited spatial differentiation despite variation in major hydrographic features (Milligan and Sutton, 2020). Adult myctophids are presumed to be less susceptible to local oceanographic conditions due to their large capacity for vertical migration, which may allow for passive advection at depth with varying currents, promoting more horizontal assemblage homogenization than would be expected with environment-driven structuring (Heino et al., 2015; Milligan and Sutton, 2020). Larval myctophids display limited vertical migration behavior compared to adults (Sassa et al., 2002) and ichthyoplankton are highly sensitive to the local environment (Kingsford, 1993; Brodeur et al., 2008; Hsieh et al., 2009), so it's possible that larval myctophid distribution patterns are quite distinct from those of their more mobile adult counterparts. It remains unknown whether increased taxonomic resolution (i.e., species-specific assemblage analyses of Myctophidae and other speciose families such as Carangidae and Scombridae) would have resulted in the detection of additional partitioning of GOM larval assemblages or aided in the ecological interpretation of defined assemblages. Regardless, when the aim is to describe overall ichthyoplankton structure or assess changes in ichthyoplankton assemblages resulting from environmental perturbations, family-level analyses have been found to be sufficient (Hernandez et al., 2013).

One goal of this study was to fill a gap in knowledge about larval fish distributions beyond the epipelagic waters of the GOM. A lack of baseline data about the early life stages of mesopelagic fishes in the GOM was apparent following the DWHOS, limiting the efficacy of subsequent damage assessment efforts. Effects of the DWHOS on epipelagic-associated larval fish populations in the GOM have been equivocal, but studies to date largely reflect resilient populations. On the continental shelf, red snapper showed declines in larval condition in the years following DWHOS (Hernandez et al., 2016), while detrimental effects on Spanish mackerel larval condition were not detected (Ransom et al., 2016); declines in abundance were not detected in either species in relation to the timing of DWHOS. In oceanic waters, declines were detected in the larval abundance of common pelagic fish species (blackfin tuna, blue marlin, dolphinfish, sailfish) in the months following DWHOS, although the declines were within the scope of interannual variability resulting from shifts in oceanographic conditions that may be unrelated to DWHOS (Rooker et al., 2013). Mesozooplankton communities were found to recover rapidly after initial DWHOS impacts (Carassou et al., 2014), perhaps contributing to food web continuity and minimizing DWHOS declines for the largely zooplanktivorous ichthyoplankton communities in the GOM.

Larval fish in the epipelagic GOM are surveyed annually (spring and fall) as part of a long-term monitoring program (Southeast Area Monitoring and Assessment Program [SEAMAP], Lyczkowski-Shultz et al., 2013), but no such survey exists for the water column beyond 200 m. This study provides the first large-scale characterization of larval fish assemblages in the GOM that encompasses epipelagic, mesopelagic, and bathypelagic portions of the water column, providing a vital description of mesopelagic-associated larval fish distributions within the full scope of their vertical habitat distribution. While the brief sampling timeframe of this study provides only a snapshot of two seasons of larval fish distributions in the GOM, our findings will provide a useful reference point for GOM ichthyoplankton communities nonetheless. We found that the vast majority of ichthyoplankton (including both epipelagic- and mesopelagic-associated families) were located in the epipelagic portion of the water column. Mesopelagic waters were dominated by larvae from four dominant mesopelagic families, which made up distinct assemblage groups that were widespread and largely structured by depth and season, not by spatial distribution. The bathypelagic GOM consisted of very few larval fish overall with limited diversity. Together, these results suggest that long-term epipelagic-focused surveys such as SEAMAP may be sufficient for characterizing the distributions of most mesopelagic-associated larval fishes and evaluating the responses of these communities to environmental perturbations. To capture variation in abundances of dominant mesopelagic-associated larval fish families associated with mesopelagic waters, the spatial scope of mesopelagic sampling for future assessments can likely be reduced considering the horizontal ubiquity of most larval assemblage groups. Tremendous resources and effort are required to assess damages to the marine environment, particularly when accounting for the logistical challenges of sampling the deep pelagic, so concentrating future evaluation efforts on epipelagic waters and reduced mesopelagic spatial extent can aid in speeding assessment, restoration, and mitigation.

DATA AVAILABILITY STATEMENT

The data are publicly available through the Gulf of Mexico Research Initiative Information and Data Cooperative (GRIIDC) at https://data.gulfresearchinitiative.org (doi: 10.7266/n7-z8ry-6j20, doi: 10.7266/n7-30jwaq82, doi: 10.7266/n7-n2t3-aa19, doi: 10.7266/n7-s18hwr95, doi: 10.7266/n7-9vcj-nf90, doi: 10.7266/n7-dp76-tz89, doi: 10.7266/n7-j6rb-dt32, doi: 10.7266/n7-7fxg-2980, doi: 10.7266/n7-qecb-7x31, doi: 10.7266/n7-rjqw-tf97, doi: 10.7266/n7-60cgk731, and doi: 10.7266/n7-1v14-fc70).

AUTHOR CONTRIBUTIONS

FH, VW, and CZ contributed to the conception and design of the study. VW and CZ organized the database. VW conducted the data analyses, prepared the figures, and wrote the first manuscript draft. All authors reviewed and edited the final draft.

FUNDING

This research was made possible by a grant from the Gulf of Mexico Research Initiative (Award No. G-231805).

ACKNOWLEDGMENTS

We are grateful to all who contributed to the Deepwater Horizon Natural Resource Damage Assessment (DWHOS NRDA) efforts, particularly Malinda Sutor (LSU), Scott Friedman (IEC), Daniel

Hahn (NOAA), Glenn Zapfe (NOAA), Joanne Lyczkowski-Schultz (NOAA), and Lauren Jackson (NOAA). Access to DWHOS NRDA data was generously provided by the Deepwater Horizon Plankton Assessment Archive and the National Centers for Environmental Information.

SUPPLEMENTARY MATERIAL

The Supplementary Material for this article can be found online at: https://www.frontiersin.org/articles/10.3389/fmars.2021.766369/full#supplementary-material

REFERENCES

Ahlstrom, E. H. (1959). Vertical distribution of pelagic fish eggs and larvae off California and Baja California. *Fish. Bull.* 60, 107–146.

Brodeur, R. D., Peterson, W. T., Auth, T. D., Soulen, H. L., Parnel, M. M., and Emerson, A. A. (2008). Abundance and diversity of coastal fish larvae as indicators of recent changes in ocean and climate conditions in the Oregon upwelling zone. *Mar. Ecol. Prog. Ser.* 366, 187–202.

Brokaw, R. J., Subrahmanyam, B., and Morey, S. L. (2019). Loop current and eddy-driven salinity variability in the gulf of Mexico. *Geophys. Res. Lett.* 46, 5978–5986. doi: 10.1029/2019GL082931

Burdett, E. A., Fine, C. D., Sutton, T. T., Cook, A. B., and Frank, T. M. (2017). Geographic and depth distributions, ontogeny, and reproductive seasonality of decapod shrimps (Caridea: Oplophoridae) from the northeastern Gulf of Mexico. *Bull. Mar. Sci.* 93, 743–767. doi: 10.5343/bms.2016.1083

Carassou, L., Hernandez, F. J., and Graham, W. M. (2014). Change and recovery of coastal mesozooplankton community structure during the Deepwater Horizon oil spill. *Environ. Res. Lett.* 9:124003.

Carassou, L., Hernandez, F. J., Powers, S. P., and Graham, W. M. (2012). Cross-shore, seasonal, and depth-related structure of ichthyoplankton assemblages in coastal alabama. *Transa. Am. Fish. Soc.* 141, 1137–1150. doi: 10.1080/00028487.2012.675920

Choy, C. A., Portner, E., Iwane, M., and Drazen, J. C. (2013). Diets of five important predatory mesopelagic fishes of the central North Pacific. *Mar. Ecol. Prog. Ser.* 492, 169–184.

Collins, M. A., Xavier, J. C., Johnston, N. M., North, A. W., Enderlein, P., Tarling, G. A., et al. (2008). Patterns in the distribution of myctophid fish in the northern Scotia Sea ecosystem. *Polar Biol.* 31, 837–851. doi: 10.1007/s00300-008-0423-2

Cook, A. B., Bernard, A. M., Boswell, K. M., Bracken-Grissom, H., D'Elia, M., deRada, S., et al. (2020). A Multidisciplinary approach to investigate deep-pelagic ecosystem dynamics in the Gulf of Mexico following Deepwater Horizon. *Front. Mar. Sci.* 7:548880. doi: 10.3389/fmars.2020.548880

Dagg, M. J., and Breed, G. A. (2003). Biological effects of Mississippi River nitrogen on the northern gulf of Mexico—a review and synthesis. *J. Mar. Syst.* 43, 133–152. doi: 10.1016/j.jmarsys.2003.09.002

Daudén-Bengoa, G., Jiménez-Rosenberg, S. P. A., Compaire, J. C., del Pilar Echeverri-García, L., Pérez-Brunius, P., and Herzka, S. Z. (2020). Larval fish assemblages of myctophids in the deep water region of the southern Gulf of Mexico linked to oceanographic conditions. *Deep Sea Res. Part I Oceanogr. Res. Pap.* 155:103181. doi: 10.1016/j.dsr.2019.103181

Davison, P. C., Checkley, D. M., Koslow, J. A., and Barlow, J. (2013). Carbon export mediated by mesopelagic fishes in the northeast Pacific Ocean. *Prog. Oceanogr.* 116, 14–30. doi: 10.1016/j.pocean.2013.05.013

De Cáceres, M., and Legendre, P. (2009). Associations between species and groups of sites: indices and statistical inference. *Ecology* 90, 3566–3574. doi: 10.1890/08-1823.1

De Cáceres, M., Legendre, P., and Moretti, M. (2010). Improving indicator species analysis by combining groups of sites. *Oikos* 119, 1674–1684. doi: 10.1111/j.1600-0706.2010.18334.x

De Forest, L., and Drazen, J. (2009). The influence of a Hawaiian seamount on mesopelagic micronekton. *Deep Sea Res. Part I Oceanogr. Res. Pap.* 56, 232–250. doi: 10.1016/j.dsr.2008.09.007

De'ath, G. (2002). Multivariate regression trees: a new technique for modeling species–environment relationships. *Ecology* 83, 1105–1117.

Dove, S., Tiedemann, M., and Fock, H. O. (2021). Latitudinal transition of mesopelagic larval fish assemblages in the eastern central Atlantic. *Deep Sea Res. Part I Oceanogr. Res. Pap.* 168:103446. doi: 10.1016/j.dsr.2020.103446

Doyle, M. J., Morse, W. W., and Kendall, J. A. W. (1993). A comparison of larval fish assemblages in the temperate zone of the northeast pacific and northwest atlantic oceans. *Bull. Mar. Sci.* 53, 588–644.

Drazen, J. C., and Sutton, T. T. (2017). Dining in the deep: the feeding ecology of deep-sea fishes. *Annu. Rev. Mar. Sci.* 9, 337–366. doi: 10.1146/annurev-marine-010816-060543

Duffy-Anderson, J. T., Busby, M. S., Mier, K. L., Deliyanides, C. M., and Stabeno, P. J. (2006). Spatial and temporal patterns in summer ichthyoplankton assemblages on the eastern Bering Sea shelf 1996–2000. *Fish. Oceanogr.* 15, 80–94. doi: 10.1111/j.1365-2419.2005.00348.x

Dufrêne, M., and Legendre, P. (1997). Species assemblages and indicator species: the need for a flexible asymmetrical approach. *Ecol. Monogr.* 67, 345–366.

Fisher, C. R., Montagna, P. A., and Sutton, T. T. (2016). How did the Deepwater Horizon oil spill impact deep-sea ecosystems? *Oceanography* 29, 182–195.

Fock, H. O., Pusch, C., and Ehrich, S. (2004). Structure of deep-sea pelagic fish assemblages in relation to the Mid-Atlantic Ridge (45°–50°N). *Deep Sea Res. Part I Oceanogr. Res. Pap.* 51, 953–978. doi: 10.1016/j.dsr.2004.03.004

Frank, T. M., Fine, C. D., Burdett, E. A., Cook, A. B., and Sutton, T. T. (2020). The vertical and horizontal distribution of deep-sea crustaceans in the order euphausiacea in the vicinity of the deepwater horizon oil spill. *Front. Mar. Sci.* 7:99. doi: 10.3389/fmars.2020.00099

Fuiman, L. A., and Werner, R.G. (eds) (2002). *Fishery Science: The Unique Contributions of Early Life Stages*. Oxford: Blackwell Science.

Grothues, T. M., and Cowen, R. K. (1999). Larval fish assemblages and water mass history in a major faunal transition zone. *Continent. Shelf Res.* 19, 1171–1198.

Hanisko, D. S., Pollack, A., Zapfe, G., and Ingram, G. W. Jr. (2017a). *King Mackerel (Scomberomorus cavalla) Larval Indices of Relative Abundance From SEAMAP Fall Plankton Surveys in the Gulf of Mexico, 1986 to 2014 SCRS/2017/095.* Washington,DC: NOAA.

Hanisko, D. S., Pollack, A. G., Zapfe, G., and Ingram, G. W. Jr. (2017b). *Spanish mackerel (Scomberomorus maculatus) Larval Indices of Relative Abundance From SEAMAP Fall Plankton Surveys in the Gulf of Mexico, 1986 to 2014 SCRS/2017/094.* Washington,DC: NOAA.

Heino, J., Melo, A. S., Siqueira, T., Soininen, J., Valanko, S., and Bini, L. M. (2015). Metacommunity organisation, spatial extent and dispersal in aquatic systems: patterns, processes and prospects. *Freshw. Biol.* 60, 845–869. doi: 10.1111/fwb.12533

Hernandez, F. J. Jr., Carassou, L., Graham, W. M., and Powers, S. P. (2013). Evaluation of the taxonomic sufficiency approach for ichthyoplankton community analysis. *Mar. Ecol. Prog. Ser.* 491, 77–90.

Hernandez, F. J., Filbrun, J. E., Fang, J., and Ransom, J. T. (2016). Condition of larval red snapper (*Lutjanus campechanus*) relative to environmental variability and the Deepwater Horizon oil spill. *Environ. Res. Lett.* 11:094019. doi: 10.1088/1748-9326/11/9/094019

Hopkins, T. L., Sutton, T. T., and Lancraft, T. M. (1996). The trophic structure and predation impact of a low latitude midwater fish assemblage. *Prog. Oceanogr.* 38, 205–239. doi: 10.1016/S0079-6611(97)00003-7

Houde, E. D. (1989). Subtleties and episodes in the early life of fishes. *J. Fish Biol.* 35, 29–38. doi: 10.1111/j.1095-8649.1989.tb03043.x

Hsieh, C.-H., Chen, C.-S., Chiu, T.-S., Lee, K.-T., Shieh, F.-J., Pan, J.-Y., et al. (2009). Time series analyses reveal transient relationships between abundance of larval anchovy and environmental variables in the coastal waters southwest of Taiwan. *Fish. Oceanogr.* 18, 102–117. doi: 10.1111/j.1365-2419.2008.00498.x

Irigoien, X., Klevjer, T. A., Røstad, A., Martinez, U., Boyra, G., Acuña, J. L., et al. (2014). Large mesopelagic fishes biomass and trophic efficiency in the open ocean. *Nat. Commun.* 5:3271. doi: 10.1038/ncomms4271

Kelly, T. B., Davison, P. C., Goericke, R., Landry, M. R., Ohman, M. D., and Stukel, M. R. (2019). The importance of mesozooplankton diel vertical migration for sustaining a mesopelagic food web. *Front. Mar. Sci.* 6:508. doi: 10.3389/fmars.2019.00508

Kingsford, M. J. (1993). Biotic and abiotic structure in the pelagic environment: importance to small fishes. *Bull. Mar. Sci.* 53, 393–415.

Koslow, J. A., Davison, P., Lara-Lopez, A., and Ohman, M. D. (2014). Epipelagic and mesopelagic fishes in the southern California Current System: ecological interactions and oceanographic influences on their abundance. *J. Mar. Syst.* 138, 20–28. doi: 10.1016/j.jmarsys.2013.09.007

Koslow, J. A., Goericke, R., Lara-Lopez, A., and Watson, W. (2011). Impact of declining intermediate-water oxygen on deepwater fishes in the California Current. *Mar. Ecol. Prog. Ser.* 436, 207–218.

Legendre, P., and Gallagher, E. D. (2001). Ecologically meaningful transformations for ordination of species data. *Oecologia* 129, 271–280. doi: 10.1007/s004420100716

Levitus, S. (1982). *Climatological Atlas of the World Ocean. US Department of Commerce, National Oceanic and Atmospheric Administration*. Washington, DC: US Department of Commerce.

Lyczkowski-Shultz, J., Hanisko, D. S., Sulak, K. J., Konieczna, M., and Bond, P. J. (2013). Characterization of ichthyoplankton in the northeastern Gulf of Mexico from SEAMAP plankton surveys, 1982-1999. *Gulf Caribb. Res.* 25, 43–98.

Meinert, C. R., Clausen-Sparks, K., Cornic, M., Sutton, T. T., and Rooker, J. R. (2020). taxonomic richness and diversity of larval fish assemblages in the oceanic gulf of mexico: links to oceanographic conditions. *Front. Mar. Sci.* 7:579. doi: 10.3389/fmars.2020.00579

Milligan, R. J., and Sutton, T. T. (2020). Dispersion overrides environmental variability as a primary driver of the horizontal assemblage structure of the mesopelagic fish family myctophidae in the Northern Gulf of Mexico. *Front. Mar. Sci.* 7:15. doi: 10.3389/fmars.2020.00015

Moser, G. H., and Smith, P. E. (1993). Larval fish assemblages of the california current region and their horizontal and vertical distributions across a front. *Bull. Mar. Sci.* 53, 645–691.

Muhling, B. A., Lamkin, J. T., and Richards, W. J. (2012). Decadal-scale responses of larval fish assemblages to multiple ecosystem processes in the northern Gulf of Mexico. *Mar. Ecol. Prog. Ser.* 450, 37–53.

Murdy, E., Matheson, R. Jr., Fechhelm, J., and McCoid, M. (1983). Midwater fishes of the Gulf of Mexico collected from the R/V Alaminos, 1965-1973 [32 families, 75 genera, 116 species]. *Texas J. Sci.* 35, 109–127.

Olivar, M. P., Contreras, T., Hulley, P. A., Emelianov, M., López-Pérez, C., Tuset, V., et al. (2018). Variation in the diel vertical distributions of larvae and transforming stages of oceanic fishes across the tropical and equatorial Atlantic. *Prog. Oceanogr.* 160, 83–100. doi: 10.1016/j.pocean.2017.12.005

Olivar, M. P., Emelianov, M., Villate, F., Uriarte, I., Maynou, F., ÁLvarez, I., et al. (2010). The role of oceanographic conditions and plankton availability in larval fish assemblages off the Catalan coast (NW Mediterranean). *Fish. Oceanogr.* 19, 209–229. doi: 10.1111/j.1365-2419.2010.00538.x

Olivar, M. P., Hulley, P. A., Castellón, A., Emelianov, M., López, C., Tuset, V. M., et al. (2017). Mesopelagic fishes across the tropical and equatorial Atlantic: biogeographical and vertical patterns. *Prog. Oceanogr.* 151, 116–137. doi: 10.1016/j.pocean.2016.12.001

Poos, M. S., and Jackson, D. A. (2012). Addressing the removal of rare species in multivariate bioassessments: the impact of methodological choices. *Ecol. Indic.* 18, 82–90. doi: 10.1016/j.ecolind.2011.10.008

R Core Team (2019). *R: A Language and Environment for Statistical Computing*. Vienna: R Foundation for Statistical Computing.

Rakocinski, C. F., Lyczkowski-Shultz, J., and Richardson, S. L. (1996). Ichthyoplankton assemblage structure in mississippi sound as revealed by canonical correspondence analysis. *Estuar. Coast. Shelf Sci.* 43, 237–257. doi: 10.1006/ecss.1996.0067

Ramirez-Llodra, E., Tyler, P. A., Baker, M. C., Bergstad, O. A., Clark, M. R., Escobar, E., et al. (2011). Man and the last great wilderness: human impact on the deep sea. *PLoS One* 6:e22588. doi: 10.1371/journal.pone.0022588

Ransom, J. T., Filbrun, J. E., and Hernandez, F. J. Jr. (2016). Condition of larval Spanish mackerel *Scomberomorus maculatus* in relation to the Deepwater Horizon oil spill. *Mar. Ecol. Prog. Ser.* 558, 143–152.

Richards, W. J. (2005). *Early Stages of Atlantic Fishes: An Identification Guide for the Western Central North Atlantic, Two Volume Set*. Boca Raton, FL: CRC Press.

Richards, W. J., McGowan, M. F., Leming, T., Lamkin, J. T., and Kelley, S. (1993). Larval fish assemblages at the loop current boundary in the Gulf of Mexico. *Bull. Mar. Sci.* 53, 475–537.

Rooker, J. R., Kitchens, L. L., Dance, M. A., Wells, R. J. D., Falterman, B., and Cornic, M. (2013). Spatial, temporal, and habitat-related variation in abundance of pelagic fishes in the Gulf of Mexico: potential implications of the Deepwater Horizon Oil Spill. *PLoS One* 8:e76080. doi: 10.1371/journal.pone.0076080

Ross, S. W., Quattrini, A. M., Roa-Varón, A. Y., and McClain, J. P. (2010). Species composition and distributions of mesopelagic fishes over the slope of the north-central Gulf of Mexico. *Deep Sea Res. Part II Top. Stud. Oceanogr.* 57, 1926–1956. doi: 10.1016/j.dsr2.2010.05.008

Sabatés, A. (2004). Diel vertical distribution of fish larvae during the winter-mixing period in the Northwestern Mediterranean. *ICES J. Mar. Sci.* 61, 1243–1252. doi: 10.1016/j.icesjms.2004.07.022

Sassa, C., and Kawaguchi, K. (2006). Occurrence patterns of mesopelagic fish larvae in Sagami Bay, central Japan. *J. Oceanogr.* 62, 143–153. doi: 10.1007/s10872-006-0040-z

Sassa, C., Kawaguchi, K., and Mori, K. (2004). Late winter larval mesopelagic fish assemblage in the Kuroshio waters of the western North Pacific. *Fish. Oceanogr.* 13, 121–133. doi: 10.1046/j.1365-2419.2003.00275.x

Sassa, C., Moser, H. G., and Kawaguchi, K. (2002). Horizontal and vertical distribution patterns of larval myctophid fishes in the Kuroshio Current region. *Fish. Oceanogr.* 11, 1–10. doi: 10.1046/j.1365-2419.2002.00182.x

Sutton, T. T., Clark, M. R., Dunn, D. C., Halpin, P. N., Rogers, A. D., Guinotte, J., et al. (2017). A global biogeographic classification of the mesopelagic zone. *Deep Sea Res. Part I Oceanogr. Res. Pap.* 126, 85–102. doi: 10.1016/j.dsr.2017.05.006

Sutton, T. T., Porteiro, F. M., Heino, M., Byrkjedal, I., Langhelle, G., Anderson, C. I. H., et al. (2008). Vertical structure, biomass and topographic association of deep-pelagic fishes in relation to a mid-ocean ridge system. *Deep Sea Res. Part II Top. Stud. Oceanogr.* 55, 161–184. doi: 10.1016/j.dsr2.2007.09.013

Watanabe, H., Moku, M., Kawaguchi, K., Ishimaru, K., and Ohno, A. (1999). Diel vertical migration of myctophid fishes (Family Myctophidae) in the transitional waters of the western North Pacific. *Fish. Oceanogr.* 8, 115–127. doi: 10.1046/j.1365-2419.1999.00103.x

Young, J. W., Hunt, B. P. V., Cook, T. R., Llopiz, J. K., Hazen, E. L., Pethybridge, H. R., et al. (2015). The trophodynamics of marine top predators: current knowledge, recent advances and challenges. *Deep Sea Res. Part II Top. Stud. Oceanogr.* 113, 170–187. doi: 10.1016/j.dsr2.2014.05.015

Conflict of Interest: The authors declare that the research was conducted in the absence of any commercial or financial relationships that could be construed as a potential conflict of interest.

frontiers in Marine Science

ORIGINAL RESEARCH
published: 07 December 2021
doi: 10.3389/fmars.2021.758089

Species Composition and Assemblages of Ichthyoplankton in Sansha Bay, Fujian Province, China

Yan Jiang[1†], Bai-an Lin[1], Hao-yang He[1], Guang-mao Ding[2], Li-ting Yan[1], Ge Zhang[3], Min Liu[1]* and Lian-ming Zheng[1]*

[1] State Key Laboratory of Marine Environmental Science, College of Ocean and Earth Sciences, Xiamen University, Xiamen, China, [2] Fishery Resources Monitoring Center of Fujian Province, Fuzhou, China, [3] Shenzhen Marine Environment Monitoring Center, State Oceanic Administration of China, Shenzhen, China

Sansha Bay (26.40–27.00°N, 119.50–120.20°E) is a typical semi-enclosed bay, located in northern Fujian Province, China, and adjacent to the East China Sea. The ichthyoplankton species composition and assemblage structure were investigated based on monthly sampling at 25 stations in April–September 2019, covering the important spring and summer spawning seasons in the region. Sampling was conducted in the first 3–5 days of the full moon or new moon phases using a standard plankton net through horizontal and vertical tows during daytime. In total, 25,819 ichthyoplankton samples were collected, of which 25,449 samples (i.e., 24,757 eggs and 692 larvae) were from horizontal tows. For horizontal tow samples, the ichthyoplankton were classified into 58 taxa in 15 orders and 23 families with a combination of external morphology and DNA barcoding analyses, from pelagic to demersal and benthic species. The dominant order was the Gobiiformes, including 23 species (39.7% of all species). The dominant taxa, in terms of relative abundance and frequency of occurrence, consisted of commercially important fishes, such as *Setipinna tenuifilis* (Valenciennes, 1848) (Engraulidae), *Epinephelus akaara* (Temminck and Schlegel, 1842) (Serraenidae), *Collichthys lucidus* (Richardson, 1844), *Nibea albiflora* (Richardson, 1846) (Sciaenidae), *Acanthopagrus schlegelii* (Bleeker, 1854), and *Pagrus major* (Temminck and Schlegel, 1843) (Sparidae), accounting for 78.9% of the horizontal tow samples. Low-valued and small-sized fishes, such as *Stolephorus commersonnii* Lacepède, 1803 (Engraulidae), *Solea ovata* Richardson, 1846 (Soleidae), *Nuchequula nuchalis* (Temminck and Schlegel, 1845), and *Photopectoralis bindus* (Valenciennes, 1835) (Leiognathidae), were also dominant species, accounting for 11.4% of the horizontal tow samples. The ichthyoplankton assemblage was categorized into five different temporal assemblages based on the cluster and nonmetric multidimensional scaling analysis, namely, April, May, June, July, and August–September (ANOSIM, Global $R = 0.656$, $p < 0.01$) with the highest density and richness of ichthyoplankton occurred in May. The spatial distribution pattern showed that the high density (ind./m^3) of ichthyoplankton occurred mainly in S12–S25 in Guanjingyang and along the Dongchong Peninsula coastline into Dongwuyang, while low density occurred mainly in S01–S11 in

Edited by:
Hui Zhang,
Institute of Oceanology, Chinese
Academy of Sciences (CAS), China

Reviewed by:
Gang Hou,
Fisheries College, Guangdong Ocean
University, China
Bruce Pfirrmann,
University of South Carolina,
United States

***Correspondence:**
Min Liu
minliuxm@xmu.edu.cn
Lian-ming Zheng
zhlm@xmu.edu.cn

†Present address:
Yan Jiang,
State Key Laboratory of Marine
Pollution, City University
of Hong Kong, Kowloon Tong,
Hong Kong SAR, China

Specialty section:
This article was submitted to
Marine Fisheries, Aquaculture
and Living Resources,
a section of the journal
Frontiers in Marine Science

Received: 13 August 2021
Accepted: 08 November 2021
Published: 07 December 2021

Citation:
Jiang Y, Lin B-a, He H-y,
Ding G-m, Yan L-t, Zhang G, Liu M
and Zheng L-m (2021) Species
Composition and Assemblages
of Ichthyoplankton in Sansha Bay,
Fujian Province, China.
Front. Mar. Sci. 8:758089.
doi: 10.3389/fmars.2021.758089

the northwest waters of Sandu Island (ANOVA, $F = 8.270$, $p < 0.05$). Temperature, salinity, and chlorophyll *a* were key factors structuring the ichthyoplankton assemblages in Sansha Bay. In addition, this study revealed the changes of the ichthyoplankton composition, density, and spatial distribution in Sansha Bay over the past three decades.

Keywords: abiotic and biotic factors, Chinese waters, DNA barcoding, fish eggs and larvae, spatial and temporal distribution

INTRODUCTION

Fishes have various life stages, and different developmental stage requires different foods, habitats, and environmental factors (Rijnsdorp et al., 2009; Hamre et al., 2013; Petitgas et al., 2013; Madeira et al., 2020). For example, ripe fishes are sensitive to the hydrological conditions of the spawning grounds, such as current, tide, water temperature, salinity and dissolved oxygen, and prey availability and preference (MacKenzie et al., 1996; Costa et al., 2002). Ichthyoplankton include fish eggs and larvae, belonging to the early life stages. Due to their absence of or weakness on independent swimming capabilities, ichthyoplankton have a drifting nature with currents and tides (Lechner et al., 2016; Downie et al., 2020). Understanding the distribution patterns of different life stages and exploring the abiotic and biotic factors influencing the distribution patterns are crucial for assessing fish recruitment and stock restoration (Costa et al., 2002; Santos et al., 2017). Achieving the sustainability of fishery resources depends highly on the abundance and survival of fish eggs and larvae (Oeberst et al., 2009; Llopiz et al., 2014).

The identification of unambiguous species from fish eggs and larvae is challenging. It is mainly because of the high diversity of species of fishes and the limitation of morphological observation on different stages of eggs and larvae before metamorphosis (Li et al., 2014; Zhang et al., 2015; Hsieh et al., 2016). For example, eggs and larvae of Sciaenidae are difficult to identify to species level through morphological features (Zhang et al., 1985; Zhan et al., 2016), besides the challenges for identification of adult sciaenids (Chu et al., 1963). DNA barcode, which delimits species using a molecular marker (e.g., mitochondrial cytochrome c oxidase subunit I gene, COI), has been widely applied to facilitate the identification in all stages from egg to adult of fishes (Ward et al., 2005; Ko et al., 2013; Becker et al., 2015; Harada et al., 2015; Hou et al., 2021a). In recent studies, Kerr et al. (2020) successfully identified 564 fish eggs to 89 taxa collected from northwestern Cuba and across the Florida Straits using DNA barcode. Hou et al. (2021a) successfully identified 931 fish eggs and 229 larvae to 75 taxa collected from the Pearl River Estuary of China using a DNA barcode. However, identifying ichthyoplankton correctly through DNA barcoding relies highly on a powerful and accurate database. It is necessary, but still challenging, to build up a DNA barcoding library in a specific area.

The transitional region between the East China Sea and the South China Sea through the Taiwan Strait, Fujian Province, has a highly sinuated coastline forming many bays with some typically semi-closed by peninsulas (Yu et al., 1988). In terms of volumes of the marine capture fisheries, Fujian Province ranks third in China, contributing to approximately 15.6% of the national total marine capture volumes or 16.8% of the national total marine fish capture volumes in the past decade, 2010−2019 (MOA, 2010–2018; MARA, 2019). Sansha Bay (26.40−27.00°N, 119.50−120.20°E) is located in Fujian Province (**Figure 1A**) and connects with the East China Sea through the narrow Dongchong Channel of about 3 km in width (**Figure 1B**). This typical semi-enclosed bay is well-known because it was one of the 12 traditional spawning grounds along Chinese coastal waters for the large yellow croaker *Larimichthys crocea* (Richardson, 1846) (Sciaenidae) before the 1990s, a commercially important species that formed large spawning aggregations (Chu, 1985; Liu and Sadovy de Mitcheson, 2008). With the mariculture and industrial development since the 1990s, marine pollution has been exacerbated in Sansha Bay (Wang et al., 2019). The current status of Sansha Bay as *L. crocea* spawning ground function is unclear.

In Sansha Bay, species composition and assemblages of ichthyoplankton, which are essential for the estimation of spawning sites, reproductive seasons, and conservative strategies (Parrish et al., 1981; Bailey and Houde, 1989; Oliveira and Ferreira, 2008), remain insufficient attention. Species composition and temporal and spatial distribution of fish eggs and larvae were investigated only four times (i.e., 1990, 2007, 2008, and 2010) historically, mainly seasonally, and the samples were identified by external morphology only (Dai, 2006; Wang et al., 2010; Shen, 2011; Xu, 2018), which may lead to the missing of certain species and underestimate the diversity of the real species. The results of these previous studies showed that Sansha Bay was important for fish reproduction, and fish egg and larva density (ind./m^3) were high in spring and summer. Moreover, the ichthyoplankton abundance of traditionally important fishery species showed dramatic declines over years. It merits further monthly and accurate studies with multiple identification methods and a high spatial coverage to evaluate the current status and long-term dynamics of ichthyoplankton assemblages in Sansha Bay.

In this study, we designed 25 stations throughout Sansha Bay for the ichthyoplankton collection. We conducted sampling monthly from April to September in 2019 covering the peak spawning seasons (i.e., spring and summer) mentioned earlier and applied DNA barcoding technique for species identification after external morphology examination, aiming to obtain a relative accurate species composition, to provide detailed characteristics of the ichthyoplankton assemblages, and to analyze the influence of abiotic and biotic variables on the distribution of ichthyoplankton in Sansha Bay. The results can be used to evaluate the current status of this traditional spawning ground and to compare the changes of

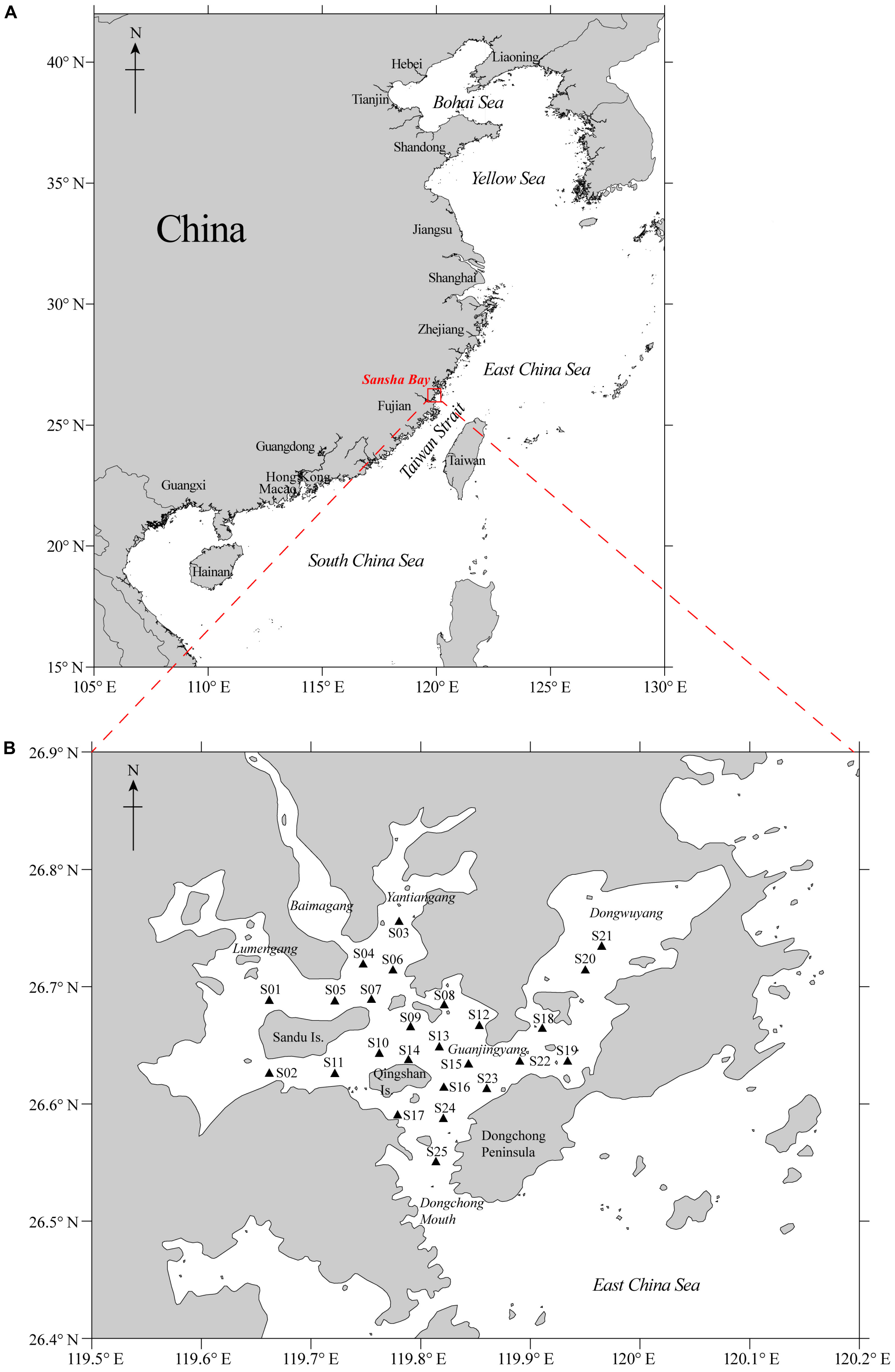

FIGURE 1 | (A) Map of mainland China and **(B)** ichthyoplankton sampling stations (*n* = 25) in Sansha Bay, Fujian Province, China.

ichthyoplankton composition and spatial distribution over the past three decades in Sansha Bay.

MATERIALS AND METHODS

Ichthyoplankton Collection

Ichthyoplankton samples were collected from 25 stations (S01−S25) (26.50−26.85°N, 119.52−120.09°E) in Sansha Bay, Fujian Province of China (**Figure 1B**). The sampling was conducted monthly from April to September 2019 within the first 3−5 days of the full moon or new moon phases during daytime.

The standard plankton net used for horizontal tows is 80 cm in net opening diameter (i.e., 0.5 m^2 net opening area) and 505 μm in net mesh size (GB/T 12763.6, 2007). At each station, the net was towed horizontally right below the sea surface with the speed of approximately 2 km for 5−10 min.

The standard plankton net used for vertical tows is 50 cm in net opening diameter (i.e., 0.2 m^2 net opening area) and 505 μm in net mesh size (GB/T 12763.6, 2007).

On board, ichthyoplankton samples collected were fixed with the formaldehyde concentration of 5%. The samples were further transferred to 95% ethanol solution within 12 h for the purpose of DNA barcoding.

Collection of Abiotic and Biotic Factors

Sea surface temperature, salinity, dissolved oxygen, and pH were measured using YSI EXO2 Multiparameter Sonde during plankton sampling at each station.

Chlorophyll *a* (Chla) samples were collected and analyzed in the laboratory through fluorospectrophotometry within 24 h. For a sampling of vertical phytoplankton, the standard plankton net used is 37 cm in net opening diameter (i.e., 0.1 m^2 net opening area) and 77 μm in net mesh size (GB/T 12763.6, 2007). On board, phytoplankton samples were fixed in Lugol's iodine solution with a concentration of 10%. For a sampling of vertical zooplankton, the standard plankton net used is the same as the vertical ichthyoplankton collection above. On board, zooplankton samples were fixed in the formaldehyde solution with a concentration of 5%.

Ichthyoplankton and Plankton Identification

In the laboratory, all fish eggs and larvae collected were sorted and pooled under a dissecting microscope (Zeiss Stemi 2000-C, Germany) according to the external morphological features (Zhang et al., 1985; Shao et al., 2001; Wan and Zhang, 2016). For each egg or larva with a specific morphological feature, photo images were collected using the Leica M165FC Fluorescent Stereo Microscope and Canon EOS 600D Digital SLR Camera, and one or more samples were selected for DNA extraction and barcode COI fragment obtaining. Sizes of eggs and larvae were not measured because they were fixed and dehydrated in 95% ethanol solution for at least 2 months before sorting.

Genomic DNA was extracted using the Takara MiniBEST Universal Genomic DNA Extraction Kit Ver. 5.0 according to manufacturer specifications and further used with no dilution for amplification and sequencing. A PCR was conducted, and the COI fragment was amplified using three universal COI gene primer pairs (i.e., LCO1490−HCO2198, FishF1−FishR1, and FishF2−FishR2) (Folmer et al., 1994; Ward et al., 2005) to obtain the target COI gene fragment (about 630 bp). For each PCR product, sequencing was performed using both corresponding forward and reverse primers that are used for PCR (Sangon Biotech, China).

Raw sequences were assembled using Bioedit 7.2. Assembled sequences of fish eggs and larvae were identified using reference sequences published in GenBank (NCBI)[1] or by the Barcode of Life Data System.[2] To assign a sequence to a species, genus, or family level, we required that the sequence matches with the database by at least 99.60, 91.29, or 85.48%, respectively (Hou et al., 2017). All sequences were further confirmed by ML and NJ phylogenetic trees with sequences from the GenBank and BOLD system using MEGA 6.06 with 1,000 bootstrap pseudo-replications. Categorization of species taxonomy was followed as suggested by Nelson et al. (2016).

Moreover, phytoplankton and zooplankton samples collected were identified based on the external morphology under a microscope (Liu et al., 2020a), following the taxonomic books in the region (Guo, 2003; Lin, 2009; Zhang et al., 2010; Ding, 2013; Slotwinski et al., 2014; Sun et al., 2015).

Plankton Calculations

In the laboratory, the densities of ichthyoplankton (i.e., eggs and larvae) from horizontal tows were standardized:

$$A = N/V$$

where A is the density of ichthyoplankton (ind./m^3), N is the number of ichthyoplankton (individuals) per plankton net, and V is the seawater volumes filtered into the plankton net (m^3).

V was calculated by a flow meter (HYDRO-BIOS) attached to the center of the plankton net:

$$V = 0.3R \times S$$

where R is the number of revolution noted from HYDRO-BIOS, $0.3R$ means that when the flow meter rotates one number, the net moves 0.3 m based on HYDRO-BIOS product manual, and S is the net opening area (m^2).

The dominant species of ichthyoplankton (i.e., eggs and larvae together) from horizontal tows were determined using the Index of Relative Importance (*IRI*) (Pinkas et al., 1971; Zhu et al., 2002):

$$IRI = N\% \times F\%$$

where $N\%$ and $F\%$ are relative abundance and frequency of occurrence of a specific species, respectively. Species with $IRI \geq 0.02$ were considered to be a dominant species.

The three diversity indices, namely, the Shannon-Wiener diversity index (H'), Pielou's evenness index (J'), and

---

[1] https://blast.ncbi.nlm.nih.gov/Blast.cgi

[2] http://www.barcodinglife.org

Margalef's richness index (d), were calculated (Margalef, 1958; Shannon and Wiener, 1963; Pielou, 1966) to evaluate the current status of ichthyoplankton in Sansha Bay:

$$H^{'} = -\sum_{i=1}^{s} P_i \ln P_i$$

$$J^{'} = H^{'}/\ln S$$

$$d = (S - 1)\big/\ln N$$

where S is the total number of ichthyoplankton species, N is the total number of individuals, and P_i is the proportion of the number of individuals for a specific ichthyoplankton species to the total number of individuals.

In addition, densities of phytoplankton and zooplankton from vertical tows were also calculated as for ichthyoplankton aforementioned:

$$A = N/V$$

where A is the density of phytoplankton (cells/m^3) or zooplankton (ind./m^3), N is the number of phytoplankton (cells) or zooplankton (individuals) per plankton net, and V is the seawater volumes filtered into the plankton net (m^3).

Data Analysis

We used only data from horizontal tows for further analyses for at least two reasons. First, the number of eggs and larvae and diversity of ichthyoplankton species from horizontal tows were much higher than those of vertical tows in sampling during every month. Second, the depths of sampling stations varied largely from as shallow as 1 m to about 40 m. Therefore, the seawater volumes filtered into the vertical tow nets varied largely that it subsequently influenced the number of eggs and larvae and the diversity of ichthyoplankton species collected. The vertical tow samples were only used for species diversity supplements.

For the data analysis below and specific calculation above (e.g., *IRI*), we combined the number of egg and larva samples together (Zhang et al., 2016; Huang et al., 2017; Hou et al., 2021a). A short hatchery period (i.e., hours to several days) and limited independent swimming capability of larvae were also the considerations for the combination of egg and larva data for analyses (Woynarovich and Horváth, 1984; Pauly and Pullin, 1988; Lechner et al., 2016; Downie et al., 2020).

The one-way ANOVA test was conducted with the IBM SPSS Statistics version 16.0 for revealing the significance of the monthly changes of environmental factors, the diversity indices, the spatial variation of average ichthyoplankton density, and the variation of average species richness among 25 stations; when necessary (ANOVA, $p < 0.05$, $n > 2$), a *post hoc* least significant difference (LSD) test was added. The cluster analysis and nonmetric multidimensional scaling (nMDS) based on the Bray-Curtis similarity and square root average density of ichthyoplankton were performed to clarify the temporal and spatial distribution patterns of the assemblages. After the cluster analysis, the tests for identifying the discrimination between two observed sample clusters (SIMPEROF) and the similarities (ANOSIM) were performed using PRIMER version 6.0 to assess the significance and discrimination between sample clusters (Clarke and Gorley, 2006).

The detrended correspondence analysis (DCA) and canonical correlation analysis (CCA) or redundancy analysis (RDA) were performed using CANOCO version 5.0 to analyze the constrained relationships between environmental factors and ichthyoplankton communities. Before the analysis, DCA was performed to determine a suitable response according to the maximum gradient of length (>4, CCA; 3–4, CCA or RDA; <3, RDA) (Šmilauer and Lepš, 2014). Because the maximum gradient length of DCA was 6.34 (>4), CCA was subsequently selected in this study. Only species that occurred in >10% of the catches, based on all species density, were included in the analysis to reduce the effect of rare species. Data of species density were log (10,000x + 1) transformed to minimize the dominant effect of some species (Clarke et al., 2014). A Monte Carlo permutation test with 999 permutations was performed to confirm the key factors significantly affecting the assemblages ($p \leq 0.05$; Arora and Mehra, 2009; Hou et al., 2021a). The variance inflation factor (VIF) was conducted to examine the collinearity between independent environment variables. VIF < 10 indicated that the environmental variables were not collinear and were fit for CCA (Graham, 2003; Huang et al., 2017). The importance of the environmental variables was measured by interset correlation coefficients, when the value of interset correlation coefficients $\geq|\pm 0.4|$ variables were regarded conservatively as biologically important (Rakocinski et al., 1996; Ramos et al., 2017).

RESULTS

Abiotic and Biotic Factors

From April to September 2019, with the significant increase of sea surface temperature (F = 290.20, $p < 0.05$), salinity also showed an upward trend (F = 36.15, $p < 0.05$), while dissolved oxygen (F = 168.23, $p < 0.05$) and pH (F = 283.25, $p < 0.05$) illustrated a downward trend (**Table 1**).

Chla peaked in July, with significant intermonth variations (F = 22.91, $p < 0.05$), and the densities of phytoplankton (F = 17.47, $p < 0.05$) and zooplankton (F = 8.908, $p < 0.05$) peaked in May and April, respectively (**Table 1**).

Ichthyoplankton Composition

A total of 25,449 ichthyoplankton samples, including 24,757 fish eggs and 692 larvae, were collected from horizontal tows. A total of 370 ichthyoplankton samples, including 315 eggs and 55 larvae, were collected from vertical tows. The numbers of eggs and larvae from horizontal tows were much higher than those of vertical tows.

According to different morphological features, 619 fish eggs and 192 larvae were selected for photography and further DNA extraction, from which high-quality COI fragments were obtained from 335 fish eggs (54.1%) and 117 larvae (60.9%). In total, 60 taxa were identified, 52 at species level, including 26 from eggs and 43 from larvae (**Supplementary Table 1**).

TABLE 1 | Temporal variation in abiotic and biotic factors (mean ± SD, *n* = 25 stations) from April to September 2019 in Sansha Bay of Fujian Province, China.

Factors	Unit	April	May	June	July	August	September
Temperature (T)	°C	17.01 ± 0.49^a	19.97 ± 0.37^b	23.18 ± 0.35^c	25.95 ± 0.45^d	28.72 ± 0.57^e	29.44 ± 0.45^f
Salinity (S)		26.66 ± 1.75^a	27.10 ± 1.66^a	27.45 ± 2.02^a	29.10 ± 1.65^b	30.75 ± 1.38^c	31.52 ± 1.28^c
Dissolved oxygen (DO)	mg/L	7.68 ± 0.18^a	7.27 ± 0.25^b	6.79 ± 0.31^c	5.83 ± 0.36^d	5.32 ± 0.65^e	5.27 ± 0.46^e
pH		8.11 ± 0.06^a	8.13 ± 0.05^a	7.98 ± 0.04^c	7.95 ± 0.06^c	8.05 ± 0.10^b	7.55 ± 0.05^d
Chlorophyll a (Chla)	μg/L	0.64 ± 0.63^a	0.28 ± 0.12^a	0.53 ± 0.39^a	2.21 ± 1.27^c	1.12 ± 0.68^b	1.33 ± 0.67^b
Phytoplankton (Phy)	10^6 cells/m^3	20.31 ± 7.30^a	81.92 ± 60.37^c	9.14 ± 3.65^a	7.95 ± 4.37^a	42.27 ± 55.93^b	11.32 ± 10.95^a
Zooplankton (Zoo)	ind./m^3	80.54 ± 89.52^a	45.44 ± 34.02^b	23.12 ± 22.87^c	17.23 ± 10.76^c	18.57 ± 16.36^c	19.71 ± 15.18^c

Values with different letters (a–f) indicate the significant difference at p ≤ 0.05 among months, and values with the same letter indicate that the difference was not significant at p > 0.05.

From horizontal tows, 58 taxa were identified from 15 orders, 23 families with 51 taxa at species level; Gobiiformes was the most diverse order, representing 39.7% of all taxa (**Supplementary Table 1** and **Supplementary Figure 1**). Additionally, four larvae were identified at the genus level (i.e., *Pseudogobius* and *Rhinogobius* in Gobiiformes, *Hyporhamphus* in Beloniformes, and *Hippichthys* in Syngnathiformes), and three larvae at the family level (i.e., Gobiidae in Gobiiformes and Blenniidae in Blenniformes).

From vertical tows, 31 taxa were identified from 9 orders, 13 families with 27 at the species level, 3 at the genus level, and 1 at the family level (**Supplementary Table 2**). Among these, 29 taxa were also recorded in horizontal tow samples, and only two species [i.e., *Acentrogobius* sp. and *Lateolabrax japonicus* (Cuvier, 1828)] were only found in vertical tow samples. Eggs and larvae of two alien species, the red drum *Sciaenops ocellatus* (Linnaeus, 1766) (Sciaenidae) in Acanthuriformes and the gilthead seabream *Sparus aurata* (Linnaeus, 1758) (Sparidae) in Spariformes, were collected in horizontal tows, *S. ocellatus* eggs in August and September and *S. aurata* larvae in June (**Supplementary Table 1**). Eggs and larvae of *L. crocea*, a critically endangered species in the IUCN Red List, were collected in April—June in horizontal and vertical tows (**Supplementary Tables 1, 2**).

Ichthyoplankton from Engraulidae (two species), Soleidae (one species), Serranidae (one species), Leiognathidae (two species), Sciaenidae (two species), and Sparidae (two species) were dominant (*IRI* ≥ 0.02; **Table 2** and **Supplementary Table 1**), accounting for 90.3% of the horizontal tow samples. The yellow drum *Nibea albiflora* (Richardson, 1846) was dominant in May—September 2019 with a peak of *IRI* in September (*IRI* = 0.51).

The three diversity indices showed significant differences from April to September (H': $F = 10.39$, $p < 0.05$; J': $F = 2.54$, $p < 0.05$; d: $F = 16.14$, $p < 0.05$; **Figure 2**). The highest H' and d were found in May, while the lowest H' and d were found in September; J' in August was significantly higher than the other months.

Temporal and Spatial Distribution Pattern of Ichthyoplankton

The ichthyoplankton richness ranged from 11 species (July) to 32 species (May) in horizontal tows (**Supplementary Table 1**). The average density of ichthyoplankton ranged from 0.18 ind./m^3 (August) to 2.10 ind./m^3 (May) (**Figure 3**).

The ichthyoplankton were classified into five representative assemblages in the Bray-Curtis similarity at 36.79% ($p = 0.001$), namely, April, May, June, July, and August—September (**Figure 4A**). The results of nMDS (**Figure 4B**) are consistent with those of the cluster analysis at the stress value < 0.2,

TABLE 2 | Dominant ichthyoplankton species (*IRI* ≥ 0.02) from April to September 2019 in Sansha Bay of Fujian Province, China.

Species	April	May	June	July	August	September
Setipinna tenuifilis			0.18	0.27	0.08	
Stolephorus commersonnii					0.05	
Solea ovata		0.14				
Epinephelus akaara			0.04			
Nuchequula nuchalis		0.07				
Photopectoralis bindus					0.27	0.03
Collichthys lucidus		0.03	0.05			
Nibea albiflora		0.48	0.43	0.32	0.04	0.51
Acanthopagrus schlegelii	0.26	0.04		0.02		
Pagrus major	0.38	0.06				

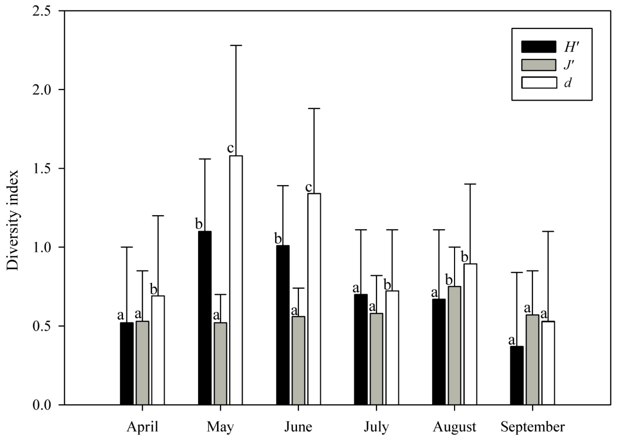

FIGURE 2 | Temporal variation of the three ichthyoplankton diversity indices (mean + standard deviation [SD], *n* = 25 stations) from April to September 2019 in Sansha Bay. H', Shannon-Wiener diversity index; J', Pielou's evenness index; d, Margalef's richness index. Values with different letters (a–c) indicate the significant difference at $p \leq 0.05$ among months, and values with the same letter indicate that the difference was not significant at $p > 0.05$.

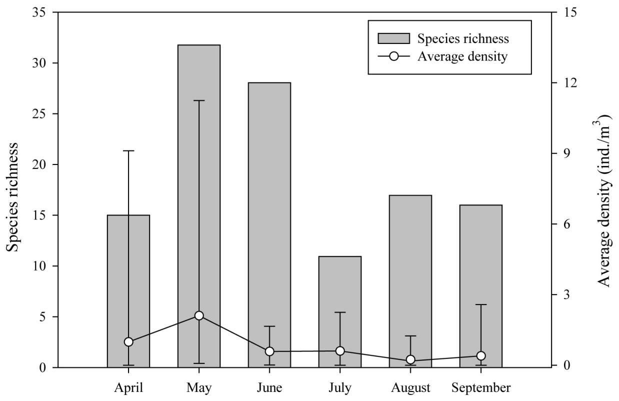

FIGURE 3 | Temporal distribution of the ichthyoplankton richness and average density (ind./m^3) (n = 25 stations) from April to September 2019 by horizontal tows in Sansha Bay of Fujian Province, China. Error bars: maximum and minimum densities.

illustrating the reliability of the results (Clarke et al., 2014). The R-statistic values by ANOSIM revealed the dissimilarity between the five assemblages over time (sample statistic: Global $R = 0.656$, $p = 0.001$; **Supplementary Table 3**). The ichthyoplankton assemblages of April, May, June, and July differed significantly from August and September, and no significant difference was found between August and September.

Although the cluster analysis of spatial assemblage was not significant (SIMPEROF, $p > 0.05$), ichthyoplankton density (total taxa) (**Figure 5**) and richness (**Figure 6**) varied by station and month. The highest density and species richness occurred in May, from May-S22 and May-S01, respectively. High density occurred mainly in S12–S25 in Guanjingyang and along the Dongchong Peninsula coastline (i.e., southeast Sansha Bay) into Dongwuyang (i.e., northeast Sansha Bay) in April—September, except for August, and low density occurred mainly in S01–S11 in northwest waters of Sandu Island in April—September (ANOVA, $F = 8.270$, $p < 0.05$). Although the spatial patterns for the species richness were not clear, it showed that around Sandu Island, especially S02, S03, S05, and S06, had a relatively high richness (ANOVA, $F = 7.953$, $p < 0.05$) during most of the sampling period.

Relationship Between Ichthyoplankton Assemblages and Abiotic and Biotic Factors

The variance inflation factor (VIF) test and Monte Carlo permutation test indicated that abiotic factors (i.e., T, S, DO, and pH) and biotic factors (i.e., Chla, Phy, and Zoo) were not collinear (VIF < 10) and contributed significantly to explain ichthyoplankton assemblage structure ($p < 0.05$; **Table 3**).

The sum of all canonical eigenvalues occupied 18.12% of the sum of all eigenvalues. The cumulative percentage variance of species was 15.79%, and cumulative percentage variance of species environment was 87.12% (**Table 4**). The first two CCA axes (i.e., axes 1 and 2) explained 73.65% of the cumulative percentage variance of species and 73.67% of the cumulative percentage variance of species environment.

Abiotic and biotic factors explained 18.1% variation in ichthyoplankton assemblages among months (**Table 3**). The main factors affecting ichthyoplankton assemblages were pH, DO, Phy, and Zoo, which were positively related with the first CCA axis in April and May, and were T, S, and Chla, which were negatively correlated with the first CCA axis while positively related with the second CCA axis in July, August, and September (**Figure 7A** and **Table 3**). Correlations between abiotic and biotic factors and the distribution of ichthyoplankton species were depicted in CCA (**Figure 7B**). *Omobranchus punctatus* (Opun) showed a close relationship with Chla; *Nibea albiflora* (Nalb), *Boleophthalmus pectinirostris* (Bpec), and *Setipinna tenuifilis* (Sten) were closely associated with S and Chla; and *Aulopareia unicolor* (Auni), *Taenioides anguillaris* (Tang), Gobiidae sp.-2 (Gibi2), and *Stolephorus niphonius* (Scom) showed a positive relationship with T but a negative relationship with pH. *Acentrogobius caninus* (Acan), *Tridentiger barbatus* (Tbar), *Parachaeturichthys polynema* (Ppol), *Konosirus punctatus* (Kpun) and *Tridentiger bifasciatus* (Tbif), *Pagrus major* (Pmaj) and *Larimichthys crocea* (Lcro) positively related with DO, pH, Phy and Zoo.

DISCUSSION

Ichthyoplankton Composition and Variation

We reported the first results combining the external morphology and DNA barcode technique to identify ichthyoplankton samples collected from April to September 2019 in Sansha Bay, which made the species richness increase significantly. In total, 60 taxa were identified from horizontal and vertical tows in this study, significantly higher than previous surveys (23—46 species in 1990—2010) from the same sampling area (**Table 5**). The high ichthyoplankton richness in this study was mainly from Gobiidae (21 species) and contributed to the application of COI gene fragment analysis with the high detection rate at the species level, rising from 39.1 to 74.2% (1990—2010) to more than 87.10% (2019) (**Table 5**).

The development of local or regional fish species COI barcodes library is highly recommended (Hou et al., 2021b). We demonstrated the importance of the accuracy and integrity of COI barcodes database in ichthyoplankton identification following the morphological feature collection. The development of a morphological database combining COI barcodes library of ichthyoplankton is needed for future investigation reference (Hubert et al., 2015; Hou et al., 2021a). In this study, we first preserved the ichthyoplankton samples in 5% neutral formalin and then transferred to 95% ethanol in less than 12 h. High-quality COI gene fragments obtained from eggs and larvae were 54.1 and 60.9%, respectively.

The 60 ichthyoplankton taxa identified in this study inferred the underestimation of the ichthyoplankton diversity in Sansha Bay because many fish larvae have a vertical distribution pattern on a diel basis (Ahlstrom, 1959; Rodríguez et al., 2006; Auth et al., 2007). Although we realized the importance of both day and night

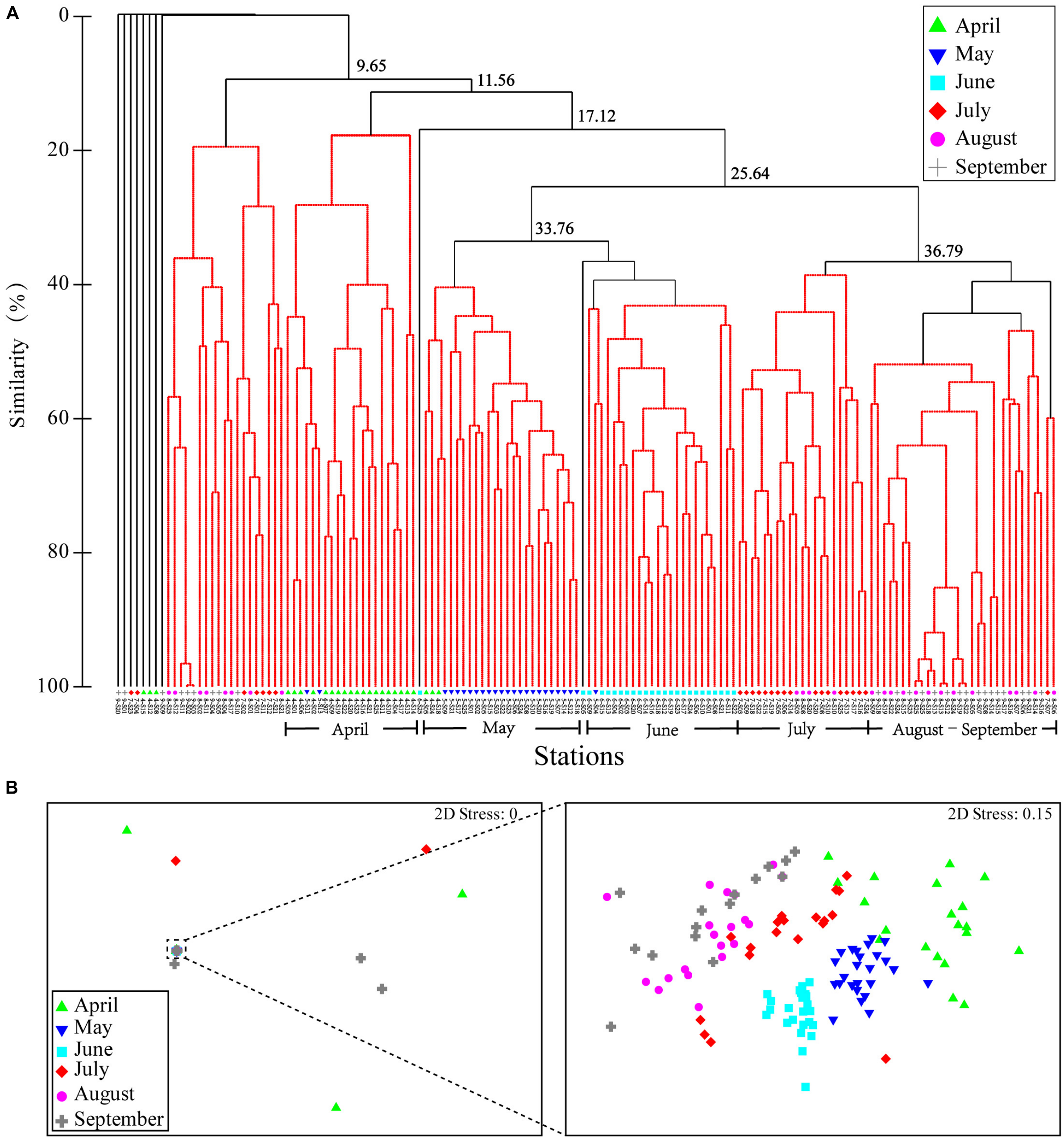

FIGURE 4 | (A) Dendrogram resulting from the cluster analysis and nonmetric multidimensional scaling (nMDS) ordination of spatial and **(B)** the temporal patterns of ichthyoplankton assemblages in Sansha Bay of Fujian Province, China. Samples were collected from April to September 2019. In panel A, the black lines indicate the significant difference at $p \leq 0.05$, and the red lines indicate no significant difference at $p > 0.05$.

sampling for understanding the ichthyoplankton composition and assemblage, night sampling was not applied mainly for safety considerations. Moreover, adhesive eggs are not able to collect using plankton nets. In the future, sampling methods need to be modified to obtain more ichthyoplankton samples.

The abundance of ichthyoplankton species (proportion of individuals) in Sansha Bay has changed over time. For example, a high abundance was found in the black sea bream *Acanthopagrus schlegelii* (Bleeker, 1854) (22%) and the bighead hairtail *Trichiurus lepturus* Linnaeus, 1758 (16%) in 1990, changed to Labridae sp. (47.1%) in 2007, to Sciaenidae spp. (80.63%) and Cynoglossidae spp. (14.18%) in 2008, and to Sciaenidae (41.19%), Sparidae (33.67%), and Engraulidae (11.36%) in this study (Dai, 2006; Wang et al., 2010; Shen, 2011). The shift of major ichthyoplankton composition may be driven by intensive fishery pressure, habitats loss, or climate change (Bui et al., 2010; Fodrie et al., 2010; Shen, 2011; McCain et al., 2016; Curran et al., 2021). In contrast, the sampling frequency (monthly

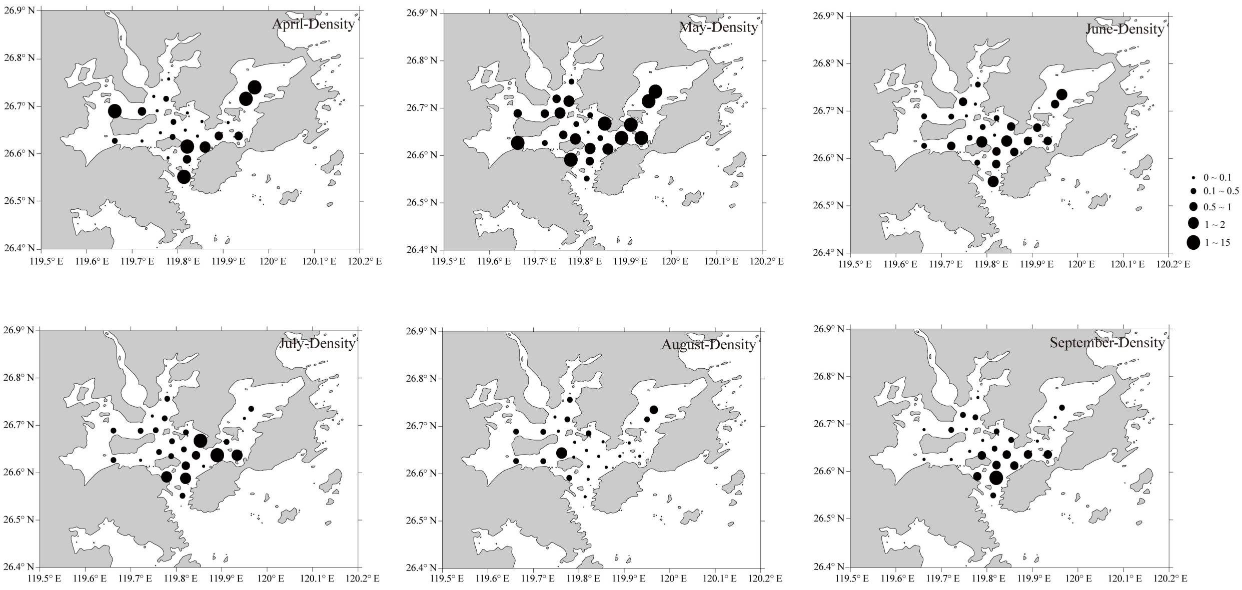

FIGURE 5 | Spatial variation of ichthyoplankton density from April to September 2019 in Sansha Bay of Fujian Province, China.

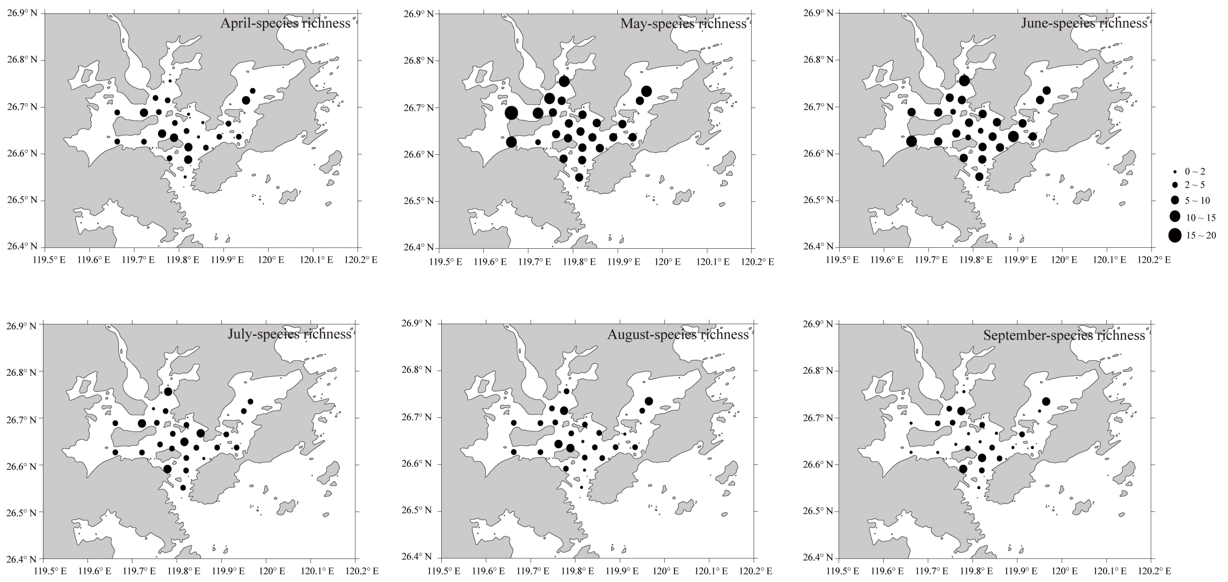

FIGURE 6 | Spatial variation of ichthyoplankton species richness from April to September 2019 in Sansha Bay of Fujian Province, China.

or seasonally), spawning ground, and station setting may also influence the ichthyoplankton composition. The temporal and spatial variation of high ichthyoplankton density was detected from 1990 to 2019 (**Figure 8**) in Sansha Bay.

Spawning Activities in Sansha Bay

This study confirmed that Sansha Bay is an important area for fish reproduction, for pelagic, demersal, and benthic species, including some commercially important species. One of the most traditionally important fishery species in Sansha Bay was *L. crocea*, a well-known species from spawning and overwintering aggregations in Chinese coastal waters (Liu and Sadovy de Mitcheson, 2008). It was documented that *L. crocea* migrated into Sansha Bay in May and June to spawn through the narrow Dongchong Channel (Chu and Wu, 1985). Eggs and larvae of *L. crocea* were collected in May, June, August, October, and November (Dai, 2006; Shen, 2011; Xu, 2018), confirming the existence of two spawning seasons (spring and autumn) in the region (Liu and Sadovy de Mitcheson, 2008). In this study, eggs and larvae of *L. crocea* were collected in April—June because only spring spawning season was focused (**Supplementary Tables 1**, **2**), and mature females and mature males were also

TABLE 3 | Results of Monte Carlo test of *F*-ratios and the interset correlations of environmental variables with the first two canonical correlation analysis (CCA) axes.

Factors	Explains %	Contribution %	*F*	*P*-value	VIF	Axis 1	Axis 2
Temperature (T)	8.6	47.5	12.1	0.002	7.35	–0.9865	0.1135
Salinity (S)	2.0	11.0	5.9	0.002	2.79	–0.5773	0.3198
Dissolved oxygen (DO)	1.1	6.1	9.0	0.002	6.90	0.8229	–0.3384
pH	1.3	7.2	6.0	0.002	2.24	0.6401	–0.0375
Chlorophyll a (Chla)	2.4	13.3	4.7	0.002	1.42	–0.4133	0.8048
Phytoplankton (Phy)	1.5	8.3	2.4	0.004	1.38	0.3291	0.0533
Zooplankton (Zoo)	1.2	6.6	2.5	0.02	1.51	0.2159	–0.2252

Explains %: the percentage of the total variation explained by the explanatory variable; contribution %: the percentage of the variable contribute to the explanatory power.

TABLE 4 | Canonical correlation analysis relating ichthyoplankton assemblages to abiotic and biotic factors in Sansha Bay of Fujian Province, China.

	Axis 1	Axis 2	Axis 3	Axis 4	Total inertia
Eigenvalues	0.5551	0.1818	0.1537	0.1097	6.3351
Species-environment correlations	0.9458	0.7120	0.7086	0.5972	
Cumulative percentage variance of species data	8.76	11.63	14.06	15.79	
Cumulative percentage variance of species-environment relation	48.35	64.18	77.57	87.12	
Sum of all unconstrained eigenvalues					6.3351
Sum of all canonical eigenvalues					1.1482

caught in April—June by fixed nets in Sansha Bay following the confirmation by gonadal histology (Liu et al., 2020a). It is the first record that *L. crocea* also spawned in April. Further understanding the reproductive dynamic and migration pattern for *L. crocea* in the Sansha Bay will help us assess the stock status of this critically endangered species (Liu et al., 2020b).

Two sciaenid species, namely, the bighead croaker *Collichthys lucidus* (Richardson, 1844) and *N. albiflora*, have been of commercial importance in Fujian waters (Chu and Wu, 1985). Juveniles and adults can be caught by fixed nets in Sansha Bay throughout the sampling period of April—September (Liu et al., 2020a). Ichthyoplankton samples (eggs as majority) of *C. lucidus* and *N. albiflora* were collected in May, June, and August and in April—September, respectively, with dominant in May and June, and in May—September, respectively (**Supplementary Table 1** and **Table 2**). However, ichthyoplankton of *C. lucidus* and *N. albiflora* were not collected in previous studies in 1990, 2007, 2008, and 2010 (Dai, 2006; Wang et al., 2010; Shen, 2011; Xu, 2018). Based on the external morphology identification of these previous studies, it was possible that the eggs and larvae of the two species were grouped as Sciaenidae species. In contrast, the reproductive dynamics of *C. lucidus* and *N. albiflora* have not been examined in Sansha Bay; therefore, it is unclear if their reproductive behavior has changed over time. For *C. lucidus*, the spawning and peak spawning seasons in Pearl River Estuary, approximately 800 km south of Sansha Bay, were December–July and May, respectively (Ou et al., 2012). For *N. albiflora*, the spawning and peak spawning seasons in Xiangshan Bay (Zhejiang Province), approximately 400 km north of Sansha Bay, were May—July and June–July, respectively (Lin et al., 2013). The variation on spawning seasons of the same species in different geological locations merits further assessments.

In Fujian waters, seabreams (Sparidae) such as *A. schlegelii* and the red seabream *Pagrus major* (Temminck and Schlegel, 1843) mainly spawned in February—April and October—December, respectively (Chu, 1985). The eggs and larvae of *A. schlegelii* were collected from April to August in Sansha Bay (Wang et al., 2010; Shen, 2011; Xu, 2018; this study), indicating the species has a longer spawning season, extending from spring to summer. For *P. major*, the eggs and larvae were collected in November 1990 (Dai, 2006) and in April and May 2019 (this study) in Sansha Bay, indicating the existence of spring and autumn spawning seasons of the species.

In the East China Sea, the spawning season of *T. lepturus* is March—August, producing pelagic eggs, and the spawning grounds are known offshore of Chinese waters (Chu, 1985; Nakamura and Parin, 1993; Xu and Chen, 2015). However, *T. lepturus* was dominant in ichthyoplankton samples (eggs) in May and August 1990 in Sansha Bay (Dai, 2006), inferring its possible spawning grounds in nearshore and semi-closed bays. It was not collected in 2007, 2008, 2010, and 2019 surveys covering its spawning season in Sansha Bay (Wang et al., 2010; Shen, 2011; Xu, 2018; this study). Nearly 100% of *T. lepturus* collected in Sansha Bay using fixed nets were young juveniles (3.2—46.1 cm total length, TL) in May—September 2019 (Liu et al., 2020a). Although the spawning ground function of *T. lepturus* in the Sansha Bay is still not clear, its nursery ground function is clear.

The Indo-Pacific king mackerel *Scomberomorus guttatus* (Bloch and Schneider, 1801) and the Japanese Spanish mackerel *S. niphonius* are pelagic, forming spawning migrations from deep waters to shallow waters in spring and spawning in May and June in Sansha Bay (Wu, 1985). Ichthyoplankton of *S. guttatus* and *S. niphonius* were collected in June 2010 (Xu, 2018), and in April and May 2019 (this study), confirming the spawning ground function of the Sansha Bay for the two species.

Ichthyoplankton of two alien species were first collected in Sansha Bay in this study; eggs of *S. ocellatus* in August

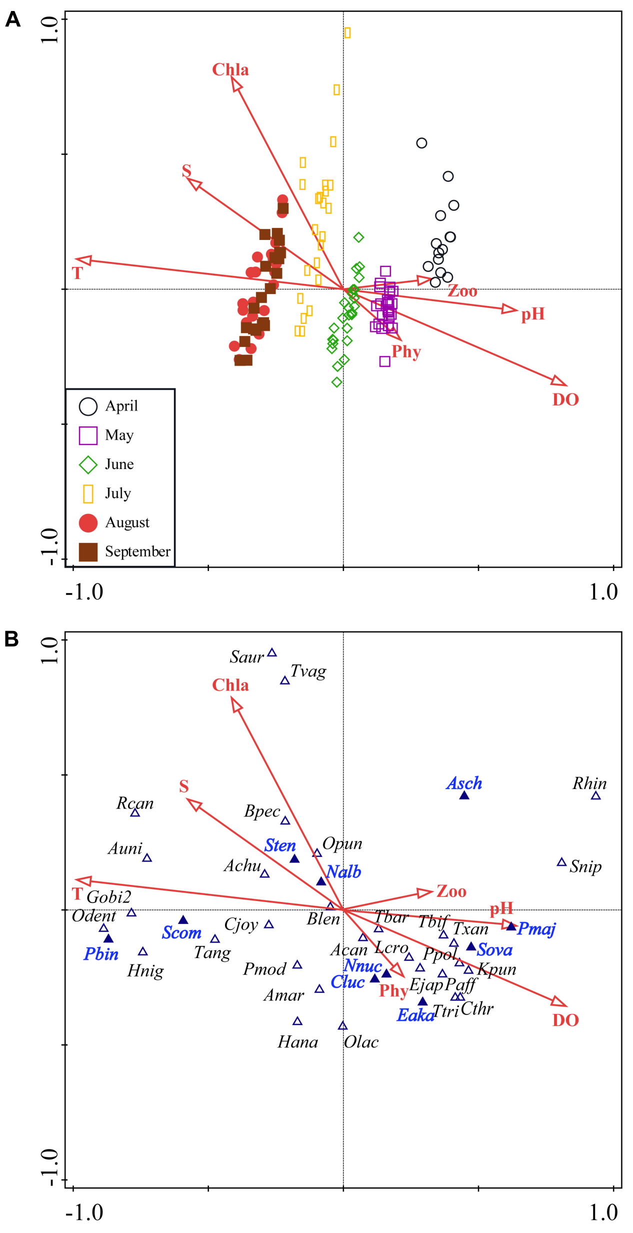

FIGURE 7 | Canonical correspondence analysis (CCA) diagram for ichthyoplankton assemblages **(A)** and species **(B)** with abiotic and biotic factors in Sansha Bay of Fujian Province, China. The abbreviations in panel **(B)** are species names shown in **Supplementary Table 1**. The dominant species are shown in blue and bold. Sten, *Setipinna tenuifilis*; Scom, *Stolephorus commersonnii*; Sova, *Solea ovata*; Eaka, *Epinephelus akaara*; Nnuc, *Nuchequula nuchalis*;, Pbin, *Photopectoralis bindus*; Cluc, *Collichthys lucidus*; Nalb, *Nibea albiflora*; Asch, *Acanthopagrus schlegelii*; Pmaj, *Pagrus major*; T, temperature; S, salinity; DO, dissolved oxygen; Chla, chlorophyll *a*; Phy, phytoplankton; Zoo, zooplankton.

and September 2019, and larvae of *S. aurata* in June 2019 (**Supplementary Table 1**). The two species were introduced into China for mariculture purposes from United States in 1991 and from France in 2001, respectively, and juveniles and adults have dispersed in coastal waters of China (Wang and Ji, 1996; Liu et al., 1998; Wang et al., 2006; Lin et al., 2020; Zhang, 2020). It is likely that *S. ocellatus* has established reproductive wild stocks in Chinese waters (Lin et al., 2020). Both species are commonly cultured in floating cages in Sansha Bay, and their juveniles (*S. ocellatus*: 35.8 cm TL, $n = 1$; *S. aurata*: 3.7—31.2 cm TL, $n = 9$) were collected using the fixed nets in 2019 (Liu et al., 2020a). This study revealed that *S. ocellatus* and *S. aurata* can reproduce and may be able to establish spawning population in Sansha Bay.

Ichthyoplankton Assemblages

Five main temporal ichthyoplankton assemblages were apparently separately in Sansha Bay. The densities of ichthyoplankton along Dongchong Peninsula coastline into Dongwuyang (S12–S25) were higher than those in the northwest waters of Sandu Island (S01–S11) with the significant high salinity (this study) and high tidal currents speed (Lin et al., 2018), and the dominant species were from Engraulidae [*S. tenuifilis*], Soleidae (*Solea ovata* Richardson, 1846), Serranidae [*Epinephelus akaara* (Temminck and Schlegel, 1842)], Sciaenidae (*N. albiflora* and *C. lucidus*), and Sparidae (*A. schlegelii* and *P. major*), including pelagic, demersal, and benthic species. The results indicated that these species may prefer spawning in waters with high salinity and strong currents, or fish eggs and larvae were dispersed to there by currents.

The spatial distribution patterns of ichthyoplankton varied over the past three decades in Sansha Bay, and three zones can be considered as core areas (Dai, 2006; Wang et al., 2010; Shen, 2011; Xu, 2018; this study; **Figure 8**). First, it is around Sandu Island. The high ichthyoplankton density area was in the north in 1990, then, shifted to the east in the late 2000s, and was not important in 2019. Second, it is in Guanjingyang waters with an extension to the Dongchong mouth. The high ichthyoplankton density was found in 2008, 2010, and 2019. Third, it is in Dongwuyang waters. The high ichthyoplankton density was found in 1990, 2007, 2010, and 2019. Overall, the high ichthyoplankton density areas remain the same in Guanjingyang and Dongwuyang over the past three decades and reduce largely from 1990 in Sandu Island water.

Influence of Abiotic and Biotic Factors

Studies revealed that both abiotic and biotic factors shaped the fish assemblages (including fish reproduction stocks and ichthyoplankton) (Olivar, 1990; Marshall and Elliott, 1998; Pombo et al., 2005; Zhang et al., 2015; Hsieh et al., 2016; Rodriguez, 2019). Temperature and salinity influence fish distribution through the different preferences and tolerances of the species. Temperature is likely to be the dominant factor influencing the variability of migration, spawning, and recruitment (Gibson et al., 1993; Marshall and Elliott, 1998) and the abundance and distribution of phytoplankton, zooplankton, and ichthyoplankton (Siokou-Frangou et al., 1998; Rautio, 2001; Hsieh et al., 2005; Gogoi et al., 2021). In this study, seven abiotic and biotic factors, including T, S, DO, pH, Chla, Phy, and Zoo, significantly structured the ichthyoplankton assemblages in Sansha Bay, and temperature was also the dominant factor and then salinity and Chla.

Fish spawning and nursing behavior could be affected by spatial and temporal distribution of preys (Cushing, 1990).

TABLE 5 | The interannual variations of the number of species and the average density (ind./m^3) (mean ± SD, n = 4 in 1990 and 2007, n = 2 in 2008, and n = 6 in 2010 and 2019) of fish eggs and larvae throughout the years in Sansha Bay of Fujian Province, China.

Survey year (survey month)	No. of species	Detection rate at species level	Average egg density (ind./m^3)	Average larva density (ind./m^3)	Sampling stations	Sampling methods	References
1990 (Feb, May, Aug, and Nov)	26	69.2%	0.042 ± 0.031*	0.036 ± 0.041*	16	Vertical Horizontal	Dai, 2006
2007 (Feb, May, Aug, and Nov)	23	39.1%	0.365 ± 0.670*	0.490 ± 0.765*	12	Vertical Horizontal	Wang et al., 2010
2008 (May and Nov)	35	51.5%	4.920 ± 9.377*	0.175 ± 0.253*	14	Vertical Horizontal	Shen, 2011
2010 (May, Jun, and Aug–Nov)	40* 31**	67.5%* 74.2%**	1.310 ± 1.2058* 4.331 ± 8.564**	0.928 ± 0.940* 0.131 ± 0.171**	41	Vertical Horizontal	Xu, 2018
2019 (Apr–Sept)	31* 58**	87.10%* 87.93%**	0.457 ± 0.305* 0.855 ± 0.686**	0.118 ± 0.073* 0.024 ± 0.011**	25	Vertical Horizontal	This study

**Data from vertical tow net.*
***Data from horizontal tow net.*

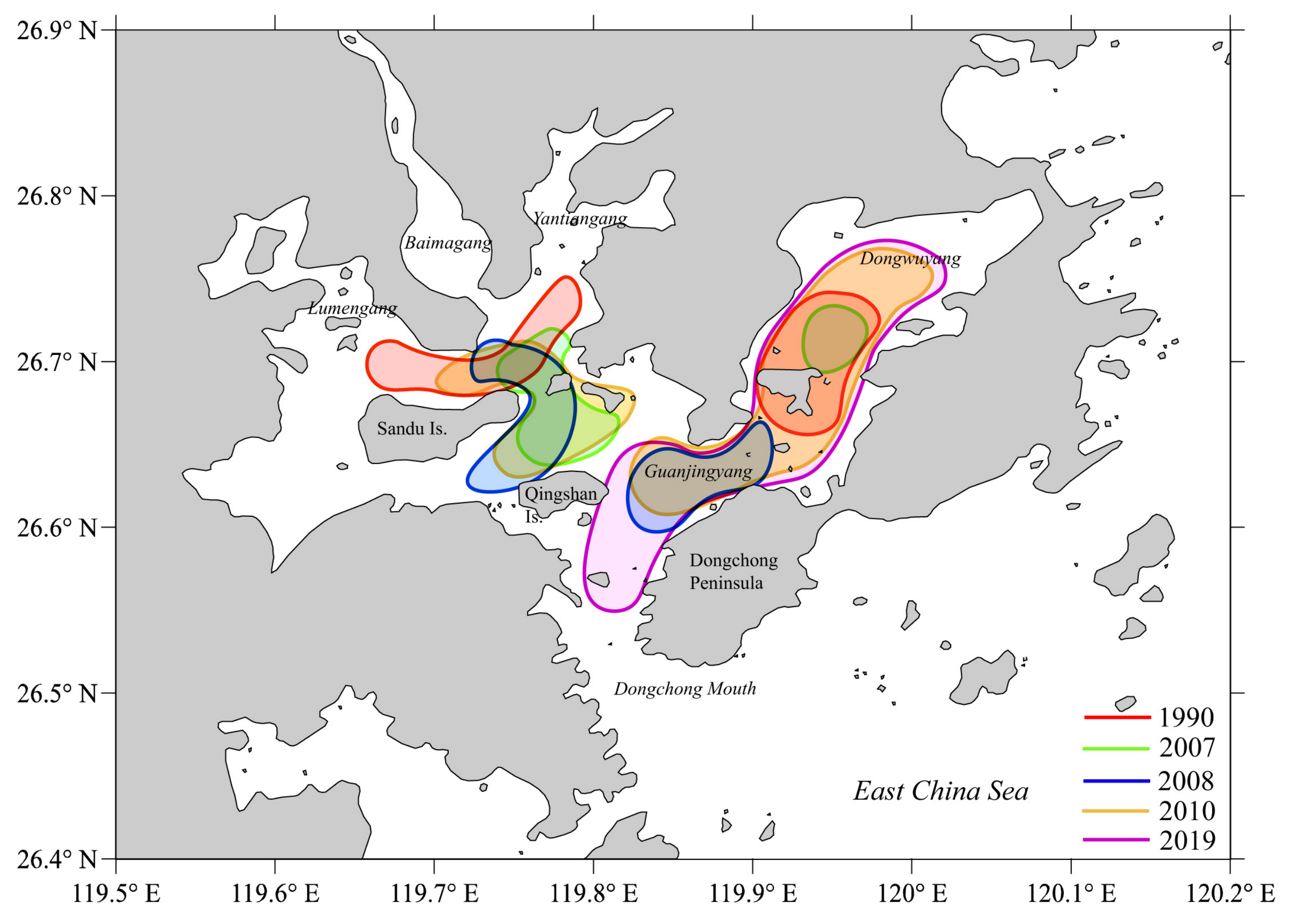

FIGURE 8 | The high ichthyoplankton density areas from 1990 to 2019 in Sansha Bay of Fujian Province, China.

Besides, food suitability and availability have been proposed as major factors to determine the survival of early-stage larval fishes, e.g., the main foods of fish larvae are phytoplankton (diatoms, flagellates, and ciliates) and zooplankton (pelecypods, euphausiids, Mysidacea, and copepods) (Govoni et al., 1983; MacKenzie et al., 1996; Platt et al., 2003; Guevara et al., 2005; Nakagawa et al., 2007; Ajiboye et al., 2011; Abo-Taleb, 2019). The dominant species of phytoplankton and zooplankton in May and June (peak spawning season) in Sansha Bay were mainly from Bacillariophyta and copepods (Liu et al., 2020a), all of which may play important roles as feeds for fish larvae and young juveniles to further impact the distribution pattern of ichthyoplankton in Sansha Bay.

Chla, representing the primary productivity, is associated with phytoplankton and zooplankton abundance and always has a positive correlation with phytoplankton abundance

(Felip and Catalan, 2000). In this study, the red tide forming species *Noctiluca scintillans* (Macartney) (Kofoid and Swezy, 1921) bloomed in May 2019, which was without chloroplast and purely phagotrophic (Balch and Haxo, 1984; Zhang et al., 2020), resulting in apparently high abundance of phytoplankton and low concentration of Chla (Nakamura, 1998). Moreover, *N. scintillas* can feed on phytoplankton, zooplankton, and even fish eggs and larvae (Nakamura, 1998; Quevedo et al., 1999; Umani et al., 2004); therefore, the impact of biotic factor Chla related with *N. scintillas* might have a negative correlation with Phy, Zoo, and certain ichthyoplankton species (**Figure 7**).

Although seven abiotic and biotic variables were integrated for analysis, only 18.1% of the variability observed in ichthyoplankton was explained (**Table 3**), which suggested that other factors could influence the ichthyoplankton assemblage, e.g., ocean currents, substrates, and human activities (Bascompte et al., 2005; Lopes et al., 2006; Daskalov et al., 2007; Muhling et al., 2008; Vilchis et al., 2009; Zhou et al., 2011; Vandendriessche et al., 2016).

CONCLUSION

In this study, 60 taxa ichthyoplankton were identified from horizontal and vertical tows by combining DNA barcoding and external morphology from April to September 2019 in Sansha Bay of Fujian Province, China. Among these, 52 taxa were identified at species level, 5 taxa at genus, and 3 taxa at family level. The 10 dominant species were from Engraulidae (*S. tenuifilis* and *Stolephorus commersonnii*), Serranidae (*E. akaara*), Leiognathidae (*Photopectoralis bindus* and *Nuchequula nuchalis*), Sciaenidae (*N. albiflora* and *C. lucidus*), and Sparidae (*P. major* and *A. schlegelii*). The temporal distribution of ichthyoplankton were divided into five assemblages, namely, April, May, June, July, and August−September with a high density occurred mainly in Guanjingyang and along the Dongchong Peninsula coastline into Dongwuyang. The temporal and spatial patterns were closely related to both abiotic and biotic factors. Temperature was the main factor influencing the assemblage structure and then Chla and salinity. Other factors, such as ocean currents, substrates, and other anthropogenic activities still need further investigation. Currently, little is explored to understand the entire life cycles of the dominant and commercially important fish species in Sansha Bay and its adjacent waters, the East China Sea. To achieve effective fishery stock management, understanding different life stages and their habitat uses, and the connectivity among different life stages are highly recommended.

DATA AVAILABILITY STATEMENT

The datasets presented in this study can be found in online repositories. The names of the repository/repositories and accession number(s) can be found below: NCBI (accession: OK012006-OK012065).

AUTHOR CONTRIBUTIONS

YJ wrote the first draft and organized the sampling trips. YJ, B-AL, H-YH, G-MD, ML, and L-MZ conducted the sample collection. B-AL, H-YH, and GZ performed the molecular analysis. YJ, B-AL, and L-TY performed the data analyses. ML and L-MZ revised the manuscript. All authors contributed to the article preparation and approved the submission.

FUNDING

This work was supported by the National Key Research and Development Program of China (2018YFD0900702-3 and 2018YFC1406501) and the Fujian Province Ocean and Fisheries Bureau of China (contract no. [3500]HTZB[GK]2019007-1-1). The funders had no role in data collection and analysis, decision to publish, or preparation of the manuscript.

ACKNOWLEDGMENTS

The authors thank Zhe-ying Lin, Qing Xu, Qing-qiang Ren, Jia-hao Song, Lv-ping Fang, Qiong Wang, and Wei-di Yang for sample collection and laboratory work and two reviewers for helpful comments.

SUPPLEMENTARY MATERIAL

The Supplementary Material for this article can be found online at: https://www.frontiersin.org/articles/10.3389/fmars.2021.758089/full#supplementary-material

REFERENCES

Abo-Taleb, H. (2019). "Importance of plankton to fish community," in *Biological Research in Aquatic Science*, ed. Y. Bozkurt (London: IntechOpen), 83–92.

Ahlstrom, E. H. (1959). Vertical distribution of pelagic fish eggs and larvae off California and Baja California. *Fish. Bul.* 161, 107–146.

Ajiboye, O. O., Yakubu, A. F., Adams, T. E., Olaji, E. D., and Nwogu, N. A. (2011). A review of the use of copepods in marine fish larviculture. *Rev. Fish. Biol. Fish.* 21, 225–246. doi: 10.1007/s11160-010-9169-3

Arora, J., and Mehra, N. K. (2009). Seasonal dynamics of zooplankton in a shallow eutrophic man-made hyposaline lake in Delhi (India): role of environmental factors. *Hydrobiologia* 626, 27–40. doi: 10.1007/s10750-009-9735-7

Auth, T. D., Brodeur, R. D., and Fisher, K. M. (2007). Diel variation in vertical distribution of an offshore ichthyoplankton community off the Oregon coast. *Fish. Bul.* 105, 313–326. doi: 10.1016/j.dsr.2016.05.014

Bailey, K. M., and Houde, E. D. (1989). Predation on eggs and larvae of marine fishes and recruitment problem. *Adv. Mar. Biol.* 25, 1–83. doi: 10.1016/S0065-2881(08)60187-X

Balch, W. M., and Haxo, F. T. (1984). Spectral properties of *Noctiluca miliaris* Suriray, a heterotrophic dinoflagellate. *J. Plankton. Res.* 6, 515–525. doi: 10.1093/plankt/6.3.515

Bascompte, J., Melián, C. J., and Sala, E. (2005). Interaction strength combinations and the overfishing of a marine food web. *Proc. Natl. Acad. Sci. U.S.A.* 102, 5443–5447.

Becker, R. A., Sales, N. G., Santos, G. M., Santos, G. B., and Carvalho, D. C. (2015). DNA barcoding and morphological identification of neotropical ichthyoplankton from Upper Paraná and São Francisco. *J. Fish Biol.* 87, 159–168. doi: 10.1111/jfb.12707

Bui, A. O. V., Ouellet, P., Castonguay, M., and Brêthes, J.-C. (2010). Ichthyoplankton community structure in the northwest Gulf of St. Lawrence (Canada): past and present. *Mar. Ecol. Prog. Ser.* 412, 189–205.

Chu, Y. (1985). *The Fishes of Fujian Province (Part II)*. Fujian: Fujian Science and Technology Press.

Chu, Y., Lo, Y., and Wu, H. (1963). *A Study on the Classification of the Sciaenoid Fishes of China, with Description of New Genera and Species*. Shanghai: Science and Technology Press.

Chu, Y., and Wu, H. (1985). "Sciaenidae," in *The Fishes of Fujian Province (Part II)*, ed. Y. Chu (Fujian: Fujian Science and Technology Press), 101–136.

Clarke, K. R., and Gorley, R. N. (2006). *PRIMER v6: User Manual/Tutorial.* Plymouth: PRIMER-E.

Clarke, K. R., Gorley, R. N., Somerfield, P. J., and Warwick, R. M. (2014). *Change in Marine Communities: An Approach to Statistical Analysis and Interpretation*. Plymouth: PRIMER-E.

Costa, M. J., Cabral, H. N., Drake, P., Economou, A. N., Fernandez-Delgado, C., Gordo, L., et al. (2002). "Chapter 3: recruitment and production of commercial species in estuaries," in *Fishes in Estuaries*, eds M. Elliott and K. Hemingway (Oxford: Blackwell Sciences Ltd), 54–123.

Curran, M. C., Wiggins, J. J., and Wilber, D. H. (2021). Flatfish habitat use of a small southeastern US Tidal Creek: long- and short-term occupancy patterns. *Estuar. Coast.* 44, 1547–1556.

Cushing, D. H. (1990). Plankton production and year-class strength in fish populations: an update of the match/mismatch hypothesis. *Adv. Mar. Biol.* 26, 249–293. doi: 10.1016/s0065-2881(08)60202-3

Dai, Y. (2006). Distribution of fish eggs, larva and juveniles in Sansha Bay. *Fujian J. Oceanogr. Taiwan* 25, 256–261.

Daskalov, G. M., Grishin, A. N., Rodionov, S., and Mihneva, V. (2007). Trophic cascades triggered by overfishing reveal possible mechanisms of ecosystem regime shifts. *Proc. Natl. Acad. Sci. U.S.A.* 104, 10518–10523. doi: 10.1073/pnas.0701100104

Ding, L. (2013). *Marine Algal Flora of China*, Vol. 4. Beijing: Science Press.

Downie, A. T., Illing, B., Faria, A. M., and Rummer, J. L. (2020). Swimming performance of marine fish larvae: review of a universal trait under ecological and environmental pressure. *Rev. Fish Biol. Fish.* 30, 93–98. doi: 10.1007/s11160-019-09592-w

Felip, M., and Catalan, J. (2000). The relationship between phytoplankton bivolume and chlorophyll in a deep oligotrophic lake: decoupling in their spatial and temporal maxima. *J. Plankton. Res.* 22, 91–105. doi: 10.1093/plankt/22.1.91

Fodrie, F. J., Heck, K. L. Jr., Powers, S. P., Graham, W. M., and Robinson, K. L. (2010). Climate-related, decadal-scale assemblage changes of seagrass-associated fishes in the northern Gulf of Mexico. *Glob. Change Biol.* 16, 48–59.

Folmer, O., Black, M., Hoeh, W., Lutz, R., and Vrijenhoek, R. (1994). DNA primers for amplification of mitochondrial cytochrome c oxidase subunit I from diverse metazoan invertebrates. *Mol. Mar. Biol. Biotech.* 3, 294–299.

GB/T 12763.6 (2007). *Specifications for Oceanographic Survey-Part 6: Marine Biological Survey*. Beijin: Standards Press of China.

Gibson, R. N., Ansell, A. D., and Robb, L. (1993). Seasonal and annual variations in abundance and species composition of fish and macrocrustacean communities on a Scottish sandy beach. *Mar. Ecol. Prog. Ser.* 98, 89–105.

Gogoi, P., Das, S. K., Sarkar, S. D., Chanu, T. N., Manna, R. K., Sengupta, A., et al. (2021). Environmental factors driving phytoplankton assemblage pattern and diversity: insights from Sundarban eco-region, India. *Ecohydro. Hydrobiol.* 21, 351–367. doi: 10.1016/j.ecohyd.2020.09.005

Govoni, J. J., Hoss, D. E., and Chester, A. J. (1983). Comparative feeding of three species of larval fishes in the Northern Gluf of Mexico: *Brevootia patronus*, *Leiostomus xanthurus*, and *Micropogonias undulatus*. *Mar. Ecol. Prog. Ser.* 13, 189–199. doi: 10.3354/meps013189

Graham, M. H. (2003). Confronting multicollinearity in ecological multiple regression. *Ecology* 84, 2809–2815. doi: 10.1890/02-3114

Guevara, M., Lodeiros, C., Donato, M. D., Graciani, C., and Freites, L. (2005). Nutritional quality of *Metamysidopsis insularis* Brattegard (Crustacea: Mysidacea). *Aquac. Nurtr.* 11, 315–319.

Guo, Y. (2003). *Marine Algal Flora of China*, Vol. 5. Beijing: Science Press.

Hamre, K., Yúfera, M., Rønnestad, I., Boglione, C., Conceição, L. E. C., and Izquierdo, M. (2013). Fish larval nutrition and feed formulation: knowledge gaps and bottlenecks for advances in larval rearing. *Rev. Aquac.* 5, S26–S58. doi: 10.1111/j.1753-5131.2012.01086.x

Harada, A. E., Lindgren, E. A., Hermsmeier, M. C., Rogowski, P. A., Terrill, E., and Burton, R. S. (2015). Monitoring spawning activity in a southern California marine protected area using molecular identification of fish eggs. *PLOS One* 10:e0134647. doi: 10.1371/journal.pone.0134647

Hou, G., Chen, W.-T., Lu, H.-S., Cheng, F., and Xie, S.-G. (2017). Developing a DNA barcode library for perciform fishes in the South China Sea: species identification, accuracy and cryptic diversity. *Mol. Ecol. Resou.* 00, 1–11. doi: 10.1111/1755-0998.12718

Hou, G., Wang, J., Liu, L., Chen, Y., Pan, C., Lin, J., et al. (2021a). Assemblage structure of the ichthyoplankton and its relationship with environmental factors in spring and autumn off the Pearl River estuary. *Front. Mar. Sci.* 8:732970. doi: 10.3389/fmars.2021.732970

Hou, G., Chen, Y., Wang, S., Wang, J., Chen, W., and Zhang, H. (2021b). Formalin-fixed fish larvae could be effectively identified by DNA barcodes: a case study on thousands of specimens in South China Sea. *Front. Mar. Sci.* 8:634575. doi: 10.3389/fmars.2021.634575

Hsieh, C.-H., Chen, C.-S., and Chiu, T.-S. (2005). Composition and abundance of copepods and ichthyoplankton in Taiwan Strait (western North Pacific) are influenced by seasonal monsoons. *Mar. Freshw. Res.* 56, 153–161. doi: 10.1071/MF04058

Hsieh, H.-Y., Lo, W.-T., Chen, H.-H., and Meng, P.-J. (2016). Larval fish assemblages and hydrographic characteristics in the coastal waters of southwestern Taiwan during non- and post-typhoon summers. *Zool. Stud.* 55, 18. doi: 10.6620/ZS.2016.55-18

Huang, D., Zhang, X., Jiang, Z., Arbi, I., Jiang, X., Huang, X., et al. (2017). Seasonal fluctuations of ichthyoplankton assemblage in the northeastern South China Sea influenced by the Kuroshio intrusion. *J. Geophys. Res. Oceans* 122, 7253–7266. doi: 10.1002/2017JC012906

Hubert, N., Espiau, B., Meyer, C., and Planes, S. (2015). Identifying the ichthyoplankton of a coral reef using DNA barcodes. *Mol. Ecol. Resour.* 15, 57–67. doi: 10.1111/1755-0998.12293

Kerr, M., Browning, J., Bønnelycke, E., Zhang, Y., Hu, C., Armenteros, M., et al. (2020). DNA barcoding of fish eggs collected off northwestern Cuba and across the Florida Straits demonstrates egg Transport by mesoscale eddies. *Fish. Oceanogr.* 29, 340–348. doi: 10.1111/fog.12475

Ko, H.-L., Wang, Y.-T., Chui, T.-S., Lee, M.-A., Leu, M.-Y., Chang, K.-Z., et al. (2013). Evaluating the accuracy of morphological identification of larval fishes by applying DNA barcoding. *PLoS One* 8:e53451. doi: 10.1371/journal.pone.0053451

Lechner, A., Keckeis, H., and Humphries, P. (2016). Patterns and processes in the drift of early developmental stages of fish in rivers: a review. *Rev. Fish Biol. Fish.* 26, 471–498. doi: 10.1007/s11160-016-9437-y

Li, K., Yin, J., Huang, L., and Lin, Z. (2014). Seasonal variations in diversity and abundance of surface ichthyoplankton in northern South China Sea. *Acta Oceanol. Sin.* 33, 145–154. doi: 10.1007/s13131-014-0533-3

Lin, B. A., Wang, Y. W., Li, J. L., Kang, B., Fang, L. P., Zheng, L. M., et al. (2020). First records of small juveniles of the red drum Sciaenops ocellatus (Linnaeus, 1766) in a subtropical mangrove habitat of China. *BioInvasions Rec.* 9, 96–102. doi: 10.3391/bir.2020.9.1.13

Lin, J., You, Y., and Liu, G. (2018). Numerical research of the tidal currents in Sansha Bay. *J. Fish. Res.* 40, 413–424. doi: 10.14012/j.cnki.fjsc.2018.06.001

Lin, N., Jiang, Y., Yuan, X., Ling, J., Yang, L., and Li, S. (2013). Reproductive biology of Nibea albiflora in Xiangshan Bay. *Mar. Fish.* 35, 389–395.

Lin, Y. (2009). *Marine Algal Flora of China*, Vol. 6. Beijing: Science Press.

Liu, H., Mao, X., and Wang, B. (1998). A preliminary study on technique for fully artificial breeding of red drum Sciaenops ocellatus. *J. Fish. Sci. China* 5, 114–116.

Liu, M., and Sadovy de Mitcheson, Y. (2008). Profile of a fishery collapse: why mariculture failed to save the large yellow croaker. *Fish Fish.* 9, 219–242. doi: 10.1111/j.1467-2979.2008.00278.x

Liu, M., Jiang, Y., Zheng, L. M., Yang, W. D., and Chen, D. (2020a). *Large Yellow Croaker (Larimichthys crocea) Stock Assessment in its Spawning Protection Area*. Xiamen: Xiamen University, 216.

Liu, M., Cheng, J.-H., Nguyen Van, Q., Sasaki, K., Hoshino, K., Sakai, T., et al. (2020b). *Larimichthys crocea. The IUCN Red List of Threatened Species 2020, e.T49182559A49239394*.

Llopiz, J. K., Cowen, R. K., Hauff, M. J., Ji, R., Munday, P. L., Muhling, B. A., et al. (2014). Early life history and fisheries oceanography: new questions in a changing world. *Oceanography* 27, 26–41. doi: 10.5670/oceanog.2014.84

Lopes, R. M., Katsuragawa, M., Dias, J. F., Montú, M. A., Muelbert, J. H., Gorri, C., et al. (2006). Zooplankton and ichthyoplankton distribution on the southern Brazilian shelf: an overview. *Sci. Mar.* 70, 189–202. doi: 10.3989/scimar.2006.70n2189

MacKenzie, B., John, M. S., and Wieland, K. (1996). Eastern Baltic cod: perspectives from existing data on processes affecting growth and survival of eggs and larvae. *Mar. Ecol. Prog. Ser.* 134, 265–281. doi: 10.3354/meps134265

Madeira, D., Madeira, C., Costa, O. M., Vinagre, C., Pörtner, H.-O., and Diniz, M. S. (2020). Different sensitivity to heatwaves across the life cycle of fish reflects phenotypic adaptation to environmental niche. *Mar. Environ. Res.* 162, 105192. doi: 10.1016/j.marenvres.2020.105192

MARA (2019). *China Fishery Statistical Yearbook 2019*. Beijing: China Agriculture Press.

Margalef, R. (1958). Information theory in ecology. *Gen. Syst.* 3, 36–71.

Marshall, S., and Elliott, M. (1998). Environmental influences on the fish assemblage of the Humber estuary. *U.K. Estuar. Coast. Shelf Sci.* 46, 175–184. doi: 10.1006/ecss.1997.0268

McCain, J. S. P., Cull, D. J., Schneider, D. C., and Lotze, H. K. (2016). Long-term shift in coastal fish communities before and after the collapse of Atlantic cod (*Gadus morhua*). *ICES J. Mar. Sci.* 73, 1415–1426. doi: 10.1093/icesjms/fsv216

MOA (2010–2018). *China Fishery Statistical Yearbooks 2010–2018*. Beijing: China Agriculture Press.

Muhling, B. A., Beckley, L. E., Koslow, J. A., and Pearce, A. F. (2008). Larval fish assemblages and water mass structure off the oligotrophic south-western Australian coast. *Fish. Oceanogr.* 17, 16–31. doi: 10.1111/j.1365-2419.2007.00452.x

Nakagawa, Y., Senoo, S., and Miyashita, S. (2007). Protozoa and diatom as primary sources for larvae of the Blue Spotted Snapper *Lutjanus rivulatus*. *Aquacult. Sci.* 55, 125–300.

Nakamura, I., and Parin, N. V. (1993). *FAO Species Catalogue: Snake Mackerels and Cutlass Fishes of the World (Families Gempylidae and Trichiuridae)*, Vol. 125. Rome: Food and Agriculture Organization of the United Nations, 99–107.

Nakamura, Y. (1998). Biomass, feeding and production of *Noctiluca scintillans* in the Seto Inland Sea. *Japan. J. Plankton. Res.* 20, 2213–2222. doi: 10.1093/plankt/20.11.2213

Nelson, J. S., Grande, T. C., and Wilson, M. V. H. (2016). *Fishes of the World*, 5th Edn. Hoboken, NJ: John Wiley & Sons, Inc.

Oeberst, R., Klenz, B., Gröhsler, T., Dichey-Collas, M., Nash, R. D. M., and Zimmermann, C. (2009). When is year-class strength determined in western Baltic herring? *ICES J. Mar. Sci.* 66, 1667–1672. doi: 10.1093/icesjms/fsp143

Olivar, M. P. (1990). Spatial patterns of ichthyoplankton distribution in relation to hydrographic features in the Northern Benguela region. *Mar. Biol.* 106, 39–48. doi: 10.1007/bf02114672

Oliveira, E. C., and Ferreira, E. J. C. (2008). Spawning areas, dispersion and microhabitats of fish larvae in the Anavilhanas Ecological Station, rio Negro, Amazonas State, Brazil. *Neotrop. Ichthyol.* 6, 559–566. doi: 10.1590/s1679-62252008000400003

Ou, Y., Liao, R., Li, J., and Gou, X. (2012). Studies on the spawning period and growth of *Collichthys lucidus* in estuary of Pearl River based on otolith daily annulus. *J. Oceanogr. Taiwan Strait.* 31, 85–88.

Parrish, R. H., Nelson, C. R., and Bakun, A. (1981). Transport mechanisms and reproductive success of fishes in the California current. *Biol. Oceanogr.* 1, 175–203.

Pauly, D., and Pullin, R. S. V. (1988). Hatching time in spherical, pelagic, marine fish eggs in response to temperature and egg size. *Environ. Biol. Fish.* 21, 261–271. doi: 10.1007/bf00004892

Petitgas, P., Rijnsdorp, A. D., Dickey-Collas, M., Engelhard, G. H., Peck, M. A., Pinnegar, J. K., et al. (2013). Impacts of climate change on the complex life cycles of fish. *Fish Oceanogr.* 22, 121–139. doi: 10.1111/fog.12010

Pielou, E. C. (1966). The measurement of diversity in different types of biological collections. *J. Theor. Biol.* 13, 131–144. doi: 10.1016/0022-5193(66)90013-0

Pinkas, L., Oliphant, M. S., and Iverson, I. L. K. (1971). Food habits of albacore, bluefin tuna and bonito in California waters. *Fish Bull.* 152, 1–105. doi: 10.1201/b18714-2

Platt, T., Fuentes-Yaco, C., and Frank, K. T. (2003). Spring algal bloom and larval fish survival. *Nature.* 423, 397–398. doi: 10.1038/423398b

Pombo, L., Elliott, M., and Rebelo, J. E. (2005). Environmental influences on fish assemblage distribution of an estuarine coastal lagoon. *Ria de Aveiro (Portugal). Sci. Mar.* 69, 143–159. doi: 10.15517/rbt.v57i1-2.11293

Quevedo, M., Gonzalez-quiros, R., and Anadon, R. (1999). Evidence of heavy predation by *Noctiluca scintillans* on *Acartia clausi* (Copepoda) eggs off the central Cantabrian coast (NW Spain). *Oceanol. Acta.* 22, 127–131. doi: 10.1016/S0399-1784(99)80039-5

Rakocinski, C. F., Lyczkowski-Shultz, J., and Richardson, S. L. (1996). Ichthyoplankton assemblage structure in Mississippi sound as revealed by canonical correspondence analysis. *Estua. Coast. Shelf Sci.* 43, 237–257. doi: 10.1006/ecss.1996.0067

Ramos, S., Paris, C., and Angélico, M. M. (2017). Larval fish dispersal along an estuarine–ocean gradient. *Can. J. Fish. Aquat. Sci.* 1, 1462–1473. doi: 10.1139/cjfas-2016-0325

Rautio, M. (2001). Zooplankton assemblages related to environmental characteristics in threeline ponds in Finnish Lapland. *Arct. Antarct. Alp. Res.* 33, 289–298. doi: 10.1080/15230430.2001.12003433

Rijnsdorp, A. D., Peck, M. A., Engelhard, G. H., Möllmann, C. and Pinnegar, J. K. (2009). Resolving the effect of climate change on fish populations. *ICES J. Mar. Sci.* 66, 1570–1583. doi: 10.1093/icesjms/fsp056

Rodríguez, J. M., Hernández-León, S., and Barton, E. D. (2006). Vertical distribution of fish larvae in the Canaries-African coastal transition zone in summer. *Mar. Biol.* 149, 885–897. doi: 10.1007/s00227-006-0270-z

Rodriguez, J. M. (2019). Assemblage structure of ichthyoplankton in the NE Atlantic in spring under contrasting hydrographic conditions. *Sci. Rep.* 9:8363. doi: 10.1038/s41598-019-44918-5

Santos, R. V. S., Ramos, S., and Bonecker, A. C. T. (2017). Environmental control on larval stages of fish subject to specific salinity range in tropical estuaries. *Reg. Stud. Mar. Sci.* 13, 42–53. doi: 10.1016/j.rsma.2017.03.010

Shannon, C. E., and Wiener, W. (1963). *The Mathematical Theory of Communication*. Champaign, IL: University of Illinois Press.

Shao, K. T., Yang, R. S., Chen, K. C., and Lee, Y. S. (2001). *An Identification Guide of Marine Fish Eggs from Taiwan*. Taipei: Institute of Zoology, Academia Sinica.

Shen, C. (2011). Species composition and abundance temporal-spatial distribution of fish egg, larvae and juveniles in Sansha Bay of Fujian. *Mar. Fish.* 33, 361–367.

Siokou-Frangou, I., Papathanassiou, E., Lepretre, A., and Frontier, S. (1998). Zooplankton assemblages and influence of environmental parameters on them in a Mediterranean coastal area. *J. Plankton. Res.* 20, 847–870. doi: 10.1093/plankt/20.5.847

Slotwinski, A., Coman, F., and Richardson, A. J. (2014). *Introductory Guide to Zooplankton Identification*. Brisbane, QID: Integrated Marine Observing System.

Šmilauer, P., and Lepš, J. (2014). *Multivariate Analysis of Ecological Data Using CANOCO 5*. Cambridge: Cambridge University Press.

Sun, S., Li, C., Cheng, F., Jin, X., and Yang, B. (2015). *Atlas Of Common Zooplankton of the Chinese Costal Seas*. Beijing: Ocean Press.

Umani, S. F., Beran, A., Parlato, S., Virgilio, D., Zollet, T., Olazabal, A. D., et al. (2004). *Noctiluca scintillans* Macartney in the Northern Adriatic Sea: long-term dynamics, relationships with temperature and eutrophication, and role in the food web. *J. Plankton. Res.* 26, 545–561. doi: 10.1093/plankt/fbh045

Vandendriessche, S., Costa, A. M., and Hostens, K. (2016). "Wind farms and their influence on the occurrence of ichthyoplankton and squid larvae," in *Environmental Impacts of Offshore Wind Farms in the Belgian Part of the North Sea: Environmental impact monitoring reloaded*, eds S. Degraer, R. Brabant, B. Rumes, and L. Vigin (Brussels: Royal Belgian Institute of Natural Sciences), 117–140.

Vilchis, L. I., Balance, L. T., and Watson, W. (2009). Temporal variability of neustonic ichthyoplankton assemblages of the eastern Pacific warm pool: Can community structure be linked to climate variability. *Deep-Sea Res. Part I.* 56, 125–140. doi: 10.1016/j.dsr.2008.08.004

Wan, R. J., and Zhang, R. Z. (2016). *Fish Eggs, Larvae and Juveniles in the Offshore Waters of China and Their Adjacent Waters*. Shanghai: Shanghai Scientific and Technical Publishers.

Wang, B., and Ji, B. (1996). On techniques for rearing fries of *Sciaenops ocellatus*. *Shandong Fish.* 13, 21–23.

Wang, J., Lin, Y., Zhou, M., and Liu, Y. (2010). The ecological distribution of fish eggs and larvae in Sansha Bay, Fujian. *J. Xiamen Univ. (Natural Science)* 49, 116–121.

Wang, X., Liu, Y., and Guo, W. (2019). Evaluation of environmental quality and change trend in Sansha Bay mariculture area in recent ten years. *J. Fish. Res.* 41, 519–525.

Wang, Y. H., Ma, Y., and Tao, B. C. (2006). Effect of temperature and salinity on the hatching rate of Gilthead Seabream, *Sparus aurata. Fish. Mod.* 5, 21–22.

Ward, R. D., Zemlak, T. S., Innes, B. H., Last, P. R., and Hebert, P. D. (2005). DNA barcoding Australia's fish species. *Phil. Trans. R. Soc. B.* 360, 1847–1857. doi: 10.1098/rstb.2005.1716

Woynarovich, E., and Horváth, L. (1984). "Chapter 4: Artificial propagation of finfish," in *The Artificial Propagation of Warm-Water Finfishes-A Manual for Extension. FAO Fish. Tech. Pap. (201)*, (Rome: FAO), 183.

Wu, H. (1985). "Scombridae," in *The Fishes of Fujian Province (Part II)*, ed. Y. Chu (Fujian: Fujian Science and Technology Press), 404–424.

Xu, Z. (2018). *Resources and Environmental Characteristics in Wild Large Yellow Croaker (Larimichthys crocea) Breeding Waters of Guanjingyang*. Beijing: Ocean Press.

Xu, Z., and Chen, J. (2015). Migratory routes of *Trichiurus lepturus* in the East China Sea, Yellow Sea and Bohai Sea. *J. Fish. China* 39, 824–835.

Yu, Z. Y., Lian, Z. S., Zhu, Y. G., Wang, W. Y., and Ni, Z. Q. (1988). "Fishery natural environment and resources," in *Fujian Province Fishery Resources*, ed. Z. Q. Ni (Fujian: Fujian Science and Technology Press), 1–65.

Zhan, W., Luo, B., Chen, R.-Y., Mao, G.-M., Liu, F., Xu, D.-D., et al. (2016). Observation of embryonic larva and juvenile development of small yellow croaker, *Larimichthys polyactis*. *Oceanol. Limnol. Sin.* 47, 1033–1039.

Zhang, G. (2020). *Study on the Diversity and Assemblage Structure of Fish Eggs and Larvae in Daya Bay and Adjacent Waters.* MSc dissertation. Xiamen: Xiamen University.

Zhang, H., Xian, W., and Liu, S. (2015). Ichthyoplankton assemblage structure of spring in the Yangtze Estuary revealed by biological and environmental visions. *PeerJ.* 3, e1186. doi: 10.7717/peerj.1186

Zhang, H., Xian, W., and Liu, S. (2016). Autumn ichthyoplankton assemblage in the Yangtze Estuary shaped by environmental factors. *PeerJ.* 4:e1922. doi: 10.7717/peerj.1922

Zhang, R. Z., Lu, S. F., and Zhao, C. Y. (1985). *Fish Eggs and Larvae in the Offshore Waters of China*. Shanghai: Shanghai Scientific and Technical Publishers.

Zhang, S., Li, C., Cheung, S., Sun, M., Song, S., Guo, W., et al. (2020). Snapshot of peptidomics of the red time forming species Noctiluca scintillans. *Front. Mar. Sci.* 7:569807. doi: 10.3389/fmars.2020.569807

Zhang, W., Zhao, N., Tao, Z., and Zhang, C. (2010). *Illustrated Guide to Marine Planktonic Copepods in China Seas*. Beijing: Science Press.

Zhou, M., Lin, Y., Yang, S., Cao, W., and Zheng, L. (2011). Composition and ecological distribution of ichthyoplankton in eastern Beibu Gulf. *Acta Oceanol. Sin.* 30, 94–105. doi: 10.1007/s13131-011-0095-6

Zhu, X., Liu, D., and Sha, X. (2002). Relationship between community structure of ichthyoplankton and environmental factors in the estuary of Changjiang River in spring. *Sutd. Mar. Sin.* 44, 169–179.

Conflict of Interest: The authors declare that the research was conducted in the absence of any commercial or financial relationships that could be construed as a potential conflict of interest.

frontiers in Marine Science

ORIGINAL RESEARCH
published: 16 December 2021
doi: 10.3389/fmars.2021.806096

Spring Ichthyoplankton Assemblage Structure in the Yangtze Estuary Under Environmental Factors

Yibang Wang[1,2,3], Cui Liang[1,2], Zhaomin Chen[1,2,3], Shude Liu[4], Hui Zhang[1,2,3,5]† and Weiwei Xian[1,2]**

[1] CAS Key Laboratory of Marine Ecology and Environmental Sciences, Institute of Oceanology, Chinese Academy of Sciences, Qingdao, China, [2] Laboratory for Marine Ecology and Environmental Science, Qingdao National Laboratory for Marine Science and Technology, Qingdao, China, [3] University of Chinese Academy of Sciences, Beijing, China, [4] Shandong Hydrobios Resources Conservation and Management Center, Yantai, China, [5] Center for Ocean Mega-Science, Chinese Academy of Sciences, Qingdao, China

Edited by:
Liping Liu,
Shanghai Ocean University, China

Reviewed by:
Sher Khan Panhwar,
University of Karachi, Pakistan
Ming Liu,
Morgan State University,
United States

***Correspondence:**
Hui Zhang
zhanghui@qdio.ac.cn
Weiwei Xian
wwxian@qdio.ac.cn

†Lead corresponding author

Specialty section:
This article was submitted to Marine Fisheries, Aquaculture and Living Resources, a section of the journal Frontiers in Marine Science

Received: *31 October 2021*
Accepted: *29 November 2021*
Published: *16 December 2021*

Citation:
Wang Y, Liang C, Chen Z, Liu S, Zhang H and Xian W (2021) Spring Ichthyoplankton Assemblage Structure in the Yangtze Estuary Under Environmental Factors. Front. Mar. Sci. 8:806096. doi: 10.3389/fmars.2021.806096

Estuaries, where fresh and salty water converge, provide abundant nutrients for ichthyoplankton. Ichthyoplankton, including fish eggs, larvae, and juveniles, are important fishery recruitment resources. The Yangtze Estuary and its adjacent waters comprise a typical large-scale estuary and supply many important fish spawning, feeding, and breeding areas. In this study, 1,291 ichthyoplankton individuals were collected in the Yangtze Estuary in spring, from 2013 to 2020. The aims of the study were to provide detailed information on characteristics of the ichthyoplankton assemblage, explore interannual variation, and evaluate the effects of environmental variables on the temporal variation in assemblage structure. Twenty-six species in seventeen families were identified. The dominant species were *Coilia mystus*, *Chelidonichthys spinosus*, *Engraulis japonicus*, *Hypoatherina valenciennei*, *Larimichthys polyactis*, *Salanx ariakensis*, *Stolephorus commersonnii*, and *Trachidermus fasciatus*. The ichthyoplankton assemblage changed significantly over time, and *Chelidonichthys spinosus* became one of the dominant species. Canonical correspondence analysis showed that temperature and chlorophyll a were the key factors affecting the assemblage structure in the Yangtze Estuary in spring.

Keywords: fish eggs, larvae and juveniles, environmental factors, assemblage structure, interannual variability

INTRODUCTION

Estuaries are semi-closed coastal water bodies that are freely connected to the open sea, in which the seawater is diluted by fresh water produced by land drainage (Day, 1981; Potter et al., 1990). The interactions of physical, chemical, biological, and geological processes lead to complex change processes and a sensitive and unique estuarine environment that differs from adjacent fresh water and marine environments (Luo, 1994; Shan et al., 2004). Estuaries are considered to be among the most productive and nutrient-rich ecosystems on earth, and provide important habitat for a variety of species (Hodgson et al., 2020). Many species complete some or all of their life histories in estuaries, and these areas are particularly important foraging and breeding habitats for many fish species (Sheaves et al., 2015; Xian et al., 2016; Lefcheck et al., 2019). As a result of their unique geographical location, estuaries have been sites of human development for thousands of years

(Limburg, 1999; Lotze, 2010). Currently, about 40% of the world's population lives in coastal areas (Barragán and de Andrés, 2015). More than 90% of economical species, including fish, have been depleted, and biomass is lower than 50% of its historical abundance in some estuaries. The main drivers of this change are resource overexploitation and habitat loss (Lotze et al., 2006).

Ichthyoplankton, including eggs, larvae, and juveniles, are significant stages during the growth and development of fish (Butler et al., 2003; Shan et al., 2004) and are the basis for the sustainable utilization of fishery resources (Miller and Kendall, 2009; Zhang et al., 2015). Although these planktonic stages can be very short, they are the most vulnerable in a fish's life history (Shao et al., 2001; Jiang et al., 2006) and can be strongly affected by environmental variability. The abundance and survival of ichthyoplankton are indicators of available biomass and interannual dynamics of fish populations in the future (Butler et al., 2003; Song et al., 2019). In addition, ichthyoplankton play a significant role in energy transfer in estuarine ecosystems (Wan and Sun, 2006), consuming and converting bioenergy as a key link in aquatic food webs (Wan and Jiang, 2000).

Ichthyoplankton assemblages, species composition, and distribution are affected by the interactions of a range of biotic and abiotic processes (Zhang et al., 2015). Biological factors include the location, timing, and modes of spawning; larval life history and behavior; rates of predation; and feeding (Azeiteiro et al., 2006). Physical factors include salinity (Wang and Zhang, 1998; Wooldridge, 1999; Campfield and Houde, 2011); temperature (Neira and Potter, 1992; Primo et al., 2011; Wang et al., 2017); turbidity (Harris and Cyrus, 1995); dissolved oxygen (Rakocinski et al., 1996); depth (Zhang et al., 2015); light (Shoji et al., 2006); and hydrographic events such as river flow (Taylor, 1982), tides (Chen et al., 1997), currents (Wu, 1989), upwelling (Ramos et al., 2006; Valencia et al., 2019), and winds (Tzeng et al., 2002). Studies of ichthyoplankton provide a foundation for understanding trends in fishery resources, determining spawning sites and cycles, and clarifying fishing mechanisms; they can also be used to monitor ecosystem health.

The Yangtze Estuary is the link between the Yangtze River and the East China Sea. The estuary is influenced by fresh water from the Yangtze River, as well as the Yellow Sea cold water mass and the Taiwan warm current. The estuary is generally considered to be important nursery habitat used by many fishes to reproduce, forage, and grow (Luo and Shen, 1994). Although researchers have previously investigated ichthyoplankton composition and distribution in the Yangtze Estuary and the relationships between ichthyoplankton assemblages and environmental factors, the duration of these studies was short (Yang et al., 1990; Zhu et al., 2002; Jiang et al., 2006; Liu et al., 2008; Zhang et al., 2019) or discontinuous (Zhang et al., 2015, 2016). A clear understanding of how the physical and chemical characteristics of the Yangtze Estuary affect ichthyoplankton assemblages is still lacking.

The present study was based on consecutive survey data from spring 2013 to 2020. The aims of the study were to provide detailed information on the characteristics of the ichthyoplankton assemblage in the Yangtze Estuary in spring, explore interannual variability in ichthyoplankton assemblages, and evaluate the effects of environmental variables on temporal variations in assemblage structure.

MATERIALS AND METHODS

Data Source

Forty stations were established in the Yangtze Estuary (30°45′-32°00′ N, 121°00′-123°20′ E), where the biological and oceanographic data were collected in eight springs (05/2013, 05/2014, 05/2015, 05/2016, 05/2017, 05/2018, 05/2019, 05/2020) (**Figure 1**).

In total, 320 ichthyoplankton samples were collected by surface tows using a plankton net (0.8 m mouth diameter, 2.8 m length, 0.505 mm mesh size) equipped with a flow meter. At each station, the net was towed against the tidal flow for 10 min at a depth of 0.5 m from the surface, with a towing speed of approximately 2–3 knots. After completion of each tow, the nets were cleaned and the samples were fixed and preserved in 5% buffered formaldehyde–seawater solution.

The geographical locations of sampling stations were determined using GPS (Magellan 315) (Zhang et al., 2016). A conductivity, temperature, and depth device (CTD) was used to measure depth (D), salinity (S), and temperature (T). Other environmental indicators, including dissolved oxygen (DO), pH, total phosphorus (TP), total nitrogen (TN), suspended particulate matter (SPM), chemical oxygen demand (COD), and chlorophyll *a* (Chla), were determined in the study according to GB/T 12763-2007 specifications for oceanographic surveys (Standardization Administration of China (SAC), 2007).

Data Analysis

Ichthyoplankton were identified in the laboratory to the lowest possible taxonomic level according to their morphological characteristics. Numerical density for each species was standardized to catch per unit effort (CPUE) as abundance per tow every 10 min.

The dominant species were determined using the index of relative importance (IRI) (Zhu et al., 2002), calculated as

$$IRI = N \times 100\% \times F \times 100\%,$$

where N 100% and F 100% are the relative abundance and frequency of occurrence, respectively. The IRI of the dominant species should be greater than 100.

To determine the significance of interannual trends in assemblage structure from 2013 to 2020, non-parametric ANOSIM analysis was performed based on a Bray–Curtis similarity matrix calculated using log(x + 1) transformed data (Clarke and Warwick, 2001). R-statistic values of paired comparisons provided by ANOSIM were used to determine differences between groups. R values close to 1 indicate that the differences between groups are greater than those within groups, and R values close to 0 indicate little difference between groups.

The ichthyoplankton assemblage structure and its relationship with environmental factors was analyzed by canonical correspondence analysis (CCA) (CANOCO

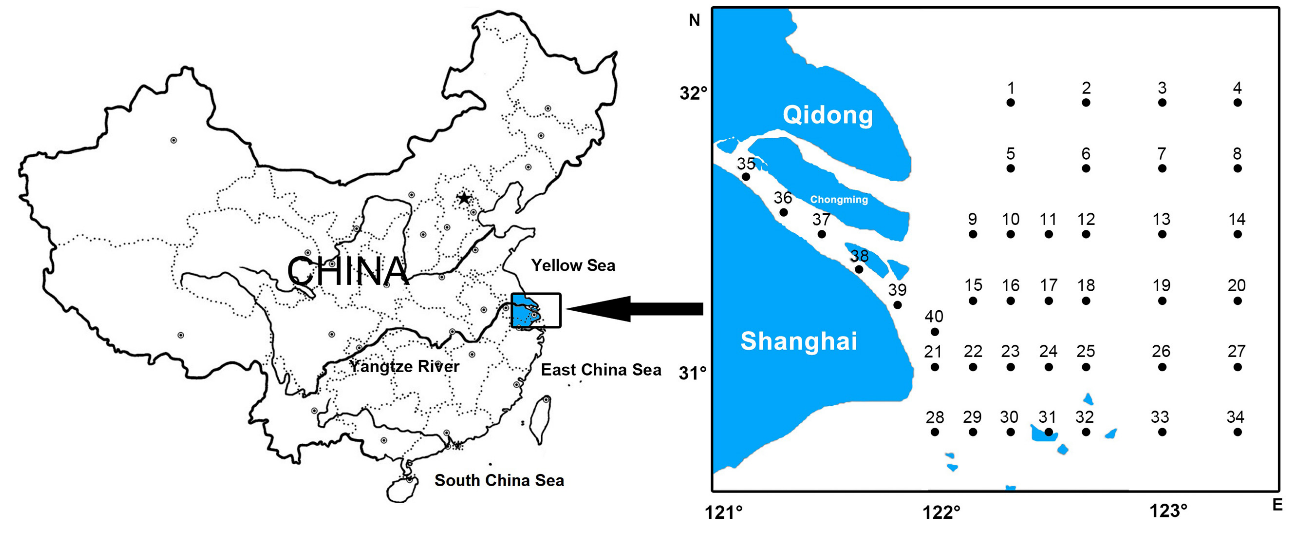

FIGURE 1 | Location of study area and sampling stations in the Yangtze Estuary from 2013 to 2020.

Software, version 5.0). Only species that occurred in $>0.5\%$ of the catches were included in the analysis. Fourteen species found between 2013 and 2020 were included in the analyses. The species abundance data were $\lg(x + 1)$ transformed to reduce the dominance effects of some species (Clarke and Warwick, 2001; Zhang et al., 2015). These 14 species and 10 environmental factors were used in the CCA.

RESULTS

Ichthyoplankton Composition

In total, 1,291 ichthyoplankton individuals, belonging to 26 species in 17 families, were captured in the Yangtze Estuary in spring 2013–2020. The scientific names, family, ecological guilds, and IRI values for the assemblages are shown in **Table 1**. The dominant species were *Coilia mystus*, *Chelidonichthys spinosus*, *Engraulis japonicus*, *Hypoatherina valenciennei*, *Larimichthys polyactis*, *Salanx ariakensis*, *Stolephorus commersonnii*, and *Trachidermus fasciatus*. Most of the species with low abundance were collected occasionally.

Interannual Variation of Assemblage Structure

The assemblage structure changed significantly in the Yangtze Estuary according to the IRI values for spring 2013–2020 (**Table 2**). Although *Engraulis japonicus* was always the dominant species in the Yangtze Estuary and adjacent waters, the composition of the other dominant species changed significantly, highlighted by the shift in the relative abundances of *Coilia mystus* and *Chelidonichthys spinosus*. The assemblage composition based on presence–absence methods varied among years and the average dissimilarity among years was very high (**Table 3**).

Ichthyoplankton Assemblages and Environmental Variables

The CCA results are shown in **Table 4**. Eigenvalues (0–1) indicate the importance of the CCA axes. The sum of all canonical eigenvalues and unconstrained eigenvalues were 1.338 and 7.729, respectively. The former only accounted for 17.31% of the latter, indicating the restrictive effect of building environmental relationships into the CCA model. The eigenvalues of the first four axes were 0.362 (CCA 1), 0.334 (CCA 2), 0.233 (CCA 3), and 0.167 (CCA 4) in the present study. The eigenvalues of the first two axes were moderately high, with correlation coefficients of 0.716 and 0.646, whereas those of the latter two were relatively low (<0.3). Consequently, the results for the first two axes were plotted (**Figure 2**), which explained 9.01 and 64.62% of the cumulative percentage variance of species and species–environment, respectively (**Table 4**).

On the basis of the Monte Carlo tests of F-ratios ($P < 0.05$), T and Chla were the most significant environmental variables affecting the ichthyoplankton assemblages (**Table 5**). In addition to these variables, the other eight environmental variables were evaluated by their inter-set correlations. There are two types of scores in this plot. (1) Environmental variable arrows, where each arrow points in the direction in which the value of the variable increases most sharply. The length of the arrow represents the strength of the environmental variable on the axis. The angle between arrows represents the correlation between the variables. More accurately, the approximate correlation between two environmental variables can be found by projecting the arrow of one variable onto an imaginary line running along the arrow direction of the other. (2) Species symbols: the distance between symbols is similar to the difference in the distribution of the relative abundance of these species in the sample, measured by chi-square distance. Adjacent points correspond to species that often occur at the same time. The species symbol can be projected vertically onto the line above the arrow of a

TABLE 1 | The basic ichthyoplankton information in the Yangtze Estuary in spring 2013–2020.

Family	Species	Abbreviation	Ecological guilds	Index of relative importance (IRI)							
				2013	2014	2015	2016	2017	2018	2019	2020
Atherinidae	*Hypoatherina valenciennei*	*Hv*	Coastal assemblage	100.86							
Clupeidae	*Sardinella zunasi*	*Sz*	Offshore assemblage			10.00			10.00		
Cottidae	*Trachidermus fasciatus*	*Tf*	Estuary assemblage	2.16	127.36						
Engraulidae	*Coilia mystus*	*Cm*	Estuary assemblage	378.24	1745.28	2.50			2.50		40.00
Engraulidae	*Coilia nasus*	*Cn*	Estuary assemblage				3.08	92.59		1.97	
Engraulidae	*Engraulis japonicus*	*Ej*	Offshore assemblage	1793.59		70.00	370.37	583.33	350.00	1970.47	665.00
Engraulidae	*Stolephorus commersonnii*	*Sc*	Coastal assemblage	18.01		35.00		27.78	35.00	236.22	
Engraulidae	*Setipinna tenuifilis*	*St*	Estuary assemblage			10.00		18.52	10.00		
Engraulidae	*Thryssa kammalensis*	*Tk*	Coastal assemblage					4.63			
Hapalogenyidae	*Hapalogenys analis*	*Ha*	Offshore assemblage	0.36							
Hemiramphidae	*Hyporhamphus sajori*	*Hs*	Estuary assemblage							15.75	5.00
Liparidae	*Liparis tanakae*	*Lt*	Offshore assemblage				3.09			1.97	
Lobotidae	*Hapalogenys kishinouyei*	*Hk*	Offshore assemblage								20.00
Salangidae	*Salanx ariakensis*	*Sar*	Estuary assemblage			150.00	870.37	9.26	187.50		15.00
Sciaenidae	*Larimichthys polyactis*	*Lp*	Offshore assemblage	90.06	7.08	250.00		74.07	250.00		5.00
Sciaenidae	*Pennahia argentata*	*Pa*	Offshore assemblage								5.00
Scombridae	*Scomber japonicus*	*Sj*	Offshore assemblage	1.44							
Sebastidae	*Sebastiscus marmoratus*	*Sm*	Offshore assemblage							1.97	
Sebastidae	*Sebastes schlegelii*	*Ss*	Offshore assemblage					4.63			
Synanceiidae	*Minous monodactylus*	*Mm*	Offshore assemblage			2.50			2.50		70.00
Syngnathidae	*Syngnathus acus*	*Sac*	Coastal assemblage					4.63			5.00
Synodontidae	*Harpadon nehereus*	*Hn*	Coastal assemblage			7.50	6.17	13.89	7.50		
Tetraodontidae	*Takifugu rubripes*	*Tr*	Estuary assemblage							11.81	
Triglidae	*Chelidonichthys spinosus*	*Cs*	Coastal assemblage		9.43	180.00	74.07	111.11	180.00	251.97	275.00
Xenocyprididae	*Pseudolaubuca engraulis*	*Pe*	Estuary assemblage			2.50			2.50		
Zoarcidae	*Zoarces elongatus*	*Ze*	Coastal assemblage			2.50			2.50		

TABLE 2 | Dominant species determined by index of relative importance (IRI) in the Yangtze Estuary in spring 2013–2020.

Species	2013	2014	2015	2016	2017	2018	2019	2020
Coilia mystus	378.24	1745.28						
Chelidonichthys spinosus			180.00		111.11	180.00	251.97	275.00
Engraulis japonicus	1793.59			370.37	583.33	350.00	1970.47	665.00
Hypoatherina valenciennei	100.86							
Larimichthys polyactis			250.00			250.00		
Salanx ariakensis			150.00	870.37		187.50		
Stolephorus commersonnii							236.22	
Trachidermus fasciatus		127.36						

specific environmental variable. These predictions can be used to approximate the optimal value of an environmental variable for a single species. The projection points for the species are arranged in the order of increasing value of the predictive variable. According to these rules, some environmental variables were inferred to be important correlates of one or both of the first two CCA axes. pH, Chla, S, and T were highly correlated with the first axis (CCA 1), while TN, SPM, TP, D, DO, and COD were strongly correlated with the second axis (CCA2). Although there was no obvious correlation between temperature and chlorophyll *a*, they both affected the interannual variation in ichthyoplankton (**Figure 2**).

Ichthyoplankton were divided into three species groups according to their ecological guilds (**Table 1** and **Figure 2**). Offshore assemblage: six species (*Chelidonichthys spinosus*, *Sardinella zunasi*, *Minous monodactylus*, *Salanx ariakensis*, *Larimichthys polyactis*, and *Engraulis japonicus*) distributed close to CCA axis 2 and mainly correlated with T. All species, except for *Sardinella zunasi* and *Minous monodactylus*, were dominant. Coastal assemblage: three species (*Hypoatherina valenciennei*, *Stolephorus commersonnii*, and *Harpadon nehereus*) distributed in brackish waters. *Hypoatherina valenciennei* and *Stolephorus commersonnii* were dominant species. Estuarine assemblage: five species (*Hyporhamphus sajori*, *Setipinna tenuifilis*, *Trachidermus*

TABLE 3 | Inter-annual comparison of the assemblage structure according to one-way ANOSIM (R value and significance level) and SIMPER analysis.

Groups	ANOSIM		SIMPER
	R	P	Average dissimilarity
2013 and 2014	0.404	0.001	91.09
2013 and 2015	0.183	0.001	89.24
2013 and 2016	0.265	0.001	87.91
2013 and 2017	0.137	0.005	85.38
2013 and 2018	0.183	0.001	89.24
2013 and 2019	0.123	0.004	82.08
2013 and 2020	0.141	0.006	85.13
2014 and 2015	0.308	0.001	97.06
2014 and 2016	0.577	0.001	98.61
2014 and 2017	0.393	0.001	98.36
2014 and 2018	0.308	0.001	97.06
2014 and 2019	0.499	0.001	98.24
2014 and 2020	0.296	0.001	92.06
2015 and 2016	–0.059	0.884	83.46
2015 and 2017	–0.019	0.673	86.52
2015 and 2018	–0.056	0.999	84.00
2015 and 2019	0.089	0.016	86.42
2015 and 2020	0.014	0.279	87.79
2016 and 2017	0.049	0.145	85.88
2016 and 2018	–0.059	0.899	83.46
2016 and 2019	0.103	0.07	82.55
2016 and 2020	0.034	0.211	84.54
2017 and 2018	–0.019	0.694	86.52
2017 and 2019	0.041	0.11	81.68
2017 and 2020	–0.002	0.441	84.21
2018 and 2019	0.089	0.019	86.42
2018 and 2020	0.014	0.256	87.79
2019 and 2020	0.013	0.253	80.01

fasciatus, *Coilia mystus*, and *Coilia nasus*) with dispersed distribution and mainly correlated with S, pH, S, and Chla. *Trachidermus fasciatus* and *Coilia mystus* were dominant species.

DISCUSSION

Variation on Ichthyoplankton Composition

The ichthyoplankton assemblage in the Yangtze Estuary is changing, as reflected in the reduction in species number and shifts in species composition. In the 1980s, 53 families and 94 species of ichthyoplankton were recorded in the Yangtze Estuary (Yang et al., 1990). By 2000–2003, the number of species collected had decreased sharply, with only 30 families and 45 species (Jiang et al., 2006). From 2012 to 2014, the number of ichthyoplankton species decreased again, with only 38 species in 18 families (Kindong et al., 2020). In this study (2013–2020), 17 families and 26 species of ichthyoplankton were collected, which is only 27.66% of the diversity observed in the 1980s. These results show that the ichthyoplankton species composition in the Yangtze Estuary has changed significantly in the last 35 years.

The abundance of ichthyoplankton in estuaries is determined by the environmental characteristics and nutritional status of the estuarine ecosystem. The community structure of ichthyoplankton in the estuary was composed of a few high abundance species and a large number of rare species, which is a common feature of estuaries (Gaughan et al., 1990; Harrison and Whitfield, 1990; Drake and Arias, 1991). For example, ichthyoplankton communities in warm water estuaries were found to be dominated by Gobiidae, which live in estuaries, and Clupeidae and Engraulidae, which lay eggs seasonally in estuaries (Talbot and Able, 1984; Drake and Arias, 1991). Our results are in accordance with those of previous studies. The eight dominant species accounted for 94.58% of all ichthyoplankton sampled. Interestingly, *Engraulis japonicus* was the dominant species in the Yangtze Estuary from 2013 to 2020 in our study, accounting for 44.15% of the total catch, which is consistent with previous reports in which this species represented 67.91% of the total catch (Shen et al., 2011; Zhang et al., 2015). In addition, *Chelidonichthys spinosus* gradually became one of the dominant species after 2015, although it accounted for only 4.96% of the total catch. As far as we know, this finding is the first report of this shift.

Interannual Variability of Assemblage Structure

Estuaries have complex and variable physical, chemical, and hydrological conditions, with environmental factors that change dramatically in time and space (Whitfield, 1994; Harris and Cyrus, 1995; Hettler and Hare, 1998). Ichthyoplankton are very sensitive to environmental conditions (Shao et al., 2001). Thus, ichthyoplankton assemblages usually show high interannual variability in abundance and composition. By comparing the shifts in dominant species between this study (2013–2020) and previous ones (1999, 2001, 2004, and 2007), it was found that the dominant species of ichthyoplankton had decreased significantly, and the species composition of dominant species had changed (**Figure 3**). During the study period, there were obvious changes in the structure of the ichthyoplankton community in the Yangtze Estuary, indicating that environmental variables have a significant effect on interannual changes in ichthyoplankton community structure. However, there were no significant differences in the structure of the ichthyoplankton community in the spring in 1999, 2001, 2004, and 2007 (Zhang et al., 2015). Distribution patterns of ichthyoplankton are closely related to the reproductive strategy and life history of the adult populations, which are often associated with oceanography and meteorology (Hernández-Miranda et al., 2003). Therefore, the ability of juvenile fish to survive in the pelagic environment and migrate to suitable adult habitats may depend on their ability to regulate their diffusion or migration (Muhling et al., 2007).

Stochastic climatic events (cyclones) can alter the community composition of ichthyoplankton in estuaries by bringing intense rainfall, which significantly changes the distribution and abundance of estuary residents and marine migratory species (Martin et al., 1992). In addition, long-term climate trends, such as climate change and El Niño events, can also drive changes in community structure (Franco-Gordoa et al., 2004;

TABLE 4 | Results of canonical correspondence analysis (CCA) relating ichthyoplankton abundance data to environmental factors in the Yangtze Estuary in spring 2013–2020.

Eigenvalues	CCA axes				Total inertia
	1	2	3	4	
Eigenvalues	0.3623	0.3339	0.2334	0.1668	7.72918
Species-environmental correlations	4.69	9.01	12.03	14.18	
Cumulative percentage variance	0.7157	0.6462	0.64	0.5049	
of species data	4.69	9.01	12.03	14.18	
of species-environment relation	27.09	52.05	69.5	81.97	
Sum of all canonical eigenvalues					1.3375
Sum of all unconstrained eigenvalues					7.72918

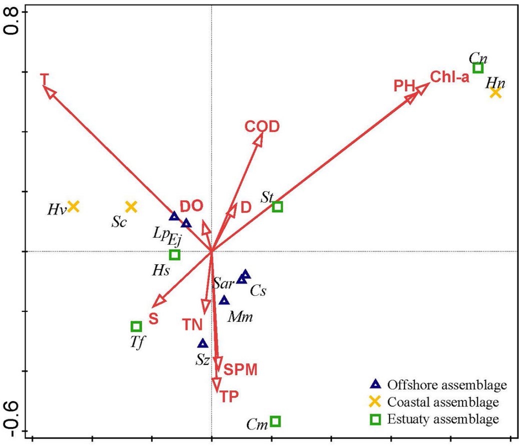

FIGURE 2 | Canonical correspondence analysis (CCA) biplot of ichthyoplankton species in the Yangtze Estuary in spring 2013–2020. The black font indicated the abbreviate name of the species as shown in **Table 1**.

Acha et al., 2012). Climate change is altering the temperature, salinity, dissolved oxygen, and other estuarine conditions, resulting in changes to the temporal and spatial distribution of ichthyoplankton (Sloterdijk et al., 2017). Increasing temperatures could lead to earlier fish spawning (Thaxton et al., 2020), extension of the spawning time (Primo et al., 2011; Acha et al., 2012), shortening of egg hatching time (Hassell et al., 2008), early gonadal maturation (Thaxton et al., 2020), and northward shift of spawning areas (Auth et al., 2018; Zhang et al., 2019), resulting in changes in ichthyoplankton community structure.

In recent years, the modernization of fishing gear and improvements in fishing technology have led to increases in fishing intensity, which now far exceeds the capacity of resource replenishment. Some important economic species have become rare, and even endangered (Zhang et al., 2009). In the Yangtze Estuary, overfishing of important economic species, such as *Trichiurus japonicus* and *Larimichthys polyactis*, has led to fish miniaturization, early maturity, and juvenile structure (Shan et al., 2004). The main reason for the miniaturization of fish communities is the uncontrolled overuse of marine resources in coastal waters (Zhu et al., 2002). Overfishing is the main reason for the significant reductions in fishery resources (Song et al., 2019). Under the joint influences of overfishing and environmental change, the population and community structure of fish resources in estuarine ecosystems have changed significantly (Bian et al., 2010), leading to loss of ecosystem resilience and integrity (Ryder et al., 1981).

TABLE 5 | Conditional effects and correlations of environmental variables with the canonical correspondence analysis (CCA) axes.

Variables	Explains (%)	Contribution (%)	pseudo-F	P
Chl-*a*	4	22.9	3.9	0.002
T	3.3	19.2	3.4	0.002
TP	1.9	10.8	1.9	0.048
S	2	11.5	2.1	0.012
D	1.7	10	1.8	0.052
DO	1.1	6.2	1.1	0.304
COD	0.9	5.2	0.9	0.46
TN	0.8	4.8	0.9	0.556
PH	0.8	4.5	0.8	0.586
SPM	0.8	4.9	0.9	0.476

Ichthyoplankton Assemblage Structure and Its Influencing Factors

The ichthyoplankton community in the Yangtze Estuary was divided into three groups: estuarine, coastal, and offshore species (Zhang et al., 2015). It is generally believed that the distribution patterns of ichthyoplankton communities is affected by both biological and environmental factors (Zhu et al., 2002). In this study, CCA was used to determine the correlations between ichthyoplankton abundance (time–abundance data) and environmental variables (time–environment data). In general, T and Chla were the most significant factors affecting community structure. The other factors, such as pH, D, COD, DO, TN, and SPM, had no significant effect on ichthyoplankton assemblage structure.

Temperature has a significant and direct effect on fish reproduction, physiology, growth, and behavior (Sabates et al., 2006; Santos and Severi, 2019), which is very important for the abundance and spatial distribution of ichthyoplankton (Bruno et al., 2014; Chermahini et al., 2021). Estuaries are generally shallow, with large temperature changes, and diurnal and seasonal changes, therefore estuarine species adapted to a wide temperature range often dominate (Yang et al., 2006).

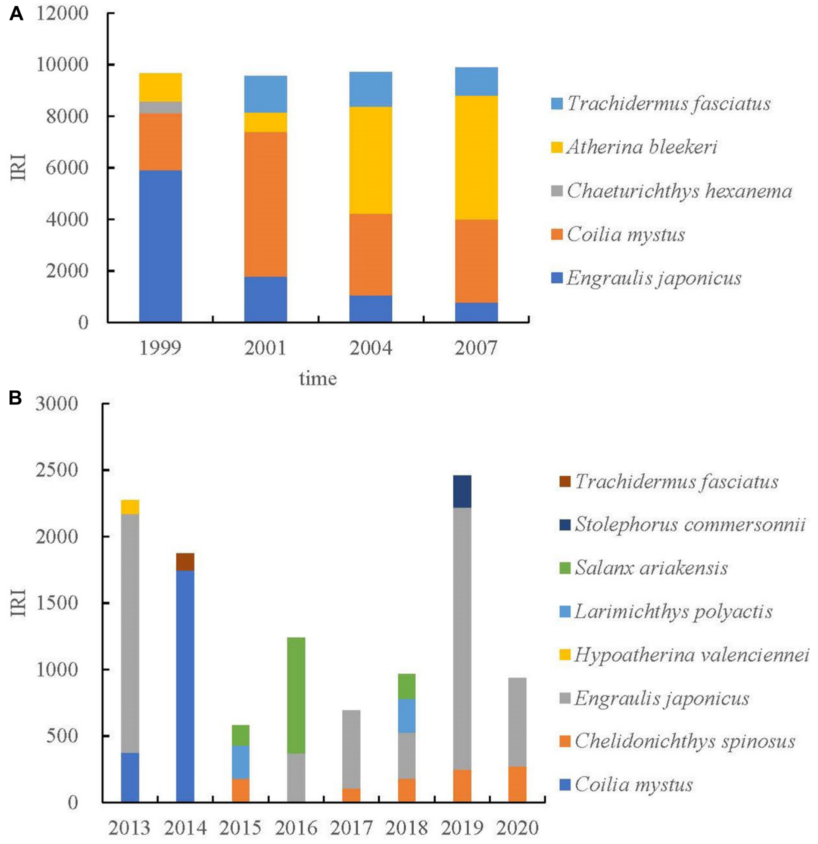

FIGURE 3 | Variations on ichthyoplankton dominance (IRI) and species composition in the Yangtze Estuary in spring. Panel **(A)** represented published data (Zhang et al., 2015); panel **(B)** represented the data of this study. Because the original abundance data were not obtained in the literature, the dominance data (IRI) were used for comparison.

In temperate and subtropical estuaries, the peak number of species usually occurs in the spring and summer because of the annual changes in temperature (Neira and Potter, 1992; Primo et al., 2011; Wang et al., 2017). Therefore, during the growth and developmental stages of larvae and juveniles, temperature could have an important influence on growth, density, and reproduction (Ramos et al., 2006). Here, interannual changes in the abundance of *Engraulis japonicus* and *Larimichthys polyactis* were closely correlated with increasing temperature, and interannual changes in *Salanx ariakensis* and *Chelidonichthys spinosus* abundance were closely associated with decreasing temperatures.

Chla is an important environmental variable that has a significant influence on ichthyoplankton community structure, and was positively correlated with pH and negatively correlated with S. Chla is a relatively accurate reflection of phytoplankton standing stock; the larger the phytoplankton biomass, the higher the primary productivity (Whitfield, 1999). Chla is closely associated with fresh water nutrient levels entering the estuary. When nutrient levels are high, the Chla level in the estuary is also high, and food resources are rich, which is necessary for the development and growth of larvae and juveniles. Abundant food resources also improved the survival rate and successful foraging rate (Zhang et al., 2015). In this study, three estuarine species (*Trachidermus fasciatus*, *Coilia nasus*, and *Setipinna tenuifilis*) were closely associated with the content of Chla (**Figure 2**). Zhang et al. (2016) also reported that Chla was closely related to the distribution of three freshwater species.

In addition to T and Chla, other environmental variables also affected the community structure of ichthyoplankton. TP and TN represent nutritional status, S, DO, COD, SPM, and pH represent water quality. Salinity is a key abiotic factor determining the structure of the ichthyoplankton community in estuaries (Wooldridge, 1999; Campfield and Houde, 2011). A decrease in salinity level can lead to peaks in fish eggs and larvae, and low salinity coastal systems have a significant influence on the hatching and development of fish eggs and larvae (Jiang et al., 2006). SPM is one of the most important factors affecting the density of estuarine species (Harris and Cyrus, 1995). Rakocinski et al. (1996) used canonical correlation analysis to analyze the changes in ichthyoplankton community structure in the Mississippi River and found that dissolved oxygen had a strong influence, as did temperature and salinity.

The variation in species distribution explained by the first four axes of the CCA was only 14.18%, which indicates that other factors are affecting the ichthyoplankton assemblage structure in the Yangtze Estuary. Biological and human factors were not included in this study and the influence of these variables should be investigated in the Yangtze Estuary.

CONCLUSION

In this study, 1,291 ichthyoplankton individuals were collected in the Yangtze Estuary from 2013 to 2020, and identified as 26 species in 17 families. The dominant species were *Coilia mystus*, *Chelidonichthys spinosus*, *Engraulis japonicus*, *Hypoatherina valenciennei*, *Larimichthys polyactis*, *Salanx ariakensis*, *Stolephorus commersonnii*, and *Trachidermus fasciatus*. The interannual ichthyoplankton assemblage has changed significantly, reflected in the replacement of some dominant species and shifts in species composition. In particular, *Chelidonichthys spinosus* became a dominant species. Temperature and chlorophyll *a* were the key factors affecting the ichthyoplankton assemblage in the Yangtze Estuary in spring. Temperature and chlorophyll *a* were closely related to the abundance of offshore and estuarine species assemblages, respectively.

DATA AVAILABILITY STATEMENT

The original contributions presented in the study are included in the article/supplementary material, further inquiries can be directed to the corresponding authors.

ETHICS STATEMENT

Ethical review and approval was not required for the animal study because this study did not involve animal ethics.

AUTHOR CONTRIBUTIONS

YW analyzed the data and completed the first draft. HZ and WX provided guidance on the structure of the manuscript. ZC and SL provided the suggestions on this manuscript. YW, CL, and HZ modified the manuscript. All authors are contributed to revise the manuscript.

FUNDING

The present work was supported by the National Natural Science Foundation of China (Nos. 41976094 and 31872568), the Key Deployment Project of Center for Ocean Mega-Science, Chinese Academy of Sciences (COMS2019Q14), and the Youth Innovation Promotion Association CAS (No. 2020211).

ACKNOWLEDGMENTS

We are grateful to the editors and reviewers for their constructive feedback and concerning on our work.

REFERENCES

Acha, E. M., Simionato, C. G., Carozza, C., and Mianzan, H. (2012). Climate-induced year-class fluctuations of whitemouth croaker *Micropogonias furnieri* (Pisces, Sciaenidae) in the Rio de la Plata estuary, Argentina-Uruguay. *Fish. Oceanogr.* 21, 58–77. doi: 10.1111/j.1365-2419.2011.00609.x

Auth, T. D., Daly, E. A., Brodeur, R. D., and Fisher, J. L. (2018). Phenological and distributional shifts in ichthyoplankton associated with recent warming in the northeast Pacific Ocean. *Glob. Chang. Biol.* 24, 259–272. doi: 10.1111/gcb.13872

Azeiteiro, U. M., Bacelar-Nicolau, L., Resende, P., Goncalves, F., and Pereira, M. J. (2006). Larval fish distribution in shallow coastal waters off North Western Iberia (NE Atlantic). *Estuar. Coast. Shelf Sci.* 69, 554–566. doi: 10.1016/j.ecss.2006.05.023

Barragán, J. M., and de Andrés, M. (2015). Analysis and trends of the world's coastal cities and agglomerations. *Ocean Coast. Manage.* 114, 11–20. doi: 10.1016/j.ocecoaman.2015.06.004

Bian, X. D., Zhang, X. M., Gao, T. X., Wan, R. J., and Zhang, P. D. (2010). Category composition and distributional patterns of ichthyoplankton in the Yellow River estuary during spring and summer 2007. *J. Fish. Sci. China* 17, 815–827.

Bruno, D. O., Delpiani, S. M., Cousseau, M. B., de Astarloa, J. M. D., Blasina, G. E., Mabragana, E., et al. (2014). Ocean-estuarine connection for ichthyoplankton through the inlet channel of a temperate choked coastal lagoon (Argentina). *Mar. Freshw. Res.* 65, 1116–1130. doi: 10.1071/Mf13128

Butler, J. L., Jacobson, L. D., Barnes, J. T., and Moser, H. G. (2003). Biology and population dynamics of cowcod (*Sebastes levis*) in the southern California Bight. *Fish. Bull.* 101, 260–280.

Campfield, P. A., and Houde, E. D. (2011). Ichthyoplankton community structure and comparative trophodynamics in an estuarine transition zone. *Fish. Bull.* 109, 1–19.

Chen, Y. H., Shaw, P. T., and Wolcott, T. G. (1997). Enhancing estuarine retention of planktonic larvae by tidal currents. *Estuar. Coast. Shelf Sci.* 45, 525–533.

Chermahini, M. A., Shabani, A., Naddafi, R., Ghorbani, R., Rabbaniha, M., and Noorinejad, M. (2021). Diversity, distribution, and abundance patterns of ichthyoplankton assemblages in some inlets of the northern Persian Gulf. *J. Sea Res.* 167:101981. doi: 10.1016/j.seares.2020.101981

Clarke, K. R., and Warwick, R. M. (2001). Changes in marine communities: an approach to statistical analysis and interpretation. *Mt. Sinai J. Med.* 40, 689–692.

Day, J. (1981). "The nature, origin and classification of estuaries," in *Estuarine Ecology with Particular Reference to Southern Africa*, ed. J. H. Day (Rotterdam: CRC Press), 1–6.

Drake, P., and Arias, A. M. (1991). Composition and seasonal fluctuations of the ichthyoplankton community in a shallow tidal channel of cadiz bay (Sw Spain). *J. Fish Biol.* 39, 245–263. doi: 10.1111/j.1095-8649.1991.tb04360.x

Franco-Gordoa, C., Godínez-Domínguezа, E., Filonovc, A. E., Tereshchenkoc, I. E., and Freireb, J. (2004). Plankton biomass and larval fish abundance prior to and during the El Niño period of 1997–1998 along the central Pacific coast of México. *Prog. Oceanogr.* 63, 99–123.

Gaughan, D. J., Neira, F. J., Beckley, L. E., and Potter, I. C. (1990). Composition, seasonality and distribution of the ichthyoplankton in the lower swan estuary, South-Western Australia. *Aust. J. Mar. Freshw. Res.* 41, 529–543. doi: 10.1071/mf9900529

Harris, S. A., and Cyrus, D. P. (1995). Occurrence of fish larvae in the St Lucia Estuary, Kwazulu-Natal, South Africa. *Afr. J. Marine Sci.* 16, 333–350. doi: 10.2989/025776195784156601

Harrison, T. D., and Whitfield, A. K. (1990). Composition, distribution and abundance of ichthyoplankton in the sundays river estuary. *Afr. J. Zool.* 25, 161–168. doi: 10.1080/02541858.1990.11448206

Hassell, K. L., Coutin, P. C., and Nugegoda, D. (2008). Hypoxia, low salinity and lowered temperature reduce embryo survival and hatch rates in black *bream Acanthopagrus butcheri* (Munro, 1949). *J. Fish Biol.* 72, 1623–1636. doi: 10.1111/j.1095-8649.2008.01829.x

Hernández-Miranda, E., Palma, A. T., and Ojeda, F. P. (2003). Larval fish assemblages in nearshore coastal waters off central Chile: temporal and spatial patterns. . *Estuar. Coast. Shelf Sci.* 56, 1075–1092. doi: 10.1016/s0272-7714(02)00308-6

Hettler, W. F. Jr., and Hare, J. A. (1998). Abundance and size of larval fishes outside the entrance to Beaufort inlet, North Carolina. *Estuaries* 21, 476–499. doi: 10.2307/1352846

Hodgson, E. E., Wilson, S. M., and Moore, J. W. (2020). Changing estuaries and impacts on juvenile salmon: a systematic review. *Glob. Chang. Biol.* 26, 1986–2001. doi: 10.1111/gcb.14997

Jiang, M., Shen, X., and Chen, L. (2006). Relationship between with abundance distribution of fish eggs, larvae and environmental factors in the Changjiang Estuary and vicinity waters in spring. *Mar. Environ. Sci.* 25, 37–39.

Kindong, R., Wu, J., Gao, C., Dai, L., Tian, S., Dai, X., et al. (2020). Seasonal changes in fish diversity, density, biomass, and assemblage alongside environmental variables in the Yangtze River Estuary. *Environ. Sci. Pollut. Res.* 27, 25461–25474. doi: 10.1007/s11356-020-08674-8

Lefcheck, J. S., Hughes, B. B., Johnson, A. J., Pfirrmann, B. W., Rasher, D. B., Smyth, A. R., et al. (2019).). Are coastal habitats important nurseries? A meta-analysis. *Conserv. Lett.* 12:e12645. doi: 10.1371/journal.pone.0114715

Limburg, K. E. (1999). Estuaries, ecology, and economic decisions: an example of perceptual barriers and challenges to understanding. *Ecol. Econ.* 30, 185–188. doi: 10.1016/s0921-8009(99)00045-2

Liu, S. D., Xian, W. W., and Liu, D. (2008). Characters of ichthyoplankton assemblages in Yangtze Estuary and adjacent waters in spring. *Chin. J. Appl. Ecol.* 19, 2284–2292. doi: 10.13287/j.1001-9332.2008.0374

Lotze, H. K. (2010). "Historical reconstruction of human-induced changes in US estuaries," in *Oceanography and Marine Biology: An Annual Review*, eds R. N. Gibson, R. J. A. Atkinson and J. D. M. Gordon (Boca Raton, FL: CRC Press), 267–338. doi: 10.1201/ebk1439821169-5

Lotze, H. K., Lenihan, H. S., Bourque, B. J., Bradbury, R. H., Cooke, R. G., Jackson, J. B. C., et al. (2006). Depletion, degradation, and recovery potential of estuaries and coastal seas. *J. Sci.* 312, 1806–1809. doi: 10.1126/science.1128035

Luo, B. Z. (1994). *Three Gorges Project and Estuarine Ecological Environment*. Beijing: Science Press.

Luo, B. Z., and Shen, H. T. (1994). *The Three Gorges Project and the Ecological Environment of Yangtze Estuary*. Beijing: Science Press.

Martin, T. J., Cyrus, D. P., and Forbes, A. T. (1992). Episodic events - the effects of cyclonic flushing on the ichthyoplankton of St-Lucia estuary on the Southeast Coast of Africa. *Neth. J. Sea Res.* 30, 273–278. doi: 10.1016/0077-7579(92)90065-M

Miller, B. S., and Kendall, A. W. (2009). *Early Life History of Marine Fishes*. Berkeley, CA: University of California Press.

Muhling, B. A., Beckley, L. E., and Olivar, M. P. (2007). Ichthyoplankton assemblage structure in two meso-scale Leeuwin current eddies, eastern Indian Ocean. *Deep Sea Res. Part II* 54, 1113–1128. doi: 10.1016/j.dsr2.2006.05.045

Neira, F. J., and Potter, I. C. (1992). Movement of larval fishes through the entrance channel of a seasonally open estuary in Western Australia. *Estuar. Coast. Shelf Sci.* 35, 213–224. doi: 10.1016/S0272-7714(05)80114-3

Potter, I. C., Beckley, L. E., Whitfield, A. K., and Lenanton, R. C. (1990). Comparisons between the roles played by estuaries in the life cycles of fishes in temperate Western Australia and Southern Africa. *Environ. Biol. Fishes* 28, 143–178. doi: 10.1007/978-94-009-2065-1_9

Primo, A. L., Azeiteiro, U. M., Marques, S. C., and Pardal, M. A. (2011). Impact of climate variability on ichthyoplankton communities: an example of a small temperate estuary. *Estuar. Coast. Shelf Sci.* 91, 484–491. doi: 10.1016/j.ecss.2010.11.009

Rakocinski, C. F., LyczkowskiShultz, J., and Richardson, S. L. (1996). Ichthyoplankton assemblage structure in *Mississippi* sound as revealed by canonical correspondence analysis. *Estuar. Coast. Shelf Sci.* 43, 237–257. doi: 10.1006/ecss.1996.0067

Ramos, S., Cowen, R. K., Paris, C., Re, P., and Bordalo, A. A. (2006). Environmental forcing and larval fish assemblage dynamics in the Lima River estuary (Northwest Portugal). *J. Plankton Res.* 28, 275–286. doi: 10.1093/plankt/fbi104

Ryder, R. A., Kerr, S. R., Taylor, W. W., and Larkin, P. A. (1981). Community consequences of fish stock diversity. *Can. J. Fish. Aquat. Sci.* 38, 1856–1866. doi: 10.1139/f81-231

Sabates, A., Martin, P., Loret, J., and Raya, V. (2006). Sea warming and fish distribution: the case of the small pelagic fish, *Sardinella aurita*, in the western Mediterranean. *Glob. Chang. Biol.* 12, 2209–2219. doi: 10.1111/j.1365-2486.2006.01246.x

Santos, R. V. S., and Severi, W. (2019). Dynamics of early life-history stages of fish along an estuarine gradient. *Fish. Oceanogr.* 28, 402–418. doi: 10.1111/fog.12420

Shan, X. J., Xian, W. W., and Wu, Y. F. (2004). Progress of studies on ichthyoplankton ecology of Changjiang river estuary. *J. Oceanol. Limnol.* 0, 87–93.

Shao, G., Yang, R., and Chen, K. (2001). *An Identification Guide of Marine Fish Eggs From Taiwan*. Taibei: Academia Sinica.

Sheaves, M., Baker, R., Nagelkerken, I., and Connolly, R. M. (2015). True value of estuarine and coastal nurseries for fish: incorporating complexity and dynamics. *Estuar. Coast.* 38, 401–414. doi: 10.1007/s12237-014-9846-x

Shen, X., Shi, Y., Chao, M., Huang, H., and Tian, F. (2011). Fish community structure of the Yangtze River Estuary in summer and autumn. *J. Fish. China* 35, 700–710.

Shoji, J., Ohta, T., and Tanaka, M. (2006). Effects of river flow on larval growth and survival of Japanese seaperch *Lateolabrax japonicus* (Pisces) in the Chikugo River estuary, upper Ariake Bay. *J. Fish Biol.* 69, 1662–1674. doi: 10.1111/j.1095-8649.2006.01235.x

Sloterdijk, H., Brehmer, P., Sadio, O., Muller, H., Doring, J., and Ekau, W. (2017). Composition and structure of the larval fish community related to environmental parameters in a tropical estuary impacted by climate change. *Estuar. Coast. Shelf Sci.* 197, 10–26. doi: 10.1016/j.ecss.2017.08.003

Song, Y. F., Zhang, L. J., and Luo, X. X. (2019). Spatiotemporal distribution of fish eggs and larvae in the Huanghe (Yellow) River estuary, China in 2005-2016. *J. Oceanol. Limnol.* 37, 1625–1637. doi: 10.1007/s00343-019-8167-0

Standardization Administration of China (SAC) (2007). *Specifications for Oceanographic Survey, Part 4: Survey of Chemical Parameters in sea Water (GB/T 12763-2007)*. Beijing: SAC.

Talbot, C. W., and Able, K. W. (1984). Composition and distribution of larval fishes in New Jersey high marshes. *Estuaries* 7, 434–443. doi: 10.2307/1351624

Taylor, R. H. (1982). "The St. Lucia estuary: the aquatic environment: physical and chemical characteristics," in *St. Lucia Research Review, Proceedings of the Natal Parks Board 1992*, ed. R. H. Taylor (South Africa), 42–56.

Thaxton, W. C., Taylor, J. C., and Asch, R. G. (2020). Climate-associated trends and variability in ichthyoplankton phenology from the longest continuous larval fish time series on the east coast of the United States. *Mar. Ecol. Prog. Ser.* 650, 269–287. doi: 10.3354/meps13404

Tzeng, W. N., Wang, Y. T., and Chang, C. W. (2002). Spatial and temporal variations of the estuarine larval fish community on the west coast of Taiwan. *Mar. Freshw. Res.* 53, 419–430. doi: 10.1071/mf01136

Valencia, B., Giraldo, A., Rivera-Gomez, M., Izquierdo-Pena, V., and Cuellar-Chacon, A. (2019). Effects of seasonal upwelling on hydrography and mesozooplankton communities in a Pacific tropical cove off Colombia. *Rev. Biol. Trop.* 67, 945–962.

Wan, R., and Jiang, Y. (2000). The species and biological characteristics of the eggs and larvae of osteichthyes in the Bohai and Yellow Sea. *J. Shanghai Fish. Univ.* 9, 290–297.

Wan, R., and Sun, S. (2006). The category composition and abundance of ichthyoplankton in the ecosystem of the Yellow Sea and the East China Sea. *J. Acta. Zool. Sin.* 52, 28–44.

Wang, H. T., and Zhang, P. J. (1998). Effects of environmental conditions on fertilized eggs and early larva of marine fishes. *Mar. Sci.* 4, 50–52.

Wang, X. G., Sun, D., and Lin, S. Q. (2017). The ecological study of fish larvae in the Yangtze River Estuary and adjacent waters. *J. Shanghai Fish. Univ.* 26, 733–742.

Whitfield, A. K. (1994). Abundance of larval and juvenile marine fishes in the lower reaches of 3 Southern African estuaries with differing fresh-water inputs. *Mar. Ecol. Prog. Ser.* 105, 257–267. doi: 10.3354/meps105257

Whitfield, A. K. (1999). Ichthyofaunal assemblages in estuaries: a South African case study. *Rev. Fish Biol. Fish.* 9, 151–186.

Wooldridge, T. (1999). *Estuarine Zooplankton Community Structure and Dynamics*. Cambridge: Cambridge University Press.

Wu, G. Z. (1989). The ecological characteristics of distribution of eggs, larvae and juveniles of the *Engraulis japonicus* (temminck & schlegel) and *Anchoviella commersonii* in the Changjiang River Estuary. *J. Oceanol. Limnol.* 3, 217–229.

Xian, W. W., Zhang, H., and Liu, S. D. (2016). Research advance in estuarine ichthyoplankton ecology. *Stud. Mar. Sin.* 2016, 167–180.

Yang, D., Wu, G., and Sun, J. (1990). The investigation ok pelagic eggs, larvae and juveniles of fishes at the mouth of the Changjiang river and adjacent areas. *J. Oceanol. Limnol.* 4, 346–355.

Yang, Y. F., Wang, Q., Chen, J. F., and Pang, S. X. (2006). Research advance in estuarine zooplankton ecology. *Acta Ecol. Sin.* 26, 576–585.

Zhang, H., Xian, W., and Liu, S. (2015). Ichthyoplankton assemblage structure of springs in the Yangtze Estuary revealed by biological and environmental visions. *PeerJ* 3:e1186. doi: 10.7717/peerj.1186

Zhang, H., Xian, W., and Liu, S. (2016). Autumn ichthyoplankton assemblage in the Yangtze Estuary shaped by environmental factors. *PeerJ* 4:e1922. doi: 10.7717/peerj.1922

Zhang, H., Xian, W., and Liu, S. (2019). Seasonal variations of the ichthyoplankton assemblage in the Yangtze Estuary and its relationship with environmental factors. *PeerJ* 7:e6482. doi: 10.7717/peerj.6482

Zhang, H., Zhu, G., and Lu, J. (2009). Fish species composition and diversity of Yangtze River estuarine wetlands. *Biodiversity Sci.* 17, 76–81. doi: 10.3724/sp.j.1003.2009.08140

Zhu, X. H., Liu, D., and Sha, X. S. (2002). Relationship between ichthyoplankton community structure and environmental factors in spring in the Yangtze River Estuary. *Stud. Mar. Sin.* 4, 169–179.

Conflict of Interest: The authors declare that the research was conducted in the absence of any commercial or financial relationships that could be construed as a potential conflict of interest.

ORIGINAL RESEARCH
published: 20 December 2021
doi: 10.3389/fmars.2021.767191

Northeast Arctic Cod and Prey Match-Mismatch in a High-Latitude Spring-Bloom System

Frode B. Vikebø[1,2]*, Ole Jacob Broch[3], Clarissa Akemi Kajiya Endo[1], Håvard G. Frøysa[1], JoLynn Carroll[4,5], Jonas Juselius[6] and Øystein Langangen[7]

[1] Institute of Marine Research, Bergen, Norway, [2] Geophysical Institute, University of Bergen, Bergen, Norway, [3] SINTEF Ocean AS, Trondheim, Norway, [4] Akvaplan-Niva, FRAM – High North Research Centre for Climate and the Environment, Tromsø, Norway, [5] Department of Geosciences, UiT The Arctic University of Norway, Tromsø, Norway, [6] High Performance Computing Group, IT Department, UiT The Arctic University of Norway, Tromsø, Norway, [7] Department of Biosciences, Centre for Ecological and Evolutionary Synthesis (CEES), University of Oslo, Oslo, Norway

OPEN ACCESS

Edited by:
Hui Zhang,
Institute of Oceanology, Chinese Academy of Sciences (CAS), China

Reviewed by:
Sophia N. Wassermann,
University of Washington, United States
Giovanni Daneri,
Patagonian Ecosystems Investigation Research Center (CIEP), Chile

***Correspondence:**
Frode B. Vikebø
frovik@hi.no

Specialty section:
This article was submitted to Marine Fisheries, Aquaculture and Living Resources, a section of the journal Frontiers in Marine Science

Received: 30 August 2021
Accepted: 30 November 2021
Published: 20 December 2021

Citation:
Vikebø FB, Broch OJ, Endo CAK, Frøysa HG, Carroll J, Juselius J and Langangen Ø (2021) Northeast Arctic Cod and Prey Match-Mismatch in a High-Latitude Spring-Bloom System. Front. Mar. Sci. 8:767191. doi: 10.3389/fmars.2021.767191

By combining an ocean model, a nutrient-phytoplankton-zooplankton-detritus-model and an individual-based model for early life stages of Northeast Arctic cod we systematically investigate food limitations and growth performance for individual cod larvae drifting along the Norwegian coast from spawning grounds toward nursery areas in the Barents Sea. We hypothesize that there is food shortage for larvae spawned early and late in the 2-monthlong spawning period, and to a larger degree to the north and south of the main spawning grounds in the Lofoten. Model results for three contrasting years (1995, 2001, and 2002) show that spawning early in the season at spawning grounds in the Lofoten and farther north is favorable for larval growth close to their size- and temperature-dependent potential. Still, both early and late spawned larvae experience slower growth than individuals originating closer to the time of peak spawning late March/early April. The reasons are low temperatures and shortage in suitable prey, respectively, and this occurs more frequent in areas of strong currents about 1–2 months post hatching. In particular, late spawned larvae grow relatively slow despite higher temperatures later in the season because they are outgrown by their preferred prey.

Keywords: Atlantic cod, match-mismatch, fish larvae, starvation, *Calanus finmarchicus*, North Atlantic, Arctic

INTRODUCTION

Early life stages of fish experience high mortality rates, associated with a range of potential drivers, that lead to high losses prior to recruitment to the stock ("recruitment-processes"). Hjort's (1914) seminal work emphasizes the need for first-feeding larvae to match prey immediately after the yolk sac is absorbed ("critical period") and being transported to favorable nursery grounds ("aberrant drift"). This has since been further developed by utilizing new observational data and methods (Cushing, 1990; Houde, 2008; Ottersen et al., 2014). After about 100 years of research on various recruitment processes there is today an understanding that a multitude of processes on various spatiotemporal scales may impact recruitment in fish and that the relative importance of these processes varies in both time and space (Gallego et al., 2012; Hare, 2014).

The typical recruitment pattern is many poor to average years with only a few highly successful years that contribute significantly to the sustainability of fish stocks (Bogstad et al., 2016). The stocks produce vast amounts of eggs, much more than what can survive to recruitment. The high egg production often leads to recruitment being more dependent on the influence of environmental conditions on the survival of young fish as compared to the size of the adult population. Several environmental factors typically play an important role in the recruitment process, including spatiotemporally varying temperatures, dispersal, light conditions, turbulence, prey availability, and predation (Ottersen et al., 2014).

The Northeast Arctic (NEA) stock of Atlantic cod (*Gadus morhua*) is a commercially exploited fish species with a typical recruitment pattern of sporadically occurring years of very high recruitment. The NEA cod stock has been subjected to moderate fishing pressure in recent years that combined with strong recruitment in 2004 and 2005 has resulted in a high spawning stock biomass and increased age diversity (Kjesbu et al., 2014). Still, only a tiny fraction of cod eggs survives to reach recruitment (Bogstad et al., 2016)—on average 6 per 1 million eggs. The highest mortality rates occur during the egg and larval stages (Houde, 2008). Recent estimates indicate that NEA cod larvae mortality rates range from 0.06 to 0.08 day^{-1} (Langangen et al., 2014a), which is on the low end of estimates previously reported by Sundby et al. (1989) of 0.08–0.15 day^{-1}. In the context of overall mortality from eggs to recruits, the largest inter-annual variability is thought to occur at the 0-group stage (developmental stage at settlement around the age of 6 months) (Langangen et al., 2014a). Considerable variability in natural mortality also occurs between juvenile stages and recruitment that may affect recruitment strength (Bogstad et al., 2016). On the other hand, density-dependent processes (e.g., competition for food and cannibalism) dampen the high variability in natural mortality rates, reducing the inter-annual variation in survivors from egg production through the early life stages until recruitment (Ottersen et al., 2014).

Sampling sufficient data at sea to obtain direct estimates of natural mortality of planktonic life stages is challenging because cohorts are dispersed by ocean currents and are therefore very difficult to track and sample repeatedly. Alternative and complimentary approaches for estimating mortality rates are therefore needed (e.g., Langangen et al., 2014b). By utilizing experimental and *in situ* data to parametrize coupled biophysical models of various complexity (e.g., Siddon et al., 2013; Daewel et al., 2015) one may investigate the relative importance of trophodynamics and variations in physical forcing at various scales (Peck and Hufnagel, 2012). For example, models combining ocean physics with nutrient-phytoplankton-zooplankton-detritus (NPZD) dynamics may quantify availability of suitable prey for larval fish. Combined with models of fish eggs and larvae, typically represented by individual-based lagrangian models (IBMs) of early life stage (ELS) (Daewel et al., 2011, 2015), the combined models allow assessment of bottom-up processes affecting growth and survival. The main prey items have pelagic free drift and exhibit diurnal vertical migration and can therefore be explicitly incorporated into the models. Predator presence is more difficult to address because adult migration behavior is less predictable than simple pelagic drift and because of the multitude of potential predators (but see end-to-end models e.g., Rose et al., 2015; Akimova et al., 2019; Daewel et al., 2019).

The adult NEA cod migrate from feeding grounds in the Barents Sea upstream along the Norwegian Coast to spawn during March through April with a peak in early April at multiple well-known spawning grounds (SGs, Sundby and Nakken, 2008; see **Figure 1**). NEA cod is a batch spawner that spawn pelagic eggs during a 2-month period from early March until late April. Pelagic eggs drift with the ocean currents toward nursery grounds in the Barents Sea and hatch after 2–3 weeks depending on temperature (Ottersen et al., 2014). Newly hatched larvae need sufficient food to cover metabolic costs and energy requirements for growth, which are additionally dependent on ambient temperature and larval size (Folkvord, 2005). The Norwegian continental shelf is a typical spring-bloom system where light conditions and structuring of the water column trigger phytoplankton and zooplankton production (Stenevik et al., 2007; Vikebø et al., 2019). NEA cod larvae and early juveniles are found to mainly feed upon various stages of *Calanus finmarchicus* from hatching in mid-March to mid-May until after metamorphosis around June (Sundby, 1995). The extended spawning time (ST) is believed to be a strategy to increase the chance of offspring to match the *C. finmarchicus* under a highly variable bloom phenology (Cushing, 1990; Solemdal, 1997). However, early spawning hampers larval visual feeding because of inadequate light conditions and low prey abundance.

Quantification of spatiotemporal variability in survival is relevant for integrated ecosystem assessments designed to consider impacts of human activities on the resilience in fish stocks (Langangen et al., 2017). A fish stock with wide-spread spawning locations and times is considered to more easily buffer

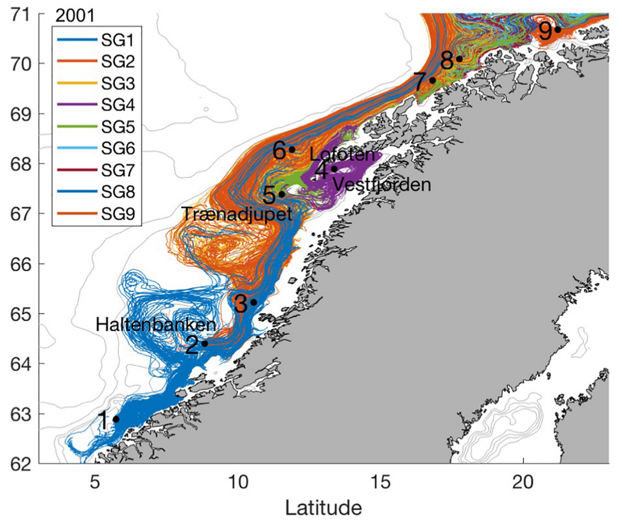

FIGURE 1 | SGs (black stars) and every 100th drift trajectory of eggs/larvae from spawning until late July during 2001.

changing environmental conditions (Hixon et al., 2014; but see Stige et al., 2017) and human activities, such as accidental oil spills (Carroll et al., 2018; Stige et al., 2018). In this context, an important question to be addressed is whether the portion of offspring successfully recruiting is systematically narrowed through match-mismatch leading to a reduction in the intrinsic buffer capacity to varying environmental conditions.

Here, we quantify how the match-mismatch between NEA larval cod and their main prey, *C. finmarchicus,* are affected by the location and timing of spawning by combining a coupled ocean- and NPZD-model with an IBM ELS for three contrasting years 1995, 2001, and 2002. We analyze the model output to address our hypothesis of a systematic lack of sufficient and suitable prey available for larvae resulting from early and late spawning, and that this lack of overlap is more pronounced at SGs to the south and north of the main SGs in the Lofoten.

METHODS AND DATA

We investigate individual growth in NEA cod larvae and pelagic juveniles as a function of SG and ST by providing stage-specific prey availability to an IBM of NEA cod ELS from the coupled open source SINMOD ocean and NPZD model thoroughly described in Alver et al. (2016). All data underlying this article will be shared on reasonable request to the corresponding author. We analyze 1995, 2001, and 2002 as these years represent contrasting conditions for NEA cod ELS development as compared to the average across 1983–2009 (Bogstad et al., 2016). In short, 1995 and 2002 had medium numbers of NEA cod eggs produced (about 102 and 103 trillion vs. a mean of 107 trillion), while 2001 only had about half of that. Subsequently, 1995 provided about 234 billion juveniles at the 0-group stage which is almost three times the long-term average of 85 billion, 2002 was close to the long-term average, and 2001 provided almost none.

SINMOD *C. finmarchicus* nauplii and copepodites are homogeneously distributed in the upper 40 and 50 m during dispersal, respectively, but only written to file as numbers per square meter surface for all 13 stages (eggs, nauplii I-VI and copepodites I-VI). When using this model output as prey for larvae, we therefore divide these numbers by 10 assuming that prey typically distribute across a 10 m water column and that larvae are able to stay within reach of their prey. We quantify which of the larvae that experience sufficient and suitable prey abundances to allow at least 90% food-unlimited growth during at least 90% of the time as a function of SG and ST. The reason why we choose to emphasize this is for two particular reasons; (i) past literature argues that the chance of survival through the early life stages is dependent on rapid growth (Houde, 1987), (ii) Folkvord (2005) reports that observed cod larvae at sea typically grow close to their size- and temperature-dependent potential, indicating that individuals unable to feed sufficiently to sustain such growth likely experience high mortality. Furthermore, we quantify ambient temperatures, larval length by the end of June and the number of days to reach 18 mm (same length used for evaluating fitness in Vikebø et al. (2007) as a function of SG and ST. The choice of 18 mm is because a major part of the individuals actually reaches this size by mid-summer, while at the same time acknowledging that mortality rates in general decrease with size. Furthermore, metamorphosis occur at lengths between 12 and 25–30 mm (Folkvord, 1997). Note that Daewel et al. (2011) used a size of 20 mm for a similar type of analysis. Finally, we investigate which areas and ages larvae grow below their growth potential and what temperature and prey conditions this occurs under. Note, that annual estimates of *C. finmarchicus* in the open ocean are based on annual survey measurements while abundance at the Norwegian shelf depends on cross-shelf transport (Opdal and Vikebø, 2015) or overwintering in the fjords and is reported to drop substantially around 2005 (Toresen et al., 2019). In general, the years in question here are considered medium to warm as compared to a long-term variability (Skagseth et al., 2015).

SINMOD Coupled Ocean and Nutrient-Phytoplankton-Zooplankton-Detritus Model

The ocean physics in SINMOD is computed by integrating the primitive Navier-Stokes equations on a grid with 4 by 4 km horizontal resolution covering the Norwegian and the Barents Sea with 34 vertical z-coordinates (Alver et al., 2016). Lateral boundary conditions from a 20 km SINMOD application covering the North Atlantic and the Arctic. Dynamics of basic nutrients and phytoplankton are described in Wassmann et al. (2006). Details of the zooplankton model representing *C. finmarchicus* can be found in Alver et al. (2016). In short, the NPZD component within SINMOD considers the basic nutrients nitrate, ammonium and silicate. The key trophic levels include compartments for bacteria, ciliates, heterotrophic nanoflagellates, diatoms and flagellates. Dissolved organic carbon and detritus are also considered. Finally, there is a stage-distributed *C. finmarchicus* model representing prey to the larval fish. *C. finmarchicus* is modeled using an Eularian stage-dependent model where growth, mortality and reproduction depends on the physical environment, food availability (modeled diatoms and ciliates), and the *C. finmarchicus* population structure. The individuals have a specified overwintering depth preference, initiated August 1st, and an ascent toward surface to spawn, initiated January 1st and ending April 1st. However, the ascent is advanced if high levels of chlorophyll appear early so that reproduction better match the peak phytoplankton bloom. The modeled abundance of *C. finmarchicus* from SINMOD is found to match well with measurements of copepodites stages at the Svinøy and Gimsøy cross-shelf sections, as well as at the weather station Mike in the Norwegian Sea (Alver et al., 2016). The oceanographic model has been shown to reproduce the circulation dynamics at the Norwegian Shelf off Northern Norway (Skarðhamar and Svendsen, 2005).

Key features of the circulation along the Norwegian Coast toward the Barents Sea are the wedge-shaped Norwegian Coastal Current (NCC) hugging the coast at about the 200-m isobath and the Norwegian Atlantic Slope Current (NASC) at the shelf edge (Skagseth et al., 2015). The former is the main carrier of fish plankton with typical velocities between 0.1 and 0.35 ms^{-1}, while the latter is typically around 0.5 ms^{-1} but up to 1.0 ms^{-1} along the narrow shelf from Lofoten and northwards. At the surface the coastal waters may extend all the way to the shelf edge depending on wind directions and strength. Cross-shelf flow are guided by bottom topography with semi-permanent eddies above bank structures and troughs such as the Haltenbanken and the Traenadjupet, and anti-clockwise circulation inside Vestfjorden. At the entrance to the Barents Sea the NCC turn east while the NASC bifurcates with branches entering the Barents Sea or continuing toward the Fram Strait.

Note that the timing of *C. finmarchicus* egg production is found to be triggered by the phytoplankton spring bloom and that nauplii do not start feeding until stage 3 (Melle and Skjoldal, 1998). According to Head et al. (2015) stage duration from spawning to nauplii stage 3 varies from about 25.5 days at 0.36°C to 12.8 days at 4.8°C. Hence, at temperatures typical for the Norwegian continental shelf during spring, increasing from about 5°C close to the coast to about 8°C near the shelf edge and the NASC, the duration from spawning until the *C. finmarchicus* offspring require food is on the order of 10 days.

Larval Northeast Arctic Cod Individual-Based Lagrangian Model

We seed cod eggs evenly out over the spawning season by releasing 1,000 particles every 3rd day at 30 m depth at each of the 9 defined SGs covering 8 by 8 km through the spawning period from March 1st to April 30th (**Figure 1**; Ellertsen et al., 1989; Sundby and Nakken, 2008) amounting to 189,000 particles. Positioning of particles representing eggs and larvae are updated every 12 min, corresponding to twice the internal time step of SINMOD, according to modeled ocean currents and a 4th order Runge-Kutta advection scheme. Particles at first resemble eggs drifting at depths according to their individual buoyancies and modeled vertical mixing following the numerical scheme by Thygesen and Ådlandsvik (2007). The temporal varying individual buoyancies of eggs are quantified as the density difference between the eggs (individual random number drawn from a normally distributed salinity equivalent with mean and standard deviation 31.25 ± 0.69 unchanged through the egg stage; Myksvoll et al., 2011) and the ambient water. The eggs hatch according to individual modeled temperature exposures (Geffen et al., 2006) and continue as larvae (see **Supplementary Information**). The larvae migrate diurnally between 5 and 40 m depth according to their individual sizes and light conditions, i.e., seeking upwards whenever ambient light is below 1.0 μmol photons $m^{-2}s^{-1}$ and down if ambient light is equal or above this threshold (Opdal et al., 2011) with a swimming speed of 1.0 body length s^{-1}. Surface light is calculated as a function of day of the year, time of the day and latitude (Skartveit et al., 1998). Individual ambient light for the larvae is a function of the surface light and the diffuse attenuation (see **Supplementary Information**).

Larvae are initiated at the size of 45 μg (Folkvord, 2005) corresponding to a length of about 4 mm. Gape size of cod larvae is set to 8% of larval length (Fiksen and MacKenzie, 2002). This allows first-feeding larvae to feed upon *C. finmarchicus* of sizes up to 0.32 mm, corresponding to nauplii stage 2 at most (see Kristiansen et al., 2007 for *C. finmarchicus* lengths). Larval cod growth is temperature-dependent according to growth models by Folkvord (2005) and Björnsson et al. (2007) combined at 400 mg (see **Supplementary Information**), if not limited by prey consumption (see **Figure 2** for larval growth for 90 days under various fixed temperatures and SI for growth equations). From 75 days post hatch the growth is set to the temperature-dependent potential as the abundance of *C. finmarchicus* no longer is limiting alone due to a more complex diet. After about 3 days of food-unlimited growth past hatch the larvae are able to feed upon nauplii stage 3 if the ambient temperature is 5°C. At 12 days past hatch in the same temperature the larvae can even feed upon nauplii stage 4. Stage-dependent size categories of *C. finmarchicus* are taken from Kristiansen et al. (2007). **Figure 2** shows the size of NEA cod larvae for fixed temperatures ranging from 1 to 11°C and the corresponding ranges of *C. finmarchicus* nauplii 2–6 and copepodites 7–12 available as prey limited by the gape size of cod. Under fixed temperatures larvae do not reach 18 mm within 90 days if not experiencing temperatures of above nearly 5°C (**Figure 2**). E.g., a larvae growing at 5°C requires about 85 days from hatching to reach 18 mm, while at 8°C this would only take about 50 days. Food is stored in the larval stomach (set to 6% of larval weight) and may to some degree buffer variable food conditions. The feeding process is formulated based on parameter values from laboratory experiments on cod in Fiksen and MacKenzie (2002) and repeated in a numerical sensitivity study in Kristiansen et al. (2007). It includes quantification of encounter and capture for each prey stage (see **Supplementary Information**). According to Fiksen and MacKenzie (2002), the capture probability is set to 1 for prey-predator length up to 0.3, thereafter decreasing linearly from 1 to 0 for ratios between 0.03 and 0.09 but set to 0 for all ratios above 0.08. Metabolic costs (see **Supplementary Information**) are calculated according to Lough et al. (2005) and increase with increasing light due to enhanced feeding activity and predator escape (Lough et al., 2005; Kristiansen et al., 2007).

The NEA larval cod IBM has been assessed by comparing model and *in situ* measurements in the Vestfjord by Kristiansen et al. (2014). The larval IBM replicates vertical positioning of larvae and demonstrate the importance of turbulence-enhanced growth necessary to maintain net growth at depth with reduced prey and light availability.

RESULTS

Drift Trajectories

Particles representing eggs/larvae drift according to the modeled currents from the SGs along the coast toward the nursery grounds in the Barents Sea (**Figure 1**, here only showing 2001, see **Supplementary Information** for additional years). Drift trajectories reflect well-known circulation features at the shelf flowing north along the coast with some cross-shelf dispersal and retention resulting from bank structures and troughs, and anti-clockwise circulation inside Vestfjorden. Dispersal from the Lofoten area and northwards features strong laminar

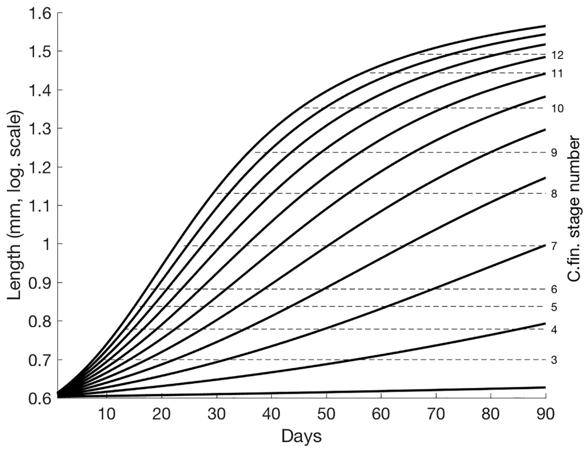

FIGURE 2 | Larval growth (logarithmic scale) according to Folkvord (2005) for fixed temperatures ranging from 1–11°C and corresponding upper threshold of available C. finmarchicus nauplii (1–6) and copepodites (7–12) stages limited by the copepod size and larval gape size. Note that newly hatched larvae are here initiated at lengths of about 4 mm. Assuming their gape size is 8% of their length enable them to initially feed upon nauplii stage 2.

flow on a narrow shelf, only about 10 km wide immediately downstream of Lofoten.

Spatial *C. finmarchicus* Abundance

Figure 3 shows smoothed modeled logarithmic abundances of nauplii stages 3 and 4 per grid cell along the Norwegian Coast in the drift routes of the NEA cod larvae at April 1st (upper panels) and May 1st (lower panels) for 1995, 2001, and 2002. The smoothing of abundances of nauplii 3 and 4 per grid cell is done by diving the number of nauplii in each grid cell across 5 by 5 grid cells according to a bell-shaped function. Abundances at April 1st, at the peak of NEA cod spawning, are mostly between 10 and 100 individuals per liter, though displaying strong horizontal gradients across eddies, filaments and fronts. North of 66°N the highest values are found in the core of the NCC and at the shelf edge, while farther south the *C. finmarchicus* are spread more out across the shelf. Downstream of the Lofoten, the elevated values coincide with a topographically steered rapid shelf edge current draining the wider upstream distributions. At May 1st, about 14 days after peak hatching of NEA cod eggs, there are still abundances up to an order of 100 per liter, but these now appear mostly off the shelf (and only to the northwest in 2001 and 2002). In particular, the areas to the south and close to the coast in the core of the NCC have low abundances of nauplii stages 3 and 4.

Temporal *C. finmarchicus* Abundance

At the SGs 2, 5 and 8 (here highlighted to contrast different latitudes) of NEA cod, the maximum abundances of stage-specific *C. finmarchicus* decrease with increasing size fractions from about 100 to 1 per liter (**Figure 4**, left panels, only showing 2001). Also, there is a clear delay in the peak of the larger size-classes of *C. finmarchicus* reflecting the time it takes to develop under the various temperature regimes, typically at a minimum around March-April before the seasonal heating starts. The single vertical lines in the panels indicate times of phytoplankton spring bloom as derived from remote sensing data (Vikebø et al., 2019). Generally, these indicate a delay in spring bloom along the coast, but the value far north (SG8) should be considered with care since it is only based on few data points due of the narrow shelf. The onsets of *C. finmarchicus* egg productions occur earlier than the phytoplankton spring bloom, but the peak of the nauplii stage 3 production is immediately after or concurrent except for SG 8.

Contrasting SGs 2, 5, and 8 shows that; (i) initiation of egg production and time to reach 10 eggs per liter is only a few days earlier in the south, (ii) to the north the development into the various nauplii stages is more gradual and the length of the stage durations are prolonged compared to the south, (iii) in particular, the tail of the curves show that presence of the various size fractions endures much longer at SG 5 representing the key spawning area of NEA cod. In fact, egg and nauplii stages 1–5 endure at concentrations above 3–4 individuals per liter until early May, almost 3 weeks longer than farther south.

Comparing nauplii stages 3 and 4 (the most relevant to first-feeding larval fish) across all years confirms that the findings for 2001 are representative also for 1995 and 2002 (**Figure 4**, right panels). However, 1995 stands out, with both nauplii stages enduring longer than for the other years at SG2. Contrary, at SG5 the concentrations of nauplii stage 3 and 4 drop late March and provide at least 3–4 individuals per liter in 2–3 weeks shorter than for 2001 and 2002. At SG8 inter-annual differences are generally low. Note that the inter-annual differences in the time of initiation of the various stages are less than the inter-stage differences, while this is opposite for the termination of the various stages.

Growth Performance as Function of Spawning Location and Time

Growth at rates above 90% of the food-unlimited potential according to present size and ambient temperature in more than 90% of the time is mainly achieved by individual larvae and pelagic juveniles spawned until the end of March for SGs from Lofoten and northwards (**Figure 5A**). The years 1995 and 2001 seem to have better conditions to support such growth rates (combination of prey availability and prey demands as a function of time-varying size and ambient temperatures) as compared to 2002.

Mean ambient temperatures from hatching until July 1st in general increase from 1995 through 2001 to a maximum in 2002 (**Figure 5B**). Also, mean ambient temperatures increase through the spawning season while decreasing with increasing latitude.

Calculating length by the end of June shows that size depends to a larger degree on ST as compared to SG (**Figure 5C**). There is a minor latitudinal effect where individuals spawned farther south grow faster than individuals to the north. Furthermore, there are only minor differences between the three years investigated.

The time it takes to reach 18 mm (**Figure 5D**) depends on both the ST and the SG. The minimum time is around 50 days and is achieved by individuals spawned during the early to mid-spawning period in the south and gradually later for SGs farther

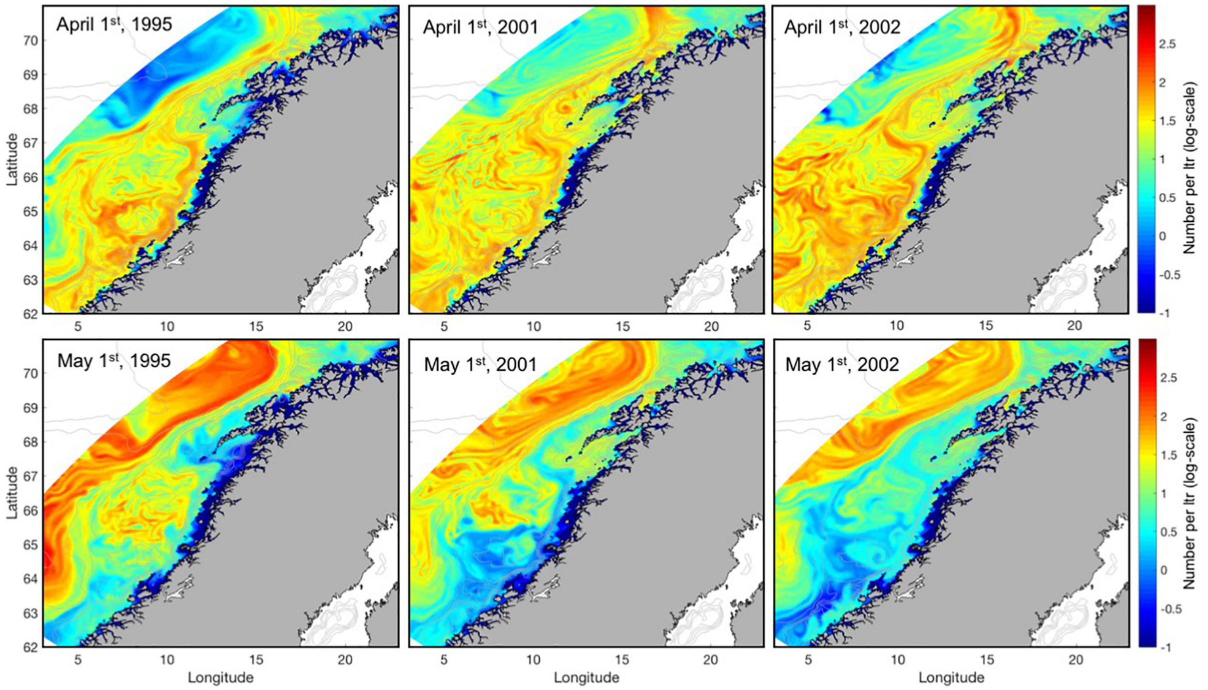

FIGURE 3 | The logarithmic sum of *C. finmarchicus* nauplii abundance per liter for stages 3 and 4 when distributed homogeneously across a 10 m water column at April 1st (upper panels) and May 1st (lower panels) for 1995, 2001, and 2002 (left to right).

north. Spawning early or late in the spawning period result in prolonged time to reach a larval size of 18 mm. In 2002 larvae reached 18 mm in fewer days than for 1995 and 2001.

Growth Performance as Function of Drift Trajectories, Temperature, and Prey Availability

The relative occurrences of prey-limited vs. prey-unlimited growth summarized within grid cells along the coast independent of larval size or time of event show that prey limitations are more frequent in areas of elevated current velocities (**Figure 6**). In such areas, there are up to 2 times more occurrences of prey-limited growth. Contrary, in areas of calmer waters, there are up to 5 times more occurrences of growth according to larval ambient temperature limitations. This is a general feature for all years though variation does occur.

The typical larval ages when growth is prey-limited (**Figure 7**) in the areas where this is most frequent (**Figure 6**) are between 40 and 60 days since spawning, i.e., about 25–45 days post hatching (**Figure 7**). Contrary, individuals experiencing prey-limited growth in areas dominated by prey-unlimited growth are on average older.

Still, most prey-limited larvae experience similar ambient temperatures as the larvae growing according to their temperature potential (**Figure 8**), though to a lesser degree in 2002 where it is on average lower. The ambient temperatures vary more for occurrences of prey-unlimited growth simply because this occurs more frequently.

However, despite that larvae generally experience high ambient biomass of *C. finmarchicus*, the larvae growing below their temperature potential are exposed to calanus stages above the size they are able to feed upon (**Figure 9**, left panel). Hence, these larvae are floating in a sea rich in prey of their preferred type but are not able to fit them in their gapes. The prey is abundant but has outgrown the cod larvae. Larvae growing prey-unlimited are floating in waters of similar prey availability, but more of this prey fit in the larval gapes (**Figure 9**, right panel).

DISCUSSION

By running a coupled ocean model, a NPZD-model, and an IBM of NEA cod ELS, we systematically investigate food limitations and growth performance for individual cod larvae drifting along the Norwegian coast for three selected years. The years represent contrasting conditions, but more years are required to generalize our findings. The cod ELS were initiated as pelagic eggs at well-known spawning grounds and drift toward nursery areas in the Barents Sea for the years 1995, 2001, and 2002. The model results confirm the expected seasonal development of *C. finmarchicus* into larger size fractions but at decreasing concentrations that drift north along the coast. The model indicates only minor delay in *C. finmarchicus* stage development across latitudes. Furthermore, the duration of stages is longer than the inter-annual variation in onset of each stage, indicating consistent feeding conditions across years. However, the latter may be an underestimate of the variability in phenology, especially since

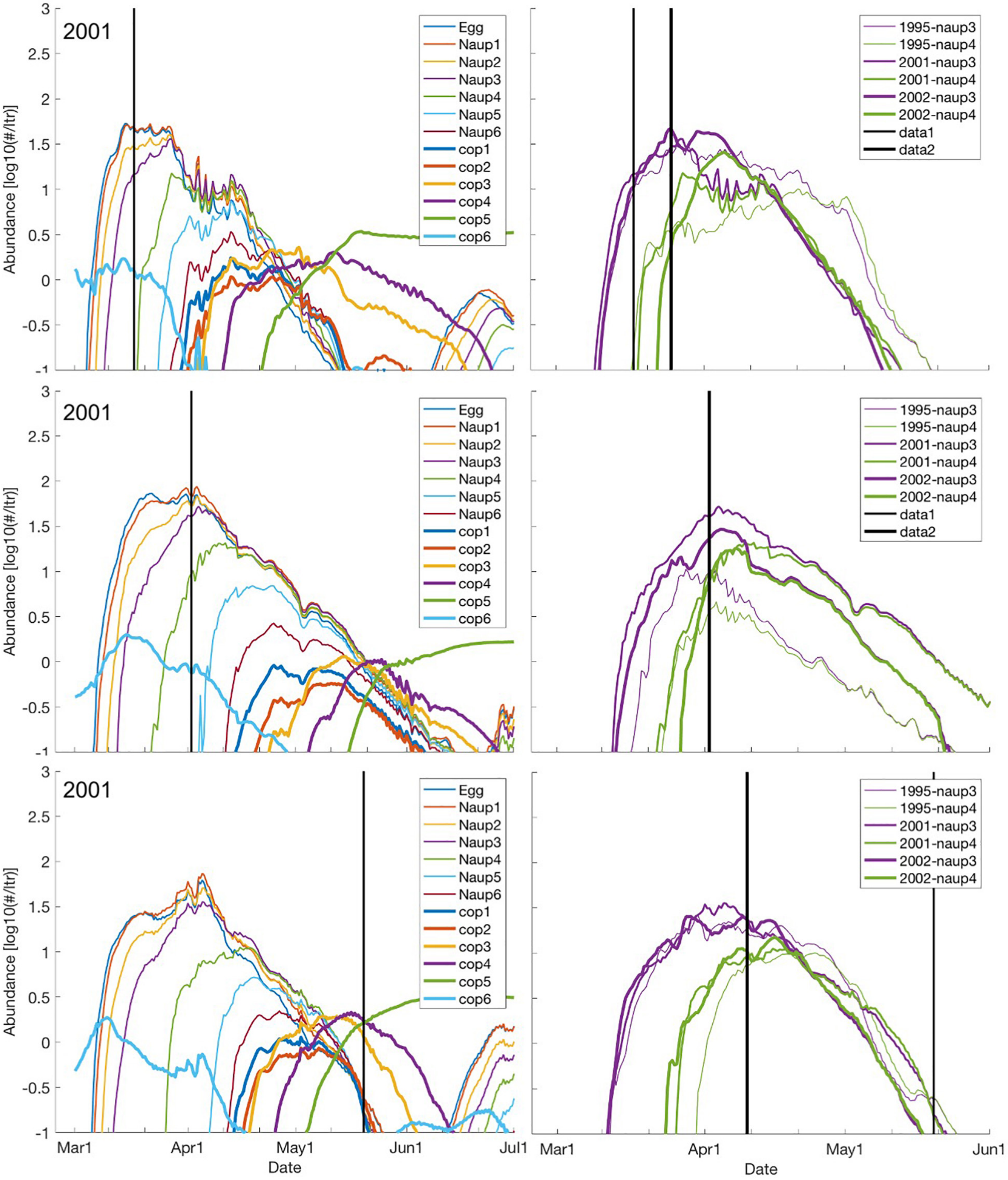

FIGURE 4 | Abundance at each nauplii and copepod stages for the SGs 2, 5, and 8 (upper, mid, and lower panels) during March through June for 2001 (left panels) when distributing *C. finmarchicus* across a 10 m water column. The vertical lines indicate time of spring bloom onset according to remote sensing data (Vikebø et al., 2019). Corresponding abundances for nauplii stages 3 and 4 but for the years 1995, 2001, and 2002 (right panels). Note that the SeaWIFS or MODIS data used here do not cover 1995, the onset of spring bloom inferred from the remote sensing data is concurrent for 2001 and 2002 at SG 5 and that the onset of spring bloom is suspiciously late at SG 8 in 2001 likely due to a combination of few data points at the narrow shelf and cloudiness.

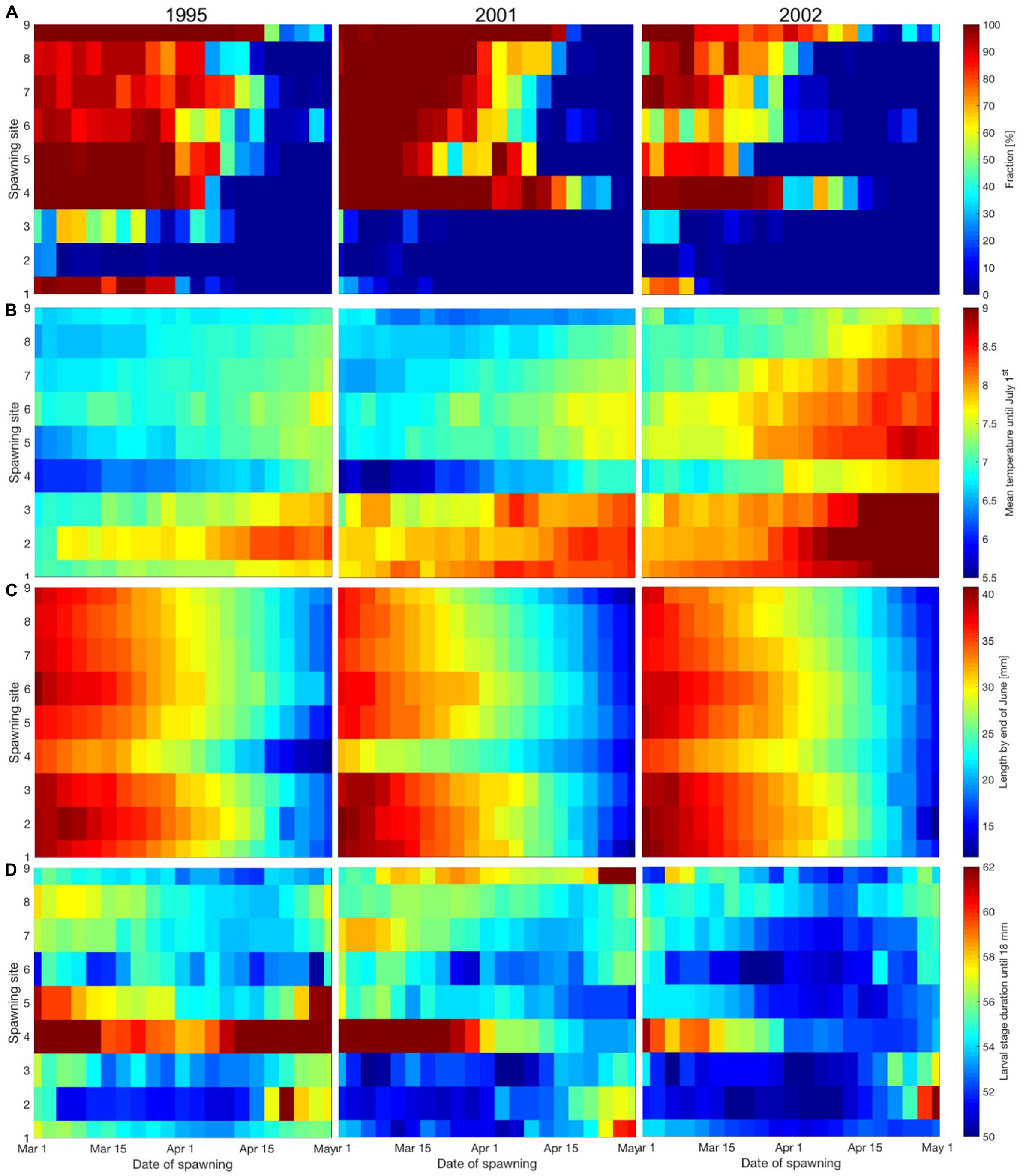

FIGURE 5 | Average (1995, 2001, and 2002) percentages of individual larvae and pelagic juveniles from each SG and ST across 1995, 2001, and 2002 that grow at more than 90% of their food-unlimited potential in more than 90% of the time **(A)**, mean larval ambient temperature **(B)**, larval length (mm) by the end of June **(C)** and larval stage duration (days) until the size of 18 mm **(D)**.

the *C. finmarchicus* egg production is reported to be tightly connected to the timing of phytoplankton spring bloom (e.g., Melle and Skjoldal, 1998) and the onset of spring bloom is shown to vary by up to a month along the Norwegian coast (Vikebø et al., 2019). More *in situ* measurements are needed to investigate this (Alver et al., 2016).

Across these years, we find that larval growth is less food-limited for spawning occurring from Lofoten and farther north for the first half of the spawning season and much less so in 1995 and 2001 than in 2002. But if rapid growth is crucial for survival (Houde, 2008) then our model results indicate that both early and late spawned larvae are performing more poorly; early

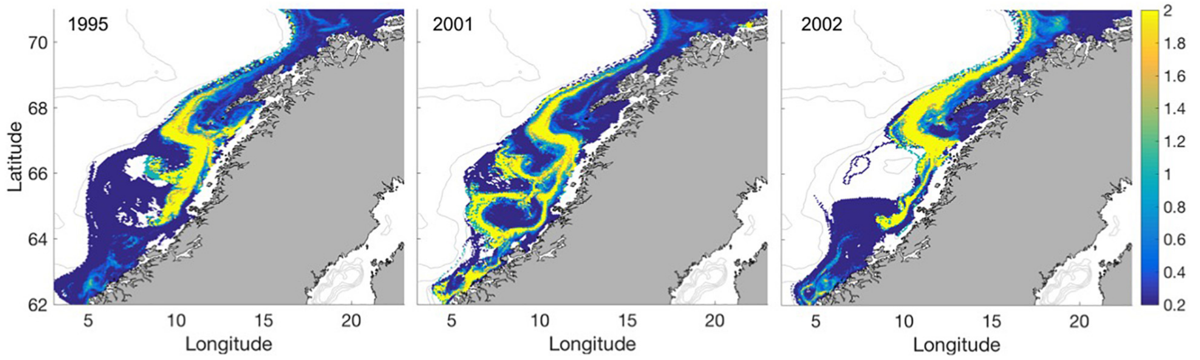

FIGURE 6 | The area-specific fraction of prey-limited growth/non-prey-limited growth for the years 1995, 2001, and 2002. Numbers at 0.2 indicate that there are 5 times more individuals not limited by prey, while 2 indicates that there is 2 times more individuals suffering from prey limitations.

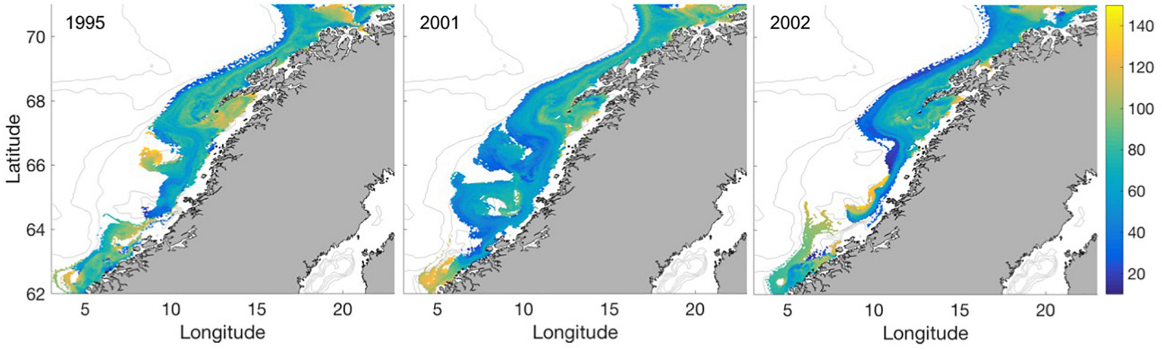

FIGURE 7 | Mean number of days after spawning when growth is prey-limited for the years 1995, 2001, and 2002.

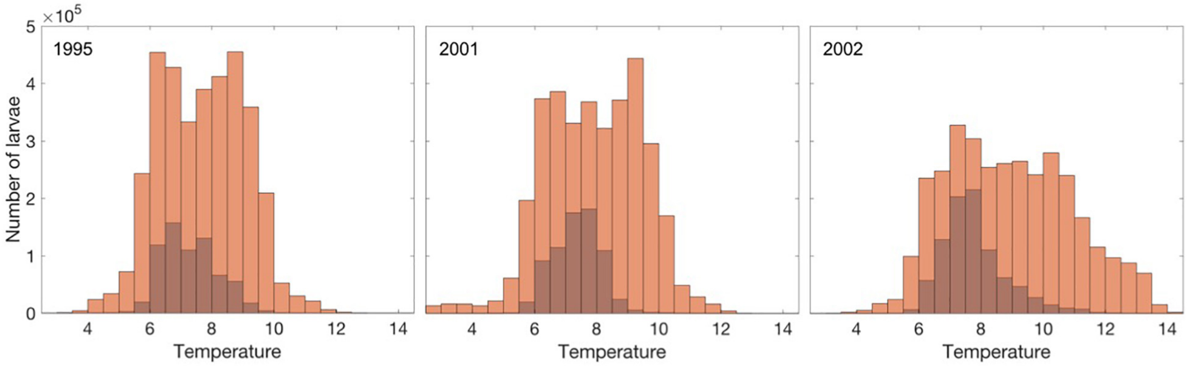

FIGURE 8 | Ambient temperature for individuals growing according to their temperature potential (light brown) and when limited by prey (dark brown) for the year 1995, 2001, and 2002.

spawned larvae because of low temperatures and late spawned larvae because of less suitable prey. Stige et al. (2019) in fact show that early life size in NEA cod is a better predictor for recruitment than abundance, underlining the importance of fast growth. Though larval size at summer reflects the age of the individual, the time available for predators to truncate the lower size-specter of the larvae is shorter for larvae spawned in the middle of the spawning period, but progressively later with increasing latitude, shifting from late March in the south to mid-April in the north.

Notably, the temperatures and thereby the growth potential is larger farther south but limited by food. Hence, additional energy spent during spawning migration is not rewarded for the offspring in stronger growth if compared to the Lofoten. Sundby and Nakken (2008) show that spawning shifts southwards only in cold periods. We have only tested years during a relatively

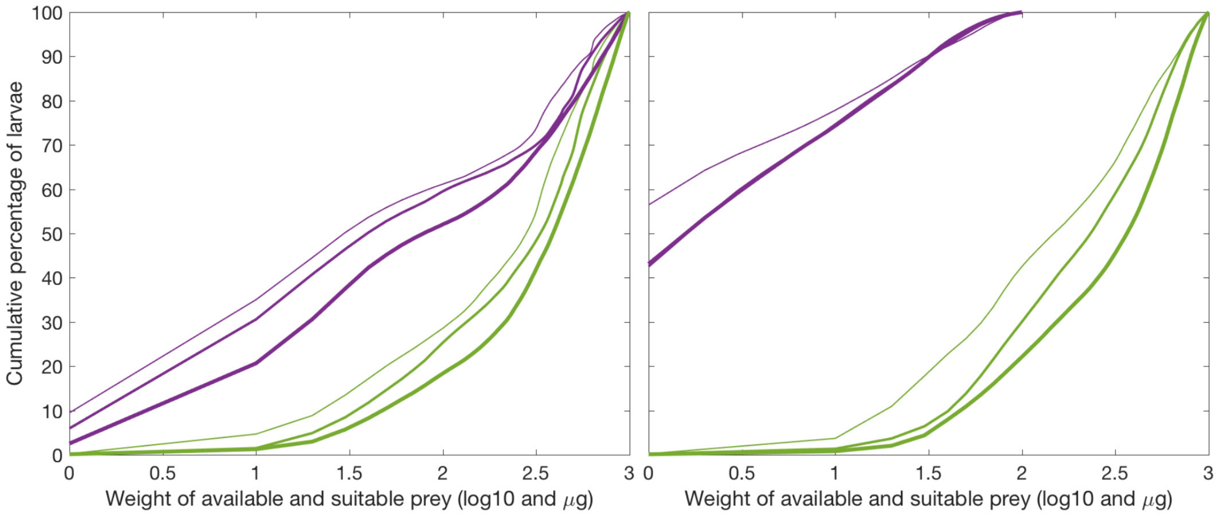

FIGURE 9 | Prey availability for starving larvae (left panel) during 1995, 2001, and 2002 (thin, medium, and thick line) accounting for suitable (magenta) and all (green) prey. Correspondingly (right panel) for non-starving larvae. E.g., left panel shows that about 43% of the larvae experiencing prey-limited growth is surrounded by between about 10–300 μg per liter but none of these have suitable size for the larvae to enable feeding.

warm period. But if prey conditions were similar during a cold period then a spawning migration to the more southern SGs could result in stronger growth than SGs farther north because prey requirements would be proportionally lower. That said, SG4 stands out with particularly low temperatures and growth rates. Strand et al. (2019) have previously shown that plankton dispersal is particularly challenging in Vestfjorden where SG 4 is located. This is due to a combination of semi-permanent eddies, tidal pumping through narrow straits, steep surrounding mountains guiding winds and freshwater runoff making it difficult to replicate transport out of the fjord.

Daewel et al. (2011, 2015) show that North Sea cod living at the southern limit of Atlantic cod with ambient temperatures close to its thermal tolerance match poorly with prey during warm years because of rapid egg and larval development and subsequent elevated food requirements while prey phenology is less affected by temperature changes and is therefore not available this early in the season. This is not the case for NEA cod according to the results here, as the model indicates that prey become available already during the first half of March, well in time to support newly hatched larvae also resulting from the earliest part of the spawning period. Contrary, in warm years late spawned cod lack food both because of higher demands under elevated temperatures and because they are partly outgrown by their prey. Hence, our results show that larval ambient temperatures increase across the years investigated here, but that NEA cod ELS are not able to utilize this through enhanced growth. As suitable prey availability does not increase proportionally to elevated temperatures a higher fraction of the larvae grows below their potential in 2002 as compared to the other 2 years.

Across years we see that areas of strong currents are less able to sustain larval growth according to the temperature potential. These areas include the core of the NCC, the shelf edge from the Lofoten and northwards, and occasionally flow around the grand bank structure of Haltenbanken. The prey-limited larvae growth occurs consistently 1–1.5 months after hatching. This shows that *C. finmarchicus* egg production has ceased and either these stages are washed out of the area or they have grown to older stages. The relatively high-water temperatures to the south will cause this transition through stages to be quicker than farther north. Results here indicate that there is sufficient prey in the waters of these larvae but not in sizes suitable for their gape size. Hence, as we know that prey-limited growth is more frequent to southern and late spawned larvae, the prey must have outgrown the larvae and is no longer available.

The study demonstrates how bottom-up processes can result in variable growth conditions of larvae, likely affecting survival, due to a mismatch in time with suitable prey resources. If survival is rather heterogeneous as compared to homogeneous, then we can expect a more pronounced impact from changes in the environment. This could be either from natural variability in ambient conditions or anthropogenic impacts that negatively affect ELS growth or survival in parts of the habitat. The current well-known spawning behavior of NEA cod (Sundby and Nakken, 2008) suggests that only low-frequency variation in environmental conditions affect spawning intensity, e.g., large-scale latitudinal shift in spawning with decadal variations in temperature. A wide temporal and spatial distribution in spawning could therefore serve the purpose of buffering high-frequency environmental variability. However, we are unable to generalize our findings further toward conclusions on the benefits of having a wide temporal and spatial distribution of spawning activities to buffer natural variability given that our results are for a limited number of years. Note though that Stige et al. (2017) have already shown that a high mean age and stock size in NEA cod result in a high abundance and wide distribution of eggs, but that this does not prove to buffer environmental variability and thereby securing strong recruitment.

The results must be interpreted with care as the models have limited resolution, especially in the spatial dimension, and simplifications of processes and ecosystem structure. These simplifications are due to lack of understanding, limitations in computational power and data to parameterize models. Predation on fish ELS might be important in areas where predators naturally aggregate, e.g., sea bird colonies (Sandvik et al., 2016). There are currently no density-dependent effects in fish ELS due to e.g., competition for *C. finmarchicus* included in the model used here. Especially at times and areas where prey become limited, here shown to be for early and late spawned individuals and in the areas of strong currents, this may result in even worse feeding conditions for the larvae. Initial conditions for eggs are based on a limited set of survey samples and though we believe this provides representative egg distributions it still introduces uncertainties. Also, we are aware that ocean models typically have challenges representing upper ocean density structures and mixing and that this affect plankton dispersal (Strand et al., 2019). Finally, we have added a diurnal vertical migration but no horizontal swimming behavior of the NEA cod ELS. Fiksen et al. (2007) have shown how dispersal may be affected by larval and juvenile behavior. However, while NEA cod larvae and juvenile diurnal behavior seems to be a feature in the ELS (e.g., Kristiansen et al., 2014), horizontal swimming in a specific direction long enough to significantly affect dispersal is yet not observed.

This work contributes to the further development of model systems for the exploration of fish population responses in connection with the impacts and outcomes of natural processes, anthropogenic stressors and their cumulative impacts (e.g., oil-spills, Langangen et al., 2017; Carroll et al., 2018). From a management perspective, the findings of the present work highlight the need for further process oriented as well as empirically based investigations of known NEA cod spawning areas, that combined with model hypothesis testing, can lead to a better understanding of why certain periods and places along the Norwegian continental shelf seem to be particularly favorable for pelagic drift stages. It is also of critical importance to focus on the role and influence of climate warming toward changing our current understanding of the patterns and processes affecting NEA cod spawning.

DATA AVAILABILITY STATEMENT

The raw data supporting the conclusions of this article will be made available by the authors, without undue reservation.

AUTHOR CONTRIBUTIONS

FV, OB, CE, and HF were responsible for formulating the hypothesis. FV, OB, CE, HF, and JJ prepared and performed most of the numerical calculations. FV, OB, CE, HF, JC, and ØL were responsible for synthesizing the literature. All authors have contributed to the discussions of hypothesis, methods and results, contributed to the work and approved it for publication.

FUNDING

Financial support for this project was provided by the Research Council of Norway (RCN# 255487/E40 and RCN #228107) and the industry-funded project—SYMBIOSES III (2019–2022).

ACKNOWLEDGMENTS

The simulations were performed on resources provided by UNINETT Sigma2—the National Infrastructure for High Performance Computing and Data Storage in Norway.

SUPPLEMENTARY MATERIAL

The Supplementary Material for this article can be found online at: https://www.frontiersin.org/articles/10.3389/fmars.2021.767191/full#supplementary-material

Supplementary Figure 1 | SGs (black stars) and every 100th drift trajectory of eggs/larvae from spawning until late July during 1995.

Supplementary Figure 2 | SGs (black stars) and every 100th drift trajectory of eggs/larvae from spawning until late July during 2002.

REFERENCES

Akimova, A., Hufnagl, M., and Peck, M. A. (2019). Spatiotemporal dynamics of predators and survival of marine fish early life stages: Atlantic cod (*Gadus morhua*) in the North Sea. *Prog. Oceanogr.* 176:102121.

Alver, M., Broch, O. J., Melle, W., Bagøien, E., and Slagstad, D. (2016). Validation of an Eularian population model for the marine copepod *Calanus finmarchicus* in the Norwegian Sea. *J. Mar. Syst.* 160, 81–93. doi: 10.1016/jmarsys.2016.04.004

Björnsson, B., Steinarsson, A., and Árnason, T. (2007). Growth model for Atlantic cod (*Gadus morhua*): effects of temperature and body weight on growth rate. *Aquaculture* 271, 216–226.

Bogstad, B., Yaragina, N. A., and Nash, R. D. M. (2016). The early life-history dynamics of Northeast Arctic cod: levels of natural mortality and abundance during the first 3 years of life. *Can. J. Fish. Aquat. Sci.* 73, 246–256. doi: 10.1139/cjfas-2015-0093

Carroll, J., Vikebø, F., Howell, D., Broch, O.-J., Nepstad, R., Augustine, S., et al. (2018). Resiliency of a healthy fish stock to recruitment losses from oil spills. *Mar. Pollut. Bull.* 126, 63–73. doi: 10.1016/j.marpolbul.2017.10.069

Cushing, D. (1990). Plankton production and year class strength in fish populations: an update of the match/mismatch hypothesis. *Adv. Mar. Biol.* 26, 249–293.

Daewel, U., Peck, M., and Schrum, C. (2011). Life history strategy and impacts of environmental variability on early life stages of two marine fishes in the North Sea: and individual-based modelling approach. *Can. J. Fish. Aquat. Sci.* 68, 426–443. doi: 10.1139/F10-164

Daewel, U., Schrum, C., and Gupta, A. K. (2015). The predictive potential of early life stage individual-based models (IBMs): an example for Atlantic cod *Gadus morhua* in the North Sea. *Mar. Ecol. Prog. Ser.* 534, 199–219. doi: 10.3354/meps11367

Daewel, U., Schrum, C., and Macdonald, J. I. (2019). Towards end-to-end (E2E) modelling in a consistent NPZD-F modelling framework (ECOSMO

E2E_v1.0): application to the North Sea and Baltic Sea. *Geosci. Model Dev.* 12, 1765–1789.

Ellertsen, B., Fossum, P., Solemdal, P., and Sundby, S. (1989). Relation between temperature and survival of eggs and first-feeding larvae of northeast Arctic cod (*Gadus morhua* L.). *Rapp. P.-v. Reun. Cons. Int. Explor. Mer* 191, 209–219.

Fiksen, Ø, and MacKenzie, B. R. (2002). Process-based models of feeding and prey selection in larval fish. *Mar. Ecol. Prog. Ser.* 243, 151–164. doi: 10.3354/meps243151

Fiksen, Ø, Jørgensen, C., Kristiansen, T., Vikebø, F., and Huse, G. (2007). Linking behavioural ecology and oceanography: larval behaviour determines growth, mortality and dispersal. *Mar. Ecol. Prog. Ser.* 347, 195–205.

Folkvord, A. (1997). "Ontogeny of cannibalism in larval and juvenile fishes with special emphasis on Atlantic cod," in *Early Life History and Recruitment in Fish Populations*, eds R. C. Chambers and E. A. Trippel (Dordrecht: Springer), 251–278.

Folkvord, A. (2005). Comparison of size-at-age of larval Atlantic cod (*Gadus morhua*) from different populations based on size- and temperature-dependent growth models. *Can. J. Fish. Aquat. Sci.* 62, 1037–1052.

Gallego, A., North, E., and Houde, E. D. (2012). Understanding and quantifying mortality in pelagic, early life stages of marine organisms – Old challenges and new perspectives. *J. Mar. Syst.* 93, 1–3. doi: 10.1016/j.jmarsys.2011.10.012

Geffen, A. J., Foc, C. J., and Nash, R. D. M. (2006). Temperature-dependent development rates of cod *Gadus morhua* eggs. *J. Fish Biol.* 69, 1060–1080. doi: 10.111/j.1095-8649.2006.01181.x

Hare, J. A. (2014). The future of fisheries oceanography lies in the pursuit of multiple hypotheses. *ICES J. Mar. Sci.* 71, 2343–2356.

Head, E. J. H., Gentleman, W. C., and Ringuette, M. (2015). Variability of mortality rates for *Calanus finmarchicus* early life stages in the Labrador Sea and the significance of egg viability. *J. Plankton Res.* 37, 1149–1165. doi: 10.1093/plankt/fbv080

Hixon, M. A., Johnson, D. W., and Sogard, S. M. (2014). BOFFFFs: on the importance of conserving old-growth age structure in fishery populations. *ICES J. Mar. Sci.* 71, 2171–2185.

Hjort, J. (1914). Fluctuations in the great fisheries of Northern Europe viewed in the light of biological research. *Rapp. P.-v. Reun. Cons. Int. Explor. Mer* 20, 1–237.

Houde, E. D. (1987). Fish early life dynamics and recruitment variability. *Am. Fish. Soc. Symp.* 2, 17–29.

Houde, E. D. (2008). Emerging from Hjort's Shadow. *J. Northwest Atlantic Fish. Sci.* 41, 53–70.

Kjesbu, O. S., Bogstad, B., Devine, J. A., Gjøsæter, H., Howell, D., Ingvaldsen, R. B., et al. (2014). Synergies between climate and management for Atlantic cod fisheries at high latitudes. *Proc. Natl. Acad. Sci. U.S.A.* 111, 3478–3483. doi: 10.1073/pnas.1316342111

Kristiansen, T., Fiksen, Ø., and Folkvord, A. (2007). Modelling feeding, growth, and habitat selection in larval Atlantic cod (*Gadus morhua*): observations and model predictions in a macrocosm environment. *Can. J. Fish. Aquat. Sci.* 64, 136–151.

Kristiansen, T., Vollset, K. W., Sundby, S., and Vikebø, F. (2014). Turbulence enhances feeding of larval cod at low prey densities. *ICES J. Mar. Sci.* 71, 2515–2529.

Langangen, Ø., Hjermann, D., Olsen, E., Stige, C., Ohlberger, J., Yaragina, N. A., et al. (2017). The effects of oil spills on marine fish: implications of spatial variation in natural mortality. *Mar. Pollut. Bull.* 119, 102–109. doi: 10.1016/j.marpolbul.2017.03.037

Langangen, Ø., Stige, L. C., Yaragina, N. A., Vikebø, F. B., Bogstad, B., and Gusdal, Y. (2014a). Egg mortality of northeast Arctic cod (*Gadus morhua*) and haddock (*Melanogrammus aeglefinus*). *ICES J. Mar. Sci.* 71, 1129–1136. doi: 10.1093/icesjms/fst007

Langangen, Ø., Stige, L. C., Yaragina, N. A., Ottersen, G., Vikebø, F. B., and Stenseth, N. C. (2014b). Spatial variations in mortality in pelagic early life stages of a marine fish (*Gadus morhua*). *Prog. Oceanogr.* 127, 96–107. doi: 10.1016/j.pocean.2014.06.003

Lough, R. G., Buckley, L. J., Werner, F. E., Quinlan, J. A., and Ed- wards, K. P. (2005). A general biophysical model of larval cod (*Gadus morhua*) growth applied to populations on Georges Bank. *Fish. Oceanogr.* 14, 241–262.

Melle, W., and Skjoldal, H. R. (1998). Reproduction and development of *Calanus finmarchicus*, C. glacialis and C. hyperboreus in the Barents Sea. *Mar. Ecol. Prog. Ser.* 169, 211–228.

Myksvoll, M. S., Sundby, S., Ådlandsvik, B., and Vikebø, F. B. (2011). Retention of coastal cod eggs in a fjord caused by interactions between egg buoyancy and circulation pattern. *Mar. Coast. Fish.* 3, 279–294. doi: 10.1080/19425120.2011.595258

Opdal, A. F., Vikebø, F. B., and Fiksen, Ø (2011). Parental migration, climate and thermal exposure of larvae: spawning in southern regions gives Northeast Arctic cod a warm start. *Mar. Ecol. Prog. Ser.* 439, 255–262.

Opdal, A., and Vikebø, F. B. (2015). Long-term stability in modelled zooplankton influx could uphold major fish spawning grounds on the Norwegian continental shelf. *Can. J. Fish. Aquat. Sci.* 73, 189–196. doi: 10.1139/cjfas-2014-0524

Ottersen, G., Bogstad, B., Yaragina, N. A., Stige, L. C., Vikebø, F., and Dalpadado, P. (2014). A review of early life history dynamics of Barents Sea cod (*Gadus morhua*). *ICES J. Mar. Sci.* 71, 2064–2087. doi: 10.1093/icesjms/fsu037

Peck, M., and Hufnagel, M. (2012). Can IBMs tell us why most larvae die in the sea? Model sensitivities and scenarios reveal research needs. *J. Mar. Syst.* 93, 77–93. doi: 10.1016/j.jmarsys.2011.08.005

Rose, K. A., Fiechter, J., Curchitser, E. N., Hedstrom, K., Bernal, M., Creekmore, S., et al. (2015). Demonstration of a fully-coupled end-to-end model for small pelagic fish using sardine and anchovy in the California current. *Prog. Oceanogr.* 138, 348–380.

Sandvik, H., Barrett, R. T., Erikstad, K. E., Myksvoll, M. S., Vikebø, F. B., Anker-Nilssen, T., et al. (2016). Drift patterns of fish larvae link coastal morphology to seabird colony distribution. *Nat. Commun.* 7:11599. doi: 10.1038/ncomms11599

Siddon, C. S., Kristiansen, T., Mueter, F. J., Holsman, K. K., Heintz, R. A., and Farley, E. V. (2013). Spatial match-mismatch between juvenile fish and prey provides a mechanism for recruitment variability across contrasting climate conditions in the eastern Bering Sea. *PLoS One* 8:e84526. doi: 10.1371/journal.pone.0084526

Skagseth, Ø, Slotte, A., Stenevik, E. K., and Nash, R. D. M. (2015). Characteristics of the Norwegian coastal current during years with high recruitment of Norwegian spring spawning herring (*Clupea harengus*, clupeidae). *PLoS One* 10:e0144117. doi: 10.1371/journal.pone.0144117

SkarÐhamar, J., and Svendsen, H. (2005). Circulation and shelf–ocean interaction off North Norway. *Cont. Shelf Res.* 25, 1541–1560. doi: 10.1016/j.csr.2005.04.007

Skartveit, A., Olseth, J. A., and Tuft, M. E. (1998). An hourly diffuse fraction model with correction for variability and surface albedo. *Sol. Energy* 63, 173–183.

Solemdal, P. (1997). Maternal effects - a link between the past and the future. *J. Sea Res.* 37, 213–227.

Stenevik, E. K., Melle, W., Gaard, E., Gislason, A., Broms, C. T. A., Prokopchuk, I., et al. (2007). Egg production of *Calanus finmarchicus*—a basin-scale study. *Deep Sea Res. II* 54, 2672–2685.

Stige, L. C., Ottersen, G., Yaragina, N. Y., Vikebø, F. B., Stenseth, N. C., and Langangen, Ø (2018). Combined effects of fishing and oil spills on marine fish: role of stock demographic structure for offspring overlap with oil. *Mar. Pollut. Bull.* 129, 336–342. doi: 10.1016/j.marpolbul.2018.02.056

Stige, L. C., Roger, L. A., Neuheimer, A. B., Hunsicker, M. E., Yaragina, N. A., Ottersen, G., et al. (2019). Density- and size-dependent mortality in fish early life stages. *Fish Fish.* 20, 962–976. doi: 10.1111/faf.12391

Stige, L. C., Yaragina, N. A., Langangen, Ø., Bogstad, B., Stenseth, N. C., and Ottersen, G. (2017). Effect of a fish stock's demographic structure on offspring survival and sensitivity to climate. *Proc. Natl. Acad. Sci.* 114, 1347–1352. doi: 10.1073/pnas.1621040114

Strand, K. O., Vikebø, F. B., Sundby, S., Sperrevik, A. K., and Breivik, Ø (2019). Subsurface maxima in buoyant fish eggs indicate vertical velocity shear and spatially limited spawning grounds. *Limnol. Oceanogr.* 64, 1239–1251.

Sundby, S. (1995). "Wind climate and foraging of larval and juvenile Arcto-Norwegian cod (Gadus morhua)," in *Climate Change and Northern Fish Populations. Can. Spec. Publ. Fish. Aquat. Sci. 121*, ed. R. J. Beamish (Ottawa, ON: National Research Council of Canada), 405–415.

Sundby, S., and Nakken, O. (2008). Spatial shifts in spawning habitats of Arcto-Norwegian cod related to multidecadal climate oscillations and climate change. *ICES J. Mar. Sci.* 65, 953–962.

Sundby, S., Bjørke, H., Soldal, A. V., and Olsen, S. (1989). Mortality rates during the early life stages and year class strength of the Arcto-Norwegian cod (*Gadus morhua* L.). *Rapp. P.-v. Reun. Cons. Int. Explor. Mer* 191, 351–358.

Thygesen, U. H., and Ådlandsvik, B. (2007). Simulating vertical turbulent dispersal with finite volumes and binned random walks. *Mar. Ecol. Prog. Ser.* 347, 145–153.

Toresen, R., Skjoldal, H. R., Vikebø, F., and Martinussen, M. B. (2019). Sudden change in long-term ocean climate fluctuations corresponds with ecosystem alterations and reduced recruitment in Norwegian spring-spawning herring (*Clupea harengus*, Clupeidae). *Fish Fish.* 20, 686–696. doi: 10.1111/faf.12369

Vikebø, F. B., Strand, K. O., and Sundby, S. (2019). Wind intensity is key to phytoplankton spring bloom under climate change. *Front. Mar. Sci.* 6:518. doi: 10.3389/fmars.2019.00518

Vikebø, F., Jørgensen, C., Kristiansen, T., and Fiksen, Ø (2007). Drift, growth, and survival of larval Northeast Arctic cod with simple rules of behaviour. *Mar. Ecol. Prog. Ser.* 347, 207–219.

Wassmann, P., Slagstad, D., Riser, C. W., and Reigstad, M. (2006). Modelling the ecosystem dynamics of the Barents Sea including the marginal ice zone: II. Carbon flux and interannual variability. *J. Mar. Syst.* 59, 1–24.

Conflict of Interest: OB was employed by the company SINTEF Ocean AS.

The remaining authors declare that the research was conducted in the absence of any commercial or financial relationships that could be construed as a potential conflict of interest.

frontiers in Marine Science

BRIEF RESEARCH REPORT
published: 06 January 2022
doi: 10.3389/fmars.2021.787765

Larval Fish Assemblages and Distribution Patterns in the Zhongsha Atoll (Macclesfield Bank, South China Sea)

Delian Huang[1,2], Jing Chen[1,3], Lei Xu[1,2], Xuehui Wang[1,2], Jiajia Ning[1,2], Yafang Li[1,2], Lianggen Wang[1,2], Shuangshuang Liu[1,2], Zhaojin Lin[1,2] and Feiyan Du[1,2]*

[1] South China Sea Fisheries Research Institute, Chinese Academy of Fishery Sciences, Guangzhou, China, [2] Guangdong Provincial Key Laboratory of Fishery Ecology and Environment, South China Sea Fisheries Research Institute, CAFS, Guangzhou, China, [3] College of Marine Science, Shanghai Ocean University, Shanghai, China

The remote coral reef in the deep sea is one of the most important nursery grounds for many marine fishes in the South China Sea. Diversity studies on larval fishes in this area are few, and the fish information on the coral reefs ecosystem is lacking. In this study, larval fishes were sampled during the summer of 2019 from the Zhongsha Atoll in the South China Sea and identified using DNA barcodes for the first time. Ninety-five larval fish species were recognized, belonging to 37 families and 12 orders based on morphological classification and DNA barcoding identification. The larval fish collected could be assigned to three categories as reef-associated, deep-sea, and pelagic. Most of the species were small fish with low commercial value but would play an essential role in the coral reef ecosystem. Some commercial fishes, including *Auxis thazard*, *Euthynnus affinis*, *Sarda orientalis*, *Decapterus macarellus*, *Lutjanus viridis*, and *Centropyge vrolikii*, were the dominant species higher than 2% total catch. The larval fish assemblage showed distinct spatial differences responding well with the geographical conditions. The most reef-associated fish occurred inside the Atoll, and the abyssal fish presented near the edge. In addition, larval fish spread over from the southwest to northeast may reflect the oceanography effect.

Keywords: larval fish assemblages, Zhongsha Atoll, South China Sea, coral reef, distribution patterns

Edited by:
Yuan Li,
Ministry of Natural Resources, China

Reviewed by:
Mohammad Reza Shokri,
Shahid Beheshti University, Iran
Kaizhi Li,
South China Sea Institute of Oceanology (CAS), China

***Correspondence:**
Feiyan Du
feiyanegg@163.com

Specialty section:
This article was submitted to Marine Fisheries, Aquaculture and Living Resources, a section of the journal Frontiers in Marine Science

Received: *01 October 2021*
Accepted: *22 November 2021*
Published: *06 January 2022*

Citation:
Huang D, Chen J, Xu L, Wang X, Ning J, Li Y, Wang L, Liu S, Lin Z and Du F (2022) Larval Fish Assemblages and Distribution Patterns in the Zhongsha Atoll (Macclesfield Bank, South China Sea).
Front. Mar. Sci. 8:787765.
doi: 10.3389/fmars.2021.787765

INTRODUCTION

Larval fish is the basis for the sustainable utilization of fishery resources, with survival directly influencing recruitment. Its investigations serve as an alternative approach for fish biodiversity, especially for some habitats, e.g., coral reefs and mangroves, where conventional fish sampling is challenging. The information on the distribution and abundance of larval fish provides a means to know the fish diversity, which is the base for fisheries management and conservation planning of the ecosystem (Almany et al., 2017).

Coral reefs are among the most biologically diverse and valuable ecosystems, providing habitat for over 4,000 species of fish at some point in their life cycle (Teh et al., 2013; Woodhead et al., 2019), especially in the early growth stages. Living coral reefs play as spawning areas, hatchery yards, nursery grounds, and recruitment sites (Jones et al., 2005; Cole et al., 2008; Almany et al., 2017).

As under increasingly exposed to the adverse effects of global climate change and human activities (Comte and Pendleton, 2018), coral reefs distinct declined, and the population and biodiversity of fish are threatened (Jones et al., 2004; De'ath et al., 2012).

The South China Sea is the largest low-latitude marginal sea, hosting some of the most productive and prosperous coral reef ecosystems and the most diverse fish on the Earth (Wang et al., 2011; Shan et al., 2021). The coral reef in the South China Sea covers ∼8,000 km^2, spreading over along its entire coastline and the islands in the deep sea, with the largest concentration around the relatively remote Zhongsha Atoll (Yu, 2012). The Zhongsha Atoll (also known as Macclesfield Bank) is one of the largest drowned atolls in the world. It locates in the central South China Sea, about 140 km away from Xisha islands and 550 km apart from Hainan Islands, comprising many submerged reefs in the seamount around by deep sea over 1,000 m in depth (**Figure 1**). The entire Zhongsha Atoll covers an area of about 23,500 km^2, with a collection of entirely submerged banks, seamounts, and shoals. Its discontinuous marginal reefs surrounded a lagoon with a water depth of up to 50–70 m. The platform slopes extend from the atoll margins to the deep-sea basin cut by submarine canyons, which promote the development of upwelling currents and may provide the hydrodynamic conditions required for reef-building corals and other organisms to flourish (Huang et al., 2020). The Zhongsha Atoll plays a vital role in the ecology and fish diversity of the South China Sea, supporting a diverse fish fauna in the sea around the Atoll (Sun et al., 2006; Chen et al., 2007).

Due to the limitation of geographical location and sampling conditions, the historical survey data of this sea area are concise, and the biology information of fish is limited. The precise nature and composition of the larval fishes across the entire Zhongsha Atoll are, as yet, poorly known (Chen, 1979). It is necessary to better understand the larval fish diversity and assemblages of the Atoll for guiding conservation policy for coral reefs of the South China Sea. The present study attempted to investigate the fish diversity in the Zhongsha Atoll using morphology and molecular tools for the first time and assess the ecological function of coral reef in the Atoll by assemblages and distribution patterns analysis to enhance our understanding of this ecosystem.

DATA AND METHODS

Sample Collection

Larval fishes were sampled from the Zhongsha Atoll aboard the *Yuezhanyuke 10* on May 9–29, 2019 (**Figure 1**). All sampling processes were conducted in the daytime. Samples were collected using a plankton net with a mouth diameter of 0.8 m, length of 2.8 m, and mesh size of 330 μm equipped with a centrally mounted flow meter (Hydro-Bios, Kiel-Holtenau, Germany). The net was trawling vertically from 200 m (or 5 m above the bottom at stations with depth <200 m) to surface with a speed of 1 m s^{-1}. After the net was retrieved, the samples were stored in 95% ethanol solution and frozen at −20°C. Each larval fish was sorted and identified to the lowest possible taxonomic level based on their morphological characteristics in the laboratory following guilds of Leis and Rennis (1983), Okiyawa (1988), and Wan and Zhang (2016).

DNA Data Collection

Then molecular identification method was performed with sample categorized (Lin et al., 2016). Before DNA extraction, larvae were macerated and then washed in ultrapure water to remove attachments. Total genomic DNA was extracted from tissue using a TIANamp Marine Animals DNA Kit (Tiangen, China) following manufacturer protocols. Partial of the mitochondrial cytochrome oxidase I (COI) sequences was amplified from total genomic DNA using the PCRs with the primers FishBCL and FishBCH (Baldwin et al., 2009).

PCRs were run in a final volume of 30 μl, containing 3 μl of 10 × PCR buffer, 3 μl of dNTPs mix (10 mM), 0.3 μl of E × *Taq* polymerase (Takara Bio. Inc.), 0.9 μl of each primer (10 μM), 2–3 μl of genomic DNA, and distilled water. PCR was carried out in an Eppendorf thermal cycler with 5 min initial denaturation at 95°C, followed by 35 cycles of 30 s at 95°C, 30 s at 52°C, 45 s at 72°C, and a final step at 72°C for 5 min on a 2720 Thermal Cycler (Applied Biosystems, Waltham, MA, USA). PCR products were visualized in 1.5% agarose gel, and samples amplified successfully were selected for sequencing. Sequences were obtained using an automated DNA sequencing device 3500 (Life Technologies, USA).

Data Analysis

The consensus DNA sequences were checked, and ambiguous bases were removed using the DNASTAR (DNASTAR, Inc., Madison, WI, USA) and then aligned in MEGA ver. 7.0.26 software (Kumar et al., 2016). Sequences were uploaded to the ORF finder (https://www.ncbi.nlm.nih.gov/orffinder/) to check for the reading frame, as no indels were observed. Identification was performed firstly by comparing with databases of National Center for Biotechnology Information (NCBI, https://www.ncbi.nlm.nih.gov/) with basic local-alignment search tool (BLAST) with a similarity threshold of 98% to assign specimens to species was followed (Ward et al., 2005). These sequences were then entered in FASTA format to the Barcode of life data systems (BOLD, http://www.boldsystems.org/) with the BOLD Identification Tool. Species-level identification would be returned when one is possible. All sequences have been deposited in GenBank (Accession Numbers OL512811—OL512944).

For those sequences that could not recognize into species, their best-matched sequences in the databases were downloaded for the following analysis. A Maximum likelihood (ML) tree of analyzed DNA barcode sequences based on the Kimura two-parameter (K2P) distance was performed using MEGA ver. 7.0.26 software, with 5,000 bootstrap replications (Kumar et al., 2016). Majority rule consensus trees were reconstructed after discarding a burn-in of 500 and displayed with TreeView v.1.6.6 (Page, 1996). The K2P genetic distances for defining the species, genus, and family levels were based on Ward et al. (2005).

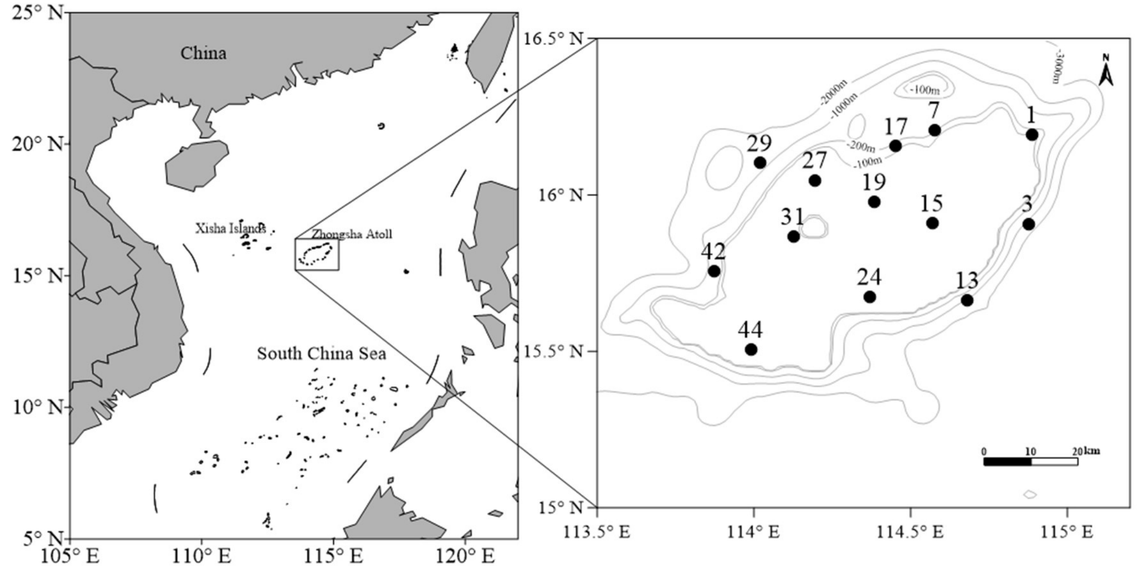

FIGURE 1 | Sampling area.

RESULTS

Species Identification and Fish Diversity

Totally 445 larval fish were collected, 146 specimens were used for molecular experiments after morphological classification, and 12 samples failed in DNA extraction and PCR process. The rest (91.78%) sequences of specimens were acquired, yielding a partial region of the COI mitochondrial gene sequences length of 648–722 bp without deletions, insertions, or stop codons. The detailed comparison was based on the aligned tool from the Genbank and BOLD systems, with the overall genetic similarity ranging from 81.87% to 100%. Comparing each of the COI sequences obtained from our samples with sequences deposited in databases online, 90 sequences (67.16%) were recovered as species of marine fish (sequence similarity > 98%). Altogether 44 sequences from 31 species showed low or no similarity matches with the databases, indicating that the reference sequences of these species were not barcoded ever. These unrecognized sequences belonged to small fishes, including *Diogenichthys* sp., *Naso* sp., and *Pseudanthias* sp. could be aligned into *Diogenichthys atlanticus*, *Naso minor,* and *Rabaulichthys squirei*, with private or early-released data in the BOLD systems (**Table 1**).

The ML tree based on K2P genetic divergence was constructed using the un-matched sequences and their most matched sequences in the databases (**Figure 2**). Most of the specimens were identified into genus without one affirmed into the family. Based on molecular identification, 95 species of fish larvae were identified from the 134 samples, of which 1, 30, and 64 were identified to family, genus, and species levels, respectively (**Table 1**). Perciformes was the most abundant order, with 69.66% of total specimens belonging to 55 taxa. Myctophiformes (10.11% of samples belonging to 17 taxa), Beryciformes (4.27% of specimens belonging to 5 taxa), and the other orders contributed 15.96% of specimens and 18 taxa (**Table 1**). Four orders contained only one species: *Histrio histrio* (Lophiiformes), *Engyprosopon latifrons* (Pleuronectiformes), *Sebastapistes* sp. (Scorpaeniformes), and *Netuma thalassina* (Siluriformes). The most diverse family was Myctophidae attributing to 17 species, followed by Gobiidae with 13 species, and Scombridae with 6 species. There were 11 and 24 predominant species with a higher than 2% and 1% of the total catch, respectively. The most dominant taxa was *Auxis thazard*, accounting for 8.99% of all specimens, followed by *Paracheilinus carpenter*, *Euthynnus affinis*, *Sarda orientalis*, and *Pseudanthias* sp., with 8.54%, 8.09%, 6.29%, and 4.72% in the catch. While about 38.95% (37 of 95) of all species were represented by a single specimen.

Most of the fish (64 of 95) collected belonged to subsistence fisheries, and only 32 taxa accounting for 46.07% of total specimens were commercial in fisheries. Twelve taxa of collected larvae were commercially valuable fishes. Taxa belonging to Scombridae (*Auxis thazard*, *Euthynnus affinis*, and *Sarda orientalis*), Carangidae (*Decapterus macarellus*, *D. macrosoma*, and *Selar crumenophthalmus*), Lutjanidae (*Lutjanus viridis*), and Lethrinidae (*Lethrinus rubrioperculatus*) accounted for 31.34% of the total specimens (**Table 1**). Account for the biology groups, 53 taxa were reef-associated fishes; 30 of them were fishes of the deep sea (such as bathy-demersal fish and bathy-mesopelagic fish), and the rest of the species collected were pelagic fishes, such as coastal-pelagic fish and oceanic-pelagic fish. Most of the un-matched specimens belonged to the reef-associated and the deep-sea fishes, whose adults were shy and tiny. They were limited to inhabiting heterogeneous coral reefs, such as species of Gobiidae, and abysmal sea (such as Myctophidae). Specimens of these fishes were hard to collect or identify by morphology.

TABLE 1 | Taxa composition and specimen proportion of the larval fishes.

No.	Order	Family	Taxa name	The best-matched species	ID in Genbank (or in BOLD with*) of the best match species	Similarity (%)	Specimens (%)
1	Aulopiformes	Scopelarchidae	*Scopelarchus michaelsarsi*	*Scopelarchus michaelsarsi*			0.22
2		Synodontidae	*Synodus jaculum*	*Synodus jaculum*			1.12
3	Beryciformes	Berycidae	*Beryx splendens*	*Beryx splendens*			0.22
4		Holocentridae	*Myripristis kuntee*	*Myripristis kuntee*			2.47
5			*Myripristis pralinia*	*Myripristis pralinia*			0.22
6		Melamphaidae	*Melamphaes polylepis*	*Melamphaes polylepis*			0.67
7			*Scopelogadus* sp.	*Scopelogadus beanii*	MG856844.1	87.52	0.67
8	Gadiformes	Bregmacerotidae	*Bregmaceros* sp.1	*Bregmaceros* sp.	ANGBF35886-19*	99.84	0.45
9			*Bregmaceros* sp.2	*Bregmaceros nectabanus*	AP004411.1	92.79	2.92
10	Lophiiformes	Antennariidae	*Histrio histrio*	*Histrio histrio*			0.45
11	Myctophiformes	Myctophidae	*Benthosema fibulatum*	*Benthosema fibulatum*			1.80
12			*Benthosema suborbitale*	*Benthosema suborbitale*			0.45
13			*Ceratoscopelus warmingii*	*Ceratoscopelus warmingii*			0.67
14			*Diaphus garmani*	*Diaphus garmani*			0.67
15			*Diaphus richardsoni*	*Diaphus richardsoni*			1.57
16			*Diaphus* sp.1	*Diaphus malayanus*	GBGCA11058-15*	97.66	0.22
17			*Diaphus* sp.2	*Diaphus mollis*	HQ564082.1	95.93	0.45
18			*Diogenichthys* sp.	*Diogenichthys atlanticus*	AP012233.1	95.13	0.22
19			*Electrona risso*	*Electrona risso*			0.22
20			*Hygophum* sp.	*Hygophum hanseni*	GBGCA11108-15*	97.72	0.22
21			*Lampadena anomala*	*Lampadena anomala*			0.22
22			*Lampanyctus* sp.1	*Lampanyctus hubbsi*	GBGCA11121-15*	91.13	0.22
23			*Lampanyctus* sp.2	*Lampanyctus turneri*	GBGCA11126-15*	96.35	0.22
24			*Lobianchia gemellarii*	*Lobianchia gemellarii*			0.22
25			*Myctophum spinosum*	*Myctophum spinosum*			1.80
26			*Symbolophorus evermanni*	*Symbolophorus evermanni*			0.45
27			*Symbolophorus* sp.	*Symbolophorus evermanni*	GU440540.1	90.19	0.45
28	Perciformes	Acanthuridae	*Acanthurus nigrofuscus*	*Acanthurus nigrofuscus*			0.22
29			*Naso annulatus*	*Naso annulatus*			0.22
30			*Naso* sp.	*Naso hexacanthus*	KF009630.1	89.64	0.22
31			*Naso thynnoides*	*Naso thynnoides*			0.22
32		Apogonidae	*Siphamia* sp.	*Siphamia tubifer*	FOAN1547-14*	90.74	1.80
33			*Pterapogon* sp.	*Pterapogon mirifica*	MK007149.1	86.09	0.22
34		Caesionidae	*Dipterygonotus balteatus*	*Dipterygonotus balteatus*			0.22
35		Callionymidae	*Callionymus kaianus*	*Callionymus kaianus*			0.90
36			*Calliurichthys australis*	*Calliurichthys australis*			1.12
37		Carangidae	*Decapterus macarellus*	*Decapterus macarellus*			2.92
38			*Decapterus macrosoma*	*Decapterus macrosoma*			0.45
39			*Selar crumenophthalmus*	*Selar crumenophthalmus*			0.22
40		Champsodontidae	*Champsodon* sp.	*Champsodon nudivittis*	MH807253.1	89.02	0.90
41		Cirrhitidae	*Paracirrhites arcatus*	*Paracirrhites arcatus*			0.90

(Continued)

TABLE 1 | Continued

No.	Order	Family	Taxa name	The best-matched species	ID in Genbank (or in BOLD with*) of the best match species	Similarity (%)	Specimens (%)
42		Coryphaenidae	*Coryphaena equiselis*	*Coryphaena equiselis*			0.22
43		Gempylidae	*Gempylus serpens*	*Gempylus serpens*			0.67
44		Gobiidae	*Ctenogobiops* sp.	*Ctenogobiops tangaroai*	HQ536632.1	85.71	0.22
45			*Eviota shimadai*	*Eviota shimadai*			0.90
46			*Eviota* sp.1	*Eviota latifasciata*	KP013247.1	91.74	0.22
47			*Eviota* sp.2	*Eviota imitata*	MF049073.1	88.77	0.22
48			*Eviota* sp.3	*Eviota cometa*	MK712446.1	84.30	1.80
49			*Eviota* sp.4	*Eviota spilota*	JX483976.1	95.33	0.67
50			*Hazeus* sp.	*Hazeus ingressus*	KY867545.1	86.74	0.90
51			Gobiidae sp.	*Sicyopterus punctissimus*	NC_044178.1*	81.87	0.67
52			*Obliquogobius* sp.	*Obliquogobius cometes*	KP244601.1	88.41	0.45
53			*Oxyurichthys* sp.	*Oxyurichthys longicauda*	MK777351.1	93.96	0.22
54			*Pleurosicya mossambica*	*Pleurosicya mossambica*			0.22
55			*Trimma okinawae*	*Trimma okinawae*			1.12
56			*Trimma* sp.	*Trimma nomurai*	RWTRM089-10*	87.50	0.90
57		Labridae	*Cirrhilabrus exquisitus*	*Cirrhilabrus exquisitus*			0.22
58			*Cirrhilabrus* sp.	*Cirrhilabrus cyanopleura*	FJ583220.1	94.48	0.45
59			*Paracheilinus carpenteri*	*Paracheilinus carpenteri*			8.54
60			*Xiphocheilus* sp.	*Xiphocheilus typus*	KM224716.1	95.89	0.22
61		Lethrinidae	*Lethrinus rubrioperculatus*	*Lethrinus rubrioperculatus*			0.22
62		Lutjanidae	*Lutjanus bengalensis*	*Lutjanus bengalensis*			0.67
63			*Lutjanus viridis*	*Lutjanus viridis*			2.02
64		Nomeidae	*Cubiceps pauciradiatus*	*Cubiceps pauciradiatus*			1.12
65		Pinguipedidae	*Parapercis rubromaculata*	*Parapercis rubromaculata*			0.22
66		Pomacanthidae	*Centropyge fisheri*	*Centropyge fisheri*			0.22
67			*Centropyge vrolikii*	*Centropyge vrolikii*			2.02
68		Pomacentridae	*Chromis margaritifer*	*Chromis margaritifer*			0.22
69			*Lepidozygus tapeinosoma*	*Lepidozygus tapeinosoma*			1.80
70		Pseudochromidae	*Pseudoplesiops* sp.	*Pseudoplesiops wassi*	FUT359-18*	88.25	0.22
71		Scaridae	*Chlorurus spilurus*	*Chlorurus spilurus*			0.90
72		Scombridae	*Auxis thazard*	*Auxis thazard*			8.99
73			*Euthynnus affinis*	*Euthynnus affinis*			8.09
74			*Grammatorcynus bilineatus*	*Grammatorcynus bilineatus*			0.45
75			*Gymnosarda unicolor*	*Gymnosarda unicolor*			0.22
76			*Sarda orientalis*	*Sarda orientalis*			6.29
77			*Thunnus albacares*	*Thunnus albacares*			0.67
78		Serranidae	*Chelidoperca margaritifera*	*Chelidoperca margaritifera*			0.22
79			*Pseudanthias hypselosoma*	*Pseudanthias hypselosoma*			0.45

(Continued)

TABLE 1 | Continued

No.	Order	Family	Taxa name	The best-matched species	ID in Genbank (or in BOLD with*) of the best match species	Similarity (%)	Specimens (%)
80			*Pseudanthias mooreanus*	*Pseudanthias mooreanus*			0.22
81			*Pseudanthias* sp.	*Pseudanthias squamipinnis*	FJ583941.1	87.40	4.72
82			*Pseudogramma polyacantha*	*Pseudogramma polyacantha*			0.45
83	Pleuronectiformes	Bothidae	*Engyprosopon latifrons*	*Engyprosopon latifrons*			1.80
84	Salmoniformes	Gonostomatidae	*Cyclothone acclinidens*	*Cyclothone acclinidens*			0.67
85			*Cyclothone pallida*	*Cyclothone pallida*			0.45
86			*Cyclothone* sp.	*Cyclothone signata*	MFC073-08*	88.02	0.67
87		Sternoptychidae	*Polyipnus ruggeri*	*Polyipnus ruggeri*			0.22
88	Scorpaeniformes	Scorpaenidae	*Sebastapistes* sp.	*Sebastapistes fowleri*	MN549776.1	92.28	1.12
89	Siluriformes	Ariidae	*Netuma thalassina*	*Netuma thalassina*			0.22
90	Stomiiformes	Phosichthyidae	*Vinciguerria attenuata*	*Vinciguerria attenuata*			0.22
91			*Vinciguerria* sp.	*Vinciguerria nimbaria*	HQ563942.1	95.64	1.80
92	Tetraodontiformes	Balistidae	*Melichthys vidua*	*Melichthys vidua*			0.45
93			*Sufflamen chrysopterum*	*Sufflamen chrysopterum*			2.02
94		Tetraodontidae	*Lagocephalus cheesemanii*	*Lagocephalus cheesemanii*			0.45
95			*Lagocephalus*	*Lagocephalus*			0.67

The ID and similarity of best-matched sequences correspond to unmatched specimens shown.
*BOLD, the Barcode of life data systems. The symbol * means the ID numbers were origined from the BOLD.*

Distribution and Assemblage Patterns

The sampling stations were divided into internal, edge, and outer groups according to their location at the Atoll, with depth <100, 100–200, and greater than 200 m, respectively (**Table 2**). The overall mean taxa amount was 15.62 ± 8.77, and the abundance was 571.85 ± 556.10 ind/1,000 m^{-3}. The lowest species number, abundance, diversity index (*H*'), and evenness index (*J*') with minimum variation ranges are presented in the edge area. The highest average abundance occurred in the outer area, while changing tremendously between stations. The species number and abundance in the internal area were relatively lower than the outer area, while higher *H*' and *J*' had a high fluctuation in these stations.

The spatial distribution of species number and abundance of larval fish is also shown in **Figure 3**. Many more species are distributed in the western (stations 31 and 42) and central area, rather than the near edge in the southern and northeastern of the Zhongsha Atoll. At the same time, a high species number also appeared in the southeastern region (stations 3 and 13) outside the edge (**Figure 3A**). The distribution of abundance was in accordance with that of species number, except for stations 3 and 13 with related low density of individuals occurred (**Figure 3B**).

The reef-associated fishes appeared in most sampling stations without station 44 on the southern edge. The species number and percentage increased from the southwestern to the inner Atoll and then decreased gradually to the northeastern (**Figure 3A**). In comparison, the abundance showed a roughly opposite trend of the species number, with a higher proportion of reef-associated fishes in the northeastern (**Figure 3B**). The pelagic fishes distributed in all the stations with the species number and their proportion were both low (**Figure 3A**), while the highest values were found in the southwestern station and lower to northeast account for the abundance and its ratio (**Figure 3B**). The deep-sea fishes occurred in all stations showing an apparent distribution pattern that most deep-sea fishes appeared at off or near the edge of the Atoll. More minor species and individuals dispersed over the Atoll internal (**Figure 3**).

DISCUSSION

Identification and Diversity of Fish

It is most commonly accepted that fish biological diversity in the coral reef of the South China Sea is immensely rich (Arai, 2015). In face to the coral decline, understanding the present status of coral reef fishes in the South China Sea in terms of their biodiversity and abundance is essential for the sustainable protection and restoration of coral reef ecosystems (Jones et al., 2004; Brandl et al., 2019). While with the limitations of sampling and habitat heterogeneity, many fish species in the coral reef are undiscovered ever, especially for small species with their all life stages confined to a minimal area (Brandl et al., 2018; Coker et al., 2018). It is

FIGURE 2 | Kimura two-parameter (K2P) distance ML tree of un-matched sequences and their best-matched sequences from the NCBI and BOLD systems with the ID of the samples and species given. Bootstrap values >50 are shown. ML, Maximum likelihood; K2P, the Kimura two-parameter; NCBI, National Center for Biotechnology Information; BOLD systems, the Barcode of life data systems.

TABLE 2 | Average species number, abundance (ind/1000 m^3), Shannon-Weaver diversity index (*H'*), and Pielou's evenness index (*J'*) of larval fishes from different areas.

Area	Station	Species number	Abundance	*H'*	*J'*
Internal	15, 19, 24, 27, 31, 44	13.17 ± 8.91	615.20 ± 426.14	6.34 ± 5.15	5.84 ± 5.65
Edge	1, 7, 17	10.00 ± 4.36	128.56 ± 64.04	2.18 ± 0.50	0.98 ± 0.02
Outer	3, 13, 29, 42	23.50 ± 7.85	839.31 ± 859.68	4.07 ± 1.11	2.95 ± 2.35
Total		15.62 ± 8.77	571.85 ± 556.10	4.68 ± 3.80	3.83 ± 4.36

hard to comprehensively understand the fish diversity by the traditional sampling gear, such as gill nets, hand-lines, long lines, hydroacoustic techniques, or visual investigation, especially in the areas that are hard to reach. The diversity of coral reefs is supposed to underestimate (Hubert et al., 2012). The ichthyoplanktons are easy to collect. Their investigation has become an alternative way of fish diversity in the coral reef (Carassou et al., 2009).

Few studies investigate the fish in the early life stage in the coral reef in the South China Sea. There is hardly any information

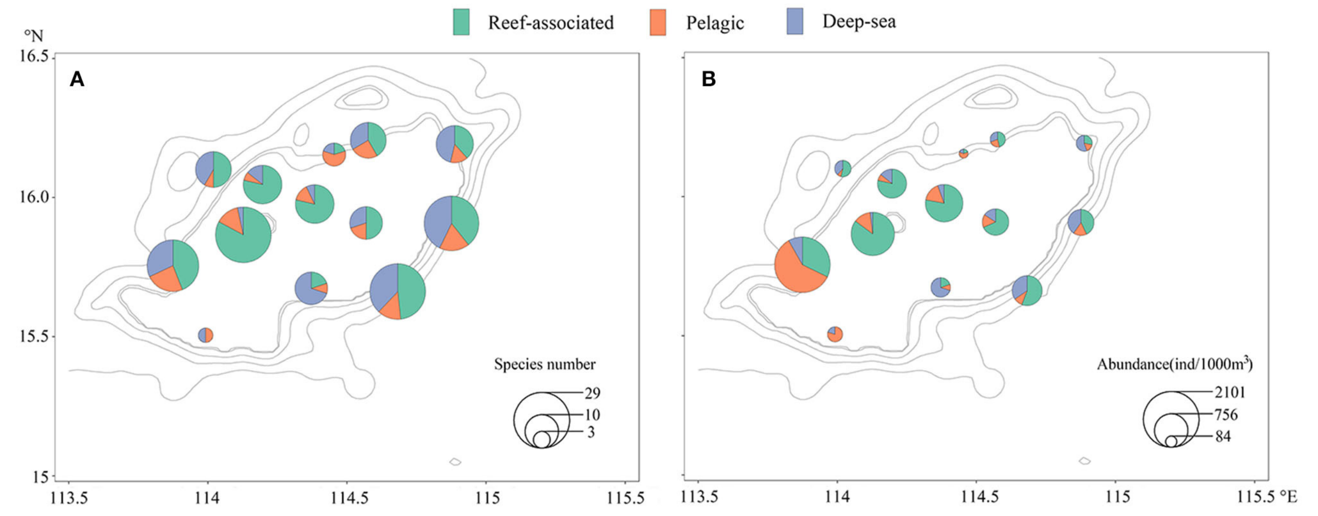

FIGURE 3 | (A,B) Distribution of species number and abundance of larval fish account for taxa groups as reef-associated, deep-sea, and pelagic fishes.

on the early life-history stages of fish from the Zhongsha Atoll, the biggest atoll in the South China Sea. The only reference we could find is about pelagic eggs and larvae of fish in the Zhongsha Islands by Chen (1979). We used DNA barcoding to identify the species in the Zhongsha Atoll for the first time and some unknown species (such as 12 taxa of Gobiidae) previously coral reef fish surveys (**Table 1**). We also found that the coral reefs support many deep-sea fish larvae, for their adult would not be collected in the shallow coral reef waters. The larval fish survey helped to improve our understanding of fish diversity on the coral reef in the Zhongsha Atoll. While 44 sequences from 31 species showed no similarity matches with the database, indicating that the reference sequences of these species were not barcoded ever. It is necessary to acquire genome information of coral reef fishes continuously. Even though we found 95 fish taxa in the Zhongsha Atoll in one cruise, the actual fish species number was likely to be far higher than this current study. More investigation is necessary to better known fish diversity in the coral reef of Zhongsha Atoll.

Distribution and Assemblage Patterns of Larval Fish

The coral reef serves as a critical ground to marine fishes for spawning, nursing, and feeding (Brandl et al., 2019; Woodhead et al., 2019; Wagner et al., 2020). Coral reefs are compound habitats, with complex water flow and water environments, with noticeable regional and temporal variations. The distribution of marine larvae could reflect the adaptation to habitats. Even though many studies focused on the distribution and community of larval fishes, the larval fish assemblage pattern in the coral reef waters is still unknown (Drew and Amatangelo, 2017; Edmunds et al., 2018).

The distribution of larval fishes changed obviously in the Atoll. More species and individuals occurred in the western and central parts of the Zhongsha Atoll (**Table 2** and **Figure 3**), respectively. Oceanographic features, such as eddies and fronts, promoted by monsoons or topography in the coral reef waters, are confirmed in enhancing the spread and survival of marine fish larvae (Shulzitski et al., 2016). The South China Sea is strongly affected by monsoon systems, influenced by the southwest monsoon causing southwest-northeast current in summer (Luo et al., 2016). The upwelling would generate at a sudden seafloor elevation in the western Zhongsha Atoll (**Figure 1**). The upwelling water might also elevate the diffusion efficiency and provide more food sources, supporting highly diverse fish larvae in the internal Atoll downstream. The habitat complexity would be afforded coral reefs as a shelter for larval fishes, maintaining a higher survival. It would make the internal Atoll a suitable habitat to live in for larval fishes, with the highest species diversity and evenness. However, taxa number, abundance, indexes *H'* and *J'* of larval fishes in the edge area were lower than the near parts (**Table 2**). It might be the integrated result of oceanographic and geomorphic over the shallow coral reef and the deep sea. The larval fishes of reef-associated, deep-sea, and pelagic co-occurrence in the Zhongsha Atoll, but their distribution patterns differed greatly (**Figure 3**). The reef-associated larval fishes seemed likely to distribute within or near the Atoll area, while most deep-sea larval fishes dispersed near the edge area. The pelagic fishes scattered in all the stations with the species number and its proportion were both low. The species number and abundance also showed a roughly consistent trend with the southwest monsoon. Therefore, the geographical variation shown from distribution and assemblage patterns of larval fish might result from topography and the monsoon effect. Faced with the deteriorating condition of deep-sea coral reefs habitats (Roberts and Hirshfield, 2004; Roder et al., 2013; Rogers, 2019), there is a pressing need to better understand reef ichthyoplankton populations, community dynamics, and the key ecological processes effects in the coral reefs.

CONCLUSION

The larval fish investigation provided an alternative way to investigate fish diversity in the coral reef of Zhongsha Atoll. Ninety-five larval fish species were identified based on morphological classification and DNA barcoding for the first time, reflecting the rich diversity of larval fish species in the Atoll. Most taxa were non-economic small fishes but would play an essential role in the coral reef ecosystem. Some commercial species, including *Auxis thazard*, *Euthynnus affinis*, *Sarda orientalis*, *Decapterus macarellus*, *Lutjanus viridis*, and *Centropyge vrolikii*, were the dominant species higher than 2% total catch. The larval fish assemblage in the Atoll was assigned categories to reef-associated, deep-sea, and pelagic, respectively. The distribution of larval fishes changed distinctly in the Atoll. The abundance of larval fish was high in the outer Atoll, indexes of species diversity and species evenness were high in the internal area, while the abundance, species number, and indexes of species diversity and species evenness were low in the edge stations. The most reef-associated fish occurred inside the Atoll, and the abyssal fish presented near the edge. The larval fish assemblage distribution might be the result of the oceanographic and geomorphologic effect.

DATA AVAILABILITY STATEMENT

The datasets presented in this study can be found in online repositories. Sequence data for specimens were submitted to the NCBI with the accession numbers as OL512811—OL512944.

ETHICS STATEMENT

The animal study was reviewed and approved by Ethics Committee of the Laboratory of Animal Welfare and Ethics of South China Sea Fisheries Research Institute.

AUTHOR CONTRIBUTIONS

DH designed the work, collected the samples, analyzed the data, and wrote the manuscript. JC performed the DNA barcoding analysis and drafted the manuscript. LX, JN, YL, LW, and SL were involved in revising critically for important intellectual content. ZL participated in the design of the work. FD participated in the work design and approved the final version. All authors contributed to the article and approved the submitted version.

FUNDING

This work was supported by the Science and Technology Basic Resources Investigation Program of China (2018FY100105 and 2017FY201405), the Central Public-interest Scientific Institution Basal Research Fund (2018YB04), and the Fund of Guangdong Provincial Key Laboratory of Fishery Ecology and Environment (FEEL-2020-11).

ACKNOWLEDGMENTS

We express our sincere thanks to the NCBI and BOLD systems for the easy access to fish barcoding data. We also thank the officers and the crew of the *Yuezhanyuke 10* for their assistance in sampling.

REFERENCES

Almany, G. R., Planes, S., Thorrold, S. R., Berumen, M. L., Bode, M., Saenz-Agudelo, P., et al. (2017). Larval fish dispersal in a coral-reef seascape. *Nat. Ecol. Evol.* 1, 1–7. doi: 10.1038/s41559-017-0148

Arai, T. (2015). Diversity and conservation of coral reef fishes in the Malaysian South China Sea. *Rev. Fish Biol. Fish.* 25, 85–101. doi: 10.1007/s11160-014-9371-9

Baldwin, C. C., Mounts, J. H., Smith, D. G., and Weigt, L. A. (2009). Genetic identification and color descriptions of early life-history stages of Belizean *Phaeoptyx* and *Astrapogon* (Teleostei: Apogonidae) with Comments on identification of adult *Phaeoptyx*. *Zootaxa* (2008) 26, 1–22. doi: 10.5281/zenodo.185742

Brandl, S. J., Goatley, C. H., Bellwood, D. R., and Tornabene, L. (2018). The hidden half: ecology and evolution of cryptobenthic fishes on coral reefs. *Biol. Rev.* 93, 1846–1873. doi: 10.1111/brv.12423

Brandl, S. J., Rasher, D. B., Cote, I. M., Casey, J. M., Darling, E. S., Lefchecku, J. S., et al. (2019). Coral reef ecosystem functioning: eight core processes and the role of biodiversity. *Front. Ecol. Environ.* 17, 445–453. doi: 10.1002/fee.2088

Carassou, L., Mellin, C., and Ponton, D. (2009). Assessing the diversity and abundances of larvae and juveniles of coral reef fish: a synthesis of six sampling techniques. *Biodiv. Conservat.* 18, 355–371. doi: 10.1007/s10531-008-9492-3

Chen, G., Li, Y., and Chen, X. (2007). Species diversity of fishes in the coral reefs of South China Sea. *Biodiv. Sci.* 15, 373–381. doi: 10.1360/biodiv.060268

Chen, Z. (1979). Floating fish eggs and larvae of Xisha and Zhongsha Islands. *Aquat. Sci. Technol. Inform.* 4, 11–13.

Coker, D. J., DiBattista, J. D., Sinclair-Taylor, T. H., and Berumen, M. L. (2018). Spatial patterns of cryptobenthic coral-reef fishes in the Red Sea. *Coral Reefs* 37, 193–199. doi: 10.1007/s00338-017-1647-9

Cole, A. J., Pratchett, M. S., and Jones, G. P. (2008). Diversity and functional importance of coral-feeding fishes on tropical coral reefs. *Fish Fisheries* 9, 286–307. doi: 10.1111/j.1467-2979.2008.00290.x

Comte, A., and Pendleton, L. H. (2018). Management strategies for coral reefs and people under global environmental change: 25 years of scientific research. *J. Environ. Manag.* 209, 462–474. doi: 10.1016/j.jenvman.2017.12.051

De'ath, G., Fabricius, K. E., Sweatman, H., and Puotinen, M. (2012). The 27–year decline of coral cover on the Great Barrier Reef and its causes. *Proc. Natl. Acad. Sci. U. S. A.* 109, 17995–17999. doi: 10.1073/pnas.1208909109

Drew, J. A., and Amatangelo, K. L. (2017). Community assembly of coral reef fishes along the Melanesian biodiversity gradient. *PLoS ONE* 12:186123. doi: 10.1371/journal.pone.0186123

Edmunds, P. J., Mcilroy, S. E., Adjeroud, M., Ang, P. O., Bergman, J. L., Carpenter, R. C., et al. (2018). Critical information gaps impeding understanding of the role of larval connectivity among coral reef islands in an era of Global Change. *Front. Mar. Sci.* 5:290. doi: 10.3389/fmars.2018.00290

Huang, X., Betzler, C., Wu, S., Bernhardt, A., Eagles, G., Han, X., et al. (2020). First documentation of seismic stratigraphy and depositional signatures of Zhongsha Atoll (Macclesfield Bank), South China Sea. *Mar. Petrol. Geol.* 117:104349. doi: 10.1016/j.marpetgeo.2020.104349

Hubert, N., Meyer, C. P., Bruggemann, H. J., Guerin, F., Komeno, R. J., Espiau, B., et al. (2012). Cryptic diversity in Indo-Pacific coral-reef fishes revealed by DNA-barcoding provides new support to the centre-of-overlap hypothesis. *PLoS ONE* 7:e28987. doi: 10.1371/journal.pone.0028987

Jones, G. P., McCormick, M. I., Srinivasan, M., and Eagle, J. V. (2004). Coral decline threatens fish biodiversity in marine reserves. *Proc. Natl. Acad. Sci. U. S. A.* 101, 8251–8253. doi: 10.1073/pnas.0401277101

Jones, G. P., Planes, S., and Thorrold, S. R. (2005). Coral reef fish larvae settle close to home. *Curr. Biol.* 15, 1314–1318. doi: 10.1016/j.cub.2005.06.061

Kumar, S., Stecher, G., and Tamura, K. (2016). MEGA7: molecular evolutionary genetics analysis version 7.0 for bigger datasets. *Mol. Biol. Evol.* 33, 1870–1874. doi: 10.1093/molbev/msw054

Leis, J. M., and Rennis, D. S. (1983). *The Larvae of Indo-Pacific Coral Reef Fishes*. Hawaii: University Hawaii Press. doi: 10.2307/1444356

Lin, H.-Y., Chiu, M.-Y., Shih, Y.-M., Chen, I.-S., Lee, M.-A., and Shao, K.-T. (2016). Species composition and assemblages of ichthyoplankton during summer in the East China Sea. *Continent. Shelf Res.* 126, 64–78. doi: 10.1016/j.csr.2016.07.016

Luo, M., Leung, Y., Graf, H. F., Herzog, M., and Zhang, W. (2016). Interannual variability of the onset of the South China Sea summer monsoon. *Int. J. Climatol.* 36, 550–562. doi: 10.1002/joc.4364

Okiyawa, M. (1988). *An Atlas of the Early Stage Fishes in Japan*. Tokyo: Tokai University Press.

Page, R. D. (1996). Tree view: an application to display phylogenetic trees on personal computers. *Bioinformatics* 12, 357–358. doi: 10.1093/bioinformatics/12.4.357

Roberts, S., and Hirshfield, M. (2004). Deep-sea corals: out of sight, but no longer out of mind. *Front. Ecol. Environ.* 2, 123–130. doi: 10.1890/1540-9295(2004)002[0123:DCOOSB]2.0.CO;2

Roder, C., Berumen, M. L., Bouwmeester, J., Papathanassiou, E., Al-Suwailem, A., and Voolstra, C. R. (2013). First biological measurements of deep-sea corals from the Red Sea. *Sci. Rep.* 3:srep02802. doi: 10.1038/srep02802

Rogers, A. D. (2019). "Chapter 23 - threats to seamount ecosystems and their management," in *World Seas: an Environmental Evaluation, 2nd Edn*, ed C. Sheppard (Cambridge, MA: Academic Press), 427–451. doi: 10.1016/B978-0-12-805052-1.00018-8

Shan, B., Liu, Y., Yang, C., Zhao, Y., Zhang, G., Wu, Q., et al. (2021). DNA barcoding of fish in mischief reef—fish diversity of a reef fish community from Nansha Islands. *Front. Mar. Sci.* 7:618954. doi: 10.3389/fmars.2020.618954

Shulzitski, K., Sponaugle, S., Hauff, M., Walter, K. D., and Cowen, R. K. (2016). Encounter with mesoscale eddies enhances survival to settlement in larval coral reef fishes. *Proc. Natl. Acad. Sci. U. S. A.* 113, 6928–6933. doi: 10.1073/pnas.1601606113

Sun, D., Qiu, Y., Lin, Z., and Wang, X. (2006). Preliminary studies on the composition of coral reef fish resources in the waters of Zhongsha Island in spring. *Trans. Oceanol. Limnol.* 3, 85–92. doi: 10.1016/j.ejps.2006.05.004

Teh, L. S., Teh, L. C., and Sumaila, U. R. (2013). A global estimate of the number of coral reef fishers. *PLoS ONE* 8:e65397. doi: 10.1371/journal.pone.0065397

Wagner, D., Friedlander, A. M., Pyle, R. L., Brooks, C. M., Gjerde, K. M., and Wilhelm, T. A. (2020). Coral reefs of the high seas: hidden biodiversity hotspots in need of protection. *Front. Mar. Sci.* 7:567428. doi: 10.3389/fmars.2020.567428

Wan, R., and Zhang, R. (2016). *Fish Eggs, Larvae and Juveniles in the Offshore Waters of China and Their Adjacent Waters*. Shanghai: Shanghai Scientific & Technical Publishers.

Wang, X., Du, F., Lin, Z., Sun, D., Qiu, Y., and Huang, S. (2011). Fish species diversity and community pattern in coral reefs of the Xisha Islands, South China Sea. *Biodiv. Sci.* 19, 463–469. doi: 10.3724/SP.J.1003.2011.07267

Ward, R. D., Zemlak, T. S., Innes, B. H., Last, P. R., and Hebert, P. D. (2005). DNA barcoding Australia's fish species. *Philos. Trans. Royal Soc. B Biol. Sci.* 360, 1847–1857. doi: 10.1098/rstb.2005.1716

Woodhead, A. J., Hicks, C. C., Norström, A. V., Williams, G. J., and Graham, N. A. J. (2019). Coral reef ecosystem services in the Anthropocene. *Funct. Ecol.* 33, 1023–1034. doi: 10.1111/1365-2435.13331

Yu, K. (2012). Coral reefs in the South China Sea: their response to and records on past environmental changes. *Sci. China Earth Sci.* 55, 1217–1229. doi: 10.1007/s11430-012-4449-5

Conflict of Interest: The authors declare that the research was conducted in the absence of any commercial or financial relationships that could be construed as a potential conflict of interest.

frontiers in Marine Science

ORIGINAL RESEARCH
published: 10 January 2022
doi: 10.3389/fmars.2021.767273

Sampling Designs for Monitoring Ichthyoplankton in the Estuary Area: A Case Study on *Coilia mystus* in the Yangtze Estuary

Xiangyu Long[1], Rong Wan[2,3,4,5], Zengguang Li[2,3,4], Dong Wang[2], Pengbo Song[1] and Fan Zhang[2]*

[1] Fisheries College, Ocean University of China, Qingdao, China, [2] College of Marine Sciences, Shanghai Ocean University, Shanghai, China, [3] National Engineering Research Center for Oceanic Fisheries, Shanghai Ocean University, Shanghai, China, [4] Key Laboratory of Sustainable Exploitation of Oceanic Fisheries Resources, Ministry of Education, Shanghai, China, [5] Laboratory for Marine Fisheries Science and Food Production Processes, Pilot National Laboratory for Marine Science and Technology (Qingdao), Qingdao, China

A fishery-independent survey can provide detailed information for fishery assessment and management. However, the sampling design for the survey on ichthyoplankton in the estuary area is still poorly understood. In this study, we developed six stratified schemes with various sample sizes, attempting to find cost-efficient sampling designs for monitoring *Coilia mystus* ichthyoplankton in the Yangtze Estuary. The generalized additive model (GAM) with the Tweedie distribution was used to quantify the "true" distribution of *C. mystus* eggs and larvae, based on the data from the fishery-independent survey in 2019–2020. The performances of different sampling designs were evaluated by relative estimation error (REE), relative bias (RB), and coefficient of variation (CV). The results indicated that appropriate stratifications with intra-stratum homogeneity and inter-stratum heterogeneity could improve precision. The stratified schemes should be divided not only between the North Branch and South Branch but between river and sea. No less than two stratifications in the South Branch could also get better performance. The sample sizes of 45–55 were considered as the cost-efficient range. Compared to other monitoring programs, monitoring ichthyoplankton in the estuary area required a more complex stratification and a higher resolution sampling. The design ideology and optimization methodology in our study would provide references to sampling designs for ichthyoplankton in the estuary area.

Keywords: sampling design, stratified scheme, sample size, ichthyoplankton, *Coilia mystus*, the Yangtze Estuary

Edited by:
Yuan Li,
Third Institute of Oceanography,
Ministry of Natural Resources, China

Reviewed by:
Morane Clavel-Henry,
University College Dublin, Ireland
Frank Hernandez,
University of Southern Mississippi,
United States

****Correspondence:***
Zengguang Li
zgli@shou.edu.cn

Specialty section:
This article was submitted to
Marine Fisheries, Aquaculture
and Living Resources,
a section of the journal
Frontiers in Marine Science

Received: *30 August 2021*
Accepted: *13 December 2021*
Published: *10 January 2022*

Citation:
Long X, Wan R, Li Z, Wang D,
Song P and Zhang F (2022) Sampling
Designs for Monitoring
Ichthyoplankton in the Estuary Area:
A Case Study on Coilia mystus
in the Yangtze Estuary.
Front. Mar. Sci. 8:767273.
doi: 10.3389/fmars.2021.767273

INTRODUCTION

A Fishery-independent survey is critical to fishery assessment and management because it can provide reliable information about spatial and temporal scales on stock abundance and distribution (Liu et al., 2009). Surveys on ichthyoplankton have been conducted worldwide, attempting to clarify their spawning habitat and monitor the dynamics of stock resources and even ecosystem structure (McClatchie et al., 2014; Doray et al., 2017). The long-term intensive surveys were enumerated but not limited to the California Cooperative Oceanic Fisheries Investigations (CalCOFI; Bjorkstedt et al., 2011) and the Pélagiques Gascogne surveys (PELGAS; Doray et al., 2000). In such areas, transect line designs for sampling ichthyoplankton were widely accepted (McClatchie, 2014;

Doray et al., 2017). Nonetheless, sampling designs in the estuary area should also be highly concerned because they can be potential spawning and nursery habitats for many fish species.

The Yangtze Estuary is one of the largest estuaries in the world, located on the west coast of the Pacific Ocean (Lin et al., 2018). The estuary area and its adjacent water had the major fisheries in China, but the resources have been rapidly reducing in the past 50 years (Xian et al., 2005; Ni and Chen, 2006). For instance, the tapertail anchovy *Coilia mystus* is a typical semi-anadromous species in the Yangtze Estuary (He et al., 2008). Annually, adult *C. mystus* migrates to brackish water to spawn in the Yangtze Estuary in late April (with spawning peaks from May to July) and descends to the sea in early September (Zhao and Zhang, 1985). It was estimated that the total catch of *C. mystus* in the Yangtze Estuary peaked at over 3,000t in 1995, but it has decreased to less than 100t since 2010 (Ni et al., 2020). The anthropological activities such as hydraulic engineering and overfishing may have disturbed its spawning or nursery habitats, resulting in a negative impact on stock recruitment (Yang et al., 2006). Fortunately, a series of resource protection measures have been taken by the Chinese government in 2019, e.g., a fishing ban (Cheng, 2021), but the status of *C. mystus* early resource is still unknown. Ichthyoplankton abundance has been proven to be a useful relative index or proxy of adult spawning stock biomass (Hsieh et al., 2005; Koslow and Davison, 2016). Thus, a targeted fishery-independent survey for *C. mystus* ichthyoplankton in the Yangtze Estuary is highly required to monitor its recruitment process and provide references for management.

The fishery management can be greatly influenced by the quantity of data from the fishery-independent survey, which is the ability to reflect the true resource distribution. Generally, the large-quantity data are obtained from high-intensity sampling, which needs to be financed and is time-consuming, especially when it targets multiple species over a broad spatiotemporal scale (Edwards et al., 2010; Blabolil et al., 2017). Thus, it is necessary to design a cost-efficient fishery-independent survey for getting adequate data with limited financial support (Puerta et al., 2018). Many pioneers have strived to optimize sampling designs with respect to sampling techniques, sampling effort, and spatial configuration (Jardim and Ribeiro, 2007; Blabolil et al., 2017). Surprisingly, there are few studies focused on sampling designs for ichthyoplankton. The surveys for ichthyoplankton were regarded as a solution to the perceived cost of fish surveys because they were more aggregated in distributions and easier to be collected (Koslow and Wright, 2016). Thus, sampling designs for ichthyoplankton should also be highly concerned.

With respect to the different objectives of fishery management, various sampling designs should be adopted to gain maximal efficiency (Bijleveld et al., 2012). Due to the complexity and variability of the seafloor in the Yangtze Estuary, there are places where sampling is not possible, and fixed-station sampling designs cannot be applied. The stratified random sampling (SRS) divides a population into different strata and samplings randomly in each stratum. It is commonly used in the fishery-independent survey to provide insights into resource status (Wang et al., 2018). The estimated precision of SRS can be improved by optimizing stratified schemes and sample sizes (Xu et al., 2015a,b). But for the fishery-independent surveys with limited funding, the optimization process should find a balance between budget and survey precision. In recent years, computer simulation has been used as an effective tool to optimize sampling designs and improve their performances. The performance is mostly defined by estimators that are unbiased, consistent, and efficient (Cochran, 1977). As the response to the uncertainty of samplings, the estimates influence the accuracy of assessment and the effect of subsequent management. Therefore, estimators that evaluate comprehensive performance should be selected to improve the assessment of fisheries.

In terms of environmental heterogeneity in the Yangtze Estuary, and the patchy distribution of *C. mystus* ichthyoplankton, the sampling design may require higher resolution sampling and more complex stratification. In this study, we developed six stratified schemes with various sample sizes for sampling *C. mystus* ichthyoplankton in the Yangtze Estuary, trying to (1) compare the performances of six sampling designs for capturing the dynamics of *C. mystus* eggs and larvae; (2) find the cost-efficient sampling designs with suitable sample sizes; and (3) develop a framework of designing and optimizing fishery-independent survey for monitoring ichthyoplankton in the estuary area. The design ideology and optimization methodology in our study would provide references to future sampling designs for ichthyoplankton in the estuary area.

MATERIALS AND METHODS

To clarify how to make sampling designs for monitoring ichthyoplankton in the estuary area, we conducted a case study of *C. mystus* ichthyoplankton in the Yangtze Estuary. Six sampling designs with various sample sizes were developed to find the cost-efficient designs for monitoring the dynamic of *C. mystus* ichthyoplankton. The performances of the designs were evaluated by relative estimation error (REE), relative bias (RB), and coefficient of variation (CV), based on the "true" distribution obtained from the generalized additive model (GAM) with the Tweedie distribution.

Study Area and the Current Sampling Design

The Yangtze Estuary is one of the most important estuaries in China and is a spawning and nursery habitat for many commercial fish species (Wan et al., 2010). It is characterized by a unique topography and the complex hydrology (Zhuang, 2013; Liu et al., 2020). Under the interaction of runoff and tide, sediments in the water settle and then form alluvial shoals and islands in the Yangtze Estuary. These lands such as Chongming island, Changxing island, and Jiuduan sandbank divide the mainstream into four passages (**Figure 1A**; Yan et al., 2001). Besides, the environmental heterogeneity extends over the whole estuarine region, especially between the North Branch and South Branch. For example, higher salinity and dissolved oxygen are found in the North Branch than in the South Branch (Luo and Shen, 1994; Meng, 2010).

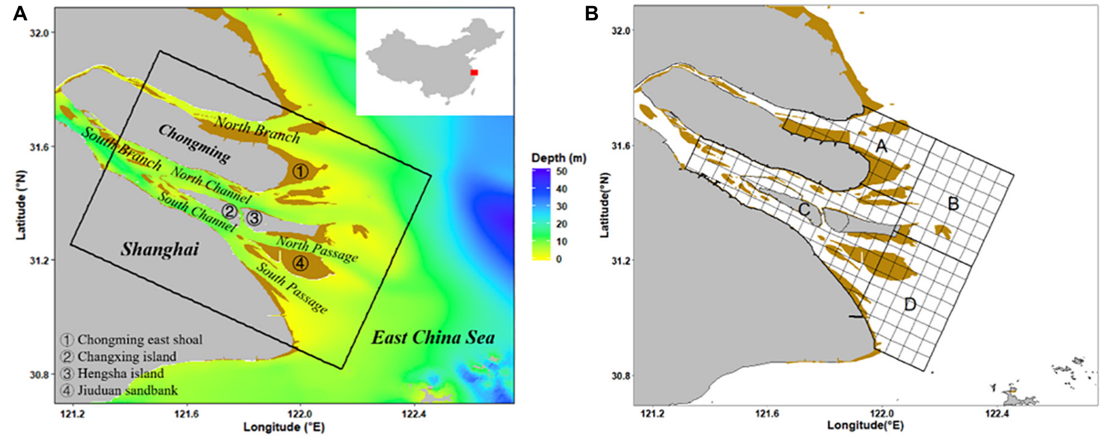

FIGURE 1 | Study area **(A)** and potential sampling stations **(B)**.

TABLE 1 | List of the sampling designs.

Designs	Stratum	Weights	Stations	Stratified rules
1	A	1	55	No stratified (**Figure 2A**).
2	A	0.36	20	Stratified with 3 latitude strata, and partly considered the branching character (**Figure 2B**).
	B	0.43	24	
	C	0.21	11	
3	A	0.11	6	Stratified with 3 longitude strata, and partly considered the area in and off the estuary (**Figure 2C**).
	B	0.33	18	
	C	0.56	31	
4	A	0.18	10	Stratified with 4 regions strata, divided the area in and off the North Branch and South Branch. (The current sampling design; A: in the North Branch, B: off the North Branch, C: in the South Branch, D: off the South Branch; **Figure 2D**).
	B	0.24	13	
	C	0.32	18	
	D	0.26	14	
5	A	0.16	9	Stratified with 6 coordinates strata, and combined Design 2 with Design 3 (**Figure 2E**).
	B	0.20	11	
	C	0.11	6	
	D	0.13	7	
	E	0.20	11	
	F	0.20	11	
6	A	0.16	9	Stratified with 6 regions strata, and separated the Chongming east shoal and the turbidity maximum zone. (A: in the North Branch, B: off the North Branch, C: Chongming east shoal, D: in the South Branch, E: turbidity maximum zone, F: off the South Branch; **Figure 2F**).
	B	0.18	10	
	C	0.09	5	
	D	0.17	9	
	E	0.25	14	
	F	0.15	8	

To clarify the distribution status of *C. mystus* ichthyoplankton, the study focused on a specific area in the Yangtze Estuary (**Figure 1A**). We conducted four fishery-independent surveys in our study area, which were in May and August of 2019 and 2020. The survey followed the SRS design, which consisted of randomly sampling 55 stations from 182 grid cells per survey. The grid was generated over our study area based on the central axis of Chongming Island, according to the sampling design of the CalCOFI (McClatchie, 2014). Grid cells had a resolution of $3' \times 3'$, and grid cells where water area occupies less than half of the grid area were not counted. We clustered the grid cells into four strata (Stratum A, B, C, and D; **Figure 1B**), according to their regions (corresponding to the area in the North Branch, off the North Branch, in the South Branch, and off the South Branch, respectively). Based on our original purpose of the survey, which was to identify the spawning habitat of *C. mystus*, more stations were allocated to Stratum C. The stations of Stratum A, B, C, and D were 12, 10, 25, and 8, respectively.

Eggs and larvae were collected using plankton nets with 280-cm net length, 80-cm mouth diameter, and 505-µm mesh size, and a General Oceanics 2030R flowmeter at the center of the net mouth. The net was dragged horizontally along the sea surface for 10 min, with a constant speed of 2–3 knots. Environmental factors, such as temperature, salinity, and depth, were also

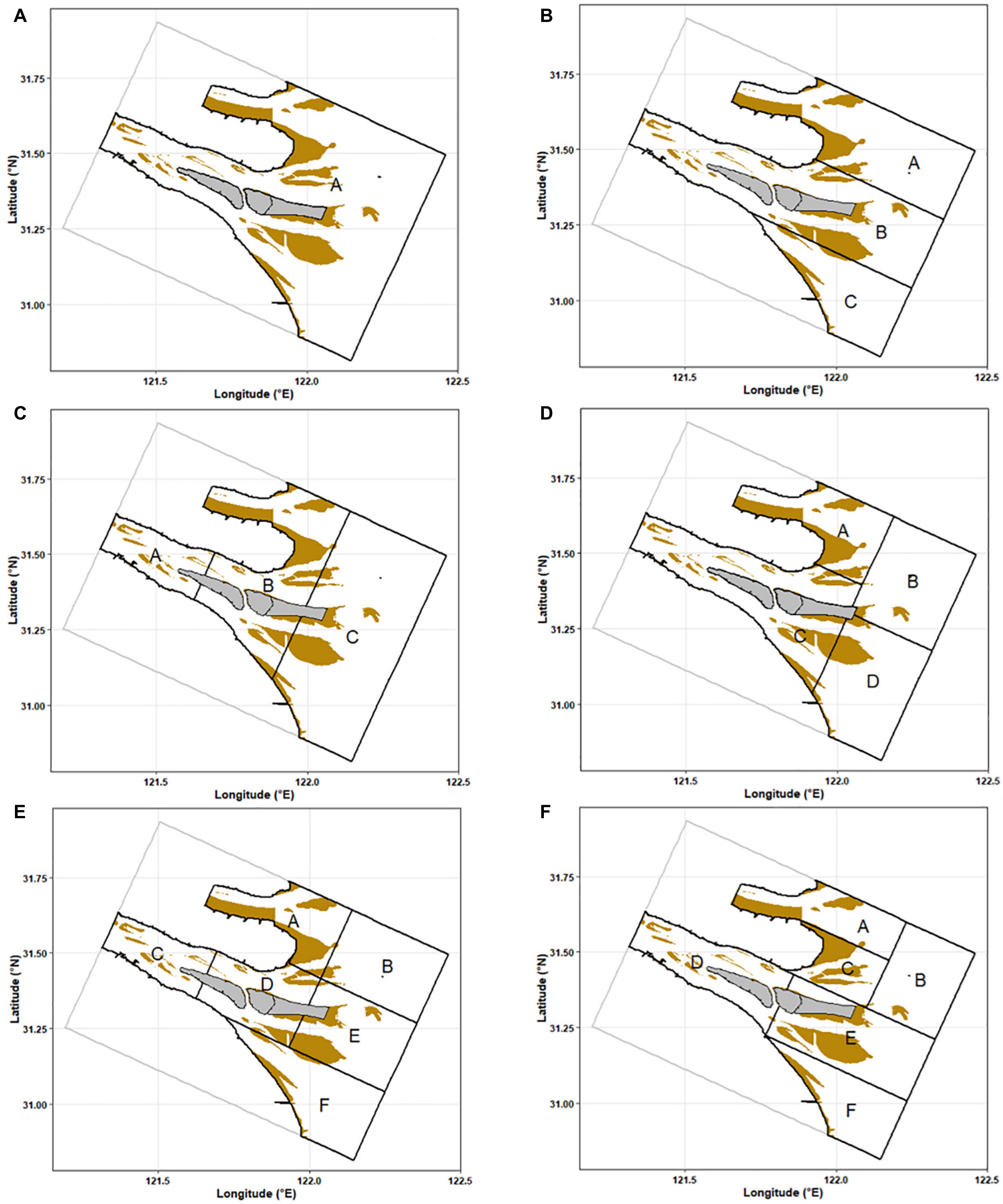

FIGURE 2 | Strata for different sampling designs. The brown areas represent shoals. The gray areas represent islands. **(A)** Design 1, **(B)** Design 2, **(C)** Design 3, **(D)** Design 4, **(E)** Design 5, and **(F)** Design 6.

recorded by the conductivity-temperature-depth system (CTD) of SBE-19plusV2 at each station. Samples were preserved in 5% buffered formalin in seawater immediately. Once in the laboratory, *C. mystus* eggs and larvae were visually identified based on existing literature and counted using a OLYMPUS SZX7 binocular microscope. According to the references, both *C. mystus* eggs and larvae are buoyant (Zhao and Zhang, 1985; Zhang et al., 2020). Eggs are transparent with a diameter of 0.83–1.03 mm and contain multiple oil globules of different sizes. Larvae can be identified by counting the number of the sarcomere and fin ray at different body lengths, but other morphological figures also contributed to their identification (Zhao and Zhang, 1985; Wan and Jiang, 2000). The five-stage eggs (Stage I–V; Thompson and Riley, 1981) and three-stage larvae (prelarva, postlarva, and juvenile; Zhao and Zhang, 1985) were found in our samples.

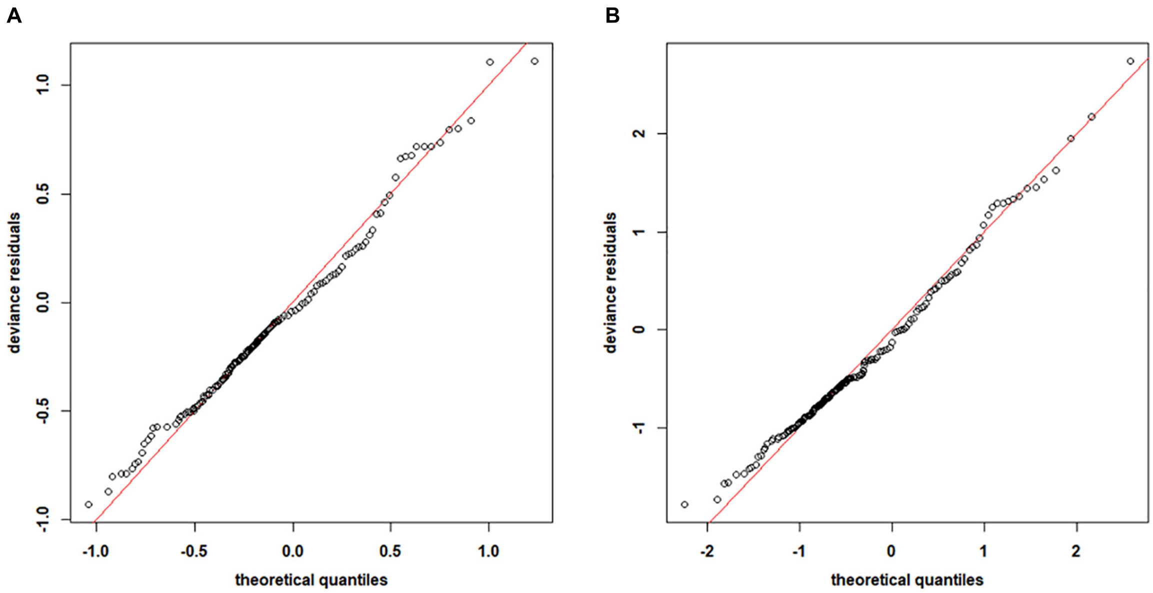

FIGURE 3 | The quantile-quantile (Q–Q) plots of the deviance residuals in optimal generalized additive models (GAMs) for *Coilia mystus* **(A)** eggs and **(B)** larvae. The red lines represent standard values.

The "True" Values

To compare and evaluate the performance of various sampling designs, the "true" distribution of *C. mystus* eggs and larvae over our study area was needed. The GAM has been widely used to fit the nonlinear relationship between species abundance and environmental factors. Combined with the Tweedie distribution, the GAM model can deal well with fishery resource data with zero inflation (Wang et al., 2017). Therefore, we developed a Tweedie-GAM to quantify the relationship between *C. mystus* egg density, larval density, and environmental factors and predicted their "true" distribution in the study area. The general GAM was expressed as follows (Hastie and Tibshirani, 1986):

$$g(\rho) = \beta_0 + \sum_{i=1}^{k} f_i(x_i) + \varepsilon \tag{1}$$

where $g(\rho)$ is the log-link function, β_0 denotes the constant intercept term, x_i denotes the explanatory variable, $f_i(x_i)$ is a smooth function that can be used to describe the relationship between $g(\rho)$ and x_i , and ε is the error term according to normal distribution. The description of the probability function of the Tweedie distribution is given by Eq. 4 in the study by Shono (2008). The Tweedie distribution can express as the compound Poisson distribution if $1 < p < 2$, which was appropriate for data with plenty of zero values (Shono, 2008).

We developed optimal models for *C. mystus* eggs and larvae with data from four surveys to improve the accuracy of optimal models. The quantity of *C. mystus* eggs and larvae was standardized to egg density and larval density, which were calculated by $\rho = A/V$, where ρ is egg density (ρ_e) or larval density (ρ_l), A denotes the number of eggs and larvae, and V is the flow volume measured with the flowmeter. Both egg density and larval density were log-transformed. The selected environmental variables were sea surface temperature (SST), sea bottom temperature (SBT), sea surface salinity (SSS), sea bottom salinity (SBS), charted depth (Dep), and a two-dimensional (2D) variable: longitude and latitude (Lon, Lat). Year and month were treated as categorical variables. The effect of shoals was represented by Dep in models.

The optimal models for eggs and larvae were selected by the lowest Akaike Information Criterion (AIC; Akaike, 1974). We interpolated spatial correlated environmental factors in the uninvestigated area by using the inverse distance weighting method (Chen, 2017). Finally, the "true" distribution of *C. mystus* eggs and larvae was predicted by the optimal models and the interpolated environmental variables. We calculated the mean of predicted egg and larval density as the "true" values in each month.

Optimization Process

A total of 182 potential sampling stations were treated as population, which was the same as the current sampling design. The stations were divided into different strata based on six sampling designs (**Table 1** and **Figure 2**). We made different stratified schemes by coordinate (Designs 2, 3, and 5) and region (Designs 4 and 6). The simple random sampling (Design 1) was treated as a design control. We compared the performance of six sampling designs with various sampling sizes, trying to find cost-efficient sampling designs to monitor the dynamics of *C. mystus* eggs and larvae.

The performances of sampling designs were evaluated by REE, RB, and CV. REE (Eq. 2) evaluated the accuracy and precision of estimated values in sampling (Chen, 1996). RB (Eq. 3) reflected the bias between estimated values and the "true" values (Jiao et al.,

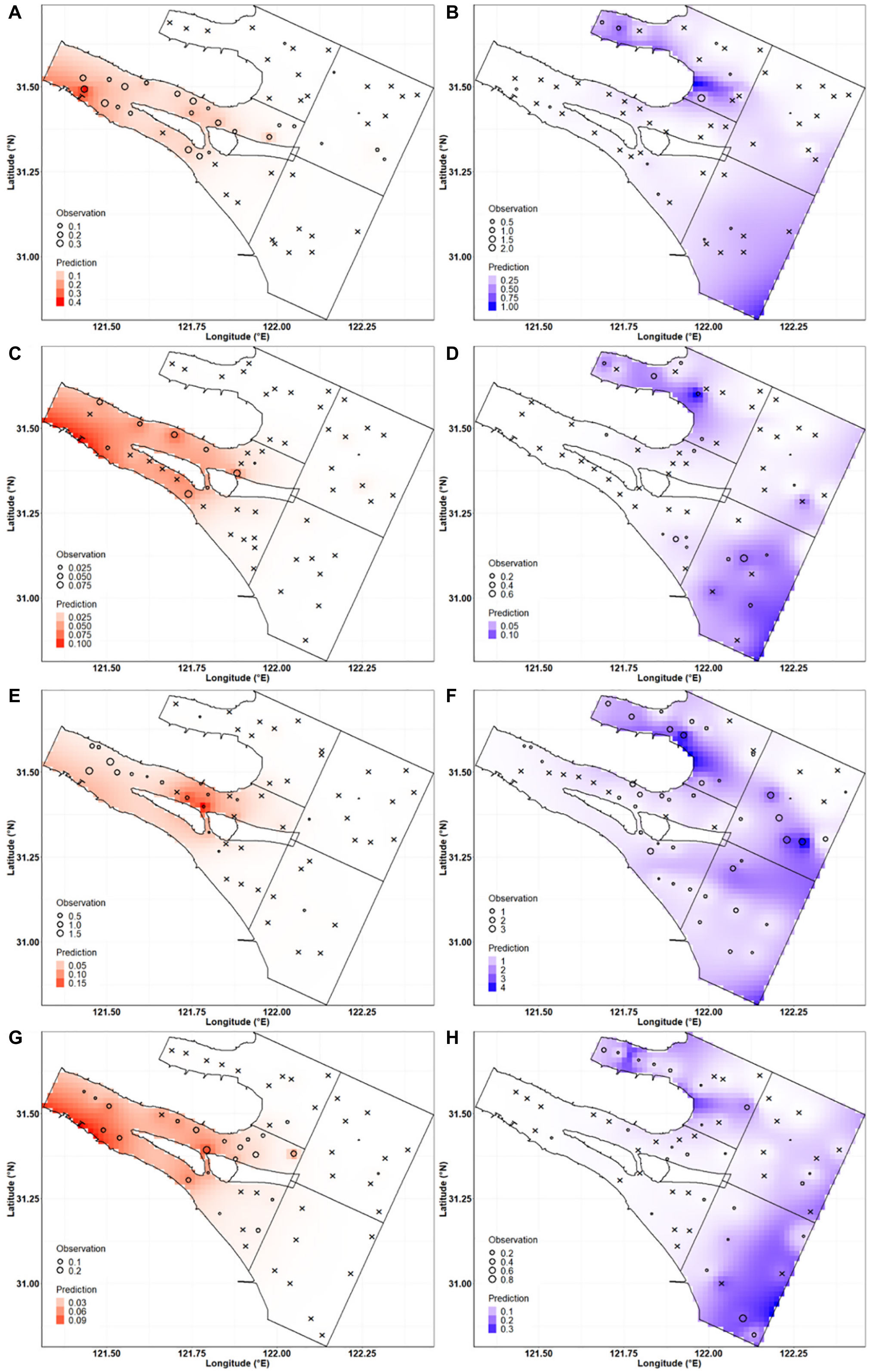

FIGURE 4 | Predicted and observed distributions of *C. mystus* egg and larval density. Red gradients represent predicted egg distribution in **(A)** May 2019, **(C)** August 2019, **(E)** May 2020, and **(G)** August 2020. Blue gradients represent predicted larval distribution in **(B)** May 2019, **(D)** August 2019, **(F)** May 2020, and **(H)** August 2020. Circle sizes represent the observed density of *C. mystus* ichthyoplankton. Cross represents no *C. mystus* eggs and larvae.

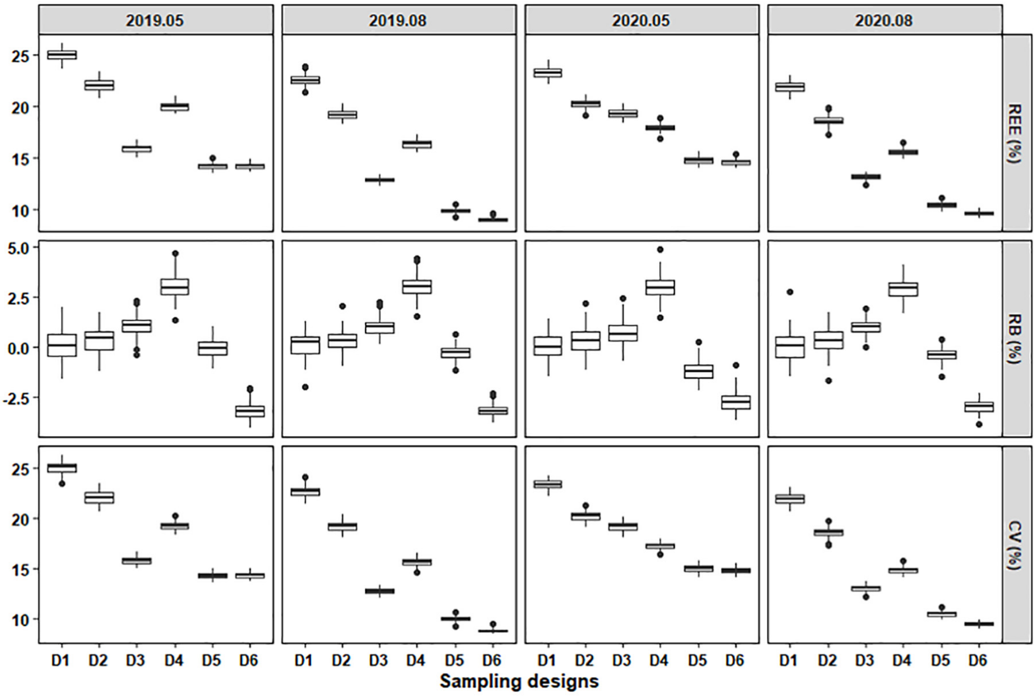

FIGURE 5 | The relative estimation error (REE), relative bias (RB), and coefficient of variation (CV) of stratified schemes for sampling *C. mystus* eggs with a sample size of 55. D1 to D6 represent Design 1 to Design 6, respectively.

2004). CV (Eq. 4) measured the relative variability of estimated values (Cochran, 1977). They were expressed as follows:

$$REE = \frac{\sqrt{\sum_{i=1}^{R}\left(Y_i^e - Y^t\right)^2/R}}{Y^t} \times 100\% \tag{2}$$

$$RB = \frac{\sum_{i=1}^{R} Y_i^e/R - Y^t}{Y^t} \times 100\% \tag{3}$$

$$CV = \sigma/\bar{Y} \times 100\% \tag{4}$$

where Y^e is the estimated value calculated by the $_{ith}$ sampling data, Y^t is the "true" values, R is the sampling times ($R{=}1000$, here), σ was an SD of the sampling data, and $\bar{Y}$ was the mean of sampling data. The performance of the sampling designs with lower REE, absolute RB, and CV was better.

We evaluated the performance of different sampling designs with various sample sizes, which were set as 25, 40, 55, 70, 85, and 100. The designs with good performances were tested in further optimization of sample size from 15 to 100 with an interval of 5. The sample sizes were proportionally allocated to each stratum by weights. It is difficult to ensure that sample sizes in each stratum were an integer, and therefore, the non-integer calculation was rounded to the nearest integer. All the processes of analysis were carried out with R software (version 3.6.0).

RESULTS

The "True" Populations

We used a preliminary variance inflation factor (VIF) analysis to check multicollinearity among variables. The environmental factors whose VIF exceeded 10 were removed from models. Based on the results of the VIF analysis and backward stepwise, GAMs with the lowest AIC values for *C. mystus* eggs and larvae were expressed as Eqs 5 and 6, respectively. Depth, SSS, SBS, and 2D longitude and latitude were selected for both the two optimal GAMs. The two models with significant variables explained 67.8 and 67.4% of the variance for egg and larval density, respectively. The quantile-quantile (Q–Q) plots of residuals were used to check the performance of the optimal GAMs (**Figure 3**). For both egg and larval models, their points were close to the straight red lines. Therefore, the optimal GAMs performed well for most of the data.

$$\begin{aligned} ln\left(\rho_e\right) = \beta_0 + year + month + s\left(Lon, Lat\right) + s\left(SSS\right) + s\left(SBS\right) \\ + s\left(Dep\right) + \varepsilon \end{aligned} \tag{5}$$

$$\begin{aligned} ln\left(\rho_l\right) = \beta_0 + year + month + s(Lon, Lat) + s\left(SSS\right) + s\left(SBS\right) \\ + s\left(Dep\right) + \varepsilon \end{aligned} \tag{6}$$

The distributions of *C. mystus* egg and larval density were predicted by the optimal GAMs on the interpolated environmental factors (**Figure 4**). The results showed that eggs

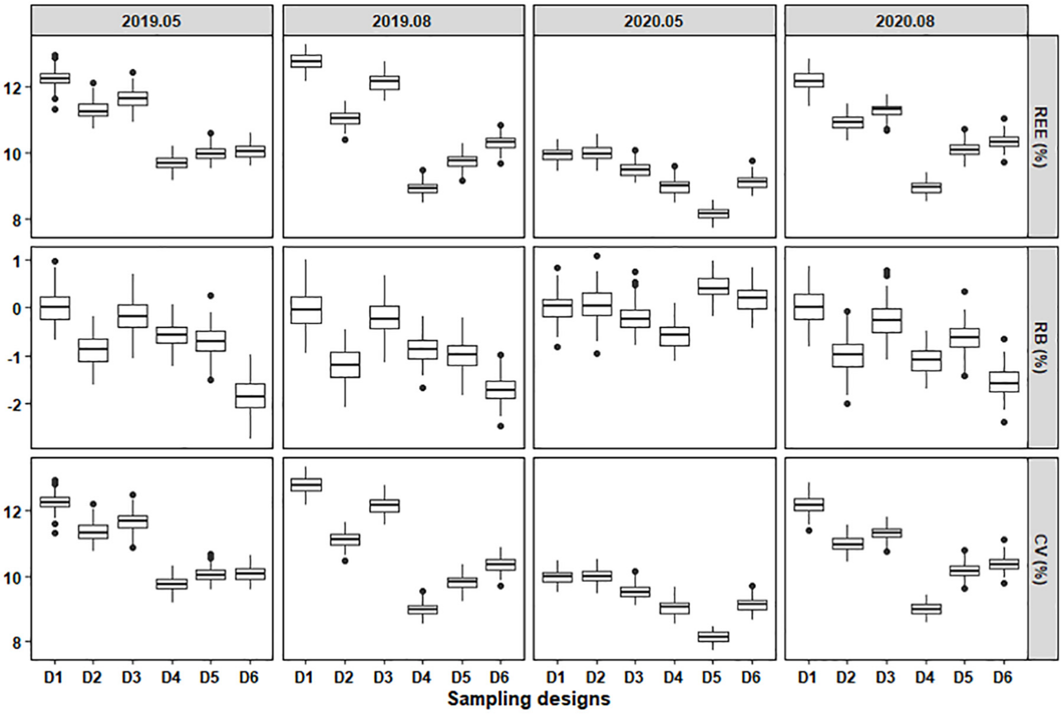

FIGURE 6 | The REE, RB, and CV of stratified schemes for sampling *C. mystus* larvae with a sample size of 55. D1 to D6 represent Design 1 to Design 6, respectively.

and larvae occurred in both May and August. Their potential spawning ground was distributed inside the Yangtze Estuary and filled in the whole South Branch. Higher egg density occurred in May rather than in August, and in 2019 rather than in 2020. The prediction indicated that *C. mystus* has more than one potential nursery ground in the Yangtze Estuary. One of which was inside the North Branch, closing to the Chongming east tidal flat. The other is located in the south of the study area, outside of the South Passage. There was another assemblage, only located in the north of the North Passage in May 2020. It was also considered as the potential nursery ground for *C. mystus*. Similarly, larval densities were higher in May than in August but lower in 2019 than 2020. In each sampling month, the density of larvae far exceeded that of eggs.

Optimization Process

The results indicated that different designs had various performances in sampling *C. mystus* eggs and larvae (**Figures 5**, **6**). For eggs, the REE and CV values of different designs fluctuated between 8.78 and 26.12% and 8.48 and 26.20%, respectively. Design 1 had the highest REE and CV values, while those of Designs 3, 5, and 6 were lower over time. Therefore, Designs 3, 5, and 6 were considered to have better precision than other sampling designs. The RB values of different designs varied from -4.07 to 4.86%. The RB values of Design 1 were distributed evenly on both sides of zero, suggesting that simple random sampling could provide unbiased measures for the population. Designs 4 and 6 were continuing overestimated and underestimated, respectively. During each survey, the absolute RB values of all sampling designs were less than 5%, which meant that they had a steady low deviation (**Figure 5**).

The results showed that REE, absolute RB, and CV of *C. mystus* larvae were obviously lower than those of eggs (**Figures 5**, **6**). For larvae, the REE values of different designs ranged from 7.72 to 13.28%, and the CV values were ranged from 7.70 to 13.35%. Design 1 with the highest REE and CV values still had the lowest accuracy among sampling designs. Conversely, Designs 4, 5, and 6 with lower REE and CV had higher precision over time. The RB values of the six designs varied from -2.75 to 1.08%. Compared with the unbiased estimate of Design 1, other designs overestimated or underestimated the “true” values. Nevertheless, the designs for larvae had a lower deviation than those for eggs (**Figure 6**).

With the increase of sample size, the REE, absolute RB, and CV of different sampling designs generally decreased, both for *C. mystus* eggs and larvae. The changing rates of mean REE and CV tended to be stable, and absolute mean RB fluctuated in a certain range (**Figures 7**, **8**). Obvious differences in performance were shown among the six designs when sampling *C. mystus*. Whenever sampling *C. mystus* eggs, Design 3 was more accurate compared to Design 2. Designs 5 and 6 performed better than others at any sample sizes in all months. They both required a sample size that exceeded 40 to get lower REE, absolute RB, and CV (**Figure 7**). The performance of the six designs was close to each other when sampling larvae. For each sample size, Designs 4, 5, and 6 have always been the better designs

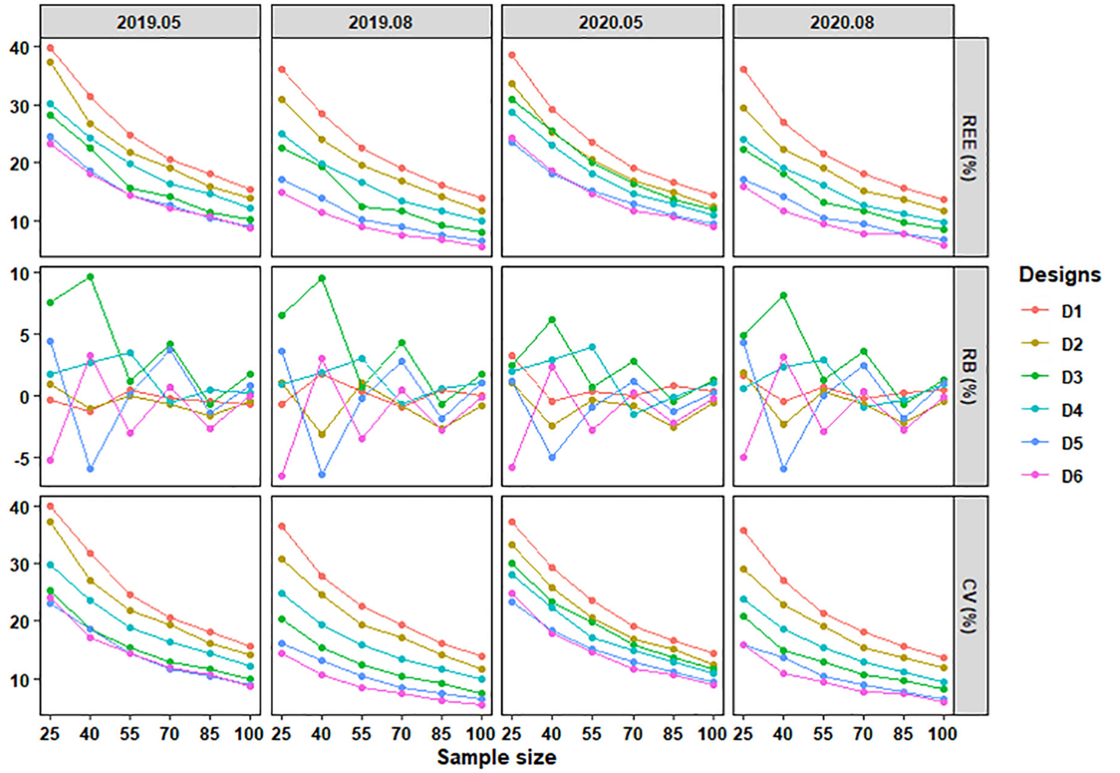

FIGURE 7 | The REE, RB, and CV of stratified schemes for sampling *C. mystus* eggs at different sample sizes. D1 to D6 represent Design 1 to Design 6, respectively.

compared to others (**Figure 8**). Although low deviation was acceptable, they still needed more sizes to ensure high precision and low dispersion. In terms of performance for sampling eggs and larvae, Designs 5 and 6 were considered as the better designs at all sample sizes.

The regression curves showed that mean of REE, absolute RB, and CV reduced with sample size increased (**Figure 9**). We found that mean of REE and CV had a similar trend. There were still differences between them with less sample size for eggs instead of larvae. The differences tended to mitigate with sample size increased. Both for Designs 5 and 6, the changing rates of regression curves were getting closer to 0 at the size of 45–55. It indicated that the three estimators reduced slightly with more sample sizes. Designs 5 and 6 with a sample size of 45–55 should be more efficient to monitor the dynamics of *C. mystus* eggs and larvae.

DISCUSSION

In this study, we compared and evaluated the performances of different stratified schemes with various sample sizes, attempting to find cost-efficient sampling designs for monitoring the dynamics of *C. mystus* ichthyoplankton. The performances were evaluated by REE, RB, and CV, which expressed their precision, deviation, and dispersion, respectively. It is well understood that simple random sampling could provide an unbiased mean of the population (Li et al., 2015; Ma et al., 2020). However, a better sampling should pay more attention to not only bias mitigation but also precision improvement (Cochran, 1977). Because the REE with SRS was lower than that with simple random sampling, we concluded that appropriate stratification could be applied to improve sampling precision. This coincided with previous studies, which indicated that SRS often improved precision and accuracy (Xu et al., 2015a; Wang et al., 2018).

It was expected that stratification should make intra-stratum homogeneity and inter-stratum heterogeneity (Manly et al., 2002; Miller et al., 2007). An appropriate stratification enhanced the ability of SRS to estimate the mean of the population (Ma et al., 2020). When sampling *C. mystus* eggs, more accuracy was found in Design 3 than in Design 2. It was because strata in Design 3 could reflect the gradient variation of egg density, which improved the stratified effect. However, the inappropriate division would translate into minimal improvement, even worse than simple random sampling (Wang et al., 2018). For example, there was hardly any difference in REE and CV between Designs 1 and 3 for sampling larvae in May and August 2019. Similarly, Design 2 performed no better than Design 1 for sampling larvae in May 2020. They divided different sizes of larval density into one stratum, resulting in the reduction of density disparity among strata.

We highlighted Designs 5 and 6 not only for their performance compatibility between *C. mystus* eggs and larvae but also for their robustness over time. The three indices used to quantify the

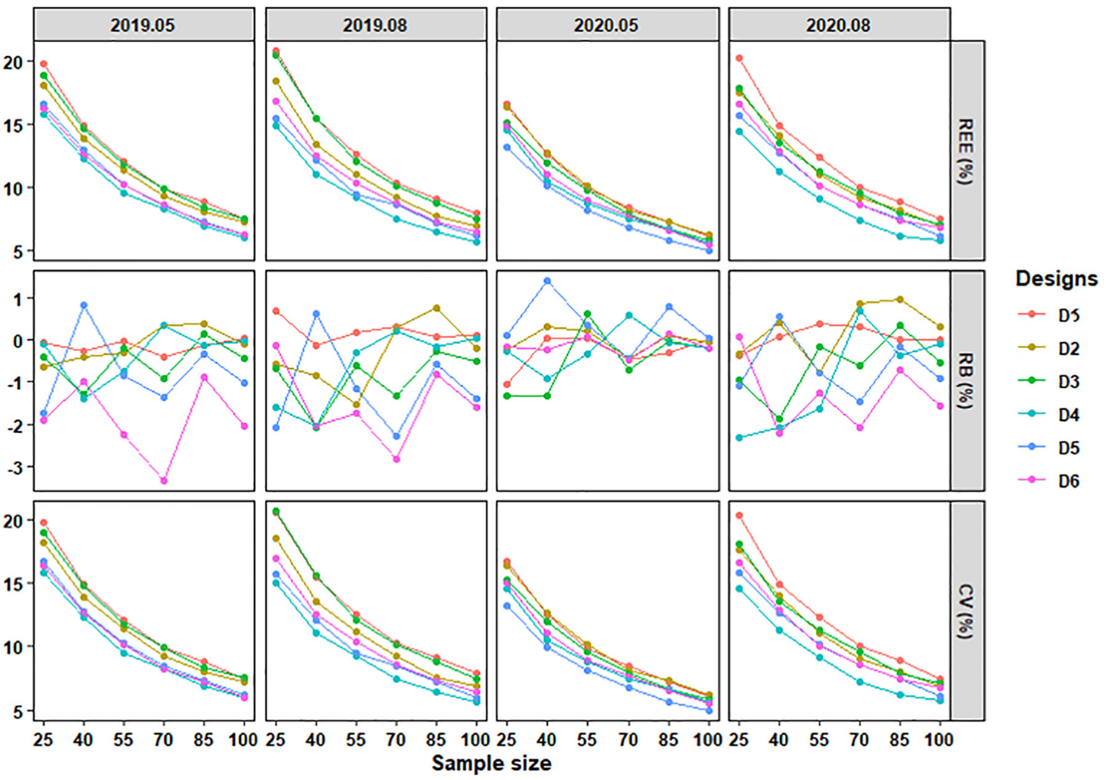

FIGURE 8 | The REE, RB, and CV of stratified schemes for sampling *C. mystus* larvae at different sample sizes. D1 to D6 represent Design 1 to Design 6, respectively.

performance of sampling designs were calculated by the "true" population, which were predicted from the fishery-independent survey data collected by Design 4. It was supposed that the used sampling design for our survey (i.e., Design 4) would perform best among different designs. However, it showed a bad performance in capturing the population of *C. mystus* eggs. Since the distribution pattern exhibited obvious spatial differences between *C. mystus* eggs and larvae, the monitoring program required a balanced consideration on both. Despite Designs 5 and 6 had slightly lower precision and higher dispersion for larvae, they were the preferred options concerning both eggs and larvae. Besides, the differences of *C. mystus* larvae have been found in May 2020, which included the increases in resources and changes in distribution. Designs 5 and 6 showed strong robustness to those changes, even exceeded Design 4, and Design 5 was especially the best. This was consistent with the studies by Cao et al. (2014) and Xu et al. (2015b), who suggested that appropriate stratified random design was robust to different distributions.

Compared to SRS in other coastal water, more stratifications are needed in the Yangtze Estuary to ensure the accuracy of sampling, even though we only focused on *C. mystus* eggs and larvae (Xu et al., 2015a; Wang et al., 2018; Wang et al., 2020). The differences might be due to the patchy distribution of ichthyoplankton or the environmental heterogeneity in the estuary area. The predicted results illustrated that *C. mystus* eggs and larvae had a patchy distribution. Specifically, eggs assembled in the South Branch, and larvae spread to the North Branch and adjacent sea. According to the performances of stratified schemes, we suggested that the study area should be stratified by not only the North Branch and South Branch but also river and sea (e.g., Design 4). No less than two stratifications were required in the South Branch (e.g., Designs 3 and 5), and further division in the North Branch and adjacent sea would also improve the precision (e.g., Designs 5 and 6).

Monitoring early resources might need a higher resolution survey to capture the patchy distribution of ichthyoplankton in the Yangtze Estuary. An increasing sample size contributed to improving the precision in different sampling designs (Wang et al., 2020). Besides, different designs had various accuracy enhancement effects under the same sample sizes. The changing rate of mean REE, absolute RB, and CV tended to be stable, which made sense to find an efficient sample size to monitor the dynamic of *C. mystus* ichthyoplankton. For a given certain precision, Designs 5 and 6 required fewer sample sizes than others. Their monitoring effects became efficient at the range of 45–55, which was considered as the optimal range of sample size. The resolution of our study (approximately 92–113 stations per 104 km^2) was higher than that of the study by Xu et al. (2015b; approximately 9–11 stations per 104 km^2), although there were differences between sampling nets.

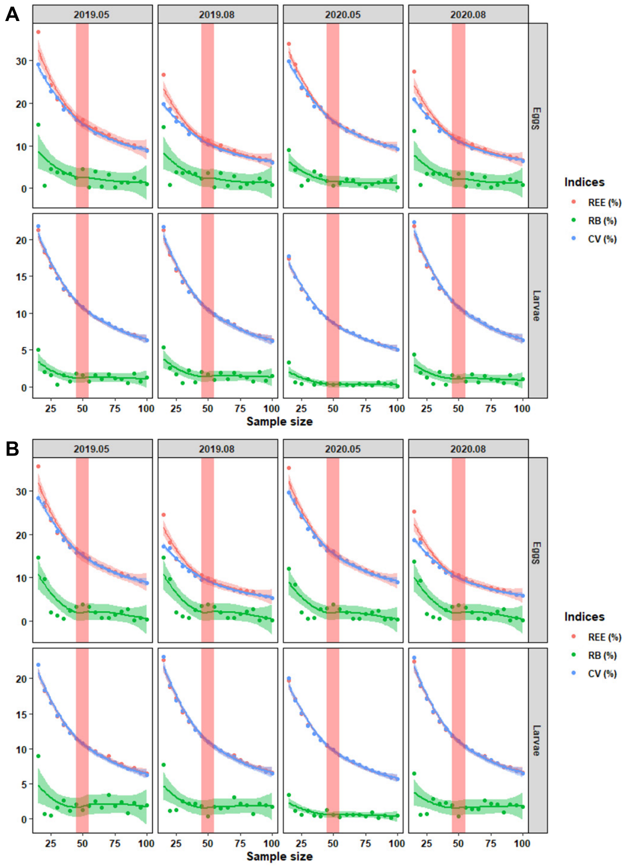

FIGURE 9 | The locally weighted regression for mean of REE, absolute RB, and CV on *C. mystus* eggs and larvae at different sample sizes. **(A)** Design 5 and **(B)** Design 6. The shadows around the lines represent 95% CIs. The red bars cover the changing rates of regression curves closing to zero.

Compared with the sampling design for adult fish, the sampling design for ichthyoplankton seemed more complicated, especially in the estuary area with complex habitats. According to the ecology of fish early life stage, most species during the egg stage were passively adrift, and their patchy distribution can be caused by diffusion and retention. Meanwhile, some species were supposed to have the potential ability to swim to their favorite places during the larval stage. Therefore, there might be some differences in the spatial distribution patterns between egg and larva stages. In this study, the optimal design scheme (e.g., Designs 5 and 6) were with more complex strata designs and were also different between egg and larva stages. However, most of the existing surveys on fish early life stage were sampled eggs and larvae simultaneously, even focused on multiple species. Their sampling designs could be very complex and should consider more potential factors. That is one of the biggest challenges, especially for the ichthyoplankton sampling, in the field of station optimization design.

The performance of SRS is usually affected by stratified scheme, sample size, and sample allocation (Gavaris and Smith, 1987; Lunsford et al., 2001). Generally, a stratified scheme should be identified by appropriate variables that are associated with the distribution of target species to improve precision by reducing sampling variation (Wilde and Fisher, 1996). In our study, strata that were divided quantitatively by environmental variables (e.g., salinity and depth) were unrealistic, because they changed rapidly (Zhao et al., 2015; Wei et al., 2021) and distributed discretely (**Figure 1** and **Supplementary Figure 1**) in the Yangtze Estuary. The strata in our study were mainly defined by coordinate and region, which could directly and indirectly associate with various environmental variables. For instance, salinity differed among strata in Design 5 (**Supplementary Figure 1**), and Stratum C was shallower (**Figure 1**) and Stratum E was more turbid (Yu et al., 2021) in Design 6. In addition, dissolved oxygen was verified as another important factor in determining the distribution of *C. mystus* ichthyoplankton (Ding, 2011; Hu et al., 2021), but it was removed from the models due to the poor data caused by instrument failure. This might affect the "true" distribution, leading to some impacts on our results. Thus, dissolved oxygen should be considered in the future study. We also evaluated the effect of sample size on sampling precision. There were exceeding 50% of potential stations considered to optimize sample size. It was sufficient because all curves have shown a stable changing rate. The stations would be given priority to the strata with high weight, most of which covered the larval density barycenter. Thus, the mean of sampling data of larvae was closer to the "true" values than that of eggs, leading to the differences between REE and CV for sampling eggs with less sample size. Fortunately, the influence tended to mitigate with sample size increased. In this study, we did not evaluate the effect of sample allocation on stratified schemes, and it deserved to be considered in the future.

CONCLUSION

We developed six stratified schemes for monitoring *C. mystus* ichthyoplankton in the Yangtze Estuary to evaluate their performances under various sample sizes. The results indicated that stratified schemes should be divided not only between the North Branch and South Branch but also between the river and sea. Also, there need more stratifications in the South Branch to improve estimated precision. Sample size at the range of 45–55 was considered as the cost-efficient design. We suggested that the complex stratification and high-resolution stations should be used for capturing the dynamic of ichthyoplankton in the estuary area. The performance of the sampling design could be greatly influenced by the distribution pattern of target species, but the design ideology and optimization methodology in our study would provide references to future sampling designs for ichthyoplankton in the estuary area.

DATA AVAILABILITY STATEMENT

The original contributions presented in the study are included in the article/**Supplementary Material**, further inquiries can be directed to the corresponding author.

ETHICS STATEMENT

The animal study was reviewed and approved by Shanghai Ocean University.

AUTHOR CONTRIBUTIONS

XL and ZL designed the study. XL and PS collected the data. XL, DW, and PS analyzed and interpreted the data. XL wrote the first draft. RW, ZL, and FZ improved the draft. All authors contributed to the final manuscript.

FUNDING

This study was supported by the Tracking Evaluation on Recovery Effect of Fishing Ban in Key Water Areas of the Yangtze River Basin (Grant No. D-8021-20-0073), the Estimation of Spawning Population Biomass of *Coilia mystus* in the Yangtze Estuary Based on Daily Egg Production Method (Grant No. A2-2006-21-200309), and the Scientific Research Foundation for the Imported Talent by RW (Grant No. A1-2006-21-7009).

ACKNOWLEDGMENTS

We thank our colleagues for their contributions to data collection and laboratory experiments. We also thank reviewers for their comments to improve our manuscript.

SUPPLEMENTARY MATERIAL

The Supplementary Material for this article can be found online at: https://www.frontiersin.org/articles/10.3389/fmars.2021.767273/full#supplementary-material

REFERENCES

Akaike, H. (1974). A new look at the statistical model identification. *IEEE Trans. Automat. Contr.* 19, 716–723.

Bijleveld, A. I., Gils, J. A. V., Meer, J. V. D., Dekinga, A., Kraan, C., and Veer, H. W. V. D. (2012). Designing a benthic monitoring programme with multiple conflicting objectives. *Methods Ecol. Evol.* 3, 526–536. doi: 10.1111/j.2041-210X.2012.00192.x

Bjorkstedt, E. P., Goericke, R., McClatchie, S., Weber, E., Watson, W., and Lo, N. (2011). State of the California current 2010–2011: regional variable responses to a strong (but fleeting?) La Niña. *Calif. Coop. Ocean. Fish. Investig. Rep.* 52, 36–68.

Blabolil, P., Boukal, D. S., Ricard, D., Kubečka, J., Říha, M., and Vašek, M. (2017). Optimal gillnet sampling design for the estimation of fish community indicators in heterogeneous freshwater ecosystems. *Ecol. Indic.* 77, 368–376. doi: 10.1016/j.ecolind.2017.02.036

Cao, J., Chen, Y., Chang, J., and Chen, X. (2014). An evaluation of an inshore bottom trawl survey design for American lobster (*Homarus americanus*) using computer simulations. *J. Northwest Atl. Fish. Sci.* 46, 27–39. doi: 10.2960/J.v46.m696

Chen, Y. (1996). A Monte Carlo study on impacts of the size of subsample catch on estimation of fish stock parameters. *Fish. Res.* 26, 207–223. doi: 10.1016/0165-7836(95)00447-5

Chen, Y. (2017). *Spatio-Temporal Variation of Fishery Resources in the Yellow Sea and Yangtze River Estuary*. Ph.D. thesis. Beijing: University of Chinses Academy of Sciences.

Cheng, X. (2021). Study on the construction of long-term mechanism of "Ten-year Fishing Ban" in major water areas of the Yangtze River basin. *J. Anhui Acad. Gov.* 6, 104–112.

Cochran, W. G. (1977). *Sampling Techniques*, 3rd Edn. New York, NY: Wiley.

Ding, Y. (2011). *The Temporal and Spatial Variation of the Fish Recruitment Resource in Yangtze River Estuary*. Ph.D. thesis. Beijing: University of Chinses Academy of Sciences.

Doray, M., Duhamel, E., Huret, M., Petitgas, P., and Massé, J. (2000). *PELGAS*. doi: 10.18142/18

Doray, M., Petitgas, P., Romagnan, J. B., Huret, M., Duhamel, E., and Dupuy, C. (2017). The PELGAS survey: Ship-based integrated monitoring of the Bay of Biscay pelagic ecosystem. *Prog. Oceanogr.* 166, 15–29. doi: 10.1016/j.pocean.2017.09.015

Edwards, M., Beaugrand, G., Hays, G. C., Koslow, A., and Richardson, A. J. (2010). Multi-decadal oceanic ecological datasets and their application in marine policy and management. *Trends Ecol. Evol.* 25, 602–610. doi: 10.1016/j.tree.2010.07.007

Gavaris, S., and Smith, S. J. (1987). Effect of allocation and stratification strategies on precision of survey abundance estimates for Atlantic cod (*Gadus morhua*) on the Eastern Scotian Shelf. *J. Northwest Atl. Fish. Sci.* 7, 137–144.

Hastie, T. J., and Tibshirani, R. J. (1986). Generalized additive models. *Stat. Sci.* 1, 297–310. doi: 10.1214/ss/1177013604

He, W., Li, Z., Liu, J., Li, Y., Murphy, B. R., and Xie, S. (2008). Validation of a method of estimating age, modelling growth, and describing the age composition of *Coilia mystus* from the Yangtze Estuary, China. *ICES J. Mar. Sci.* 65, 1655–1661. doi: 10.1093/icesjms/fsn143

Hsieh, C. H., Reiss, C., Watson, W., Allen, A. J., Hunter, J. R., and Lea, R. N. (2005). A comparison of long-term trends and variability in populations of larvae of exploited and unexploited fishes in the Southern California region: a community approach. *Prog. Oceanogr.* 67, 160–185. doi: 10.1016/j.pocean.2005.05.002

Hu, L., Song, C., Geng, Z., Zhao, F., Jiang, J., Liu, R., et al. (2021). Temporal and spatial distribution of *Coiliamystus* larvae and juveniles in the Yangtze Estuary during the main breeding season. *J. Fish. Sci. China* 28, 1152–1161.

Jardim, E., and Ribeiro, P. J. (2007). Geostatistical assessment of sampling designs for Portuguese bottom trawl surveys. *Fish. Res.* 85, 239–247. doi: 10.1016/j.fishres.2007.02.014

Jiao, Y., Chen, Y., Schneider, D., and Wroblewski, J. (2004). A simulation study of impacts of error structure on modeling stock-recruitment data using generalized linear models. *Can. J. Fish. Aquat. Sci.* 61, 122–133. doi: 10.1139/f03-149

Koslow, J. A., and Davison, P. C. (2016). Productivity and biomass of fishes in the California current large marine ecosystem: comparison of fishery-dependent and -independent time series. *Environ. Dev.* 17, 23–32. doi: 10.1016/j.envdev.2015.08.005

Koslow, J. A., and Wright, M. (2016). Ichthyoplankton sampling design to monitor marine fish populations and communities. *Mar. Policy* 68, 55–64. doi: 10.1016/j.marpol.2016.02.011

Li, B., Cao, J., Chang, J., Wilson, C., and Chen, Y. (2015). Evaluation of effectiveness of fixed-station sampling for monitoring American Lobster settlement. *N. Am. J. Fish. Manag.* 35, 942–957. doi: 10.1080/02755947.2015.1074961

Lin, N., Chen, Y., Jin, Y., Yuan, X., Ling, J., and Jiang, Y. (2018). Distribution of the early life stages of small yellow croaker in the Yangtze River estuary and adjacent waters. *Fish. Sci.* 84, 357–363. doi: 10.1007/s12562-018-1177-6

Liu, Q., Chen, J., Liu, H., and Zhang, D. (2020). Study of surface sediment characteristics in the south and north passages of the Yangtze estuary in 2019 flood and dry seasons. *Ocean Eng.* 38, 100–108.

Liu, Y., Chen, Y., and Cheng, J. (2009). A comparative study of optimization methods and conventional methods for sampling design in fishery-independent surveys. *ICES J. Mar. Sci.* 66, 1873–1882. doi: 10.1093/icesjms/fsp157

Lunsford, C., Haldorson, L., Fujioka, J. T., and Quinn, T. J. (2001). Distribution patterns and survey design considerations of Pacific Ocean perch (*Sebastes alutus*) in the Gulf of Alaska. *Spat. Process. Manag. Mar. Popul.* 17, 281–302.

Luo, B., and Shen, H. (1994). *The Three Gorges Project and Estuarine Ecological Environment*. Beijing: China Science Publishing & Media Ltd.

Ma, J., Tian, S., Gao, C., Kindong, R., and Zhao, J. (2020). Evaluation of sampling designs for different fishery groups in the Yangtze River estuary, China. *Reg. Stud. Mar. Sci.* 38, 1–8.

Manly, B. F. J., Akroyd, J. A. M., and Walshe, K. A. R. (2002). Two-phase stratified random surveys on multiple populations at multiple locations. *N. Z. J. Mar. Freshw. Res.* 36, 581–591. doi: 10.1080/00288330.2002.9517114

McClatchie, S. (2014). *Regional Fisheries Oceanography of the California Current System: The CalCOFI Program*. London: Springer.

McClatchie, S., Duffy-Anderson, J., Field, J. C., Goericke, R., Griffith, D., and Hanisko, D. S. (2014). Long time series in US fisheries oceanography. *Oceanography* 27, 48–67. doi: 10.5670/oceanog.2014.86

Meng, F. (2010). *Material Transport and Study of Dynamic Mechanism in the Yangtze River Estuary*. Ph.D. thesis. Shenyang: Shenyang Ligong University.

Miller, T. J., Skalski, J. R., and Ianelli, J. N. (2007). Optimizing a stratified sampling design when faced with multiple objectives. *ICES J. Mar. Sci.* 64, 97–109. doi: 10.1093/icesjms/fsl013

Ni, J., Guo, H., Tang, W., Zhang, Y., and Zhang, X. (2020). On interannual variations of *Coilia mystus* catches in the Yangtze River Estuary. *Mar. Fish.* 42, 192–204.

Ni, Y., and Chen, Y. (2006). Fishery resources, ecological environment, production status and fishery position and adjustment in the Yangtze Estuary. *Fish. Sci. Technol. Inform.* 33, 121–127.

Puerta, P., Johnson, B., Ciannelli, L., Helser, T., and Lauth, R. (2018). Subsampling populations with spatially structured traits: a field comparison of stratified and random strategies. *Can. J. Fish. Aquat. Sci.* 76, 511–522. doi: 10.1139/cjfas-2017-0248

Shono, H. (2008). Application of the Tweedie distribution to zero catch data in CPUE analysis. *Fish. Res.* 93, 154–162. doi: 10.1016/j.fishres.2008.03.006

Thompson, B. M., and Riley, J. D. (1981). Egg and larval development studies in the North Sea cod (*Gadus morhua* L.). *Rapp. P.-V. Reun. Cons. Int. Explor. Mer* 178, 553–559.

Wan, R., and Jiang, Y. (2000). The species and biological characteristics of the eggs and larvae of osteichthyes in the Bohai Sea and Yellow Sea. *J. Shanghai Fish. Univ.* 9, 290–297.

Wan, R., Zhou, F., Shan, X., and Sun, S. (2010). Impacts of variability of habitat factors on species composition of ichthyoplankton and distribution of fish spawning ground in the Changjiang River estuary and its adjacent waters. *Acta Ecol. Sin.* 30, 155–165. doi: 10.1016/j.chnaes.2010.04.006

Wang, H., Dai, X., Guan, W., and Fan, Y. (2017). Relationship between the environmental factors and the CPUE (catch per unit effort) of *Pseudocarcharias kamoharai* in tropical Atlantic Ocean based on the GAM-Tweedie model. *Chin. J. Appl. Ecol.* 28, 2024–2032.

Wang, J., Xu, B., Zhang, C., Xue, Y., Chen, Y., and Ren, Y. (2018). Evaluation of alternative stratifications for a stratified random fishery-independent survey. *Fish. Res.* 207, 150–159. doi: 10.1016/j.fishres.2018.06.019

Wang, J., Zhang, C., Xue, Y., Xu, B., Ren, Y., and Chen, Y. (2020). Comparison of different sampling designs for macrozoobenthos survey in a tidal flat. *Reg. Stud. Mar. Sci.* 35, 1–15. doi: 10.1016/j.rsma.2020.101113

Wei, W., Luo, B., and Ding, L. (2021). Three decadal morphodynamic response of Hengsha island tidal flat wetland to adjacent engineering in Yangtze Estuary. *J. Jilin Univ. (Earth Sci. Ed.)* 51, 1193–1203.

Wilde, G. R., and Fisher, W. L. (1996). Reservoir fisheries sampling and experimental design. *Am. Fish. Soc. Symp.* 16, 397–409.

Xian, W., Kang, B., and Liu, R. (2005). Jellyfish blooms in the Yangtze Estuary. *Science* 307, 41–41. doi: 10.1126/science.307.5706.41c

Xu, B., Ren, Y., Chen, Y., Xue, Y., Zhang, C., and Wan, R. (2015a). Optimization of stratification scheme for a fishery-independent survey with multiple objectives. *Acta Oceanol. Sin.* 34, 154–169. doi: 10.1007/s13131-015-0739-z

Xu, B., Zhang, C., Xue, Y., Ren, Y., and Chen, Y. (2015b). Optimization of sampling effort for a fishery-independent survey with multiple goals. *Environ. Monit. Assess.* 187, 1–16. doi: 10.1007/s10661-015-4483-9

Yan, Y., Gao, J., Zhu, Y., and Zheng, J. (2001). Preliminary study on relationship between deepwater channel regulation and riverbed evolution. *J. Hohai Univ.* 29, 7–12.

Yang, J., Arai, T., Liu, H., Miyazaki, N., and Tsukamoto, K. (2006). Reconstructing habitat use of *Coilia mystus* and *Coilia ectenes* of the Yangtze River estuary, and of *Coilia ectenes* of Taihu Lake, based on otolith strontium and calcium. *J. Fish Biol.* 69, 1120–1135. doi: 10.1111/j.1095-8649.2006.01186.x

Yu, S., He, Q., Chen, Y., and Deng, Z. (2021). Response of suspended sediment particle size to sediment reduction in the Yangtze Estuary turbidity maximum zone. *J. Sediment Res.* 46, 60–67.

Zhang, Z., Mammola, S., Xian, W., and Zhang, H. (2020). Modelling the potential impacts of climate change on the distribution of ichthyoplankton in the Yangtze Estuary, China. *Divers. Distrib.* 26, 126–137. doi: 10.1111/ddi.13002

Zhao, C., and Zhang, R. (1985). *Fish Eggs and Larvae in Offshore Waters of China*. Shanghai: Shanghai Scientific and Technical Publishers.

Zhao, K., Wu, B., You, Q., Ren, J., and Wang, Q. (2015). Spatio-temporal distribution of zooplankton and its relation with environmental factors in Jiuduansha inshore waters of Yangtze estuary. *J. Saf. Environ.* 15, 374–379.

Zhuang, P. (2013). *The Diverse Habitats and Aquatic Animals of the Yangtze Estuary*. Beijing: China Science Publishing & Media Ltd.

Conflict of Interest: The authors declare that the research was conducted in the absence of any commercial or financial relationships that could be construed as a potential conflict of interest.

ORIGINAL RESEARCH
published: 10 January 2022
doi: 10.3389/fmars.2021.786724

Shifting Feeding Habits During Settlement Among Small Yellow Croakers (*Larimichthys polyactis*)

Yuange Chen[1†], Weilong Wang[2†], Wei Zhou[3], Fen Hu[1] and Meiqin Wu[4*]

[1] East China Sea Fisheries Research Institute, Chinese Academy of Fishery Sciences, Shanghai, China, [2] Centre for Research on Environmental Ecology and Fish Nutrition of the Ministry of Agriculture, Shanghai Ocean University, Shanghai, China, [3] National University of Singapore, Singapore, Singapore, [4] College of Marine Ecology and Environment, Shanghai Ocean University, Shanghai, China

The small yellow croaker, *Larimichthys polyactis*, is a keystone species in the Yellow Sea and the East China Sea, with significant impacts on the regional ecosystem, but has experienced decades of population decline as a result of environmental changes and overfishing. The settlement of post-larval *L. polyactis* is a period of high mortality, with impacts on population recruitment and survival. This study examines the feeding habits of 49 post-larval and early juvenile *L. polyactis* in the Yangtze River estuary, in order to reveal diet composition before and after the settlement period. DNA barcoding methods (MiSeq and TA cloning) were used to examine gastrointestinal contents in detail. Both methods revealed that dietary breadth increased with increasing body length, while the dominance of copepods in the diet decreased as the body length increased. Post-larva (body length < 17 mm in this study) primarily fed on copepods. At the beginning of settlement (body length between 17 and 19 mm), *L. polyactis* began to ingest larger organisms, such as fishes and mysids, along with copepods. Larger early juveniles (body length > 20 mm) demonstrated a much wider dietary breadth, implying that successful settlement had occurred. Diet species richness in the MiSeq group was significantly greater than species richness in the TA cloning group, making the trend more pronounced within the MiSeq group. This indicates that the MiSeq method was more efficient than TA cloning in this study. We recommend that future research to investigate the feeding habits of fish larvae should combine MiSeq and visual examination methods.

Keywords: *Larimichthys polyactis*, shifting feeding habits, MiSeq sequencing, settlement, TA cloning

Edited by:
Chen Jiang,
Dalian Ocean University, China

Reviewed by:
Jin-Xian Liu,
Institute of Oceanology, Chinese Academy of Sciences (CAS), China
Osamu Nishimiya,
Ehime University, Japan

Correspondence:
Meiqin Wu
keer0316@hotmail.com

† These authors have contributed equally to this work and share first authorship

Specialty section:
This article was submitted to Marine Fisheries, Aquaculture and Living Resources, a section of the journal Frontiers in Marine Science

Received: *30 September 2021*
Accepted: *26 November 2021*
Published: *10 January 2022*

Citation:
Chen Y, Wang W, Zhou W, Hu F and Wu M (2022) Shifting Feeding Habits During Settlement Among Small Yellow Croakers (Larimichthys polyactis). Front. Mar. Sci. 8:786724. doi: 10.3389/fmars.2021.786724

INTRODUCTION

The small yellow croaker (*Larimichthys polyactis*) is a demersal marine fish, mainly distributed in marginal seas in eastern China, around southern Japan, and the Korean Peninsula (Froese and Pauly, 2017). As a keystone species in the Yellow Sea and the East China Sea, its population dynamics and interactions with the abiotic and biotic environments have a more significant impact than many other species on the regional ecosystem (Tang and Su, 2000; Zheng et al., 2003; Jin et al., 2005). Over the last seven decades, yellow croaker populations in the Yellow Sea and the East

China Sea have experienced a long-term decline in L_{50} (body length at median sexual maturity) and A_{50} (age at median sexual maturity). This is thought to be caused by environmental changes, such as rising sea surface temperature and overfishing (Li et al., 2011). Most small yellow croakers caught in the Yellow Sea and the East China Sea over recent years have been less than 1 year old (Jin et al., 2005; Lin et al., 2011). As a result, there is increasing concern over the longer-term survival of yellow croaker populations and potential impacts on the sustainability of the regional ecosystem and fishery.

Food quantity, quality, and timing are essential to the recruitment and survival of larval fish populations (Cushing, 1990; Beaugrand et al., 2003; Burrow et al., 2011; Swalethorp et al., 2014). Thus, research on fish feeding habits could provide important information on the survival and sustainability of local small yellow croaker populations. The ontogenetic, diel, seasonal, and spatial variations in the feeding habits of the small yellow croaker have been analyzed by visual gastrointestinal content analysis (Lin, 1962; Xue et al., 2005; Guo et al., 2010). However, visual identification of prey from gastrointestinal contents requires comprehensive taxonomic expertise, and a significant proportion of unrecognizable remains is often excluded from subsequent analysis (Xue et al., 2005; Guo et al., 2010; Landaeta et al., 2015). Detecting just one or two additional prey species from stomach contents could lead to different conclusion about the feeding strategy of a species (Boling et al., 2012; Leray et al., 2013; Huang et al., 2014), so unidentified components should never be disregarded during gastrointestinal content analysis. Several techniques have been adopted to enhance diet analysis, among which DNA-based techniques are widely used, due to their significant efficiency and versatility (Symondson, 2002; King et al., 2008; Navarrete et al., 2009). Depending on the particular study objectives, prey-specific DNA may be identified using PCRs with species-specific, group-specific, or universal primers. Although universal primers are the most efficient for identifying prey items, they usually simultaneously amplify a vast amount of host DNA due to low species-specificity (Suzuki et al., 2006, 2008). PCR clamping could be the most promising approach to improve this situation by including a predator species-specific annealing blocking primer in the PCR to prevent the amplification of predator DNA (Vestheim and Jarman, 2008; Leray et al., 2013).

The technical advances of next-generation sequencing (NGS, also known as high-throughput sequencing) enable the sequencing of vast quantities of different DNA or RNA segments, from different species simultaneously, by performing “massive parallel analysis” (Liu et al., 2013). This allows the most comprehensive description of the composition of the tested sample. Previous studies have adopted the advantages of MiSeq in investigating the intestinal microbiome of fishes (Franchini et al., 2014; Li et al., 2014); however, no studies have reported using this technique to elucidate complex shifts in the feeding habits of fish larvae or juveniles.

As a demersal fish, the settlement of the small yellow croaker involves a movement from open to coastal water, as pelagic larvae become benthic juveniles (Chen et al., 2015; Lin et al., 2018). The Yangtze River estuary is a vital nursery ground for the small yellow croaker, where post-larva and juveniles dominate the developmental stages (Lin et al., 2018). High mortality during settlement is observed in coral reef fishes (Doherty et al., 2004), which may partially attribute to the poor availability of suitable prey and shifts in feeding habits during the settlement period. The prosperous prey organisms in the Yangtze River estuary may thus be an important factor in the successful settlement of small yellow croakers. This study uses molecular techniques to examine the gastrointestinal contents of post-larval and early juvenile small yellow croakers in the region to reveal their feeding habits during the settlement period.

MATERIALS AND METHODS

Fish Sampling Techniques

Samples were collected every month by conducting horizontal tows (at speeds of 1–2 knots) with a plankton net (1.3 m diameter, 6 m length, and 0.5 mm mesh) in the East China Sea, from April to July 2017. At two of the survey sites in the Yangtze River Estuary region (**Figure 1**), between April and June, a total of 49 post-larval and juvenile small yellow croakers (*L. polyactis*) were collected and stored in absolute ethanol at −20°C. The specimens were sorted into post-larva and juvenile, based on their morphology, using the method of Kendall et al. (1984), and their body length was measured. Then, individual animals were allocated to one of the 11 groups, distinguished by developmental stage and average body length. Then, 6 groups were allocated to analysis using TA cloning, and 5 groups were allocated to analysis using MiSeq sequencing (**Table 1**).

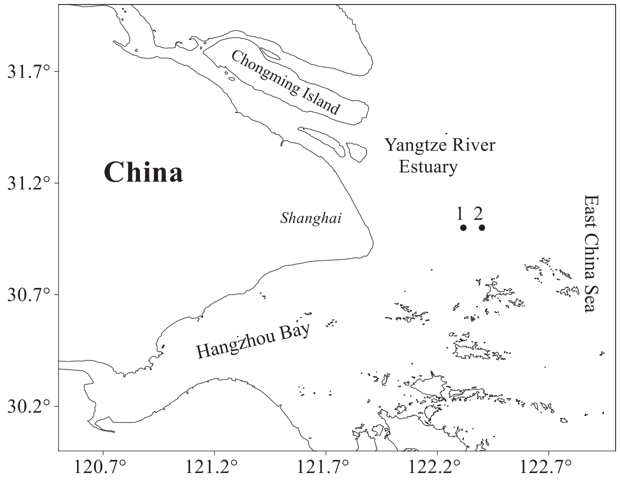

FIGURE 1 | Locations of sampling sites in the Yangtze River Estuary region. Numbers 1 and 2 are sampling locations.

TABLE 1 | *Larimichthys polyactis* samples, developmental stages, analysis methods, and body lengths.

Sample	Development stage	Method	Average body length (mm)	Standard deviation (mm)	Number of specimens
A	Post-larvae	TA cloning	14.06	1.22	7
B	Post-larvae	TA cloning	15.92	0.33	4
C	Post-larvae	TA cloning	17.92	0.87	3
D	Juveniles	TA cloning	22.01	0.59	3
E	Juveniles	TA cloning	25.31	0.63	3
F	Juveniles	TA cloning	32.14	2.56	3
G	Post-larvae	Miseq	13.54	0.42	14
H	Post-larvae	Miseq	17.77	0.40	3
J	Juveniles	Miseq	19.00	0.46	3
K	Juveniles	Miseq	21.21	1.21	3
L	Juveniles	Miseq	31.89	1.17	3

DNA Extraction From Gastrointestinal Contents

Each specimen was carefully washed with sterile ddH$_2$O (double-distilled water) to eliminate contaminants from the body surface. Then, the entire gastrointestinal tract was exposed, on a clean bench, and the gastrointestinal contents were removed using a fine acupuncture needle under a stereoscope. Gastrointestinal contents from all animals in the same group (groups A–L) were pooled for DNA analysis. Then, genome DNA was extracted from each group using a TaKaRa MiniBEST Universal Genomic DNA Extraction Kit (Takara Biomedical Technology Co., Ltd., China).

TA Cloning

To prevent co-amplification of predator DNA, during PCR, we included an *L. polyactis*-specific annealing blocking primer as used by Leray et al. (2013). Three primers were designed as below: 5′-GGWACWGGWTGAACWGTWTAYCCYCC-3′ (mlCOIintF), 5′-TANACYTCNGGRTGNCCRAARAAYCA-3′ (jgHCO2198), and 5′-GTCTACCCCCCACTTGCTGGAAATCT-3′ (annealing primer, with Spacer C3 CPG to 3′).

The PCR was performed using a TaKaRa Ex Taq® Kit (Takara), in a volume of 50 μl, which contained 1 μl each of mlCOlintF primer (10 μM), jgHCO2198 primer (10 μM) and annealing primer (100 μM), 0.25 μl of ExTaq (5 U/μl), 5 μl of 10× Ex Taq Buffer (Mg^{2+} Plus), 4 μl of dNTP (2.5 mM), and 1 μl of genome DNA. Touchdown PCR programs were carried out at 95°C for 4 min followed by 5 cycles of 95°C for 30 s, then 60°C for 45 s (-1°C per cycle), and 72°C for 45 s, followed by 30 cycles of 55°C with the annealing primer, and a final extension at 72°C for 10 min.

The amplified products were analyzed using a 2% agarose gel electrophoresis and purified using a TIANgel Midi Purification Kit [TIANGEN Biotech (Beijing) Co., Ltd., China]. The isolated fragments were ligated into the pGEM-T Easy vector (Promega, Madison, WI, United States) and transformed into DH5α strain of *Escherichia coli* [TIANGEN Biotech (Beijing) Co., Ltd., China]. Recombinant clones were incubated overnight at 37°C in Luria-Broth, containing 1.5% agar and ampicillin (50 μg/ml), following selection of colonies by blue-white plaque screening. A total of 30 white colonies were picked up and analyzed by PCR, to screen the size of inserted fragments. After overnight culturing, the colonies were sent to Sangon Biotech Company (Shanghai, China) for plasmid DNA extraction and DNA sequencing.

MiSeq Sequencing

The genome DNA of samples in MiSeq groups were also amplified using PCR (95°C for 4 min, 30 cycles of 95°C for 30 s, 60°C for 45 s, and 72°C for 45 s, followed by a final extension at 72°C for 10 min) using the primers mlCOIintF and jgHCO2198, where a barcode was an eight-base sequence unique to each sample. PCR reactions were performed in a triplicate 20 μl mixture containing 4 μl of 5× FastPfu buffer, 2 μl of 2.5 mM dNTPs, 0.8 μl of each primer (5 μM), 0.4 μl of FastPfu polymerase, and 10 ng of template DNA. The amplicons were extracted from a 2% agarose gel and then purified using the AxyPrep DNA Gel Extraction Kit (Axygen Biosciences, Union City, CA, United States) and quantified using QuantiFluor$^{\text{TM}}$-ST (Promega) according to the protocol of the manufacturer.

Purified amplicons were pooled in equimolar and paired-end sequenced (2 × 300) on an Illumina MiSeq platform (Illumina, San Diego, CA, United States), according to the standard protocols by Majorbio Bio-Pharm Technology Co. Ltd. (Shanghai, China). When processing sequencing data, raw FASTQ files were demultiplexed, quality-filtered by Trimmomatic, and merged by FLASH with the following criteria: (i) the reads were truncated at any site receiving an average quality score <20 over a 50 bp sliding window; (ii) primers were matched exactly, allowing 2 nucleotide mismatches, and reads containing ambiguous bases were removed; and (iii) sequences whose overlap was longer than 10 bp were merged according to their overlap sequence. Operational taxonomic units (OTUs) were clustered with 97% similarity cutoff using UPARSE (version 7.1[1]), and chimeric sequences were identified and removed using UCHIME. The taxonomy of each COI gene sequence was analyzed using the RDP Classifier algorithm[2] against the FGR database (release 7.3) using a confidence threshold of 70%.

---

[1] http://drive5.com/uparse/

[2] http://rdp.cme.msu.edu/

TABLE 2 | Prey species of post-larval and juvenile *L. polyactis.*

Kingdom	Phylum	Class	Order	Family	Species name	Spp. Abbrev.*	MiSeq†	TA†
Chromista	Ochrophyta	Eustigmatophyceae	Eustigmatales	Monodopsidaceae	*Nannochloropsis limnetica*	nl	+	
		Bacillariophyceae	Paraliales	Paraliaceae	*Paralia sulcata*	ps	+	
Animalia	Cnidaria	Hydrozoa	Anthoathecata	Bougainvilliidae	*Nemopsis bachei*	nb	+	
			Limnomedusae	Geryoniidae	*Liriope tetraphylla*	lt	+	
	Ctenophora				*Ctenophora* sp.1	ct	+	+
	Rotifera	Eurotatoria	Philodinida	Philodinidae	*Macrotrachela* sp.1	ma	+	
					Rotifera sp.1	ro	+	
	Mollusca	Gastropoda	Neogastropoda	Nassariidae	*Nassarius variciferus*	nv	+	
	Annelida	Polychaeta			*Polychaeta* sp.1	po		+
	Arthropoda	Hexanauplia	Calanoida	Paracalanidae	*Paracalanus aculeatus*	pa	+	
					Paracalanus parvus	pp	+	+
				Pontellidae	*Labidocera euchaeta*	le	+	+
				Pseudodiaptomidae	*Pseudodiaptomus poplesia*	pd	+	+
				Tortanidae	*Tortanus vermiculus*	tv	+	+
			Cyclopoida	Corycaeidae	*Ditrichocorycaeus affinis*	da		+
					Unclassified copepoda sp.1	u1	+	+
		Thecostraca	Sessilia	Balanidae	*Amphibalanus* sp.1	am	+	
		Malacostraca	Euphausiacea	Euphausiidae	*Pseudeuphausia sinica*	pu	+	
			Decapoda	Sesarmidae	*Orisarma dehaani*	od		+
				Varunidae	*Helice tientsinensis*	ht	+	
					Neoeriocheir leptognathus	ne	+	
			Amphipoda		Gammaridea sp.1	ga		+
			Mysida	Mysidae	*Hyperacanthomysis brevirostris*	hb		+
					Iiella pelagica	ip	+	+
					Mysida sp.1	my	+	
	Chaetognatha	Sagittoidea	Aphragmophora	Sagittidae	*Zonosagitta nagae*	zn	+	
	Chordata	Actinopteri	Syngnathiformes	Callionymidae	*Callionymus olidus*	co	+	+
			Gobiiformes	Gobiidae	*Chaeturichthys stigmatias*	cs	+	
			Mugiliformes	Mugilidae	*Planiliza haematocheilus*	ph	+	
			Acropomatiformes	Lateolabracidae	*Lateolabrax japonicus*	lj	+	
Unclassified					Unclassified sp.1	u2	+	

**Spp. Abbrev, species name abbreviations.*
† *"+" indicates species occurrence.*

Data Analysis

Operational taxonomic units belonging to *L. polyactis*, fungi, parasites, and obvious contaminants were excluded from further analysis. Species taxonomic ranks mainly referred to the Worms database (WoRMS Editorial Board, 2021) and Eschmeyer's Catalog of Fishes Online Database (Fricke et al., 2021). Diversity was represented by species richness (number of species) and the Shannon-Wiener index. Some of the data did not conform to a normal distribution (Shapiro-Wilk test), so the Mann-Whitney *U* test was used to test for differences in body length, species richness, and Shannon-Wiener index. Non-metric Multidimensional Scaling (NMDS) and analysis of similarities (ANOSIM) were performed on the square-rooted species matrix. The *Vegan package* (Oksanen et al., 2020) and *Tidyverse package*

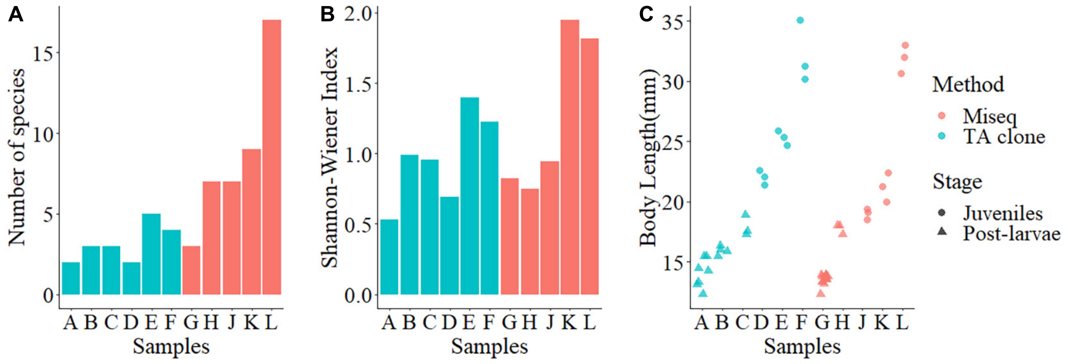

FIGURE 2 | Prey species richness, prey diversity, and body length of post-larval and juvenile small yellow croakers *(Larimichthys polyactis)*. **(A)** Prey species richness; **(B)** Prey diversity; **(C)** Body length. Red indicates samples analyzed using MiSeq, and blue indicates samples analyzed using TA cloning. In panels **(A,B)**, bars A, B, C, G, and H show post-larva, and bars D, E, F, J, K, and L show juveniles. In panel **(C)**, triangles represent post-larva, and dots represent juveniles.

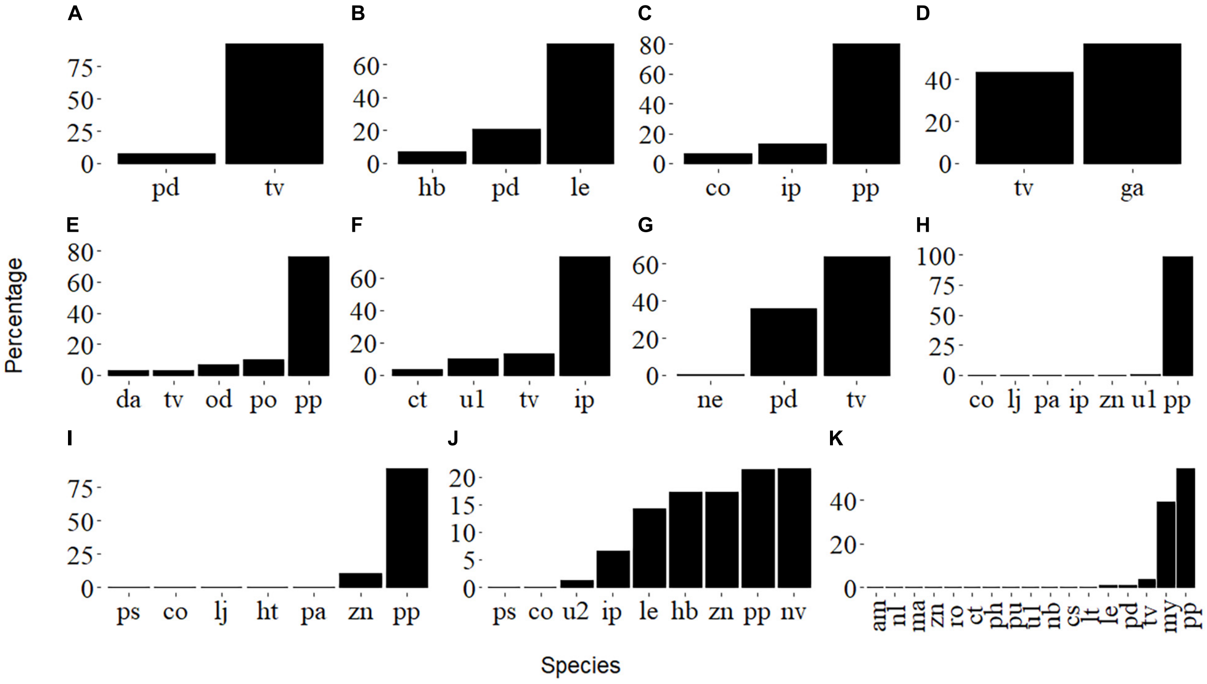

FIGURE 3 | Percentage of prey amplicons for post-larval (i.e., **(A–C,G,H)**) and juvenile (i.e., **(D–F,I–K)**) *L. polyactis*. See **Table 2** for the species abbreviations.

(Wickham et al., 2019) were used for data analysis. All statistical analyses were performed with R 4.1.0 (R Core Team, 2021).

Ethical Statement

The present experimental procedures were carried out in strict accordance with the recommendations in the ethical guidelines of EU Directive 2010/63/EU for animal experiments.

RESULTS

After removing the amplicons of *L. polyactis*, possible contaminants (i.e., *Homo sapiens*) and parasites (i.e., *Hematodinium* sp.1), 26, 29, 30, 30, 30, and 30 amplicons remained for each sample of the TA cloning group (samples A–F), respectively, and 9881, 21223, 10526, 10506, and 18761 amplicons remained for each sample of the MiSeq group (samples G, H, J, K, and L), respectively. Algae and rotifers were not excluded (*Nannochloropsis limnetica* and *Paralia sulcata*) because it was difficult to determine whether they were (actively or incidentally) consumed from surrounding water or indirectly ingested through other herbivorous zooplankton, especially bearing in mind that freshwater species can be washed out of an estuary in the runoff. As a result, 31 prey species were identified across different taxonomic orders belonging to nine phyla. MiSeq sequencing identified 27 prey species, compared to 13 species by the TA cloning, showing an enhanced ability to detect rare OTUs. *L. polyactis* feeds on plankton (e.g., copepods, jellyfish, mysids, arrow worms, and krill), co-occurring larval fishes or possibly fish eggs, even sessile larva (e.g., barnacles), and benthic organisms (e.g., mud snails, and crabs). Most of these are dominant species or common species in the Yangtze River Estuary. Copepods have the highest species richness of all taxa in the prey list, followed by fishes, crabs, and mysids (**Table 2**).

Species richness ranged between 2 and 17 species, with a Shannon-Wiener index ranging from 0.53 to 1.95. Species richness and Shannon-Wiener index tended to increase with body length, meaning that prey species diversity was generally greater for larger *L. polyactis*, but the trend was more pronounced in the MiSeq group (**Figures 2A,B**). There was no significant difference in the body length (Mann-Whitney *U* test, $W = 225$, $P > 0.05$) or Shannon-Wiener index (Mann-Whitney *U* test, $W = 18$, $P > 0.05$) between the TA cloning group and the MiSeq group (**Figures 2B,C**). However, species richness was significantly greater in the MiSeq group than in the TA cloning group (Mann-Whitney *U* test, $W = 27$, $P < 0.05$). Pearson correlations of the body length with species richness and body length with the Shannon-Wiener index for the TA cloning group were 0.65 and 0.68, respectively, compared with 1.00 and 0.74 for the MiSeq group, suggesting that food richness was closely associated with the developmental stages. In this study, we found that larval *L. polyactis* began to grow scales at ca. 18 mm body length, representing the beginning of the juvenile stage. Prey species richness and diversity began to rise from samples E and K onward, when body length exceeded 20 mm (**Figure 3**), displaying a successful shift of feeding habits into the juvenile stage. It should be noted that the transitional body lengths mentioned above may not apply to *L. polyactis* living in other regions or populations, or during other seasons.

The prey species composition for groups A, B, and G, with average body lengths below 17 mm, were dominated by copepods, mainly *Tortanus vermiculus*, *Labidocera euchaeta*, and *Pseudodiaptomus poplesia*. Samples C, H, and J, with average body lengths between 17 and 19 mm, mainly fed on copepods (*Paracalanus parvus*). However, they also consumed larger organisms such as fishes (probably eggs or larvae of *Callionymus olidus*, *Lateolabrax japonicus*, etc.) and mysids (*Iiella pelagica*, etc.), and this probably represents a transitional stage between post-larva and juvenile. Groups with body lengths greater than 20 mm displayed a more diverse diet, including plankton (*Copepoda*, *Sagittidae*), polychaetes (*Polychaeta*), jellyfish (*Hydrozoa*, *Ctenophora*), mud snails (*Nassarius variciferus*), barnacles (*Amphibalanus* sp.), krill (Mysida), mullet (*Planiliza haematocheilus*), etc.; this may be an indication of successful settlement (**Figure 3**). There were significant differences in prey composition among the three body length groups (ANOSIM, $R = 0.34$, $P < 0.05$). However, samples on the Non-metric Multidimensional Scaling ordination plot (**Figure 4**) are not well clustered due to many shared prey species, indicating that the changes in feeding habits between post-larval and juvenile *L. polyactis* occur progressively.

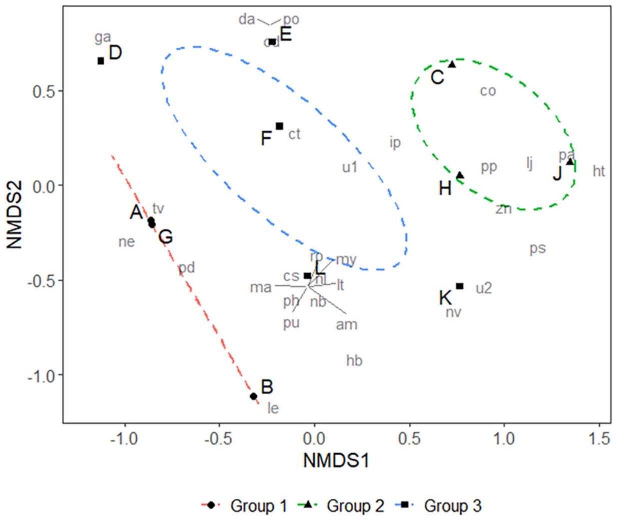

FIGURE 4 | Non-metric Multidimensional Scaling (NMDS) of prey animals of larval and juvenile *L. polyactis.* Stress = 0.09, and confidence limit for the ordination ellipse is 90%. Analysis of similarity (ANOSIM) on three groups: $R = 0.34$, $P < 0.05$. Group 1 represents animals with an average body length <17 mm (post-larva); Group 2 represents animals between 17 and 19 mm (post-larva or juvenile at the transitional stage); Group 3 represents animals >20 mm (juvenile).

DISCUSSION

In this study, we examined the gastrointestinal contents of post-larval and juvenile small yellow croakers using DNA barcoding and revealing how feeding habits shift from post-larva to early juvenile during settlement. The same trend was recognized by Llopiz (2013) who reported that the dominant prey types of higher latitude larvae were nauplii and calanoid copepods, with a shift from smaller to larger prey through larval ontogeny. Lin (1962) identified 19 OTUs from prey in 2,593 small yellow croaker samples with body lengths ranging from 9 to 140 mm. Twelve OTUs were identified from 11 to 35 mm samples (similar to this study), with eight to species level (*Sagitta crassa*, *Calanus pacificus*, *L. euchaeta*, *Acartia bifilosa*, *Acanthomysis longirostris*, *Themisto gracilipes*, *Leptochela gracilis*, and *Crangon affinis*). Bai (1966) identified 17 OTUs from prey in more than 1,300 samples measuring 4 mm–80 mm, and Guo et al. (2010) identified 34 OTUs from prey in 731 samples measuring 20 mm–109 mm. However, in the previous studies of *L. polyactis* feeding habits, the less accurate identification of preys species and grouping strategies did not allow a good observation on the critical period of feeding habits transition. Robert et al. (2014) recommended that, research on the survival and recruitment of larval fish should investigate diet composition at the species level. The difficulty of species-level diet analysis lies in the identification of food remnants. For example, it is difficult to identify the source of plankton chitin debris, remnants of soft-bodied organisms such as jellyfish and fish larvae, and even protozoa (Montagnes et al., 2010). This challenge can be solved by molecular approaches, which are able to identify fragments without obvious morphological features; however, molecular approaches also bearing the disadvantage in quantifying the relative abundance of preys. Combining visual identification and metabarcoding (Kodama et al., 2017) might be an optimal solution in the future to improve dietary research on larval fish.

Next-generation sequencing showed a superior ability to reveal wider dietary breadth than TA cloning in this study. Further studies should apply NGS techniques to a broader list of predators. Besides, several other NGS techniques have been used to identify fish gut microbiome and/or content (as reviewed in Ghanbari et al., 2015). Comparative studies with different sequencing methods can also be conducted to identify the optimum method with the greatest efficiency. The most exciting outcome of this research is that when early stage larvae are obtained, prey selection during initial feeding can be revealed in detail by these molecular approaches, even if samples sizes are small, which will be of particular benefit to research on fish breeding.

DATA AVAILABILITY STATEMENT

The data presented in the study are deposited in the NCBI Sequence Read Archive (SRA) database, accession number PRJNA784007.

ETHICS STATEMENT

Ethical review and approval was not required for the animal study because the present experimental procedures were carried out in strict accordance with the recommendations in the ethical guidelines of EU Directive 2010/63/EU for animal experiments.

AUTHOR CONTRIBUTIONS

YC and FH conducted the sampling and experimental analysis. WW and WZ analyzed the data and revised the manuscript. MW advised on experimental design.

FUNDING

This study was supported by the Central Public-interest Scientific Institution Basal Research Fund, ECSFR, CAFS (2015T04), and the Special Funds for Survey of Nearshore Spawning Ground by the Ministry of Agriculture and Rural Affairs (125C0505).

SUPPLEMENTARY MATERIAL

The Supplementary Material for this article can be found online at: https://www.frontiersin.org/articles/10.3389/fmars.2021.786724/full#supplementary-material

REFERENCES

Bai, X. E. (1966). "Feeding habits of larval and juvenile small yellow croaker (*Pseudosciaena polyactis*) in the Bohai Sea and the Yellow Sea," in *Proceedings of the Western Pacific Fisheries Commission 8th Symposium*, ed. Chinese Office of the Pacific West Fisheries Commission (Beijing: China Science Press), 18–30.

Beaugrand, G., Brander, K. M., Lindley, J. A., Souissi, S., and Reid, P. C. (2003). Plankton effect on cod recruitment in the North Sea. *Nature* 426, 661–664. doi: 10.1038/nature02164

Boling, W. B., Sinclair, G. A., and Wawrik, B. (2012). Identification of calanoid copepod prey species via molecular detection of carbon fixation genes. *Mar. Biol.* 159, 1165–1171. doi: 10.1007/s00227-011-1877-2

Burrow, J. F., Horwood, J. W., and Pitchford, J. W. (2011). The importance of variable timing and abundance of prey for fish larval recruitment. *J. Plankton Res.* 33, 1153–1162. doi: 10.1371/journal.pone.0017456

Chen, Y., Zhong, J., Xu, Z., and Chen, J. (2015). Spatio-temporal distribution of larval and juvenile fishes at frequent harmful algal blooms (HABs) areas of the East China Sea in spring. *Haiyang Xuebao* 37, 44–54.

Cushing, D. H. (1990). "Plankton production and year-class strength in fish populations: an update of the match/mismatch hypothesis," in *Advances in Marine Biology*, Vol. 26, eds J. H. S. Blaxter and A. Southward (Cambridge, MA: Academic Press), 249–293.

Doherty, P. J., Dufour, V., Galzin, R., Hixon, M. A., Meekan, M. G., and Planes, S. (2004). High mortality during settlement is a population bottleneck for a tropical surgeonfish. *Ecology* 85, 2422–2428. doi: 10.1890/04-0366

Franchini, P., Fruciano, C., Frickey, T., Jones, J. C., and Meyer, A. (2014). The gut microbial community of Midas cichlid fish in repeatedly evolved limnetic–benthic species pairs. *PLoS One* 9:e95027. doi: 10.1371/journal.pone.0095027

Fricke, R., Eschmeyer, W. N., and van der Laan, R. (2021). *Eschmeyer's Catalog of Fishes: Genera, Species, References*. Available online at: https://researcharchive.calacademy.org/research/ichthyology/catalog/fishcatmain.asp (Accessed August 05, 2021)

Froese, R., and Pauly, D. (2017). *FishBase*. Available online at: https://www.fishbase.org (Accessed August 05, 2021)

Ghanbari, M., Kneifel, W., and Domig, K. J. (2015). A new view of the fish gut microbiome: advances from next-generation sequencing. *Aquaculture* 448, 464–475.

Guo, B., Zhang, B., and Jin, X. S. (2010). Diet composition and ontogenetic variation in feeding habits of juvenile small yellow croaker *Pseudosciaena polyactis* Bleeker in the Yellow Sea. *J. Fish. Sci. China* 17, 289–297.

Hixon, M. A. (1991). "Predation as a process structuring coral reef fish communities," in *The Ecology of Fishes on Coral Reefs*, ed. P. F. Sale (San Diego, CA: Academic Press), 475–508. doi: 10.1016/b978-0-08-092551-6.50022-2

Huang, Y. S., Xu, D. H., and Chen, H. J. (2014). PCR-based in situ dietary analysis of *Calanus sinicus* Brodsky in Yellow River Estuary and adjacent waters. *J. Ocean Univ. China* 44, 83–91.

Jin, X. S., Zhao, X. Y., Meng, T. X., and Cui, Y. (2005). *Biology Resource and Environment in the Bohai Sea and Yellow Sea*. Beijing: China Science Press.

Kendall, A. W. Jr., Ahlstrom, E. H., and Moser, H. G. (1984). "Early life history stages of fishes and their characters," in *Ontogeny and Systematics of Fishes. Special Publication 1*, eds H. G. Moser, W. J. Richards, D. M. Cohen, M. P. Fahay, A. W. Kendall Jr., and S. L. Richardson (Lawrence, KS: Allen press), 11–22.

King, R. A., Read, D. S., Traugott, M., and Symondson, W. O. C. (2008). Invited review: molecular analysis of predation: a review of best practice for DNA-based approaches. *Mol. Ecol.* 17, 947–963. doi: 10.1111/j.1365-294X.2007.03613.x

Kodama, T., Hirai, J., Tamura, S., Takahashi, T., Tanaka, Y., Ishihara, T., et al. (2017). Diet composition and feeding habits of larval Pacific bluefin tuna *Thunnus orientalis* in the Sea of Japan: integrated morphological and metagenetic analysis. *Mar. Ecol. Prog. Ser.* 583, 211–226. doi: 10.3354/meps12341

Landaeta, M. F., Bustos, C. A., Contreras, J. E., Salas-Berríos, F., Palacios-Fuentes, P., Alvarado-Niño, M., et al. (2015). Larval fish feeding ecology, growth and mortality from two basins with contrasting environmental conditions of an inner sea of northern Patagonia. *Chile. Mar. Environ. Res.* 106, 19–29. doi: 10.1016/j.marenvres.2015.03.003

Leray, M., Agudelo, N., Mills, S. C., and Meyer, C. P. (2013). Effectiveness of annealing blocking primers versus restriction enzymes for characterization of generalist diets: unexpected prey revealed in the gut contents of two coral reef fish species. *PLoS One* 8:e58076. doi: 10.1371/journal.pone.0058076

Li, X. M., Zhu, Y. J., Yan, Q. Y., Ringø, E., and Yang, D. G. (2014). Do the intestinal microbiotas differ between paddlefish (*Polyodon spathula*) and bighead carp (*Aristichthys nobilis*) reared in the same pond? *J. Appl. Microbiol.* 117, 1245–1252. doi: 10.1111/jam.12626

Li, Z. L., Shan, X. J., Jin, X. S., and Dai, F. Q. (2011). Long-term variations in body length and age at maturity of the small yellow croaker (*Larimichthys polyactis* Bleeker, 1877) in the Bohai Sea and the Yellow Sea. *China Fish. Res.* 110, 67–74.

Lin, J. Q. (1962). "Study on the feeding habit and condition of young and adult small yellow croaker," in *Proceedings of Marine Fishery Resource*, eds S. P. Zhu, X. W. Zhang, X. S. Liu, and G. Z. Xu (Beijing: China Agriculture Press), 34–43.

Lin, L. S., Liu, Z. L., Jiang, Y. Z., Huang, W., and Gao, T. X. (2011). Current status of small yellow croaker resources in the southern Yellow Sea and the East China Sea. *Chin. J. Oceanol. Limnol.* 29, 547–555. doi: 10.1007/s00343-011-0182-8

Lin, N., Chen, Y. G., Jin, Y., Yuan, X. W., Ling, J. Z., and Jiang, Y. Z. (2018). Distribution of the early life stages of small yellow croaker in the Yangtze River estuary and adjacent waters. *Fish. Sci.* 84, 357–363. doi: 10.1007/s12562-018-1177-6

Liu, L., Li, Y. H., Li, S. L., Hu, N., He, Y. M., Pong, R., et al. (2013). "Comparison of next-generation sequencing systems," in *Biofuel Production: Algae and Aquatic Plants*, ed. B. Gikonyo (Palm Bay, FL: Apple Academic Press), 279–303.

Llopiz, J. K. (2013). Latitudinal and taxonomic patterns in the feeding ecologies of fish larvae: a literature synthesis. *J. Mar. Syst.* 109, 69–77. doi: 10.1016/j.jmarsys.2012.05.002

Montagnes, D. J., Dower, J. F., and Figueiredo, G. M. (2010). The Protozooplankton-ichthyoplankton trophic link: an overlooked aspect of aquatic food webs. *J. Eukaryotic Microbiol.* 57, 223–228. doi: 10.1111/j.1550-7408.2010.00476.x

Navarrete, P., Espejo, R. T., and Romero, J. (2009). Molecular analysis of microbiota along the digestive tract of juvenile Atlantic salmon (*Salmo salar* L.). *Microb. Ecol.* 57, 550–561. doi: 10.1007/s00248-008-9448-x

Oksanen, J., Blanchet, F. G., Kindt, R., Legendre, P., Minchin, P. R., O'hara, R. B., et al. (2020). *Vegan: Community Ecology Package. R Package Version 2.5-7*. Available online at: https://cran.r-project.org/package=vegan (accessed August 15, 2021).

R Core Team (2021). *R: A Language and Environment for Statistical Computing*. Vienna: R Foundation for Statistical Computing.

Robert, D., Murphy, H. M., Jenkins, G. P., and Fortier, L. (2014). Poor taxonomical knowledge of larval fish prey preference is impeding our ability to assess the existence of a "critical period" driving year-class strength. *ICES J. Mar. Sci.* 71, 2042–2052.

Suzuki, N., Hoshino, K., Murakami, K., Takeyama, H., and Chow, S. (2008). Molecular diet analysis of phyllosoma larvae of the Japanese spiny lobster *Panulirus japonicus* (Decapoda: Crustacea). *Mar. Biotechnol.* 10, 49–55. doi: 10.1007/s10126-007-9038-9

Suzuki, N., Murakami, K., Takeyama, H., and Chow, S. (2006). Molecular attempt to identify prey organisms of lobster phyllosoma larvae. *Fish. Sci.* 72, 342–349.

Swalethorp, R., Kjellerup, S., Malanski, E., Munk, P., and Nielsen, T. G. (2014). Feeding opportunities of larval and juvenile cod (*Gadus morhua*) in a Greenlandic fjord: temporal and spatial linkages between cod and their preferred prey. *Mar. Biol.* 161, 2831–2846. doi: 10.1007/s00227-014-2549-9

Symondson, W. O. C. (2002). Molecular identification of prey in predator diets. *Mol. Ecol.* 11, 627–641. doi: 10.1046/j.1365-294x.2002.01471.x

Tang, Q. S., and Su, J. L. (2000). *Global Ocean Ecosystem Dynamic of China. I. Key Scientific Problems and Strategy of Development*. Beijing: China Science Press.

Vestheim, H., and Jarman, S. N. (2008). Blocking primers to enhance PCR amplification of rare sequences in mixed samples–a case study on prey DNA in Antarctic krill stomachs. *Front. Zool.* 5:12. doi: 10.1186/1742-9994-5-12

Wickham, H., Averick, M., Bryan, J., Chang, W., McGowan, L. D., Froncois, R., et al. (2019). Welcome to the tidyverse. *J. Open Source Softw.* 4:1686. doi: 10.21105/joss.01686

WoRMS Editorial Board (2021). *World Register of Marine Species*. Available online at: https://www.marinespecies.org (Accessed August 05, 2021)

Xue, Y., Jin, X., Zhang, B., and Liang, Z. (2005). Seasonal, diel and ontogenetic variation in feeding patterns of small yellow croaker in the central Yellow Sea. *J. Fish Biol.* 67, 33–50. doi: 10.1111/j.0022-1112.2005.00677.x

Zheng, Y. J., Chen, X. Z., Cheng, J. H., Wang, Y. L., Shen, X. Q., Chen, W. Z., et al. (2003). *The Living Resources and the Environment in the Continental Shelf of the East China Sea*. Shanghai: Shanghai Science and Technology Press.

Conflict of Interest: The authors declare that the research was conducted in the absence of any commercial or financial relationships that could be construed as a potential conflict of interest.

frontiers in Marine Science

ORIGINAL RESEARCH
published: 28 January 2022
doi: 10.3389/fmars.2021.806208

Molecular Identification of Species Diversity Using Pelagic Fish Eggs in Spring and Late Autumn-Winter in the Eastern Beibu Gulf, China

Gang Hou[1], Yanying Chen[1], Jinrun Wang[1], Chuanhao Pan[1], Jianbin Lin[1], Bo Feng[1] and Hui Zhang[2,3,4]*†*

[1] College of Fisheries, Guangdong Ocean University, Zhanjiang, China, [2] CAS Key Laboratory of Marine Ecology and Environmental Sciences, Institute of Oceanology, Chinese Academy of Sciences, Qingdao, China, [3] Center for Ocean Mega-Science, Chinese Academy of Sciences, Qingdao, China, [4] Laboratory for Marine Ecology and Environmental Science, Qingdao National Laboratory for Marine Science and Technology, Qingdao, China

Edited by:
Huang Wei,
Second Institute of Oceanography,
Ministry of Natural Resources, China

Reviewed by:
Jiaguang Xiao,
Third Institute of Oceanography,
Ministry of Natural Resources, China
Liandong Yang,
Institute of Hydrobiology, Chinese
Academy of Sciences (CAS), China

***Correspondence:**
Bo Feng
fengb@gdou.edu.cn
Hui Zhang
zhanghui@qdio.ac.cn

†Lead author

Specialty section:
This article was submitted to
Marine Fisheries, Aquaculture
and Living Resources,
a section of the journal
Frontiers in Marine Science

Received: 31 October 2021
Accepted: 08 December 2021
Published: 28 January 2022

Citation:
Hou G, Chen Y, Wang J, Pan C,
Lin J, Feng B and Zhang H (2022)
Molecular Identification of Species
Diversity Using Pelagic Fish Eggs
in Spring and Late Autumn-Winter
in the Eastern Beibu Gulf, China.
Front. Mar. Sci. 8:806208.
doi: 10.3389/fmars.2021.806208

The Beibu Gulf is considered as one of China's four major fishing grounds, although the substantial overexploitation of fisheries has led to the collapse of many fish stocks, and to changes to spawning grounds in recent decades. Classifying fish eggs is an important way to monitor the recruitment process and identify the spawning sites of fish. However, the lack of a basis for morphological identification and difficulties in correctly identifying fish eggs based on morphological characteristics has limited scientific studies. In the present study, we identified fish eggs using molecular detection of cytochrome c oxidase subunit I and cytochrome b fragments. Ichthyoplankton surveys were conducted in the spring and late autumn–winter of 2020 in the eastern Beibu Gulf. Among the DNA extracted from the 873 chosen fish eggs, we successfully obtained 541 high-quality cytochrome c oxidase subunit I sequences and 41 high-quality cytochrome b sequences. We successfully identified 212 fish eggs (36.4%) from 32 species; 291 eggs (50.0%) showed ambiguous species delimitation, and 79 eggs (13.6%) could not be identified. Among the identified species, we found 25 species in spring and 25 species in late autumn–winter, out of which 18 species occurred in both seasons. We also obtained high resolution photographs of fish eggs at the species level for further morphological analysis and identification. The present study confirms the efficacy of using molecular methods to identify fish species from eggs and provides valuable information for protecting the spawning ground of economically valuable fish and for managing fishery resources.

Keywords: fish eggs, molecular species identification, spawning site, fish conservation, Beibu Gulf

INTRODUCTION

Eggs represent the earliest phase in the life cycle of fish. Because eggs cannot move unaided, they can provide valuable information about the reproductive biology, preferred spawning times, spawning sites, and recruitment success rates within fish populations (Baumgartner et al., 2004; Cao et al., 2007; Hou et al., 2021a; Takeuchi et al., 2021). Information on the composition and spatial and temporal distribution of fish eggs is vital for determining closed fishing zones, fishing moratoriums, fishery resource management strategies, marine protection areas, and even environmental evaluation of sea/fresh water-related construction and engineering (Rakocinski et al., 1996; Cao et al., 2007; Oliveira and Ferreira, 2008; Ahern et al., 2018). Although the importance of the fish egg pool has been long recognized, species-level information on the occurrence of fish eggs and their distributional patterns is lacking because of the difficulties in identifying fish egg stages (Baumgartner et al., 2004; Bui et al., 2011; Burrows et al., 2018; Hou et al., 2021a).

The paucity of species-level information on fish eggs occurs mainly because of the complex dynamic changes in the ontogeny of fish eggs (Zhang et al., 1985; Cao et al., 2007; Ikeda et al., 2014). There are nearly 30 stages of embryonic development, from fertilized eggs to newly hatched larvae (Zhang et al., 2006; Cao et al., 2007). In the early egg stages before early gastrula, there are strong morphological similarities among different species, while after the muscle burl stages potential morphological classification characteristics may be detected at the taxa level (Cao et al., 2007; Ikeda et al., 2014; Wan and Zhang, 2016). It is not easy to collect all the morphological ontogenetic stages of fish eggs and larvae within a limited time period through field surveys, especially for oceanic fish which are difficult to hatch and rear to juvenile/adult stages to confirm the species (Zhang et al., 1985; Ikeda et al., 2014; Wan and Zhang, 2016). Thus, the marked ontogenetic changes that occur within and among the fish species and the lack of morphological data make it difficult to precisely identify fish eggs at the species level.

In the last decade, molecular identification methods have been widely applied to identify fish eggs, including use of mitochondrial DNA fragments such as cytochrome c oxidase subunit I (COI) (Valdez-Moreno et al., 2010; Lewis et al., 2016; Leyva-Cruz et al., 2016; Ahern et al., 2018; Kerr et al., 2020; Chen et al., 2021), cytochrome b (*cytb*) (Liu et al., 2018), mtDNA PCR restriction fragment length polymorphism (RFLP) (Karaiskou et al., 2007; Stéphanie et al., 2010; Bui et al., 2011; Fitzcharles, 2012; Lelievre et al., 2012), and mtDNA control region (D-loop) (Shao et al., 2002). The DNA barcode method (COI) has been widely applied to define fish species, and facilitate the identification of fish eggs and larvae. For instance, Leyva-Cruz et al. (2016) identified fish eggs from 42 taxa collected from the waters surrounding Banco Chinchorro in the Mexican Caribbean. Burrows et al. (2018) applied a DNA barcode to identify fish eggs in the Gulf of Mexico, and allocated 709 eggs to 62 species. Kerr et al. (2020) successfully identified 564 fish eggs in 89 taxa collected from northwestern Cuba and across the Florida Straits using DNA barcodes. These studies demonstrate that molecular techniques can be used effectively to identify fish eggs, and they illustrate the potential for searching for spawning sites and relevant studies.

The Beibu Gulf (17–21.75°N, 105.67–110.17° E), situated in the northwestern South China Sea (SCS), covers an area of 12.88×10^3 km^2 with an average depth of 38 m. It has a number of habitats, including mangrove forests, coral reefs, and numerous estuaries (such as the Red River and Nanliu River). This heterogeneity provides suitable habitats for a high diversity of marine organisms. More than 600 fish species have been reported in the Beibu Gulf, with 60 commercially important fish taxa supporting a substantial fishery (Sun et al., 2010; Wang et al., 2011; Sun and Chen, 2013). The Beibu Gulf is one of China's four major fishing grounds, playing an important role in food security, the economy, and employment (Qiu et al., 2008). However, the marine system in the Beibu Gulf has been heavily disturbed and degraded, especially in the last few decades, owing to global climate change and various human activities, including overexploitation, illegal fishing, coastal mangrove damage, and habitat loss. Consequently, the fish diversity in the Beibu Gulf has been threatened, the fish trophic levels and assemblages have changed significantly, and fishery resources and catch rates have declined substantially (Sun and Lin, 2004; Qiu et al., 2008; Wang et al., 2010; Zhang et al., 2020).

Ranked as one of the most important fishery grounds in China and SCS, the Beibu Gulf is also an important spawning and nursing ground for numerous fish species. Studies on fish eggs and larvae can be traced to 1959–1962 and 1997–1999, although they did not analyze the fish egg and larvae separately (Jia et al., 2004; Zhou et al., 2008, 2011). Jia et al. (2004) and Zhou et al. (2008) described the fish eggs and larvae abundance and/or composition in partial season. Zhou et al. (2011) morphologically identified 153 taxa of fish eggs and larvae in the eastern Beibu Gulf, although only 11 taxa were identified at the species level from fish eggs. Hou et al. (2021b) used molecular identification of 53 species of fish larvae fixed in formalin from the Beibu Gulf. However, owing to the difficulties of identifying fish egg stages, information on most spawning sites of fish in the Beibu Gulf on the basis of ichthyoplankton surveys is still limited.

Given the present conditions of fishery resources in the Beibu Gulf, there is an urgent need to document the current spawning grounds of fish species, from a perspective of both fishery management and fish biodiversity protection perspectives. We undertook ichthyoplankton surveys in the spring and late autumn–winter of 2020 in the eastern Beibu Gulf. In the present study, our aims were to: (i) identify the pelagic eggs collected in these surveys using molecular techniques; (ii) determine the diversity of fish eggs during the study period; and (iii) evaluate the effectiveness of the molecular method in identifying fish eggs in the Beibu Gulf. Our findings will contribute to improved management and conservation of fish species and their spawning grounds in the Beibu Gulf.

MATERIALS AND METHODS

Study Area and Sample Collection

Two surveys were conducted in the area of the eastern Beibu Gulf (17.75–21.25°N, 107.25–109.75°E) in the spring (April) and late autumn–winter (November–December) of 2020 (**Figure 1**). Ichthyoplankton samples were collected by zooplankton nets (0.8 m diameter, 2.7 m long, 505 μm mesh, with a cod-end container mesh of 400 μm). Four zooplankton net deployments were made at each survey station: two simultaneous horizontal tows at fixed depth (10 min at 1.5–2.2 knots), and two vertical hauls ($\sim$ sea bed to the surface, hauled at 1.5 m/s).

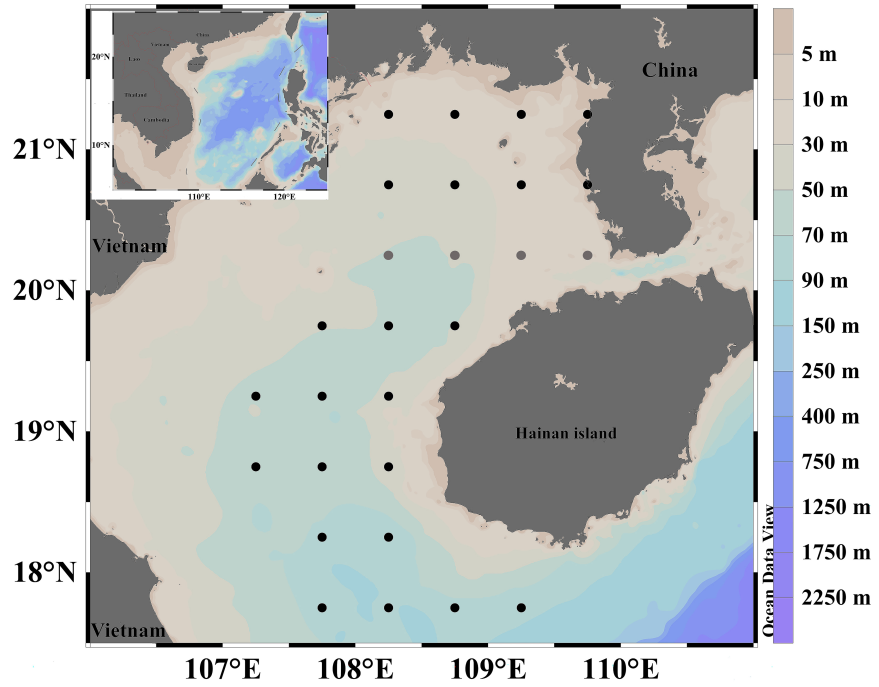

FIGURE 1 | Sampling stations of fish eggs in the eastern Beibu Gulf. The black dots indicate the stations where the spring and late autumn-winter survey was conducted, the gray dots indicate the stations where only the spring survey was conducted.

Specimens from one horizontal and one vertical tow were quickly preserved in 75% ethanol–sea water solution, and then stored in cold storage (<0°C). The other specimens were preserved in 4% formalin solution. The horizontal and vertical nets were fitted with General Oceanic flowmeters for estimating filtered water volume.

Photography and Molecular Experiment

In the laboratory, all fish eggs from each station were examined using a stereomicroscope. Because we could not amplify and sequence all the collected eggs, we randomly selected partial samples for molecular identification. Up to 30 eggs were randomly selected at a survey station, if there were more than 30 eggs, and photographed. If there were <30, all the eggs were selected, and 15 eggs were selected each time; this was done twice in each station to give a total of 30 eggs. We also selected eggs with different morphological features to identify more fish species or taxa.

Each egg was first numbered, rehydrated in hydrogen peroxide for 5–8 min for cleaning, and then photographed using a Zeiss microscope (Axioplan 2 imaging E; **Figure 2**). The primer treating processes and DNA extraction followed Hou et al. (2020). Total genomic DNA was extracted using an Axygen DNA Extraction Kit (Axygen, Shanghai, China). A partial fragment of the 5'-end of COI sequences (∼648 bp) was firstly amplified, using the universal primers FishF1 and FishR1 (Ward et al., 2005). If COI sequences were not obtained, then fragments of *cytb* were amplified, using the primers L14724 and H15915 (Xiao et al., 2001). The polymerase chain reaction (PCR) conditions of COI were as follows: 94°C for 3 min, 35 cycles at 94°C for 30 s, 51°C for 30 s, 72°C for 1 min, and a final extension at 72°C for 10 min (Hou et al., 2020). The PCR conditions of *cytb* were as follows: 96°C for 5 min; 35 cycles at 96°C for 30 s, 58°C for 30 s, 72°C for 1.5 min; and a final extension at 72°C for 5 min. The amplification products of PCR reactions were purified using 1% low-melting agarose by electrophoresis, and sequenced bidirectionally on an ABI 3730 XL DNA system, following the manufacturer's protocols.

Data Analyses

The tracer files were initially checked and sequences assembled using SEQMAN in Lasergene v 7.0 (DNASTAR Inc., Madison, WI, United States). High-quality sequences were aligned and manually edited using MEGA v6.0 (Tamura et al., 2013). Fish egg identification was performed in the Barcode of Life Data System (BOLD, V4). We retained reference sequences of both the best and second-best interspecific matches in BOLD and documented the percentages of sequence matches. Three criteria similar to those used in Hubert et al. (2015) were adopted in our study: (i) sequences of the COI fragment with >98% similarity to the best sequence match and <98% similarity to the nearest neighbor species, exhibiting >2% genetic divergence between sequences and the nearest neighbor species were unambiguously tagged with that species name. If the top 99 matches were blasted to single species within the above threshold, the sequences were delimited to the matches species (Case I). (ii) If the genetic divergence was more than 98% similarity, or less than the 2% threshold to the best matched species and nearest neighbor

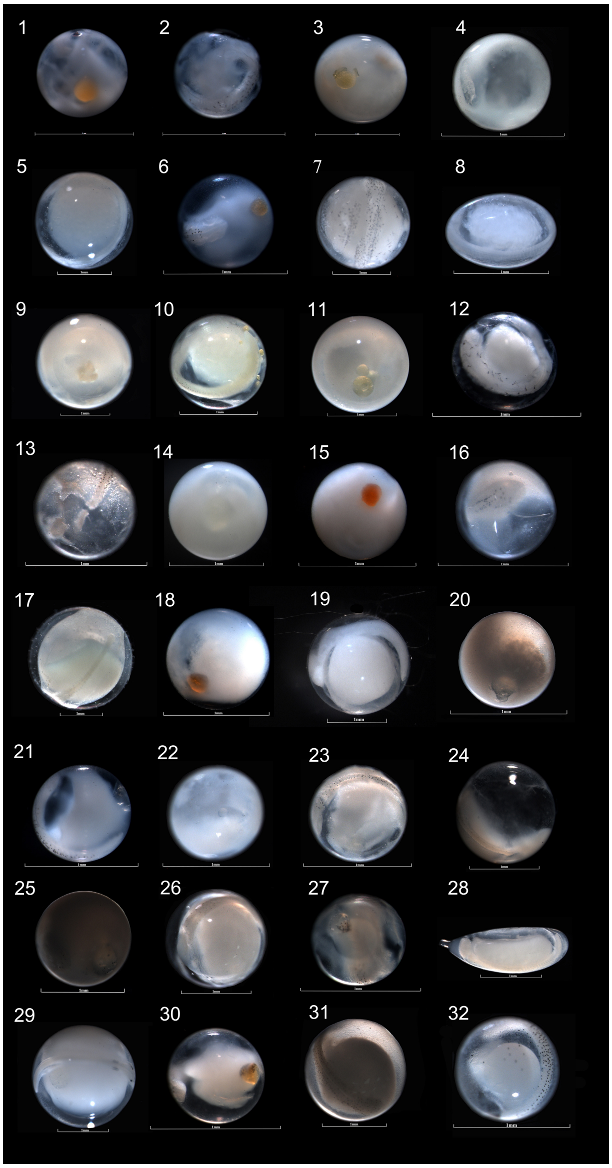

FIGURE 2 | Photographs of the egg specimens that were identified to species level by COI and *cytb* sequences in the eastern Beibu Gulf. (1) *Acropoma japonicum*, GDYH16088, 0.923 mm; (2) *Atropus Atropos*, GDYH16147, 0.719 mm; (3) *Branchiostegus albus*, GDYH15795, 1.106 mm; (4) *Carangoides malabaricus*, GDYH13119, 0.790 mm; (5) *Chirocentrus dorab*, GDYH13103, 1.784 mm; (6) *Chrysochir aureus*, GDYH16116, 0.766 mm; (7) *Coryphaena hippurus*, GDYH13118, 1.641 mm; (8) *Encrasicholi heteroloba*, GDYH12984, 1.178 × 0.792 mm; (9) *Fistularia petimba*, GDYH14150, 1.912 mm; (10) *Hilsa kelee*, GDYH13042, 1.234 mm; (11) *Ilisha melastoma*, GDYH13028, 1.401 mm; (12) *Leiognathus ruconius*, GDYH15838, 0.707 mm; (13) *Megalaspis cordyla*, GDH12789, 1.085 mm; (14) *Mene maculate*, GDYH13073, 1.085 mm; (15) *Moolgarda perusii*, GDYH16099, 0.833 mm; (16) *Nemipterus marginatus*, GDYH12936, 0.731 mm; (17) *Oxyporhamphus micropterus*, GDYH13048, 2.407 mm; (18) *Parapercis lutevittata*, GDYH15760, 0.976 mm; (19) *Parexocoetus mento*, GDYH13132, 1.719 mm; (20) *Penhia anea*, GDYH12757, 0.833 mm; (21) *Penhia microcephalus*, GDYH16123, 0.867 mm; (22) *Penhia pawak*, GDYH12932, 0.859 mm; (23) *Pomadasys maculatus*, GDYH12791, 0.897 mm; (24) *Saurida elongate*, GDYH15780, 1.430 mm; (25) *Scomberomorus commerson*, GDYH12756, *(Continued)*

FIGURE 2 | 1.193 mm; (26) *Seriolina nigrofasciata*, GDYH12880, 1.393 mm; (27) *Sillago sihama*, GDYH15562, 0.782 mm; (28) *Stolephorus waitei*, GDYH12913, 1.950 × 0.736 mm; (29) *Tentoriceps cristatus*, GDYH13107, 2.006 mm; (30) *Terapon jarbua*, GDYH15866, 0.726 mm; (31) *Trachicephalus uranoscopus*, GDYH12765, 1.583 mm; and (32) *Scomberoides tol*, GDYH13111, 0.899 mm. Among them, egg specimens of serial number 1–31 were identified by COI sequences, and 32 was identified by *cytb* sequence.

species, the two matched species were in the same genus, and the sequences were delimited to genus level; if not in the same genus, and the sequences were identified as species uncertain (Case II). (iii) Sequences with matches <98% were deemed unidentified (Case III).

The sequences of the *cytb* fragment were blasted in the GenBank nucleotide database using the Basic Local Alignment Search Tool (BLAST).[1] Sequences with >99% similarity were tagged with that species name. Genetic distance was calculated in MEGA6 based on the Kimura 2-parameter model (K2P, Kimura, 1980). A neighbor-joining (NJ) tree based on the K2P model was reconstructed to illustrate lineage diversity *via* the phylogenetic topology. The NJ tree was constructed with 1,000 bootstrap replicates using MEGA v6.0.

To accumulate description morphological characteristics of fish eggs in the waters of the eastern Beibu Gulf, the egg diameter and oil diameter were measured (to the nearest 0.001 mm). To assess whether the sampling effort was sufficient to describe the species richness of fish eggs, species accumulation curves were created for each survey using the "random" method as an accumulator function to determine the means and standard deviations of species accumulation curves from random subsampling of the data without replacement (Gotelli and Colwell, 2001). The species accumulation curves were fitted in the "vegan" package implemented in R version 4.0.5 (Oksanen et al., 2020).

RESULTS

Sequence Information

In all, 13,984 individual alcohol-preserved fish eggs were collected in spring, including 11,239 individual eggs in horizontal trawls, and 2,745 individuals in vertical trawls. A further 527 alcohol-preserved fish eggs were collected and preserved in late autumn–winter, including 392 individuals eggs in horizontal trawls, and 135 in vertical trawls. The mean total abundance in spring was 191.49 ind./100 m^3 in horizontal tows and 1067.55 ind./100 m^3 in vertical hauls. The mean total abundance in late autumn-winter was 8.75 ind./100 m^3 in horizontal tows and 3.08 ind./100 m^3 in vertical hauls (**Supplementary Figure 1**). A total of 873 fish eggs were chosen for DNA extraction and molecular identification. The COI fragment in the fish eggs was first sequenced. If it failed to be amplified after three attempts, the *cytb* fragment was then sequenced. Owing to the delays and difficulties in the laboratory experiments because of the coronavirus disease outbreak, 291 eggs (33.33%) failed to

---

[1] https://blast.ncbi.nlm.nih.gov/Blast.cgi

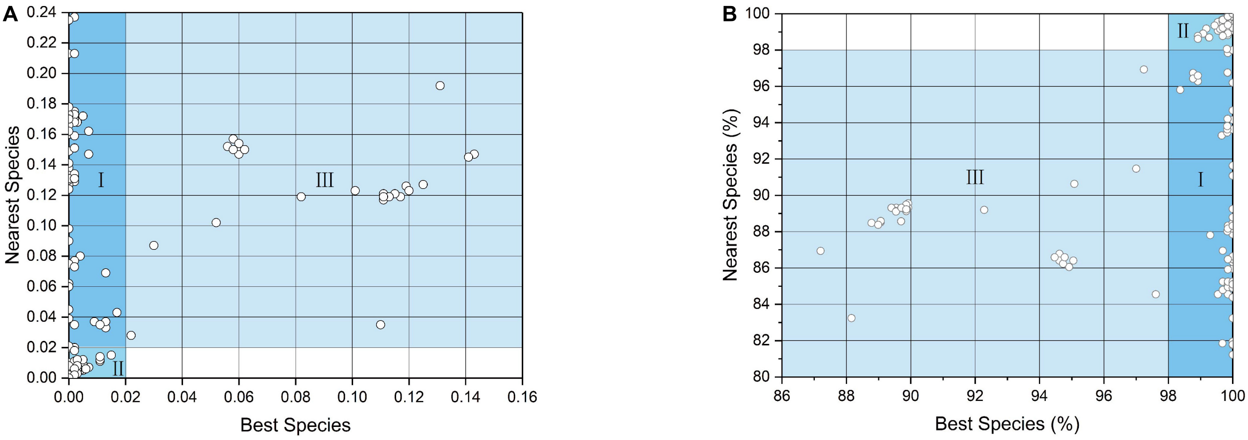

FIGURE 3 | The best match compared with the nearest neighbor for each specimen. **(A)** Genetic distance, **(B)** similarity percentage. Case I, delimited to species level; Case II, delimited to genus or uncertain; Case III, unidentified.

yield high-quality sequences. In summary, we finally obtained high-quality COI sequences from 541 fish eggs and 41 *cytb* sequences (66.67%).

Molecular Identification of Fish Eggs

Using the 2% genetic divergence and 98% similarity thresholds to represent species boundaries in the BOLD platform, approximately 89.5% of the COI sequences (484/541) had a match of 88–100%. Among the 484 COI sequences, 193 sequences (~35.7%) were successfully categorized as Case I, and were assigned to 31 species. A total of 291 (~53.8%) sequences were categorized as Case II, and 57 sequences (~10.5%) were categorized as Case III (**Figure 3** and **Supplementary Table 1**). Using an identification threshold of more than 99%, 19 *cytb* sequences were successfully assigned to five species, i.e., *Ilisha melastoma* (Bloch and Schneider, 1801), *Terapon jarbua* (Forsskål, 1775), *Fistularia petimba* (Lacepède, 1803), *Scomberomorus commerson* (Lacepède, 1800), and *Scomberoides tol* (Cuvier, 1832), and 22 sequences could not be identified at the species level (**Supplementary Table 2**). In total, 212 fish eggs (36.4%) were successfully identified to 32 species (**Table 1**), 291 eggs (50.0%) had ambiguous species delimitation, and 79 eggs (13.6%) could not be identified using the BOLD and NCBI platforms.

The 32 species that were identified belonged to 24 families. The most abundant families were Carangidae (5 species, 14 individuals), Sciaenidae (4 species, 15 individuals), and Engraulidae (2 species, 57 individuals). Among these, the eggs of 15 economically important species were identified, i.e., *Sillago sihama* (Forsskål, 1775), *Pomadasys maculatus* (Bloch, 1793), *Megalaspis cordyla* (Linnaeus, 1758), *Chirocentrus dorab* (Forsskål, 1775), *Chrysochir aureus* (Richardson, 1846), *Pennahia pawak* (Richardson, 1846), *Pennahia macrocephalus* (Tang, 1937), *Pennahia anea* (Bloch, 1793), *Branchiostegus albus* (Dooley, 1978), *Mene maculate* (Bloch and Schneider, 1801), *T. jarbua*, *Saurida elongata* (Temminck and Schlegel, 1846), *Coryphaena hippurus* (Linnaeus, 1758), *S. commerson*, and *F. petimba*.

The NJ tree of COI sequences suggested that the identified species of fish eggs based on the BOLD and GenBank databases generated 80 independent lineages (**Figure 4**). The NJ tree of *cytb* sequences generated nine independent lineages (**Supplementary Figure 2**), suggesting that at least 81 distinct species/taxa were collected and occurred in the study period. In spring, the fish eggs of 25 fish taxa were successfully identified at the species level, and the same number were identified in late autumn–winter. Among them, the eggs of 18 fish species occurred in both the spring and late autumn–winter surveys, and seven species occurred only in spring or in late autumn-winter (**Table 1**). Using the habitat data for adult fish species cited in Fishbase,[2] 11, 8, 7, 4, 1, and 1 species were reef-associated, demersal, pelagic-neritic, benthopelagic, bathypelagic, and pelagic-oceanic, respectively, indicating that the spawning activities of multiple ecological groups of fish occurred in the semi-closed gulf. The species accumulation curves of fish eggs were non-asymptotic, indicating that substantially more taxa would have been encountered with increased sampling effort in both seasons (**Figure 5**).

Morphological Characteristics of Fish Eggs

The egg diameters of 582 fish eggs identified by COI and *cytb* sequences were measured. Most of the eggs were <2.500 mm in diameter, with 29.55% belonging to the 0.630–1.000 mm size class and 60.48% belonging to the 1.010–2.000 mm size class. Altogether, 97.42% of the eggs were <2.500 mm, while the remaining 2.58% belonged to 2.510–3.190 mm and 4.350–4.920 mm classes (**Figure 6**). For the 32 identified species, the shapes of eggs were spherical for 30 species, 1 species was elliptical (**Figure 2**, **8**th), and 1 species was elliptical with a knob (**Figure 2**, **28**th). The egg diameters ranged from 0.660 to 2.694 mm. The smallest eggs at the species level were those of *Leiognathus ruconius* (Hamilton, 1822), and the largest were those of *Oxyporhamphus micropterus* (Valenciennes, 1847), while the smallest eggs at the family level were those of Leiognathidae,

---

[2] https://www.fishbase.com

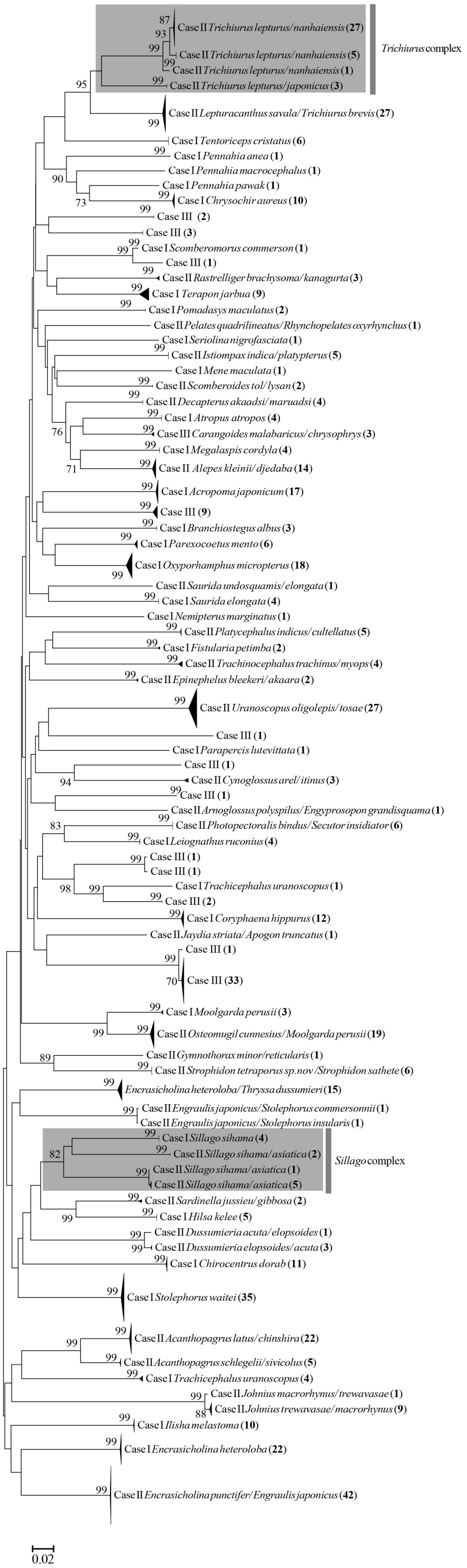

FIGURE 4 | The neighbor-joining tree of COI sequences of fish eggs. The bootstrap values are given at nodes.

and the largest were those of Hemiramphidae (**Figure 7**). The average egg diameters of 16 fish species were <1.000 mm (i.e., 50%), while 10 of 24 families were <1.000 mm (38.5%; **Figure 7**). This indicated that a large proportion of fish species in the eastern Beibu Gulf produced small eggs. Most of the eggs had a transparent and smooth chorion. However, a chorion surface structure was observed in two species. The eggs of *O. micropterus* had numerous short spines (ca. 0.030–0.050 mm) uniformly scattered (**Figure 2**, **17**th), while the eggs of *Parexocoetus mento* (Valenciennes, 1847) had many long filaments all over the surface (ca. 0.410–1.540 mm; **Figure 2**, **19**th).

DISCUSSION

Sequencing Success Rate of Fish Eggs

Preserving fish eggs in formaldehyde allows the visual characteristics of development for morphological classification to be retained, but this method can cause fragmentation and denaturation of DNA (Akimoto et al., 2002; Srinivasan et al., 2002; Karaiskou et al., 2007). Ethanol-preserved eggs may shrink, obscuring the developmental stages, lose pigmentation, and turn opaque (Espeland and Sannæs, 2018). Because there is little morphology literature on fish eggs in the Beibu Gulf, we preferred to preserve the eggs in ethanol with the primary aim of identifying them. In the present study, the sequencing success rate of fish eggs was low (66.78%). The high failure rate was most likely due to poor preservation at sea, the long time needed to pick out eggs preserved in low concentrations in ethanol, and the delayed DNA extraction process affected by the coronavirus epidemic in 2020. In previous studies, the sequencing success rate for fish eggs varied considerably, i.e., Ahern et al. (2018) selected 6,422 eggs out of which 2,354 were sequenced successfully (COI/16S fragments, 36.66%); Liu et al. (2018) selected 8,983 drifting eggs and obtained 7,933 *cytb* sequences (88.31%); and Chen et al. (2021) selected 641 eggs and obtained 397 high-quality sequences (61.93%). It is considered that a low ethanol concentration and long storage in ethanol (>6 months) both negatively affect DNA stability and lead to DNA degradation (Zimmermann et al., 2008; Michaud and Foran, 2011; Marquina et al., 2021). However, highly concentrated ethanol (95–100%) was found to induce albefaction, brittleness, dissolution of oil globules, and damage to the morphology (Marquina et al., 2021; Zheng et al., 2021). In this study, we preserved the specimens in 75% ethanol–sea water solution to balance a relatively good morphology preservation and sequencing success rate. This ethanol concentration can also reduce potential bacterial pollution in the specimens and reduce the amplification of DNA fragments of non-target species. However, timely DNA extraction should be conducted to increase the success rate in future studies.

Performance of Molecular Techniques for Identifying Fish Eggs

In the present study, we identified 81 distinct taxa using COI and *cytb* sequences, out of which 32 taxa (39.51%) were identified at the species level (**Figures 2**, **4**). However, nearly

TABLE 1 | The fish eggs identified in species level using molecular methods.

Family	Species	Common name	Number of specimens identified by COI/*Cytb*	Egg diameter/mm	Oil diameter/mm	Spring	Late autumn-winter	Gene used	Habitat
Acropomatidae	*Acropoma japonicum*	Glowbelly	5	0.923–0.950	0.244–0.251	+	+	COI	Bathypelagic
Carangidae	*Megalaspis cordyla*	Torpedo scad	4	0.760–1.085	0.23	+		COI	Reef–associated
Carangidae	*Atropus atropos*	Cleftbelly trevally	4	0.719–0.748	0.166–0.209	+	+	COI	Pelagic–neritic
Carangidae	*Seriolina nigrofasciata*	Blackbanded trevally	2	1.393–1.393		+		COI	Reef–associated
Carangidae	*Scomberoides tol*	Needlescaled queenfish	2	0.853–0.899	0.156	+		*Cytb*	Reef–associated
Carangidae	*Carangoides malabaricus*	Malabar trevally	2	0.790–0.869		+	+	COI	Reef–associated
Chirocentridae	*Chirocentrus dorab*	Dorab wolf–herring	11	1.656–2.039		+	+	COI	Reef–associated
Clupeidae	*Hilsa kelee*	Kelee shad	5	1.101–1.242	0.041–0.122*	+		COI	Pelagic–neritic
Coryphaenidae	*Coryphaena hippurus*	Common dolphinfish	12	1.446–1.641	0.260–0.463	+	+	COI	Pelagic–neritic
Engraulidae	*Encrasicholina heteroloba*	Shorthead anchovy	22	1.073–1.408 ×0.692–0.842		+	+	COI	Reef–associated
Engraulidae	*Stolephorus waitei*	Spotty–face anchovy	35	1.727–2.158 ×0.772–1.047	0.053–0.177	+	+	COI	Pelagic–neritic
Exocoetidae	*Parexocoetus mento*	African sailfin flyingfish	6	1.685–1.788		+	+	COI	pelagic–neritic
Fistulariidae	*Fistularia petimba*	Red cornetfish	2/3	1.759–1.976	0.513	+	+	COI/*Cytb*	Reef–associated
Haemulidae	*Pomadasys maculatus*	Saddle grunt	2	0.848–0.897		+	+	COI	Reef–associated
Hemiramphidae	*Oxyporhamphus micropterus*	Bigwing halfbeak	18	2.112–2.694		+	+	COI	Pelagic–oceanic
Latilidae	*Branchiostegus albus*	Null	3	1.059–1.106	0.221–0.257	+	+	COI	Benthopelagic
Leiognathidae	*Leiognathus ruconius*	Deep pugnose ponyfish	4	0.660–0.732		+	+	COI	Demersal
Menidae	*Mene maculata*	Moonfish	1	1.085			+	COI	Reef–associated
Mugilidae	*Moolgarda perusii*	Longfinned mullet	3	0.799–0.919	0.198–0.200	+		COI	Reef–associated
Nemipteridae	*Nemipterus marginatus*	Red filament threadfin bream	1	0.731			+	COI	Demersal
Pinguipedidae	*Parapercis lutevittata*	Yellow–striped sandperch	1	0.976	0.223		+	COI	Demersal
Pristigasteridae	*Ilisha melastoma*	Indian ilisha	10/1	1.125–1.443	0.227–0.348	+	+	COI/*Cytb*	Pelagic–neritic
Sciaenidae	*Chrysochir aureus*	Reeve's croaker	10	0.766–0.846	0.129–0.214	+		COI	benthopelagic
Sciaenidae	*Pennahia anea*	Donkey croaker	1	0.833	0.229		+	COI	Demersal
Sciaenidae	*Pennahia macrocephalus*	Big–head pennah croaker	3	0.848–0.897	0.206	+		COI	Demersal
Sciaenidae	*Pennahia pawak*	Pawak croaker	1	0.859	0.099		+	COI	Benthopelagic
Scombridae	*Scomberomorus commerson*	Narrow–barred Spanish mackerel	1/12	1.116–1.257	0.238–0.450		+	COI/*Cytb*	Pelagic–neritic
Sillaginidae	*Sillago sihama*	Silver sillago	4	0.709–0.802	0.138–0.164	+	+	COI	Reef–associated
Synanceiidae	*Trachicephalus uranoscopus*	Stargazing stonefish	4	1.499–1.590			+	COI	Demersal
Synodontidae	*Saurida elongata*	Slender lizardfish	4	1.427–1.511		+	+	COI	Demersal
Terapontidae	*Terapon jarbua*	Jarbua terapon	9/1	0.683–0.775	0.143–0.264	+	+	COI/*Cytb*	Demersal
Trichiuridae	*Tentoriceps cristatus*	Crested hairtail	6	1.764–2.006		+	+	COI	Benthopelagic

*Information of egg diameter, oil diameter, the occurrence season and habitat of adult are also shown. * indicate numerous oil globules occur in each fish egg.*

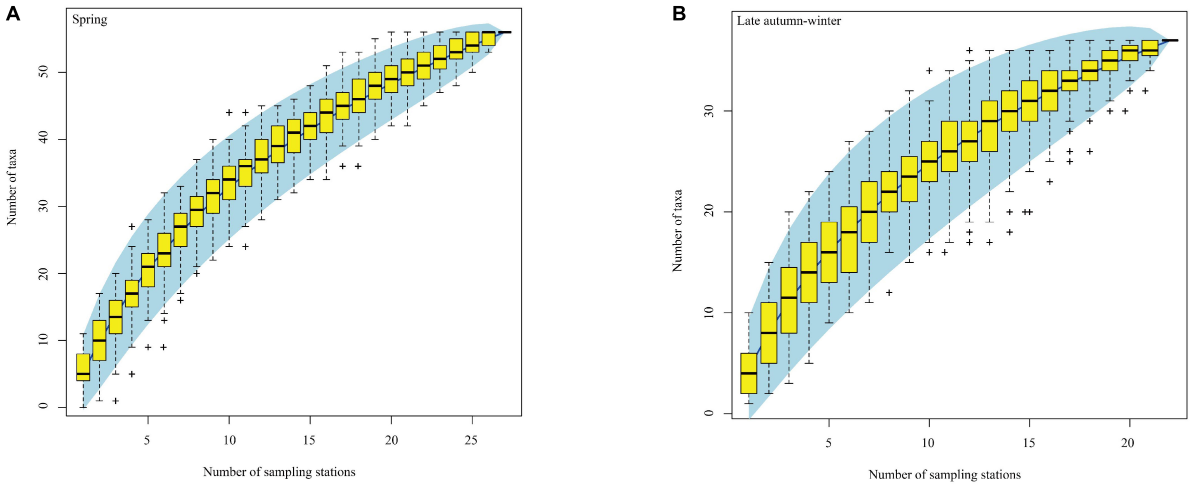

FIGURE 5 | Species accumulation curves of fish eggs taxa identified by molecular methods in the eastern Beibu Gulf. **(A)** Spring; **(B)** late autumn-winter. The light blue area indicates 95% confidence intervals. Yellow boxes are the interquartile ranges, the central bold mark on each box indicates the median, and the bottom and top edges of the box indicate the 25th and 75th percentiles, respectively. The whiskers extend to the most extreme data points not considered outliers, and the outliers are plotted individually using the "+"symbol.

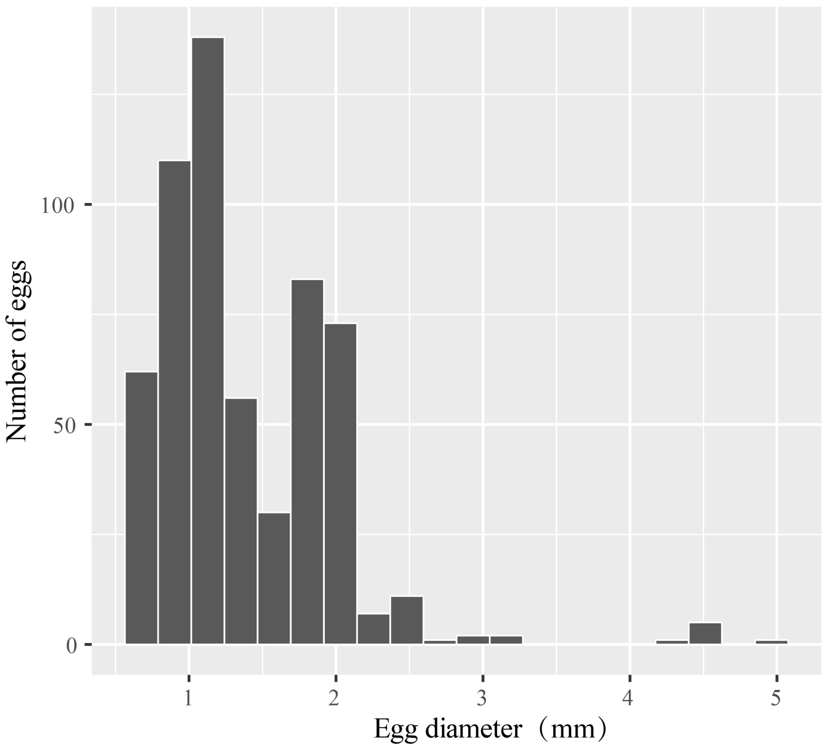

FIGURE 6 | The egg diameter distribution of identified fish eggs in the eastern Beibu Gulf.

36 taxa (44.44%) were ambiguous, and could only be identified at the genus or family level (**Figure 4** and **Supplementary Table 1**). The high ratio (53.89% of COI sequences) of ambiguous identification potentially limited the performance of species identification in the informatics platforms, BOLD and NCBI (Meiklejohn et al., 2019; Pentinsaari et al., 2020). For the two platforms, BOLD mines barcode sequences from GenBank periodically, and sequences in BOLD are submitted to GenBank when preparing for publication. The percentage of sequences on BOLD originating from GenBank are lower than the barcodes in GenBank, and include unverified sequences mined from GenBank. In addition, the taxonomic classifications or scientific

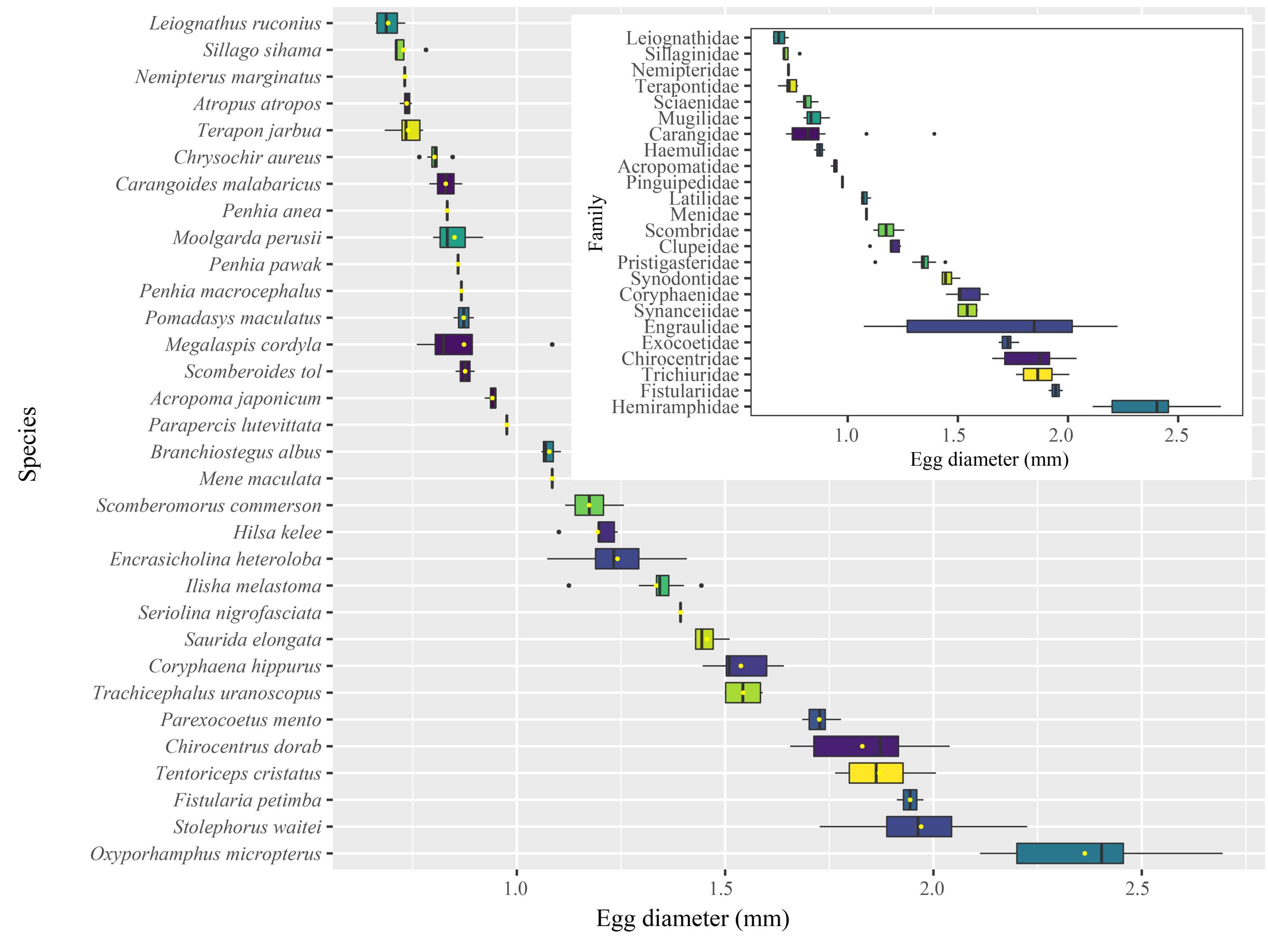

FIGURE 7 | The egg diameter of identified fish eggs at the species level.

name changes for fish specimens that are submitted in BOLD can be updated and amended freely before being submitted to NCBI. The database managers regularly undertake taxonomic checks in BOLD. Therefore, BOLD provided a more informative platform for the fish eggs in this study than GenBank, given the contemporary COI sequencing of candidate species in the present study. Despite using the delineation criteria for those sequences with GenBank accession numbers, the high ratio of Case II findings introduced caution about fish species identification.

As mitochondrial DNA is maternally inherited, DNA barcoding has limitations in identifying species associated with incomplete lineage sorting, introgression hybridization, or ancestral polymorphism. In addition, the method can be affected by misidentification in the reference libraries or in the query sequences in the platforms (Pentinsaari et al., 2020). The misidentifications that occur during the process of developing the DNA barcode library of fish are normal because of morphological characteristics, i.e., phenotypic plasticity, new species, cryptic diversity, genotypic variation, or different life stages. In the present study, ambiguous delineation mainly appeared in the taxa or genera *Alepes*, *Acanthopagrus*, *Johnius*, *Istiompax*, *Scomberoides*, *Rastrelliger*, *Decapterus*, *Carangoides*, *Saurida*, *Platycephalus*, *Epinephelus*, *Uranoscopus*, *Cynoglossus*, *Sillago*, and *Sardinella*, and families Apogonidae, Bothidae, Clupeidae, Theraponidae, Trichiuridae, Mugilidae, and Engraulidae, among which misidentifications, cryptic diversity, and new species were common (Mat Jaafar et al., 2012; Qin et al., 2013; Gon et al., 2015; Tucker et al., 2016; Fricke, 2018; Hata and Motomura, 2018; Chao et al., 2019; Frable et al., 2019; Huang et al., 2020; Prokofiev, 2021; Xiao et al., 2021). Developing a reliable DNA barcode library for these taxa, with correct species identifications *via* morphology, or using multiple DNA fragments is recommended in future studies (Chakraborty et al., 2006; Hsu et al., 2009).

Species Composition, Spawning Periods, and Occurrence in Spring and Late Autumn–Winter

On the basis of the COI and *cytb* sequences obtained, we successfully identified 32 species in 81 taxa, belonging to 30 genera and 24 families (**Table 1**). Five and four identified fish species from their eggs (29 sequences, 13.48%) were Carangidae and Sciaenidae, respectively, indicating that these two families were the dominant fish groups in the eastern

Beibu Gulf. The other 23 species belonged to 22 families (29 sequences, 86.52%), suggesting a high species diversity distribution pattern in the study area. In previous studies, the dominant species were *Acropoma japonicum* (Günther, 1859), *Photopectoralis bindus* (Valenciennes, 1835) (also known as *Leiognathus bindus*), *Trachurus japonicus* (Temminck and Schlegel, 1844), *Evynnis cardinalis* (Lacepède, 1802) (also known as *Parargyrops edita*), and *P. macrocephalus* (also known as *Argyrosomus microcephalus*) based on the quarterly otter trawl surveys (Wang et al., 2011), and *A. japonicum*, *E. cardinalis*, *T. japonicus*, *Decatperus maruadsi*, and *L. ruconius* using acoustic measurement with ordinary kriging in the Beibu Gulf (Wang et al., 2012; Sun et al., 2019). In the present study, the eggs of the dominant fish species (*A. japonicum*, *L. ruconius*, and *P. microcephalus*) were also detected using the DNA barcode method (**Table 1**, **Figure 4**, and **Supplementary Table 1**). For *D. maruadsi and P. bindus*, 4 and 6 COI sequences of *Decatperus* sp. and Leiognathidae sp. were categorized as Case II (i.e., *D. akaadsi/maruadsi* and *P. bindus/Secutor insidiator*, respectively) following the criteria. These eggs may need to be analyzed further in combination with the local DNA barcode library (Hou et al., 2018, 2020). For *E. cardinalis*, although the fish's spawning period occurred in the winter season, we did not collect eggs from this species in either of the two surveys, indicated that more surveys should be conducted. In addition, given that we only used zooplankton nets to collect drifting and suspended eggs in surveys, we chose a partial set of specimens for molecular identification, and we had a high failure rate of amplification, it is likely that the species diversity of the egg pool in the eastern Beibu Gulf was underestimated, and a random sampling error may have occurred. Accordingly, the composition of the fish community was biased, and did not include the entire fish community known from the waters. In addition, a strong La Niña phenomenon in 2020 affected fish reproduction in the autumn and winter seasons, which correspondingly reduced the eggs of potential fish species that were collected. However, we did find several unexpected and important taxa, i.e., the first identification of *Stolephorus waitei* (Jordan and Seale, 1926) eggs with morphological characteristics of an elliptical shape, with a knob on the egg membrane (Gao et al., 2016); the potentially new species *Strophidon tetraporus* sp. nov (Case II, **Supplementary Table 1**; Huang et al., 2020); and the economically important species *B. albus*, *C. aureus*, *M. cordyla*, *M. maculate*, and *S. sihama*, and genus *Pennahia*. The spawning ground of these species are not well-known in the Beibu Gulf.

Among the 32 species identified, 25 species were found in spring and 25 species in late autumn–winter, out of which 18 species (56.25%) were found in both surveys. This finding indicated that these species spawned both in spring and late autumn–winter, which are the main spawning seasons in the Beibu Gulf. The Beibu Gulf is located in a subtropical/tropical sea area, with a sea surface temperature ranging between 18 and 32°C through the year (Huang et al., 2008; Gao et al., 2017; Shen et al., 2018). The typical hatching time of pelagic fish eggs in this sea area is between 18 and 70 h (Zhang et al., 1985). Although these planktonic fish eggs can disperse some distance on the ocean current, the main current in the Beibu Gulf is circular, because of the dynamics of coastal water, mixing with oceanic water, and a cold upwelling water mass (Su, 2005; Gao et al., 2017). Thus the complicated hydrological conditions do not transport the fish eggs a long distance prior to hatching. In addition, with a background trend of ocean warming, the hatching time of fertilized fish eggs is becoming shorter (Pauly and Pullin, 1988). Therefore, most eggs collected in the current study probably participated in local spawning events, and the sampling sites can be determined as the spawning grounds of these species.

The average egg diameters of 50% of the fish species (38.5% families) were <1 mm (**Figure 7**). Small eggs hatch into small fish larvae, which tend to have a high mortality rate in conditions of marine environmental change (Ware, 1975; Fuiman, 2003). This indicates that the population recruitment and assemblage structure in this marine area may fluctuate substantially, which corresponds to the current fishery status in the Beibu Gulf (Sun and Lin, 2004; Wang et al., 2010). In the present study, the smallest eggs were from *L. ruconius*, which have become the dominant species following the decline of large economically valuable fish species. The increase in fish eggs from this family cannot be regarded as a manifestation of improved fish resources (Jia et al., 2004).

CONCLUSION

Although our surveys and collection period were limited, we were able to use molecular identification to discern 32 species in 81 taxa, belonging to 24 families in the present study, which facilitates the delimitation of fish eggs based on morphological features. The number of taxa identified corresponded to nearly 27% of teleost fish referred to in the recent fish assemblage status study by Wang et al. (2010, 2011)) in the Beibu Gulf. The use of informatics platforms for species identification generated many ambiguous and unidentified taxa. To overcome this limitation, substantial efforts shall be made to improve the completeness of DNA barcode reference libraries for fish in the Beibu Gulf. However, we identified, for the first time, the spawning sites of economically important fish species proved by molecular methods. Our study provides new insights into the ichthyoplankton in the eastern Beibu Gulf, and will benefit the protection of spawning grounds and fishery management.

DATA AVAILABILITY STATEMENT

The original contributions presented in the study are included in the article/**Supplementary Material**, further inquiries can be directed to the corresponding author/s.

ETHICS STATEMENT

The animal study was reviewed and approved by the Guangdong Ocean University.

AUTHOR CONTRIBUTIONS

GH, JW, and HZ analyzed the data and completed the first draft. BF, CP, and JW performed the field survey. GH, YC, CP, and JW conducted the laboratory experiments. GH and HZ provided guidance on the data analysis and structure. All authors contributed to the article and approved the submitted version.

FUNDING

This study was supported by the National Key R&D Program of China (No. 2018YFD0900906), the National Natural Science Foundation of China (Nos. 31702347 and 42090044), the Youth Innovation Promotion Association CAS (No. 2020211), the Undergraduate Innovation and Entrepreneurship Training Program of Guangdong province (S202010566005), and the Start-up Project of Guangdong Ocean University (R19006).

ACKNOWLEDGMENTS

We would like to thank the editor and reviewers for their constructive comments on our manuscript. We thank numerous survey ship members for their help.

SUPPLEMENTARY MATERIAL

The Supplementary Material for this article can be found online at: https://www.frontiersin.org/articles/10.3389/fmars.2021.806208/full#supplementary-material

REFERENCES

Ahern, A. L. M., Gómez-Gutiérrez, J., Aburto-Oropeza, O., Saldierna-Martínez, R. J., Johnson, A. F., Harada, A. E., et al. (2018). DNA sequencing of fish eggs and larvae reveals high species diversity and seasonal changes in spawning activity in the southeastern Gulf of California. *Mar. Ecol. Prog. Ser.* 592, 159–179. doi: 10.3354/meps12446

Akimoto, S., Kinoshita, S., Sezaki, K., and Mitami, I. (2002). Identification of alfonsino and related fish species belonging to the genus *Beryx* with mitochondrial 16S rRNA gene and its application on their pelagic eggs. *Fish. Sci.* 68, 1242–1249. doi: 10.1046/j.1444-2906.2002.00561.x

Baumgartner, G., Nakatani, K., Gomes, L. C., Bialetzki, A., Sanches, P. V., and Makrakis, M. C. (2004). Identification of spawning sites and natural nurseries of fishes in the upper Paraná River, Brazil. *Environ. Biol. Fish.* 71, 115–125. doi: 10.1007/s10641-004-0098-z

Bui, A. O. V., Castonguay, M., Ouellet, P., and Sévigny, J. M. (2011). Searching for Atlantic cod (*Gadus morhua*) spawning sites in the northwest Gulf of St Lawrence (Canada) using molecular techniques. *ICES J. Mar. Sci.* 68, 911–918. doi: 10.1093/icesjms/fsr016

Burrows, M., Browing, J. S., Breitbart, M., and Murawski, S. A. (2018). DNA barcoding reveals clear delineation between spawning sites for neritic versus oceanic fishes in the Gulf of Mexico. *Fish. Oceanogr.* 28, 228–239. doi: 10.1111/fog.12404

Cao, W., Chang, J., Qiao, Y., and Duan, Z. (2007). *Fish Resources of Early Life History Stages in Yangtze River*. Beijing: China waterpower press.

Chakraborty, A., Aranishi, F., and Iwatsuki, Y. (2006). Genetic differentiation of *Trichiurus japonicus* and T. *lepturus* (Perciformes: trichiuridae) based on mitochondrial DNA analysis. *Zool. Stud.* 45, 419–427.

Chao, N. L., Chang, C. W., Chen, M. H., Guo, C. C., Lin, B. A., Liou, Y. Y., et al. (2019). *Johnius taiwanensis*, a new species of Sciaenidae from the Taiwan Strait, with a key to *Johnius* species from Chinese waters. *Zootaxa* 4651, 259–270. doi: 10.11646/zootaxa.4651.2.3

Chen, W. T., Zhu, S. L., Yang, J. P., Li, X. H., Li, Y. F., and Li, J. (2021). DNA barcoding reveals the temporal community composition of drifting fish eggs in the lower Hongshui River, China. *Ecol. Evol.* 11, 11507–11514. doi: 10.1002/ece3.7943

Espeland, S. H., and Sannæs, H. (2018). Estimating cod egg developmental stage based on DNA concentration. *ICES J. Mar. Sci.* 75, 825–830. doi: 10.1093/icesjms/fsx172

Fitzcharles, E. M. (2012). Rapid discrimination between four Antarctic fish species, genus *Macrourus*, using HRM analysis. *Fish. Res.* 12, 166–170. doi: 10.1016/j.fishres.2012.02.002

Frable, B. W., Tucker, S. J., and Walker, H. (2019). A new species of grouper, *Epinephelus craigi* (Perciformes: epinephelidae), from the South China Sea. *Ichthyol. Res.* 66, 215–224. doi: 10.1007/s10228-018-0669-9

Fricke, R. (2018). Two new species of stargazers of the genus *Uranoscopus* (Teleostei: uranoscopidae) from the western Pacific Ocean. *Zootaxa* 4476, 157–167. doi: 10.11646/zootaxa.4476.1.15

Fuiman, L. A. (2003). "Special considerrations of fish eggs and larvae," in *Fishery Science: The Unique Contributions of Early Life Stages*, eds L. A. Fuiman and R. G. Werner (Hoboken, NJ: Blackwell Science), 1–32.

Gao, D., Wan, R., Ma, Q., Zhang, X., and Bian, X. (2016). Development of eggs and larvae of *Stolephorus commersonnii* and taxonomic key to fish eggs of the Clupeidae and Engraulidae off China. *Mar. Biol. Res.* 12, 255–267. doi: 10.1080/17451000.2015.1125004

Gao, J., Wu, G., and Ya, H. (2017). Review of the circulation in the Beibu gulf, South China Sea. *Cont. Shelf Res.* 138, 106–119. doi: 10.1080/17451000.2015.1125004

Gon, O., Liao, Y. C., and Shao, K. T. (2015). A new species of the cardinalfish genus *Jaydia* (Teleostei: apogonidae) from the Philippines. *Zootaxa* 3980, 286–292. doi: 10.11646/zootaxa.3980.2.9

Gotelli, N. J., and Colwell, R. K. (2001). Quantifying biodiversity: procedures and pitfalls in the measurement and comparison of species richness. *Ecol. Lett.* 4, 379–391. doi: 10.1046/j.1461-0248.2001.00230.x

Hata, H., and Motomura, H. (2018). *Stolephorus continentalis*, a new anchovy from the northwestern South China Sea, and redescription of *Stolephorus chinensis* (Günther 1880)(Clupeiformes: engraulidae). *Ichthyol. Res.* 65, 374–382. doi: 10.1007/s10228-018-0621-z

Hou, G., Chen, W. T., Lu, H. S., Cheng, F., and Xie, S. G. (2018). Developing a DNA barcode library for perciform fishes in the South China Sea: species identification, accuracy and cryptic diversity. *Mol. Ecol. Resour.* 18, 137–146. doi: 10.1111/1755-0998.12718

Hou, G., Xu, Y., Chen, Z., Zhang, K., Huang, W., Wang, J., et al. (2021a). Identification of eggs and spawning zones of Hairtail fishes *Trichiurus* (Pisces: trichiuridae) in northern South China Sea, using DNA Barcoding. *Front. Env. Sci.* 9:703029. doi: 10.3389/fenvs.2021.703029

Hou, G., Chen, Y., Wang, S., Wang, J., and Zhang, H. (2021b). Formalin-fixed fish larvae could be effectively identified by DNA Barcodes: a case study on thousands of specimens in South China Sea. *Front. Mar. Sci.* 8:634575. doi: 10.3389/fmars.2021.634575

Hou, G., Wang, J., Chen, Z., Zhou, J., Huang, W., and Zhang, H. (2020). Molecular and morphological identification and seasonal distribution of eggs of four *Decapterus* fish species in the northern South China Sea: a key to conservation of spawning ground. *Front. Mar. Sci.* 7:970. doi: 10.3389/fmars.2020.590564

Hsu, K. C., Shih, N. T., Ni, I. H., and Shao, K. T. (2009). Speciation and population structure of three *Trichiurus* species based on mitochondrial DNA. *Zool. Stud.* 48, 851–865.

Huang, W. C., Mohapatra, A., Thu, P. T., Chen, H. M., and Liao, T. Y. (2020). A review of the genus *Strophidon* (Anguilliformes: muraenidae), with description of a new species. *J. Fish. Biol.* 97, 1462–1480. doi: 10.1111/jfb.14514

Huang, Y., Li, Y., Shan, H., and Li, Y. (2008). Seasonal variations of sea surface temperature, chlorophyll a and turbidity in Beibu Gulf, MODIS imagery study. *J. Xiamen Univ.* 47, 856–863.

Hubert, N., Espiau, B., Meyer, C., and Planes, S. (2015). Identifying the ichthyoplankton of a coral reef using DNA barcodes. *Mol. Ecol. Resour.* 15, 57–67. doi: 10.1111/1755-0998.12293

Ikeda, T., Hirai, A., Tabata, S., Onishi, Y., and Mito, S. (2014). "Key to fish eggs in Japan," in *An Atlas of the Early Stage Fishes In Japan*, 2nd Edn, ed. M. Okiyama (Kanagawa: Tokai University Press), 1–108.

Jia, X. P., Li, Y. Z., Li, C. H., Qiu, Y. S., and Gan, J. L. (2004). *Fishery Ecology Environment and Fishery Resources in the South China Sea Exclusive Economic Zone Adn Continental Shelf*. Beijing: Science Press.

Karaiskou, N., Triantafyllidis, A., Alvarez, P., Lopes, P., Garcia-Vazquez, E., and Triantaphyllidis, C. (2007). Horse mackerel egg identification using DNA methodology. *Mar. Ecol.* 28, 429–434. doi: 10.1111/j.1439-0485.2007.00190.x

Kerr, M., Browning, J., Bønnelycke, E. M., Zhang, Y., Hu, C., Armenteros, M., et al. (2020). DNA barcoding of fish eggs collected off northwestern Cuba and across the Florida Straits demonstrates egg transport by mesoscale eddies. *Fish. Oceanogr.* 29, 340–348. doi: 10.1111/fog.12475

Kimura, M. (1980). A simple method for estimating evolutionary rates of base substitutions through comparative studies of nucleotide sequences. *J. Mol. Evol.* 16, 111–120. doi: 10.1007/BF01731581

Lelievre, S., Jerome, M., Maes, G. E., Vaz, S., Calaivany, S., and Verrez-Bagnis, V. (2012). Integrating molecular identification of pelagic eggs with geostatistical mapping to improve the delineation of North Sea fish spawning grounds. *Mar. Ecol. Prog. Ser.* 445, 161–172. doi: 10.3354/meps09443

Lewis, L. A., Richardson, D. E., Zakharov, E. V., and Hanner, R. (2016). Integrating DNA barcoding of fish eggs into ichthyoplankton monitoring programs. *Fish. Bull. Natl Oceanic Atmos. Adm.* 114, 153–168. doi: 10.7755/FB.114.2.3

Leyva-Cruz, E., Vásquez-Yeomans, L., Carrillo, L., and Valdez-Moreno, M. (2016). Identifying pelagic fish eggs in the southeast Yucatan Peninsula using DNA barcodes. *Genome* 59, 1117–1129. doi: 10.1139/gen-2015-0151

Liu, M. D., Wang, D. W., Gao, L., Tian, H. W., Liu, S. P., Chen, D. P., et al. (2018). Species diversity of drifting fish eggs in the Yangtze River using molecular identification. *PeerJ* 6:e5807. doi: 10.7717/peerj.5807

Marquina, D., Buczek, M., Ronquist, F., and Łukasik, P. (2021). The effect of ethanol concentration on the morphological and molecular preservation of insects for biodiversity studies. *PeerJ* 9:e10799. doi: 10.7717/peerj.10799

Mat Jaafar, T. N. A., Taylor, M. I., Mohd Nor, S. A., De Bruyn, M., and Carvalho, G. R. (2012). DNA barcoding reveals cryptic diversity within commercially exploited Indo-Malay Carangidae (Teleosteii: perciformes). *PLoS One* 7:e49623. doi: 10.1371/journal.pone.0049623

Meiklejohn, K. A., Damaso, N., and Robertson, J. M. (2019). Assessment of BOLD and GenBank- their accuracy and reliability for the identification of biological materials. *PLoS One* 14:e0217084. doi: 10.1371/journal.pone.0217084

Michaud, C. L., and Foran, D. R. (2011). Simplified field preservation of tissues for subsequent DNA analyses. *J. Forensic Sci.* 56, 846–852. doi: 10.1111/j.1556-4029.2011.01771.x

Oksanen, J., Blanchet, F. G., Friendly, M., Kindt, R., and Wagner, H. H. (2020). *Package 'vegan': Community Ecology Package. R package Version 2.5-6.*

Oliveira, E. C. D., and Ferreira, E. J. (2008). Spawning areas, dispersion and microhabitats of fish larvae in the Anavilhanas Ecological Station, rio Negro, Amazonas State, Brazil. *Neotrop. Ichthyol.* 6, 559–566. doi: 10.1590/s1679-62252008000400003

Pauly, D., and Pullin, R. S. (1988). Hatching time in spherical, pelagic, marine fish eggs in response to temperature and egg size. *Environ. Biol. Fish.* 22, 261–271. doi: 10.1007/BF00004892

Pentinsaari, M., Ratnasingham, S., Miller, S. E., and Hebert, P. D. (2020). BOLD and GenBank revisited-Do identification errors arise in the lab or in the sequence libraries? *PLoS One* 15:e0231814. doi: 10.1371/journal.pone.0231814

Prokofiev, A. (2021). To the taxonomy of the stargazers of the genus *Uranoscopus* of the Indo-Pacific waters with a description of three new species (Uranoscopidae). *J. Ichthyol.* 61, 655–679. doi: 10.1134/S0032945221050131

Qin, Y., Song, N., Zou, J., Zhang, Z., Cheng, G., Gao, T., et al. (2013). A new record of a flathead fish (Teleostei: platycephalidae) from China based on morphological characters and DNA barcoding. *Chin. J. Oceanol. Limnol.* 31, 617–624. doi: 10.1007/s00343-013-2186-z

Qiu, Y., Zeng, X., Chen, T., Yuan, W., and Wang, Y. (2008). *Fishery Resources and Management in South China Sea*. Beijing: The Ocean Press.

Rakocinski, C. F., Lyczkowski-Shultz, J., and Richardson, S. L. (1996). Ichthyoplankton assemblage structure in Mississippi Sound as vevealed by canonical correspondence analysis. *Estuar. Coast. Shelf Sci.* 43, 237–257. doi: 10.1006/ecss.1996.0067

Shao, K. T., Chen, K. C., and Wu, J. H. (2002). Identification of marine fish eggs in Taiwan using light microscopy, scanning electric microscopy and mtDNA sequencing. *Mar. Freshw. Res.* 53, 355–365. doi: 10.1071/MF01141

Shen, C. Y., Yan, Y. R., Zhao, H., Pan, J. Y., and Devlin, A. T. (2018). Influence of monsoonal winds on chlorophyll-α distribution in the Beibu Gulf. *PLoS One* 13:e0191051. doi: 10.1371/journal.pone.0191051

Srinivasan, M., Sedmak, D., and Jewell, S. (2002). Effect of fixatives and tissue processing on the content and integrity of nucleic acids-sciencedirect. *Am. J. Pathol.* 161, 1961–1971. doi: 10.1016/S0002-9440(10)64472-0

Stéphanie, L., Véronique, V. B., Marc, J., and Sandrine, V. (2010). PCR-RFLP analyses of formalin-fixed fish eggs for the mapping of spawning areas in the Eastern Channel and Southern North Sea. *J. Plankton Res.* 32, 1527–1539. doi: 10.1093/plankt/fbq067

Su, J. (2005). *The Offshore Hydrology in China*. Beijing: China Ocean Press, 285–296.

Sun, D. F., Zhu, W. C., Ai, H., Li, N. N., Dong, L. N., Shi, Y. R., et al. (2010). Taxonomic diversity of fish species in Beibu Gulf. *Guangdong Agric. Sci.* 37, 4–7. doi: 10.16768/j.issn.1004-874x.2010.06.099

Sun, D. R., and Chen, Z. (2013). *Fish Categories Books in the South China Sea*, Vol. 1. Beijing: Maritime Press.

Sun, D. R., and Lin, Z. J. (2004). Variations of major commercial fish stocks and strategies for fishery management in Beibu Gulf. *J. Trop. Oceanogr.* 23, 62–68. doi: 10.3724/sp.j.1118.2012.00062

Sun, M. S., Chen, Z. J., Zhang, J., and Zhang, K. (2019). Analysis of fish abundance and distribution pattern in the Beibu Gulf using fishery acoustic measurement combined with ordinary Kriging method. *Fresen. Environ. Bull.* 28, 9058–9069.

Takeuchi, A., Higuchi, T., Watanabe, S., Miller, M. J., Yama, R., Fukuba, T., et al. (2021). Several possible spawning sites of the Japanese eel determined from collections of their eggs and Preleptocephali. *Fish. Sci.* 87, 339–352. doi: 10.1007/s12562-021-01519-4

Tamura, K., Stecher, G., Peterson, D., Filipski, A., and Kumar, S. (2013). MEGA6: molecular evolutionary genetics analysis version 6.0. *Mol. Biol. Evol.* 30, 2725–2729. doi: 10.1093/molbev/mst197

Tucker, S. J., Kurniasih, E. M., and Craig, M. T. (2016). A new species of grouper (Epinephelus; Epinephelidae) from the Indo-Pacific. *Copeia* 104, 658–662. doi: 10.1643/CI-16-398

Valdez-Moreno, M., Vásquez-Yeomans, L., Elías-Gutiérrez, M., Ivanova, N. V., and Hebert, P. D. N. (2010). Using DNA barcodes to connect adults and early life stages of marine fishes from the Yucatan Peninsula, Mexico: potential in fisheries management. *Mar. Freshw. Res.* 61, 665–671. doi: 10.1071/MF09222

Wan, R. J., and Zhang, R. J. (2016). *Fish Eggs, Larvae and Juveniles in the Offshore Waters of China and Their Adjacent Waters*. Shanghai: Shanghai Scientific and Technological Press.

Wang, X., Qiu, Y., Du, F., Lin, Z., Sun, D., and Huang, S. (2010). Fish community pattern and its relation to environmental factors in the Beibu Gulf. *J. Fish. China* 34, 1579–1586. doi: 10.3724/SP.J.1231.2010.06827

Wang, X., Qiu, Y., Du, F., Lin, Z., Sun, D., and Huang, S. (2011). Spatio-temporal variability of fish diversity and dominant species in the Beibu Gulf. *J. Fish. Sci. China* 18, 427–436. doi: 10.3724/SP.J.1011.2011.00415

Wang, X., Qiu, Y., Du, F., Lin, Z., Sun, D., and Huang, S. (2012). Dynamics of demersal fish species diversity and biomass of dominant species in autumn in the Beibu Gulf, northwestern South China Sea. *Acta Ecol. Sin.* 32, 333–342. doi: 10.5846/stxb201011291700

Ward, R. D., Zemlak, T. S., Innes, B. H., Last, P. R., and Hebert, P. D. (2005). DNA barcoding Australia's fish species. *Philos. Trans. R. Soc. B* 360, 1847–1857. doi: 10.1098/rstb.2005.1716

Ware, D. (1975). Relation between egg size, growth, and natural mortality of larval fish. *J. Fish. Board Can.* 32, 2503–2512. doi: 10.1139/f75-288

Xiao, J. G., Yu, Z. S., Song, N., and Gao, T. X. (2021). Description of a new species, *Sillago nigrofasciata* sp. nov. (Perciformes, Sillaginidae) from the southern coast of China. *ZooKeys* 1011, 85–100. doi: 10.3897/zookeys.1011.57302

Xiao, W., Zhang, Y., and Liu, H. (2001). Molecular systematics of *Xenocyprinae* (Teleostei : cyprinidae): taxonomy, biogeography, and coevolution of a special group restricted in east Asia. *Mol. Phylogenet. Evol.* 18, 163–173. doi: 10.1006/mpev.2000.0879

Zhang, H. F., Liu, X. C., Zhong, L. Y., Xing, W. Y., Li, L., Huang, G. G., et al. (2006). Embryonic development, morphological development of larva, juvenile and young fish of *Epinephelus coioides*. *J. Fish. Sci. China* 13, 689–699.

Zhang, K., Cai, Y., Liao, B., Jiang, Y. E., Sun, M., Su, L., et al. (2020). Population dynamics of threadfin porgy *Evynnis cardinalis*, an endangered species on the IUCN red list in the Beibu Gulf, South China Sea. *J. Fish Biol.* 97, 1–11. doi: 10.1111/jfb.14398

Zhang, R., Lu, S., Zhao, C., Chen, L., Zang, Z., and Zhang, X. (1985). *Fish Eggs and Larvae in the Offshore Waters of China*. Shanghai: Shanghai Scientific and Technological Press.

Zheng, Y. J., Li, X. Q., Yang, Z. X., Cai, W. X., Lou, Q. S., and Tao, W. (2021). The identification of fish eggs of two species, the ovate sole *Solea ovata* and black porgy *Acanthopagrus schlegelii*. *J. Fish. Biol.* 99, 1746–1751. doi: 10.1111/jfb.14854

Zhou, M. Y., Lin, Y. S., and Hou, T. T. (2008). "The abundance and distribution of ichthyoplankton in the Gulf of Tonkin in summer, 2006," in *Proceedings of the Symposium of Marine Science Research in Beibu Gulf*, eds J. Hu, S. Yang, et al. (Beijing: China Ocean Press), 264–271.

Zhou, M., Lin, Y., Yang, S., Cao, W., and Zheng, L. (2011). Composition and ecological distribution of ichthyoplankton in eastern Beibu Gulf. *Acta Ecol. Sin.* 30, 94–105. doi: 10.1007/s13131-011-0095-6

Zimmermann, J., Hajibabaei, M., Blackburn, D. C., Hanken, J., Cantin, E., Posfai, J., et al. (2008). DNA damage in preserved specimens and tissue samples: a molecular assessment. *Front. Zool.* 5:18. doi: 10.1186/1742-9994-5-18

Conflict of Interest: The authors declare that the research was conducted in the absence of any commercial or financial relationships that could be construed as a potential conflict of interest.

frontiers in Marine Science

ORIGINAL RESEARCH
published: 09 February 2022
doi: 10.3389/fmars.2022.767290

Two Decades of Match-Mismatch in Northeast Arctic Cod – Feeding Conditions and Survival

Clarissa Akemi Kajiya Endo[1,2]*, Leif Christian Stige[2,3], Morten D. Skogen[1], Lorenzo Ciannelli[4] and Frode V. Vikebø[1,5]

[1] Institute of Marine Research, Bergen, Norway, [2] Centre for Ecological and Evolutionary Synthesis (CEES), Department of Biosciences, University of Oslo, Oslo, Norway, [3] Norwegian Veterinary Institute, Ås, Norway, [4] College of Earth, Ocean, and Atmospheric Sciences, Oregon State University, Corvallis, OR, United States, [5] Geophysical Institute, University of Bergen, Bergen, Norway

OPEN ACCESS

Edited by:
Hui Zhang,
Institute of Oceanology, Chinese
Academy of Sciences (CAS), China

Reviewed by:
Cui Liang,
Institute of Oceanology, Chinese
Academy of Sciences (CAS), China
Gang Hou,
Guangdong Ocean University, China

***Correspondence:**
Clarissa Akemi Kajiya Endo
clarissa.endo@hi.no

Specialty section:
This article was submitted to
Marine Fisheries, Aquaculture
and Living Resources,
a section of the journal
Frontiers in Marine Science

Received: 30 August 2021
Accepted: 17 January 2022
Published: 09 February 2022

Citation:
Endo CAK, Stige LC, Skogen MD,
Ciannelli L and Vikebø FV (2022) Two
Decades of Match-Mismatch
in Northeast Arctic Cod – Feeding
Conditions and Survival.
Front. Mar. Sci. 9:767290.
doi: 10.3389/fmars.2022.767290

The successful recruitment of Northeast Arctic (NEA) cod is thought to depend on sufficient and suitable prey for the newly hatched larvae, in particular the *nauplii* stages of the lipid-rich calanoid copepod species *Calanus finmarchicus*. The role of spatial and temporal variations in prey availability in combination with temperature and other factors in influencing growth and survival of cod larvae is, however, incompletely understood. By combining an individual based model for NEA cod larvae at the Norwegian coast with a high-resolution ocean model and a nutrient-phytoplankton-zooplankton-detritus model providing 18 years of daily environmental conditions and prey availability we assessed larval growth and survival until they settle in their feeding habitat in the Barents Sea in early fall. We find on average a two-week delay from the peak timing of first-feeding cod larvae to the peak in prey availability. In warm years, more larvae experience food limitation than in normal years. The positive effects of high temperature on growth, survival and ultimately recruitment are nonetheless larger than the negative effects of food limitation. Food limitation mainly affects larvae spawned in southern areas or late in the spawning season as these larvae experience the highest temperatures and have the highest energy requirements. Our findings highlight the spatial and temporal differences in mechanisms that regulate growth and survival of early life stages of NEA cod and suggest that spatially resolved data may be essential for understanding match-mismatch dynamics.

Keywords: Atlantic cod, individual-based model (IBM), dispersal, climate, recruitment, larval growth, Barents Sea, prey availability

INTRODUCTION

Variability in the number of individuals in adult fish populations results mainly from the loss of individuals through natural and fishing mortality, and recruitment of individuals through the reproduction process (Payne et al., 2009). The survival until recruitment to the harvestable stock is a complex process that encompasses all conditions experienced by the fish including the variability in physical and biological conditions (Hjort, 1914). Numerous hypotheses have been developed to explain the observed variability in year-class success, mostly related to the early life stages of fish development. The "Critical Period" hypothesis explains year-class survival variability through the success or failure in finding enough suitable prey after the yolk-sac has been exhausted. Meanwhile, the "Aberrant Drift" hypothesis states that larvae survival is dependent on the dispersal to favorable areas, i.e., with enough prey and suitable abiotic conditions (Hjort, 1914; Houde, 2008). The "Match-mismatch" hypothesis explains the year-class survival variability through phenology and extends the critical period from the first-feeding stage until after metamorphosis (Cushing, 1969, 1990). This hypothesis highlights mechanisms that connect the temporal overlap between prey and predators as a key for the survival of the predators, assuming spatial overlap is present. Mismatch with prey results in slower growth and development and may lead to enhanced mortality because the larval fish are more susceptible to predation (Hjort, 1914; Durant et al., 2007; Ferreira et al., 2020). The three above mentioned hypotheses account for many underlying processes of various spatial and temporal resolutions that affect survival of the early life stages of fish, including starvation, transport to and from favorable habitats, and metabolic rates due to varying ambient conditions. Moreover, the relative importance of these processes to recruitment varies in space and time (Gallego et al., 2012; Hare, 2014).

Natural variability and ongoing climate change significantly influence the spatial and temporal distributions of predators and prey and may alter phenology and trophic interactions (Durant et al., 2007). It can also modify the costs and benefits associated with different spawning times and areas, and cause constraints at spawning grounds and shifts in the feeding areas, potentially through climate-driven changes in prey distribution (Fossheim et al., 2015). Changes in temperature affect the habitat selection of the spawners (Sundby and Nakken, 2008; Höffle et al., 2014; Sandø et al., 2020). Offspring transport may also be affected by changing ocean currents and cross-shelf exchange due to changes in ambient temperature, wind patterns and stratification that affects vertical egg distribution and spring bloom dynamics through nutrient availability (Vikebø et al., 2010, 2021; Skagseth et al., 2015; Strand et al., 2017).

Demographic structure and biological condition of the spawners may also influence the survival and distribution of the eggs and larvae of fish. The age and size composition of the spawning stock can influence spawning location, time, and duration (Sundby and Nakken, 2008; Opdal and Jørgensen, 2015; Langangen et al., 2019). For example, when there are older and bigger fish in the spawning stock of Northeast Arctic (NEA) cod, there is higher egg abundance and a spatially more widespread egg distribution (Stige et al., 2017). Furthermore, maternal characteristics affect egg quality, which in turn can impact larval susceptibility to starvation (Marteinsdottir and Steinarsson, 1998).

The diet of first-feeding larvae of NEA cod is mainly composed of copepod *nauplii* and for older larvae copepodites of *Calanus finmarchicus* (Dalpadado et al., 2009; Ottersen et al., 2014). Larvae are restricted to forage on prey smaller than their gape size, so it is important that the larvae are in a favorable place and time regarding prey concentrations of suitable sizes. The development of their main prey item *C. finmarchicus* is dependent on the onset of the seasonal spring bloom, which varies considerably (weeks) between years (Ellertsen et al., 1987; Vikebø et al., 2019; Dalpadado et al., 2020). Observations of prey availability are limited in space and time and can only provide a snapshot of the processes occurring in the ecosystem, but recently there are indications of a shift towards lower abundance, especially of *C. finmarchicus*, at the Norwegian continental shelf (Toresen et al., 2019).

Species-environment interactions are non-linear, and interannual dynamics cannot be reliably inferred from spatially averaged data (Ciannelli et al., 2007). On the other hand, individual based models (IBMs) coupled with ocean hydrodynamics models and nutrient, primary production, zooplankton, and detritus (NPZD) models represent complementary information about availability of suitable and sufficient prey items. The high spatial and temporal resolution of such models allow studying how local-scale processes translate into population-scale dynamics. In this study, we quantify availability of suitable prey items by combining the results from an IBM of NEA cod early life stages with an ocean hydrodynamics model and a NPZD model across the period 2000-2017. This approach enables quantification of intra- and interannual variations in match-mismatch and survival of NEA cod larvae through considerations of individual prey catches along individual drift trajectories for integration across the entire population (Kristiansen et al., 2009; Daewel et al., 2011; Strand et al., 2017). The analyses of the simulation results also enable investigation of the underlying spatio-temporal mechanisms regulating dispersal, feeding and development of individual NEA cod spawned along the Norwegian coast. We specifically address the following questions:

(I) Does prey availability (timing, size, and abundance) affect individual larval growth, spatially, seasonally and interannually?
(II) How does this effect on growth impact survival through early life stages until recruitment?
(III) What are the key mechanisms and their relative importance that control growth and survival until settlement at favorable nursery grounds?

MATERIALS AND METHODS

Individual NEA cod larval growth was investigated using offline coupled models. Overall, the model results were calculated by using an ocean hydrodynamics model, a nutrient-phytoplankton-zooplankton-detritus model including an individual based model for *Calanus finmarchicus*, and an individual based model for NEA cod eggs and larvae. The simulations were run from 2000 to 2017, for the period between the 15th of January to the 30th of September each year. The results from the simulations were used to analyse growth and survival of the individuals from the egg stage until the larvae reaches the Barents Sea. We also account for size-dependent survival through the first winter after settlement in the Barents Sea.

Model Species

The Northeast Arctic Cod

The Northeast Arctic (NEA) stock of Atlantic cod (*Gadus morhua*) is one of the world's largest and most studied cod stocks due to its commercial importance and of high commercial and ecological importance (Yaragina et al., 2011; Ottersen et al., 2014). NEA cod inhabits the Barents Sea, a shallow shelf sea and a transition zone for warm and saline waters between the Atlantic Ocean and the Arctic. Mature NEA cod individuals migrate long distances during winter-spring from their feeding habitats in the Barents Sea towards the south to spawn along the Norwegian coast (**Figure 1**), from Finnmark (71°N) to Møre (63°N), with the highest spawning activity in the Lofoten archipelago (69°N) (Opdal et al., 2008; Sundby and Nakken, 2008).

The main spawning season lasts from early March until the end of April with a peak in early April (Ottersen et al., 2014). After spawning, the offspring drift northeastward in the upper layers of the water column and are transported by the Norwegian Coastal current (NCC) and the Norwegian Atlantic current (NAC) from the spawning grounds back to the Barents Sea (Vikebø et al., 2005). Egg development until hatching is highly dependent on ambient temperature, but it usually lasts from 2 to 5 weeks (Ellertsen et al., 1989; Yaragina et al., 2011). The NEA cod larvae yolk sac provides nutrition for about 5–7 days, whereafter the larvae switch to exogenous feeding about 3–6 weeks after spawning (on average late April) (Ottersen et al., 2014). By August - September successful offspring have reached the nursery grounds in the Barents Sea and are denoted 0-group. During the autumn (September - October) the 0-group descend towards the bottom and switch from the pelagic to the demersal phase in the Barents Sea. Surviving individuals are recruited to the harvested stock when they reach 3 years age.

Calanus finmarchicus

Calanus finmarchicus is one of the dominant species in the meso-zooplankton in the Atlantic water masses of the Norwegian Sea and Barents Sea. *C. finmarchicus* is an herbivore species and an

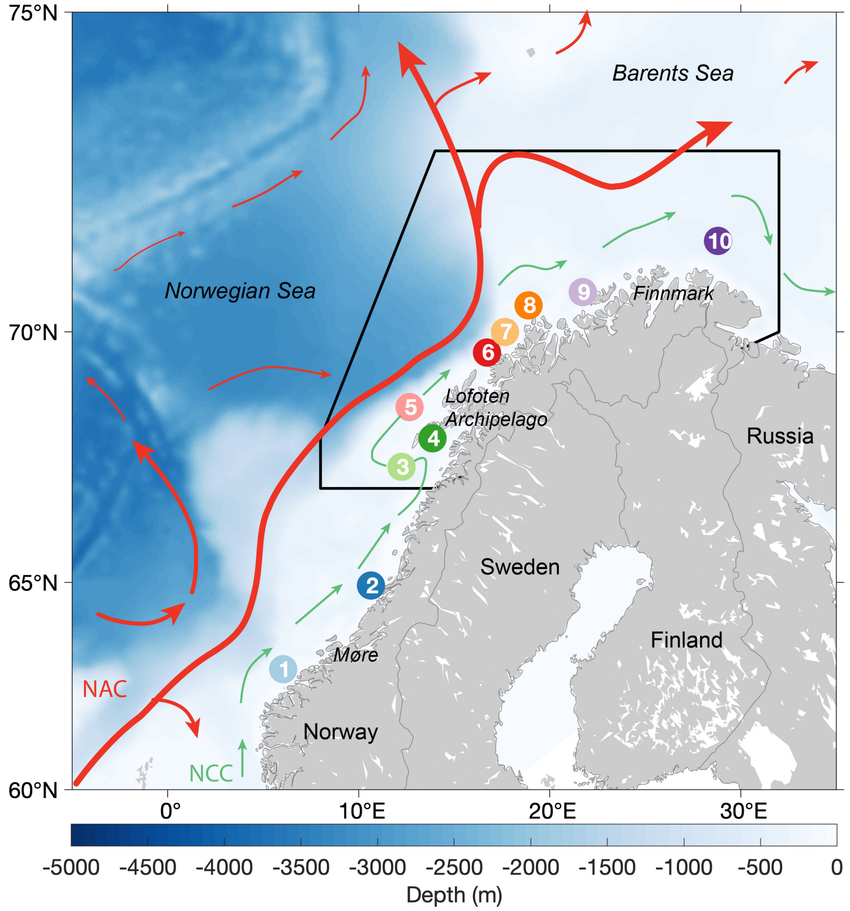

FIGURE 1 | Northeast Arctic cod spawning sites and origins of particle dispersal: 1- Møre, 2 - Vikna, 3 - Røst, 4- Lofoten, 5 - Moskenesgrunnen, 6 - Senja, 7 - Malangsgrunnen, 8 -Torsvåg, 9 - Breivikbotn and 10 - East Finnmark. The black polygon represents the area where 95% of the larvae (2000-2017) are located when they are 15 days post hatch. Main surface ocean currents pattern in the Norwegian and Barents Sea is illustrated by the arrows: Norwegian Coastal Current (NCC – green arrows) and Norwegian Atlantic Current (NAC - red arrows).

important link between the phytoplankton and higher trophic levels (Melle et al., 2004), e.g., larvae of NEA cod that feed upon *C. finmarchicus nauplii* and copepodites (Ellertsen et al., 1989). The *C.* life cycle consists of an egg stage, 6 *nauplii* stages (denoted N1 to N6), 5 copepodites stages and the adult stage (male or female). *C. finmarchicus* usually has a one-year life cycle, but this species can develop more than one generation in warmer regions, as in the southernmost parts of the Norwegian Sea (Broms and Melle, 2007). The reproduction of *C. finmarchicus* is linked to the seasonal development of the phytoplankton (Melle and Skjoldal, 1998; Stenevik et al., 2007). *C. finmarchicus* release their eggs in the upper layers of the water column during spring and develop with the spring bloom to reach the overwintering stage (mainly copepodites stage five) in mid-late summer. Overwintering occurs in deep ($>$500 m) cold water and lasts until late winter, when the overwintered individuals ascend to surface waters to reproduce (Skjoldal et al., 1992).

Numerical Model Components

The Hydrodynamical Model Component

Ocean physics were modeled using the Regional Ocean Modelling System (ROMS). ROMS is a three-dimensional free surface, baroclinic, primitive equations ocean model with topography following s-coordinates in the vertical (Shchepetkin and McWilliams, 2005). In the present study, the Nordic Seas numerical ocean model hindcast (SVIM) archive with 4 km horizontal resolution and 32 sigma coordinates in the vertical was used. It covers the Nordic, Barents and Kara seas and parts of the Arctic Ocean (for further information we refer to Lien et al., 2013, 2016).

The NORWegian ECOlogical Model (NORWECOM)

NORWECOM is a coupled physical, chemical, biological model system (Skogen et al., 1995; Skogen and Søiland, 1998) applied to study primary production, nutrient budgets and dispersion of particles such as fish larvae and pollution. In the present study it was run in offline mode using physics (light, wind, hydrography, horizontal and vertical movement of the water masses) from the SVIM archive. The NORWECOM model includes an ordinary NPZD model with processes such as primary production, respiration, algal death, remineralization of inorganic nutrients from dead organic matter, self-shading, turbidity, sedimentation, resuspension, sediment burial and denitrification. In addition, the model has an IBM for *C. finmarchicus* (Hjøllo et al., 2012).

The *Calanus finmarchicus* Individual Based Model

The three-dimensional IBM for *C. finmarchicus* includes feeding, growth, mortality, movement, reproduction, and adaptive traits that control the interaction with the environment. The entire life cycle of *C. finmarchicus* is included in the model, resolving the 13 life stages and their features, also including a genetic model algorithm which allows the model to evolve individual traits. Up until the third *nauplius* stage the development and stage longevity is based on temperature. From the third *nauplius* stage (N3) *C. finmarchicus* starts feeding and is 2-way coupled to the NPZD model. Growth is a function of phytoplankton density, temperature and size based on a bioenergetics model. A more detailed description of the model can be found in Hjøllo et al. (2012) and Huse et al. (2018).

The NEA Cod Egg and Larvae Individual Based Model

The IBM for NEA cod eggs and larvae is a Lagrangian dispersal model, and it includes dynamical vertical positioning of eggs dependent on buoyancy and turbulence, prey- and temperature dependent larval growth, predator-prey encounter rates and capture, larvae ingestion rate and metabolism, and larval vertical migration (Vikebø et al., 2005, 2007; Kristiansen et al., 2007).

The NEA cod IBM was run offline based on daily ROMS currents and hydrography, and NORWECOM 2D fields of the *C. finmarchicus* from the Lagrangian IBM in addition to 3D Eularian fields of mesozooplankton for the period January 15th until September 30th, 2000–2017.

Individual particles were initiated as eggs at 10 known spawning sites along the Norwegian coast (**Figure 1** – colored circles; Sundby and Nakken, 2008). While the spawning season lasts from early March until the end of April, we initiated eggs from February 15th to May 15th to enable consideration of conditions also outside the main spawning period. For some of the analysis model results were adjusted according to the observed spawning intensities in space and time (Strand et al., 2017). Specifically, the relative importance of each individual particle was weighted by a gaussian function of spawning date with a peak on April 1st and a standard deviation of 14 days, and by year- and spawning site-specific weights that scaled the spatial relative importance of spawning sites according to egg surveys and observations of spawning adults (following Strand et al., 2017).

A total of one hundred eggs were released at each of the ten spawning sites (SS) per spawning date (SD), amounting to 90 000 particles per year. Particles were released initially as eggs at about 30 m depth. Individual particle position was updated every 30 min according to a 4^{th} order Runge-Kutta advection scheme and vertical egg positioning in the water column was based on the density difference between the eggs and the ambient water and turbulence (Thygesen and Ådlandsvik, 2007). Eggs were initiated with a buoyancy of 31.25 and a population standard deviation of 0.69 (Sundby, 1997). Individual hatching time followed Geffen et al. (2006)– see **Supplementary Information** (SI) for details.

After hatching, eggs continued as larvae with an initial weight of 45 μg and a length of approximately 4 mm (Folkvord, 2005). Larvae performed diel vertical migration at a third of a body length per second, ascending during night and descending during day (see Vikebø et al. (2007) for more details). Light decays exponentially with depth and depends on surface irradiance and the attenuation coefficient (see SI for details). Hence, each egg and larva experienced unique abiotic and biotic conditions through the period of pelagic drift.

After hatching, the larvae immediately started feeding in our model, and thus they did not go through the stage of yolk-sac larvae. It is estimated that yolk-sac cod larvae have a duration of 5–7 days in nature. Within this period, the larvae were feeding mostly on *nauplii* N2, and included *nauplii* N3 about 10-15 days after hatching depending on temperatures in the range 4-6°C (**Supplementary Figure 1**).

Larval growth in the IBM was potentially food limited, depending on available prey concentration, the metabolic costs and egestion/excretion losses. Larvae fed on mesozooplankton from the NPZD model and from the *C. finmarchicus* IBM, which together provided prey field concentrations per stage [ind/m^2]. Unlike in the *C. finmarchicus* IBM, mesozooplankton in the NPZD model is not stage resolved. They were therefore converted to *C. finmarchicus* equivalents assuming a similar relative stage distribution (see SI for equations and details).

Cod larvae may feed on prey stages limited by their respective gape size, here 8 % of the larval length according to Otterå and Folkvord (1993). Feeding was parameterized according to Fiksen and MacKenzie (2002), already included in an IBM and tested for sensitivity in a numerical study by Kristiansen et al. (2007) - see SI for details. Stomach content [μg] was assumed to reach a maximum of 6 % of the body weight of the larva according to Lough et al. (2005).

Larval growth potential (i.e., growth assuming unlimited food) was limited by temperature according to Folkvord (2005) and may only be reached if sufficient prey is ingested (**Supplementary Figure 1**) - see SI for details.

The higher the ambient temperature, the higher the metabolic requirements. Consequently, a higher quantity of food is needed. If the food requirement is met the larvae may grow faster and prey composition more quickly diversifies (**Supplementary Figure 1**). Note that larval weight may decrease while larval length may not. This was also considered in the model.

Data Analyses

Annual averages of individual larval net distance from SS and ambient temperatures 30 days post-spawning were compiled in a scatter plot to indicate inter-annual varying conditions for NEA cod early life stages. In addition, we extracted annual average modeled temperatures during March-August in the upper 50 m of the water column in a polygon (**Figure 1**, black contour) containing 95 % of 15 days post-hatch (dph) larvae across all years. This calculation allowed inter-annual comparison of environmental conditions independent of egg and larva dispersal trajectories. The polygon extracted mean temperature was used to separate warm and normal years using the median value (**Table 1**). Here, we used the nomenclature normal years instead of cold years because the temperature anomalies (not shown) for the period from 1921 to 2018 based on the Kola section showed there are no actual cold years in our study period 2000-2017 (Yashayaev and Seidov, 2015).

Survival

Cumulative survival until the end of the simulation (September 30th) was calculated as a product of several factors. In short, survival at the end of the experiment was the product of survival through hatching, not starving (nonSt), reaching the Barents Sea (inBS), stage-dependent mortality, and size-dependent mortality.

To be considered alive the eggs must have hatched before the end of the simulation. Also, we required the larvae to reach the Barents Sea, the NEA cod nursery grounds, implemented as being east of 19°E. Furthermore, we required that the individuals did not starve at any time throughout the drift period.

TABLE 1 | Mean yearly temperature (T) in the main distribution area of cod larvae (the polygon in **Figure 1**) from March until August in the upper 50 m in the water column.

Normal years	T (°C)	Warm years	T (°C)
2000	5.61	2002	6.65
2001	5.38	2004	6.52
2003	6.24	2005	6.56
2008	6.12	2006	6.58
2009	6.16	2007	6.54
2010	5.48	2012	6.30
2011	5.91	2015	6.68
2013	6.16	2016	6.61
2014	6.24	2017	6.48

The median temperature value, 6.27°C, was used to separate normal and warm years.

Starvation was defined as weighing 20% less than its expected weight (i.e., only temperature dependent weight - potential weight) given its length (see Folkvord (2005) for function relating length and weight). As larvae cannot become shorter, this may occur if larvae are unable to ingest prey that at least match metabolic costs and assimilation losses.

We also calculated stage-specific survival for each individual that accounted for baseline natural mortality from, e.g., predation. Instantaneous natural mortality rates (M) for each stage were: for eggs (M_{egg}) 0.169 d^{-1}, for larvae (M_{lar}) 0.075 d^{-1} and for early juveniles (M_{eju}) 0.023 d^{-1} (Langangen et al., 2014b; Bogstad et al., 2016). Individuals were larvae if they were within 4.2 and 24 mm in length and early juveniles within 25 - 99 mm (Herbing et al., 1996; Folkvord, 1997; Hamre, 2006). Cumulative baseline natural mortality as a function of time is therefore;

$$N_t = N_0 * exp^{[-M_{egg} * t_{egg} - M_{lar} * t_{lar} - M_{ejuv} * t_{ejuv})]}$$

where the different M's are daily instantaneous stage-specific mortality rates, N_t is the abundance at time t and N_0 is the abundance at time 0 and t_{egg}, t_{lar} and t_{ejuv} are the number of days spent in the different stages.

We also accounted for size-dependent survival through the first winter. Specifically, we calculated a proxy for size-corrected abundance at age 1 (N_{1age}) based on the abundance (N_{0age}) and mean length (L_{0age}) at the end of the simulation. The size-corrected abundance was calculated for each SS and SD using the following equation: $N_{1age} = N_{0age} * \exp(c_1 * [\ln(L_{0age}) - \ln(L_{mean})])$. Here, the coefficient $c_1 = 9.78$ was estimated by Stige et al. (2019, Table S6) based on year-class survival of NEA cod through the first winter. The scaling factor L_{mean} was the mean length of all individuals through all the years in the simulation.

Food Sufficiency Index (FSI)

In addition, we quantified a food sufficiency index (FSI) to find which individuals might have suffered from food limitation but are not food limited enough to be considered starved. FSI reports the fraction of individuals that grew at rates above 90 % of the food-unlimited temperature dependent growth potential for more than 90 % of the time until the end of the simulation. The

FSI was included as a more sensitive measure than starvation of food-limitations on larval growth through the planktonic stages.

RESULTS

Drift and Development of Egg and Yolk-Sac Larvae

Egg stage duration until hatching varies with ambient temperatures, which in turn depends on SS, SD, year, and individual drift trajectory. Individuals spawned late and to the south generally experience higher temperatures (∼ 7.0 ± 0.3 °C) than those spawned to the north (∼ 4.8 ± 0.2 °C) (**Figure 2A**), while inter-annual variability (**Figure 2B**) is highest early in the season likely because of variation in the onset of seasonal heating. Individuals originating from SS 4 (inside the Lofoten archipelago) experience anomalously low ambient temperatures (∼ 4.9 ± 0.4°C) (**Figure 2C**) compared with other SS at similar latitudes, likely because of less influence of relatively warm Atlantic Water, retention, and runoff. Warm years generally result in less variable ambient temperatures between SSs, with 2012 as a good example.

Duration of the egg stage affects both the time and location in which the larvae start feeding. With average egg stage duration of 18.7 ± 5.3 (s.d.) days in our model and yolk sac absorption (not included in the model) of another 5–7 days the first feeding of larvae typically occurs within the first 30 days after spawning. Low ambient temperatures (< 4.5 °C) experienced by the offspring correspond to long distance traveled, while elevated ambient temperatures (> 4.5°C) may correspond to a variety of mean distances from SS (**Figure 3**). The association between low ambient temperature and long distance traveled may be linked to a general trend of decreasing temperature with increasing distance from the spawning grounds. The absence of clear dispersal patterns for the individuals experiencing higher ambient temperatures is likely due to more variable circulation features. We believe that due to a constant NCC, low ambient temperatures result in a prolonged drift period until 30 days after spawning and a longer distance traveled from the SS. In warmer years (annual average polygon temperatures) the individuals generally experience higher ambient (5.2 ± 0.3°C) temperatures along their drift routes than in normal years (4.6 ± 0.1°C). In 2004, the individuals on average travelled the farthest

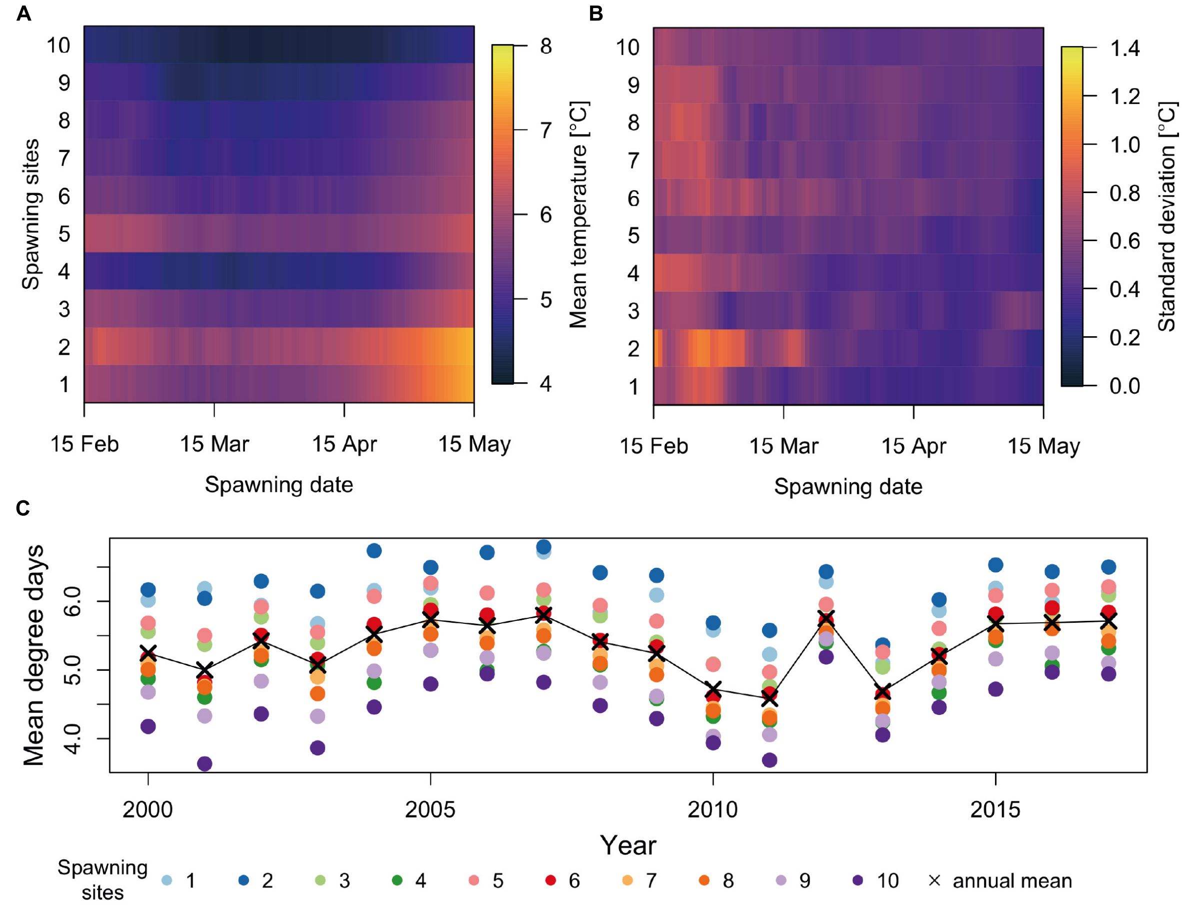

FIGURE 2 | (A) Mean modeled ambient temperature of eggs until hatching from 2000 to 2017 by spawning site and spawning date. **(B)** Corresponding standard deviation for between-year variation of temperature. **(C)** Time series of annual mean ambient temperatures until hatching from 2000 to 2017 (black line connecting x's) along with the annual mean ambient spawning site specific temperatures (colored circles).

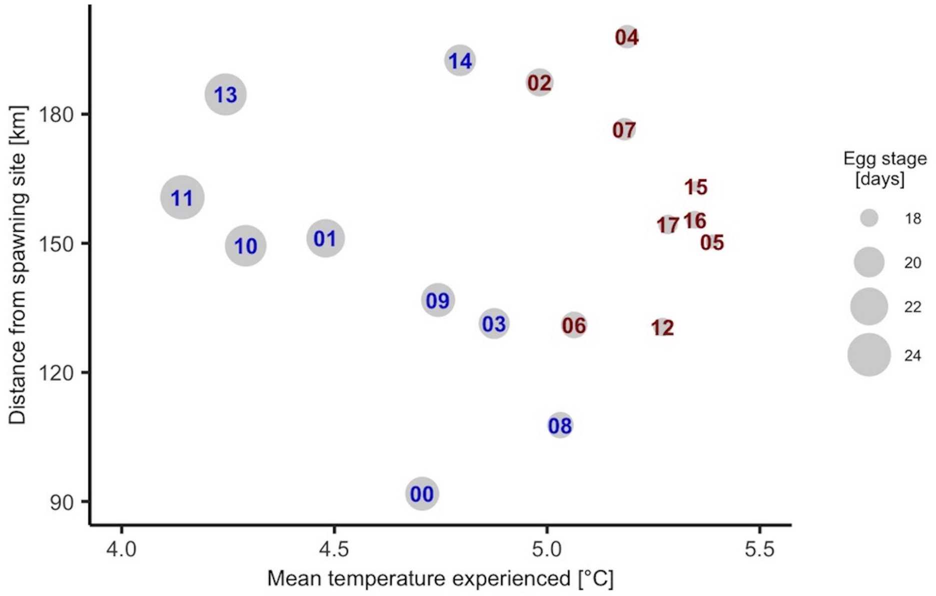

FIGURE 3 | Annual mean net distance from spawning sites to positions of eggs or larvae thirty days after spawning and corresponding ambient temperatures along the drift routes. Note that these values are weighted according to the temporal and spatial spawning intensity (see Materials and Methods). The size of the circles represents the yearly mean egg stage duration, while the numbers denote the year in the simulation period. Years in red and blue denote warm and normal, respectively.

(∼ 198 km), more than double the distance traveled in the year 2000 (∼ 91 km).

Feeding Conditions for Larvae

In our simulation results, the peak timing in the abundance of larvae at 15 dph in the polygon occurred on average about 15 days before the peak timing of prey of suitable size (**Figure 4**).

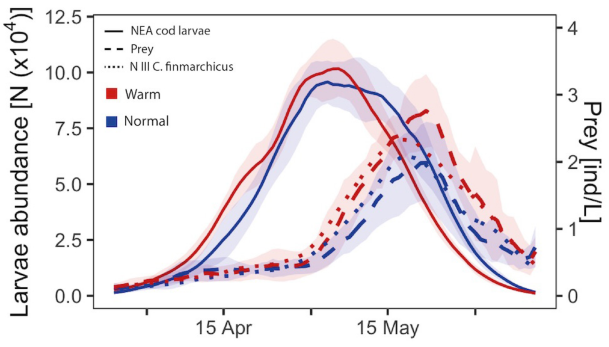

FIGURE 4 | Mean seasonal pattern in abundances of cod larvae at 15 days post hatch (unbroken lines), all prey of suitable size for the larvae (dashed lines) and the dominant prey *C. finmarchicus nauplii* stage N3 (dotted lines). The mean values were calculated for the main distribution area of cod larvae (the polygon in **Figure 1**) for warm (red) and normal (blue) years. The shading for larval and prey abundances shows the interannual variation (± 1 standard deviation) for warm or normal years. The lines have been smoothed by a moving mean of 5 days to emphasize trends. For a detailed year by year curves with the mean for all years see **Supplementary Figure 2**.

Abundance of 15 dph larvae appear on average 8 days later in normal than warm years (**Figure 4**, solid lines). Meanwhile, prey abundance of suitable sizes peaks almost at the same time in warm and normal years (**Figure 4**, dashed lines), but the abundance of prey is on average 31% lower in normal years than in warm years (non-significantly lower, $t = 1.17$, $p = 0.28$). *C. finmarchicus nauplii* at stage N3 constitutes a major part of the food of the correct size for cod larvae at this age (**Supplementary Figure 3**), and the seasonal curve for N3 abundance resembles the seasonal curve in prey of suitable size (**Figure 4**).

Match between larvae and suitable prey is higher for warm years than normal years (**Figure 4** - area below intersection of solid and broken red lines vs. blue lines; for interannual variability see **Supplementary Figure 3**). Both normal and warm years (e.g., 2003 and 2002) may have higher abundances of N3 than the mean, and curiously, the year 2016 (warm) presented a delayed peak of N3 as compared to other years (**Supplementary Figure 2B**). Elevated abundances of *C. finmarchicus* progress northwards along the coast with time before becoming limited to only the southern part of the model domain from early June and onwards (**Supplementary Figures 2A,C**). In higher latitudes it is possible to observe two peaks of elevated *C. finmarchicus* N3 concentrations (**Supplementary Figure 2A** - area I and II), whereas in the southernmost area III, *C. finmarchicus* N3 is available throughout the entire simulated months.

Mechanisms of Survival of the Early Juveniles

The FSI shows that on average early spawned larvae experience sufficient and suitable prey conditions to support growth according to their temperature potential (**Figure 5A**). Later in the year, as temperature and thereby prey requirements increase, larvae experience growth limited by food availability, and this is particularly strong for late spawning far south. FSI is more variable for the individuals spawned far south and early in the spawning season, and at all spawning sites for those spawned around the main spawning period from late March to early April (**Figure 5B**).

Mean ambient temperature along egg and larval drift routes and the FSI have a negative relationship (**Figure 6A**). Consistently, most warm years, according to mean polygon temperature from March – August (**Table 1**), tend to have a lower FSI, while normal years tend to have a higher FSI (**Figure 6A**). Note, however, that 2012 and 2017 are warm years, with median ambient temperatures along drift routes and high FSI. Larval length (and weight - not shown) against FSI (**Figure 6B**) displays similar patterns as for ambient temperature against FSI (**Figure 6A**). Larval length (and weight – not shown) is positively correlated with ambient temperature (**Figure 6C**).

Modeled stage-specific cumulative survival until the 0-age group displays little variation between years. Slightly elevated survival occurs in 2002 (warm), 2007 (warm), 2010 (normal) and 2013 (normal) (**Figure 7** – yellow line with triangles). Adding the requirement of also reaching the Barents Sea makes little difference, except for slightly reduced survival in 2011 (**Figure 7** – light green line with triangles). If starvation is considered fatal, survival decreases resulting in particularly low survival in 2010, 2011 (normal) and 2013 (**Figure 7** – dark green line with diamonds). If also accounting for size-dependent survival through the first winter from age 0 to age 1 (Stige et al., 2019), survival decreases even further still, resulting in particularly low survival in the same years as before (**Figure 7** – green petrol line with filled diamonds). The calculated survival to age 1 and the field data for the 0-age group (age-0 fish per spawning stock biomass) have a non-significant weak negative correlation ($r = -0.12$, $p = 0.64$). However, although also non-significant, calculated survival to age one is weakly positively correlated with recruitment success at age three (recruits per spawning stock biomass, from assessment reports of the Arctic Fisheries Working Group (ICES, 2020), $r = 0.29$, $p = 0.25$). The recruitment at age 3 showed a long-term decline through the study period, which was not seen in the age-0 data or in the modeled survival (**Figure 7**). Short-term variability in survival to age-1 and recruitment, represented by year-to-year differences, were also non-significantly weakly positively correlated ($r = 0.07$, $p = 0.78$).

Correlations Between Key Variables Concerning Cod Survival and Prey Interactions

Cumulative modeled survival to age 1 is negatively correlated with the FSI ($r = -0.72$, $p < 0.001$), positively correlated with modeled 0-age length ($r = 0.87$, $p < 0.001$) and weight ($r = 0.98$, $p < 0.001$) and significantly positively correlated with the annual peak abundance of *C. finmarchicus* N3 available to 15 dph larvae ($r = 0.58$, $p = 0.01$) (**Figure 8**). Weight correlates negatively with the FSI ($r = -0.67$, $p = 0.002$), positively with N3 abundance ($r = 0.56$, $p = 0.017$) and positively with length (as weight and length are functionally interlinked here). Length on the other hand correlates positively with starvation ($r = 0.66$, $p = 0.003$) and negatively with the FSI ($r = -0.49$, $p = 0.045$).

The latitudes of NEA cod larvae at 15 dph are significantly positively correlated with starvation ($r = 0.51$, $p = 0.03$) and with 0-age length ($r = 0.52$, $p = 0.03$). The strong correlation between larval latitude and longitude is because of the northeasterly orientation of the coast between spawning and nursery grounds.

The day of the year with the highest larvae abundance naturally correlates positively with their mean latitude ($r = 0.83$, $p < 0.001$) and longitude 15 dph ($r = 0.71$, $p < 0.001$) because

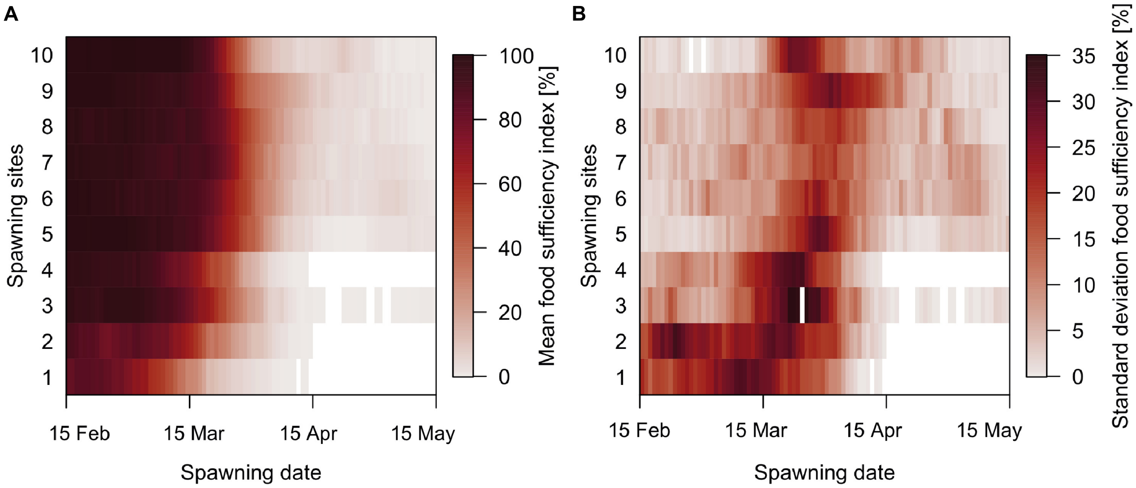

FIGURE 5 | Fraction of individuals that grow 90% or more than their temperature-dependent potential if the prey is unlimited for more than 90% of the time since hatching until the 30th of September (food sufficiency index), per spawning site and spawning date. **(A)** Mean and **(B)** standard deviation. Blank spaces represent no individuals (food sufficiency index = 0).

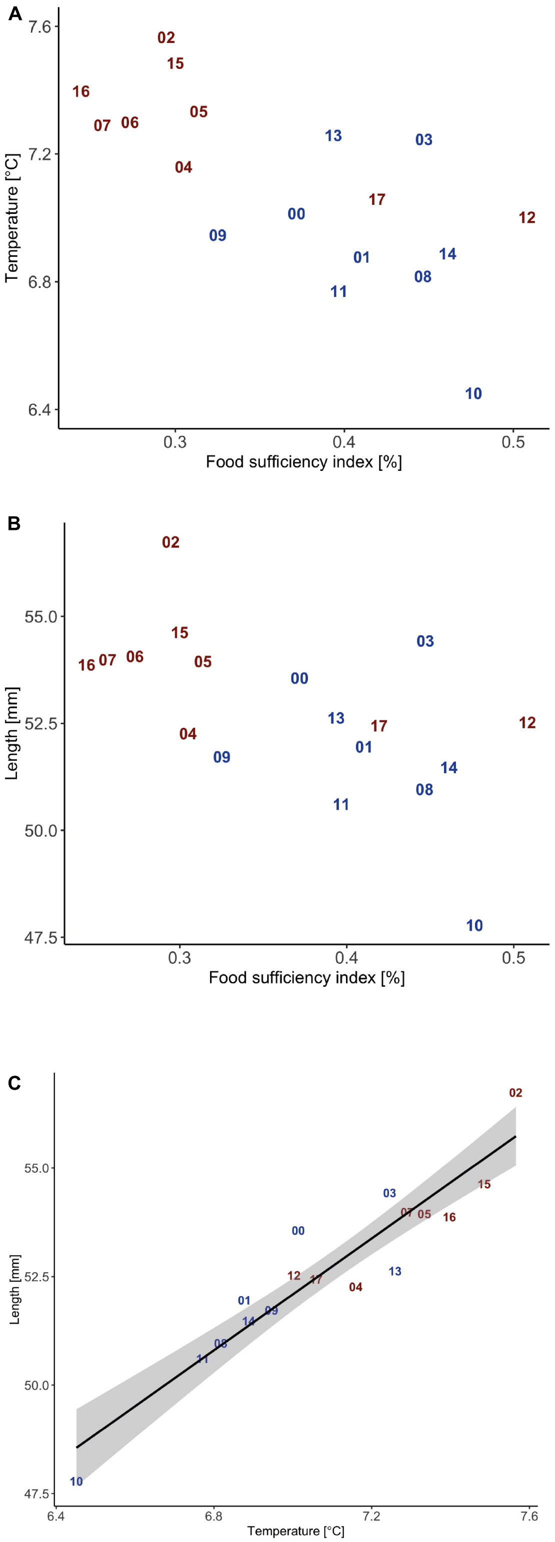

FIGURE 6 | (A,B) Annual mean food sufficiency index weighted by spawning intensity vs. ambient temperature and length also weighted by spawning intensity at September 30th. **(C)** Annual mean ambient temperature vs. length along with the 95 % confidence interval for the regression. Red are warm years and blue are normal years.

a prolonged stage duration allows a longer drift period until the date of 15 dph. The time difference between peak abundance of 15 dph cod larvae and *C. finmarchicus* N3 is positively correlated with northward drift and day of peak abundance *C. finmarchicus* N3. Peak abundance of 15 dph larvae is on average 15 days prior to the peak of *C. finmarchicus* N3 and a delayed peak indicates a prolonged egg stage duration and therefore prolonged dispersal time to reach 15 dph. Latitude of the highest concentration of N3 has a positive correlation with cod survival to age 1 ($r = 0.5$, $p = 0.035$).

DISCUSSION

Key Findings and Implications

The results presented here shed light on the processes and mechanisms that affect larval growth, distribution and survival from NEA cod egg and larval stages until arrival of juveniles in their nursery grounds in the Barents Sea and through the first winter by considering previously established empirical-based size-dependent survival prospects. Using a coupled ocean hydrodynamical model, a NPZD model including a *C. finmarchicus* IBM and an IBM for pelagic stages of NEA cod, it was possible to analyse the importance of abiotic conditions and food availability for growth and survival through all early life stages until settlement of juveniles at nursery grounds in the Barents Sea for 18 consecutive years. Observational-based abundance estimates were also added at multiple stages and statistical correlations were performed with the modeled larval abundances. In comparison a similar study focused on hydrodynamical processes along the coast that affect spatial-temporal overlap between NEA cod larvae and prey for a few selected years (Vikebø et al., 2021). On the whole, the two studies provide complimentary information on key physical processes along the Norwegian coast that are important to NEA cod larvae feeding and to what extent combined biophysical models may predict the population size at different development stages.

We found that the time of peak abundance of 15 dph larvae is around two weeks before the peak timing of prey, with considerable interannual variability both in timing and amplitude. Because of this mismatch in peak timing, the NEA cod larvae seem to depend more strongly on the time of the increase in prey concentration than on the time of peak or decrease in prey. A delay between cod larvae and their prey is consistent with observations from Vestfjorden in the Lofoten archipelago, where an early peak of *C. finmarchicus* copepodite stage C1 in warm years tended to coincide with large mean size of NEA cod larvae around 15 dph, presumably because of a good temporal match between predators and prey (Ellertsen et al., 1987, 1989; Cushing, 1990).

Most larvae grow at or close to their temperature potential except for late-spawned individuals. Late spawned cod eggs hatch into first-feeding larvae with better temporal match with suitable prey, at the same time as seasonal heating allows for a higher growth potential and thereby elevated feeding requirements to support growth and metabolic costs. In fact, our model results show that fast-growing larvae experience more often insufficient

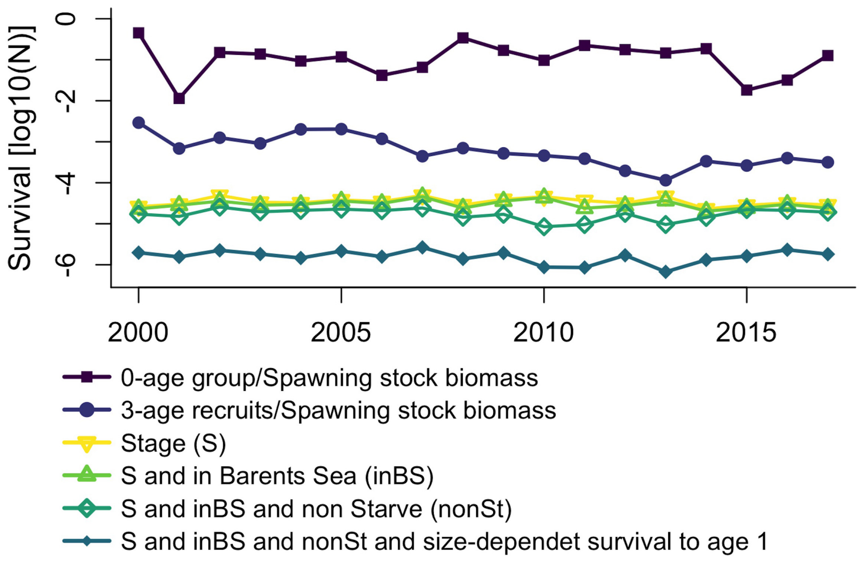

FIGURE 7 | Cumulative modeled survival until the 30th of September only including fixed stage-specific mortality rates (yellow line with upside-down triangles), also adding requirement that individuals need to reach the Barents Sea (green with triangles), also requiring that individuals do not starve (dark green with open diamond) and including size-dependent survival until age 1 (blue line with filled diamonds). For comparison we show observed 0-age group abundance divided by spawning stock biomass (purple line with filled squares) and abundance of 3-year olds from Virtual Population Analysis back-calculated to spawning year divided by spawning stock biomass (SSB - dark blue line with filled circles). Units for the latter two variables are thousands per tones, data from the ICES (2020).

prey conditions to match their growth potential depending on their size and ambient temperature. March - August mean temperature during the early life stages of NEA cod in the core area of appearance has positive correlations with the length and weight at 0-age ($r = 0.80$, $p < 0.001$; $r = 0.88$, $p < 0.001$, respectively) and a negative correlation with the FSI ($r = -0.62$, $p = 0.005$). This is also the reason why they are more prone to experience starvation as they have elevated metabolic costs and therefore require an elevated steady supply of suitable prey which in our model is not always available. However, the reward of finding sufficient food is rapid growth and high cumulative survival.

First-feeding and young larvae depend on a narrow selection of *C. finmarchicus* stages. The results here show that the abundances of prey for these stages are still significantly affecting NEA cod weight and survival at the 0-age group and 1-year old individuals. Our results further suggest that this association at the population level is mainly driven by the food conditions experienced by a minority of individuals that have high growth potential because of high temperatures, as these are the ones that are potentially food-limited. Despite having sufficient food, the individuals that originate from early spawning and northern spawning grounds develop slowly and have low survival because of low ambient temperatures. Individuals that originate from late spawning and southern spawning grounds have higher growth potential because of higher temperature, but also higher risks of food limitation and of not reaching the Barents Sea nursery grounds. An implication of this spatial heterogeneity in which mechanisms regulate growth and survival is that the dynamics are not necessarily well represented by spatially averaged data (as pointed out by, e.g., Ciannelli et al., 2008). For example, average food and temperature conditions may not be the most relevant for year-class survival, but rather food levels in the water masses with high temperature.

Dispersal to the north is necessary to reach the NEA cod nursery grounds but also impose an enhanced risk of mismatch because suitable *C. finmarchicus* nauplii abundance is only present at the shelf towards the entrance to the Barents Sea during a much more limited period than farther south. This is likely also the explanation why we find a positive correlation between larval latitude and starvation. During spring (April - May) *C. finmarchicus* N3 individuals are abundant both inside the polygon encompassing 95 % of 15 dph cod larvae and even farther north. However, toward summer (June-July) *C. finmarchicus* N3 are almost absent in the polygon and farther north, and only present at latitudes farther south.

We find that the southern spawned eggs from spawning from around late March to mid-April have the highest survival, but also the highest variability between years. This spatial gradient is different from what we would expect as observed spawning is centered around Lofoten (SS 3-5) but indicates that there are additional drivers that shape spawning behavior not addressed in our model. Such drivers could be spawning migration costs (e.g., Jørgensen et al., 2008), spatial patterns in predation pressure (Langangen et al., 2016) and predation avoidance (e.g., Husebø et al., 2009). The seasonal pattern in modeled offspring survival resembles the seasonal pattern in the spawning of NEA cod (peaking around 1st of April, Ottersen et al., 2014), supporting that this timing provides the best balance for offspring to be spawned late enough to benefit from high temperature and fast development but early enough to reach the Barents Sea and

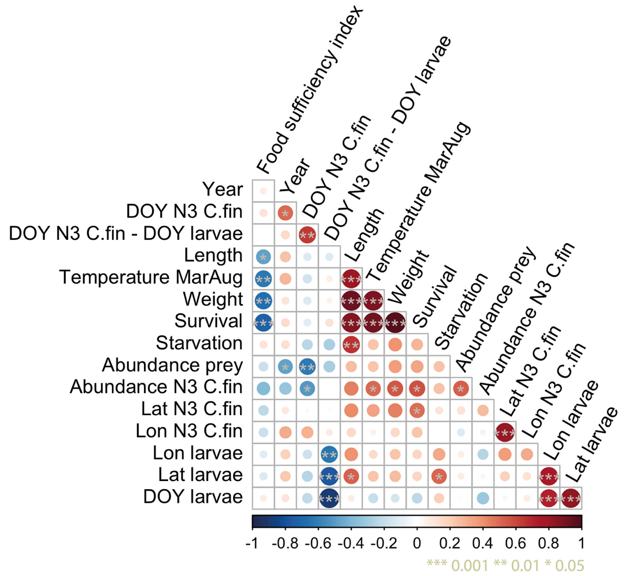

FIGURE 8 | Correlation matrix between variables that indicate survival and match-mismatch between the cod larvae 15 days post-hatch within the polygon and their prey of correct size, *Calanus finmarchicus* (C. fin) *nauplii* stage III (N3) abundance, larval length and weight at the end of simulation (30th of September) and survival from the egg stage to age 1 (accounting for size-dependent survival through the first winter). Temperature included in this analysis is the mean temperature from March until August within the main distribution area of cod larvae (the polygon in **Figure 1**) and it is based on the ocean model. DOY corresponds to the day of the year where highest abundance was observed.

have enough food to take advantage of the high growth potential (consistent with, e.g., Kristiansen et al., 2007).

Temperature and Prey, and Their Effects on Growth and Survival

Our findings are consistent with literature indicating that low temperatures result in prolonged stage duration and enhanced mortality independent of prey availability (Pepin et al., 1997; Otterlei et al., 1999). Most larvae are not food-limited within our model simulations. It is mainly the late- and southern-spawned larvae that experience food limitation. The high temperatures these larvae experience imply that the larvae require higher food concentration than other larvae to grow optimally. High temperatures have the potential to secure rapid growth and development (Daewel et al., 2011) and thereby to reduce the number of potential predators, but success requires high food abundance, otherwise high temperatures may be prejudicial (Fouzai et al., 2015). Our results suggest that late-spawned larvae experience higher prey abundance in warm than normal years, but that the food requirements increase more than the food concentrations, leading to increasing food limitations on growth. The food limitations are, however, not so large that the high temperatures are prejudicial for survival.

We find in our model results that the bigger the size at 0-age the higher the survival from spawning to age 1. However, the modeled survival is weakly but positively correlated with recruitment success at age 3 and not significantly, so it is not possible to establish a linear relation between modeled survival and recruitment success. Yet, it is known that larger mean size of larvae and juveniles is associated with higher survival through the first winter and recruitment later at age 3 (Ottersen and Loeng, 2000; Stige et al., 2015, 2019). Growing fast and becoming bigger may increase survival because individuals have outgrown their predator diet size range, due to enhanced ability to escape predators, and to the ability to exploit a wider size range of prey (Cushing, 1995). Larger individuals tend to have higher energy reserves and to be more resilient to starvation than smaller individuals, and a larger body size can also be an advantage when dealing with physical stress (Sogard, 1997; Marteinsdottir and Steinarsson, 1998).

Match-Mismatch

We observe a difference in mean time of peak abundance of 15 dph larvae and their suitable prey, but apparently prey availability does not limit survival or growth of most larvae until the 0-age group. In our model we observe that at the date of peak abundance of 15 dph larvae, the maximum concentration of *C. finmarchicus* is a little below the minimum concentration found by Cushing (1990, page 280), who writes "Above a density of 5 nauplii/L, the cod larvae are well fed." On the other hand, Folkvord (2005) found that most NEA cod larvae in the sea have a size that is near the maximum for their temperature, suggesting that surviving larvae have not suffered food limitation. Our findings are in accordance with Folkvord (2005), and apparently small larvae need less than 5 ind/L to survive without food limitations.

Our results partly support previous studies that have suggested that in warm years, NEA cod larvae grow and survive better than in cold years because of a better temporal match between the first-feeding larvae and their prey (Ellertsen et al., 1987, 1989; Cushing, 1990). Our results are consistent with empirical findings that *C. finmarchicus* nauplii abundance in spring is higher in warm than normal or cold years (Kvile et al., 2014; Stige et al., 2015), but do not support temperature-driven shifts in the peak timing of the nauplii (Ellertsen et al., 1987, 1989) and also show large variability in nauplii levels between years with similar temperatures. Our results are also consistent with empirical findings that link high nauplii levels in spring with large size of NEA cod larvae (Ellertsen et al., 1987, 1989; Cushing, 1990; Stige et al., 2015) and between large larval and juvenile size and high survival to later ages (Ottersen and Loeng, 2000; Stige et al., 2015, 2019). Our model results thereby support that the statistical associations between temperature and recruitment through match-mismatch dynamics have a mechanistic basis, but also highlight that these associations are complex and involve temperature-dependent interactions between processes at different spatial and temporal scales.

Model Refinements, Sensitivity to the Results and Future Studies

The current parameterization in the NEA cod IBM includes egg buoyancy but does not differentiate between eggs according to quality and size as a function of e.g., spawning time or spawning adult conditions. An increased egg diameter supports bigger hatched larvae and has positive effects also on yolk-sac larvae (Pepin et al., 1997). However, egg development, time to hatch, size of the larvae at hatching and time of yolk absorption are more significantly affected by temperature than by egg size (Pepin et al., 1997; Steinarsson and Björnsson, 1999). Since biological parameters for the egg and larva development are more affected by temperature than by egg size, we believe our model provides a fair representation of the natural world.

The success of the feeding process and prey selection depend on many parameters such as prey encounter rate, prey, and predator (larvae) size, light, capture success, ingestion rate, prey selection and others. Wind generated turbulence may also affect feeding conditions. Turbulence contributes to the maintenance of the larvae at depths where there is less predation risk than closer to the surface, and that also increases prey encounter rates, suggesting that turbulence can be important to avoid starvation of first-feeding larvae, especially in low prey densities (Sundby, 1997; Kristiansen et al., 2014). On the other hand, turbulence can have a detrimental impact on encounter rates when being too high through the advection of the prey out of the visual range of the larvae (Fiksen and MacKenzie, 2002). Turbulence is not included in the cod larvae IBM used in this study. As food seems to be limiting growth only for the late spawned individuals, we believe that turbulence-enhanced predator-prey contact rates would only have importance for these individuals.

Predation and cannibalism mortality varies in space and time and consequently can affect the spatio-temporal dynamics of survival and future recruitment. These sources of mortality are not included in the models coupled here. The natural mortality rates of NEA cod larvae have been found to vary spatially (Langangen et al., 2014a). In this regard, it is important to understand the spatial heterogeneity of mortality and survival. Age-0 NEA cod has decreased survival when the overlap between juvenile and adult cod increases, likely due to cannibalism (Ciannelli et al., 2007). For the Atlantic cod stock in the North Sea, not only the number of predators is important, but also how they are distributed and at what larval life stage they affect survival rates (Akimova et al., 2019). Akimova et al. (2019) also highlights the importance of the patchiness distribution of both predators and prey.

The predator-prey interaction occurs at much finer spatial-temporal scales in marine ecosystems than the scales modeled here, which can cause uncertainty in predator-prey interactions. Considering the uncertainty in predator-prey and cannibalism interactions mentioned above, it is important to ponder adding further biological features to the early life stages of individuals, as well as further sources of mortality. As topics of future studies, we also suggest analyzing the effect of the spawning adult stock and the variation in demographic characteristics and how this can affect growth and survival of the offspring.

DATA AVAILABILITY STATEMENT

Data can be made available upon reasonable request.

AUTHOR CONTRIBUTIONS

CE contributed with evaluation of model, model analyses, and writing of the manuscript. MS contributed with model runs and model analysis. LS, LC, and FV contributed with constructive discussions, suggestions for model analysis and feedback on the manuscript writing. All authors contributed to the work and contributed to the discussions of hypothesis, methods, and results.

FUNDING

This work was supported by the Research Council of Norway (project number 280468) under the project "Drivers and effects of Spatial shifts in early life stages of marine fish (SpaceShift)." The simulations were performed on resources provided by UNINETT Sigma2—the National Infrastructure for High-Performance Computing and Data Storage in Norway under grant NN2984K.

SUPPLEMENTARY MATERIAL

The Supplementary Material for this article can be found online at: https://www.frontiersin.org/articles/10.3389/fmars.2022.767290/full#supplementary-material

REFERENCES

Akimova, A., Hufnagl, M., and Peck, M. A. (2019). Spatiotemporal dynamics of predators and survival of marine fish early life stages: atlantic cod (*Gadus morhua*) in the North Sea. *Prog. Oceanogr.* 176:102121. doi: 10.1016/j.pocean.2019.102121

Bogstad, B., Yaragina, N. A., and Nash, R. D. M. (2016). The early life-history dynamics of Northeast Arctic cod: levels of natural mortality and abundance during the first 3 years of life. *Can. J. Fish. Aquat. Sci.* 73, 246–256. doi: 10.1139/cjfas-2015-0093

Broms, C., and Melle, W. (2007). Seasonal development of *Calanus finmarchicus* in relation to phytoplankton bloom dynamics in the Norwegian Sea. *Deep. Res. Part II Top. Stud. Oceanogr.* 54, 2760–2775. doi: 10.1016/j.dsr2.2007.08.021

Ciannelli, L., Dingsør, G. E., Bogstad, B., Ottersen, G., Chan, K. S., Gjøsæter, H., et al. (2007). Spatial anatomy of species survival: effects of predation and climate-driven environmental variability. *Ecology* 88, 635–646. doi: 10.1890/05-2035

Ciannelli, L., Fauchald, P., Chan, K. S., Agostini, V. N., and Dingsør, G. E. (2008). Spatial fisheries ecology: recent progress and future prospects. *J. Mar. Syst.* 71, 223–236. doi: 10.1016/j.jmarsys.2007.02.031

Cushing, D. (1995). *Population Production and Regulation in the Sea: A Fisheries Pesperctive*. Cambridge: Cambridge University Press.

Cushing, D. H. (1969). The Regularity of the spawning season of some fishes. *J. Mar. Sci.* 33, 81–92. doi: 10.1093/icesjms/33.1.81

Cushing, D. H. (1990). Plankton production and year-class strength in fish populations: an update of the match/mismatch hypothesis. *Adv. Mar. Biol.* 26, 249–293. doi: 10.1016/S0065-2881(08)60202-3

Daewel, U., Peck, M. A., and Schrum, C. (2011). Life history strategy and impacts of environmental variability on early life stages of two marine fishes in the North Sea: an individual-based modelling approach. *Can. J. Fish. Aquat. Sci.* 68, 426–443. doi: 10.1139/F10-164

Dalpadado, P., Arrigo, K. R., van Dijken, G. L., Rune Skjoldal, H., Bagøien, E., Dolgov, A., et al. (2020). Climate effects on temporal and spatial dynamics of phytoplankton and zooplankton in the Barents Sea. *Prog. Oceanogr.* 185:102320. doi: 10.1016/j.pocean.2020.102320

Dalpadado, P., Bogstad, B., Eriksen, E., and Rey, L. (2009). Distribution and diet of 0-group cod (*Gadus morhua*) and haddock (*Melanogrammus aeglefinus*) in the Barents Sea in relation to food availability and temperature. *Polar Biol.* 32, 1583–1596. doi: 10.1007/s00300-009-0657-

Durant, J. M., Hjermann, D., Ottersen, G., and Stenseth, N. C. (2007). Climate and the match or mismatch between predator requirements and resource availability. *Clim. Res.* 33, 271–283. doi: 10.3354/cr033271

Ellertsen, B., Fossum, P., Solemdal, P., and Sundby, S. (1989). Relation between temperature and survival of eggs and first-feeding larvae of northeast Arctic cod (*Gadus morhua L.*). *Cons. int. Explor. M er* 191, 209–219.

Ellertsen, B., Fossum, P., Solemdal, P., Sundby, S., and Tilseth, S. (1987). "The effect of biological and physical factors on the survival of Arcto-Norwegian cod and the influence on recruitment variability," in *The Effect of Oceanographic Conditions on the Distribution and Population Dynamics of Commercial Fish Stocks in the Barents Sea. Proceedings of the 3rd Soviet-Norwegian Symposium Murmansk, 26–28 May 1986*, ed H. Loeng (Bergen: Institute of Marine Research), 101–126.

Ferreira, A. S. A., Stige, L. C., Neuheimer, A. B., Bogstad, B., Yaragina, N., Prokopchuk, I., et al. (2020). Match - mismatch dynamics in the Norwegian - Barents Sea system. *Mar. Ecol. Prog. Ser.* 650, 81–94.

Fiksen, Ø, and MacKenzie, B. R. (2002). Process-based models of feeding and prey selection in larval fish. *Mar. Ecol. Prog. Ser.* 243, 151–164. doi: 10.3354/meps243151

Folkvord, A. (1997). "Ontogeny of cannibalism in larval and juvenile fishes with special emphasis on Atlantic cod," in *Early Life History and Recruitment in Fish Populations*, eds R. C. Chambers and E. A. Trippel (Dordrecht: Springer), 251–278. doi: 10.1007/978-94-009-1439-1_9

Folkvord, A. (2005). Comparison of size-at-age of larval Atlantic cod (*Gadus morhua*) from different populations based on size- and temperature-dependent growth models. *Can. J. Fish. Aquat. Sci.* 62, 1037–1052. doi: 10.1139/f05-008

Fossheim, M., Primicerio, R., Johannesen, E., Ingvaldsen, R. B., Aschan, M. M., and Dolgov, A. V. (2015). Recent warming leads to a rapid borealization of fish communities in the Arctic. *Nat. Clim. Chang.* 5, 673–677. doi: 10.1038/nclimate2647

Fouzai, N., Opdal, A. F., Jørgensen, C., and Fiksen, Ø (2015). Effects of temperature and food availability on larval cod survival: a model for behaviour in vertical gradients. *Mar. Ecol. Prog. Ser.* 529, 199–212. doi: 10.3354/meps11326

Gallego, A., North, E. W., and Houde, E. D. (2012). Understanding and quantifying mortality in pelagic, early life stages of marine organisms – Old challenges and new perspectives. *J. Mar. Syst.* 93, 1–3. doi: 10.1016/j.jmarsys.2011.10.012

Geffen, A. J., Fox, C. J., and Nash, R. D. M. (2006). Temperature-dependent development rates of cod *Gadus morhua* eggs. *J. Fish Biol.* 69, 1060–1080. doi: 10.1111/j.1095-8649.2006.01181.x

Hamre, K. (2006). Nutrition in cod (*Gadus morhua*) larvae and juveniles. *ICES J. Mar. Sci.* 63, 267–274. doi: 10.1016/j.icesjms.2005.11.011

Hare, J. A. (2014). The future of fisheries oceanography lies in the pursuit of multiple hypotheses. *ICES J. Mar. Sci.* 71, 2343–2356.

Herbing, I. H. V., Miyake, T., Hall, B. K., and Boutilier, R. G. (1996). Ontogeny of feeding and respirantion in larval Atlantic cod *Gadus morhua* (Teleostei, *Gadiformes*): I. Morphology. *J. Morphol.* 227, 15–35.

Hjøllo, S. S., Huse, G., Skogen, M. D., and Melle, W. (2012). Modelling secondary production in the Norwegian Sea with a fully coupled physical/primary production/individual-based *Calanus finmarchicus* model system. *Mar. Biol. Res.* 8, 508–526. doi: 10.1080/17451000.2011.642805

Hjort, J. (1914). *Fluctuations in the Great Fisheries of Northen Europe Viewed in the Light of Biological Research. Rapports et Procès – Verbaux.* Copenhagen: Andr. Fred. Host & Sons.

Höffle, H., Solemdal, P., Korsbrekke, K., Johannessen, M., Bakkeplasss, K., and Kjesbu, O. S. (2014). Variability of northeast Arctic cod (*Gadus morhua*) distribution on the main spawning grounds in relation to biophysical factors. *ICES J. Mar. Sci.* 71, 1317–1331.

Houde, E. D. (2008). Emerging from Hjort's shadow. *J. Northwest Atl. Fish. Sci.* 41, 53–70. doi: 10.2960/J.v41.m634

Huse, G., Melle, W., Skogen, M. D., Hjøllo, S. S., Svendsen, E., and Budgell, W. P. (2018). Modeling emergent life histories of copepods. *Front. Ecol. Evol.* 6:23. doi: 10.3389/fevo.2018.00023

Husebø, Å, Stenevik, E. K., Slotte, A., Fossum, P., Salthaug, A., Vikebø, F., et al. (2009). Effects of hatching time on year-class strength in Norwegian spring-spawning herring (*Clupea harengus*). *ICES J. Mar. Sci.* 66, 1710–1717. doi: 10.1093/icesjms/fsp150

ICES (2020). *Arctic Fisheries Working Group (AFWG). ICES Scientific Reports*. Copenhagen: ICES.

Jørgensen, C., Dunlop, E. S., Opdal, A. F., and Fiksen, Ø (2008). The evolution of spawning migrations: state dependence and fishing-induced changes. *Ecology* 89, 3436–3448. doi: 10.1890/07-1469.1

Kristiansen, T., Fiksen, Ø, and Folkvord, A. (2007). Modelling feeding, growth, and habitat selection in larval Atlantic cod (*Gadus morhua*): observations and model predictions in a macrocosm environment. *Can. J. Fish. Aquat. Sci.* 64, 136–151. doi: 10.1139/F06-176

Kristiansen, T., Vikebø, F., Sundby, S., Huse, G., and Fiksen, Ø (2009). Modeling growth of larval cod (*Gadus morhua*) in large-scale seasonal and latitudinal environmental gradients. *Deep. Res. Part II Top. Stud. Oceanogr.* 56, 2001–2011. doi: 10.1016/j.dsr2.2008.11.011

Kristiansen, T., Vollset, K. W., Sundby, S., and Vikebø, F. B. (2014). Turbulence enhances feeding of larval cod at low prey densities. *ICES J. Mar. Sci.* 9, 2515–2529.

Kvile, K. Ø, Dalpadado, P., Orlova, E., Stenseth, N. C., and Stige, L. C. (2014). Temperature effects on *Calanus finmarchicus* vary in space, time and between developmental stages. *Mar. Ecol. Prog. Ser.* 517, 85–104. doi: 10.3354/meps11024

Langangen, Ø, Färber, L., Stige, L. C., Diekert, F. K., Barth, J. M. I, Matschiner, M., et al. (2019). Ticket to spawn: combining economic and genetic data to evaluate the effect of climate and demographic structure on spawning distribution in Atlantic cod. *Glob. Chang. Biol.* 25, 134–143. doi: 10.1111/gcb.14474

Langangen, Ø, Ottersen, G., Ciannelli, L., Vikebø, F. B., and Stige, L. C. (2016). Reproductive strategy of a migratory fish stock: implications of spatial variations in natural mortality. *Can. J. Fish. Aquat. Sci.* 73, 1742–1749. doi: 10.1139/cjfas-2015-0321

Langangen, Ø, Stige, L. C., Yaragina, N. A., Vikebø, F. B., Bogstad, B., and Gusdal, Y. (2014b). Egg mortality of northeast Arctic cod (*Gadus morhua*) and haddock (*Melanogrammues aegleginus*). *ICES J. Mar. Sci.* 71, 1129–1136.

Langangen, Ø, Stige, L. C., Yaragina, N. A., Ottersen, G., Vikebø, F. B., and Stenseth, N. C. (2014a). Spatial variations in mortality in pelagic early life stages of a marine fish (*Gadus morhua*). *Prog. Oceanogr.* 127, 96–107. doi: 10.1016/j.pocean.2014.06.003

Lien, V. S., Gusdal, Y., Albretsen, J., Melsom, A., and Vikebø, F. B. (2013). *Evaluation of a Nordic Seas 4 km Numerical Ocean Model Hindcast Archive (SVIM), 1960-2011. Fisken og Havet, 7-2013.* Bergen: Havforskningsinstituttet.

Lien, V. S., Hjøllo, S. S., Skogen, M. D., Svendsen, E., Wehde, H., Bertino, L., et al. (2016). An assessment of the added value from data assimilation on modelled Nordic Seas hydrography and ocean transports. *Ocean Model.* 99, 43–59. doi: 10.1016/j.ocemod.2015.12.010

Lough, R. G., Buckley, L. J., Werner, F. E., Quinlan, J. A., and Pehrson Edwards, K. (2005). A general biophysical model of larval cod (*Gadus morhua*) growth applied to populations on Georges Bank. *Fish. Oceanogr.* 14, 241–262. doi: 10.1111/j.1365-2419.2005.00330.x

Marteinsdottir, G., and Steinarsson, A. (1998). Maternal influence on the size and viability of Iceland cod *Gadus morhua* eggs and larvae. *J. Fish Biol.* 52, 1241–1258. doi: 10.1006/jfbi.1998.0670

Melle, W., Ellertsen, B., and Skjoldal, H. R. (2004). "Zooplankton: the link to higher trophic levels," in *The Norwegian Sea ecosystem*, ed. H. R. Skjoldal (Trondheim: Tapir Academic Press), 559.

Melle, W., and Skjoldal, H. R. (1998). Reproduction and development of *Calanus finmarchicus*, *C. glacialis* and *C. hyperboreus* in the Barents Sea. *Mar. Ecol. Prog. Ser.* 169, 211–228. doi: 10.3354/meps169211

Opdal, A. F., and Jørgensen, C. (2015). Long-term change in a behavioural trait: truncated spawning distribution and demography in Northeast Arctic cod. *Glob. Chang. Biol.* 21, 1521–1530. doi: 10.1111/gcb.12773

Opdal, A. F., Vikebø, F. B., and Fiksen, Ø (2008). Relationships between spawning ground identity, latitude and early life thermal exposure in Northeast Arctic cod. *J. Northwest Atl. Fish. Sci.* 41, 13–22. doi: 10.2960/J.v41.m621

Otterå, H., and Folkvord, A. (1993). Allometric growth in juvenile cod (*Gadus morhua*) and possible effects on cannibalism. *J. Fish Biol.* 43, 643–645. doi: 10.1111/j.1095-8649.1993.tb00447.x

Otterlei, E., Nyhammer, G., Folkvord, A., and Stefansson, S. O. (1999). Temperature- and size-dependent growth of larval and early juvenile Atlantic cod (*Gadus morhua*): a comparative study of Norwegian coastal cod and northeast Arctic cod. *Can. J. Fish. Aquat. Sci.* 56, 2099–2111. doi: 10.1139/cjfas-56-11-2099

Ottersen, G., Bogstad, B., Yaragina, N. A., Stige, L. C., Vikebø, F. B., and Dalpadado, P. (2014). A review of early life history dynamics of Barents Sea cod (*Gadus morhua*). *ICES J. Mar. Sci.* 71, 2064–2087.

Ottersen, G., and Loeng, H. (2000). Covariability in early growth and year-class strength of Barents Sea cod, haddock, and herring: the environmental link. *ICES J. Mar. Sci.* 57, 339–348. doi: 10.1006/jmsc.1999.0529

Payne, M. R., Hatfield, E. M. C., Dickey-Collas, M., Falkenhaug, T., Gallego, A., Gröger, J., et al. (2009). Recruitment in a changing environment: the 2000s North Sea herring recruitment failure. *ICES J. Mar. Sci.* 66, 272–277. doi: 10.1093/icesjms/fsn211

Pepin, P., Orr, D. C., and Anderson, J. T. (1997). Time to hatch and larval size in relation to temperature and egg size in Atlantic cod (*Gadus morhua*). *Can. J. Fish. Aquat. Sci.* 54, 2–10. doi: 10.1139/f96-154

Sandø, A. B., Johansen, G. O., Aglen, A., Stiansen, J. E., and Renner, A. H. H. (2020). Climate change and new potential spawning sites for Northeast Arctic cod. *Front. Mar. Sci.* 7:28. doi: 10.3389/fmars.2020.00028

Shchepetkin, A. F., and McWilliams, J. C. (2005). The regional oceanic modeling system (ROMS): a split-explicit, free-surface, topography-following-coordinate oceanic model. *Ocean Model.* 9, 347–404. doi: 10.1016/j.ocemod.2004.08.002

Skagseth, Ø, Slotte, A., Stenevik, E. K., and Nash, R. D. M. (2015). Characteristics of the Norwegian coastal current during years with high recruitment of Norwegian spring spawning herring (*Clupea harengus L.). PLoS One* 10:e0144117. doi: 10.1371/journal.pone.0144117

Skjoldal, H. R., Gjosaeter, H., and Loeng, H. (1992). The Barents Sea ecosystem in the 1980s: ocean climate, plankton, and capelin growth. *ICES J. Mar. Sci.* 195, 278–290.

Skogen, M. D., and Søiland, H. (1998). *A User's Guide to NORWECON V2.0: The Norwegian Ecological Model System*. Bergen: Fisken og Havet.

Skogen, M. D., Svendsen, E., Berntsen, J., Aksnes, D., and Ulvestad, K. B. (1995). Modelling the primary production in the North Sea using a coupled three-dimensional physical-chemical-biological ocean model. *Estuar. Coast. Shelf Sci.* 41, 545–565.

Sogard, S. M. (1997). Size-selective mortality in the juvenile stage of teleost fishes: a review. *Bull. Mar. Sci.* 60, 1129–1157.

Steinarsson, A., and Björnsson, B. (1999). The effects of temperature and size on growth and mortality of cod larvae. *J. Fish Biol.* 55, 100–109. doi: 10.1006/jfbi.1999.1053

Stenevik, E. K., Melle, W., Gaard, E., Gislason, A., Broms, C. T., Prokopchuk, I., et al. (2007). Egg production of *Calanus finmarchicus*-A basin-scale study. *Deep. Res. Part II Top. Stud. Oceanogr.* 54, 2672–2685. doi: 10.1016/j.dsr2.2007.08.027

Stige, L. C., Langangen, Ø, Yaragina, N. A., Vikebø, F. B., Bogstad, B., Ottersen, G., et al. (2015). Combined statistical and mechanistic modelling suggests food and temperature effects on survival of early life stages of Northeast Arctic cod (*Gadus morhua*). *Prog. Oceanogr.* 134, 138–151. doi: 10.1016/j.pocean.2015.01.009

Stige, L. C., Rogers, L. A., Neuheimer, A. B., Hunsicker, M. E., Yaragina, N. A., Ottersen, G., et al. (2019). Density- and size-dependent mortality in fish early life stages. *Fish Fish.* 20, 962–976. doi: 10.1111/faf.12391

Stige, L. C., Yaragina, N. A., Langangen, Ø, Bogstad, B., Stenseth, N. C., and Ottersen, G. (2017). Effect of a fish stock's demographic structure on offspring survival and sensitivity to climate. *Proc. Natl. Acad. Sci. U.S.A.* 114, 1347–1352. doi: 10.1073/pnas.1621040114

Strand, K. O., Sundby, S., Albretsen, J., and Vikebø, F. B. (2017). The Northeast Greenland Shelf as a Potential Habitat for the Northeast Arctic Cod. *Front. Mar. Sci.* 4:304. doi: 10.3389/fmars.2017.00304

Sundby, S. (1997). Turbulence and ichthyoplankton: influence on vertical distributions and encounter rates. *Sci. Mar.* 61, 159–176.

Sundby, S., and Nakken, O. (2008). Spatial shifts in spawning habitats of Arcto-Norwegian cod related to multidecadal climate oscillations and climate change. *ICES J. Mar. Sci.* 65, 953–962.

Thygesen, U. H., and Ådlandsvik, B. (2007). Simulating vertical turbulent dispersal with finite volumes and binned random walks. *Mar. Ecol. Prog. Ser.* 347, 145–153. doi: 10.3354/meps06975

Toresen, R., Skjoldal, H. R., Vikebø, F., and Martinussen, M. B. (2019). Sudden change in long-term ocean climate fluctuations corresponds with ecosystem alterations and reduced recruitment in Norwegian spring-spawning herring (*Clupea harengus, Clupeidae*). *Fish Fish.* 20, 686–696. doi: 10.1111/faf.12369

Vikebø, F., Jørgensen, C., Kristiansen, T., and Fiksen, Ø (2007). Drift, growth, and survival of larval Northeast Arctic cod with simple rules of behaviour. *Mar. Ecol. Prog. Ser.* 347, 207–219. doi: 10.3354/meps06979

Vikebø, F., Sundby, S., Ådlandsvik, B., and Fiksen, Ø (2005). The combined effect of transport and temperature on distribution and growth of larvae and pelagic juveniles of Arcto-Norwegian cod. *ICES J. Mar. Sci.* 62, 1375–1386. doi: 10.1016/j.icesjms.2005.05.017

Vikebø, F. B., Broch, O. J., Endo, C. A. K., Frøysa, H. G., Carroll, J., Juselius, J., et al. (2021). Northeast Arctic Cod and prey match-mismatch in a high-latitude spring-bloom system. *Front. Mar. Sci.* 8:767191. doi: 10.3389/fmars.2021.767191

Vikebø, F. B., Husebø, A. S., Slotte, A., Stenevik, E. K., and Lien, V. S. (2010). Effect of hatching date, vertical distribution, and interannual variation in physical forcing on northward displacement and temperature conditions of Norwegian spring-spawning herring larvae. *ICES J. Mar. Sci.* 67, 1948–1956. doi: 10.1093/icesjms/fsq084

Vikebø, F. B., Strand, K. O., and Sundby, S. (2019). Wind intensity is key to phytoplankton spring bloom under climate change. *Front. Mar. Sci.* 6:518. doi: 10.3389/fmars.2019.00518

Yaragina, N. A., Aglen, A., and Sokolov, K. M. (2011). "Cod," in *The Barents Sea: Ecosystem, Resources, Management*, eds T. Jakobsen and V. K. Ozhigin (Trondheim: Tapir Academic Press), 225–270.

Yashayaev, I., and Seidov, D. (2015). The role of the Atlantic Water in multidecadal ocean variability in the Nordic and Barents Seas. *Prog. Oceanogr.* 132, 68–127. doi: 10.1016/j.pocean.2014.11.009

Conflict of Interest: The authors declare that the research was conducted in the absence of any commercial or financial relationships that could be construed as a potential conflict of interest.

frontiers | Frontiers in Marine Science

REVIEW
published: 24 May 2022
doi: 10.3389/fmars.2022.794433

Estuarine Ichthyoplankton Studies – A Review

Hui Zhang[1,2,3,4*†], **Yibang Wang**[1,2,3†], **Cui Liang**[1,3], **Shude Liu**[5] and **Weiwei Xian**[1,2,3*]

[1] CAS Key Laboratory of Marine Ecology and Environmental Sciences, Institute of Oceanology, Chinese Academy of Sciences, Qingdao, China, [2] University of Chinese Academy of Sciences, Beijing, China, [3] Laboratory for Marine Ecology and Environmental Science, Qingdao National Laboratory for Marine Science and Technology, Qingdao, China, [4] Center for Ocean Mega-Science, Chinese Academy of Sciences, Qingdao, China, [5] Shandong Hydrobios Resources Conservation and Management Center, Yantai, China

Edited by:
Çetin Keskin,
Istanbul University, Turkey

Reviewed by:
Alan Whitfield,
South African Institute for Aquatic Biodiversity, South Africa
Yuan Li,
Ministry of Natural Resources, China
Jose Henrique Muelbert,
Universidade Federal do Rio Grande, Brazil

***Correspondence:**
Hui Zhang
zhanghui@qdio.ac.cn
Weiwei Xian
wwxian@qdio.ac.cn

[†]These authors have contributed equally to this work and share first authorship

Specialty section:
This article was submitted to Marine Fisheries, Aquaculture and Living Resources, a section of the journal Frontiers in Marine Science

Received: 13 October 2021
Accepted: 26 April 2022
Published: 24 May 2022

Citation:
Zhang H, Wang Y, Liang C, Liu S and Xian W (2022) Estuarine Ichthyoplankton Studies – A Review. Front. Mar. Sci. 9:794433. doi: 10.3389/fmars.2022.794433

Estuaries are nutrient-rich environments with a gradient of fresh to salt water. They support high primary productivity and an abundance of zooplankton. Estuaries are used by many fish as nursery grounds because their environmental conditions provide abundant food for larval and adult fish. Ichthyoplankton, which comprise fish eggs and larvae, are important for the recruitment of fish species. At present, there are no systematic reviews on ichthyoplankton in estuaries from a global perspective. Here, research on ichthyoplankton over the last 60 years (1951–2022) was reviewed, focusing on three aspects: evaluation of ichthyoplankton published studies, community structure, and factors affecting community structure. The results show that research on estuarine ichthyoplankton has increased, from less than 1 article per year in the 1950s to more than 30 articles per year in the 2020s. The keyword used most commonly was 'community structure' and 'dynamics' and the word used most recently was 'climate change'. Regarding the geographical distribution of the studies carried out on estuarine ichthyoplankton, USA had the most (32.9% of all studies), followed by Australia (8.1%), South Africa (6.1%), Brazil (5.6%), Japan (5.1%), China (4.9%), Canada (4.8%), and Portugal (4.8%). Salinity and turbidity were the main factors affecting the ichthyoplankton community structure in estuaries. Climate change indirectly affected the community structure of estuarine ichthyoplankton by changing the spawning time, spawning location, and hatching time of species. The movement of spawning sites poleward and the advance of spawning time showed a consistent trend. In addition, the development of DNA barcoding techniques will be a useful supplement to traditional taxonomic methods for identifying ichthyoplankton and will provide new opportunities for the development of systematic taxonomy in this field. Our review contributes to a broader understanding of estuarine ichthyoplankton and provides theoretical support for estuarine environmental protection and the sustainable use of estuarine fishery resources.

Keywords: estuary, environmental factors, human activities, climate change, DNA barcoding, fish eggs, community structure, larvae

1 INTRODUCTION

Estuaries are the most productive and nutrient-rich ecosystems on Earth. Many species complete part or all of their life history in estuaries, and they are especially important foraging and breeding habitats for many fish species (Sheaves et al., 2015; Xian et al., 2016; Lefcheck et al., 2019). However, owing to their unique geographical location, they have been subject to human development for millennia (Limburg, 1999; Lotze, 2010). At present, approximately 40% of the world's population lives in coastal areas (Barragán and de Andrés, 2015). In some estuarine areas, the populations of more than 90% of economically important species, including fish, have been exhausted, and the overall biomass is less than 50% of the historical abundance. The main driving factors of this change are the overexploitation of resources and the loss of habitat (Lotze et al., 2006). Therefore, to improve decision-making for estuarine ecological management and sustainable use of resources, more baseline information is needed.

The ichthyoplankton stage (including fish eggs and larvae) is important for the growth and development of estuarine communities and can change quickly in response to environmental variations (Shan et al., 2004). Although this stage in the fish life history is short, it is the most vulnerable stage in the whole development cycle (Shao et al., 2001; Jiang et al., 2006a). The quantity and survival of ichthyoplankton reflects the biomass and interannual dynamics of future fish stocks (Butler et al., 2003; Song et al., 2019). It provides the basis for the recruitment of fish stocks and the sustainable use of fishery resources (Chambers and Trippel, 1997; Cao et al., 2007). Moreover, as a major predator and important consumer of planktonic (especially zooplankton) of secondary production (Monteiro et al., 2021), ichthyoplankton play an important role in the energy transfer of estuarine ecosystems (Wan and Sun, 2006). Ichthyoplankton are, thus, a key link in the aquatic food web (Wan and Jiang, 2000). Investigating and evaluating the ichthyoplankton community not only lays a foundation for understanding the status of fish stocks, determining spawning sites and spawning cycles, and clarifying fishery management, but also helps to clarify the energy flow and material circulation of estuarine ecosystems.

Owing to the limitations of previous scientific and technological methods, early research reports on estuarine ichthyoplankton were mainly descriptions of ecological habits, species composition and distribution (Jones and Menon, 1951; Chandra, 1962). After the 1970s, studies began to focus on the life history and morphological functions (Hickling, 1970), ecological habits (Blaber, 1997), species composition and distribution characteristics (Able, 1978; Melvillesmith and Baird, 1980) of estuarine ichthyoplankton. Since the 1980s, factors affecting the distribution of ichthyoplankton have been considered. For example, turbidity was found to be one of the main factors affecting their distribution (Boehlert and Morgan, 1985). Salinity was also an important environmental factor affecting the distribution of ichthyoplankton in estuaries (Locke and Courtenay, 1995; Zhang et al., 2016). In addition, the quantity and distribution of copepods, which are the main food source for ichthyoplankton, played an important role (Islam et al., 2006; Jiang et al., 2006). What's more, the breeding migration of offshore fishes was one of the important recruitment sources for estuarine nursery areas (Schilling et al., 2021). Therefore, the distribution of ichthyoplankton in estuaries was jointly determined by a variety of environmental factors such as temperature, salinity, dissolved oxygen, food, runoff and climate (Xiao et al., 2013; Sloterdijk et al., 2017).

Human activities, such as overfishing, dam construction and environmental pollution, are also important factors affecting estuarine ichthyoplankton (Shan et al., 2004). Overfishing reduces the adult stocks, which weakens the function of estuarine nurseries (Yu et al., 2018). Dam construction changes the amount of sediment—especially fine sediment—entering the sea from the estuary, which leads to a decline in the self-purification capacity of the estuary (Yang et al., 1992). Environmental pollution, caused by the discharge of industrial wastewater and domestic sewage (Guan et al., 1992), has changed the nutritional structure of estuarine water bodies (Pombo et al., 2002), thus destroying the spawning and breeding grounds of fish (Yao, 1995). Recently, climate change has been shown to have a subtle influence on the distribution of ichthyoplankton in estuaries (Thaxton et al., 2020). For example, the increase in the sea surface temperature has led to a northward movement of spawning sites and an advance of the spawning period (Zhang Z. et al., 2020). Therefore, exploring the impact of climate change on changes in ichthyoplankton community structure in estuaries has become a new research focus.

Although ichthyoplankton play an important ecological role, identifying individual species is still difficult (Zhang et al., 2015). At present, more than 36,058 fish species have been identified as adults (Fricke et al., 2021), but only approximately 10% of these can be identified as larvae and postlarvae, while less than 10% of eggs can be identified to species (Shao et al., 2001). Owing to the lack of specific features that can be used for morphological classification, little research has been carried out on the morphological classification of ichthyoplankton (Peterson and Lietz, 2017). Generally, eggs from different species are collectively referred to as 'fish eggs' in the investigation and assessment of fishery resources, resulting in inaccuracies in related work such as resource assessment, population dynamics research and spawning site identification (Shao et al., 2001; Zhang et al., 2015). Understanding how to identify ichthyoplankton species efficiently and accurately is essential for fishery-related research.

Scientific and technological progress has greatly improved the accuracy of ichthyoplankton identification. For example, the development of scanning electron microscope technology allows researchers to observe the egg membrane structure of fish eggs and identify species (Gao, 2015). In recent years, DNA barcoding has become an effective method for fish identification (Hebert et al., 2003). Tautz first proposed that DNA sequences could be used for species identification or classification (Tautz et al., 2002). Subsequently, studies have found that the application of DNA barcoding can greatly improve the accuracy of species identification (Pegg et al., 2006;

Valdez-Moreno et al., 2010; Ko et al., 2013; Zhou et al., 2017; Liu et al., 2021). The growth of various fish genetic sequences collected by global shared gene databases, such as DNA Data Bank of Japan, European Molecular Biology Laboratory and GenBank, has provided a substantial number of comparable adult fish homologous DNA sequences which can be used to identify ichthyoplankton, and the accuracy of DNA barcoding techniques in this field will continue to increase (Lin et al., 2018). The simplicity and efficiency of DNA barcoding is helping its growth as a new technique to study ichthyoplankton.

The aim of this review is to evaluate the status of research on ichthyoplankton in estuarine ecosystems, explore changes in the ichthyoplankton community structure and its influencing factors. The research gaps and recommendations for future research are also presented.

2 METHODS

A scientometric and systematic review was carried out using the 'Web of Science' 'China National Knowledge Infrastructure', 'PubMed', 'Scopus' and 'Engineering Village' databases. The following terms were used to identify in the title or abstract or keywords, refine and organize existing literature: ('ichthyoplankton' or 'egg' or 'larva' or 'larvae') and ('fish') and ('estuary' or 'estuarine' or 'estuaries'). The detailed search conditions used in this study and output results from each database are showed in **Supplementary Materials 1** (**Table S1**) and **Supplementary Materials 2** respectively. Papers published up to April 2022 were considered, while technical reports, academic theses, book chapters and scientific events summaries were excluded (**Figure 1**). A total of 2, 314 articles were retrieved from the databases. After screening and exclusion (reviews, technical reports, protocols, grey literature, did not fit the objectives, letters or short communications and duplicate articles), 836 articles were systematically analyzed according to the following parameters: 1) year of publication; 2) authors; 3) geographical location of the study (according to the location of the corresponding author); 4) subject (according to keywords); and 5) citations. The data concerning community structure (i.e., ecological categorization, species composition, temporal and spatial distribution), affecting factors (i.e., temperature, salinity, overfishing, pollution and climate changes) were also summarized.

To understand the relationship between the countries and the most influential researchers concerned with ichthyoplankton in estuarine ecology, a cluster analysis among (i) the countries and (ii) the most influential researchers in the study area were performed using the VOSviewer software (version 1.6.15; Centre for Science and Technology Studies, the Netherlands). The inclusion criteria for this analysis were that the country (occurrence) and author (citation) were recorded at least 5 time and 50 times, respectively, among the analyzed studies. The VOSviewer software generates a network whose visualization is based on nodes and connections, with the diameter of each node indicating the volume of (i) publications per country and (ii) citations of the referred author, while the distance between two nodes indicates the approximate intensity of the relationship between them (the stronger the relationship, the shorter the connection distance). Clusters are grouped by different colors (van Eck et al., 2014).

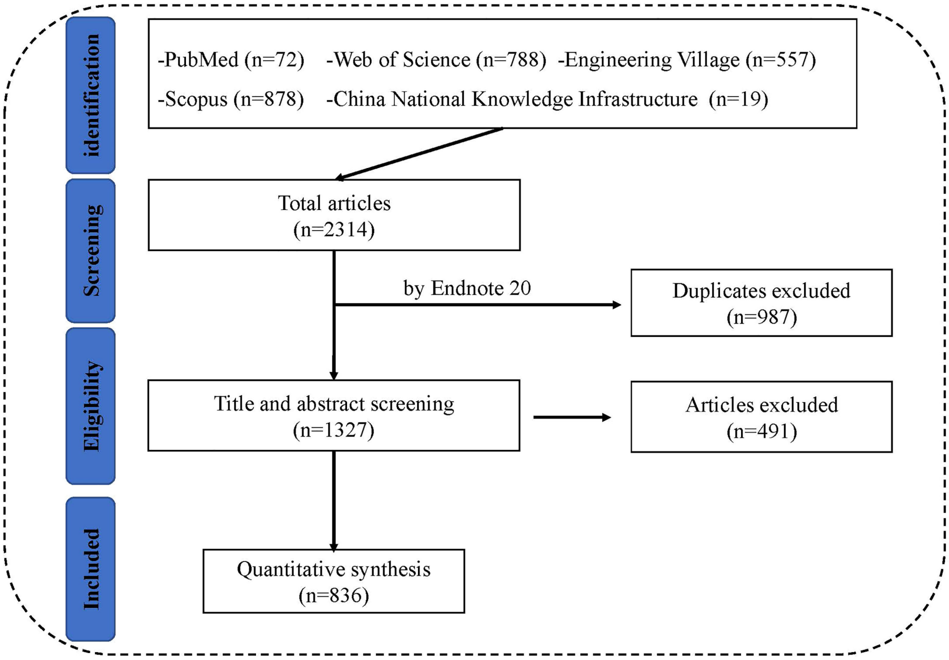

FIGURE 1 | Systematic review methodology used in this study.

3 EVALUATION OF ICHTHYOPLANKTON IN ESTUARINE ECOSYSTEMS

3.1 Historical Overview

Figure 2 represents the absolute and cumulative number of papers published until April 2022. The number of papers on estuarine ichthyoplankton increased year by year, especially after 1990s. The earliest full text in the database appeared in 1951 and it described and illustrated the larval development of the Indian shad until it became a juvenile (Jones and Menon, 1951). **Figure 3** represents the clustering relationship between keywords (appearing more than 10 times). The diameter of the node indicates the volume of publications, and the connections indicate the intensity of the relationship between the countries. Colors represent the time when keywords appeared. The keyword used most was 'community structure' and 'dynamics' (the largest node diameter), and the keyword used latest was 'climate change' (the lightest color), mainly because the impact of climate change on estuarine ichthyoplankton is a long-term process (Zhang Z. et al., 2020). The cluster analysis with the greatest centrality among the researchers in this study area can be seen in **Figure 4**. The most cited authors (largest node diameter) among all the studies examined were A.K. Whitfield (n = 341; 10.94%), followed by S.J.M. Blaber (n = 162; 5.20%), K.W. Able (n = 143; 4.59%) and N.A. Strydom (n = 142; 4.56%).

3.2 Geographical Overview

Regarding the geographical distribution of all studies carried out on estuarine ichthyoplankton, USA stands out (32.9% of the studies), followed by Australia (8.1%), South Africa (6.1%), Brazil (5.6%), Japan (5.1%), China (4.9%), Canada (4.8%), and Portugal (4.8%) (**Figure 5**). Another 66 countries have articles published on the topic; however, 23 countries (34%) presented only one publication. The cluster analysis performed with these data showed a strong relationship among USA, Australia and Brazil, for which the nodes were more expansive and had stronger connectivity (**Figure 6**). Interestingly, among the 26 countries with more than five publications evaluating estuarine ichthyoplankton, 18 countries (69%) were classified as developed countries, suggesting a lack of investment in education, science and technology in developing countries worldwide. **Figure 7** represents the research status of ichthyoplankton in estuaries around the world and systematically classifies the reports from countries with more than 30 articles (i.e., the top 10 countries with the largest number of articles). The results show that among these 10 countries, the research focus is on the impact of environmental factors on the community structure of estuarine ichthyoplankton, especially in China, France, Brazil and Portugal (accounting for more than 60% of the total number of articles published in the top 10 countries). At present, there are few studies on the impact of climate change on community structure, and the application of DNA barcoding for the identification of ichthyoplankton has not been popularized.

4 STUDIES ON THE COMMUNITY STRUCTURE OF ESTUARINE ICHTHYOPLANKTON

Community structure is one of the important studies on the estuarine ichthyoplankton. In this study, the ecological

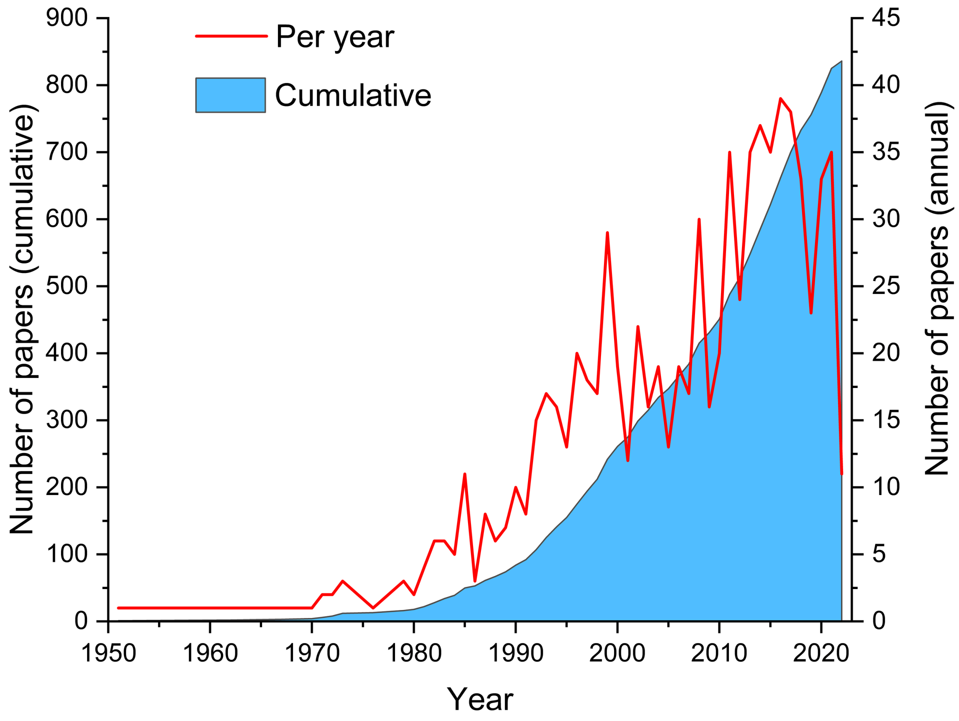

FIGURE 2 | Number of included estuarine ichthyoplankton papers (annual and cumulative) published between 1951 and 2022.

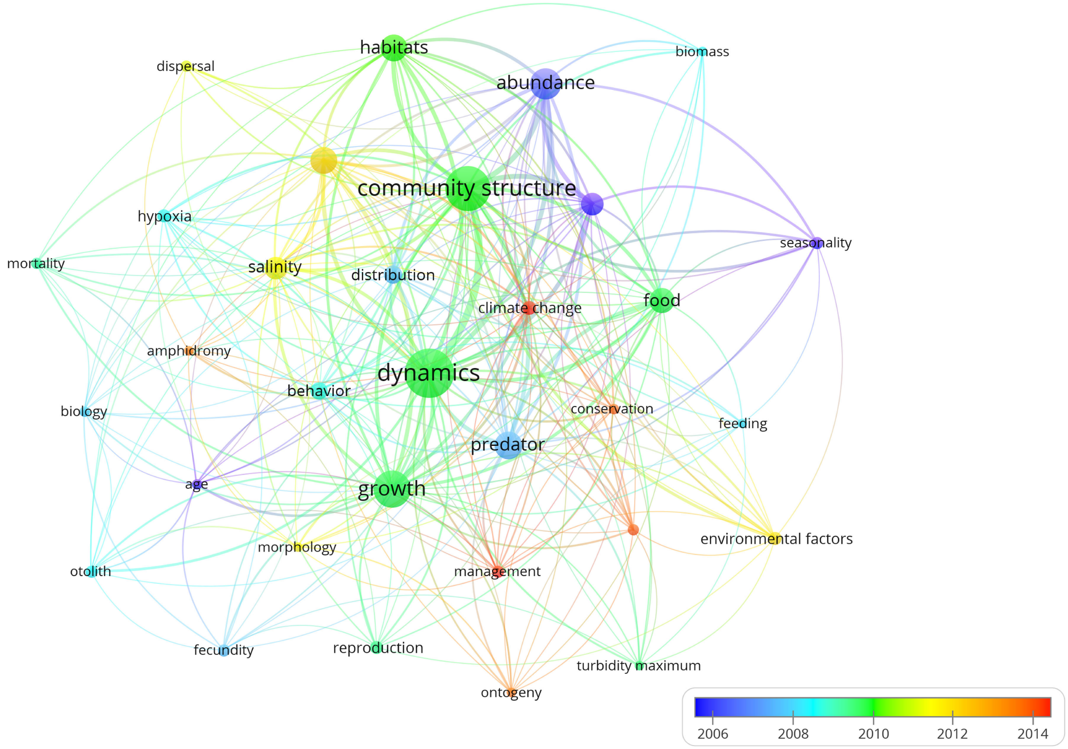

FIGURE 3 | Cluster analysis showing the most important estuarine ichthyoplankton related keywords used in research papers a minimum of 10 times. The diameter of the node indicates the volume of occurrences and the connections indicate the intensity of the relationship between the keywords.

categorization, species composition, temporal and spatial distribution of ichthyoplankton and the application of emerging identification methods (DNA barcoding) were classified under the broad topic of community structure. 480 of total 836 literature results were reported on community structure, including 20 on ecological categorization, 159 on species composition, 266 on temporal and spatial distribution, and 37 on application of DNA barcoding (**Table 1**).

4.1 The Ecological Categorization of Estuarine Ichthyoplankton

There are many biological classifications of estuarine ichthyoplankton communities in many different types of estuaries. Generally, communities can be divided into different ecological or functional groups according to different characteristics such as spawning habits, temperature and salinity tolerance, migratory habits and spatial distribution (Xian et al., 2016). For example, Yang et al. (1990) and Luo (1994) divided the ichthyoplankton in the Yangtze Estuary into four ecological categories according to the ecological habits and distribution characteristics of larvae and juvenile stages. These categories are generally recognized by other Chinese researchers (Liu et al., 2008; Zhang et al., 2015). Potter et al. (1990) and Whitfield (1989) classified ichthyoplankton into five types according to their habits and the relationship between spawning area of estuarine fish and estuaries, respectively. Islam and Tanaka (2006) classified the ichthyoplankton of the Chikugo estuary in Japan into four groups according to different types of salinity adaptation. Wang et al. (2020) classified the ichthyoplankton of Shijiu Port (China) into warm-temperature and cold-temperature species according to the parental thermophily and into demersal fish and pelagic fish according to space distribution characteristics. The first two classification methods are the most commonly used, and they both have similar classification criteria and high similarity of classification results (**Table S2** in **Supplementary Materials 1**). However, there is no international common classification standard on the ecological categorization of estuarine ichthyoplankton. Therefore, there is a need to integrate an understanding of community structure in terms of ecological categorization to provide more comprehensive information.

4.2 Species Composition of Estuarine Ichthyoplankton

As estuaries are the sites where rivers enter the ocean and they reflect land–sea interactions (Zhuang, 2006), they are rich in nutrients and food sources, which provide suitable conditions for the breeding of fish (Huang et al., 2017). Thus, the species and number of ichthyoplankton living in an estuary are determined by the environmental characteristics and material sources (Shan et al., 2004). The specific ichthyoplankton communities formed in estuaries differ from other marine areas owing to the interaction of freshwater runoff and tidal currents (Whitfield, 1994). A common characteristic of ichthyoplankton communities in

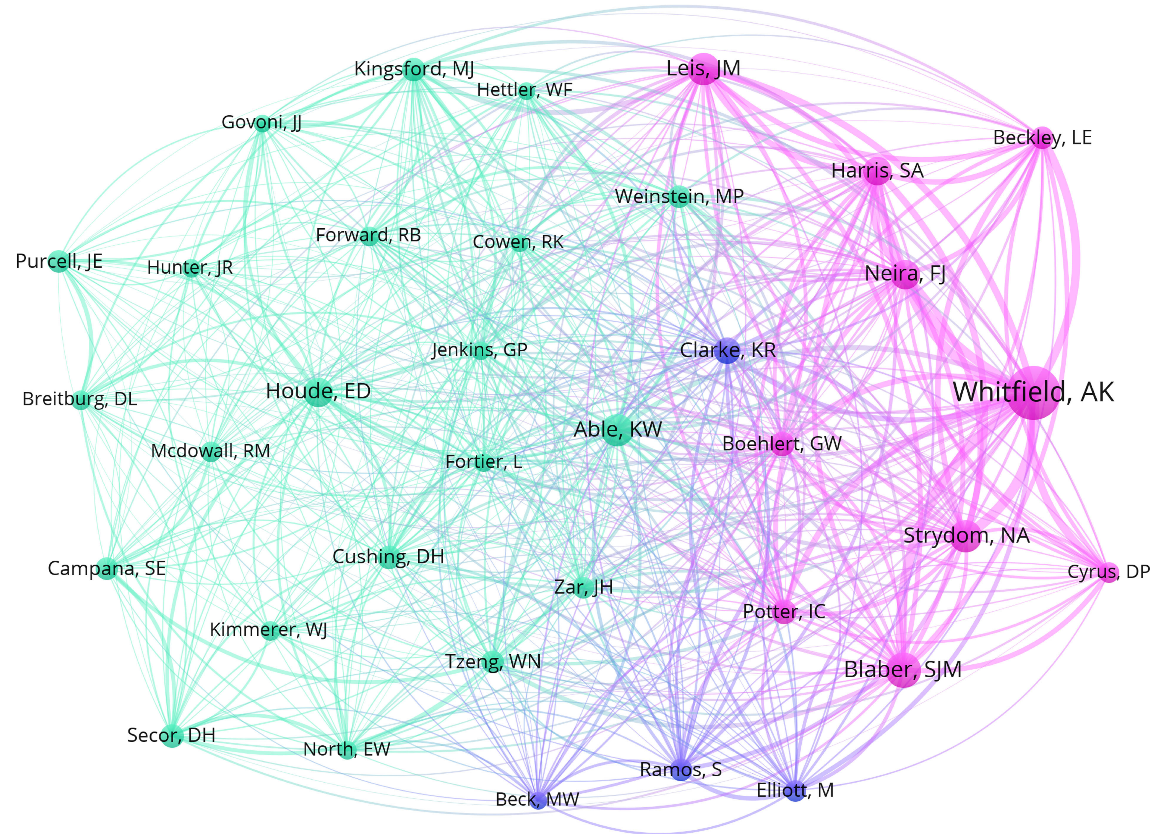

FIGURE 4 | Cluster analysis of ichthyoplankton scientists with more than fifty citations between 1951 and 2022. The diameter of each node represents the total number of citations by each scientist and the connections indicate the intensity of collaboration between researchers.

estuaries is a mix of rare and highly abundant species (Gaughan et al., 1990; Harrison and Whitfield, 1990; Pfirrmann et al., 2021). Many studies have shown that ichthyoplankton communities in warm water estuaries are dominated by Gobiidae, which live in estuaries, and Clupeidae and Engraulidae, which lay eggs seasonally in estuaries (Talbot and Able, 1984; Drake and Arias, 1991; Monteleone, 1992; Harris and Cyrus, 2000; Strydom et al., 2003; Bonecker et al., 2019; Zhang et al., 2019; Amezcua et al., 2020; Chermahini et al., 2021).

The species composition of ichthyoplankton communities varies according to the environmental conditions of each estuary (Shan et al., 2004). The Yangtze Estuary has the most comprehensively studied ichthyoplankton communities in China (Zhang et al., 2015). Since the 1980s, abundant work has been done on the community structure of ichthyoplankton in this area. By comparing the research results from the 1980s with more recent work, it is clear that the quantity of existing ichthyoplankton species has declined sharply in the Yangtze Estuary. Although Engraulidae is still the dominant species in this region, some other species, such as Sciaenidae, have begun to increase in the past decade (**Table 2**). These surveys show that the species composition and community structure of ichthyoplankton in the Yangtze Estuary have changed remarkably, mainly through the reduction in species numbers and the replacement of dominant species (see examples in **Table 2**). However, there are relatively few research reports on ichthyoplankton in other estuaries in China, except in the Jiujiang Estuary (Jiang and Chen, 1993), Taiwan (Tzeng and Wang, 1993), Laizhou Bay (Song et al., 2010), the Pearl River Estuary (Xiao et al., 2013) and the Yellow River Estuary (Bian et al., 2010; Song et al., 2019). Therefore, more attention should be paid to the study of these estuaries in the future, to understand the community structure of their ichthyoplankton.

The dominance of the estuarine ichthyoplankton assemblages by members of the Engraulidae, Clupeidae and Gobiidae can be attributed to these taxa spawning in estuaries and being represented mainly by preflexion and flexion larvae that are easily sampled by plankton nets. Many marine taxa that recruit into estuaries as early juveniles are seldom sampled because they tend to be able to avoid most plankton nets. So, the ichthyoplankton community structure as recorded by plankton nets is biased towards those species that are represented in estuaries by early larval stages (**Table 3**). Moreover, the species composition and abundance in two regions with similar environmental conditions and geographical locations is also similar (de Morais and de Morais, 1994; Korsman et al., 2017). For example, a report compared the composition of several estuarine areas in southwestern Australia and southeastern Africa, which were at

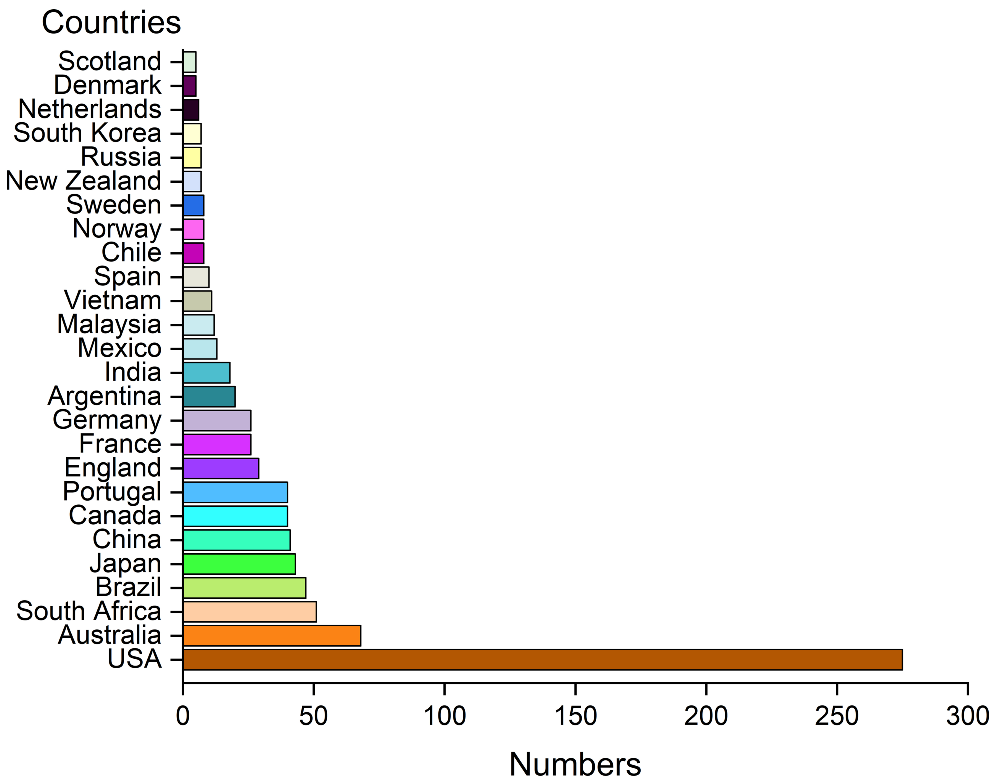

FIGURE 5 | Number of papers per country evaluating estuarine ichthyoplankton, from 1951 to 2022, with at least five occurrences.

similar latitudes (lower than 30°S) and flowed into the Indian Ocean, and found that Clupeidae, Mugilidae, Atherinidae and Gobiidae were important families in these areas (Potter et al., 1990). Similarly, a study comparing the composition of ichthyoplankton in seven permanently open estuaries and five temporarily open estuaries along the coastline of the Eastern Cape of South Africa found that the majority of ichthyoplankton appearing in the two types of estuaries were Clupeidae and Gobiidae (Strydom et al., 2003). New research has confirmed this conclusion (Korsman et al., 2017; Pfirrmann et al., 2021). However, other studies have reported different results. The species richness in the mangrove estuaries of the Western Indo-Pacific was higher than that of tropical Atlantic mangrove estuaries (Robertson and Alongi, 1992). The diversity of larvae in the Sine-Saloum Delta (Senegal) was lower than that of other tropical estuaries (Sloterdijk et al., 2017). This may be caused by large differences between one or more environmental conditions such as temperature, salinity or climate change. Therefore, the ichthyoplankton community structure presents particular distribution characteristics because of the differing adaptability of ichthyoplankton to diverse types of estuaries.

4.3 Temporal and Spatial Distribution of Ichthyoplankton in Estuaries

Estuarine areas have complex and variable physical, chemical and hydrological conditions, with environmental factors that change dramatically in time and space (Harris and Cyrus, 1995; Hettler and Hare, 1998). The estuarine ichthyoplankton communities also change in time and space in line with different fish reproductive seasons and environmental factors (Harris et al., 2001; Ren et al., 2021).

There are notable seasonal variations in the composition, abundance and spatial distribution of ichthyoplankton communities (Harris et al., 1999). Generally, the abundance of estuarine ichthyoplankton reaches its peak in spring or summer (Kindong et al., 2020; Monteiro et al., 2021), because these are the reproductive seasons for most fish (Sabates et al., 2007; Primo et al., 2012; Korsman et al., 2017). For example, in the Yangtze Estuary, fish eggs, larvae and juveniles appeared throughout the year, but mainly in spring and summer (Liu and Xian, 2010; Jiang et al., 2013). The number of fish eggs was highest in spring, while the number of larvae and juveniles was relatively small; in summer, the number of fish eggs decreased, while larvae and juveniles increased. The species composition of eggs, larvae and juveniles in different seasons was also notably different (Xian and Luo, 2015; Zhang et al., 2019). Seasonal variation and changes in the quantity of ichthyoplankton species in the Yangtze River were all restricted by changes in hydrological factors, such as runoff and interactions among the Yangtze River, the Yellow Sea cold water mass and the Taiwan warm current (Yang et al., 1990). In addition, the seasonal rhythm of variations in ichthyoplankton was also an adaptation in the distribution of

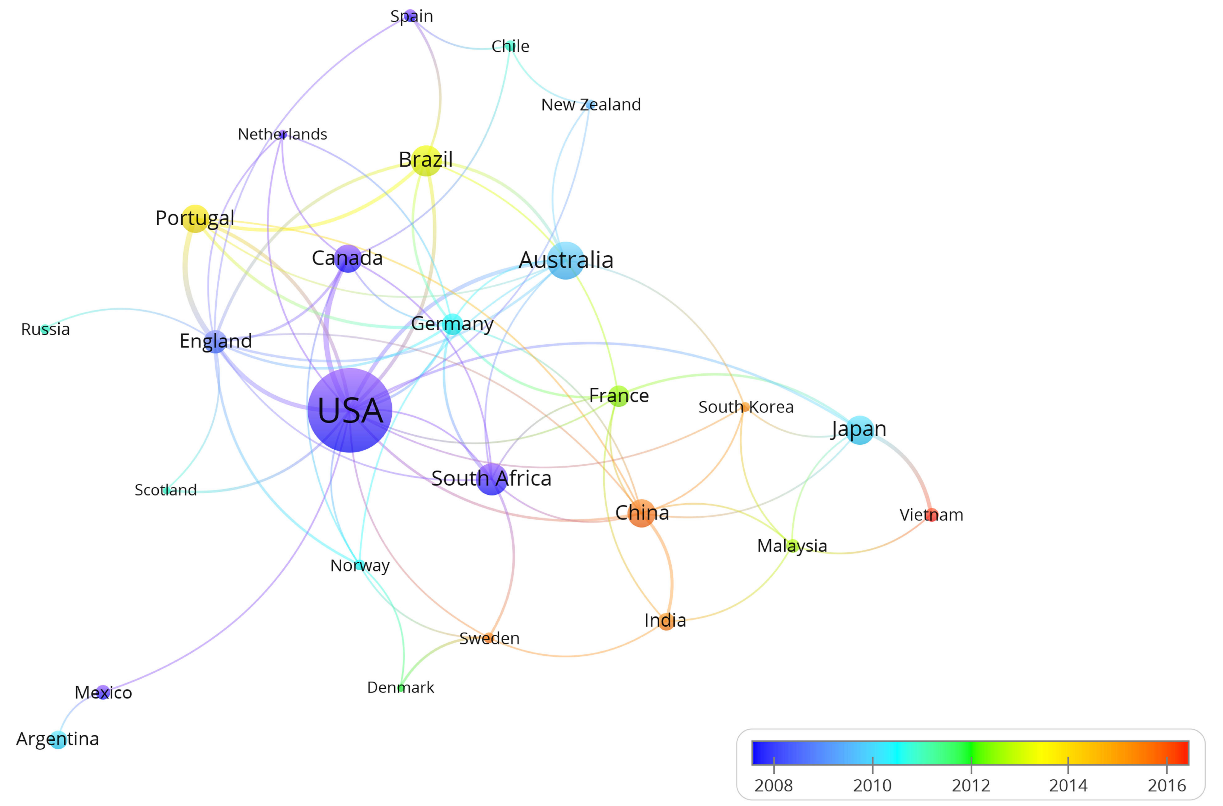

FIGURE 6 | Cluster analysis of the countries with studies (more than 5 literatures) evaluating estuarine ichthyoplankton. The diameter of the node indicates the volume of publications and the connections indicate the intensity of the relationship between the countries.

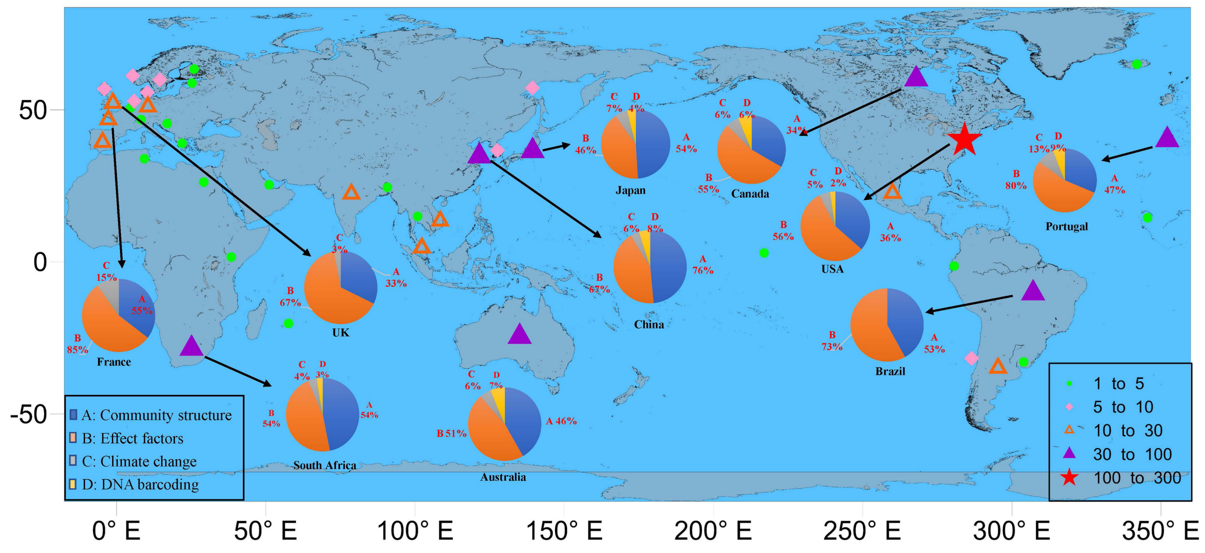

FIGURE 7 | The research status of ichthyoplankton in estuaries around the world and systematically classifies the reports of countries with more than 30 articles (i.e. the top 10 countries with the largest number of articles).

TABLE 1 | Number of relevant literatures on different topics.

Topics	Minor topics	Numbers
Community structure	Ecological categorization	20
	Species composition	159
	Temporal and spatial distribution	266
	DNA barcoding	37
Effect factors		
a. Natural factors	Temperature or salinity	310
	Turbidity	56
	Hydrodynamic	177
	Food	128
	Predator	53
	Climate change	30
b. Anthropogenic factors	Construction of dams	6
	Overfishing	13
	Pollution	47

dominant species in time to avoid intense competition and make full use of food resources (Shan et al., 2004). The seasonal distribution of ichthyoplankton was also closely related to environmental factors such as temperature, salinity, depth, chlorophyll a and freshwater input (Wang et al., 2017; Gao et al., 2018).

The spatial distribution of ichthyoplankton is often characterized by the heterogeneity of the horizontal distribution and vertical stratification. This is related to the ecological habits and physiological changes (such as species and development period) of larvae and juveniles, as well as to changes in the external environment (such as prey, light, runoff and tides) (Yang et al., 2006). The difference in horizontal distribution is related to variations in the species and abundance in different regions, as well as to the ecological categorization of species in different regions (Zhang et al., 2016). For example, most of the ichthyoplankton in the Yangtze Estuary in spring belong to the brackish water type, which mainly propagated in the lower Yangtze River channel and the marine area near the estuary with water temperatures of 12.0–22.0°C and salinity of 0.1–12.0 (Yang et al., 1990). In autumn, the ichthyoplankton in the Yangtze Estuary are mainly coastal species, followed by brackish water and inshore species; freshwater ichthyoplankton are the least common (Ding and Xian, 2011). In addition, the ichthyoplankton in the lower estuary mostly belong to marine spawning fish, while those in the upper estuary belong to estuarine spawning fish (Neira and Potter, 1992).

The number of ichthyoplankton species in the estuarine area decreases substantially from the downstream to the upstream. For example, it was found that the monthly average number of species in the lower reaches of the Swan Estuary in Southwestern Australia was far higher than that in the upper reaches of the estuary (Neira and Potter, 1992). However, this distribution pattern is not universal. For example, the highest abundance of ichthyoplankton was found in the upper Lima Estuary (Portugal) (Ramos et al., 2006). Similarly, in the Caeté Estuary (Brazil), the peak density of larvae and juveniles occurred in the upper estuary in the dry season, and the peak number of species occurred in the upper estuary between the dry and wet seasons (Barleta-Bergan et al., 2002). The results in the Jiulong River Estuary (China) showed that the highest number of fish eggs was in the upper estuary, and the highest number of species was in the lower estuary. The larvae and juveniles with the highest number and the greatest diversity of species were relatively concentrated in the middle of the estuary (Jiang and Chen, 1993). Therefore, the horizontal distribution pattern of ichthyoplankton in estuaries is related to both salinity and runoff (Sanvicente-Anorve et al., 2000; Costa et al., 2016).

The difference in the vertical distribution is not only related to the ecological preferences of different species but also to the water structure and fluctuation; for example, the herring family generally live in the upper and middle layer of the estuary, while Gobiidae inhabit the bottom of estuarine and coastal waters (Muhling et al., 2007). In addition to examining the vertical

TABLE 2 | Species composition and dominant species of ichthyoplankton in different periods in the Yangtze estuary.

Survey time	Results	Dominant	References
1985-1986	53 families, 82 genera, 94 species	Engraulidae	Yang et al., 1990
2002	9 orders, 15 families, 19 genera, 20 species	Engraulidae	Zhu et al., 2002
2000-2003	10 orders, 30 families, 45 species	Engraulidae, Synodontidae and Sciaenidae	Jiang et al., 2006
1999 and 2001	11 orders, 18 families, 32 species	*Coilia mystus, Engraulis japonicus, Chaeturichthys hexanema, Allanetta bleekeri*, and *Trachidermis fasciatus*	Liu et al., 2008
2007	12 orders, 28 families, 45 species	Engraulidae	Liu and Xian, 2010
1998, 2000, 2002, 2003, 2004, 2007 and 2009	10 orders, 19 families, 33 species	Engraulidae, Gobiidae and Salangidae	Zhang et al., 2016
2006-2007	16 orders, 48 families	*Engraulis japonicas, Coilia mystus*, and *Benthosema pterotum*	Wang et al., 2017
2012	5 orders, 9 families, 15 species	*Engraulis japonicus*	Zhang et al., 2019
2012-2014	18 family, 38 species	Sciaenidae	Kindong et al., 2020

TABLE 3 | Species composition and dominant species of ichthyoplankton in different periods and regions.

Survey time	Study areas	Results	Dominant	References
1973-1975	St. Lawrence estuary, Canada	14 families, 25 species	Osmerids, Gadids, Cottids, Cyclopterids, and Pleuronectids	Able, 1978
1983	the Hillsborough, USA and St. Lawrence estuaries, Canada	14 families, 22 species	Limanda ferruginea, Alosa pseudoharengus, Scomber scombrus and Autogolabrus adspersus	Powles et al., 1984
1992	the Miramichi estuary, Canada	14 families, 20 species (or genus)	Osmerus mordax, Alosa pseudoharengus and Alosa aestivalis	Locke and Courtenay, 1995
1995	St Lucia estuary, South Africa	44 families, 85 species	Gobiidae and the Clupeidae	Harris and Cyrus, 1995
2016	the estuary of North Inlet-Winyah Bay, USA	59 species	Gobiidae	Pfirrmann et al., 2021
1990s	The Presidio River estuary, USA	none	Engraulidae and Clupeidae	Amezcua et al., 2020
2002	The Caeté estuary, northern Brazil	28 families, 63 genera	Anchovia clupeoides (Sciaenidae) and Stelifer microps (Engraulidae)	Barleta-Bergan et al., 2002
2004	The La Plata estuary, South America	none	Sciaenidae, Clupeidae, Engraulidae, Cynoglossidae and Decapteridae	Berasategui et al., 2004
2012	Guayaquil Bay, South America	3 families, 36 species	Engraulidae	Calderón-Peralta et al., 2020
2006	The Lima estuary, Portugal	20 families, 50 genera	Gobiidae and herring	Ramos et al., 2006
2018	The Mahury estuary, France	13 families, 67 species	Engraulidae, Gobiidae, Chancellidae and Sciaenidae	Rousseau et al., 2018
2003-2004	The northern Persian Gulf estuary, India	30 families	Clupeidae, Gobiidae and Sillago	Chermahini et al., 2021

distribution of the ichthyoplankton community in estuaries, studies are currently focusing on individual activities such as the depth trend of some species and their diurnal periodic vertical movement. For example, the larvae of *Anchoa mitchilli* and *Gobiosoma bosc* in the Hudson estuary (America) showed periodic vertical movement behavior over the day and night (Schultz et al., 2003). The vertical migration of larvae and juveniles may be used to avoid cold and low-salinity surface water (Ramos et al., 2006). In addition, vertical migration could help the larvae and juveniles use the two-layer circulation to maintain a dynamic balance and avoid being washed out of the estuary (Weinstein et al., 1980).

4.4 Application of DNA Barcoding in Estuarine Ichthyoplankton Identification

DNA barcoding is an effective method for species identification based on molecular biology techniques. It identifies species through differences in the sequence of standardized short gene fragments (Chu et al., 2019). Identification is possible if, first, the fragment is conservative enough to be amplified in a wide range with universal primers, and second, the fragment has enough variation to distinguish the DNA sequences of different species (Hebert et al., 2003). Compared with the traditional morphological classification methods, the biggest advantage of the DNA barcoding technique is that it can accurately identify individuals at different development stages, as well as species with high morphological similarity and individuals that are difficult to distinguish owing to the lack of morphological classification data (Liu et al., 2021). The application of this technique to the identification of ichthyoplankton can solve many problems that cannot be solved by traditional morphological classification methods. For example, Bian et al. used cytochrome oxidase subunit I sequence to identify fish eggs collected from seaweed in the Yellow Sea area, and determined that they were *Hyporhamphus sajori*, rather than *Strongylura anastomella*, which has a similar egg morphology, spawning time and geographical distribution (Bian et al., 2007).

However, DNA barcoding is not applicable for the identification of all fish. Some fishes, such as Epinephelinae and *Sillago*, are prone to hybridization (Lin et al., 2014). Therefore, it is difficult to identify them only from the cytochrome oxidase subunit I sequence, and joint labeling with other genes is required. In addition, because the databases are incomplete, some fish records have only 16S and 12S fragments, and the cytochrome oxidase subunit I gene cannot be identified to the species level (Li et al., 2017). For some related species, DNA barcoding needs to be combined with morphology, geography and molecular genetics to identify them accurately. A combination of traditional morphological identification and DNA barcoding can improve the accuracy and efficiency of ichthyoplankton species identification (Zhang G et al., 2020; Liu et al., 2021).

In summary, the development of DNA barcoding techniques will become a powerful supplement to the traditional taxonomy of ichthyoplankton and provide new opportunities for the development of systematic taxonomy in this field. The application of DNA barcoding techniques in ichthyoplankton can address the limitations of traditional morphological classification. Because DNA barcoding is a digital format, the sample identification process can be automated and standardized, reducing the need for expert input and establishing an easy-to-use database in a short time. Both taxonomists and non-professionals will be able to find species information on ichthyoplankton rapidly through the international database and identify potential hidden species or new species. The development of DNA barcoding techniques will greatly alleviate the limitations of ichthyoplankton morphological identification and the shrinking number of traditional taxonomists.

5 FACTORS INFLUENCING ICHTHYOPLANKTON COMMUNITY STRUCTURE IN ESTUARIES

The factors affecting the community structure of estuarine ichthyoplankton have been one of the most important concerns of researchers. In this study, we artificially divided the influencing factors into natural and anthropogenic factors. Natural factors include temperature, salinity, turbidity, hydrodynamic conditions, food, predators, and climate change. And the anthropogenic factors include construction of dams, overfishing and pollution. The results showed that 540 of 836 literatures were on factors affecting community structure, with temperature and salinity (310) being the most documented, followed by hydrodynamics (177) and food (128) (**Table 1**).

There are differing views on the reasons for changes in the ichthyoplankton community structure in estuaries. Many researchers believe that the regional change in fish communities is mainly caused by gradients of temperature, salinity and depth as well as different sediment types (Liu et al., 2008; Monteiro et al., 2021; Chermahini et al., 2021). However, other studies propose that individual behavior plays an important role in the distribution of ichthyoplankton (Costa et al., 2011; Munk et al., 2014). A few studies suggest that the spatiotemporal variation of the ichthyoplankton community is mainly related to the meteorological and seasonal characteristics of the ocean, especially in the middle latitudes (Hernández-Miranda et al., 2003; Thaxton et al., 2020). There are also reports that the horizontal distribution of larvae and juveniles in temperate coastal waters is related to the distribution of adults, as well as the location and type of spawning (floating or sinking) (Azeiteiro et al., 2006; Ribeiro et al., 2015). Other studies have found that in addition to temperature and salinity, suspended solids, suspended organic matter, chlorophyll a and runoff all affect the spatial structure of ichthyoplankton in estuaries (Faria et al., 2006; Ramos et al., 2006; Zhang et al., 2015). In addition, the annual cyclical changes of climate and hydrodynamics also have a strong impact on ichthyoplankton communities in estuaries (Sloterdijk et al., 2017; Gao et al., 2018). To review the contribution of each factor affecting the ichthyoplankton community structure in the estuary more clearly, we divided the factors into two types (natural factors and anthropogenic factors) to discussion.

5.1 Natural Factors

5.1.1 Temperature and Salinity

Temperature has a major and direct impact on fish reproduction, recruitment, physiology, growth and behavior (Sabates et al., 2006; Doring et al., 2018). These are important for the quantity and spatial distribution of ichthyoplankton (Bruno et al., 2014; Chermahini et al., 2021). Estuaries are generally shallow, and the temperature varies greatly, with both diurnal and seasonal variations. Thus, estuarine species that can adapt to a wide range of temperatures tend to be dominant (Yang et al., 2006). In temperate and subtropical estuaries, the peak of species numbers generally occurs in spring and summer (Primo et al., 2011; Wang et al., 2017). In other words, temperature affects the reproductive cycle and timing of adult fish (Holmes and Henderson, 1990; Palomera, 1992). Taking a simple example, in the Yangtze Estuary, the water temperature rose from spring (average of 19.9°C) to summer (average of 29.9°C), the food supply was plentiful, many fish spawned in the estuary, and the species and quantity of fish eggs and juveniles in the estuary increased greatly. In winter, the water temperature dropped (average of 16.6°C), the food supply was scarce, and the number of spawning fish and the species and quantity of fish eggs, larvae and juveniles was greatly reduced (Jiang and Chen, 1993). The peak abundance of larvae and juveniles usually occurred just before or after the maximum water temperature (Newton, 1996). Thus, the seasonal variation of temperature played a key role in the temporal variation of the juvenile fish community (Demirel, 2015).

Salinity is also an important environmental factor affecting estuarine organisms. For example, it affects the hatching period of fish. In some species, the hatching period is shortened with an increase in salinity, while in others it is prolonged with an increase in salinity; a few species are not affected by salinity (Wang and Zhang, 1998). Salinity not only affects the growth, development and reproduction of ichthyoplankton, but also the spatiotemporal distribution and abundance of species (Jiang et al., 2013; Lima et al., 2019). Salinity is a key abiotic factor determining the structure of the ichthyoplankton community in estuaries (Wooldridge, 1999; Campfield and Houde, 2011; Song et al., 2019). In estuarine areas, salinity is affected by runoff, wind, waves and tidal current, and has complex temporal and spatial variations. The special geographical conditions of estuaries and the inflow of potentially large amounts of fresh water determine that the salinity gradually increases with distance from the river mouth, and the different ecological categorizations and distributions of estuarine organisms often reflect the salinity gradient (Mouny and Dauvin, 2002). Generally, estuarine salinity is high in the dry season and low in the flood season. In the Caeté Estuary (Brazil), seasonal fluctuations in salinity caused changes in the number of ichthyoplankton species and community composition (Barleta-Bergan et al., 2002). Reduced salinity levels may cause a peak in the number of fish eggs and larvae, and low salinity coastal systems have a marked impact on the hatching and development of fish eggs and larvae in the Yangtze Estuary (Jiang et al., 2006). In addition, salinity can interact with organic compounds and modulate their toxicity, which is essential to ichthyoplankton growth in estuaries (Segarra et al., 2021).

5.1.2 Turbidity

Estuarine water carries substantial quantities of suspended particles, which result in high turbidity, especially when there is a large inflow of river water. Turbidity has an important impact on the temporal and spatial distribution of ichthyoplankton in estuaries (Costa et al., 2011). The most abundant species in the Large Swan Estuary

(Australia) were estuarine resident larvae and juveniles because of the turbid conditions in the upper estuary (Neira and Potter, 1992). Thus, turbidity can be considered as one of the most important factors affecting the density of estuarine species (Harris and Cyrus, 1995). The maximum turbidity zone of estuaries has been widely studied because it is a universal feature of estuarine dynamics (Schubel, 1968; Jager, 1999; Islam et al., 2006). This zone also has a high proportion of food organisms and is therefore more conducive for the feeding of ichthyoplankton (Shideler and Houde, 2014). In high turbidity areas, the probability of ichthyoplankton encountering predators is also reduced, which improves the survival rate (Parrish, 1989). Many fish rely on vision to catch their prey, and the level of light in turbid water can affect the behavior and predation of larvae and juveniles (Shoji et al., 2006; Bradbury et al., 2006; Chicharo et al., 2009). Accordingly, the maximum turbidity zone of estuaries often has the highest abundance of larvae and juveniles (North and Houde, 2003). In contrast, Faria et al. found a low density and abundance of ichthyoplankton in the maximum turbidity zone of the Guadiana Estuary on the Iberian Peninsula. However, this may have been caused by: a) high turbidity hindering feeding by some species; b) large mesh sizes in the net allowing many small individuals to escape; and c) the larvae and juveniles in the maximum turbidity zone moving deeper in the water during the day when the trawl was carried out (Faria et al., 2006). The maximum turbidity zone of the estuary can change over a short time scale in some seasons owing to the injection of fresh water and the effect of wind (North and Houde, 2003); this leads to an associated change in the ichthyoplankton community.

5.1.3 Hydrodynamic Conditions

Many marine fish migrate from open ocean spawning grounds to estuarine nursery grounds in their early life cycle stage (Churchill et al., 1999; Islam et al., 2007). Because estuaries are at the confluence of rivers and the ocean, the migration of ichthyoplankton is affected by complex hydrodynamic conditions, such as river runoff, tides, water masses and ocean currents. Estuaries pose a special challenge to the migration of ichthyoplankton because the speed of river runoff is usually faster than the swimming speed of larvae and juveniles (Forward and Tankersley, 2001; Schultz et al., 2003). Freshwater injection and the tidal action of seawater were found to be the two main factors determining the physical and chemical properties of estuarine ecosystems (Yang et al., 2006). Consequently, changes in estuarine hydrodynamic conditions not only affect the migration of ichthyoplankton, but also affect their community structure and distribution.

River runoff is a key factor in adjusting the structure and function of estuarine systems (Taylor, 1982). The change in estuarine runoff can cause many effects, including floodplain development, accelerated transport of organic matter, dilution and movement of pollutants, shifts in peak salinity and the formation of density gradients, changes in the residence time of some particles and biota in the estuary (Kimmerer, 2002), changes in topography, and changes in turbidity and dissolved oxygen levels. These effects influence the abundance and distribution pattern of estuarine organisms (Drinkwater and Frank, 1994; Grange and Allanson, 1995; Chiappa-Carrara et al., 2003; Monteiro et al., 2021). The location of the spawning center in the Yangtze Estuary tends to move nearshore or offshore depending on the amount of fresh water entering the sea, salinity and transparency (Yang et al., 1990).

Runoff was the main factor affecting the abundance and distribution of ichthyoplankton in the Guadiana Estuary (Spain and Portugal) before the construction of the Alqueva Dam (Portugal) (Faria et al., 2006). Although the inflow of fresh water is basically stable year after year, it can still affect the recruitment of some species of larvae and change the composition of the ichthyoplankton community (de Morais and de Morais, 1994). The relationship between species abundance and river runoff also varies because different species have different adaptations to the flow and time of runoff (Costa et al., 2007). For example, the abundance and survival rate of several estuary-dependent species increased with the injection of fresh water (Kimmerer, 2002). Whitfield found that ichthyoplankton abundance in Eastern Cape estuaries (southern Africa) increased with increasing riverine input (Whitfield, 1994). In Japan, the runoff from Chikugo River affected the recruitment of *Lateolabrax japonicus* in two ways: a) recruitment was increased by increasing the temperature and accelerating the growth of larvae and juveniles; and b) high inflows of runoff reduced the possibility of migration to the estuary by dispersing larvae and juveniles in the ocean, enhanced the predation activities of other organisms by reducing turbidity, and reduced the availability of predated zooplankton (Shoji et al., 2006).

The water level and currents in estuaries fluctuate periodically owing to the influence of tides in nearby coastal waters. A substantial quantity of seawater can flow into estuarine areas driven by the wind, thus changing the original habitat conditions for estuarine organisms and affecting their community pattern (Tzeng and Wang, 1993). The resulting estuary tides are usually larger and more complex than tides in the open ocean. Under the action of tides, the salinity of estuaries increases, especially in the middle and lower reaches, and the water body is relatively stratified with a high abundance of shallow marine organisms. If the effect of flushing water is strong, the salinity of the estuary decreases, and the water is better mixed. In this case, the dominant species of the biological community are mainly estuarine species, or even freshwater species (Yang et al., 2006). According to the relationship between tidal influences and species abundance, fish could be divided into two groups: a) at low tide, they are mainly freshwater species; and b) at high tide, they are mainly marine species. In general, at high tide, more species are found in the lower reaches of the estuary because many marine species enter the estuary with the tide (‘selective tidal stream transport’), increasing the species diversity (Kingsford and Suthers, 1996; Faria et al., 2006; Primo et al., 2012).

Tides not only affect the distribution and structure of ichthyoplankton communities, but also considerably influence the migration, predation, avoidance and reproduction of larvae and juveniles (Gibson, 2003). Seasonal species can be carried from the ocean to the estuary by tidal currents, but migration to the estuary can be hindered by high-throughput runoff, especially in the surface water layer. This effect often occurs in the subtropical estuaries of South America (Garcia et al., 2003). In tidal regions, animals with weak swimming abilities may accomplish efficient directed transport by ascending in the water column during the appropriate tidal phase and holding position on the bottom during the opposite tide. The behavior of modulating horizontal transport through timed vertical migration is termed 'selective tidal stream transport' (Walker et al., 1978) and is used by a number of species, including ichthyoplankton, living in tidally energetic regions. The interaction between tidal currents and larval behavior (vertical migration) also plays an important role in the upwelling movement and retention of plankton in the original habitat (Chen et al., 1997). Larvae and juveniles appeared in the upper layer of a water body at high tide and in the lower layer of a water body at low tide, which indicated that the larvae and juveniles were using the tide as a retention mechanism (Islam et al., 2007). For example, in the Swartkops estuary (South Africa), early juveniles of marine species which utilize the estuary as a nursery ground, such as *Rhabdosargus holubi*, *Liza richardsoni* and *Heteromycteris capensis*, enter the estuary on the flood-tide and actively migrate towards the banks to prevent being swept back out to sea (Beckley, 1985). Similarly, in Swartvlei estuary (South Africa), *Rhabdosargus holubi* enter the estuary mainly as postlarvae, and congregate along the margins or on the bottom where water current speeds are reduced (Whitfield, 1989b).

In addition to runoff and tides, other hydrodynamic conditions also affect ichthyoplankton in estuaries. For example, the reproduction of Engraulidae is restricted by the specific geographical location of the Yangtze Estuary and the variation of water potential in various other systems, such as the Yangtze River runoff, the Kuroshio warm current and the Yellow Sea cold water mass (Wu, 1989). Upwelling can make the nearshore seawater flow toward the ocean, thus delaying the replenishment of seawater farming land to the estuary as well as reducing the species diversity in the lower estuary (Ramos et al., 2006; Valencia et al., 2019). Hydrodynamic conditions such as the Kuroshio Current and upwelling can increase food supplies for the ichthyoplankton in estuaries, thus affecting their community structure (Huang et al., 2017).

5.1.4 Food

In the early life stages after hatching, fish rely on yolk as a food resource for a very short time. After a brief period of mixed nutrition, they switch completely to external food sources. For example, the larvae of marine fish mainly feed on copepods (Dagg and Govoni, 1996), while freshwater fish mainly feed on rotifers (Wang et al., 2006). Individual fish species select different food organisms at different growth and development stages. For example, in the Yangtze Estuary (China), the larvae and juveniles of *Coilia mystus* feed on zooplankton such as Cladocera and Amphipoda. And then their food composition changes gradually to the eggs and juveniles of fish such as *Larimichthys polyactis*, *Chaetorichthys stigmatias* and H*arpadon nehereus*, shrimps, copepods and Amphipoda, and other small animals, such as squid and squilla (Wang et al., 2006). Similarly, in the Sundays Estuary (South Africa), larvae also showed changes in diet at different stages of development (Strydom et al., 2014). From the perspective of spatial distribution, larvae and juveniles prefer to live in marine areas with a stable and reliable food supply of plankton (Whitfield, 1999).

In the Mira and Guadiana Estuaries (Portugal), the spatial and diurnal distribution of larvae and juveniles was related to the vertical and horizontal migration of food organisms (Esteves et al., 2000). The species and quantity of food organisms have an important impact on the ichthyoplankton community. Larvae and juveniles were found to gather in deep areas with a high food concentration (Shideler and Houde, 2014). According to Drake et al., stepwise multiple regression analysis of the spatial and temporal distribution of *Engraulis encrasicolus* showed that its main food source, *Mesopodopsis slabberi*, could explain 45% of its change in density (Drake et al., 2007). The peak abundance of larvae and juveniles in spring and summer was related to the large-scale reproduction of zooplankton after the flood season, because a large number of zooplankton provided a good food supply for young fish larvae and juveniles (Newton, 1996). In some estuarine ecosystems, the peak abundance of larvae and juveniles coincides with the peak of phytoplankton productivity and biomass (Livingston et al., 1997; Garcia et al., 2003).

5.1.5 Predators

In estuarine and marine ecosystems, adult fish, invertebrates, mammals and some zooplankton have a strong predation effect on ichthyoplankton. The complex feeding relationship has an important impact on ichthyoplankton communities, especially abundance. In the Yangtze Estuary, the feeding relationship between planktonic copepods and fish eggs and larvae determines that changes in abundance affect the quantity of fish eggs and larvae (Jiang et al., 2006). According to Esteves et al., the abundance of larvae and juveniles in the Mira and Guadiana Estuaries (Portugal) was positively correlated with the abundance of several invertebrates that prey on fish eggs and larvae (Esteves et al., 2000). Jellyfish are important predators of larvae and juveniles, and they are also important regulators of the zooplankton community structure in several ecosystems (Pereira et al., 2014). For example, the monthly decline in ichthyoplankton community abundance in 2002 (Guadiana Estuary, Portugal) was closely related to the increase in jellyfish abundance (Faria et al., 2006).

5.2 Climate Change

Ichthyoplankton are thought to be sensitive to climate change, and a number of studies have focused on the impact of climate change on the distribution and interannual change of ichthyoplankton communities (Zhang Z. et al., 2020). Stochastic climate events (cyclones) changed the community composition of ichthyoplankton in estuaries by bringing intense rainfall, which caused the distribution and abundance of estuary resident species and marine migratory species to change substantially (Martin et al., 1992). The seasonal changes in temperature and precipitation caused by climate change were the main reasons for the temporal differences of larvae and juveniles, which strengthens the supposition that interannual climate and hydrodynamic changes have a strong impact on the composition of estuarine ichthyoplankton communities (Ramos et al., 2006).

Global warming causes changes in the temperature, salinity, dissolved oxygen and other environmental factors, resulting in changes to the temporal and spatial distribution of ichthyoplankton (Sloterdijk et al., 2017). The increase in temperature may lead to earlier fish spawning (Thaxton et al., 2020), extension of the spawning time (Primo et al., 2011; Acha et al., 2012), shortening of egg hatching time (Hassell et al., 2008), early gonadal maturation (Thaxton et al., 2020) and northward expansion of spawning areas (Auth et al., 2018; Zhang et al., 2019).

Droughts and water shortages may reduce river runoff to the extent that the salinity stratification in estuaries is reduced, resulting in a decline in fish with strong dependence on estuary conditions, such as *Acanthopagrus butcheri* (Williams et al., 2013). This may have a substantial impact on the development and supply of larvae and juveniles (Primo et al., 2011). Climate change also causes hypoxia and ocean acidification, which greatly reduces the survival rate of ichthyoplankton embryos (Hassell et al., 2008; Valencia et al., 2019). The impacts of climate variability on ichthyoplankton assemblages will have consequences for marine pelagic food webs and fish population biology, namely recruitment (Monteiro et al., 2021).

The El Niño–Southern Oscillation is an irregular fluctuation that can affect the entire tropical Pacific as well as the global climate. It is a manifestation of ocean–atmosphere interactions, which leads to fluctuations in the wind, rainfall, thermocline depth and circulation, and ultimately affects the biological productivity and changes the feeding and reproduction of fish, birds and mammals (Fiedler, 2002). El Niño can affect the cold water mass of the Yellow Sea and the Taiwan warm current, altering the ocean temperature, salinity and food sources, and changing the location of the central spawning grounds and hence the temporal and spatial distribution pattern of ichthyoplankton in estuaries (Shan et al., 2004). A similar conclusion was reached in a study of the Central Gulf of California (Sánchez-Velasco et al., 2004). In addition, the El Niño phenomenon can affect the rate of recruitment of larvae and juveniles to the adult fish community. In an El Niño year, the recruitment rate is higher than the average level, but in the years before and after El Niño, the recruitment rate is lower than the average level (Franco-Gordoa et al., 2004; Acha et al., 2012). Therefore, under the influence of global climate change, the community structure, distribution range and life history characteristics of ichthyoplankton will undergo major changes.

5.3 Anthropogenic Factors

5.3.1 Construction of Dams

Over the past few decades, many large-scale dam construction projects have occurred in or near rivers and estuaries. These projects play an important role in economic development and social progress, but also have a considerable impact on the ecological environment of estuaries (Burns et al., 2006). The construction of dams in the main stream of a river can change the flow pattern of the whole river, particularly the distribution of runoff and sediment downstream of the dam, which results in changes in the amount of runoff, sediment and nutrients flowing into the estuary and sea (Shan et al., 2004). This alters the hydrological dynamics and sediment deposition processes of estuaries and their adjacent coasts, thus changing the spatial pattern of ichthyoplankton in the estuary (Faria et al., 2006). For example, large-scale water conservancy projects in the main stream of the Yangtze River altered the original seasonal distribution of runoff. The flow velocity, sediment discharge, salinity distribution and bottom material conditions were all changed (Shan et al., 2004). Owing to the backflow of seawater, the salinity in the Yangtze Estuary has increased, which affects the distribution of fish species in the estuary. The distribution area of offshore species has expanded and that of estuarine fish has contracted (Xian and Luo, 2015). Owing to the increase in transparency in estuarine waters caused by the decreased inflow of sediment, areas with high phytoplankton productivity have expanded, and the position of spawning and feeding grounds of many fish has changed accordingly (Luo, 1994; Gao et al., 2018).

After the Aswan Dam was built on the Nile River in Egypt, the nutrients transported to the waters of the Nile Estuary decreased by more than 90%, resulting in the serious depletion of fishery resources in the coastal waters (Nixon, 2004). Similarly, the Alqueva Dam has affected the abundance and community structure of ichthyoplankton in the estuary by changing the river runoff (Faria et al., 2006). Thirty years after the completion of the dam in the upper Petitcodiac River in Canada, the representative anadromous species had disappeared (Aube et al., 2005).

5.3.2 Overfishing

The combination of nutrient-rich fresh and saline aquatic habitats in estuaries makes them extremely productive for fisheries; for this reason, many large fishing grounds are located near estuaries (Shan et al., 2004). In recent years, fishing intensity has increased annually owing to the modernization of fishing gear and the improvement of fishing technology, far exceeding the capacity of resource recruitment (Song et al., 2019). This has greatly impacted ichthyoplankton as the recruitment source for fisheries and has changed the community composition. Some economically valuable species have disappeared from their original habitats, fishery resources have been degraded, and many traditional fishing grounds have been become uneconomic (Hale et al., 2016). For example, in the Yangtze Estuary, overfishing of *Trichiurus japonicus*, *Larimichthys polyactis* and other important economic species has led to fish miniaturization, early maturity and a young age structure (Shan et al., 2004). The primary reason for the miniaturization of the fish community is the uncontrolled overuse of marine biological resources in coastal waters (Zhu et al., 2002).

Overfishing is the main cause of the substantial reduction of fishery resources (Song et al., 2019). Consequently, overfishing and environmental degradation lead to a loss of ecosystem resilience and integrity. Because the fishery yield is dependent on ecosystem productivity, a more unstable ecosystem leads to unpredictable changes in both quality and quantity (Ryder et al., 1981). Overfishing greatly reduces the survival rate of adult fish and affects spawning, resulting in a reduction of ichthyoplankton abundance. Therefore, under the combined effect of overfishing and environmental change, the population and community structure of ichthyoplankton in estuarine ecosystems has changed markedly (Bian et al., 2010).

5.3.3 Pollution

Human activities are highly concentrated in estuarine areas, and environmental changes have a profound impact. The development of modern industry and agriculture has led to a substantial quantity of industrial wastewater and domestic sewage being discharged into estuaries through various pathways. The discharge volume and the concentration of pollutants are increasing year by year, causing eutrophication and declining water quality of estuaries and their adjacent coastal waters.

In addition to red tides, eutrophication may also lead to oxygen deficiency or even anoxia in estuaries and nearby waters. Oxygen deficiency can destroy the biological community structure in affected waters, which changes fish food resources, including the species composition and quantity of plankton, aquatic plants, benthos and other food organisms, disrupting the food chain of fish (Liu et al., 2008). In addition, oil pollution from factories and shipping is becoming more serious. Sedimentary oil can also cause secondary pollution, leading to long-term pollution of water bodies and damaging the normal biochemical processes. This, in turn, destroys the spawning and feeding grounds of fish over a large area, damaging the self-renewal mechanism of fish resources and leading to an imbalance in fish community niches. Fish larval physiology has been changed by pollution, leading to increased tissue damage and decreased survival rates, all of which affect the structure of estuarine fishery resources (Shan et al., 2004; Bajo et al., 2020).

Microplastics (particle size < 5 mm) do great harm to juvenile fish. While ingestion of microplastics leads to intestinal obstruction of juvenile fish, which affects their feeding, microplastics also have a high capacity to absorb pollutants, which leads to the accumulation of pollutants in the body (Rodrigues et al., 2019). However, the specific impact of microplastics on the ichthyoplankton community structure of estuarine fish is unclear.

6 CONCLUSION

This review contributes important theoretical and practical information for estuarine environmental protection and the sustainable use of estuarine resources. We found an increase in the amount of research on estuarine ichthyoplankton over time, but it was mainly concentrated in developed countries. Salinity and turbidity are the main factors affecting changes in ichthyoplankton community structure in estuaries. Climate change indirectly affects the community structure of estuarine ichthyoplankton by altering the spawning time, spawning location and egg hatching time of adult fish. The movement of spawning sites poleward and the advance of spawning time have become a consistent trend. Although there is little research on the DNA barcoding of ichthyoplankton, evidence suggests that the wide use of DNA barcoding will provide an effective solution for the accurate identification of ichthyoplankton.

Therefore, strengthening the research on estuarine ichthyoplankton in developing countries can further deepen the understanding of estuarine ichthyoplankton ecology and help to provide references for the protection of fishery resources in these countries. The impact of climate change on ichthyoplankton in estuaries has attracted more and more attention, but its potential driving mechanism needs to be further explored. The impact of human activities (such as overfishing, environmental pollution and dam construction) on ichthyoplankton in estuaries is often ignored, and more attention should be paid to it. DNA barcoding has broad development prospects in the identification of ichthyoplankton. The identification method combining molecular and morphology may become the mainstream method in the future.

Although this study systematically reviews the research on ichthyoplankton in estuaries all over the world, there are still many limitations. On the one hand, many non-English literature sources are excluded, which leads to some deviations in the statistical results. On the other hand, this study focuses on the community structure and influencing factors of estuarine ichthyoplankton, but does not discuss its potential driving mechanism in detail. Thus, to strengthen the study of estuarine ichthyoplankton ecology, we need to fully understand the structure and function of estuarine ecosystems and the impact of human activities on estuarine resources so that we can develop protective countermeasures.

AUTHOR CONTRIBUTIONS

HZ and YW analyzed the literatures and completed the first draft. HZ and WX provided guidance on the structure of the paper. SL provided the suggestions on this paper, and YW, CL and HZ modified the paper. All authors were involved in the revision of the original manuscript. All authors contributed to the article and approved the submitted version.

FUNDING

The present work was supported by National Natural Science Foundation of China (No. 41976094 and 31872568); Key Deployment Project of Center for Ocean Mega-Science, Chinese Academy of Sciences (COMS2019Q14); Youth Innovation Promotion Association CAS (No.2020211).

ACKNOWLEDGMENTS

We thank Leonie Seabrook, PhD, from Liwen Bianji (Edanz) (www.liwenbianji.cn/), for editing the English text of a draft of this manuscript.

SUPPLEMENTARY MATERIAL

The Supplementary Material for this article can be found online at: https://www.frontiersin.org/articles/10.3389/fmars.2022.794433/full#supplementary-material

REFERENCES

Able, K. W. (1978). Ichthyoplankton of the St. Lawrence Estuary - Composition, Distribution, and Abundance. *J. Fish. Res. Board Can.* 35 (12), 1518–1531. doi: 10.1139/f78-241

Acha, E. M., Simionato, C. G., Carozza, C., and Mianzan, H. (2012). Climate-Induced Year-Class Fluctuations of Whitemouth Croaker Micropogonias Furnieri (*Pisces, Sciaenidae*) in the Rio De La Plata Estuary, Argentina-Uruguay. *Fish. Oceanogr.* 21 (1), 58–77. doi: 10.1111/j.1365-2419.2011.00609.x

Amezcua, F., Rodriguez-Preciado, J. A., Calderon-Perez, A., Rendon-Rodriguez, S., Green, L., and Chazarreta, C. J. (2020). Larval Fish Assemblages in Nearshore Waters of Southeast Gulf of California: Vertical and Temporal Patterns. *Neotrop. Ichthyol.* 18 (1), e190102. doi: 10.1590/1982-0224-2019-0102

Aube, C. I., Locke, A., and Klassen, G. J. (2005). Zooplankton Communities of a Dammed Estuary in the Bay of Fundy, Canada. *Hydrobiologia* 548, 127–139. doi: 10.1007/s10750-005-4730-0

Auth, T. D., Daly, E. A., Brodeur, R. D., and Fisher, J. L. (2018). Phenological and Distributional Shifts in Ichthyoplankton Associated With Recent Warming in the Northeast Pacific Ocean. *Glob. Change Biol.* 24 (1), 259–272. doi: 10.1111/gcb.13872

Azeiteiro, U. M., Bacelar-Nicolau, L., Resende, P., Goncalves, F., and Pereira, M. J. (2006). Larval Fish Distribution in Shallow Coastal Waters Off North Western Iberia (NE Atlantic). *Estuarine Coastal Shelf Sci.* 69 (3-4), 554–566. doi: 10.1016/j.ecss.2006.05.023

Bajo, B. A., Castro, L. R., and Costalago, D. (2020). Elucidating Trophic Pathways of the Most Abundant Fish Larvae in Northern Patagonia Using δ13c and δ15n Isotopes. *Mar. Ecol.: Prog. Ser.* 650, 253–267. doi: 10.3354/meps13374

Barleta-Bergan, A., Barletta, M., and Saint-Paul, U. (2002). Structure and Seasonal Dynamics of Larval Fish in the Caete River Estuary in North Brazil. *Estuarine Coastal Shelf Sci.* 54 (2), 193–206. doi: 10.1006/ecss.2001.0842

Barragán, J. M., and de Andrés, M. (2015). Analysis and Trends of the World's Coastal Cities and Agglomerations. *Ocean Coast. Manage.* 114, 11–20. doi: 10.1016/j.ocecoaman.2015.06.004

Beckley, L. E. (1985). Tidal Exchange of Ichthyoplankton in the Swartkops Estuary Mouth, South Africa. *South Afr. J. Zool.* 20, 15–20. doi: 10.1080/02541858.1985.11447906

Berasategui, A. D., Acha, E. M., and Araoz, N. C. F. (2004). Spatial Patterns of Ichthyoplankton Assemblages in the Rio De La Plata Estuary (Argentina-Uruguay). *Estuarine Coastal Shelf Sci.* 60 (4), 599–610. doi: 10.1016/j.ecss.2004.02.015

Bian, X. D., Zhang, X. M., Gao, T. X., Wan, R. J., and Zhang, P. D. (2010). Category Composition and Distributional Patterns of Ichthyoplankton in the Yellow River Estuary During Spring and Summer 2007. *J. Fish. Sci. China* 17 (4), 815–827. doi: CNKI:SUN:ZSCK.0.2010-04-024

Bian, X. D., Zhang, X. M., Gao, T. X., Xiao, Y. S., and Wan, R. J. (2007). Identification of Fish Eggs of Japanese Halfbeak (*Hyporhamphus Sajori*) Using mtDNA Sequencing. *J. Ocean Univ. China* 37, 111–116. doi: 10.16441/j.cnki.hdxb.2007.s1.018

Blaber, S. J. M. (1997). Fish and Fisheries of Tropical Estuaries. *Trans. Am. Fish. Soc.* 128 (1), 183–184. doi: 10.1577/1548-8659(1999)128<0183:FAFOTE>2.0.CO;2

Boehlert, G. W., and Morgan, J. B. (1985). Turbidity Enhances Feeding Abilities of Larval Pacific Herring, *Clupea Harengus Pallasi*. *Hydrobiologia* 123 (2), 161–170. doi: 10.1007/BF00018978

Bonecker, A. C. T., de Castro, M. S., Costa, P. G., Bianchini, A., and Bonecker, S. L. C. (2019). Larval Fish Assemblages of the Coastal Area Affected by the Tailings of the Collapsed Dam in Southeast Brazil. *Reg. Stud. Mar. Sci.* 32, 100848. doi: 10.1016/j.rsma.2019.100848

Bradbury, I. R., Gardiner, K., Snelgrove, P. V. R., Campana, S. E., Bentzen, P., and Guan, L. (2006). Larval Transport, Vertical Distributions and Localized Recruitment in Anadromous Rainbow Smelt (*Osmerus Mordax*). *Can. J. Fish. Aquat. Sci.* 63 (12), 2822–2836. doi: 10.1139/F06-164

Bruno, D. O., Delpiani, S. M., Cousseau, M. B., de Astarloa, J. M. D., Blasina, G. E., Mabragana, E., et al. (2014). Ocean-Estuarine Connection for Ichthyoplankton Through the Inlet Channel of a Temperate Choked Coastal Lagoon (Argentina). *Mar. Freshw. Res.* 65 (12), 1116–1130. doi: 10.1071/Mf13128

Burns, M. D. M., Garcia, A. M., Vieira, J. P., Bemvenuti, M. A., Marques, D., and Condini, V. (2006). Evidence of Habitat Fragmentation Affecting Fish Movement Between the Patos and Mirim Coastal Lagoons in Southern Brazil. *Neotrop. Ichthyol.* 4 (1), 69–72. doi: 10.1590/s1679-62252006000100006

Butler, J. L., Jacobson, L. D., Barnes, J. T., and Moser, H. G. (2003). Biology and Population Dynamics of Cowcod (*Sebastes Levis*) in the Southern California Bight. *Fish. Bull.* 101 (2), 260–280.

Calderón-Peralta, G., Ayora-Macias, G., and Solís-Coello, P. (2020). Variación Espacio-Temporal De Larvas De Peces En El Golfo De Guayaquil, Ecuador. *J. Coast. Res.* 49 (1), 135–156. doi: 10.25268/bimc.invemar.2020.49.1.778

Campfield, P. A., and Houde, E. D. (2011). Ichthyoplankton Community Structure and Comparative Trophodynamics in an Estuarine Transition Zone. *Fish. Bull.* 109 (1), 1–19. doi: 10.1007/s12562-010-0303-x

Cao, W., Chang, J., and Duan, Z. (2007). *Fish Resources of Early Life Stages in Yangtze River* (Beijing, China: Waterpower Press).

Chambers, R. C., and Trippel, E. A. (1997). "Early Life History and Recruitment: Legacy and Challenges," in *Early Life History and Recruitment in Fish Populations* (London: Chapman and Hall), 515–549. doi: 10.1007/978-94-009-1439-1_19

Chandra, R. (1962). A Preliminary Account of Distribution and Abundance of Fish Larvae in Hooghly Estuary. *Indian J. Fish. Sect. A.* 9 (1), 48. doi: 10.1007/978-1-4020-2792-5_6

Chen, Y. H., Shaw, P. T., and Wolcott, T. G. (1997). Enhancing Estuarine Retention of Planktonic Larvae by Tidal Currents. *Estuarine Coastal Shelf Sci.* 45 (4), 525–533. doi: 10.1006/ecss.1996.0217

Chermahini, M. A., Shabani, A., Naddafi, R., Ghorbani, R., Rabbaniha, M., and Noorinejad, M. (2021). Diversity, Distribution, and Abundance Patterns of Ichthyoplankton Assemblages in Some Inlets of the Northern Persian Gulf. *J. Sea Res.* 167, 101981. doi: 10.1016/j.seares.2020.101981

Chiappa-Carrara, X., Sanvicente-Anorve, L., Monreal-Gomez, A., and De Leon, D. S. (2003). Ichthyoplankton Distribution as an Indicator of Hydrodynamic Conditions of a Lagoon System in the Mexican Caribbean. *J. Plankton Res.* 25 (7), 687–696. doi: 10.1093/plankt/25.7.687

Chicharo, L., Faria, A., Morais, P., Amaral, A., Mendes, C., and Chicharo, M. A. (2009). How to Sample Larval Fish for Taxonomical and Ecophysiological Studies in Shallower Temperate Coastal Ecosystems? *Cah. Biol. Mar.* 50 (4), 311–318. doi: 10.1007/978-0-387-89959-6_39

Chu, C., Loh, K. H., Ng, C. C., Ooi, A. L., Konishi, Y., Huang, S. P., et al. (2019). Using DNA Barcodes to Aid the Identification of Larval Fishes in Tropical Estuarine Waters (Malacca Straits, Malaysia). *Zool. Stud.* 58, e30. doi: 10.6620/zs.2019.58-30

Churchill, J. H., Forward, R. B., Luettich, R. A., Hench, J. L., Hettler, W. F., Crowder, L. B., et al. (1999). Circulation and Larval Fish Transport Within a Tidally Dominated Estuary. *Fish. Oceanogr.* 8, 173–189. doi: 10.1046/j.1365-2419.1999.00025.x

Costa, A. J. G., Costa, K. G., Pereira, L. C. C., Sampaio, M. I., and da Costa, R. M. (2011). Dynamics of Hydrological Variables and the Fish Larva Community in an Amazonian Estuary of Northern Brazil. *J. Coastal Res.* 64, 1960–1964.

Costa, M. D. P., Possingham, H. P., and Muelbert, J. H. (2016). Incorporating Early Life Stages of Fishes Into Estuarine Spatial Conservation Planning. *Aquat. Conserv.* 26 (6), 1013–1030. doi: 10.1002/aqc.2584

Costa, M. J., Vasconcelos, R., Costa, J. L., and Cabral, H. N. (2007). River flow Influence on the fish Community of the Tagus Estuary (Portugal). *Hydrobiologia* 587, 113–123. doi: 10.1007/s10750-007-0690-x

Dagg, M. J., and Govoni, J. J. (1996). Is Ichthyoplankton Predation an Important Source of Copepod Mortality in Subtropical Coastal Waters? *Mar. Freshw. Res.* 47 (2), 137–144. doi: 10.1071/mf9960137

Demirel, N. (2015). Ichthyoplankton Dynamics in a Highly Urbanized Estuary. *Mar. Biol. Res.* 11 (7), 677–688. doi: 10.1080/17451000.2015.1007873

de Morais, T. A., and de Morais, T. L. (1994). The Abundance and Diversity of Larval and Juvenile fish in a Tropical Estuary. *Estuaries* 17, 216–225. doi: 10.2307/1352571

Ding, Y. W., and Xian, W. W. (2011). Temporal and Spatial Structure of Ichthyoplankton Assemblages in the Yangtze Estuary During Autumn. *J. Ocean Univ. China* 41 (10), 67–74. doi: 10.16441/j.cnki.hdxb.2011.10.011

Doring, J., Neumann, S. I., Sloterdijk, H., and Ekau, W. (2018). Seasonal Growth Differences of Larval *Hyporhamphus Picarti* (Hemiramphidae) in the Sine Saloum Estuary, Senegal. *J. Appl. Ichthyol.* 34 (1), 97–102. doi: 10.1111/jai.13528

Drake, P., and Arias, A. M. (1991). Composition and Seasonal Fluctuations of the Ichthyoplankton Community in a Shallow Tidal Channel of Cadiz Bay (Sw Spain). *J. Fish Biol.* 39 (2), 245–263. doi: 10.1111/j.1095-8649.1991.tb04360.x

Drake, P., Borlan, A., Gonzalez-Ortegon, E., Baldo, F., Vilas, C., and Fernandez-Delgado, C. (2007). Spatio-Temporal Distribution of Early Life Stages of the European Anchovy *Engraulis Encrasicolus L.* Within a European Temperate Estuary With Regulated Freshwater Inflow: Effects of Environmental Variables. *J. Fish Biol.* 70 (6), 1689–1709. doi: 10.1111/j.1095-8649.2007.01433.x

Drinkwater, K. F., and Frank, K. T. (1994). Effects of River Regulation and Diversion on Marine fish and Invertebrates. Aquatic Conservation: Freshwater and Marine. *Ecosystems* 4, 135–151. doi: 10.1002/aqc.3270040205

Esteves, E., Pina, T., Chícharo, M. A., and Andrade, J. P. (2000). The Distribution of Estuarine fish Larvae: Nutritional Condition and Co-Occurrence With Predators and Prey. *Acta Oecol.* 21 (3), 161–173. doi: 10.1016/S1146-609X(00)01078-X

Faria, A., Morais, P., and Chicharo, M. A. (2006). Ichthyoplankton Dynamics in the Guadiana Estuary and Adjacent Coastal Area, South-East Portugal. *Estuarine Coastal Shelf Sci.* 70 (1-2), 85–97. doi: 10.1016/j.ecss.2006.05.032

Fiedler, P. C. (2002). Environmental Change in the Eastern Tropical Pacific Ocean: Review of ENSO and Decadal Variability. *Mar. Ecol.: Prog. Ser.* 244, 265–283. doi: 10.3354/meps244265

Forward, R. B., and Tankersley, R. A. (2001). Selective Tidal–Stream Transport of Marine Animals. *Oceanogr. Mar. Biol. Ann. Rev.* 39, 305–353. doi: 10.1080/00049185908702346

Franco-Gordoa, C., Godínez-Domínguez, E., Filonovc, A. E., Tereshchenkoc, I. E., and Freireb, J. (2004). Plankton Biomass and Larval Fish Abundance Prior to and During the El Niño Period of 1997–1998 Along the Central Pacific Coast of México. *Prog. Oceanogr.* 63 (3), 99–123. doi: 10.1016/j.pocean.2004.10.001

Fricke, R., Eschmeyer, W. N., and van der, R. L. (2021). "Eschmeyer's Catalog of Fishes," in *Genera, Species, References*. San Francisco: California Academy of Sciences, Internet publication. Available at: http://researcharchive.calacademy.org/research/ichthyology/catalog/fishcatmain.asp.

Gao, D. (2015). *Applying Basic Research on the Morphological and Molecular Approaches to Identifying the Ichthyoplankton* (D. Qingdao: Ocean University of China).

Gao, L., Cheng, F., Song, Y. Q., Jiang, W., Feng, G. P., Luo, Y. M., et al. (2018). Patterns of Larval Fish Assemblages Along the Direction of Freshwater Input Within the Southern Branch of the Yangtze Estuary, China: Implications for Conservation. *J. Freshw. Ecol.* 33 (1), 97–114. doi: 10.1080/02705060.2018.1426503

Garcia, A. M., Vieira, J. P., and Winemiller, K. O. (2003). Effects of 1997-1998 El Nino on the Dynamics of the Shallow-Water Fish Assemblage of the Patos Lagoon Estuary (Brazil). *Estuarine Coastal Shelf Sci.* 57, 489–500. doi: 10.1016/S0272-7714(02)00382-7

Gaughan, D. J., Neira, F. J., Beckley, L. E., and Potter, I. C. (1990). Composition, Seasonality and Distribution of the Ichthyoplankton in the Lower Swan Estuary, South-Western Australia. *Aust. J. Mar. Freshw. Res.* 41 (4), 529–543. doi: 10.1071/MF9900529

Gibson, R. N. (2003). Go With the flow: Tidal Migration in Marine Animals. *Hydrobiologia* 503, 153–161. doi: 10.1023/B:HYDR.0000008488.33614.62

Grange, N., and Allanson, B. R. (1995). The Influence of Freshwater Inflow on the Nature, Amount and Distribution of Seston in Estuaries of the Eastern Cape, South Africa. *Estuarine Coastal Shelf Sci.* 40, 403–420. doi: 10.1006/ecss.1995.0028

Guan, X., Du, X., Lin, Y., and Tang, R. (1992). Effects of Sewage Discharge on Fishery Water Environment in Yangtze River Estuary in Summer. *Shanghai J. Water Resour.* 2, 15–20. doi: CNKI:SUN:HYHJ.0.1992-04-004

Hale, E. A., Park, I. A., Fisher, M. T., Wong, R. A., Stangl, M. J., and Clark, J. H. (2016). Abundance Estimate for and Habitat Use by Early Juvenile Atlantic Sturgeon Within the Delaware River Estuary. *Trans. Am. Fish. Soc.* 145 (6), 1193–1201. doi: 10.1080/00028487.2016.1214177

Harris, S. A., and Cyrus, D. P. (1995). Occurrence of Fish Larvae in the St Lucia Estuary, Kwazulu-Natal, South Africa. *S. Afr. J. Mar. Sci.* 16, 333–350. doi: 10.2989/025776195784156601

Harris, S. A., and Cyrus, D. P. (2000). Comparison of Larval Fish Assemblages in Three Large Estuarine Systems, KwaZulu-Natal, South Africa. *J. Mar. Biol.* 137 (3), 527–541. doi: 10.1007/s002270000356

Harris, S. A., Cyrus, D. P., and Beckley, L. E. (1999). The Larval Fish Assemblage in Nearshore Coastal Waters Off the St Lucia Estuary, South Africa. *Estuarine Coastal Shelf Sci.* 49 (6), 789–811. doi: 10.1006/ecss.1999.0554

Harris, S. A., Cyrus, D. P., and Beckley, L. E. (2001). Horizontal Trends in Larval Fish Diversity and Abundance Along an Ocean-Estuarine Gradient on the Northern KwaZulu-Natal Coast, South Africa. *Estuarine Coastal Shelf Sci.* 53 (2), 221–235. doi: 10.1006/ecss.2001.0803

Harrison, T. D., and Whitfield, A. K. (1990). Composition, Distribution and Abundance of Ichthyoplankton in the Sundays River Estuary. *S. Afr. J. Zool.* 25 (3), 161–168. doi: 10.1080/02541858.1990.11448206

Hassell, K. L., Coutin, P. C., and Nugegoda, D. (2008). Hypoxia, Low Salinity and Lowered Temperature Reduce Embryo Survival and Hatch Rates in Black Bream *Acanthopagrus Butcheri* (Munrol 1949). *J. Fish Biol.* 72 (7), 1623–1636. doi: 10.1111/j.1095-8649.2008.01829.x

Hebert, P. D. N., Cywinska, A., Ball, S., and deWaard, J. R. (2003). Biological Identifications Through DNA Barcodes. *Philos. Trans. R. Soc. Lond. B. Biol. Sci.* 270, 313–321. doi: 10.1098/rspb.2002.2218

Hernández-Miranda, E., Palma, A. T., and Ojeda, F. P. (2003). Larval fish Assemblages in Nearshore Coastal Waters Off Central Chile: Temporal and Spatial Patterns. *Estuarine Coastal Shelf Sci.* 56, 1075–1092. doi: 10.1016/S0272-7714(02)00308-6

Hettler, W. F.Jr., and Hare, J. A. (1998). Abundance and Size of Larval fishes Outside the Entrance to Beaufort Inlet, North Carolina. *Estuaries* 21, 476–499. doi: 10.2307/1352846

Hickling, C. F. (1970). A Contribution to the Natural History of the English Grey Mullets [Pisces, Mugilidae]. *J. Mar. Biol. Assoc. U. K.* 50 (3), 609–633. doi: 10.1017/S0025315400004914

Holmes, R. H. A., and Henderson, P. A. (1990). High fish Recruitment in the Severn Estuary: The Effect of a Warm Year. *J. Fish Biol.* 36, 961–963. doi: 10.1111/j.1095-8649.1990.tb05641.x

Huang, D. L., Zhang, X., Jiang, Z. J., Zhang, J. P., Arbi, I., Jiang, X., et al. (2017). Seasonal Fluctuations of Ichthyoplankton Assemblage in the Northeastern South China Sea Influenced by the Kuroshio Intrusion. *J. Geophys. Res. Oceans* 122 (9), 7253–7266. doi: 10.1002/2017jc012906

Islam, M. S., Hibino, M., and Tanaka, M. (2006). Distribution and Diets of Larval and Juvenile fishes: Influence of Salinity Gradient and Turbidity Maximum in a Temperate Estuary in Upper Ariake Bay, Japan. *Estuarine Coastal Shelf Sci.* 68, 62–74. doi: 10.1016/j.ecss.2006.01.010

Islam, M. S., Hibino, M., and Tanaka, M. (2007). Tidal and Diurnal Variations in Larval fish Abundance in an Estuarine Inlet in Ariake Bay, Japan: Implication for Selective Tidal Stream Transport. *Ecol. Soc Jpn.* 22, 165–171. doi: 10.1007/s11284-006-0001-4

Islam, M. S., and Tanaka, M. (2006). Spatial Variability in Nursery Functions Along a Temperate Estuarine Gradient: Role of Detrital Versus Algal Trophic Pathways. *Can. J. Fish. Aquat. Sci.* 63 (8), 1848–1864. doi: 10.1139/f06-086

Jager, Z. (1999). Selective Tidal Stream Transport of Flounder Larvae (*Platichthys Flesus L.*) in the Dollard (Ems Estuary). *Estuarine Coastal Shelf Sci.* 49 (3), 347–362. doi: 10.1006/ecss.1999.0504

Jiang, S., and Chen, F. (1993). Studies on Estuarine Ecology of Ichthyoplankton of Jiulong River. *J. Oceanogr. Taiwan Strait* 12 (4), 351–358. doi: CNKI:SUN:TWHX.0.1993-04-007

Jiang, M., Shen, X., and Chen, L. (2006). Relationship Between With Abundance Distribution of Fish Eggs, Larvae and Environmental Factors in the Changjiang Estuary and Vicinity Waters in Spring. *Mar. Environ. Sci.* 25 (2), 37–39. doi: 10.3969/j.issn.1007-6336.2006.02.010

Jiang, M., Shen, X. Q., Li, L., and Quan, W. M. (2013). Annual Variability of Ichthyoplankton in the Yangtze Estuary of China From August 2002 to 2009. *Oceanol. Hydrobiol. Stud.* 42 (1), 59–69. doi: 10.2478/s13545-013-0060-4

Jiang, M., Shen, X. Q., Wang, Y. L., Yuan, Q., and Chen, L. F. (2006a). Species of Fish Eggs and Larvae and Distribution in Changjiang Estuary and Vicinity Waters. *Acta Oceanol. Sin.* 28 (2), 171–174. doi: 10.1007/978-94-017-9136-6_8

Jones, S., and Menon, P. M. G. (1951). Observations on the Life-History of the Indian Shad, *Hilsa Ilisha* (Hamilton). *P. Indian Natl. Sci. Ac. Sect. B.* 33 (3), 101–124. doi: 10.1007/BF03049975

Kimmerer, W. J. (2002). Physical, Biological, and Management Responses to Variable Freshwater Flow Into the San Francisco Estuary. *Estuaries* 25 (6B), 1275–1290. doi: 10.1007/BF02692224

Kindong, R., Wu, J., Gao, C., Dai, L., Tian, S., Dai, X., et al. (2020). Seasonal Changes in Fish Diversity, Density, Biomass, and Assemblage Alongside Environmental Variables in the Yangtze Estuary. *Environ. Sci. Pollut. Res.* 27 (20), 25461–25474. doi: 10.1007/s11356-020-08674-8

Kingsford, M. J., and Suthers, I. M. (1996). The Influence of Tidal Phase on Patterns of Ichthyoplankton Abundance in the Vicinity of an Estuarine Front, Botany Bay, Australia. *Estuarine Coastal Shelf Sci.* 43 (1), 33–54. doi: 10.1006/ecss.1996.0056

Korsman, B. M., Kimball, M. E., and Hernandez, F. J. (2017). Spatial and Temporal Variability in Ichthyoplankton Communities Ingressing Through Two Adjacent Inlets Along the Southeastern US Atlantic Coast. *Hydrobiologia* 795 (1), 219–237. doi: 10.1007/s10750-017-3131-5

Ko, H. L., Wang, Y. T., Chiu, T. S., Lee, M. A., Leu, M. Y., Chang, K. Z., et al. (2013). Evaluating the Accuracy of Morphological Identification of Larval Fishes by Applying DNA Barcoding. *PloS One* 8 (1), e53451. doi: 10.1371/journal.pone.0053451

Lefcheck, J. S., Hughes, B. B., Johnson, A. J., Pfirrmann, B. W., Rasher, D. B., Smyth, A. R., et al. (2019). Are Coastal Habitats Important Nurseries? A Meta-Analysis. *Conserv. Lett.* 12 (4), e12645. doi: 10.1111/conl.12645

Lima, A. R. A., Ferreira, G. V. B., and Barletta, M. (2019). Estuarine Ecocline Function and Essential Habitats for Fish Larvae in Tropical South Western Atlantic Estuaries. *Mar. Environ. Res.* 151, 104786. doi: 10.1016/j.marenvres.2019.104786

Limburg, K. E. (1999). Estuaries, Ecology, and Economic Decisions: An Example of Perceptual Barriers and Challenges to Understanding. *Ecol. Econ.* 30 (1), 185–188. doi: 10.1016/S09218009(99)00045-2

Lin, S., Wang, L., Zheng, L., Dong, Y., Liu, S., and Ding, S. (2014). Current Status and Future Prospect of DNA Barcoding in Marine Biology. *Acta Ocean. Sinica.* 36 (12), 1–17. doi: 10.3969/j.issn.0253-4193.2014.12.001

Lin, J., Wu, H., Chen, K., Du, Q., Huang, Z., Huang, K., et al. (2018). Identification of Ichthyoplankton Using DNA Barcoding in Xiamen Bay. *J. Fish. Res.* 40 (5), 340–348. doi: 10.14012/j.cnki.fjsc.2018.05.002

Liu, S., and Xian, W. (2010). Ichthyoplankton Community Structure Characteristics During Spring in Yangtze Estuary Before and After Impoundment of Three Gorges Reservoir. *J. Yangtze River Sci. Res. Institute* 27 (10), 82–87. doi: 10.3969/j.issn.1001-5485.2010.10.017

Liu, S. D., Xian, W. W., and Liu, D. (2008). Characteristics of Ichthyoplankton Assemblages in Yangtze Estuary and Adjacent Waters in Spring. *J. Appl. Ecol.* 19 (10), 2284–2292. doi: CNKI:SUN:YYSB.0.2008-10-029

Liu, S., Yang, Y., He, Y., Ji, X., Wang, Y., and Zhang, H. (2021). Morphological Classification of Ichthyoplankton in the Changjiang River Estuary Based on DNA Barcoding. *Haiyang Xuebao* 43 (8), 93–104. doi: 10.12284/hyxb2021062

Livingston, R. J., Niu, X., Lewis, F. G., and Woodsum, G. C. (1997). Freshwater Input to a Gulf Estuary: Long-Term Control of Trophic Organization. *Ecol. Appl.* 7, 277–299. doi: 10.1890/1051-0761(1997)007[0277:FITAGE]2.0.CO;2

Li, Y., Zhang, Y., Zhang, R., Song, P., Wang, L., and Zhang, L. (2017). Identification of Several Fish Larvae Based on DNA Barcoding Int the Investigated Waters of Cangnan. *J. Ocean Univ. China* 36 (12), 1–17. doi: 10.16441/j.cnki.hdxb.20160343

Locke, A., and Courtenay, S. C. (1995). Effects of Environmental-Factors on Ichthyoplankton Communities in the Miramichi Estuary, Gulf of St-Lawrence. *J. Plankton Res.* 17 (2), 333–349. doi: 10.1093/plankt/17.2.333

Lotze, H. K. (2010). "Historical Reconstruction of Human-Induced Changes in US Estuaries," in *Oceanography and Marine Biology: An Annual Review*, vol. Vol. 48 . Eds. R. N. Gibson, R. J. A. Atkinson and J. D. M. Gordon (Boca Raton, FL: CRC Press), 267–338.

Lotze, H. K., Lenihan, H. S., Bourque, B. J., Bradbury, R. H., Cooke, R. G., Jackson, J. B. C., et al. (2006). Depletion, Degradation, and Recovery Potential of Estuaries and Coastal Seas. *J. Sci.* 312 (5781), 1806–1809. doi: 10.1126/science.1128035

Luo, B. Z. (1994). *Three Gorges Project and Estuarine Ecological Environment* (China: Science Press).

Martin, T. J., Cyrus, D. P., and Forbes, A. T. (1992). Episodic Events - the Effects of Cyclonic Flushing on the Ichthyoplankton of St-Lucia Estuary on the Southeast Coast of Africa. *Neth. J. Sea Res.* 30, 273–278. doi: 10.1016/0077-7579(92)90065-M

Melvillesmith, R., and Baird, D. (1980). Abundance, Distribution and Species Composition of Fish Larvae in the Swartkops Estuary. *S. Afr. J. Zool.* 15 (2), 72–78. doi: 10.1080/02541858.1980.11447689

Monteiro, M., Azeiteiro, U. M., Martinho, F., Pardal, M. A., and Primo, A. L. (2021). Long-Term Changes of Ichthyoplankton Communities in an Iberian Estuary are Driven by Varying Hydrodynamic Conditions. *J. Plankton Res.* 43 (1), 33–45. doi: 10.1093/plankt/fbaa057

Monteleone, D. M. (1992). Seasonality and Abundance of Ichthyoplankton in Great South Bay, New York. *Estuaries* 15, 230–238. doi: 10.2307/1352697

Mouny, P., and Dauvin, J. C. (2002). Environmental Control of Mesozooplankton Community Structure in the Seine Estuary (English Channe1). *Acta Oceanol. Sin.* 25 (1), 13–22. doi: 10.1016/S0399-1784(01)01177-X

Muhling, B. A., Beckley, L. E., and Olivar, M. P. (2007). Ichthyoplankton Assemblage Structure in Two Meso-Scale Leeuwin Current Eddies, Eastern Indian Ocean. *Deep Sea Res. Part II* 54, 1113–1128. doi: 10.1016/j.dsr2.2006.05.045

Munk, P., Cardinale, M., Casini, M., and Rudolphi, A. C. (2014). The Community Structure of Over-Wintering Larval and Small Juvenile Fish in a Large Estuary. *Estuarine Coastal Shelf Sci.* 139, 27–39. doi: 10.1016/j.ecss.2013.12.024

Neira, F. J., and Potter, I. C. (1992). Movement of Larval Fishes Through the Entrance Channel of a Seasonally Open Estuary in Western Australia. *Estuarine Coastal Shelf Sci.* 35 (2), 213–224. doi: 10.1016/S0272-7714(05)80114-3

Newton, G. M. (1996). Estuarine Ichthyoplankton Ecology in Relation to Hydrology and Zooplankton Dynamics in a Salt-Wedge Estuary. *Mar. Freshwater Res.* 47 (2), 99–111. doi: 10.1071/Mf9960099

Nixon, S. W. (2004). The Artificial Nile. *Am. Sci.* 92, 158–165. doi: 10.1511/2004.46.927

North, E. W., and Houde, E. D. (2003). Linking ETM Physics, Zooplankton Prey and Fish Early-Life Histories to White Perch (*Morone Americana*) and Striped Bass (*M. Saxatilis*) Recruitment Success. *Mar. Ecol.: Prog. Ser.* 260, 219–236. doi: 10.3354/meps260219

Palomera, I. (1992). Spawning of Anchovy *Engraulis Encrasicolus* in the North-Western Mediterranean Relative to Hydrographic Features in the Region. *Mar. Ecol.: Prog. Ser.* 79, 215–223. doi: 10.3354/meps079215

Parrish, J.D. (1989). Fish Communities of Interacting Shallow Water Habitats in Tropical Oceanic Regions. *Mar. Ecol.: Prog. Ser.* 58, 143–160.

Pegg, G. G., Sinclair, W. T., Briskey, L., and William, J. A. (2006). mtDNA Barcode Identification of Fish Larvae in the Southern Great Barrier Reef, Australia. *Sci. Marina* 70 (S2), 7–12. doi: 10.3989/scimar.2006.70s27

Pereira, R., Teodosio, M. A., and Garrido, S. (2014). An Experimental Study of Aurelia Aurita Feeding Behaviour: Inference of the Potential Predation Impact on a Temperate Estuarine Nursery Area. *Estuarine Coastal Shelf Sci.* 146, 102–110. doi: 10.1016/j.ecss.2014.05.026

Peterson, G. S., and Lietz, J. E. (2017). Identification of Ruffe Larvae (*Gymnocephalus Cernua*) in the St. Louis River, Lake Superior: Clarification and Guidance Regarding Morphological Descriptions. *J. Great Lakes Res.* 43 (1), 205–210. doi: 10.1016/j.jglr.2016.10.005

Pfirrmann, B. W., Kimball, M. E., Mace, M. M.III, and Turley, B. D. (2021). Summer Ichthyoplankton Assemblage Diversity Within a Southeastern United States Estuary. *Estuaries Coasts* 44 (1), 253–268. doi: 10.1007/s12237-020-00777-2

Pombo, L., Ellio, M., and Rebelo, E. (2002). Changes in the Fish Faunal of the Ria De Aveiro Estuarine Lagoon (Portugal) During the Twentieth Century. *J. Fish Biol.* 61, 167–181. doi: 10.1111/j.1095-8649.2002.tb01769.x

Potter, I. C., Beckley, L. E., Whitfield, A. K., and Lenanton, R. C. (1990). Comparisons Between the Roles Played by Estuaries in the Life Cycles of Fishes in Temperate Western Australia and Southern Africa. *Environ. Biol. Fishes* 28, 143–178. doi: 10.1007/BF00751033

Powles, H.Auger, F.Fitzgerald, G. J. (1984). Nearshore Ichthyoplankton of a North Temperate Estuary. *Can. J. Fish. Aquat. Sci.* 41 (11), 1653–1663. doi: 10.1139/f84-204.

Primo, A. L., Azeiteiro, U. M., Marques, S. C., and Pardal, M. A. (2011). Impact of Climate Variability on Ichthyoplankton Communities: An Example of a Small Temperate Estuary. *Estuarine Coastal Shelf Sci.* 91 (4), 484–491. doi: 10.1016/j.ecss.2010.11.009

Primo, A. L., Azeiteiro, U. M., Marques, S. C., Re, P., and Pardal, M. A. (2012). Seasonal, Lunar and Tidal Control of Ichthyoplankton Dynamics at the Interface Between a Temperate Estuary and Adjacent Coastal Waters (Western Portugal). *Sci. Mar.* 76 (2), 237–246. doi: 10.3989/scimar.03415.18A

Ramos, S., Cowen, R. K., Paris, C., Re, P., and Bordalo, A. A. (2006). Environmental Forcing and Larval Fish Assemblage Dynamics in the Lima

River Estuary (Northwest Portugal). *J. Plankton Res.* 28 (3), 275–286. doi: 10.1093/plankt/fbi104

Ren, P., Schmidt, B. V., Fang, D. A., and Xu, D. P. (2021). Spatial Distribution Patterns of Fish Egg and Larval Assemblages in the Lower Reach of the Yangtze River: Potential Implications for Conservation and Management. *Aquat. Conserv.* 31 (8), 1929–1944. doi: 10.1002/aqc.3595

Ribeiro, F., Hale, E., Hilton, E. J., Clardy, T. R., Deary, A. L., Targett, T. E., et al. (2015). Composition and Temporal Patterns of Larval Fish Communities in Chesapeake and Delaware Bays, USA. *Mar. Ecol.: Prog. Ser.* 527, 167–180. doi: 10.3354/meps11265

Robertson, A. I., and Alongi, D. M. (1992). *Tropical Mangrove Ecosystems* (Washington, D.C: American Geophysical Union).

Rodrigues, S. M., Almeida, C. M. R., Silva, D., Cunha, J., Antunes, C., Freitas, V., et al. (2019). Microplastic Contamination in an Urban Estuary: Abundance and Distribution of Microplastics and Fish Larvae in the Douro Estuary. *Sci. Total. Environ.* 659, 1071–1081. doi: 10.1016/j.scitotenv.2018.12.273

Rousseau, Y., Blanchard, F., and Gardel, A. (2018). Spatiotemporal Dynamics of Larval Fish in a Tropical Estuarine Mangrove: Example of the Mahury River Estuary (French Guiana). *Can. J. Fish. Aquat. Sci.* 75 (2), 235–246. doi: 10.1139/cjfas-2016-0267

Ryder, R. A., Kerr, S. R., Taylor, W. W., and Larkin, P. A. (1981). Community Consequences of Fish Stock Diversity. *Can. J. Fish. Aquat. Sci.* 38, 1856–1866. doi: 10.1139/f81-231

Sabates, A., Martin, P., Loret, J., and Raya, V. (2006). Sea Warming and fish Distribution: The Case of the Small Pelagic fish, *Sardinella Aurita*, in the Western Mediterranean. *Glob. Change Biol.* 12, 2209–2219. doi: 10.1111/j.1365-2486.2006.01246.x

Sabates, A., Olivar, M. P., Salat, J., Palomera, I., and Alemany, F. (2007). Physical and Biological Processes Controlling the Distribution of fish Larvae in the NW Mediterranean. *Prog. Oceanogr.* 74, 355–376. doi: 10.1016/j.pocean.2007.04.017

Sánchez-Velasco, L., Avalos-García, C., Rentería-Cano, M., and Shirasago, B. (2004). Fish Larvae Abundance and Distribution in the Central Gulf of California During Strong Environmental Changes (1997–1998 El Niño and 1998–1999 La Niña). *Deep Sea Res. Part II* 51 (6-9), 711–722. doi: 10.1016/j.dsr2.2004.05.021

Sanvicente-Anorve, L., Flores-Coto, C., and Chiappa-Carrara, X. (2000). Temporal and Spatial Scales of Ichthyoplankton Distribution in the Southern Gulf of Mexico. *Estuarine Coastal Shelf Sci.* 51 (4), 463–475. doi: 10.1006/ecss.2000.0692

Schilling, H. T., Hinchliffe, C., Gillson, J. P., Miskiewicz, A. G., and Suthers, I. M. (2021). Coastal Winds and Larval Fish Abundance Indicate a Recruitment Mechanism for Southeast Australian Estuarine Fisheries. *Fish. Oceanogr.* 31 (1), 40–55. doi: 10.1111/fog.12561

Schubel, J. R. (1968). Turbidity Maximum of the Northern Chesapeake Bay. *Science* 161, 1013–1015. doi: 10.1126/science.161.3845.1013

Schultz, E. T., Lwiza, K. M. M., Fencil, M. C., and Martin, J. M. (2003). Mechanisms Promoting Upriver Transport of Larvae of Two Fish Species in the Hudson River Estuary. *Mar. Ecol.: Prog. Ser.* 251, 263–277. doi: 10.3354/meps251263

Segarra, A., Mauduit, F., Amer, N. R., Biefel, F., Hladik, M. L., Connon, R. E., et al. (2021). Salinity Changes the Dynamics of Pyrethroid Toxicity in Terms of Behavioral Effects on Newly Hatched Delta Smelt Larvae. *Toxics* 9 (2), 40. doi: 10.3390/toxics9020040

Shan, X. J., Xian, W. W., and Wu, Y. F. (2004). Progress of Studies on Ichthyoplankton Ecology of Changjiang River Estuary. *J. Oceanol. Limnol.* 0 (4), 87–93. doi: 10.13984/j.cnki.cn37-1141.2004.04.015

Shao, G., Yang, R., and Chen, K. (2001). *An Identification Guide of Marine Fish Eggs From Taiwan* (M. Taibei: Academia Sinica).

Sheaves, M., Baker, R., Nagelkerken, I., and Connolly, R. M. (2015). True Value of Estuarine and Coastal Nurseries for Fish: Incorporating Complexity and Dynamics. *Estuaries Coasts* 38 (2), 401–414. doi: 10.1007/s12237-014-9846-x

Shideler, A. C., and Houde, E. D. (2014). Spatio-Temporal Variability in Larval-Stage Feeding and Nutritional Sources as Factors Influencing Striped Bass (Morone Saxatilis) Recruitment Success. *Estuaries Coasts* 37 (3), 561–575. doi: 10.1007/s12237-013-9696-y

Shoji, J., Ohta, T., and Tanaka, M. (2006). Effects of River Flow on Larval Growth and Survival of Japanese Seaperch *Lateolabrax Japonicus* (Pisces) in the Chikugo River Estuary, Upper Ariake Bay. *J. Fish Biol.* 69 (6), 1662–1674. doi: 10.1111/j.1095-8649.2006.01235.x

Sloterdijk, H., Brehmer, P., Sadio, O., Muller, H., Doring, J., and Ekau, W. (2017). Composition and Structure of the Larval Fish Community Related to Environmental Parameters in a Tropical Estuary Impacted by Climate Change. *Estuarine Coastal Shelf Sci.* 197, 10–26. doi: 10.1016/j.ecss.2017.08.003

Song, X. K., Liu, A. Y., Yang, Y. Y., Yang, J. M., Ren, L. H., Liu, L. J., et al. (2010). Distributing of Ichthyoplankton and the Correlation With Environmental Factors in Laizhou Bay. *J. Oceanol. Limnol.* 41 (3), 378–385. doi: 10.11693/hyhz201003013013

Song, Y. F., Zhang, L. J., and Luo, X. X. (2019). Spatiotemporal Distribution of Fish Eggs and Larvae in the Huanghe (Yellow) River Estuary, China in 2005-2016. *J. Oceanol. Limnol.* 37 (5), 1625–1637. doi: 10.1007/s00343-019-8167-0

Strydom, N. A., Sutherland, K., and Wooldridge, T. H. (2014). Diet and Prey Selection in Late-Stage Larvae of Five Species of Fish in a Temperate Estuarine Nursery Area. *Afr. J. Mar. Sci.* 36, 85–98. doi: 10.2989/1814232X.2014.895420

Strydom, N. A., Whitfield, A. K., and Wooldridge, T. H. (2003). The Role of Estuarine Type in Characterizing Early Stage Fish Assemblages in Warm Temperate Estuaries, South Africa. *Zool. Afr.* 38 (1), 29–43. doi: 10.1080/15627020.2003.11657192

Talbot, C. W., and Able, K. W. (1984). Composition and Distribution of Larval fishes in New Jersey High Marshes. *Estuaries* 7, 434–443. doi: 10.2307/1351624

Tautz, D., Arctander, P., Minelli, A., Thomas, R., and Vogler, A. (2002). DNA Points the Way Ahead in Taxonomy. *Nature* 418, 479. doi: 10.1038/418479a

Taylor, R. H. (1982). "The St. Lucia Estuary: The Aquatic Environment: Physical and Chemical Characteristics," in *St. Lucia Research Review, Proceedings of the Natal Parks Board 1992.* Ed. R. H. Taylor (South Africa: Symposium), 42–56.

Thaxton, W. C., Taylor, J. C., and Asch, R. G. (2020). Climate-Associated Trends and Variability in Ichthyoplankton Phenology From the Longest Continuous Larval Fish Time Series on the East Coast of the United States. *Mar. Ecol.: Prog. Ser.* 650, 269–287. doi: 10.3354/meps13404

Tzeng, W. N., and Wang, Y. T. (1993). Hydrography and Distribution Dynamics of Larval and Juvenile Fishes in the Coastal Waters of the Tanshui River Estuary, Taiwan, With Reference to Estuarine Larval Transport. *J. Mar. Biol.* 116, 205–217. doi: 10.1007/BF00350010

Valdez-Moreno, M., Vásquez-Yeomans, L., Elías-Gutiérrez, M., Natalia, V., and Pauly, D. N. H. (2010). Using DNA Barcodes to Connect Adults and Early Life Stages of Marine Fishes From the Yucatan Peninsula, Mexico: Potential in Fisheries Management. *Mar. Freshw. Res.* 61 (6), 655–671. doi: 10.1071/MF09222

Valencia, B., Giraldo, A., Rivera-Gomez, M., Izquierdo-Pena, V., and Cuellar-Chacon, A. (2019). Effects of Seasonal Upwelling on Hydrography and Mesozooplankton Communities in a Pacific Tropical Cove Off Colombia. *Rev. Biol. Trop.* 67 (4), 945–962. doi: 10.15517/rbt.v67i4.35489

van Eck, N. J., Waltman, L., Ding, Y., and Wolfram, D. (2014). "Visualizing Bibliometric Networks," in *Measuring Scholarly Impact: Methods and Practice.* Ed. R. Rousseau (London: Springer).

Walker, M. G., Jones, F. R. H., and Arnold, G. P. (1978). Movements of Plaice (Pleuronectes-Platessa L) Tracked in Open Sea. *J. Du Conseil* 38 (1), 58–86. doi: 10.1093/icesjms/38.1.58

Wang, J. W., Huang, J., and Tao, H. H. (2020). Investigation on Ichthyoplankton in Offshore Area of Shijiu Port in Spring. *J. Anhui Agric. Sci.* 48 (21), 91–94. doi: 10.3969/j.issn.0517-6611.2020.21.024

Wang, X., Ma, A., and Zhang, X. (2006). A Review on Feeding Behavior Ecology of Early Development Stage of Marine Fish. *Stud. Mar. Sin.* 30 (11), 69–75. doi: 10.3969/j.issn.1000-3096.2006.11.015

Wang, X. G., Sun, D., and Lin, S. Q. (2017). The Ecological Study of Fish Larvae in the Yangtze Estuary and Adjacent Waters. *J. Shanghai Fish. Univ.* 26 (5), 733–742. doi: 10.12024 /jsou.20170301964

Wang, H. T., and Zhang, P. J. (1998). Effects of Environmental Conditions on Fertilized Eggs and Early Larva of Marine Fishes. *Mar. Sci.* 04, 50–52. doi: 10.1017/S0266078400010713

Wan, R., and Jiang, Y. (2000). The Species and Biological Characteristics of the Eggs and Larvae of Osteichthyes in the Bohai and Yellow Sea. *J. Shanghai Fish. Univ.* 9 (4), 290–297. doi: 10.11964/jfc.20210512867

Wan, R., and Sun, S. (2006). The Category Composition and Abundance of Ichthyoplankton in the Ecosystem of the Yellow Sea and the East China Sea. *Curr. Zool.* 52 (1), 28–44. doi: 10.3969/j.issn.1674-5507.2006.01.004

Weinstein, M. P., Weiss, S. L., Hodson, R. G., and Gerry, L. R. (1980). Retention of Three Taxa of Post Larval fishes in a Intensively flushed Tidal Estuary, Cape Fear River, North Carolina. *Fish. Bull.* 78, 419–436.

Whitfield, A. K. (1999). Ichthyofaunal Assemblages in Estuaries: A South African Case Study. *Rev. Fish Biol. Fish.* 9, 151–186. doi: 10.1023/A:1008994405375

Whitfield, A. K. (1989). Ichthyoplankton Interchange in the Mouth Region of a Southern African Estuary. *Mar. Ecol. Prog. Ser.* 54, 25–33. doi: 10.3354/meps054025

Whitfield, A. K. (1994). Abundance of Larval and Juvenile Marine Fishes in the Lower Reaches of 3 Southern African Estuaries With Differing Fresh-Water Inputs. *Mar. Ecol.: Prog. Ser.* 105 (3), 257–267. doi: 10.3354/meps105257

Williams, J., Jenkins, G. P., Hindell, J. S., and Swearer, S. E. (2013). Linking Environmental Flows With the Distribution of Black Bream *Acanthopagrus Butcheri* Eggs, Larvae and Prey in a Drought Affected Estuary. *Mar. Ecol.: Prog. Ser.* 483, 273–287. doi: 10.3354/meps10280

Wooldridge, T. (1999). *Estuarine Zooplankton Community Structure and Dynamics.* (Cambridge, U.K: Cambridge University Press).

Wu, G. Z. (1989). The Ecological Characteristics of Distribution of Eggs, Larvae and Juveniles of the *Engraulis Japonicus* (Temminck & Schlegel) and *Anchoviella Commersonii* in the Changjiang River Estuary. *J. Oceanol. Limnol.* 3 (20), 217–229. doi: CNKI:SUN:HYFZ.0.1989-03-002

Xian, W. W., and Luo, B. Z. (2015). *Estuarine Ecology and Environment Before the Impoundment of the Three Gorges Project* (Beijing: China Ocean Press).

Xian, W. W., Zhang, H., and Liu, S. D. (2016). Research Advance in Estuarine Ichthyoplankton Ecology. *Stud. Mar. Sin.* 00, 167–180. doi: 10.12036/hykxjk20160718001

Xiao, Y. Z., Wang, R., Zheng, Y. J., and He, W. (2013). Species Composition and Abundance Distribution of Ichthyoplankton in the Pearl River Estuary. *J. Trop. Oceanogr.* 32 (6), 80–87. doi: 10.3969/j.issn.1009-5470.2013.06.012

Yang, Y. F., Wang, Q., Chen, J. F., and Pang, S.X.J.A.E.S. (2006). Research Advance in Estuarine Zooplankton Ecology. *Acta Ecol. Sin.* 26 (2), 576–585. doi: 10.3321/j.issn:1000-0933.2006.02.034

Yang, G., Wu, J., and Gao, M. (1992). Effects of the Three Gorges Project on Sedimentary Structure and Geochemical Characteristics in the Yangtze Estuary. *Study Marina Sin.* 33, 69–108.

Yang, D., Wu, G., and Sun, J. (1990). The Investigation Ok Pelagic Eggs, Larvae and Juveniles of Fishes at the Mouth of the Changjiang River and Adjacent Areas. *J. Oceanol. Limnol.* 4 (21), 346–355.

Yao, Y. (1995). Investigation of Petroleum Pollution in Yangtze River Estuary. *J. Dalian Univ.* 4 (3), 225–230. doi: CNKI:SUN:SSDB.0.1995-03-007

Yu, G., Dong, J., Li, Y., Fu, J., Li, Y., and Wang, A. (2018). Species Composition and Protection of Fish Eggs and Larvae in the Coastal Waters in Liaodong Bay. *J. Dalian Univ.* 33 (3), 370–378. doi: 10.16535/j.cnki.dlhyxb.2018.03.015

Zhang, Z., Mammola, S., Xian, W., and Zhang, H. (2020). Modelling the Potential Impacts of Climate Change on the Distribution of Ichthyoplankton in the Yangtze Estuary, China. *Divers. Distrib.* 26 (1), 126–137. doi: 10.1111/ddi.13002

Zhang, H., Xian, W., and Liu, S. (2015). Ichthyoplankton Assemblage Structure of Springs in the Yangtze Estuary Revealed by Biological and Environmental Visions. *PeerJ* 3, e1186. doi: 10.7717/peerj.1186

Zhang, H., Xian, W., and Liu, S. (2016). Autumn Ichthyoplankton Assemblage in the Yangtze Estuary Shaped by Environmental Factors. *PeerJ* 4, e1922. doi: 10.7717/peerj.1922

Zhang, H., Xian, W., and Liu, S. (2019). Seasonal Variations of the Ichthyoplankton Assemblage in the Yangtze Estuary and its Relationship With Environmental Factors. *PeerJ* 7, e6482. doi: 10.7717/peerj.6482

Zhang, G., Zheng, L., He, H., Lin, H., Zhan, X., and Li, K. (2020). The Continuous Observation of Ichthyoplankton Species Composition and Diversity in Summer in Yangtze Estuary. *J. Fish. Res.* 42 (1), 10–21. doi: 10.14012/j.cnki.fjsc.2020.01.002

Zhou, X., Guo, S., Song, NA, and Zhang, X. (2017). Identification of *Cynoglossus Joyneri* Eggs and Larvae by DNA Barcoding and Morphological Method. *Biodiversity Sci.* 25 (8), 847–855. doi: 10.17520/biods.2017094

Zhuang, P. (2006). *Fishes of the Yangtze Estuary.* (Shanghai: Shanghai Scientific & Technical Publishers).

Zhu, X. H., Liu, D., and Sha, X. S. (2002). Relationship Between Ichthyoplankton Community Structure and Environmental Factors in Spring in the Yangtze Estuary. *Stud. Mar. Sin.* 00, 169–179. doi: CNKI:SUN:HKJK.0.2002-00-022

Conflict of Interest: The authors declare that the research was conducted in the absence of any commercial or financial relationships that could be construed as a potential conflict of interest.

The reviewer YL is currently organizing a Research Topic with the author HZ.

Advantages of publishing in Frontiers

OPEN ACCESS
Articles are free to read
for greatest visibility
and readership

FAST PUBLICATION
Around 90 days
from submission
to decision

HIGH QUALITY PEER-REVIEW
Rigorous, collaborative,
and constructive
peer-review

TRANSPARENT PEER-REVIEW
Editors and reviewers
acknowledged by name
on published articles

Frontiers
Avenue du Tribunal-Fédéral 34
1005 Lausanne | Switzerland

Visit us: www.frontiersin.org
Contact us: frontiersin.org/about/contact

REPRODUCIBILITY OF RESEARCH
Support open data
and methods to enhance
research reproducibility

DIGITAL PUBLISHING
Articles designed
for optimal readership
across devices

FOLLOW US
@frontiersin

IMPACT METRICS
Advanced article metrics
track visibility across
digital media

EXTENSIVE PROMOTION
Marketing
and promotion
of impactful research

LOOP RESEARCH NETWORK
Our network
increases your
article's readership